Mutational analysis of the yeast chromatin modulator complex FACT

by

Allyson F. O'Donnell

Submitted in partial fulfillment of the requirements
for the degree of Doctor of Philosophy

at

Dalhousie University
Halifax, Nova Scotia
August, 2004

© Copyright by Allyson F. O'Donnell, 2004

National Library
of Canada

Acquisitions and
Bibliographic Services

395 Wellington Street
Ottawa ON K1A 0N4
Canada

Bibliothèque nationale
du Canada

Acquisisitons et
services bibliographiques

395, rue Wellington
Ottawa ON K1A 0N4
Canada

Your file Votre référence
ISBN: 0-612-94033-0
Our file Notre référence
ISBN: 0-612-94033-0

The author has granted a non-exclusive licence allowing the National Library of Canada to reproduce, loan, distribute or sell copies of this thesis in microform, paper or electronic formats.

The author retains ownership of the copyright in this thesis. Neither the thesis nor substantial extracts from it may be printed or otherwise reproduced without the author's permission.

L'auteur a accordé une licence non exclusive permettant à la Bibliothèque nationale du Canada de reproduire, prêter, distribuer ou vendre des copies de cette thèse sous la forme de microfiche/film, de reproduction sur papier ou sur format électronique.

L'auteur conserve la propriété du droit d'auteur qui protège cette thèse. Ni la thèse ni des extraits substantiels de celle-ci ne doivent être imprimés ou aturement reproduits sans son autorisation.

In compliance with the Canadian Privacy Act some supporting forms may have been removed from this dissertation.

While these forms may be included in the document page count, their removal does not represent any loss of content from the dissertation.

Conformément à la loi canadienne sur la protection de la vie privée, quelques formulaires secondaires ont été enlevés de ce manuscrit.

Bien que ces formulaires aient inclus dans la pagination, il n'y aura aucun contenu manquant.

Canada

DALHOUSIE UNIVERSITY

To comply with the Canadian Privacy Act the National Library of Canada has requested that the following pages be removed from this copy of the thesis:

Preliminary Pages

Examiners Signature Page (pii)

Dalhousie Library Copyright Agreement (piii)

Appendices

Copyright Releases (if applicable)

For my grandmother, Edna O'Donnell
who taught me what it means to persevere.

TABLE OF CONTENTS

		page
I.	**INTRODUCTION**	**1**
1.	Regulation of chromatin structure	**1**
	i) Chromatin structure	**1**
	ii) ATP-dependent nucleosome remodelling	**4**
	iii) Nuclesome modifications	**6**
	iv) Histone protein substitutions	**8**
	v) Histone chaperones	**10**
2.	Yeast FACT structure and function	**13**
	i) FACT complex structure	**14**
	ii) A role for FACT in transcription	**16**
	iii) The involvement of FACT in DNA replication and repair	**24**
II.	**MATERIALS AND METHODS**	**28**
1.	Media and growth conditions	**28**
2.	Yeast strains and plasmids	**37**
	i) KanB and derivatives	**37**
	ii) *YNL035c* deletion strains	**40**
	iii) Generating *natMX4*-tagged mutant *cdc68* alleles	**42**
	iv) Strains for 'classical' synthetic-lethal screening	**50**
	v) Plasmids	**51**
	a) pRS316-A4 and pRS426-B2	**51**
	b) Plasmids used in yeast two-hybrid analysis	**51**
	c) Plasmids used to generate recombinant Cdc68 and Pob3 proteins	**53**
	d) pRS425-SSD1 and pRS315-SSD1	**54**
	e) pRS315-UTRSSD1, pRS315-YI50SSD1, and pRS315-KanBSSD1	**55**
	f) pRS425-SRP101	**56**
	g) p315-ΔNTDFLAG and p316-ΔNTDFLAG	**56**
	h) 316-ΔNTD-3'68	**56**
	i) p316-ΔNTD plasmids containing the *cdc68-ΔNTD* allele with additional C-terminal point mutations	**56**
	j) p426-TF128 plasmids	**57**
	k) pRS314-YNL and pRS424-YNL	**57**
3.	DNA manipulations	**58**
	i) Restriction endonuclease digestion, calf intestinal alkaline phosphatase treatment, and DNA ligations	**58**
	ii) Plasmid isolation	**58**
	iii) Plasmid transformations	**59**
	iv) DNA sequencing	**60**
	v) Polymerase chain reaction (PCR)	**60**
	a) PCR using *Taq* DNA polymerase	**61**
	b) Mutagenic PCR	**62**

c) Colony PCR 62
d) High-fidelity PCR 62
4. Protein analyses 63
i) Yeast protein extracts 63
a) Glass-bead disruption method 63
b) TCA extractions 64
ii) Co-immunoprecipitation 65
iii) Purification of recombinant Cdc68 and Pob3 polypeptides 65
a) Isolation of GST fusion proteins 66
b) Isolation of His-tagged recombinant Cdc68 proteins 66
iv) GST-pulldown assays 67
v) SDS-polyacrylamide gel electrophoresis and western blot analysis 68
5. Gene-expression analysis 69
i) Northern blotting 69
ii) Microarray experiments 70
a) Microarray slides 70
b) RNA extractions, labelling, and microarray hybridization 72
c) Signal intensities and data normalization 73
d) Identifying genes with significantly altered expression in *cdc68* mutant cells 74
iii) β-galactosidase assays 76
a) Filter lifts 76
b) Permeabilized-cell assays 80
6. Synthetic genetic array (SGA) analysis 81

III. RESULTS 84
1. Characterization of yFACT complex physical interactions 84
i) Cdc68 and Pob3 fail to interact in the yeast two-hybrid system 84
ii) *In vitro* pull-down assays show that the middle domain of Cdc68 is responsible for binding Pob3 99
iii) *In vivo* assessment of Cdc68-mini and Cdc68-ΔNTD association with Pob3 108
iv) Assessment of CP multimerization 112
2. Isolation and characterization of novel *cdc68* mutant alleles 118
i) Generation of dominant *cdc68* alleles that cause defects in chromatin structure 118
ii) New Cdc68 mutants supply essential function 131
iii) New Cdc68 mutant proteins are present at wild-type levels in cells grown at 30°C 132
iv) Cdc68 N-terminal and C-terminal mutations cause similar phenotypes 132
v) Cdc68 N-terminal mutations produce unstable protein products 141
vi) The temperature-sensitive phenotype of Cdc68 N-terminal mutants can be suppressed by elevated gene dosage 142

vii) The hydroxyurea sensitivities of *cdc68* mutations are not due to defects in the activation of the DNA-replication checkpoint 145
viii) Rad53 activation in response to hydroxyurea treatment is impaired in certain *cdc68* mutant strains 149
ix) *RNR1* and *RNR3* gene expression in response to hydroxyurea is altered in *cdc68* mutants 152
x) Increased dosage of *RNR1* or *RNR3* cannot suppress the hydroxyurea sensitivity of *cdc68* mutants 156
xi) Genetic analysis of chimeric *cdc68* mutant alleles 159
xii) Chimeric N- and C-terminally mutated alleles generate stable protein products 165
xiii) Global alterations in transcription caused by *cdc68* mutations 168
a) Genes with altered transcript abundance in *cdc68-mini* cells 168
b) Genes with altered transcript abundance in *cdc68-312* cells 175
c) Genes with altered transcript abundance in *cdc68-319* cells 181
i. Genes with increased transcript abundance in *cdc68-319* cells 181
ii. Genes with decreased transcript abundance in *cdc68-319* cells that are also regulated during the diauxic shift 206
iii. Genes with decreased transcript abundance in *cdc68-319* cells that are induced by stress-response transcription factors Msn2/4 and/or Hsf1 207
iv. Genes with decreased transcript abundance in *cdc68-319* cells that are regulated by the Ssn6-Tup1 repressor complex 208
v. Genes with decreased transcript abundance in *cdc68-319* cells that encode proteins involved in vesicular transport 209
vi. Genes with decreased transcript abundance in *cdc68-319* cells that encode proteins involved in cell integrity 210
3. Genetic and phenotypic characterization of *cdc68* mutant alleles implicate a role for FACT in mediating cell integrity 213
i) Complementation of the temperature sensitivity of *cdc68 ssd1-d* cells by *SSD1* 213
ii) Cells containing *cdc68* mutation exhibit phenotypes consistent with defects in cell integrity 220
iii) Genetic interactions between genes encoding Pkc1-signalling components and *cdc68-312* and *cdc68-319* indicate a role for Cdc68 in maintaining cell integrity 226
iv) *cdc68* mutations alter the activity of SBF but do not alter transcript levels for *SWI4* and *SWI6* 235

4. Synthetic lethal interactions with novel *cdc68* mutant alleles 242
i) Identification of synthetic lethal interactions with *cdc68-E857K* using a 'classical' synthetic-lethal approach 245
ii) Synthetic genetic array analysis of *cdc68* mutant alleles 257
iii) SGA analysis of *CDC68::natMX4* 259
iv) SGA analysis using *cdc68-E857K::natMX4* 268
a) *cdc68-E857K* SGA interactions with genes involved in transcription 268
b) *cdc68-E857K* SGA interactions with genes involved in DNA metabolism 278
c) Additional *cdc68-E857K* SGA interactions and conclusions 282
v) Synthetic genetic array analysis with *cdc68-E763G::natMX4* 283
a) *cdc68-E763G* SGA interactions with genes involved in transport 284
b) *cdc68-E763G* SGA interactions with genes involved in cell integrity and morphogenesis 305
c) *cdc68-E763G* SGA interactions with genes involved in transcription 307
vi) Synthetic genetic array analysis with *cdc68-312::natMX4* 311
a) Common interactions found using SGA for both *cdc68-E763G* and *cdc68-312* with genes involved in transport, cell integrity and morphogenesis 311
b) *cdc68-312* SGA interactions with genes involved in transcription 322
vii) Synthetic genetic array analysis with *cdc68-319::natMX4* 325
a) *cdc68-319* SGA interactions with genes involved in transcription 325
b) *cdc68-319* SGA interactions with genes involved in DNA replication and repair 341
viii) Synthetic genetic array analysis with *cdc68-ΔNTD-FLAG::natMX4* 345
a) *cdc68-ΔNTD* SGA interactions with genes involved in transcription 360
b) *cdc68-ΔNTD* SGA interactions with genes involved in DNA replication and repair 362
ix) Classification of *cdc68* mutant alleles based on synthetic genetic array analysis 366
x) Comparison of synthetic genetic interactions identified with *cdc68* mutants to those for other genes 369
5. Identification of Ynl035c as a novel interacting partner with Cdc68 372
i) Ynl035c physically interacts with the Cdc68(436-1035) polypeptide *via* the yeast two-hybrid assay 372
ii) Phenotypic analysis of *ynl035cΔ* 379
iii) Characterization of genetic interactions for *YNL035c* and *CDC68* 380
iv) Synthetic genetic array analysis of *ynl035cΔ* 382

IV. DISCUSSION **387**
1. FACT structure **387**
i) Domain structure of FACT **387**
ii) Domains responsible for the association of Cdc68 and Pob3 **387**
iii) FACT multimerization **391**
iv) FACT physical associations with other proteins **393**
2. FACT functional studies **393**
i) Mechanism generating the Spt phenotype in Cdc68 mutants **393**
ii) *cdc68* alleles categorized by impact on FACT functions **398**
iii) C-terminal substitutions show that the Cdc68 C-terminal and N-terminal domains share an overlapping function **403**
iv) FACT and cell integrity **405**
3. Concluding remarks **407**

APPENDIX 1 **409**
Summary of random spore verification of genetic interactions with *cdc68* alleles employed in SGA analysis

APPENDIX 2 **419**
Colour indexes for genetic interactions webs.

REFERENCES **420**

LIST OF FIGURES

		page
1.	The nucleosome	3
2.	Model for FACT activity in transcription	23
3.	PCR verification of *kanMX4* replacement at *CDC68* chromosomal locus	39
4.	Chromosomal integration of *cdc68* alleles containing the downstream *natMX4* tag	47
5.	Spotted microarray methodology	71
6.	Comparison of *cdc68-312* transcription profiles from two microarray hybridizations	77
7.	Comparison of *cdc68-319* transcription profiles from two microarray hybridizations	78
8.	Comparison of *cdc68-mini* transcription profiles from two microarray hybridizations	79
9.	Yeast two-hybrid system	86
10.	Two-hybrid interactions	92
11.	Gal4 BD and AD fusion proteins	95
12.	Summary of interactions between Cdc68 and Pob3 as determined by *in vitro* pull-down studies	100
13.	Purified recombinant GST-Pob3 polypeptides used in pull-downs	101
14.	Purified recombinant pET-Cdc68 polypeptides used in pull-downs	103
15.	GST-Pob3 pull-downs of recombinant pET-Cdc68 polypeptides	104
16.	GST pull-downs of pET-Cdc68 recombinant polypeptides with GST-Pob3, GST-NTDPob3, GST-CTDPob3 and GST alone	105
17.	pET-Cdc68(436-786) pull-downs with GST-Pob3, GST-NTDPob3, GST-CTDPob3, and GST	106
18.	CP structure	109
19.	Competitive co-immunoprecipitation of full length Cdc68 versus (A) Cdc68-mini or (B) Cdc68-ΔNTD with Pob3	111
20.	Pob3-Pob3 interaction	116
21.	Spt reporter genes	120
22.	Regions of *CDC68* subjected to PCR mutagenesis	121
23.	Spt− phenotype of the sequenced *cdc68* alleles generated in this study	124
24.	Alignment of Cdc68 protein homologues	126
25.	Summary of sequence changes in eleven of the Cdc68 mutant proteins generated in this study	129
26.	Western blot of total protein extracts from cells containing Cdc68 mutant proteins	133
27.	*cdc68-312* and *cdc68-319* temperature sensitivity	134
28.	Hydroxyurea sensitivity of *cdc68-312* and *cdc68-319* mutant cells	136
29.	Phenotypes caused by Cdc68 mutant proteins with of N-terminal substitutions	138
30.	N-terminal deletion mutations of Cdc68	139
31.	Phenotypes caused by Cdc68 mutant proteins with N-terminal deletions	140
32.	Stability of mutant Cdc68 proteins at elevated temperature	143

33.	Dosage suppression of the temperature-sensitive phenotype for Cdc68 mutations	**144**
34	Acute hydroxyurea sensitivity tested at 30°C	**147**
35	Acute hydroxyurea sensitivity tested at 35°C	**148**
36	Rad53 phosphorylation in response to hydroxyurea treatment	**151**
37.	*RNR1* and *RNR3* transcript levels in response to hydroxyurea treatment are altered in *cdc68* mutant cells	**153**
38.	Overexpression of *RNR1* or *RNR3* does not suppress the hydroxyurea sensitivity of *cdc68* mutants	**158**
39.	*sml1Δ* is unable to alleviate the hydroxyurea sensitivity of *cdc68-ΔNTD*	**160**
40.	Phenotypes of *cdc68* chimeric mutants containing an NTD deltion and C-terminal point mutation(s)	**163**
41.	Chimeric Cdc68 proteins are stable in the presence of wild-type Cdc68 protein	**166**
42.	Chimeric Cdc68 proteins are stable at 38°C	**167**
43.	Alleviation of *cdc68-312* and *cdc68-319* temperature sensitivities	**216**
44.	*SSD1* increases the maximal permissive growth temperature for cells containing *cdc68* mutant cells	**221**
45.	Sorbitol-remedied temperature sensitivity of *cdc68* mutant cells	**224**
46.	Sodium dodecyl sulfate (SDS) sensitivity of *CDC68 ssd1-d* mutant cells	**225**
47.	Abnormal cell morphologies associated with *cdc68 ssd1* mutant cells	**227**
48.	Suppression of the temperature sensitivity of *cdc68-312* and *cdc68-319* by over-expression of genes encoding components of the Pkc1 signaling pathway	**229**
49.	Tetrad analysis of segregants from heterozygous *cdc68-319::natMX4* diploids deleted for genes encoding Pkc1-pathway components	**234**
50.	Synthetic growth defect at 37°C for *cdc68-319* cells deleted for genes encoding Pkc1-pathway components	**236**
51.	Effects of *cdc68* mutations on MBF, SBF, and Swi4 activation of transcription	**239**
52.	*SWI4* and *SWI6* transcript abundances are not altered in *cdc68* mutant cells	**241**
53.	Mechanisms for synthetic lethal interactions	**243**
54.	Classical synthetic lethal screening with *cdc68-E857K*	**246**
55.	Synthetic genetic array (SGA) analysis	**248**
56.	Growth of *cdc68-E857K* synthetic-lethal candidate cells on 5-fluoroorotate acid medium	**253**
57.	Two *cdc68-E857K* synthetic-lethal candidates are further confirmed	**254**
58.	Synthetic genetic interactions web with *cdc68-E857K*	**277**
59.	Tetrad analysis of segregants from diploids containing gene deletions identified by SGA analysis as synthetically lethal with *cdc68-E763G::natMX4*	**285**
60.	Synthetic-genetic-interactions web involving *cdc68-E763G*	**296**
61.	Connectivity of synthetic genetic interactions web with *cdc68-E763G*	**297**

62.	Synthetic-genetic-interactions web of genes involved in vesicular transport identified as synthetically sick or lethal in combination with *cdc68-E763G*	**298**
63.	Synthetic genetic interactions web with *cdc68-312*	**320**
64.	Connectivity of synthetic genetic interactions web with *cdc68-312*	**321**
65.	Gene deletions identified as causing a growth defect with both *cdc68-E763G* and *cdc68-312*	**323**
66.	Synthetic genetic interactions web with *cdc68-319*	**326**
67	Connectivity of synthetic genetic interactions web with *cdc68-319*	**337**
68.	Tetrad analysis to verify chromosomal location of the *natMX4* cassette in cells from the *cdc68-ΔNTD::natMX4* query strain	**346**
69.	Synthetic genetic interactions web with *cdc68-ΔNTD*	**348**
70.	Connectivity of synthetic genetic interactions web with *cdc68-ΔNTD*	**359**
71.	Synthetic genetic interactions web for *cdc68*	**370**
72.	Common genetic interactions identified in SGA screens with *cdc68* mutant alleles and with *cdc73Δ*	**371**
73.	Common genetic interactions identified in SGA screens with *cdc68* mutant alleles and with *cdc45*	**373**
74.	BD-Cdc68(436-1035) interacts with AD-Ynl035c	**378**
75.	Over-expression of *YNL035c* causes a synthetic growth defect in *cdc68-319* cells	**381**
76.	FACT physical associations	**394**

LIST OF TABLES

		page
1.	Chemical additions to growth media used to assess sensitivities in yeast cells	29
2.	Yeast strains used in this study	31
3.	Plasmids used in this study	43
4.	DNA sequencing primers and templates	52
5.	Microarray slide identification numbers, labelled cell extracts employed for each, and normalization factors	75
6.	Plasmid-encoded fusions of Cdc68 and Pob3 to Gal4 DB and Gal4 AD	87
7.	Summary of Cdc68 *vs* Pob3 two-hybrid results	93
8.	Summary of Cdc68 *vs* Cdc68 and Pob3 *vs* Pob3 two-hybrid results	113
9.	Summary of Cdc68 mutants generated and verifications performed	122
10.	Summary of sequence changes in novel *cdc68* alleles	125
11.	Phenotypes for N-terminal and C-terminal Cdc68 mutants	137
12.	Phenotypes for *cdc68* mutant alleles containing deletions of the NTD combine with C-terminal mutations	164
13.	Genes with expression changes greater than two-fold in *cdc68-mini* cells as determined by microarray analysis	170
14.	Genes with expression changes greater than two-fold in *cdc68-312* cells as determined by microarray analysis	176
15.	Genes with expression changes greater than two-fold in *cdc68-319* cells as determined by microarray analysis	182
16.	Additional SGA false positive gene deletions identified in the Singer/Johnston lab	261
17.	Number of synthetic-lethal or –sick genetic interactions identified with each *cdc68* allele using SGA analysis and random spore	269
18.	Gene deletions that are synthetically sick or lethal in combination with *cdc68-E857K*	270
19.	Gene deletions that are synthetically sick or lethal in combination with *cdc68-E763G*	286
20.	Gene deletions that are synthetically sick or lethal in combination with *cdc68-312*	312
21.	Gene deletions that are synthetically sick or lethal in combination with *cdc68-319*	327
22.	Gene deletions that are synthetically sick or lethal in combination with *cdc68-ΔNTD*	349
23.	Overlap between SGA analyses datasets for each allele of *cdc68*	367
24.	Summary of two-hybrid library screening	375
25.	Gene deletions identified as synthetic-lethal with *ynl035cΔ* by SGA analysis	383

ABSTRACT

FACT (facilitates chromatin transactions) is an essential conserved complex for chromatin modulation, and in yeast is comprised of the Cdc68 and Pob3 proteins. My thesis research has identified novel mutations of the Cdc68 subunit of FACT that result in defects in chromatin structure. These mutations cluster in the C-terminal region of Cdc68 which in addition to the identification of an N-terminal deletion mutation of *cdc68* (missing approximately 40% of the coding sequence), has facilitated a concerted approach to understand the structure/function relationships for Cdc68, particularly in the context of the Cdc68-binding partner, Pob3. In particular, the regions responsible for Cdc68/Pob3 interaction(s) were determined. Additional genetic experiments to elucidate structure/function relationships for several mutant alleles of *cdc68* were also carried out, including characterization of phenotypes associated with a range of mutant alleles, a dosage-suppressor selection approach, and screens for synthetic-lethal interactions of *cdc68* N-terminal and C-terminal mutations. The conclusions from these studies include 1) identification of a role for the N-terminal domain of Cdc68 in FACT-mediated DNA replication and repair, 2) classification of Cdc68 C-terminal point mutations based on the ability to influence transcription-related processes or intracellular transport, 3) characterization of an overlapping essential function for the N-terminal and C-terminal domains of Cdc68, and 4) identification of Pkc1-signalling components as dosage suppressors of defective Cdc68 function that implicates FACT in regulation of cell integrity and morphogenesis.

I. INTRODUCTION

A nuclear complex in eukaryotes known as FACT mediates transcription, DNA repair and replication, and exerts its effects on these processes mainly through modulation of chromatin structure (reviewed in Belotserkovskaya *et al.* 2004). Recent research into FACT function has yielded several new and exciting findings, and the synthesis of these findings has allowed a model of FACT function in modulating chromatin structure to be generated (reviewed in Belotserkovskaya *et al.* 2004). During the course of the research presented here I have furthered our understanding of FACT structure and pursued investigations to allow functional assignments for specific regions of the Cdc68 protein, the largest subunit of the FACT complex. Presented below is a review of pertinent features of chromatin structure and its regulation, with a focus on the role of FACT in mediating chromatin structural changes during processes requiring access to the DNA template.

1. Regulation of chromatin structure

i) Chromatin structure

Chromatin refers to the protein/DNA package within the nucleus of eukaryotic cells. The functions of this protein packaging involve more than just compaction of the large chromosomal DNA molecules; chromatin is involved in the organization of the DNA template, and as a result influences all biochemical and molecular transactions that occur with the DNA. The basic unit of chromatin is the nucleosome, which is comprised of an octamer of histone proteins around which 1.65 turns, or approximately 147 bp, of DNA are wrapped (White *et al.* 2001). Association of DNA with the histone octamer results in a 7-fold compaction of the DNA (reviewed in Nemeth and Langst 2004). Nucleosomes in yeast are spaced at approximately 162-bp intervals and the inter-nucleosomal DNA interacts with the histone tails from the octamer, leading to further compaction and organization of chromatin structure (Horz and Zachau 1980; Luger *et al.* 1997; Nemeth and Langst 2004). A considerable amount of research focusing on nucleosomal structure and how it is regulated has been reported, and the crystal structure of the nucleosome has been solved (Luger *et al.* 1997; White *et al.* 2001). In contrast, little is known about higher-order chromatin structures and their regulation. Non-histone proteins as well as the histone tails, and in most eukaryotes an additional histone protein, known as the

'linker' histone H1, assist in the organization of nucleosomes into arrays that comprise the 10-nm and 30-nm fibres (reviewed in Nemeth and Langst 2004). Two models account for the arrangement of these 30-nm fibres into higher-order chromatin structures: the first is that the 30-nm fibre is 'coiled' to form higher-order fibres ranging from 60 nm to 300 nm in diameter (Belmont and Bruce 1994), while the second is that the 30-nm fibre is arranged into long loops that radiate off a 'scaffold' structure, resulting in further condensation of chromatin structure (Boy de la Tour and Laemmli 1988). Undoubtedly these higher-order chromatin structures have roles to play in regulating gene expression and access to the DNA template, but this area remains largely unstudied. The impact of the nucleosomal package on gene expression and DNA transactions in general is well characterized and this nucleosomal packaging is directly influenced by the FACT complex.

Each histone that makes up the protein core of the nucleosome is comprised of two unstructured 'tail' regions, one at each of the protein termini, and a central portion that is organized into three α-helices that form the 'histone-fold' structure (Arents *et al.* 1991); (Luger *et al.* 1997). The histone fold is responsible for the dimerization of histone proteins as well as for interactions between these dimers that assist in forming the stable nucleosomal package (Luger *et al.* 1997). The histone octamer is comprised of two dimers of histones H3 and H4 at its core with a dimer of histones H2A and H2B flanking each side of the core tetramer (Figure 1). The crystal structure of the nucleosome revealed that the amino and carboxy-termini or 'tails' of these dimers are not tightly associated with the nucleosome, but protrude from its surface (Luger *et al.* 1997). In the cases of histones H3 and H2B the tails are threaded out through aligned minor grooves of the helically wrapped DNA surrounding the histone octamer, where they are free to make contacts with an array of other protein factors (Luger *et al.* 1997). The amino-terminal tails of the H4 histones are thought to be important for inter-nucleosomal interactions and stabilizing higher-order chromatin structures (Luger *et al.* 1997).

Chromatin structure can be both an obstacle and an ally to DNA transactions such as transcription, replication and repair, but in either case alterations in chromatin structure play key roles in the regulation of these processes. There is a myriad of cellular factors whose roles' center on altering the interaction between DNA and the histone octamer by

A.

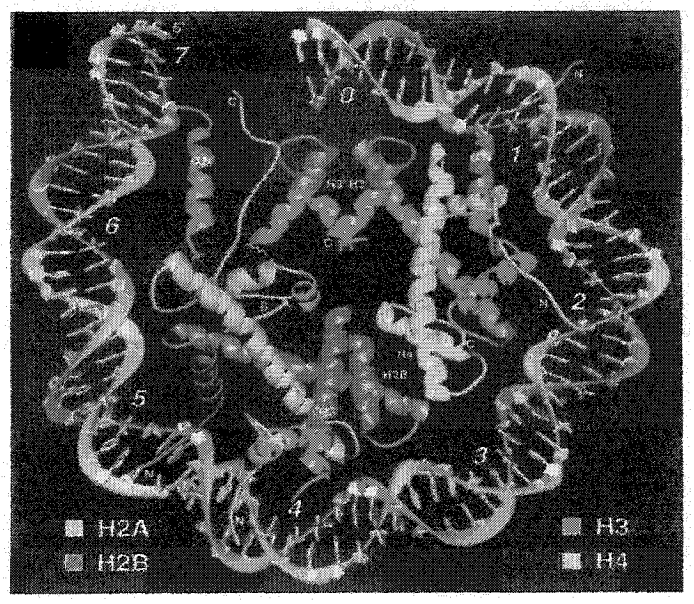

B.

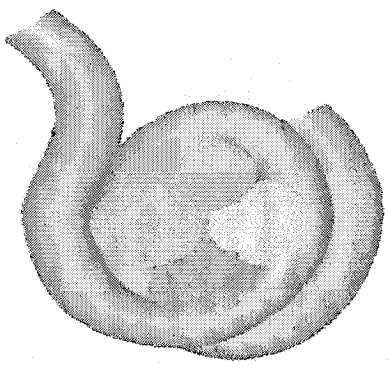

Figure 1. The nucleosome. **A.** Cross-section of a nucleosome based on crystal structure (modified from Luger *et al.* 1997). The DNA helix is shown in green and brown wrapped around half of a nucleosome (one H2A/H2B and one H3/H4). **B.** Half of the histone octamer is visible (colour-coded to match the histones in (A) around which the 1.6 loops of DNA (shown in brown) are wrapped (modified from Formosa, 2003).

remodelling or modifiying the histone proteins to decondense chromatin structure, or by folding and depositing histones onto DNA. Substitutions of the canonical histone proteins for 'variant' histones can also lead to specialized chromatin structures that promote specific nuclear functions. Thus regulation of chromatin structure impinges on all transactions with the DNA, including transcription, replication and repair. As a result, complexes that modulate chromatin structure often have an impact on each of these processes as well. The key mechanisms employed to regulate chromatin, and specifically nucleosomal, structure are described in the following sections.

ii) ATP-dependent nucleosome remodelling

DNA wrapped around the histone octamer forms non-covalent associations approximately every 10 bp, and these mediate the stability of the nucelosome structure (Luger *et al.* 1997; Rhodes 1997). Chromatin-remodelling complexes employing the energy derived from the hydrolysis of ATP to weaken the histone/DNA association in the nucleosome often facilitates access to the DNA template (reviewed in Peterson and Workman 2000; Peterson 2002; Martens and Winston 2003). Recent findings also implicate ATP-dependent chromatin-remodelling complexes in the repression of gene expression, indicating that the activities of these complexes do not always facilitate access to the DNA template but may also inhibit access (Martens and Winston 2002; reviewed in Martens and Winston 2003). ATP-dependent chromatin-remodelling complexes contain multiple protein subunits but may be classified into four groups, including SWI/SNF, ISWI, CHD, or INO80-related, based on the similarity of the ATPase domain and the presence of 'accessory domains' involved in chromatin and DNA binding in each of the catalytic proteins (Martens and Winston 2003; Langst and Becker 2004; Mellor and Morillon 2004).

The mechanism(s) of ATP-dependent nucleosome remodelling catalyzed by these different complexes has been the subject of extensive research and there have been several models proposed based on *in vitro* and *in vivo* studies (Havas *et al.* 2000; Gavin *et al.* 2001; Langst and Becker 2001; Narlikar *et al.* 2001; Fazzio and Tsukiyama 2003) reviewed in Langst and Becker 2004). Recently described 'torsional' changes in the DNA wound around the nucleosome as a result of ATP-dependent remodelling are thought to create 'bulges' or loops of DNA that have lost contact with the histone octamer. The size

of the DNA loop and its position on the nucleosome surface then determines the fate of the nucleosome remodelling. The detachment of a loop of DNA may lead to sliding of the nucleosome, thereby altering the position of the DNA with respect to the histone octamer and exposing a new region of template DNA to cellular factors. Members of the ISWI family of remodelling complexes appear to operate in this fashion by sliding the nucleosome along the DNA template (Fazzio and Tsukiyama 2003; Mellor and Morillon 2004). Alternatively, the loop of DNA may lose contact with only a small region of the octamer surface, resulting in a 'bulge' of DNA that is not bound to the nucleosome and is therefore free to interact with other proteins to mediate DNA transactions (Peterson 2002; Langst and Becker 2004). The SWI/SNF family of remodelling complexes is thought to act in this fashion, given that they do not alter the position of the histone octamer with respect to the DNA and that they may allow access to DNA that is bound to the central-most region of the nucleosome (Narlikar *et al.* 2001; Langst and Becker 2004). A common aspect of all proposed ATP-dependent chromatin-remodelling models is that the energy of ATP hydrolysis is used to generate torsional strain which somehow disrupts histone/DNA contacts within the nucleosome, leading to altered accessibility of the DNA template. The induction of torsional strain to alter the topology of the DNA bound to the nucleosome may occur in subtly different ways, and this has been proposed to account for the observed differences in the effects of ATP-dependent nucleosome-remodelling complexes on the structure of the nucleosome (reviewed in Flaus and Owen-Hughes 2001; Langst and Becker 2004).

While the FACT complex does not require ATP for its chromatin-related activities (Orphanides *et al.* 1998; Wittmeyer *et al.* 1999), FACT has been shown to interact physically with the Chd1 ATP-dependent chromatin-modifying factor (LeRoy *et al.* 1998; Kelley *et al.* 1999; Krogan *et al.* 2002; Simic *et al.* 2003). *In vitro* studies of RNA polymerase II transcription using a nucleosome template have also tied FACT to ATP-dependent chromatin remodelling by showing that the human ISWI homologue RSF is required for promoter-proximal chromatin remodelling prior to FACT-assisted transcription elongation (LeRoy *et al.* 1998). In addition to these physical and functional interactions with ATP-dependent chromatin-remodelling complexes, I show here that mutations in the Cdc68 component of FACT cause synthetic growth defects in

combination with gene deletions eliminating components of SWR-C or INO80, which are ATP-dependent chromatin-remodelling complexes. These findings suggest that while FACT may not possess intrinsic ATP-dependent remodelling activity of its own, it shares important functions with ATP-dependent remodelling complexes.

iii) Nucleosome modifications

Another way to regulate or modify nucleosome structure is by changing the biochemical nature of the histones. The histone tails extend from the surface of the nucleosome at 20-bp intervals (Luger *et al.* 1997) and are therefore easily accessible targets for modification by and association with cellular factors. The histone tails are unstructured, highly basic, and range from 15 to 30 amino acids in length (Luger *et al.* 1997; Kornberg and Lorch 1999). Several multi-subunit complexes target the histone tails as substrates for covalent modifications including acetylation, phosphorylation, methylation, ubiquitination, and ADP-ribosylation (Iizuka and Smith 2003). These modifications occur frequently, and the combination of modifications present on the histone tails is crucial in mediating DNA transactions within the region. For example, acetylated histone tails are generally associated with 'open' chromatin conformations that are involved in active transcription processes (reviewed in Grunstein; 1997; Struhl 1998; Kornberg and Lorch 1999), while unacetylated or hypoacetylated histone tails are associated with 'silenced' or transcriptionally repressed regions of the DNA (reviewed in Grunstein, 1997; Struhl 1998; Kornberg and Lorch 1999; Strahl and Allis 2000; Iizuka and Smith 2003). The ordered accumulation of covalent modifications on histone tails and the recognition of specific sets of alterations by other protein factors is referred to as the 'histone code' (Strahl and Allis 2000). An example of this type of recruitment to histone tails by a specific covalent modification is the association of chromodomain proteins to histone tails containing a methylated lysine residue (Jacobs and Khorasanizadeh 2002; Nielsen *et al.* 2002; Min *et al.* 2003). Many proteins containing chromodomains also have histone-modifying or -remodelling functions. In this way the initial methylation of a lysine residue assists in recruiting other complexes that further alter chromatin structure. Another example of the combinatorial control of histone-tail modifications and their impact on DNA transactions involves the requirement for ubiquitination of histone H2B (mediated by Rad6 in yeast) prior to methylation of histone H3 (by either the COMPASS

or Dot1 methyltransferase complexes in yeast) during the formation of silenced chromatin structures at the telomeres (Dover *et al.* 2002; Sun and Allis 2002; Wood *et al.* 2003). There are numerous examples of this type of ordered recruitment of chromatin-modifying or -remodelling complexes by specific covalent modifications of histones (reviewed in Fischle *et al.* 2003).

In yeast, as in other eukaryotes, there exist many large, multi-subuint complexes responsible for the covalent modifications of histone tails. At least five complexes in yeast, known as Elongator, SAGA, ADA, NuA3, and NuA4, posess histone acetyltransferase activity (reviewed in Brown *et al.* 2000). The process of histone acetylation is reversed by histone deacetylases, of which there are several in yeast including Rpd3, Hda1, and Sir2 (Rundlett *et al.* 1996; Landry *et al.* 2000; Shore 2000; Smith *et al.* 2000). Unlike acetylation, the covalent addition of a methyl group to histone tails is not reversible. The catalytic subunits of methyltransferase complexes in yeast include Set1 (COMPASS), Set2, Set3, and Dot1, among others (Jenuwein 2001; Khan and Hampsey 2002; Ng *et al.* 2002; Min *et al.* 2003). Ubiquitination of histones is mediated by Rad6 and Ubc2 in yeast and this process, like acetylation, is reversible, with ubiquitin hydrolases removing ubiquitin from histone proteins (Osley 2004). ADP-ribosylation is another type of covalent modification that occurs on histone tails, but the regulation of this modification is not well characterized. Many histone-modifying complexes contain more than one catalytic activity. For example, the Set3 complex in yeast contains both a histone-methyltansferase component and proteins that contain histone-deacetylase activity (Pijnappel *et al.* 2001), and the SAGA complex contains both histone-acetyltransferase and ubiqitin-hydrolase activities (Henry *et al.* 2003). These modifications not only regulate chromatin structure during the process of transcription, which may be the best-understood function, but also play significant roles in DNA repair, replication and recombination (Boulikas 1990; Megee *et al.* 1995; Qin and Parthun 2002; Carrozza *et al.* 2003; Pappas *et al.* 2004).

The FACT complex is not known to possess any histone-modifying activity (Wittmeyer *et al.* 1999), but has been shown to interact physically with the catalytic subunit of the NuA3 histone acetyltransferase complex (John *et al.* 2000), and genetic interactions between mutations in genes encoding FACT subunits and deletions of genes

encoding proteins involved in histone modification have been reported (Formosa *et al.* 2001), identified by Neil Brewster in our lab (N. K. Brewster, unpublished observations) and are demonstrated in this study. Thus, while FACT does not itself covalently modify histones it does share overlapping functions with these complexes, most likely by influencing chromatin structure.

iv) Histone protein substitutions

Substitutions of the canonical histone proteins in the nucleosome for 'variant' histone proteins can result in altered chromatin structures which have been associated with specific cellular functions. While variant histones may not differ greatly in sequence from the canonical histones, incorporation of histone variants into nucleosomes can have a definite impact on nucleosomal structure (Glowczewski *et al.* 2000; Suto *et al.* 2000), which undoubtedly leads to changes in higher-order chromatin structures as well. Histone variants also differ in nucleosome-remodelling and -modifying characteristics and associate with a different subset of protein partners than do the canonical histone proteins, resulting in further alterations to chromatin structure that impact DNA transactions in these regions (Redon *et al.* 2002; Smith *et al.* 2002).

In yeast there are two genes, *CSE4* and *HTZ1*, that encode variant versions of histones H3 and H2A, respectively. The *CSE4* gene encodes a histone variant protein resembling human CENP-A that is selectively incorporated into the histone octamer associated with the 125-bp stretch of centromeric DNA on each yeast chromosome (Meluh *et al.* 1998; Keith *et al.* 1999; reviewed in Smith *et al.* 2002). The association of this modified centromeric nucleosome with centromeric DNA sequences forms the fundamental building block for recruitment of other protein factors involved in the production of the kinetochores (Van Hooser *et al.* 2001), which in turn serve as attachment sites for microtubules and are crucial for mitotic chromosome segregation (reviewed in Smith *et al.* 2002). The mechanism of incorporation of the *CSE4*-encoded CENP-A histone variant in to the centromeric nucleosome is unclear; however, the RSC histone-remodelling complex as well as the chromatin-assembly Hir family of histone chaperone proteins (Introduction 1, v) have been shown to be important for this process (Tsuchiya *et al.* 1998; Sharp *et al.* 2002). Genetic interactions between genes encoding the Hir histone chaperones involved in the deposition of CENP-A and mutations in the genes encoding

FACT subunits have been reported (Formosa *et al.* 2002). These findings are further supported by genetic evidence identified here for a functional relationship between the Hir proteins and FACT. Additionally, the Cbf1 protein recognizes a specific sequence element in centromeric DNA, known as CDE1, and assists in the positioning of the centromeric nucleosome containing the CENP-A histone H3 variant (Niedenthal *et al.* 1993). Genetic interactions have been reported between mutations in the Cbf1 binding site and *cse4* mutations, consistent with an important role for Cbf1 in centromere function (Keith and Fitzgerald-Hayes 2000). I show here that deletion of *CBF1* in cells containing a mutation in the *CDC68* gene, which encodes a FACT subunit, results in a synthetic growth defect. These findings suggest that FACT may play a role in chromatin organization at the centromere; however, additional interpretations are possible, as Cbf1 has been implicated in other activities as well (Ferreiro *et al.* 2004; Kent *et al.* 2004).

A second histone variant found in yeast has been the subject of a flurry of recent publications which focused on the mechanism of histone variant H2A.Z incorporation into nucleosomes and the location of these nucleosomes in the yeast genome (Krogan *et al.* 2003b; Kobor *et al.* 2004; Mizuguchi *et al.* 2004). Genome-wide studies have found approximately 25 locations containing H2A.Z-bearing nucleosomes and, consistent with these findings, gene expression in many of these regions appears to be influenced by H2A.Z (Krogan *et al.* 2003b; Kobor *et al.* 2004; Mizuguchi *et al.* 2004). One of the key locations for H2A.Z incorporation is adjacent to the silenced chromatin found at the telomeres. Telomeric silencing is mediated by the Sir proteins, which form a complex with the chromatin at telomeric regions (reviewed in Gartenberg 2000). Incorporation of H2A.Z into nucleosomes adjacent to these silenced regions assists in blocking the spread of Sir-mediated silencing, thereby permitting active gene expression from these DNA templates (Meneghini *et al.* 2003; reviewed in Rusche *et al.* 2003). The recently identified SWR-C histone-remodelling complex has been shown to play a critical role in regulating the exchange of histone H2A/H2B dimers for H2A.Z/H2B dimers (Krogan *et al.* 2003b; Kobor *et al.* 2004; Mizuguchi *et al.* 2004). Deletions of genes encoding SWR-C members or of the gene encoding H2A.Z are shown here to result in growth defects when combined with FACT mutations. These novel findings implicate FACT in histone

exchange, which is consistent with the current model for FACT function (Introduction 2, ii).

v) Histone chaperones

Histone-gene expression is regulated in a cell-cycle-dependent fashion to coordinate maximal synthesis of histone proteins with DNA replication (Osley 1991). Histone-gene expression outside of S phase is responsive to histone protein dosage (Osley and Hereford 1981; Moran *et al.* 1990) and is repressed by the Hir family of proteins and by Asf1 (Osley and Lycan 1987; Xu *et al.* 1992; Sutton *et al.* 2001a). In addition to regulating histone-gene expression, the Hir proteins and Asf1 have the added role of histone chaperones, assisting in nucleosome assembly during DNA transactions (Tyler *et al.* 1999; Ray-Gallet *et al.* 2002; reviewed in Loyola and Almouzni 2004). Histone chaperones, including the CAF-1 complex, Hir-family proteins, Nap1 and Asf1 in yeast, ensure that histone proteins are properly folded and reach the appropriate locations. Mutations in many proteins involved in histone-chaperone activities result in phenotypes consistent with a role for these proteins in maintaining chromatin structure, including defects in chromatin silencing, centromere function, transcription, regulation of recombination, and repair (reviewed in Loyola and Almouzni 2004). An example of histone-chaperone-mediated function would include the disassembly of nucleosomes in front of elongating RNA and DNA polymerases and then the efficient reassembly or deposition of nucleosomes in the wake of these complexes. Recent evidence (Introduction 2, ii) generates a model for FACT activity consistent with histone-chaperone activity for this complex (reviewed in Belotserkovskaya and Reinberg 2004; Belotserkovskaya *et al.* 2004).

Histone chaperones may be divided into two classes: 1) replication-coupled (RC) chaperones which, as the name implies, assemble and disassemble nucleosomes during replication (Krude and Keller 2001), and 2) replication-independent (RI) chaperones, which are involved in the assembly and disassembly of nucleosomes that occur during other DNA transactions, such as transcription (Altheim and Schultz 1999). The CAF-1 complex, comprised of Cac1, Cac2, and Cac3, is a RC histone chaperone (Smith and Stillman 1989; Gaillard *et al.* 1996) whose primary role appears to be the deposition of nucleosomes on newly synthesized DNA during replication and certain types of repair

(reviewed in Ridgway and Almouzni 2000; Mello and Almouzni 2001). Histone chaperones typically show some degree of specificity in the histones they associate with, and consistent with this, CAF-1 shows a preference for binding histone H3/H4 dimers (Verreault *et al.* 1996). To assist in chromatin assembly on newly synthesized DNA, CAF-1 is targeted to the replication fork *via* associations with proliferating cell nuclear antigen (PCNA) (Krude 1995; Shibahara and Stillman 1999; Moggs *et al.* 2000). Mutations in the CAF-1 complex that result in disruptions in nucleosome assembly on newly replicated DNA have recently been shown to cause DNA polymerase stalling that can result in DNA damage (Ye *et al.* 2003). Despite the crucial role of CAF-1 in establishing chromatin structure on newly synthesized DNA, the genes encoding CAF-1 components are not essential. Several lines of investigation have indicated that other histone chaperones, including Asf1 and the Hir proteins, may share an overlapping function with CAF-1.

Asf1 has been shown to function in both RC and RI nucleosome assembly (Tyler *et al.* 1999; Robinson and Schultz 2003). Like CAF-1, Asf1 preferentially associates with the H3/H4 dimer and is able to assist in histone deposition on newly synthesized DNA during both replication and repair processes (Tyler *et al.* 1999; Mello *et al.* 2002). It has been proposed that since Asf1 has not been shown to assemble nucleosomes independently, it may act as an intermediate in nucleosome assembly, passing histone H3/H4 dimers to CAF-1 or to the Hir proteins, which then load them onto the DNA (Mello and Almouzni 2001; Sharp *et al.* 2001; Sutton *et al.* 2001a; Loyola and Almouzni 2004). However, there is genetic evidence suggesting a role for Asf1 in CAF-1- and Hir-independent functions (Emili *et al.* 2001; Krawitz *et al.* 2002). In addition to its CAF-1- and Hir-associated functions, Asf1 has been shown to interact with the phosphorylated form of Rad53, a DNA-damage-activated kinase, thus providing a link between the DNA-damage response and chromatin assembly (Emili *et al.* 2001; Hu *et al.* 2001; Schwartz *et al.* 2003). The details of this interaction are still unclear, but perhaps the Rad53-mediated DNA-damage signal activates or targets Asf1 to the site of DNA damage, where Asf1 may alter chromatin structure to allow access by repair enzymes (Hu *et al.* 2001). My Synthetic Genetic Array (SGA) analysis employing mutant alleles of *cdc68* has revealed genetic interactions with *asf1* deletion, consistent with a role for

FACT in chromatin assembly. Additionally, synthetic growth defects in cells containing *cdc68* or *pob3* mutant alleles in combination with *asf1*deletion have been previously reported (Formosa *et al.* 2002).

The Hir proteins represent a third class of histone chaperones that have been shown to bind histones H2B, H3, and H4 *in vitro* and are primarily involved in RI nucleosome-assembly processes (Lorain *et al.* 1996; Sutton *et al.* 2001a; Ray-Gallet *et al.* 2002). The Hir chaperones also show significant functional overlap with CAF-1 and Asf1, suggesting that when these other chaperones are defective the Hir chaperones may be able to functionally substitute (Kaufman *et al.* 1998; Sharp *et al.* 2001, 2002). Synthetic genetic relationships between mutations in genes encoding FACT subunits and deletions of *HIR* genes have been reported (Formosa *et al.* 2002). Our lab has also identified similar synthetic genetic effects between *cdc68* alleles and *HIR* gene deletions (Results 4; J. R. Stevens, unpublished observations). Not all *cdc68* mutations result in growth defects when combined with mutations in the *HIR* genes, suggesting functional distinctions among the proteins encoded by different *cdc68* alleles (Results 4; Formosa *et al.* 2002; J. R. Stevens, unpublished observations). Further evidence for the genetic interplay between *HIR*s and genes encoding FACT subunits is provided here.

The Nap1 histone chaperone preferentially interacts with dimers of histones H2A/H2B and has been shown to shuttle in and out of the nucleus in a cell-cycle-dependent fashion (Ito *et al.* 1996; Mosammaparast *et al.* 2002). It is thought that the Nap1 histone chaperone regulates the accumulation of H2A/H2B dimers within the nucleus *via* this shuttling (Mosammaparast *et al.* 2002; reviewed in Loyola and Almouzni 2004). Recently, Nap1 was shown to co-purify with SWR-C and the variant histone H2A.Z. While Nap1 does not appear to be a subunit of SWR-C, given this physical association, perhaps Nap1 is important for the nuclear import of the variant histone H2A.Z in addition to the canonical H2A protein (Kobor *et al.* 2004). Nbp2 (Nap1-binding protein) has been shown to interact physically with Nap1 and therefore may assist in Nap1 histone-chaperone and nuclear shuttling functions. In this study I have found that deletion of the *NBP2* gene results in synthetic growth impairments when cells contain *cdc68* mutant alleles, which may imply that FACT shares an overlapping role in chromatin assembly processes with Nbp2 and Nap1 proteins.

In summary, FACT shares overlapping function with many of the histone chaperones involved in chromatin assembly. This genetic evidence strongly suggests a role for FACT as a histone chaperone itself, a view that is supported by biochemical and genetic findings related to FACT function (discussed below; reviewed in Belotserkovskaya *et al.* 2004; Belotserkovskaya and Reinberg 2004). In addition to genetic interactions with histone chaperones, mutations affecting FACT subunits also show genetic interactions with mutations in genes encoding histone-remodelling and -modifying complexes. Alterations to chromatin structure can be cumulative and there are many instances where more than one type of chromatin alteration (*i.e.* histone remodelling, histone modifications, and histone-chaperone activity) is required to produce the desired effect. As a result, mutations influencing chromatin-modifying complexes may impede the function of chromatin-remodelling agents or histone chaperones. This dynamic interplay between the types of chromatin-modulating complexes is reflected in the array of genetic interactions reported here for mutations affecting FACT.

2. Yeast FACT structure and function

One of the initial goals of my research was to identify novel mutant alleles of *cdc68* with a specific impact on transcription. These alleles were isolated based on the ability to alter transcription of Spt (suppressor of Ty) reporter genes. Sequence analysis of the alleles generated in this way revealed mutational clustering in the 3' end of the *CDC68* gene. This finding, coupled with the identification of a *cdc68* deletion mutation missing approximately 42% of the N-terminal coding sequence that still encodes a protein with essential Cdc68 function (J. Kurniawan, unpublished observations) spurred our interest in the structure of the Cdc68 protein and of FACT.

Studies characterizing the protein domain structures of FACT components were undertaken by N. K. Brewster in our lab, and experiments designed to identify regions responsible for the association between FACT subunits are described here. The combination of findings from these two approaches has enabled us to generate a picture of FACT structure. In addition to these structural studies, several genetic studies designed to identify the impact of specific *cdc68* mutant alleles on FACT-mediated functions were also carried out. These investigations are described here and were performed to try to associate functions with specific structural regions of the Cdc68 protein. From these

studies it appears that certain *cdc68* mutations generate protein products that are impaired for a subset of Cdc68 functions, while other mutational changes do not influence these specific functions. The non-essential yet highly conserved N-terminal domain of the Cdc68 protein shares some functional overlap with the C-terminal domain of the protein, while the middle domain of Cdc68 is responsible for the association of Cdc68 with Pob3 to generate FACT.

i) FACT complex structure

One goal of my research was to elucidate the structure of the *Saccharomyces cerevisiae* FACT complex, with particular attention to identifying the regions responsible for the physical association of Cdc68, the largest subunit of FACT, with Pob3. Together Cdc68 and Pob3 form a sub-complex of yeast FACT known as the CP complex. In a parallel line of investigation N. K. Brewster of our lab was identifying the domain structures of both Cdc68 and Pob3. These studies are complementary and have led to a model of CP structure that is most likely representative of metazoan FACT structure as well, given the highly conserved nature of the proteins that comprise these complexes.

Metazoan FACT is made up of two proteins, SPT16 (suppressor of Ty) and SSRP1 (structure-specific recognition protein-1), and was originally purified from human cells as an *in vitro* co-factor required for RNA polymerase II transcription elongation on a nucleosomal template (LeRoy *et al.* 1998; Orphanides *et al.* 1998). *Xenopus* FACT was purified a short time later from oocyte extracts based on its ability to unwind DNA (Okuhara *et al.* 1999). These findings assigned functional roles to FACT and provided further insight into potential molecular mechanisms for previously observed phenotypes associated with mutations in yeast FACT genes, such as alterations in gene expression and genetic interactions with components of the DNA replication machinery (Malone *et al.* 1991; Rowley *et al.* 1991; Lycan *et al.* 1994; Wittmeyer and Formosa 1997).

Unlike metazoan FACT, the *Saccharomyces cerevisiae* FACT complex is comprised of three proteins, Cdc68/Spt16 (referred to here as Cdc68), Pob3, and Nhp6 (Wittmeyer and Formosa 1997; Brewster *et al.* 1998; Wittmeyer *et al.* 1999; Brewster *et al.* 2001; Formosa *et al.* 2001). The yeast Cdc68 and human Spt16 proteins share 36% sequence identity (Orphanides *et al.* 1999), and the Cdc68 protein is highly conserved across its length in many eukaryotes (Figures 24 and 25; Evans *et al.* 1998). Interestingly, the Pob3

(Pol1-binding protein) and Nhp6 (non-histone protein) proteins are structurally homologous to different regions of the metazoan SSRP1 protein (Wittmeyer and Formosa 1997; Orphanides *et al.* 1999; Brewster *et al.* 2001; Formosa *et al.* 2001). The N-terminal 75% of SSRP1 is homologous to the entire length of the Pob3 protein, while the C-terminal 25% of the SSRP1 protein is homologous to Nhp6 (Wittmeyer and Formosa 1997; Brewster *et al.* 2001; Formosa *et al.* 2001). Thus SSRP1 is the metazoan structural homologue for both the Pob3 and Nhp6 proteins.

The Cdc68 and Pob3 proteins co-purify from yeast cells as a stable heterodimeric complex (known as CP) even under highly stringent purification conditions, indicating an avid association between these two proteins (Brewster *et al.* 1998; Wittmeyer *et al.* 1999). The domain structure of yeast CP, as identified by proteolytic analysis of the complex (N. K. Brewster, unpublished observations), and the regions responsible for the physical association of Cdc68 and Pob3, as determined by the *in vitro* pull-downs performed in this study, are shown in Figure 18A. In contrast, the association of Nhp6 with this complex is not as robust, with only about 5% of Nhp6 protein found associated with the CP dimer when purifications are performed under low-stringency conditions (Brewster *et al.* 2001; Formosa *et al.* 2001). However, when a gene fusion of *POB3* to *NHP6A* was constructed to mimic the SSRP1 gene in both layout and sequence, the resulting Pob3-Nhp6 fusion protein was able to provide essential Pob3 function and complemented many but not all of the growth defects associated with *nhp6aΔ nhp6bΔ* mutant cells (Brewster *et al.* 2001). These findings indicate that while Nhp6 has a role as a member of the FACT complex, this protein may also have FACT-independent functions (Brewster *et al.* 2001; Formosa *et al.* 2001).

The Cdc68 and Pob3 proteins are both essential in yeast, while the Nhp6 protein is not. The critical function of facilitating RNA polymerase II transcription elongation on a chromatin template could explain the essential natures of Cdc68 and Pob3 (Orphanides *et al.* 1998, 1999). Nhp6 is encoded by two genes, *NHP6A* and *NHP6B*, whose protein products share 88% sequence identity and contain a high-mobility group (HMG) box (Kolodrubetz and Burgum 1990). Proteins containing HMG boxes are associated with chromatin structure and with DNA-binding and -bending activities (Bustin 1999), which is consistent with the functions associated with FACT. There are several other HMG-box

proteins in the yeast cell that could have overlapping functions with Nhp6, which may explain why cells containing deletions of both *NHP6A* and *NHP6B* are viable. Alternatively, the function of Nhp6 or other HMG-box proteins may assist Cdc68 and Pob3 in mediating their essential function(s) but may not be required for these activities.

No specific association between Nhp6 and Pob3 in the absence of Cdc68 has been reported. A weak two-hybrid interaction has been observed between a Gal4 DNA-binding-domain fusion to Cdc68 and a Gal4 transactivation-domain fusion to Nhp6 (Formosa *et al.* 2001). This interaction may be indirect, occurring *via* a bridge of other nuclear proteins, or it may represent one of the ways Nhp6 is associated with Cdc68 and Pob3 to form FACT in yeast. The *in vitro* binding studies performed by Shimojima *et al.* (2003) using recombinant *Drosophila* SPT16 and SSRP1 polypeptides showed that a recombinant polypeptide comprised mainly of the HMG-box domain from SSRP1 was able to associate with full-length SPT16. However, studies performed by Keller and Liu (2002), where a human SSRP1 polypeptide encoding predominantly the HMG box domain was not able to associate with recombinant human SPT16 protein, contradict this finding. Therefore, the regions responsible for the association of Nhp6 and/or Nhp6-like domains with the rest of FACT remain uncertain.

ii) A role for FACT in transcription

Some of the initial characterizations of the Cdc68 component of FACT revealed a role for this protein in transcription. Three independent identifications of a single-point-mutant allele, known variously as *cdc68-1*, *spt16-197*, and *cdc68-11*, each described different influences of this allele on transcription, including a decline in transcript abundance for several genes, alteration of Spt-reporter-gene expression, and altered *HO::lacZ* reporter-gene expression (Malone *et al.* 1991; Rowley *et al.* 1991; Lycan *et al.* 1994). This association with transcription was further substantiated by the identification of suppressor mutations in the *SAN1* gene, involved in repression of transcription, that were able to alleviate some of the observed transcription deficits found in *cdc68* cells (Xu *et al.* 1993; Xu 1995). Further studies involving the *cdc68-Δ922* allele, which encodes a protein missing the N-terminal 30%, showed that this mutation also causes alterations in transcription by allowing altered expression of the Spt reporter genes and bypassing the need for upstream activation sequences for *SUC2* gene expression (Evans *et al.* 1998).

The finding that transcript abundance is decreased for several genes when *cdc68* mutant alleles are present indicated that Cdc68 plays a positive role in activating gene expression (Rowley *et al.* 1991; Xu *et al.* 1993; Lycan *et al.* 1994; Xu 1995). However, there were several lines of evidence indicating that Cdc68 also functioned in repression of gene expression. The first line of evidence was that *cdc68* mutant alleles allow expression of the Spt reporter genes. These Spt reporter genes contain DNA sequence insertions, known as δ elements, that cause alterations in transcription of these genes. As a result, no transcript that can be tranaslated into functional protein product is generated. Loss of repression at alternative transcription initiation sites in the Spt reporters allows the production of additional transcripts from these reporters that may be translated into functional proteins, and *cdc68* mutations permit this type of activation of Spt-reporter-gene expression (Malone *et al.* 1991; Evans *et al.* 1998). The second line of evidence was that the *cdc68-1* allele allows *HO::lacZ* reporter-gene expression in cells lacking the normal activators of *HO* transcription, Swi4 and Swi6, suggesting that *cdc68-1* causes a loss of repression when the activators are absent (Lycan *et al.* 1994). Finally, the third line of evidence supporting a role for Cdc68 in repression of transcription comes from the observation that *cdc68* mutant cells are able to bypass the requirement for upstream activating sequences in expression of the *SUC2* gene. An allele of *SUC2* called *suc2ΔUAS* lacks the DNA sequences responsible for binding transcriptional activators, and therefore is not typically expressed. However, when *cdc68* is mutated repression of the *suc2ΔUAS* gene is lost, once again implying that the Cdc68 protein mediates repression (Evans *et al.* 1998). These findings imply that Cdc68 mediates both activation and repression of gene expression. Many of the phenotypes observed for *cdc68* mutant cells were also observed for cells with defects in chromatin structure. As a result, it was proposed that the alterations in transcription in *cdc68* mutant cells may be due to chromatin structural changes, suggesting a role for Cdc68 in regulating gene expression by alterations in chromatin structure.

Consistent with these findings for Cdc68, Pob3 has also been shown to mediate transcription processes. A similar set of phenotypes observed for cells containing *cdc68* mutations was also observed for cells containing *pob3* mutations or increased dosage of the *POB3* gene (Brewster *et al.* 1998; Costa and Arndt 2000; Schlesinger and Formosa

2000). Thus it appears that both the Cdc68 and Pob3 components of FACT are able to alter gene expression, but how does this complex exert its influence?

Insight into the role of FACT in transcription came from *in vitro* studies of RNA polymerase II transcription elongation using recombinant purified proteins and reconstituted chromatin templates (LeRoy *et al.* 1998; Orphanides *et al.* 1998, 1999). As reported in a series of publications, the human homologue of FACT was purified as a co-factor required for RNA polymerase II transcription elongation, but not initiation, on a chromatin template. Promoter-proximal remodelling to allow transcription initiation in these assays required additional factors in the forms of transcription factors or DNA-binding factors and an ATP-dependent chromatin-remodelling factor (RSF) (LeRoy *et al.* 1998; Orphanides *et al.* 1998, 1999). These *in vitro* findings were further substantiated by genetic interactions identified between *cdc68* yeast mutations and mutations of genes encoding proteins with known functions in transcription elongation, namely *DST1* and *SPT4*. The *DST1* gene encodes the TFIIS component of the RNA polymerase II transcription machinery involved in overcoming transcriptional pauses (Izban and Luse 1992; reviewed in Wind and Reines 2000), while *SPT4* encodes one subunit of the Spt4/Spt5 (*a.k.a.* DSIF in human cells) complex which has been shown to regulate transcription elongation (Hartzog *et al.* 1996, 1998; Wada *et al.* 1998a, 1998b). Deletions of *DST1* or *SPT4* result in sensitivity 6-azauracil, an analog that impedes the production of UTP and GTP. This reduction in UTP and GTP levels slows the progression of the elongating RNA polymerase II enzyme and thereby sensitizes cells to further perturbations in transcription elongation (Hampsey 1997). When deletions of *DST1* or *SPT4* were combined with the *cdc68-1* mutation, cell growth was enhanced on medium containing 6-azauracil (Orphanides *et al.* 1999). This result indicates that Cdc68 would normally pose a block to transcription elongation in cells lacking the Dst1 or Spt4 transcription elongation factors, thereby supporting the idea that Cdc68 functions to regulate transcription elongation.

The role of FACT in transcription elongation was further dissected using *in vitro* transcription-elongation assays with purified components and various combinations of elongation factors (Wada *et al.* 2000). Results from these assays indicated that FACT and the RNA polymerase II carboxy terminal domain (CTD) kinase termed pTEFb (which

corresponds to the Ctk1/Ctk2 CTD kinase complex in yeast) are required to counteract the inhibitory effects of DSIF (Spt4/Spt5 complex in yeast) (Wada *et al.* 2000). In the transition from transcription initiation to elongation the CTD of the largest subunit of RNA polymerase II is phosphorylated by both TFIIH and pTEFb or Ctk1/Ctk2 in yeast (Komarnitsky *et al.* 2000; Cho *et al.* 2001). Therefore, finding that FACT and pTEFb cooperate is significant evidence of a common role in facilitating the transition from initiation to elongation.

In addition to these biochemical findings, genetic and physical interactions have been identified in yeast between FACT and components involved in elongation (Costa and Arndt 2000; Lindstrom and Hartzog 2001; Squazzo *et al.* 2002). For example, the Paf1 complex in yeast is associated with RNA polymerase II and is involved in both transcription initiation and elongation (Shi *et al.* 1996, 1997; Wade *et al.* 1996; Costa and Arndt 2000; Pokholok *et al.* 2002; Squazzo *et al.* 2002; Rondon *et al.* 2004). FACT co-purifies with the Paf1 complex (Krogan *et al.* 2002; Squazzo *et al.* 2002) and many synthetic genetic interactions between mutations in genes encoding FACT and Paf1 subunits have been found, indicating that these two complexes share an overlapping role. A *pob3* mutation was identified in a screen for synthetic-lethal mutations with *rtf1Δ*, eliminating a subunit of the Paf1 complex (Costa and Arndt 2000), and deletion of *PAF1* or *CTR9*, genes encoding two other Paf1 components, also results in synthetic lethality with *cdc68-1* (Squazzo *et al.* 2002). I have also identified several novel genetic interactions between *cdc68* mutant alleles and deletions of genes encoding Paf1-complex proteins. These findings indicate that the Paf1 and FACT complexes operate in parallel to mediate transcription elongation.

Recent findings demonstrating the association of FACT with actively transcribed regions of DNA have cemented the association of FACT with RNA polymerase II transcription elongation (Mason and Struhl 2003; Saunders *et al.* 2003). Comparisons of hybridization patterns for RNA polymerase II and FACT on *Drosophila* polytene chromosomes revealed that FACT co-localizes with RNA polymerase II (Saunders *et al.* 2003). Further analysis of polytene-chromosome hybridization patterns and chromatin immunopreciptation studies of RNA polymerase II and FACT in post-heat-shock conditions also demonstrated that RNA polymerase II and FACT are recruited to and

remain associated with the gene in temporally and spatially similar patterns (Saunders *et al.* 2003). In contrast, similar studies examining the association of the heat-shock transcription factor HSF showed a distinct difference between the regions bound by HSF and FACT, with FACT associating downstream of the HSF-binding site at the promoter (Saunders *et al.* 2003). These findings showed that FACT is recruited to genes and travels along with the RNA polymerase II enzyme during transcription elongation, but is not present at promoter regions. Further experiments by Mason and Struhl (2003) supported these conclusions and showed that FACT and RNA-polymerase-II gene occupancy is temporally and spatially similar in yeast. These authors further showed that the association of FACT with a gene requires functional TFIIH. The transition of RNA polymerase II from initiation to elongation also requires TFIIH; therefore this failure of FACT to associate with the transcribed region when TFIIH activity is absent may be an indirect effect of loss of transcription elongation (Mason and Struhl 2003).

For what purpose is FACT associated with the elongating RNA polymerase? The answer to this question appears to be that FACT is required to disrupt nucleosome structure in front of the elongating polymerase and also is needed to redeposit nucleosomes behind the polymerase (Orphanides *et al.* 1999; Belotserkovskaya *et al.* 2003; Kaplan *et al.* 2003; Mason and Struhl 2003; Saunders *et al.* 2003). In this model, FACT serves as a histone chaperone to displace an H2A/H2B dimer from the nucleosome so that RNA polymerase may gain access to the DNA template, and then in the wake of RNA polymerase passage FACT is thought to be responsible for replacing this dimer to regenerate a stable nucleosome structure (Belotserkovskaya and Reinberg 2004; Belotserkovskaya *et al.* 2004).

In support of this model, the SPT16 (homologue of yeast Cdc68) component of human FACT has been shown to interact physically with both purified nucleosomes and the H2A/H2B dimer (Orphanides *et al.* 1999; Belotserkovskaya *et al.* 2003). The C-terminal 20% of the SPT16 protein seems to be responsible for these interactions and this region is highly acidic, a feature ascribed to both transcription factors and histone chaperones (Rowley *et al.* 1991; Belotserkovskaya *et al.* 2003). The ability of FACT to assist in the transcription elongation process on a nucleosome-bound template can be abrogated by covalently crosslinking the histone proteins within the nucleosome

(Orphanides *et al.* 1999). This finding suggests that the FACT-mediated assistance in transcription elongation requires removal of the histone proteins from the nucleosome (Orphanides *et al.* 1999). Consistent with this model, more recent *in vitro* work has shown that FACT-assisted transcription results in loss of one H2A/H2B dimer from nucleosomes to form a 'hexasome' (a nucleosome containing a dimer of H3/H4 dimers and one H2A/H2B dimer). Additionally, human FACT has been shown to have histone-chaperone activity based on its ability to deposit histones on a DNA template, generating nucleosomes *in vitro* (Belotserkovskaya *et al.* 2003).

While the SPT16 component of FACT has been shown to bind histone H2A/H2B dimers, the SSRP1 component of metazoan FACT is able to bind H3/H4 dimers (Belotserkovskaya *et al.* 2003). This observation raises the possibility that the SSRP1 subunit of FACT tethers the FACT complex to the H3/H4 nucleosomal core while the SPT16 component removes the H2A/H2B dimer to allow polymerase passage and then redeposits the dimer afterwards (reviewed in Belotserkovskaya and Reinberg 2004; Belotserkovskaya *et al.* 2004). In yeast it has been shown that the Nhp6 protein is required for the association of the Cdc68/Pob3 dimer with nucleosomes, suggesting that it may be the HMG-box domain that mediates metazoan SSRP1 association with the nucleosome (Formosa *et al.* 2001; Ruone *et al.* 2003). Recent work indicates that yeast FACT is also able reorganize the nucleosome, but the details of this nucleosomal reorganization are still unclear (Ruone *et al.* 2003; Rhoades *et al.* 2004).

In addition to the *in vitro* work indicating that human FACT has histone-chaperone activity and is able to remove a dimer of histone H2A/H2B to assist in RNA polymerase transcription (Belotserkovskaya *et al.* 2003), FACT studies from yeast have provided the supporting evidence for a role for FACT in reassembling nucleosomes behind the polymerase (Kaplan *et al.* 2003; Mason and Struhl 2003). Research from the Winston lab has provided a breakthrough in our understanding of how FACT ensures repression of transcription from cryptic promoter elements, like those found in the Spt reporters (Kaplan *et al.* 2003). Cells containing *cdc68* mutant alleles have been shown to generate truncated transcripts for certain genes (Xu 1995; Kaplan *et al.* 2003). These shortened transcripts are not the result of premature termination of transcription, but instead are due to the initiation of RNA polymerase II transcription at promoter sites within the gene

(Kaplan *et al.* 2003; Mason and Struhl 2003). RNA polymerase II enzyme and TATA-binding protein accumulate at regions within the coding sequence of genes when FACT mutations are present, indicating that in these mutant cells a decrease in FACT activity results in loss of repression at cryptic promoters within gene sequences (Mason and Struhl 2003). This loss of repression, seen as access to cryptic promoters, in cells mutant for another transcription elongation factor, Spt6, was shown to correspond to a decrease in the density of nucleosomes associated with the coding sequence of the gene (Kaplan *et al.* 2003). It is likely that mutations in *cdc68* have a similar effect. This outcome would indicate that while these *cdc68* mutations are able to assist transcription elongation, the nucleosome-reassembly function after RNA polymerase II passage is impaired (reviewed in Belotserkovskaya and Reinberg 2004; Belotserkovskaya *et al.* 2004). This impairment would result in a decrease in nucleosome density, exposing sites within the coding DNA sequence for binding by RNA polymerase II and initiation factors. These cryptic promoter sites would not be exposed for potential binding and transcription initiation if chromatin structure is uncompromised.

In summary, these findings indicate that FACT mediates RNA polymerase II transcription by regulating chromatin structural changes. It has been shown that FACT associates with the coding region of genes in a temporally and spatially similar way as does RNA polymerase II, suggesting that FACT moves across a gene at the same time as this enzyme. The purpose of FACT association with the elongating polymerase is to facilitate polymerase passage through the nucleosmes. FACT has been shown to bind nucleosomes and remove a dimer of histone H2A/H2B, which is thought to 'loosen' chromatin structure to allow transcription elongation. Further evidence suggests that FACT then assists in replacing the H2A/H2B dimer in the wake of polymerase passage to re-establish proper chromatin conformation. Mutations in FACT result in transcription initiation from cryptic promoters within the coding sequence of genes. This may be a result of improper reassembly of nucleosomes behind RNA polymerase II, which then allows access by initiation factors to binding sites that would otherwise be blocked by repressive chromatin structure. This current model for FACT as a histone chaperone and its influence on the process of transcription is shown in Figure 2.

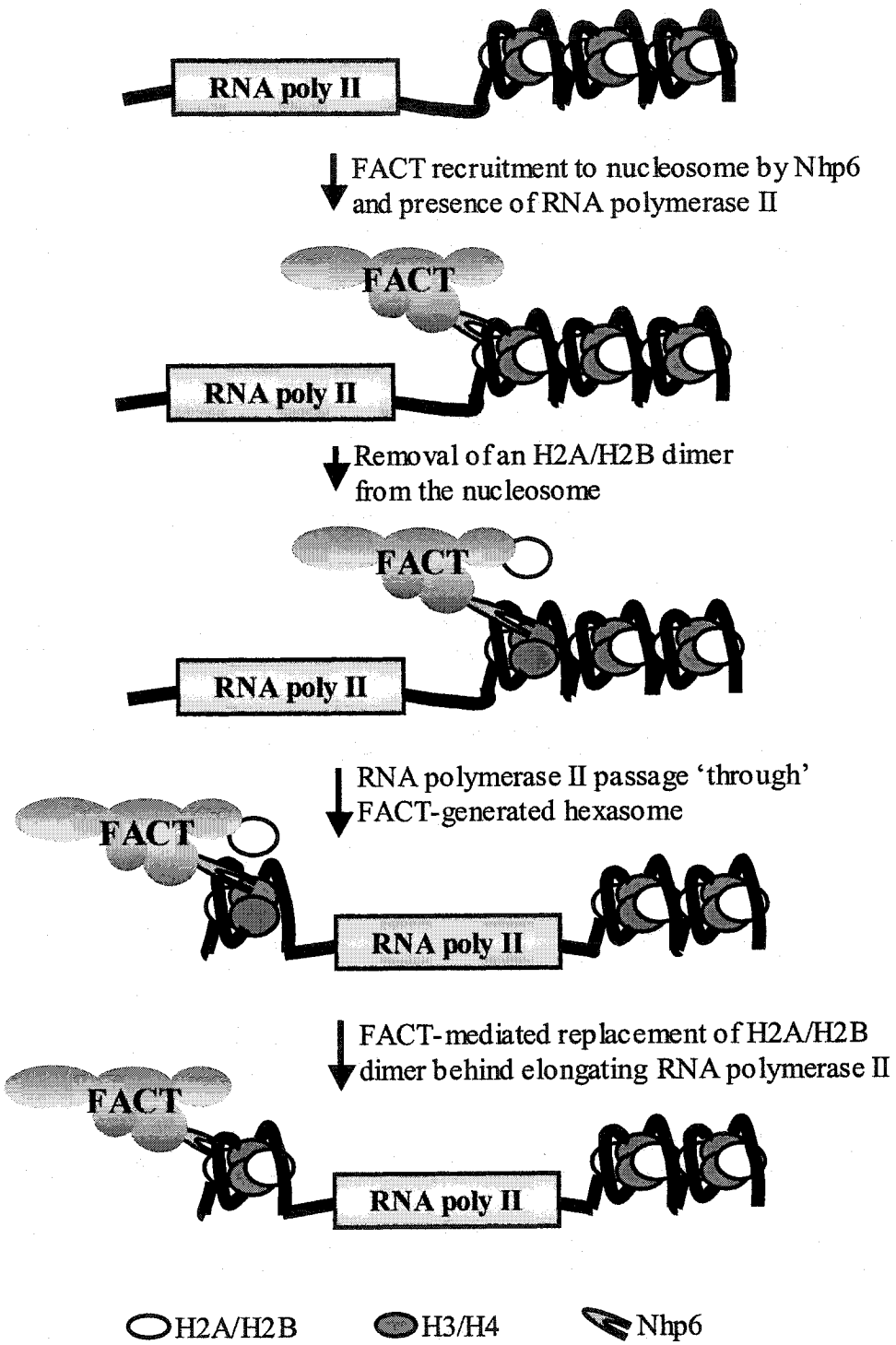

Figure 2. Model for FACT activity in transcription.

iii) The involvement of FACT in DNA replication and repair

Given the model outlined above for FACT as a histone chaperone, it is not surprising that, in addition to its role in transcription, FACT has also been implicated in DNA repair and replication. It would seem likely that FACT would function in a similar fashion as a histone chaperone during these processes as well, although no direct evidence supporting this view has been reported.

The initial characterization of the interaction between Cdc68 and Pob3 stemmed from the finding that these two proteins co-purified from an affinity matrix comprised of the Pol1 subunit of DNA polymerase α (Wittmeyer and Formosa 1997). DNA polymerase α is part of the primase complex involved in synthesizing the RNA primer required in theinitiation of DNA replication. With this job completed, DNA polymerase α is replaced by DNA polymerase δ, which performs the lion's share of DNA replication. The association of Cdc68 and Pob3 with DNA polymerase α was enhanced by the absence of Ctf4, a protein also identified based on its ability to associate with Pol1 (Miles and Formosa 1992). Ctf4 has since been shown to function in sister-chromatid cohesion, and is involved in the maintenance of genome stability (Hanna *et al.* 2001). While the absence of Ctf4 permitted tighter physical associations between FACT and DNA polymerase α, deletion of *CTF4* in combination with *cdc68* or *pob3* mutations results in cellular growth defects (Wittmeyer and Formosa 1997; Wittmeyer *et al.* 1999). In addition to the physical association of FACT with a component of the replication machinery, other genetic interactions between genes encoding FACT and those encoding proteins involved in replication functions have also been identified (Wittmeyer and Formosa 1997; Wittmeyer *et al.* 1999; Schlesinger and Formosa 2000). These genetic interactions include synthetic growth defects when mutations in *cdc68* or *pob3* are combined with mutations in *pol1*, although no similar effects were observed when these same *cdc68* and *pob3* mutations were combined with a mutant allele of *cdc2*, the gene encoding a DNA polymerase δ subunit (Wittmeyer and Formosa 1997; Wittmeyer *et al.* 1999). Additional synthetic genetic interactions were observed between *cdc68* and mutations in *cdc6*, which encodes a component of the pre-replicative complex involved in the initiation of replication (Cocker *et al.* 1996), and in *cdc9*, which encodes the DNA ligase involved in Okazaki-fragment joining during replication (Johnston and Johnson

1993; Wittmeyer and Formosa 1997). Mutations in *pob3* were shown to cause synthetic growth defects in combination with mutation of *DNA2*, encoding a helicase and nuclease involved in Okazaki-fragment processing (Budd and Campbell 1997; Bae *et al.* 2002), and of *CTF18*, which encodes a component of an alternative replication-factor-C complex important for sister-chromatid cohesion and chromosome-transmission fidelity (Schlesinger and Formosa 2000; Hanna *et al.* 2001; Mayer *et al.* 2001). I have identified several novel genetic interactions between *cdc68* mutations and genes involved in replication, further providing evidence that FACT has a role to play in DNA replication.

FACT isolated from *Xenopus* was named DUF (DNA unwinding factor) for its ability to unwind or alter the supercoiling of DNA plasmids (Okuhara *et al.* 1999). This function has been attributed to the HMG-box domain of the SSRP1 homologue of Pob3, since HMG-box proteins are known to be able to associate with and bend DNA, which can alter the supercoiled nature of the DNA molecule (Jung and Lippard 2003). However, a striking finding from this work was that depletion of *Xenopus* FACT from the oocyte resulted in a block to DNA replication, suggesting that FACT is involved in DNA replication (Okuhara *et al.* 1999).

The processes of DNA replication and repair often share components, as some forms of repair rely on the replication machinery to assist in replacing DNA at the damage site. Several lines of evidence implicate FACT in DNA repair. The first is that human FACT binds preferentially to DNA-damage sites caused by cisplatin, and that this binding occurs primarily through the HMG-box domain of the SSRP1 component (Yarnell *et al.* 2001). More compelling evidence for FACT involvement in repair comes from a series of experiments from the Lu lab which identified human FACT as a component of a DNA-damage-induced p53-phosphorylating complex containing casein kinase II (CKII). In these studies they show that FACT physically associates with CKII and that this association changes the specificity of CKII so that it now preferentially targets serine 392 of p53 for phosphorylation (Keller *et al.* 2001; Keller and Lu 2002). p53 is a tumor-suppressor protein involved in regulating cell fate in response to a number of different stimuli, including DNA damage (reviewed in Sherr 2004; Slee *et al.* 2004). The increased phosphorylation of p53 enhanced its DNA-binding affinity, and since many of the responses in which p53 is involved require its regulation of transcription, this is consitent

with the ideat that not only does the FACT/CKII complex target p53 for phosphorylation, but this phosphorylation event changes the activity of p53 (Keller *et al.* 2001; Keller and Lu 2002). In addition to p53, CKII has been shown to target the SSRP1 subunit of FACT for phosphorylation (Keller *et al.* 2001) and there are CKII target sequences in the C-terminal domain of both human SPT16 and yeast Cdc68 proteins (Rowley *et al.* 1991; Orphanides *et al.* 1999). The phosphorylation of SSRP1 has been linked to the ability of SSRP1 to bind DNA that has been damaged by ultraviolet radiation. Thus these interactions with CKII not only activate p53 in a DNA-damage response-specific fashion, but also alter the properties of FACT so that it has increased binding affinity for sites of DNA damage (Krohn *et al.* 2003).

While no similar observations have been made in yeast regarding a role for FACT in DNA-damage responses, yeast FACT has been shown to co-purify with caseine kinase II, suggesting that this association, and therefore most likely function, is conserved (Krogan *et al.* 2002). During my research I have examined the influence of FACT mutations on the activation of the DNA-damage-response kinase Rad53 and found that under DNA-damage conditions at least one of the *cdc68* mutations alters the phosphorylation of Rad53 and subsequently results in decreased cell viability. Rad53 signals DNA damage, stimulating checkpoint responses and DNA-repair activities. The histone chaperone Asf1 has been shown to associate with Rad53 in a DNA-damage-dependent fashion (Emili *et al.* 2001; Hu *et al.* 2001). This interaction may target Asf1 to sites of DNA damage, where it may assist by altering chromatin structure to allow repair processes to proceed (Hu *et al.* 2001). FACT may play a similar role in response to DNA damage, in damage detection and signalling, or in repair. I have identified many genetic interactions between *cdc68* mutations and deletions of genes encoding proteins that function in DNA repair. The vast majority of these synthetic lethal interactions were identified using the *cdc68-ΔNTD* allele, which encodes a Cdc68 protein missing the N-terminal domain. This domain corresponds to a region of the human homologue SPT16 that has been shown to associate with the CKII enzyme. Perhaps loss of the N-terminal domain of Cdc68 impairs the interaction between FACT and CKII in yeast, an interaction that has been shown to play an important role in DNA-damage responses in human cells.

The findings outlined above indicate FACT is an important player in DNA replication and repair. This is an area of FACT function that bears further investigation and will undoubtedly receive considerable attention in the future.

In summary, like many other proteins that influence chromatin structure, FACT has been shown to participate in an array of processes involving the DNA template. FACT is a histone chaperone, and this activity is important for minimizing the nucleosome block during the process of transcription (Orphanides *et al.* 1999; Belotserkovskaya *et al.* 2003). Given the findings that FACT is also involved in DNA replication and repair, it is not unreasonable to predict that FACT may play a similar role in these processes, altering chromatin structure to facilitate these DNA transactions as well. The isolation of novel mutations in the *CDC68* gene led us to explore the relationship between FACT structure and the functions it mediates. Here I present findings that elucidate the structure of yeast FACT and genetic data showing that certain *cdc68* mutations are more influential in a subset of FACT-mediated processes than others. The plethora of genetic interactions identified for FACT in my study certainly supports the idea that FACT facilitates a wide range of chromatin-related transactions.

II. MATERIALS AND METHODS

1. Media and growth conditions

Yeast cells employed in this study were grown in two types of liquid medium. YM1 rich medium contained 1% succinic acid, 0.6% sodium hydroxide, 1% bactopeptone, 2% glucose and 0.67% yeast nitrogen base without amino acids (Hartwell 1967). YNB synthetic minimal medium contained 1% succinic acid, 0.6% sodium hydroxide, 2% glucose, and 0.67% yeast nitrogen base without amino acids or ammonium sulphate (Johnston *et al.* 1977), which was then supplemented with 0.1% ammonium sulphate, amino acids (40 μg/ml) and nucleoside bases (20 μg/ml). This same formulation was employed for solid synthetic complete (SC) medium, with the addition of 2% agar. The following amino acids and nucleoside bases were added to both solid and liquid YNB medium prior to use, except those whose absence would maintain selection pressure during growth: arginine, aspartic acid, histidine, isoleucine, leucine, lysine, methionine, phenylalanine, serine, tryptophan, threonine, tyrosine, valine, adenine, and uracil. The components excluded from minimal liquid or solid media are indicated for each case (*i.e.*, SC-Ura is synthetic complete YNB medium supplemented with all amino acids and bases except uracil). YEPD was employed for growth on rich solid medium and contained 2% glucose, 2% bactopeptone, 1% yeast extract, and 2% agar (Hartwell 1967). Cells were routinely grown at 30°C unless otherwise indicated.

Sporulation of diploid cells was performed by growing cells consecutively in 'pre-sporulation' and then sporulation liquid medium. For cells maintaining a plasmid during the sporulation process, pre-sporulation medium was SC lacking the appropriate amino acid or base for plasmid selection, and sporulation liquid medium was 1% potassium acetate, 0.05% dextrose, amino acids at 40 μg/ml (arginine, aspartic acid, histidine, isoleucine, leucine, lysine, methionine, phenylalanine, serine, tryptophan, threonine, tyrosine, and valine), and bases at 20 μg/ml (uracil and adenine), where once again the appropriate amino acid or base for plasmid selection was omitted. Rich pre-sporulation medium contained 0.8% bacto-yeast extract, 0.3% bacto-peptone, and 10% dextrose; sporulation medium was 1% potassium acetate, 0.1% bacto-yeast extract, and 0.05% dextrose (Guthrie 1991). Cells were grown in pre-sporulation medium at 23°C to a density of approximately 5×10^6 to 1×10^7 cells per ml and then cultures were

Table 1. Chemical additions to growth media used to assess cell sensitivities.

Chemical	Concentration(s)	Medium
Sodium chloride	0.9 M	YEPD
Potassium chloride	1.5 M	YEPD
Glycerol	2.5 M	YEPD
Formamide	3%	YEPD
Ethanol	6 %	YEPD
Sorbitol	1 M	YEPD
Hydroxyurea	50 mM and 100 mM	YEPD
Mycophenolic acid	50 μg/ml	SC-Ura
6-azauracil	50 μg/ml and 100 μg/ml	SC-Ura
Methyl methane sulphonate	0.02% and 0.04%	YEPD
Phleomycin	1.25 μg/ml	YEPD
4-nitroquinoline oxide	0.5 μM, 1 μM, and 2 μM	YEPD
Cisplatin	1 μM	YEPD
Sodium dodecyl sulphate	0.02%	YEPD
Caffeine	10 mM	YEPD

centrifuged to form a cell pellet. The pre-sporulation medium was then removed, the pellet was resuspended in sporulation medium, and the resulting cell suspension was incubated for 4 to 7 days at 23°C.

Several chemicals were added to growth media to determine if different genetic combinations resulted in growth impairments under certain conditions. Table 1 lists these supplements and the medium they were added to as well as the concentrations routinely employed for each. Many of these additions were based on recommendations found in Hampsey (1997).

5-fluoro-orotic acid (5-FOA) allows counterselection against cells containing plasmids bearing the *URA3* gene. 5-FOA medium was YNB solid medium containing all amino acids and bases (listed above) with 5-FOA (Sigma) added to 0.33 g per litre. *Escherichia coli* (*E. coli*) cultures were typically grown in 2xYT (1.6% bacto-tryptone, 1% bacto-yeast extract, and 0.5% sodium chloride) liquid medium or on 2xYT solid medium (2xYT liquid medium with the addition of 2% agar) (Messing 1983). Supplementation with antibiotics (ampicillin or kanamycin at 50 μg/ml) was performed as required for plasmid maintenance. For blue/white *E. coli* colony-colour screening for plasmids, 40 μl of 2% 5-bromo-4-chloro-3-indolyl-beta-D-galactopyranoside (X-gal) stock solution and 4 μl of 100 mM isopropyl-beta-D-thiogalactopyranoside (IPTG) stock solution were spread over the surface of solid 2xYT medium, containing the appropriate antibiotic, in a standard-size Petri plate.

To select for the presence of *LEU2* yeast plasmids, strain JF1754 (*Dlac, gal, metB, leuB, hisB436, hsdR*) *E. coli* cells were employed, with growth on M9 medium lacking leucine (Sambrook 1989). To make M9 medium, an M9 salt stock solution (30 g/l sodium phosphate (Na_2HPO_4), 15 g/l potassium phosphate (KH_2PO_4), 5 g/l NH_4Cl, 2.5g/l NaCl, and 15 mg/l $CaCl_2$ was made and 200 ml of this stock solution was used per litre of M9 medium, with the addition of 2% agar. This mixtures was then supplemented with 2% glucose, 5 x 10^{-4}% thiamine, 1 mM magnesium sulphate, ampicillin to 50 μg/ml, amino acids to 40 μg/ml (arginine, aspartic acid, histidine, isoleucine, lysine, methionine, phenylalanine, serine, tryptophan, threonine, tyrosine, and valine), and bases to 20 μg/ml (uracil and adenine). Leucine was omitted, and therefore the only JF1754 *E. coli* cells

Table 2. Yeast strains used in this study.

Strain	Description and Genotype	Source
BM403	*MATa his4-912δ lys2-128δ ura3-52 suc2ΔUAS cdc68-1*	Malone *et al.* 1991
AW11-9a	*MATα his4-912δ lys2-128δ leu2-3,112 trp1-Δ1 ura3-52 suc2ΔUAS CDC68*	Amy Wheeler, unpublished
AFO1-I2	*MATa his4-912δ lys2-128δ leu2-3,112 trp1-Δ1 ura3-52 suc2ΔUAS cdc68-1*	BM403 x AW11-9A segregant
BM64	*MATa/α his4-912δ lys2-128δ leu2-3,112 trp1-Δ1 ura3-52 ssd1-d/? CDC68/ cdc68-101::LEU2* (homozygous unless otherwise indicted)	Malone *et al.* 1991
KanB	*MATa/α his4-912δ lys2-128δ leu2-3,112 trp1-Δ1 ura3-52 ssd1-d/? CDC68/cdc68Δ::kanMX4* (homozygous unless otherwise indicted)	BM64 derivative
KanB 316-A4 HA	*MATα his4-912δ lys2-128δ leu2-3,112 trp1-Δ1 ura3-52 ssd1-d cdc68Δ::kanMX4* [pRS316-A4]	KanB haploid derivative
KanB 316-A4 Hα[2]	*MATa his4-912δ lys2-128δ leu2-3,112 trp1-Δ1 ura3-52 ssd1-d cdc68Δ::kanMX4* [pRS316-A4]	KanB haploid derivative
KanB 316[2]	*MATα his4-912δ lys2-128δ leu2-3,112 trp1-Δ1 ura3-52 ssd1-d CDC68* [pRS316]	KanB haploid derivative
KanB 316-E763G	*MATα his4-912δ lys2-128δ leu2-3,112 trp1-Δ1 ura3-52 ssd1-d cdc68Δ::kanMX4* [pRS316-*cdc68-E763G*]	KanB haploid derivative
KanB 316-E857K	*MATα his4-912δ lys2-128δ leu2-3,112 trp1-Δ1 ura3-52 ssd1-d cdc68Δ::kanMX4* [pRS316-*cdc68-E857K*]	KanB haploid derivative
KanB 316-312[2]	*MATα his4-912δ lys2-128δ leu2-3,112 trp1-Δ1 ura3-52 ssd1-d cdc68Δ::kanMX4* [pRS316-*cdc68-312*]	KanB haploid derivative
KanB 316-319[2]	*MATα his4-912δ lys2-128δ leu2-3,112 trp1-Δ1 ura3-52 ssd1-d cdc68Δ::kanMX4* [pRS316-*cdc68-319*]	KanB haploid derivative
KanB128	*MATα his4-912δ lys2-128δ leu2-3,112 trp1-Δ1 ura3-52 ssd1-d cdc68Δ::kanMX4* [pTF128]	KanB haploid derivative
KanB128-8	*MATα his4-912δ lys2-128δ leu2-3,112 trp1-Δ1 ura3-52 ssd1-d cdc68Δ::kanMX4* [pTF128-8]	KanB haploid derivative
KanB128-12	*MATα his4-912δ lys2-128δ leu2-3,112 trp1-Δ1 ura3-52 ssd1-d cdc68Δ::kanMX4* [pTF128-12]	KanB haploid derivative
KanB128-16A	*MATα his4-912δ lys2-128δ leu2-3,112 trp1-Δ1 ura3-52 ssd1-d cdc68Δ::kanMX4* [pTF128-16ABC]	KanB haploid derivative
KanB128-24	*MATα his4-912δ lys2-128δ leu2-3,112 trp1-Δ1 ura3-52 ssd1-d cdc68Δ::kanMX4* [pTF128-24]	KanB haploid derivative
JK122-3B[3]	*MATα his4-912δ lys2-128δ leu2-3,112 trp1-Δ1 ura3-52 ssd1-d cdc68Δ::kanMX* [pRS316-A4]	KanB haploid derivative, J. Kurnawan, unpublished
JK120-6A[3]	*MATα his4-912δ lys2-128δ leu2-3,112 trp1-Δ1 ura3-52 ssd1-d cdc68Δ::kanMX* [YEpDE-MC4] *cdc68-Δ922*	KanB haploid derivative, J. Kurnawan, unpublished
JK121-10B	*MATa his4-912δ lys2-128δ leu2-3,112 trp1-Δ1 ura3-52 ssd1-d cdc68Δ::kanMX* [JKpmini68]	KanB haploid derivative, J. Kurnawan, unpublished

JK121-10D	*MATα his4-912δ lys2-128δ leu2-3,112 trp1-Δ1 ura3-52 ssd1-d cdc68Δ::kanMX* [JKpmini68]	KanB haploid derivative, J. Kurnawan, unpublished
JK124-14C[3]	*MAT*a *his4-912δ lys2-128δ leu2-3,112 trp1-Δ1 ura3-52 ssd1-d cdc68Δ::kanMX* [JKpd369] *cdc68-Δ369*	KanB haploid derivative, J. Kurnawan, unpublished
JK123-2D[3]	*MAT*a *his4-912δ lys2-128δ leu2-3,112 trp1-Δ1 ura3-52 ssd1-d cdc68Δ::kanMX* [YEpDE68-1]	KanB haploid derivative, J. Kurnawan, unpublished
KanB 315-A4[4]	*MATα his4-912δ lys2-128δ leu2-3,112 trp1-Δ1 ura3-52 ssd1-d cdc68Δ::kanMX4* [pRS315-A4]	KanB haploid derivative
KanB 315-E763G	*MATα his4-912δ lys2-128δ leu2-3,112 trp1-Δ1 ura3-52 ssd1-d cdc68Δ::kanMX4* [pRS315-*cdc68-E763G*]	KanB haploid derivative
KanB 315-E857K	*MATα his4-912δ lys2-128δ leu2-3,112 trp1-Δ1 ura3-52 ssd1-d cdc68Δ::kanMX4* [pRS315-*cdc68-E763G*]	KanB haploid derivative
KanB 315-312[4]	*MATα his4-912δ lys2-128δ leu2-3,112 trp1-Δ1 ura3-52 ssd1-d cdc68Δ::kanMX4* [pRS315-*cdc68-312*]	KanB haploid derivative
KanB 315-319[4]	*MATα his4-912δ lys2-128δ leu2-3,112 trp1-Δ1 ura3-52 ssd1-d cdc68Δ::kanMX4* [pRS315-*cdc68-319*]	KanB haploid derivative
KanB 314-A4	*MATα his4-912δ lys2-128δ leu2-3,112 trp1-Δ1 ura3-52 ssd1-d cdc68Δ::kanMX4* [pRS314-A4]	KanB haploid derivative
KanB 314-E763G	*MATα his4-912δ lys2-128δ leu2-3,112 trp1-Δ1 ura3-52 ssd1-d cdc68Δ::kanMX4* [pRS314-*cdc68-E763G*]	KanB haploid derivative
KanB 314-E857K	*MATα his4-912δ lys2-128δ leu2-3,112 trp1-Δ1 ura3-52 ssd1-d cdc68Δ::kanMX4* [pRS314-*cdc68-E857K*]	KanB haploid derivative
KanB 314-312	*MATα his4-912δ lys2-128δ leu2-3,112 trp1-Δ1 ura3-52 ssd1-d cdc68Δ::kanMX4* [pRS314-*cdc68-312*]	KanB haploid derivative
KanB 314-319	*MATα his4-912δ lys2-128δ leu2-3,112 trp1-Δ1 ura3-52 ssd1-d cdc68Δ::kanMX4* [pRS314-*cdc68-319*]	KanB haploid derivative
KanB 426-B2	*MATα his4-912δ lys2-128δ leu2-3,112 trp1-Δ1 ura3-52 ssd1-d cdc68Δ::kanMX4* [pRS426-B2]	KanB haploid derivative
KanB 426-E763G	*MATα his4-912δ lys2-128δ leu2-3,112 trp1-Δ1 ura3-52 ssd1-d cdc68Δ::kanMX4* [pRS426-*cdc68-E763G*]	KanB haploid derivative
KanB 426-E857K	*MATα his4-912δ lys2-128δ leu2-3,112 trp1-Δ1 ura3-52 ssd1-d cdc68Δ::kanMX4* [pRS426-*cdc68-E857K*]	KanB haploid derivative
KanB 426-312	*MATα his4-912δ lys2-128δ leu2-3,112 trp1-Δ1 ura3-52 ssd1-d cdc68Δ::kanMX4* [pRS426-*cdc68-312*]	KanB haploid derivative
KanB 426-319	*MATα his4-912δ lys2-128δ leu2-3,112 trp1-Δ1 ura3-52 ssd1-d cdc68Δ::kanMX4* [pRS426-*cdc68-319*]	KanB haploid derivative
KanB 316-ΔNWT	*MATα his4-912δ lys2-128δ leu2-3,112 trp1-Δ1 ura3-52 ssd1-d cdc68Δ::kanMX* [316-ΔNTD-3'68]	KanB haploid derivative
KanB 316-ΔN,763	*MATα his4-912δ lys2-128δ leu2-3,112 trp1-Δ1 ura3-52 ssd1-d cdc68Δ::kanMX* [316-ΔNTD E763G]	KanB haploid derivative
KanB 316-ΔN,857	*MATα his4-912δ lys2-128δ leu2-3,112 trp1-Δ1 ura3-52 ssd1-d cdc68Δ::kanMX* [316-ΔNTD E857K]	KanB haploid derivative
KanB 316-ΔN,312	*MATα his4-912δ lys2-128δ leu2-3,112 trp1-Δ1 ura3-52 ssd1-d cdc68Δ::kanMX* [316-ΔNTD 312]	KanB haploid derivative
KanB 316-ΔN,319	*MATα his4-912δ lys2-128δ leu2-3,112 trp1-Δ1 ura3-52 ssd1-d cdc68Δ::kanMX* [316-ΔNTD 319]	KanB haploid derivative

BM64 ynl035cΔ	*MAT*a/α *his4-912δ lys2-128δ leu2-3,112 trp1-Δ1 ura3-52 ssd1-d CDC68/ cdc68-101::LEU2 ynl035cΔ::natMX4/YNL035c*	BM64 derivative
YNL035c NAT1 KO *MAT*a (7A) and *MAT*α (7B)	*his4-912δ lys2-128δ leu2-3,112 trp1-Δ1 ura3-52 ssd1-d CDC68 ynl035cΔ::natMX4*	Haploid derivatives of BM64 ynl035cΔ
YNLK 122	Haploid segregants of genotype *his4-912δ lys2-128δ leu2-3,112 trp1-Δ1 ura3-52 ssd1-d cdc68Δ::kanMX4 ynl035cΔ::natMX4* [pRS316-A4] were also obtained, with the identities 1C, 5A, 7B, and 10A	YNL035c NAT1 KO x JK122-3B
YNLK 123	Haploid segregants of genotype *his4-912δ lys2-128δ leu2-3,112 trp1-Δ1 ura3-52 ssd1-d cdc68Δ::kanMX4 ynl035cΔ::natMX4* [YEpDE68-1] were also obtained with the identities 1D, 8C, 15D, and 17B.	YNL035c NAT1 KO x JK123-2D
YNLK 319	Haploid segregants of genotype *his4-912δ lys2-128δ leu2-3,112 trp1-Δ1 ura3-52 ssd1-d cdc68Δ::kanMX4 ynl035cΔ::natMX4* [pRS316-*cdc68-319*] were also obtained with the identities 8B, 8D, 15B, and 15D.	YNL035c NAT1 KO x KanB 316-319
YNLK A4	Haploid segregants of genotype *his4-912δ lys2-128δ leu2-3,112 trp1-Δ1 ura3-52 ssd1-d cdc68Δ::kanMX4 ynl035cΔ::natMX4* [pRS316-A4] were also obtained with the identitites 3A, 3B, 7C, and 7D.	YNL035c NAT1 KO x KanB 316-A4
YNLK 120	Haploid segregants of genotype *his4-912δ lys2-128δ leu2-3,112 trp1-Δ1 ura3-52 ssd1-d cdc68Δ::kanMX4 ynl035cΔ::natMX4* [YEpDEMC4] were also obtained with the identities 1A, 13A, 9B, and 7D.	YNL035c NAT1 KO x JK120-6A
YNLK 316	Haploid segregants of genotype *his4-912δ lys2-128δ leu2-3,112 trp1-Δ1 ura3-52 ssd1-d CDC68 ynl035cΔ::natMX4* [pRS316] were also obtained with the identities 1D and 4C.	YNL035c NAT1 KO x KanB 316
YNLK 121B	Haploid segregants of genotype *his4-912δ lys2-128δ leu2-3,112 trp1-Δ1 ura3-52 ssd1-d cdc68Δ::kanMX4 ynl035cΔ::natMX4* [JKpmini68] were also obtained with the identities 4A, 9A, 10B, and 11C.	YNL035c NAT1 KO x JK121-10B
YNLK 121D	Haploid segregants of genotype *his4-912δ lys2-128δ leu2-3,112 trp1-Δ1 ura3-52 ssd1-d cdc68Δ::kanMX4 ynl035cΔ::natMX4* [JKpmini68] were also obtained with the identities 4C, 10D, 11D, and 15A.	YNL035c NAT1 KO x JK121-10D
YNLK 312	Haploid segregants of genotype *his4-912δ lys2-128δ leu2-3,112 trp1-Δ1 ura3-52 ssd1-d cdc68Δ::kanMX4 ynl035cΔ::natMX4* [pRS316-*cdc68-312*] were also obtained with the identities 7B, 9A, 10C, and 16C.	YNL035c NAT1 KO x KanB 316-312
QXT101	*MAT*a *sug1-1 leu2-3,112 trp1-Δ1 ura3-52 ade2 cdc68-1[cdc68-210N::URA3]*	Xu *et al.* 1995
PJ69-4a [1]	*MAT*a *his3-200 LYS2::GAL1-HIS3 leu2-3, 112 trp1-901 ura3-52 gal4Δ gal80Δ met2::GAL7-lacZ GAL2-ADE2*	James *et al.* 1996
Y2454	*MAT*α *mfa1Δ::MFA1pr-HIS3 can1Δ his3Δ1 leu2Δ0 ura3Δ0 MET15 lys2Δ0*	Tong *et al.* 2001
Y2454 312-8 c1	*MAT*α *mfa1Δ::MFA1pr-HIS3 can1Δ his3Δ1 leu2Δ0 ura3Δ0 MET15 lys2Δ0 cdc68-312::natMX4*	Y2454 derivative
Y2454 319-5 c1	*MAT*α *mfa1Δ::MFA1pr-HIS3 can1Δ his3Δ1 leu2Δ0 ura3Δ0 MET15 lys2Δ0 cdc68-319::natMX4*	Y2454 derivative
Y2454 ΔNTD c4 or c8	*MAT*α *mfa1Δ::MFA1pr-HIS3 can1Δ his3Δ1 leu2Δ0 ura3Δ0 MET15 lys2Δ0 cdc68-ΔNTD::natMX4*	Y2454 derivative

Y2454 E763G-3 c3	*MATα mfa1Δ::MFA1pr-HIS3 can1Δ his3Δ1 leu2Δ0 ura3Δ0 MET15 lys2Δ0 cdc68-E763G::natMX4*	Y2454 derivative
Y2454 E857K-7 c3	*MATα mfa1Δ::MFA1pr-HIS3 can1Δ his3Δ1 leu2Δ0 ura3Δ0 MET15 lys2Δ0 cdc68-E857K::natMX4*	Y2454 derivative
Y2454 WT68 c1	*MATα mfa1Δ::MFA1pr-HIS3 can1Δ his3Δ1 leu2Δ0 ura3Δ0 MET15 lys2Δ0 CDC68::natMX4*	Y2454 derivative
Y2454 YNL NAT	*MATα mfa1Δ::MFA1pr-HIS3 can1Δ his3Δ1 leu2Δ0 ura3Δ0 MET15 lys2Δ0 ynl035cΔ::natMX4*	Y2454 derivative
GHY1088	*MATα ade2Δ::hisG ade3Δ::hisG his4-912δ lys2-128δ leu2-Δ1 ura3-52*	Grant Hartzog (Santa Cruz, CA)
SNL5A	*MATa ade2Δ ade3Δ his4-912δ lys2-128δ leu2-3,112 trp1-Δ1 ura3-52 cdc68Δ::kanMX4* [pRS316-A4]	KanB 316-A4 HA x GHY1088 segregant
SNL-58D	*MATa ade2Δ ade3Δ his4-912δ lys2-128δ leu2-3,112 trp1-Δ1 ura3-52 cdc68Δ::kanMX4* [pRS316-A4]	produced by backcrossing a SNL5A-type segregant to GHY1088 (see Materials and Methods text)
SNL-51B	*MATα ade2Δ ade3Δ his4-912δ lys2-128δ leu2-3,112 trp1-Δ1 ura3-52 cdc68Δ::kanMX4* [pRS316-A4]	produced by backcrossing a SNL5A-type segregant to GHY1088 (see Materials and Methods text)
SNL-58D plA4	*MATa ade2Δ ade3Δ his4-912δ lys2-128δ leu2-3,112 trp1-Δ1 ura3-52 cdc68Δ::kanMX4* [pRS316-A4] [pRS315-A4]	Derivative of SNL-58D
SNL-58D plE763G	*MATa ade2Δ ade3Δ his4-912δ lys2-128δ leu2-3,112 trp1-Δ1 ura3-52 cdc68Δ::kanMX4* [pRS316-A4] [pRS315-E763G]	Derivative of SNL-58D
SNL-58D plE857K	*MATa ade2Δ ade3Δ his4-912δ lys2-128δ leu2-3,112 trp1-Δ1 ura3-52 cdc68Δ::kanMX4* [pRS316-A4] [pRS315-E857K]	Derivative of SNL-58D
SNL-58D pl312	*MATa ade2Δ ade3Δ his4-912δ lys2-128δ leu2-3,112 trp1-Δ1 ura3-52 cdc68Δ::kanMX4* [pRS316-A4] [pRS315-312]	Derivative of SNL-58D
SNL-58D pl319	*MATa ade2Δ ade3Δ his4-912δ lys2-128δ leu2-3,112 trp1-Δ1 ura3-52 cdc68Δ::kanMX4* [pRS316-A4] [pRS315-319]	Derivative of SNL-58D
SNL-51B plA4	*MATα ade2Δ ade3Δ his4-912δ lys2-128δ leu2-3,112 trp1-Δ1 ura3-52 cdc68Δ::kanMX4* [pRS316-A4] [pRS314-A4]	Derivative of SNL-51B
SNL-51B plE763G	*MATα ade2Δ ade3Δ his4-912δ lys2-128δ leu2-3,112 trp1-Δ1 ura3-52 cdc68Δ::kanMX4* [pRS316-A4] [pRS314-E763G]	Derivative of SNL-51B
SNL-51B plE857K	*MATα ade2Δ ade3Δ his4-912δ lys2-128δ leu2-3,112 trp1-Δ1 ura3-52 cdc68Δ::kanMX4* [pRS316-A4] [pRS314-E857K]	Derivative of SNL-51B
SNL-51B pl312	*MATα ade2Δ ade3Δ his4-912δ lys2-128δ leu2-3,112 trp1-Δ1 ura3-52 cdc68Δ::kanMX4* [pRS316-A4] [pRS314-312]	Derivative of SNL-51B

SNL-51B pl319	*MATα ade2Δ ade3Δ his4-912δ lys2-128δ leu2-3,112 trp1-Δ1 ura3-52 cdc68Δ::kanMX4* [pRS316-A4] [pRS314-319]	Derivative of SNL-51B
SNL-58D 315-A4	*MAT*a *ade2Δ ade3Δ his4-912δ lys2-128δ leu2-3,112 trp1-Δ1 ura3-52 cdc68Δ::kanMX4* [pRS315-A4]	Derivative of SNL-58D
SNL-58D 315-E763G	*MAT*a *ade2Δ ade3Δ his4-912δ lys2-128δ leu2-3,112 trp1-Δ1 ura3-52 cdc68Δ::kanMX4* [pRS315-E763G]	Derivative of SNL-58D
SNL-58D 315-E857K	*MAT*a *ade2Δ ade3Δ his4-912δ lys2-128δ leu2-3,112 trp1-Δ1 ura3-52 cdc68Δ::kanMX4* [pRS315-E857K]	Derivative of SNL-58D
SNL-58D 315-312	*MAT*a *ade2Δ ade3Δ his4-912δ lys2-128δ leu2-3,112 trp1-Δ1 ura3-52 cdc68Δ::kanMX4* [pRS315-312]	Derivative of SNL-58D
SNL-58D 315-319	*MAT*a *ade2Δ ade3Δ his4-912δ lys2-128δ leu2-3,112 trp1-Δ1 ura3-52 cdc68Δ::kanMX4* [pRS315-319]	Derivative of SNL-58D
SNL-51B 314-A4	*MATα ade2Δ ade3Δ his4-912δ lys2-128δ leu2-3,112 trp1-Δ1 ura3-52 cdc68Δ::kanMX4* [pRS314-A4]	Derivative of SNL-51B
SNL-51B 314-E763G	*MATα ade2Δ ade3Δ his4-912δ lys2-128δ leu2-3,112 trp1-Δ1 ura3-52 cdc68Δ::kanMX4* [pRS314-E763G]	Derivative of SNL-51B
SNL-51B 314-E857K	*MATα ade2Δ ade3Δ his4-912δ lys2-128δ leu2-3,112 trp1-Δ1 ura3-52 cdc68Δ::kanMX4* [pRS314-E857K]	Derivative of SNL-51B
SNL-51B 314-312	*MATα ade2Δ ade3Δ his4-912δ lys2-128δ leu2-3,112 trp1-Δ1 ura3-52 cdc68Δ::kanMX4* [pRS314-312]	Derivative of SNL-51B
SNL-51B 314-319	*MATα ade2Δ ade3Δ his4-912δ lys2-128δ leu2-3,112 trp1-Δ1 ura3-52 cdc68Δ::kanMX4* [pRS314-319]	Derivative of SNL-51B
SNL-58D 315-A4 SL	*MAT*a *ade2Δ ade3Δ his4-912δ lys2-128δ leu2-3,112 trp1-Δ1 ura3-52 cdc68Δ::kanMX4* [pRS315-A4] [pSLCDC68]	Derivative of SNL-58D
SNL-58D 315-E763G SL	*MAT*a *ade2Δ ade3Δ his4-912δ lys2-128δ leu2-3,112 trp1-Δ1 ura3-52 cdc68Δ::kanMX4* [pRS315-E763G] [pSLCDC68]	Derivative of SNL-58D
SNL-58D 315-E857K SL	*MAT*a *ade2Δ ade3Δ his4-912δ lys2-128δ leu2-3,112 trp1-Δ1 ura3-52 cdc68Δ::kanMX4* [pRS315-E857K] [pSLCDC68]	Derivative of SNL-58D
SNL-58D 315-312 SL	*MAT*a *ade2Δ ade3Δ his4-912δ lys2-128δ leu2-3,112 trp1-Δ1 ura3-52 cdc68Δ::kanMX4* [pRS315-312] [pSLCDC68]	Derivative of SNL-58D
SNL-58D 315-319 SL	*MAT*a *ade2Δ ade3Δ his4-912δ lys2-128δ leu2-3,112 trp1-Δ1 ura3-52 cdc68Δ::kanMX4* [pRS315-319] [pSLCDC68]	Derivative of SNL-58D
SNL-51B 314-A4 SL	*MATα ade2Δ ade3Δ his4-912δ lys2-128δ leu2-3,112 trp1-Δ1 ura3-52 cdc68Δ::kanMX4* [pRS314-A4] [pSLCDC68]	Derivative of SNL-51B
SNL-51B 314-E763G SL	*MATα ade2Δ ade3Δ his4-912δ lys2-128δ leu2-3,112 trp1-Δ1 ura3-52 cdc68Δ::kanMX4* [pRS314-E763G] [pSLCDC68]	Derivative of SNL-51B

SNL-51B 314-E857K SL	*MATα ade2Δ ade3Δ his4-912δ lys2-128δ leu2-3,112 trp1-Δ1 ura3-52 cdc68Δ::kanMX4* [pRS314-E857K] [pSLCDC68]	Derivative of SNL-51B
SNL-51B 314-312 SL	*MATα ade2Δ ade3Δ his4-912δ lys2-128δ leu2-3,112 trp1-Δ1 ura3-52 cdc68Δ::kanMX4* [pRS314-312] [pSLCDC68]	Derivative of SNL-51B
SNL-51B 314-319 SL	*MATα ade2Δ ade3Δ his4-912δ lys2-128δ leu2-3,112 trp1-Δ1 ura3-52 cdc68Δ::kanMX4* [pRS314-319] [pSLCDC68]	Derivative of SNL-51B
NB6247	*his3-1 leu2-3, 112 trp1-1 ura3-52 CDC68 POB3-V5::TRP1* [p314-M68]	N. K. Brewster
NB6247 ΔN	*his3-1 leu2-3, 112 trp1-1 ura3-52 CDC68 POB3-V5::TRP1* [p315-ΔNTDFLAG]	Derivative of NB6247

1) Many yeast strains were made by transforming various combinations of yeast two-hybrid plasmids into cells of strain PJ69-4a. The plasmid combinations tested for two-hybrid interactions are indicated in Tables 7 and 8 by the fusion proteins they express. For two-hybrid plasmids made in this study see Table 3.

2) These stains were transformed with the following plasmids: YEpSH68, YEpMPT5, YEpPKC1, pWSC1, pBA1036, pBA958, pBA251, pBA487, pRS424-YNL, pRS425-SSD1, pRS315-SSD1, pRS425-SRP101, and appropriate vector controls.

3) These strains were transformed with the following plasmids: pRS315-SSD1, pRS424-YNL and appropriate vector controls.

4) These strains were transformed with pBA314 and pRS426.

that were able to grow on the M9 medium were those that had a plasmid-borne yeast *LEU2* gene which complements the *leuB* auxotrophy.

2. Yeast strains and plasmids

The *Saccharomyces cerevisiae* strains employed in this research are listed in Table 2.

i) KanB and derivatives

The majority of strains employed in this work are derivatives of the KanB diploid strain. The KanB diploid was generated from diploid BM64, a strain with an S288c genetic background (Malone *et al.* 1991), by replacing the *LEU2*-marked *cdc68* disruption with a *kanMX4* cassette, deleting the entire coding region for *CDC68*. To assist in generating this deletion/replacement of the *cdc68::LEU2* chromosomal sequence, the pRS316-CDC68kanMX4 plasmid was made. This plasmid was generated by ligation of the following four DNA molecules: 1) a *Kpn*I- and *Xba*I-digested pRS316 vector (Sikorski and Hieter 1989); 2) a *Kpn*I- and *Bgl*II-digested PCR product consisting of approximately 510 basepairs of genomic DNA upstream of the *CDC68* start codon generated using the primer pairs 5'UTR68 A (5'GGGGTACCCATTCCCGCCGTGTTTACTGACCC), which contains a *Kpn*I recognition site, and 5'UTR68 B (5'CCCAGATCTCGCGACTTCCGGGTATTAGTATCG), which contains a *Bgl*II recognition site; 3) an *Eco*RI- and *Xba*I-digested PCR product consisting of approximately 369 basepairs of genomic DNA sequence downstream of the *CDC68* stop codon generated using the primers 3'UTR68 C (5'CCCAGATCTGAATTCGGTCAAGGTCATAGGACGTTTGCG), which contains an *Eco*RI recognition site, and 3'UTR68 D (5'GGGTCTAGAAACCTTTGATGCTGATGAACAGCG), which contains an *Xba*I recognition site; and 4) a *Bgl*II- and *Eco*RI-digested PCR product consisting of the *kanMX4* cassette (Wach *et al.* 1994) generated using the primers 5'KanMX4 (5'CGCGCCAGATCTGTTTAGCTTGCC), which contains a *Bgl*II site, and 3'KanMX4 (5'CCCAGATCTTCGATGAATTCGAGCTCGTTTTCG), which contains an *Eco*RI site. The end result of this ligation was the pRS316-CDC68kanMX4 plasmid, which contains the *kanMX4* cassette flanked by approximately 510 and 369 basepairs of DNA sequence from upstream and downstream of the *CDC68* coding sequence, respectively, in the pRS316 vector backbone.

Plasmid pRS316-CDC68kanMX4 was next digested with *Kpn*I and *Xba*I and a 2.3-kbp fragment containing the *kanMX4* cassette flanked by the *CDC68* upstream and downstream sequences was purified and used to transform BM64 diploid cells. Transformants were then spread on YEPD medium containing geneticin at 200 mg/l (also known as G418; Invitrogen) and allowed to grow at 30°C for 5 to 7 days to select for cells that contained integrations of the *kanMX4* cassette. Large transformant colonies were re-inoculated onto solid YEPD medium containing geneticin. Growth of cells on SC-Leu medium was also tested to determine the status of the *cdc68::LEU2* chromosomal locus. Cells that were resistant to growth inhibition by geneticin, indicating that the *kanMX4* cassette had integrated, and leucine auxotrophs, indicating that the *LEU2* marker at the *cdc68* disruption chromosomal locus had been lost, were chosen for further verifications.

The insertion of the *kanMX4* cassette at the *CDC68* chromosomal locus, resulting in loss of the *CDC68* coding sequence as well as the disrupting *LEU2* sequence, was verified using PCR in a scheme similar to that described (Wach *et al.* 1994) Colony PCR (described below) used the *kanMX4* replacement candidates as template and the following primer sets: 1) 5'KanMX4 primer (described above), 3' CDC68 primer (used to generate the pRS316-A4 plasmid as described below), and GAP3 TOP primer (used in sequencing *cdc68* alleles as described below); and 2) 3'KanMX4 primer (described above), V1 primer (5'GTGAAGCTAAGGCTGCTTCCAGGC), and GAP1 primer (5'CAACTCCTCGTCAACTGCCCG) (Figure 3). The KanB diploid verified in this way to contain the *kanMX4* cassette as a replacement for the *cdc68::LEU2* coding sequences at the chromosomal locus was then employed in subsequent studies.

The KanB diploid was transformed with a *URA3*-marked wild-type *CDC68* plasmid (pRS316-A4) as well as a *URA3* vector (pRS316) as a control. These two resultant strains were then sporulated and tetrad analysis was performed to verify that 1) tetrads from the KanB diploid plus vector showed a 2:2 segregation pattern of live spores to dead spores (where none of the live spores were resistant to geneticin), indicating that the essential, undisrupted *CDC68* chromosomal copy has been maintained, and 2) all of the live segregants from the *CDC68* transformants that were geneticin-resistant (a phenotype conferred by the *kanMX4* cassette) could not survive loss of the plasmid-borne *CDC68*

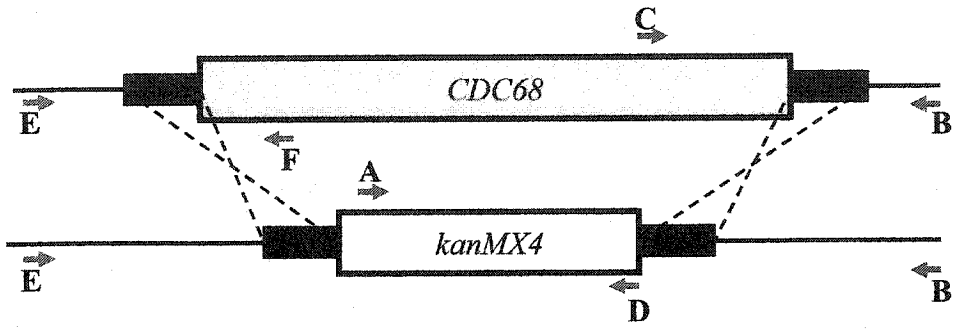

Figure 3. PCR verification of *kanMX4* replacement at *CDC68* chromosomal locus. The new KanB diploids that have the *cdc68::LEU2* locus in the BM64 progenitor cells with the *kanMX4* cassette have replaced one wild-type *CDC68* gene (coding sequence shown as a grey box) and one *kanMX4* deletion/replacement at the second chromosomal locus (shown as a white box). Black boxes indicate the non-coding *CDC68* flanking sequences used to target the *kanMX4* cassette to the *CDC68* locus. Colony PCR to verify the insertion site of the *kanMX4* cassette made use of the red primer set (A) 5'KanMX4, (B) 3' CDC68, (C) GAP2 TOP and the blue primer set (D) 3'KanMX4, (E) V1, and (F) GAP1 to verify the 5' and 3' insertion points, respectively. Primers A and B yielded a diagnostic DNA product of 2.0 kbp that verified the 3' insertion site of the *kanMX4* cassette at the *CDC68* locus, while the primer combination C and B gave a 1.1-kbp product (an internal control for the PCR reaction). Primers D and E generate a 2.3-kbp product that verified the 5' insertion site of the *kanMX4* cassette at the *CDC68* locus, while the primer combination F and E gave a 1.7-kbp band (as an internal PCR control). This combination of PCR products was observed when cells from the KanB diploid strain were used as template for colony PCR with the above primers, indicating that in cells of strain KanB the *kanMX4* cassette is integrated as a replacement of the *cdc68::LEU2* coding sequences at the *CDC68* chromosomal locus.

gene, as determined by uracil prototrophy. These features helped ensure that the *kanMX4* cassette had not integrated at any other chromosomal location in addition to the *CDC68* locus. With this final verification that the KanB diploid contains only a single *kanMX4* integration that replaces the *cdc68::LEU2* coding sequence, the KanB diploid was then ready for use as the progenitor of a multitude of haploid derivatives (Table 2).

The KanB diploid cells were transformed with *URA3* plasmids bearing mutant alleles of *cdc68* and then were sporulated to generate haploid *cdc68::kanMX4* segregants with the *URA3 cdc68* plasmid (Table 2). These haploid progeny were used for plasmid shuffling with mutant *cdc68* plasmids marked with other biosynthetic genes (like *LEU2* and *TRP1*) to introduce these alleles as the only form of *CDC68* in the cell (Table 2). While each of these haploid derivatives bears the KanB designation, the addition of a *MAT*a or *MAT*α notation designates the haploid nature of these cells (Table 2).

ii) *YNL035c* deletion strains

A similar strategy was used to create *natMX4* (Goldstein and McCusker 1999) replacements of the *YNL035c* gene in derivatives of strain Y2454 or strain BM64, known as Y2454 YNL NAT or BM64 ynl035cΔ, respectively (Table 2). The pRS314-YNL NAT plasmid was generated by ligation of the following DNA molecules: 1) a *Cla*I- and *Not*I-digested pRS314 (Sikorski and Hieter 1989) vector; 2) a *Cla*I- and *Bam*HI-digested 167-basepair PCR product from the genomic DNA upstream of the *YNL035c* start codon that was amplified using the V1 5'UTR YNL035c primer (5'GCGATCGATTTTTGCATTGGCAATGTGA), which contains a *Cla*I recognition site, and the V2 5'UTR YNL035c primer (5'GCGGGATCCGCTCTAGAAGTTAATTTGAGATTCTCG), which contains a *Bam*HI recognition site; 3) a *Bam*HI- and *Not*I-digested 291-basepair PCR product of the genomic DNA downstream of the *YNL035c* stop codon that was amplified using the V3 3'UTR YNL035c primer (5'GCTGGATCCCATAAAGACAATACATCTAAAGAGATGCC), which contains a *Bam*HI recognition sequence, and the V4 3'UTR YNL035c primer (5'GATGCGGCCGCTTCACCATCAACGTGGTGTTTC), which contains a *Not*I recognition site; and 4) a *Bam*HI-digested 1.2-kbp PCR-amplified *natMX4* cassette (Goldstein and McCusker 1999) amplified using the *Bam*HI MX4 NAT FOR primer (5'CGCGGATCCACATGGAGGCCCAGAATACCC) and the *Bam*HI MX4 NAT REV primer

(5'CGCGGATCCCAGTATAGCGACCAGCATTCAC), which both contain *Bam*HI recognition sequences. The pRS314-YNL NAT plasmid that is the product of this ligation contains the *natMX4* cassette flanked by 167 bp of *YNL035c* upstream DNA sequence and 291 bp of *YNL035c* downstream DNA sequence, cloned into the *Cla*I and *Not*I sites of the pRS314 vector.

The pRS314-YNL NAT plasmid was digested with *Cla*I and *Not*I to release a 1.6-kbp DNA fragment that was purified and used to transform cells from both the Y2454 and BM64 strains. Transformants were spread on YEPD medium containing Nat (100 μg/ml; also known as clonNAT; Werner BioAgents) and grown for 5 to 7 days at 30°C. The *natMX4* cassette encodes a gene that allows yeast cells to grow in the presence of nourseothricin (Nat); therefore only cells that had a *natMX4* integration were able to grow on the Nat-containing medium. Large Nat-resistant colonies were then re-inoculated onto YEPD medium containing Nat and grown at 30°C for a further 2 to 3 days to verify the Nat-resistance phenotype.

To verify the insertion site of the *natMX4* cassette at the *YNL035c* genomic locus a PCR strategy was employed using the following primer pairs: 1) 5UPS YNL (5'GGAGGGTTGCTTGGTTAATAC) with ALLY NAT MID FOR (5'GGACTCCCGGACGTTCGTCGC), and 2) 3DNS YNL (5'TGGTATGATTCTCGCTTTGG) with STEVE NAT MID REV (5'ACGAACGTCCGGGAGTCC). In each case, one of the primers anneals within the *natMX4* cassette while the other primer anneals to genomic DNA flanking the *YNL035c* locus but outside of the region used for construction of the pRS314-YNL NAT plasmid. PCR amplification using these primers gave in each case a DNA fragment of approximately 1 kbp, the expected size product if the *natMX4* cassette was successfully integrated to replace the *YNL035c* coding sequence in the chromosome.

The Y2454 YNL NAT strain was used in SGA analysis, while the BM64 *ynl035cΔ* diploid was sporulated and haploid segregants (strains YNL035c NAT1 KO 7A and 7B in Table 2) were mated to several KanB haploid derivatives containing various mutant alleles of *cdc68* to generate a series of diploid strains (strains with YNLK designations in Table 2). These double-mutant diploids, containing the *ynl035cΔ::natMX4* gene replacement and the *cdc68Δ::kanMX4* deletion as well as a plasmid-borne allele of

cdc68, were then sporulated and double-mutant haploid progeny (Table 2) were assessed for growth under a variety of conditions (Results, section 5).

iii) Generating *natMX4*-tagged mutant *cdc68* alleles

Chromosomally integrated *cdc68* mutant alleles that were *natMX4*-tagged downstream of the stop codon for *CDC68* were generated in derivatives of strain Y2454 for use in SGA analysis. Several plasmids were built to assist in the construction of these strains, which each contain a mutant allele of *cdc68* with the *natMX4* cassette inserted at the *Bsr*GI site downstream of the *CDC68* stop codon. The *natMX4* cassette was PCR-amplified using the *Bsr*GI MX4 NAT FOR primer (5'CGCTCTACAACATGGAGGCCCAGAATACCC) and the *BsrG*I MX4 NAT REV primer (5'CGCTGTACACAGTATAGCGACCAGCATTCAC), which each contain a *BsrG*I restriction endonuclease cleavage sequence. The following plasmids were digested with *Bsr*GI and used in ligations with *Bsr*GI-digested PCR-amplified *natMX4* cassette: 1) pRS316-*cdc68-E763G*, 2) pRS316-*cdc68-E857K*, 3) pRS316-*cdc68-312*, 4) pRS316-*cdc68-319*, and 5) 316-ΔNTD-3'68 (which contains a FLAG-epitope tagged version of the *cdc68-ΔNTD* allele; Table 3). The new plasmids generated from these ligations were named pRS316-E763G NATc3, pRS316-E857K NATc7, pRS316-312 NATc8, pRS316-319c5 and pRS316-ΔNTD NATc1, respectively, and the orientation of the *natMX4* cassette insertion was determined for each plasmid by analyzing the pattern of DNA fragments produced from restriction endonuclease digestion. The orientation of the *natMX4* cassette with respect to the *CDC68* gene is shown in Figure 4. Each of these new *natMX4* plasmids was then digested with *Bam*HI and *Sst*I, and the 5.5-kbp DNA fragment (except in the case of pRS316-ΔNTD NATc1, which was digested with *Bam*HI alone and generated a 4.4-kbp DNA fragment used in transformations) containing the *CDC68* coding sequence for each mutant allele plus the *natMX4* cassette and 462 bp upstream and 776 bp downstream of the *CDC68* coding sequence, was gel-purified and employed in transformations of Y2454 cells.

Transformation mixtures were spread on YEPD medium containing Nat (100 μg/ml) and grown for 5 to 7 days at 30°C. Large Nat-resistant colonies were then re-inoculated on YEPD medium containing Nat and grown for 2 to 3 days at 30°C to verify the Nat-resistance phenotype. Several measures were taken then to ensure that 1) the chromosomal integration of the *natMX4* marker and the flanking *CDC68* sequences had

Table 3. Plasmids used in this study.

Plasmid name	Description	Source
pRS316	*URA3 CEN amp*^{R} vector	Sikorski and Hieter 1989
pRS315	*LEU2 CEN amp*^{R} vector	Sikorski and Hieter 1989
pRS314	*TRP1 CEN amp*^{R} vector	Sikorski and Hieter 1989
pRS425	*LEU2* 2μ *amp*^{R} vector	Christianson *et al.* 1992
pRS424	*TRP1* 2μ *amp*^{R} vector	Christianson *et al.* 1992
pRS426	*URA3* 2μ *amp*^{R} vector	Christianson *et al.* 1992
YEp351	*LEU2* 2μ *amp*^{R} vector	Hill *et al.* 1986
pGEX2T	*tac* promoter-glutathione-S-transferase (GST) *lacI amp*^{R}	Pharmacia Biotech
pET32-mLIC	T7 promoter-thioredoxin-His_6-S-protein *amp*^{R} vector modified multiple cloning site pET32-LIC; Novagen	Paul Liu (Dept. Biochem. & Mol Bio., Dalhousie University)
pGAD424	*GAL4-AD TRP1* 2μ *amp*^{R}	Bartel *et al.* 1993
pGBT9	*GAL4-BD LEU2* 2μ *amp*^{R}	Bartel *et al.* 1993
p68-BS-XI	*CDC68 URA3* 2μ *amp*^{R}	Brian Smith, unpublished
pRS316-A4	*CDC68 URA3 CEN*	This study
pRS315-A4	*CDC68 LEU2 CEN*	This study
pRS314-A4	*CDC68 TRP1 CEN*	This study
pRS426-B2	*CDC68 URA3* 2μ	This study
YEpSH68	*CDC68 LEU2* 2μ	Sally Harvie, unpublished
pRS316-cdc68-E763G	*cdc68-E763G URA3 CEN*	This study
pRS315-cdc68-E763G	*cdc68-E763G LEU2 CEN*	This study
pRS314-cdc68-E763G	*cdc68-E763G TRP1 CEN*	This study
pRS426-cdc68-E763G	*cdc68-E763G URA3* 2μ	This study
pRS316-cdc68-E857K	*cdc68-E857K URA3 CEN*	This study
pRS315-cdc68-E857K	*cdc68-E857K LEU2 CEN*	This study
pRS314-cdc68-E857K	*cdc68-E857K TRP1 CEN*	This study
pRS426-cdc68-E857K	*cdc68-E857K URA3* 2μ	This study
pRS316-cdc68-312	*cdc68-312 URA3 CEN*	This study
pRS315- cdc68-312	*cdc68-312 LEU2 CEN*	This study
pRS314- cdc68-312	*cdc68-312 TRP1 CEN*	This study
pRS426- cdc68-312	*cdc68-312 URA3* 2μ	This study
pRS316-cdc68-319	*cdc68-319 URA3 CEN*	This study

pRS315- cdc68-319	*cdc68-319 LEU2 CEN*	This study
pRS314- cdc68-319	*cdc68-319 TRP1 CEN*	This study
pRS426- cdc68-319	*cdc68-319 URA3* 2μ	This study
pRS316-cdc68-121	*cdc68-121 URA3 CEN*	This study
pRS316-cdc68-122	*cdc68-122 URA3 CEN*	This study
pRS316-cdc68-123	*cdc68-123 URA3 CEN*	This study
pRS316-cdc68-124	*cdc68-124 URA3 CEN*	This study
pRS316-cdc68-131	*cdc68-131 URA3 CEN*	This study
pRS316-cdc68-134	*cdc68-134 URA3 CEN*	This study
JKpmini68	*cdc68-mini URA3 CEN*	Joelius Kurniawan, unpublished
p314-cdc68-mini	*cdc68-mini TRP1 CEN*	Neil Brewster, unpublished
YEpDE68-1	*cdc68-1 URA3 CEN*	Evans *et al.* 1998
YEpDE-MC4	*cdc68-Δ922 URA3 CEN*	Evans *et al.* 1998
JKpd369	*cdc68-Δ369 URA3 CEN*	Joelius Kurniawan, unpublished
p314-ΔNTDFLAG	*cdc68-ΔNTD-FLAG TRP1 CEN*	Neil Brewster, unpublished
p316-ΔNTDFLAG	*cdc68-ΔNTD-FLAG URA3 CEN*	This study
p315-ΔNTDFLAG	*cdc68-ΔNTD-FLAG LEU2 CEN*	This study
pTF128	*SPT16/CDC68 LEU2 CEN*	Formosa *et al.* 2001
p426-TF128-WT	*SPT16/CDC68 URA3* 2μ	This study
pTF128-8	*spt16-8 LEU2 CEN*	Formosa *et al.* 2001
p426-TF128-8	*spt16-8 URA3* 2μ	This study
pTF128-12	*spt16-12 LEU2 CEN*	Formosa *et al.* 2001
p426-TF128-12	*spt16-12 URA3* 2μ	This study
pTF128-16ABC	*spt16-16a LEU2 CEN*	Formosa *et al.* 2001
p426-TF128-16ABC	*spt16-16a URA3* 2μ	This study
pTF128-24	*spt16-24 LEU2 CEN*	Formosa *et al.* 2001
p426-TF128-24	*spt16-24 URA3* 2μ	This study
p314-M68	*cdc68-mini TRP1 CEN*	Neil Brewster, unpublished
pRS425-SRP101	*SRP101 LEU2* 2μ	This study
pRS425-SSD1	*SSD1 LEU2* 2μ	This study
pRS315-SSD1	*SSD1 LEU2* CEN	This study
pRS315-UTRSSD1	300 bp upstream and 350 bp downstream of the *SSD1* coding sequence *LEU2 CEN*	This study
pRS315-YI50SSD1	*ssd1-d* (allele from strain Y150) *LEU2 CEN*	This study
pRS315-KanBSSD1	*ssd1-d* (allele from KanB haploid strain) *LEU2 CEN*	This study
YEpMPT5	*MPT5 LEU2* 2μ	Leonard Guarente; Hata *et al.* 1998
YEpPKC1	*PKC1 LEU2* 2μ	Leonard Guarente; Hata *et al.* 1998
pWSC1	*WSC1 LEU2* 2μ	Leonard Guarente; Verna and Ballester 1999
pBA1036	*SWI6 LEU2* 2μ	Brenda Andrews (University of Toronto)
pBA314	*SWI4 URA3* 2μ	Costanzo *et al.* 2003
pBA958	*SLT2 LEU2* 2μ	Costigan *et al.* 1992
pBA251	4x*SCB::lacZ URA3* 2μ	Andrews and Herskowitz 1989

pBA487	4x*MCB::lacZ URA3* 2μ	Verma *et al.* 1992
pBA537	*prPCL1-lacZ URA3* 2μ	Ogas *et al.* 1991
pYES2-POB3	T7-promoter-*POB3-V5-His$_6$ URA3* 2μ	Invitrogen
pRS316-E763G NATc3	*cdc68-E763G::natMX4 URA3 CEN*	This study
pRS316-E857K NATc7	*cdc68-E857K::natMX4 URA3 CEN*	This study
pRS316-312 NATc8	*cdc68-312::natMX4 URA3 CEN*	This study
pRS316-319 NATc5	*cdc68-319::natMX4 URA3 CEN*	This study
316-ΔNTD-3'68	*cdc68-ΔNTD-FLAG URA3 CEN*	This study
pRS316-ΔNTD NATc1	*cdc68-ΔNTD-FLAG::natMX4 URA3 CEN*	This study
pRS314-YNL NAT	*natMX4* cassette flanked by 167 bp and 291 bp of genomic DNA sequence from upstream and downstream, respectively, of the YNL035c gene *TRP1 CEN*	This study
pRS316-CDC68kanMX4	*kanMX4* cassette flanked by 510 bp and 369 bp of genomic DNA sequence from upstream and downstream, respectively, of the *CDC68* gene *URA3 CEN*	This study
p316- ΔNTD E763G	*cdc68-ΔNTD,763 URA3 CEN*	This study
p316-ΔNTD E857K	*cdc68-ΔNTD,857 URA3 CEN*	This study
p316-ΔNTD 312	*cdc68-ΔNTD,312 URA3 CEN*	This study
p316-ΔNTD 319	*cdc68-ΔNTD,319 URA3 CEN*	This study
pRS314-YNL	*YNL035c TRP1 CEN*	This study
pRS424-YNL	*YNL035c TRP1* 2μ	This study
YEp352-POB3	*POB3 URA3* 2μ	Neil Brewster
pBD-CDC68	*GAL4-BD-CDC68 LEU2* 2μ	This study
pBD-68(1-436)	*GAL4-BD-cdc68* (ORF nucleotides 1-1308) *LEU2* 2μ	This study
pBD-68(436-1035)	*GAL4-BD-cdc68* (ORF nucleotides 1308-3105) *LEU2* 2μ	This study
pBD-68(626-1035)	*GAL4-BD-cdc68* (ORF nucleotides 1867-3105) *LEU2* 2μ	This study
pBD-68(308-642)	*GAL4-BD-cdc68* (ORF nucleotides 924-1926) *LEU2* 2μ	This study
pBD-POB3	*GAL4-BD-POB3 LEU2* 2μ	This study
pAD-CDC68	*GAL4-AD-CDC68 TRP1* 2μ	This study
pAD-68(1-436)	*GAL4-AD-cdc68* (ORF nucleotides 1-1308) *TRP1* 2μ	This study
pAD-68(436-1035)	*GAL4-AD-cdc68* (ORF nucleotides 1308-3105) *TRP1* 2μ	This study
pAD-68(626-1035)	*GAL4-AD-cdc68* (ORF nucleotides 1867-3105) *TRP1* 2μ	This study
pAD-68(308-642)	*GAL4-AD-cdc68* (ORF nucleotides 924-1926) *TRP1* 2μ	This study
pSE1111	*GAL4-AD-SNF4 TRP1* 2μ	Bai and Elledge 1997
pSE1112	*GAL4-BD-SNF1 LEU2* 2μ	Bai and Elledge 1997
pPP381.39	*GAL4-AD-SNC2 TRP1* 2μ	Pak Poon,
pPP269.8	*GAL4-BD-GCS1 LEU2* 2μ	Pak Poon,
pGST-Pob3	*tac* promoter-GST-*POB3 lacI amp^R*	This study
pGST-Pob3NTD	*tac* promoter-GST-*pob3* (ORF nucleotides 1-645) *lacI amp^R*	This study

pGST-Pob3CTD	*tac* promoter-GST-*pob3* (ORF nucleotides 534-1656) *lacI* amp^R	This study
pET-68(1-435)	T7 promoter-thioredoxin-His_6-S-protein-*cdc68* (ORF nucleotides 1-1305) amp^R	This study
pET-68(436-1035)	T7 promoter-thioredoxin-His_6-S-protein-*cdc68* (ORF nucleotides 1308-3105) amp^R	This study
pET-68(436-821)	T7 promoter-thioredoxin-His_6-S-protein-*cdc68* (ORF nucleotides 1308-2463) amp^R	This study
pET-68(436-786)	T7 promoter-thioredoxin-His_6-S-protein-*cdc68* (ORF nucleotides 1308-2358) amp^R	This study
pET-68(308-642)	T7 promoter-thioredoxin-His_6-S-protein-*cdc68* (ORF nucleotides 924-1926) amp^R	This study
pET-68(635-1035)	T7 promoter-thioredoxin-His_6-S-protein-*cdc68* (ORF nucleotides 1905-3105) amp^R	This study
pET-68(771-1035)	T7 promoter-thioredoxin-His_6-S-protein-*cdc68* (ORF nucleotides 2313-3105) amp^R	This study
pET-68(710-1035)	T7 promoter-thioredoxin-His_6-S-protein-*cdc68* (ORF nucleotides 2130-3105) amp^R	This study
pIC19R	*SWI4* amp^R	Brenda Andrews
pUC19-SWI6	*SWI6* amp^R	Brenda Andrews
pBR1.129	*TUB2 YPT1* amp^R	Alan Wildeman (University of Guelph)
pBAD054	*prGAP TRP1* 2μ	Desany *et al.* 1998
pBAD070	*prGAP-RNR1 TRP1* 2μ	Desany *et al.* 1998
pBAD079	*prGAP-RNR3 TRP1* 2μ	Desany *et al.* 1998

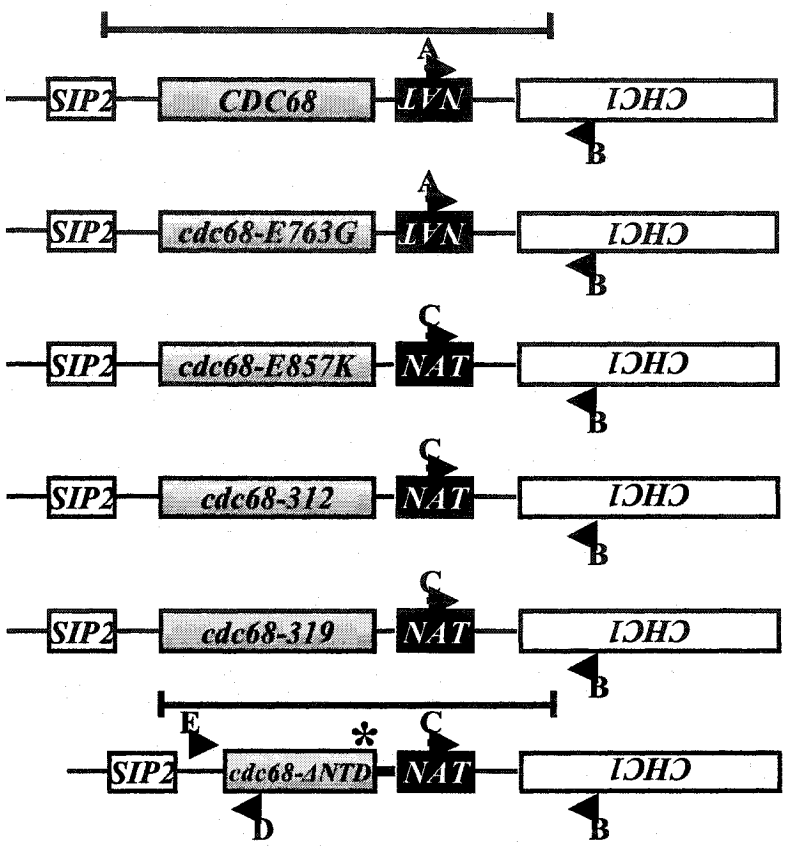

Figure 4. Chromosomal integration of *cdc68* alleles containing the downstream *natMX4* tag. The Watson strand of the chromosome VII is shown (inverted lettering indicates that the gene is encoded on the Crick strand). The black *NAT* box indicates the location and orientation of the *natMX4* cassette inserted into the *Bsr*GI site 132 bp downstream of the stop codon for *CDC68* and 335 bp downstream of the stop codon for *CHC1*. Arrows indicate locations of primers used for PCR verifications, with primer A = Steve NAT MID REV, B = 68DS 891, C = Ally NAT MID FOR, D = GAP2 BOT, and E = Primer F ATG-128. The black bars indicate the regions of DNA employed during the transformation process to generate each of the *natMX4*-tagged gene replacements. The * indicates the presence of the DNA sequences encoding the FLAG epitope in the *cdc68-ΔNTD* allele. The DNA sequence between the *cdc68-ΔNTD* stop codon and the *natMX4* cassette is not that typically found downstream of the *CDC68* gene.

indeed occurred at the *CDC68* genomic locus, and 2) the mutational changes characterizing each allele of *cdc68* that originally was transformed in conjunction with the *natMX4* were intact, and had not been repaired by recombination events that excluded the mutational changes.

To ensure that the *natMX4* cassette chromosomal integration had occurred at the *CDC68* genomic locus, colony PCR was employed using either the STEVE NAT MID REV or ALLY NAT MID FOR primer (depending on the orientation of the *natMX4* cassette with respect to the *CDC68* sequence) plus the 68 DS 891 primer (5'TCAAGAAAATAGGAGCCCTGT) to verify the location of the *natMX4* cassette with respect to the genomic DNA flanking the *CDC68* locus. In each instance, a 1.3-kbp DNA product was expected from the PCR reaction if the *natMX4* cassette was integrated at the appropriate location downstream of the *CDC68* gene. Only those yeast cells that generated a PCR product of the expected size were employed in further studies. It should be noted that the 68 DS 891 primer binds outside of the sequences employed during the integration event, approximately 425 basepairs upstream of the stop codon of the *CHC1* gene (Figure 4). Therefore, any gross alterations of the 3' 425 basepairs of *CHC1* coding sequence or in downstream non-coding sequences that may have been caused by the integration event would have been detected as a failure to generate a PCR product of the anticipated size.

To verify that the mutational changes present in the *cdc68* alleles employed were intact, two strategies were used. For *cdc68* alleles containing point mutations (like *cdc68-E763G*, *cdc68-E857K*, *cdc68-312* and *cdc68-319*), the DNA of the region with the mutational change was sequenced to verify that the inserted allele still contained the original mutations. Chromosomal DNA was isolated from cells for each of the strains shown to contain the *natMX4* cassette at the appropriate chromosomal location. This DNA was used as template in PCR amplifications employing 1) the 5'*Hin*dIII flank (5'GATTTCAATCCCCACTAAGGA) and GAP3 BOT primers (5'GATTGTTGAGACAGTGTAAGG), which amplified nucleotides 2116 to 2777 of the coding sequence of the *cdc68* genes, or 2) the 5' *Hin*dIII flank primer and 2H 3' FULL *CDC68* primer (5'GCGCTGCAGGCTAATCTCTAAAGTTTGCACCCCTATCA), which amplified nucleotides 2116 to the end of the *CDC68* coding sequence (991 bp in total).

PCR reaction (1) used template from cells containing *cdc68-E763G* and *cdc68-E857K*, as the mutational changes for these alleles reside within this stretch of amplified DNA, while PCR reaction (2) used template from *cdc68-312* and *cdc68-319* cells, as the mutational changes in these alleles span a broader region of DNA sequence (Table 10). Sequencing of these purified PCR products using the 5' *Hin*dIII flank primer or the GAP3 BOT primer (for PCR products from the *cdc68-E857K* cells only) was performed by the Robarts Research Institution DNA Sequencing Facility (London, Ontario). In all but one instance, the sequence changes originally identified for each allele were also found in the PCR products generated from the newly integrated alleles. One of the two isolates analyzed from the *cdc68-E763G::natMX4* insertion no longer contained the A2288G nucleotide substitution, but instead had the original wild-type DNA sequence. Since this was the only mutational change in the *cdc68-E763G* allele, the reversion of this DNA sequence to the wild-type DNA sequence makes the *CDC68* gene present in these cells wild-type. Thus, this isolate is a wild-type *CDC68* gene tagged downstream with the *natMX4* cassette in the same fashion as the other mutant alleles described here. Each of these new strains is named as follows: Y2454 312-8 c1, Y2454 319-5 c1, Y2454 E763G 3 c3, Y2454 E857K 7 c3, and Y2454 WT68 c1 (Table 2).

PCR was used to ensure that the DNA sequence encoding the N-terminal domain of Cdc68 are not present in the *cdc68-ΔNTD-FLAG::natMX4* integrated allele. The PCR product generated from a *cdc68-ΔNTD* allele is expected to be significantly smaller than that of the intact *CDC68* gene. Colony PCR was performed using cells from *cdc68-ΔNTD-FLAG::natMX4* candidates and the Primer F 68 ATG-128 (5'TGGTGAGAAGAGGAATAAAAGT) and GAP2 BOT primers (5'TTCCTCATACGGCAATTCCTCC), which amplify the DNA sequence from 128 bp upstream of the start codon for *CDC68* to nucleotide 1847 of the *CDC68* open reading frame. This PCR reaction would amplify a product of 1975 bp from the wild-type *CDC68* sequence, but for the *cdc68-ΔNTD* allele, which is missing the sequences encoding the N-terminal domain, a PCR product of 534 bp was expected. Cells from Nat-resistant colonies that produced the expected PCR product indicating the proper location for the *natMX4* integration and that also generated the 534-bp product from this PCR were then considered verified as having the *cdc68-ΔNTD-FLAG::natMX4* chromosomal integration

replacing the wild-type *CDC68* gene. These new strains are called Y2454 ΔNTD c4 and c8 (c4 and c8 refer to the two different isolates employed), and were used in SGA analysis (Table 2).

iv) Strains for 'classical' synthetic-lethal screening

The strains SNL-58C and SNL-51B used in classical synthetic-lethal screening (Results 4, i) were generated through a series of genetic crosses. Haploid strains containing the *cdc68Δ::kanMX4* deletion and with the *ade2Δ* and *ade3Δ* deletions required for this type of synthetic-lethal analysis, along with *ura3*, *leu2*, and *trp1* mutations (for selection of plasmids) were the objectives of these crosses. Initially, the haploid KanB 316-A4 HA was mated to GHY1088 (provided by G. A. Hartzog, University of Callifornia at Santa Cruz) and the resultant diploid cells were sporulated, tetrads dissected, and the genotypes of segregants were determined based on growth patterns on SC media lacking the appropriate supplements or on YEPD medium containing geneticin. Even though the KanB 316-A4 HA and GHY1088 strains are both of the S288c lineage, backcrossing was performed to ensure that the genetic backgrounds of strains used in subsequent experiments were homogeneous. Cells from a single spore product, SNL5A (Table 2), were backcrossed with GHY1088, and a segregant with the same genotype as SNL5A was then backcrossed again with GHY1088. Segregants from this cross of genotype *MAT*a or *MATα ade2Δ ade3Δ his4-912δ lys2-128δ leu2-3,112 trp1-Δ1 ura3-52 cdc68Δ::kanMX4* [pRS316-A4], known as SNL-58D or SNL-51B, respectively, were selected. SNL-58D cells were transformed with pRS315-based plasmids containing the *CDC68*, *cdc68-E763G*, *cdc68-E857K*, *cdc68-312*, or *cdc68-319* allele, and SNL-51B cells were transformed with pRS314-based plasmids containing these same *CDC68* alleles (Table 2). The SNL-58D and SNL-51B transformants were then grown in SC liquid medium lacking leucine or tryptophan, respectively, but containing uracil. These growth conditions selected for the presence of the plasmids containing a pRS315 (*LEU2*) or pRS314 (*TRP1*) backbone but did not select for the presence of the pRS316-A4 (*URA3*) plasmid. Cells containing only the pRS315-based or pRS314-based plasmids were selected, while cells that did not maintain the pRS316-A4 plasmid would not have experienced any growth impairments. In this way a series of SNL-58D and SNL-51B derivatives containing only the version of *CDC68* present on the pRS315 or pRS314

vectors was generated. Cells from these strains were then transformed with pSLCDC68 and subsequently employed in classical synthetic-lethal screening.

v) Plasmids

The plasmids employed in this study are shown in Table 3. Plasmid construction not described above is outlined below.

a) pRS316-A4 and pRS426-B2: PCR was performed using Vent DNA polymerase (New England Biolabs), the p68-BS-XI plasmid as template, the 5' CDC68 primer (5'GCGGAGCTCCTTTGTGTAGCCTCCATC), which contains an *Sst*I recognition sequence, and 3'CDC68 primer (5'GCGGGTACCGGATCCAAAGGTAGTGGA), which contains a *Kpn*I recognition sequence. The PCR product generated from this reaction contains the coding region of the *CDC68* gene (which in plasmid p68-BS-XI had been modified to contain an *Xba*I site by changing nucleotide 3098 from a cytosine to a thymine, thus altering codon 1033 from serine to phenylalanine; B. Smith, unpublished data) plus 462 bp upstream and 776 bp downstream genomic DNA sequence. This PCR product was digested with *Kpn*I and *Sst*I and used in ligation reactions with *Kpn*I- and *Sst*I-digested pRS316 (Sikorski and Hieter 1989) or pRS426 (Christianson *et al.* 1992) to generate plasmids pRS316-A4 and pRS426-B2, respectively. pRS316-A4 was used extensively in this work as a wild-type *CDC68* control, and also as the base from which many of the plasmids bearing mutant alleles of *cdc68* were produced.

b) Plasmids used in yeast two-hybrid analysis: Eleven plasmids were generated containing the DNA sequences required for expression of Cdc68 or Pob3 polypeptides fused in frame with either the Gal4 DNA-binding domain (BD) or Gal4 transactivation domain (AD). The methodology used to generate these plasmids was similar. In each case the region of *CDC68* or *POB3* coding sequence to be fused to the GAL4-BD in a derivative of plasmid pGBT9 or to GAL4-AD in a derivative of plasmid pGAD424 was PCR-amplified using Platinum *Pfx* DNA polymerase (Invitrogen), using either pRS316-A4 or YEp352-POB3 as template and the primer pairs indicated in Table 4. All of the 2H 5' primers used for amplification of *CDC68* sequences and the 2H POB3 3' primer contain a *Bam*HI recognition sequence. All of the 2H 3' primers used for amplifications of *CDC68* sequenced contain a *Pst*I recognition sequence. The PCR products were digested with either *Bam*HI (for the *POB3* PCR product) or with *Bam*HI and *Pst*I (for all

Table 4. DNA sequencing primers and templates.

DNA template	Primer(s) name and sequence
pRS316-cdc68-E763G	GAP2 TOP (5'CAAAGTTACGTGGCGAAGCCCG) GAP2 BOT (5'TTCCTCATACGGCAATTCCTCC) 5' ClaI flank (5'CTCCAATCATTCAGTCCGGG) 3' SpeI flank (5'TTAAAGCAGTCACCGCGTTGG) 5' HindIII flank (5'GATTTCAATCCCCACTAAGG)
pRS316-cdc68-E857K	GAP2 TOP, GAP2 BOT 5', 5' ClaI flank, 3' SpeI flank, 5' HindIII flank
pRS316-cdc68-312	GAP3 TOP (5'AGCAGTGGTTAACAGATATGG) GAP3 BOT (5'GATTGTTGAGACAGTGTAAGG) 5' HindIII flank 3' BsrGI flank (5'CTGAGGGGATTTCAAAATGCC)
pRS316-cdc68-319	GAP3 TOP, GAP3 BOT , 5' HindIII flank, 3' BsrGI flank
pRS316-cdc68-121	GAP2 TOP, GAP2 BOT 5', 5' ClaI flank, 3' SpeI flank, 5' HindIII flank
pRS316-cdc68-122	GAP2 TOP, GAP2 BOT 5', 5' ClaI flank, 3' SpeI flank, 5' HindIII flank
pRS316-cdc68-123	GAP2 TOP, GAP2 BOT 5', 5' ClaI flank, 3' SpeI flank, 5' HindIII flank
pRS316-cdc68-124	GAP2 TOP, GAP2 BOT 5', 5' ClaI flank, 3' SpeI flank, 5' HindIII flank
pRS316-cdc68-131	GAP3 TOP, GAP3 BOT , 5' HindIII flank, 3' BsrGI flank
pRS316-cdc68-134	GAP3 TOP, GAP3 BOT , 5' HindIII flank, 3' BsrGI flank
Library plasmid SUP Q	NEW 213F (5'TACTTGGAGCCACTATCGACTACG) NEW 213R (5'CGGCGATATAGGCGCCAGCAACCG)
pRS315-SSD1	SEQ SSD1 #1 (5'CAGGCTTATTTTCGCCAT) SEQ SSD1 #551 (5'CAGGAAATTCTGGCTCTA) SEQ SSD1 #1101 (5'TCCAGGCATTAATTCCAA) SEQ SSD1 #1651 (5'ACTGCTGCAACAAGCAAC) SEQ SSD1 #2201 (5'TTTTAGTTTCCGAACTTG) SEQ SSD1 #2754 (5'CGAAAAATTATCTACTGG) SEQ SSD1 #3301 (5'TACGCTGATCATGTCGTT) SEQ SSD1 #3851 (5'TAAGGCTACCATCTGCAA)
pRS315-YI50SSD1	SEQ SSD1 #1, SEQ SSD1 #551, SEQ SSD1 #1101, SEQ SSD1 #1651, SEQ SSD1 #2201, SEQ SSD1 #2754, SEQ SSD1 #3301, SEQ SSD1 #3851
pRS315-KanBSSD1	SEQ SSD1 #1, SEQ SSD1 #551, SEQ SSD1 #1101, SEQ SSD1 #1651, SEQ SSD1 #2201, SEQ SSD1 #2754, SEQ SSD1 #3301, SEQ SSD1 #3851
pMH1	OPP976 (Pak Poon) OPP977 (Pak Poon)
Y2454 *cdc68-E763G::natMX4* (PCR prod. using 5' HindIII flank and GAP3 BOT)	5' HindIII flank
Y2454 *cdc68-E857K::natMX4* (PCR prod. using 5' HindIII flank and GAP3 BOT)	5' HindIII flank
Y2454 *cdc68-312::natMX4* (PCR prod. using 5' HindIII flank and 2H 3'FULL CDC68)	5' HindIII flank
Y2454 *cdc68-319::natMX4* (PCR prod. using 5' HindIII flank and 2H 3'FULL CDC68)	5' HindIII flank

CDC68 PCR products). The pGBT9 plasmid was digested with either *Bam*HI (for the reaction containing the *POB3* PCR product) or with *Bam*HI and *Pst*I (for reactions containing *CDC68* PCR products), and then ligated to the appropriately digested PCR product to generate plasmids pBD-CDC68, pBD-68(1-436), pBD-68(436-1035), pBD-68(308-642), pBD-68(626-1035), and pBD-POB3 (Table 3). The pGAD424 plasmid was digested with *Bam*HI and *Pst*I and then ligated to the appropriately digested PCR product to generate plasmids pAD-CDC68, pAD-68(1-436), pAD-68(436-1035), pAD-68(308-642), and pAD-68(626-1035) (Table 3). Plasmids were transformed into cells of strain PJ69-4a and tested in various combinations (Tables 7 and 8) for activation of two-hybrid reporter genes.

c) Plasmids used to generate recombinant Cdc68 and Pob3 proteins: DNA sequences encoding various polypeptides from Cdc68 and Pob3 were cloned into plasmid pET32-mLIC and the pGEX2T, respectively. To generate genes that would express in-frame fusions of the Cdc68 polypeptides with the various tags encoded in pET32-mLIC, the region of *CDC68* sequence encoding each polypeptide was PCR-amplified using Platinum *Pfx* DNA polymerase (Invitrogen), pRS316-A4 plasmid DNA as template, and a primer pair in which one primer contains a *Bam*HI recognition sequence and the other primer contains an *Sst*I recognition sequence. The PCR products were then digested with *Bam*HI and *Sst*I and used in ligation reactions with *Bam*HI- and *Sst*I-digested pET32-mLIC plasmid. The resulting plasmids and the primer pairs employed to make each were as follows: 1) primers 5' FULL CDC68 (5'GCGGGATCCATGGAAGAGCTGAATATTGATTTTGACG) and 3' MEGA CDC68 (5'GCGGAGCTCATTTGTTAAGAAGCGTGGAGGCTCTGTT) were used to generate pET-68(1-435); 2) primers 5' MINI CDC68 (5'GCGGGATCCTACACCAAAGCCAAATCCCAGATATCAT) and 3' FULL CDC68 (5'GCGGAGCTCCTAATCTCTAAAGTTTGCACCCCTATCA) were used to generate pET-68(436-1035); 3) primers 5' MUT CDC68 (5'GCGGGATCCATTACACTAAGATCCAAAGATGGTGACC) and 3' FULL CDC68 were used to generate pET-68(635-1035); 4) primers 5' MID CDC68 (5'GCGGGATCCGATCCATCTGAAGAATTGGCCAACAACT) and 3' MID CDC68 (5'GCGGAGCTCTTGTTTAAAGGTTTCACTCATGCGGTCAC) were used to generate pET-

68(308-642); 5) primers 5' MINI CDC68 and 3' MID 786 (5'GCGGAGCTCACCATATCTTCTGAATCTGGATTGACC) were used to generate pET-68(436-786); 6) primers 5' MINI CDC68 and 3' MID 821 (5'GCGGAGCTCACCGTTTGATGCTTCTGCGATTGCGTC) were used to generate pET-68(436-821); 7) primers 5' CTD 771 (5'GCGGGATCCGAAACTGGAGGTGGAAGACGAGGTCAATCC) and 3' FULL CDC68 were used to make pET-68(771-1035); and 8) primers 5' CTD 710 (5'GCGGGATCCCCACTAAGGACTGATAGCAGAATAGAC) and 3' FULL CDC68 were used to make pET-68(710-1035). Each of these plasmids was transformed into *E. coli* BL21-DE3 cells for the expression of recombinant polypeptides.

To make genes that would generate in-frame fusions of the glutathione-S-transferase protein and Pob3 polypeptides, the *POB3* DNA sequences encoding these polypeptides were PCR-amplified using Platinum *Pfx* DNA polymerase (Invitrogen), YEp352-Pob3 plasmid as template, and a pair of PCR primers. The entire coding sequence of *POB3* was amplified using the 5' BamHI POB3 primer (5'GCGGGATCCATCGAGTACCGACTTTGATAGAATT) and the 3' BamHI POB3 primer (5'GCGGGATCCCTATTCTACCTTAGGCTTCTTCGA), and this PCR product was then digested with *Bam*HI and used in a ligation reaction with *Bam*HI-digested and calf intestinal alkaline phosphatase-treated pGEX2T vector DNA, generating pGST-Pob3 (Table 3). The pGST-Pob3NTD plasmid was made by amplifying the DNA sequence encoding the N-terminal domain of Pob3 using PCR with primers 5' BamHI POB3 and 3' EcoRI NTD Pob3 (5'GCGGAATTCCTACTGCCATTTGTACATCTTCTCC). The pGST-Pob3CTD plasmid was made by amplifying the DNA sequence encoding the C-terminal domain of Pob3 using PCR with primers 5'CTERM POB3 178 primer (5'GCGGGATCCGGTGTTATTCAAACAAACGTCGATC) and the 3' EcoRI END Pob3 primer (5'GCGGAATTCCCTATTCTACCTTAGGCTTCTTCGAAGG). Each of these PCR products was then digested with *Bam*HI and *Eco*RI and used in ligation reactions with *Bam*HI- and *Eco*RI-digested pGEX2T vector. Plasmids were transformed into *E. coli* TOP10 cells for expression of recombinant polypeptides.

d) pRS425-SSD1 and pRS315-SSD1: A PCR reaction was carried out using Platinum *Pfx* DNA polymerase (Invitrogen), the yeast genomic library plasmid Q

(Results 3, i) as template, the PSTI 5'SSD1 primer (5'GCGGCTGCAGCAGGCTTATTTTCGCCATACCA), which contains a *Pst*I recognition site, and the XHOI 3'SSD1 primer (5'GCGGCTCGAGGATGATATTTGTACAGCAAAAGGG), which contains an *Xho*I recognition sequence. The PCR product, which contains the coding region for *SSD1* plus 300 bp and 350 bp of genomic sequence upstream and downstream, respectively, was digested with *Pst*I and *Xho*I and used in ligation reactions with *Pst*I- and *Xho*I-digested pRS315 (Sikorski and Hieter 1989) or pRS425 (Christianson *et al.* 1992). These reactions generated plasmids pRS425-SSD1 and pRS315-SSD1 (Table 3).

e) pRS315-UTRSSD1, pRS315-YI50SSD1, and pRS315-KanBSSD1: To clone the chromosomal *SSD1* genes from cells of the KanB haploid strain (S288c background) and the Y150 strain (W303 background), the plasmid pRS315-UTRSSD1 was made. This plasmid contains 300 bp and 350 bp of genomic DNA sequence from upstream and downstream of the *SSD1* coding sequence. The 300 bp of DNA from upstream of the *SSD1* coding sequence was amplified using PCR with the PSTI 5'SSD1 primer and the 5'REV UTR SSD1 primer (5'CGCAAGCTTAGTGTATAAAGATGGAATAATTGGGCC), while the 350 bp of DNA downstream of the *SSD1* coding sequence was amplified using PCR with the XHOI 3'SSD1 primer and the 3'FOR UTR SSD1 primer (5'CGCAAGCTTTCTCTTCTACCAATATCGTCATTGC). The 5'REV UTR SSD1 and 3'FOR UTR SSD1 primers each contain a *Hin*dIII recognition sequence. These PCR products were digested with *Pst*I and *Hin*dIII for the upstream sequence and *Xho*I and *Hin*dIII for the downstream sequence, and then used in ligation reactions with *Xho*I- and *Pst*I-digested pRS315 vector. In this way plasmid pRS315-UTRSSD1 was generated.

This plasmid was then digested with *Hin*dIII and the linearized DNA molecule was transformed into Y150 cells and KanB haploid cells. Cells from these transformations that were leucine prototrophs were selected by growth on SC medium lacking leucine. These cells must have repaired the linearized pRS315-UTRSSD1 plasmid; one mechanism of this repair is homologous recombination between the ends of the linearized plasmid and homologous chromosomal sequences upstream and downstream of the *SSD1* gene. This type of repair results in a plasmid-borne copy of the chromosomal *SSD1* gene. In this way the plasmids pRS315-YI50SSD1 and pRS315-KanBSSD1 (Table 3) were

identified and used in sequencing reactions (see below) to determine the *SSD1* gene sequence present in cells from each of these strains.

f) pRS425-SRP101: A PCR reaction was performed using Platinum *Pfx* DNA polymerase, the yeast genomic library plasmid Q (Results 3, i) as template, and the PSTI 5' SRP101 primer (5'GCGGCTGCAGCTTTTGCTGTACAAATATCATCAAAG) and the XHOI 3'SRP101 primer (5'GCGGCTCGAGCTGTTATTCCTGTGTCAGAGCATG). The PCR product, which contained the coding region of *SRP101* plus 302 bp and 307 bp of genomic sequence upstream and downstream, respectively, was digested with *Pst*I and *Xho*I and used in a ligation reaction with *Pst*I- and *Xho*I-digested pRS425. This reaction generated plasmid pRS425-SRP101 (Table 3).

g) p315-ΔNTDFLAG and p316-ΔNTDFLAG: Plasmid p314-ΔNTDFLAG (N. K. Brewster, unpublished) was digested with *Bam*HI to generate 2.8-kbp and 5.0-kbp DNA fragments. These DNA fragments were resolved by agarose gel electrophoresis and the 2.8-kbp fragment containing the *cdc68-ΔNTD-FLAG* coding and regulatory sequence was purified and used in a ligation reaction with a *Bam*HI-digested and calf intestinal alkaline phosphatase-treated pRS315 and pRS316 vectors, generating the p315-ΔNTDFLAG and p316-ΔNTDFLAG plasmids (Table 3).

h) 316-ΔNTD-3'68: This plasmid was generated to place the genomic DNA sequence typically found downstream of the *CDC68* gene downstream of the *cdc68-NTD-FLAG* allele found in the p316-ΔNTDFLAG plasmid. To do this, the pRS316-E857K NATc7 plasmid was digested with *Bsr*GI and *Bam*HI, resulting DNA fragments were resolved by agarose gel electrophoresis, and the 644-bp *Bsr*GI/*Bam*HI fragment was purified. Plasmid p316-ΔNTDFLAG was also digested with *Bsr*GI and *Bam*HI and the 2.5-kbp DNA fragment was isolated. These two DNA fragments were then used in a ligation with *Bam*HI-digested and calf intestinal alkaline phosphate-treated pRS316 vector, producing 316-NTD-3'68 (Table 3). This plasmid was used as a base to insert the *natMX4* cassette (section iii above) and also to generate the plasmids described in the next section.

i) p316-ΔNTD plasmids containing the *cdc68-ΔNTD* allele with additional C-terminal point mutations: Plasmids p316-ΔNTD E763G, p316-ΔNTD E857K, p316-ΔNTD 312, and p316-ΔNTD 319 were made through a fragment-swap procedure,

replacing the 3' end of the *cdc68-ΔNTD* gene with the 3' end of the *cdc68-E763G*, *cdc68-E857K*, *cdc68-312*, and *cdc68-319* allele, respectively. To generate these plasmids, plasmids pRS316-cdc68-E763G, pRS316-cdc68-E857K, pRS316-cdc68-312, and pRS316-cdc68-319 were digested with *Eco*RI, the products were resolved by agarose gel electrophoresis, and the 2.1-kbp fragment was isolated. Plasmid 316-ΔNTD-3'68 was also digested with *Eco*RI and the 5.8-kbp piece of DNA generated from this digest was treated with calf intestinal alkaline phosphatase. The 5.8-kbp and 2.1-kbp DNA fragments were then used in ligation reactions to generate the p316-ΔNTD E763G, p316-ΔNTD E857K, p316-ΔNTD 312, and p316-ΔNTD 319 plasmids (Table 3).

j) p426-TF128 plasmids: The pTF128 series of plasmids (pTF128, pTF128-8, pTF128-12, pTF128-16ABC, and pTF128-24) contain alleles of *CDC68* generated in the Formosa lab (Formosa *et al.* 2001). Each of these *CDC68* alleles was sub-cloned from the YCplac111 plasmid backbone (*CEN LEU2*) (Gietz and Sugino 1988) into the pRS426 plasmid backbone (2μ *URA3*). The pTF128 plasmids were digested with *Hin*dIII and *Sst*I, the products were resolved by gel electrophoresis, and the resultant 3.0-kbp product was purified. This product corresponds to DNA sequence upstream of the coding sequence of *CDC68* and the first three quarters of the coding sequence of the gene. Plasmid pRS426-B2 was also digested with *Hin*dIII and *Sst*I, the products were resolved by gel electrophoresis, and the resultant 7.3-kbp product was purified. This 7.3-kbp DNA fragment contains the pRS426 vector backbone, the 3' quarter of the *CDC68* coding sequence, and some genomic DNA sequence downstream of the *CDC68* gene. The 3.0-kbp *Hin*dIII/*Sst*I fragments from the pTF128 plasmids were then used in a ligation reaction with the 7.3-kbp *Hin*dIII/*Sst*I DNA fragment from pRS426-B2, producing p426-TF128-WT, p426-TF128-8, p426-TF128-12, p426-TF128-16ABC, and p426-TF128-24 (Table 3).

k) pRS314-YNL and pRS424-YNL: Colony PCR using Platinum *Pfx* DNA polymerase, cells of strain BM64 as template, and the V1 5'UTR YNL035c and V4 3'UTR YNL035c primers was used to obtain the *YNL035c* gene sequence. The *YNL035c* coding sequence plus 167 bp and 291 bp of genomic sequence upstream and downstream, respectively, were present in this PCR product, which was then digested with *Cla*I and *Not*I (the PCR primers contain the recognition sites for these restriction endonucleases)

and ligated with *Cla*I- and *Not*I-digested pRS314 and pRS424 vector DNA, producing pRS314-YNL and pRS424-YNL (Table 3).

3. DNA manipulations

i) Restriction endonuclease digestion, calf intestinal alkaline phosphatase treatment, and DNA ligations

DNA was cleaved by restriction endonucleases (Invitrogen; New England Biolabs) as per the suppliers recommended conditions. Calf intestinal alkaline phosphatase (New England Biolabs) was used to treat DNA that had been digested with restriction endonuclease(s) prior to use in ligation reactions. Typically, 1 μl of this enzyme preparation would be added to a 20-μl restriction endonuclease digestion mixture and incubated at 37°C for 30 minutes. To remove enzymes from DNA samples prior to use in cloning procedures, the DNA sample was either resolved by agarose gel electrophoresis and the appropriate DNA molecule excised from the gel and purified from the agarose using the QIAquick Gel Extraction kit (Qiagen), or the enzyme(s) was removed from the DNA sample using a QIAquick PCR purification kit (Qiagen). Ligation reactions were carried out using T4 DNA ligase (Invitrogen). A typical reaction would include 1 μl T4 DNA ligase, 2 μl 5x ligase buffer, 5 μl of 'insert DNA', and 2 μl of vector DNA. Reactions were incubated at room temperature from one hour to overnight.

ii) Plasmid isolation

Plasmids were isolated from *E. coli* cells using three methods: 1) standard alkaline-lysis preparations followed by phenol:chloroform extractions to remove residual proteinaceous material and ethanol precipitation to concentrate the DNA (Sambrook 1989); 2) GenElute plasmid Miniprep kit (Sigma); or 3) Qiaprep Spin Miniprep kit (Qiagen), when plasmid DNA was to be used in sequencing reactions.

The glass-bead disruption method (Hoffman 1997) was used to extract plasmid DNA from yeast cells. In this protocol, the cell pellet from 1.5 ml of stationary-phase culture was resuspended in 300 μl of glass-bead disruption buffer (100 mM NaCl, 10 mM Tris-Cl pH 8.0, 1 mM EDTA, and 0.1% SDS) to which approximately 300 μl of acid-washed glass beads and 300 μl of phenol:chloroform were added. This mixture was then vortexed at the maximum setting for 6 minutes at room temperature. The resulting cell debris and phenol mixture was then discarded and the aqueous phase was further extracted with

chloroform. The DNA was ethanol-precipitated from the aqueous phase and resuspended in ddH_2O for use in *E. coli* electroporation. This method does not differentiate between plasmids; therefore, if there are multiple plasmids in the yeast cells, further manipulations are required to distinguish one plasmid from another. The biosynthetic marker on a yeast plasmid may often be selected in the appropriate *E. coli* host through complementation of an *E. coli* auxotrophy. This method was used repeatedly to distinguish *LEU2* plasmids from other plasmids in a mixture. The yeast plasmid extract was transformed into strain JF1754 *E. coli* cells, and transformants containing a *LEU2* plasmid were selected based on growth on M9 medium lacking leucine.

iii) Plasmid transformations

Plasmid DNA was transformed into *E. coli* cells using electroporation. Electroporation-competent *E. coli* cells were first made (Ausubel 1991). *E. coli* cells were grown to an OD_{600} of 0.6-0.8, placed at 4°C or chilled on ice for a minimum of one hour (all subsequent handling of cells occurred at 4°C or on ice, and all solutions were pre-chilled at 4°C) and subjected to centrifugation at 2800 x g for 20 minutes. The cell pellet was washed twice with ddH_2O (distilled and deionized) and once with 10% glycerol, resuspended in an equal volume of 10% glycerol, and apportioned to microfuge tubes and stored at –80°C.

For electroporation, an 80-μl sample of competent *E. coli* cells was thawed on ice, the DNA to be transformed was added (typically 1-2 μl of plasmid DNA), and this mixture was placed in a pre-chilled electroporation cuvette (BioRad). An electric current was then applied to the sample using a Gene Pulser (BioRad) according to the manufacturer's specifications. 800 μl of 2xYT medium was then added to the mixture, which was incubated at 37°C for 20 minutes for recovery and then spread on 2xYT solid medium containing the appropriate antibiotic for selection.

Yeast cell transformations were performed using two slightly different lithium-acetate methods (modified from Ito *et al.* 1983). For large-scale yeast transformations, 50 ml to 250 ml of yeast culture grown to a density of ~5 x 10^6 cells/ml were centrifuged and the resulting cell pellets were resuspended in one volume of 0.1 M lithium acetate, 10 mM Tris-Cl, pH 8.0, and 1 mM EDTA, and two volumes of 50% polyethylene glycol. 1 ml of this cell suspension was then placed in a microfuge tube and 33 μl denatured salmon

sperm carrier DNA (10 μg/ml) was added along with 5 to 15 μl of the DNA to be transformed. These cells were then incubated at 30°C for 30 minutes followed by a 10-minute incubation at 45°C. At this point, 100 μl of 95% ethanol was added and the 45°C incubation was continued for a further 5 minutes. Cells were centrifuged at 5000 x g for 10 seconds, resuspended in 300 μl of 10 mM Tris-Cl pH 8.0 and 1 mM EDTA, and spread on the appropriate solid selective medium for plasmid maintenance.

This transformation protocol was modified when transforming linear fragments containing the *natMX4* or *kanMX4* cassette (Wach *et al.* 1998). The cell pellets generated after the 45°C incubation were resuspended in 3 ml of pre-warmed 30°C YM1 medium. These cell suspensions were then incubated at 30°C for 5 to 8 hours prior to transfer to selective medium (YPD+clonNat or YPD+geneticin).

For small-scale lithium-acetate yeast transformations, cells from a 5-ml overnight YM1 culture were pelleted by centrifugation, washed twice in ddH_2O, once with 1 ml of 0.1 M lithium acetate, 10 mM Tris-Cl pH 8.0, 1 mM EDTA, and finally resuspended in the same solution. 100 μl of this cell suspension was employed in each transformation along with 10 μl of denatured salmon sperm carrier DNA (10 μg/ml), 2 to 5 μl of the plasmid DNA to be transformed, and 700 μl of 50% polyethylene glycol. This mixture was treated as described above except that only 80 μl of 95% ethanol was added.

iv) DNA sequencing

Sequencing primers and templates (Table 4) were provided to DNA sequencing facilities (NRC, Halfiax, Nova Scotia; Cortec DNA Service Laboratories Inc., Kingston, Ontario; Robarts Research Institution, London, Ontario) that employed automated dideoxynucleotide triphosphate terminator sequencing chemistry (Sanger *et al.* 1977) to determine DNA sequences. SeqEd software (Applied Biosystems) was used to view, edit, align, and generate consensus sequences from raw sequence data files.

v) Polymerase chain reaction (PCR)

Depending on the application, four different types of PCR were employed. PCR with Taq DNA polymerase (Invitrogen), which lacks a proof-reading or error-correction capacity, was used if the amplification was to verify the size or insertion point of a DNA molecule rather than the nucleotide sequence of the molecule. This type of PCR was not employed during cloning steps unless the purpose of the cloning was to generate novel mutational

changes (*i.e.* mutagenic PCR). PCR using high-fidelity DNA polymerases, such as Vent DNA polymerase (New England Biolabs) or Platinum *Pfx* DNA polymerase (Invitrogen), that contain proof-reading and error-correction mechanisms was used for DNA cloning or sequencing applications. PCR was also performed using yeast colonies as template (colony PCR). Each type of PCR is described below.

a) **PCR using *Taq* DNA polymerase:** these PCR mixtures included the following:

10 μl 10x PCR buffer (200 mM Tris-KCl pH 8.4, 500 mM KCl)

10 μl 10x PCR Enhancer Solution (Invitrogen) (optional)

10 μl 100 mM Tris-Cl, pH 9.4

6 μl 50 mM $MgCl_2$

2 μl 10 mM dNTPs

0.5 μl *Taq* DNA polymerase (5 units/μl)

2 μl 1st primer stock (50 ng/μl)

2 μl 2nd primer stock (50 ng/μl)

5-10 μl template DNA (~0.1 μg/ml)

Reaction volume to 100 μl with ddH_2O

Reactions were prepared on ice in 0.5-ml microcentrifuge tubes and then incubated in a hot-bonnet thermocycler (MJ Research) under the following conditions:

1) 94°C, 5 minutes

2) 94°C, 45 seconds

3) 45-60°C, 90 seconds (range reflects different primer annealing temperatures)

4) 72°C, 1 minute per kbp of DNA amplified (from 0.5 minutes to 4 minutes)

5) Cycle to step (2) 35 times

6) 72°C, 5 minutes

This type of PCR was employed for several applications. One specific application, however, was its use with the modification of omitting the PCR Enhancer from the reaction mixture, to generate the DNA fragments employed in the PCR-mutagenesis strategy to isolate novel mutant alleles of *CDC68*. Sequence analysis indicated that, on average, PCR performed in this way generated one mutational change per kilobase of

DNA amplified. This approach generated *cdc68-E763G* (both isolates), *cdc68-E857K*, *cdc68-121*, *cdc68-123*, *and cdc68-131* (Table 10).

b) Mutagenic PCR: In addition to using the standard *Taq* DNA polymerase PCR protocol given above to generate nucleotide substitutions in the *CDC68* coding sequence, a mutagenic PCR strategy was also employed (Muhlrad *et al.* 1992). In this approach, the concentration of dATP was four-fold lower in the PCR mixture than that of the three other dNTPs. Based on sequence analysis, this method introduced an average of 6 nucleotide substitutions per kilobase of DNA sequence amplified. This type of PCR generated *cdc68-122*, *cdc68-124*, *cdc68-134*, *cdc68-312* and *cdc68-319* (Table 10).

c) Colony PCR: Colony PCR employed the same reaction mixtures as the Taq DNA polymerase or Platinum *Pfx* DNA polymerase protocols, with the exception that the DNA template was omitted. Instead, cells from a yeast colony were used as the template. The cells were from a freshly grown colony and only a small colony or small portion of a large colony was used. The yeast cells were placed at the bottom of a 0.5 ml-microcentrifuge tube, which was then microwaved at the maximum setting for 1-2 minutes and placed on ice; the PCR mixture was then added and thermocycling as described above for Taq DNA polymerase or below for Platinum *Pfx* DNA polymerase, was carried out.

d) High-fidelity PCR: Two high-fidelity DNA polymerases were used; Vent DNA polymerase (New England Biolabs) and Platinum *Pfx* DNA polymerase (Invitrogen).

Vent DNA polymerase PCR mixtures included the following:

10 μl 10x Vent PCR buffer (New England Biolabs)

2 μl 100 mM MgSO4

3 μl 10 mM dNTPs

1 μl Vent DNA polymerase (2 units/μl)

2 μl 1st primer stock (50 ng/μl)

2 μl 2nd primer stock (50 ng/μl)

5-10 μl template DNA (~0.1 μg/ml)

Reaction volume to 100 μl with ddH_2O.

Thermocycling of Vent DNA polymerase PCRs was carried out as described above for Taq DNA polymerase.

Platinum *Pfx* DNA polymerase PCR mixtures included the following:

10 μl 10x *Pfx* PCR buffer (Invitrogen)

10 μl 10x PCR Enhancer Solution (Invitrogen)

2 μl 50 mM $MgSO_4$

2 μl 10 mM dNTPs

1 μl Platinum *Pfx* DNA polymerase (2.5 units/μl)

2 μl 1st primer stock (50 ng/μl)

2 μl 2nd primer stock (50 ng/μl)

5-10 μl template DNA (~0.1 μg/ml)

Reaction volume to 100 μl with ddH_2O.

Reactions were prepared on ice in 0.5-ml microcentrifuge tubes and then incubated in a hot-bonnet thermocycler (MJ Research) under the following conditions:

1) 94°C, 5 minutes

2) 94°C, 30 seconds

3) 50-60°C, 45 seconds (range reflects different primer annealing temperatures)

4) 68°C, 1 minute per kbp of DNA amplified (from 0.5 minutes to 4 minutes)

5) Cycle to step (2) 35 times

6) 68°C, 5 minutes

DNA molecules generated using Vent or Platinum Pfx DNA polymerases are suitable for cloning and sequencing applications and were routinely used for these procedures.

4. Protein analyses

i) Yeast protein extracts

Whole-cell yeast protein extracts were prepared by glass-bead disruption under denaturing conditions or non-denaturing conditions (Ausubel 1991), and by trichloroacetic acid (TCA) protein preparations (Foiani 1999).

a) Glass-bead disruption method: Sodium azide was added to a final concentration of 10 mM to yeast cells grown to mid-log phase (~5 x 10^6 cells/ml), which were then centrifuged to produce a concentrated pellet that was washed in cold ddH_2O and resuspended in an equal volume (approximately 300 μl for 50-ml of culture) of either

glass-bead disruption buffer (20 mM Tris-Cl pH 7.9, 10 mM $MgCl_2$, 1 mM EDTA, 5% glycerol, 0.3 M ammonium sulphate) or co-immunoprecipitation buffer (CO-IP) (50 mM Tris-Cl pH 7.4, 15 mM EGTA, 100 mM NaCl, 0.1% v/v Triton X-100). Both buffers had 1 mM PMSF and a protease-inhibitor cocktail added just prior to use. The resuspended cells were added to ~300 μl of acid-washed glass beads and vortexed at maximum setting for 6-8 minutes at 4°C. The beads and cell debris were allowed to settle and the resulting supernatant was placed in a new microcentrifuge tube and centrifuged at 12 500 x g for 20 minutes to remove insoluble material. The soluble cell lysate was then transferred to a new microcentrifuge tube and the protein concentration was determined using the BioRad protein assay and a bovine serum albumin standard (BioRad). If the samples were to be used directly in western blot analysis (typically the case with samples generated in glass-bead disruption buffer) with no further manipulations, an equal volume of 2x Laemmli buffer (Ausubel *et al.* 1991) was added to the samples and they were boiled for 5 minutes and stored at −20°C. Extracts to be used in co-immunoprecipitation experiments (Materials and Methods 4, ii) were stored at 4°C.

b) TCA extractions: Denatured protein extracts were prepared essentially as described by Foiani *et al.* (1999). Sodium azide was added to a final concentration of 10 mM to 50 ml of cell culture at approximately 1 x 10^7 cells/ml. The cells were pelleted by centrifugation, washed in 10 ml of ddH_2O followed by 10 ml of 20% TCA (at room temperature), resuspended in 300 μl of 20% TCA to which an equal volume of acid-washed glass beads was added, and vortexed at the maximum setting for 4 minutes at room temperature. The beads were allowed to settle and the supernate was transferred to a new microcentrifuge tube. The glass beads were then washed twice with 300 μl of 5% TCA and the three supernates were pooled to produce a protein extract with a final concentration of 10% TCA. This extract was then centrifuged at 700 x g for 10 minutes at room temperature and the pellet was resuspended in a modified 1x Laemmli buffer (Laemmli buffer lacking bromophenol blue to which 0.6 M Tris, pH 10, had been added to neutralize residual TCA). The protein samples were then boiled for 3 minutes and centrifuged at 700 x g for 10 minutes to removed insoluble debris. The soluble protein extract was transferred to a new microcentrifuge tube and the protein concentration was determined using BioRad protein assays (BioRad). The protein sample used for these

concentration determinations was diluted at least five-fold in PBS for use in the BioRad protein assay. Protein samples were stored at −20°C.

ii) Co-immunoprecipitation

Co-immunoprecipitations used 2 mg of cell extracts made using the glass-bead disruption method and co-immunoprecipitation buffer (Materials and Methods 4, i-a). For the competitive co-immunoprecipitation experiment, cell extracts were from strain NB6247 cells containing either the p314-cdc68-mini plasmid or the p315-ΔNTDFLAG plasmid. NB6247 cells contain a chromosomally integrated *POB3* gene that expresses a Pob3-V5-His_6 tagged protein. 5 μl of anti-V5-HRP antibody (0.9 mg/ml; Invitrogen) was added to 2 mg of each extract and, as a control, other tubes containing 2 mg of the same extracts were incubated without antibody. The extracts with or without antibody were then incubated at 4°C for 90 min with gentle rocking, after which time 50 μl of 50% Protein-A agarose-bead slurry that had been pre-equilibrated in co-immunoprecipitation buffer (Invitrogen) was added to each sample. The samples were then incubated for 1 hour at 4°C with gentle rocking and centrifuged and the supernate was saved for analysis of the unbound protein fraction. An equal volume of 2x Laemmli buffer was added to the unbound protein fraction and the samples were boiled for 10 minutes and stored at −20°C. The Protein-A agarose beads were washed three times in 1 ml of co-immunoprecipitation buffer, and after the final wash the Protein-A agarose beads along with the associated bound proteins were resuspended in 50 μl of 2x Laemmli buffer, boiled for 10 minutes and stored at −20°C until analyzed by SDS-PAGE and western blotting.

iii) Purification of recombinant Cdc68 and Pob3 polypeptides

Several plasmids were created to express various polypeptides of Cdc68 or Pob3 fused to different peptide tags. Regions of the *CDC68* gene were fused to the DNA encoding thioredoxin, His_6, and S-protein tags in the pET32-mLIC vector (Table 3). The resulting *CDC68* fusion genes were expressed and the polypeptides were purified from *E. coli* BL21-DE3 cells. Similarly, regions of the *POB3* gene were fused to the sequence encoding glutathione-S-transferase in the pGEX2T vector (Table 3) and the resulting fusion polypeptides were purified from *E. coli* TOP10 cells. The details for these recombinant protein purifications are presented below.

a) Isolation of GST fusion proteins: The pGEX2T, pGST-Pob3, pGST-Pob3NTD, and pGST-Pob3CTD plasmids were transformed into *E. coli* Top10 cells and were grown overnight in 2xYT medium containing ampicillin (50 μg/ml). These cultures were then diluted 500-fold in fresh medium and grown at 37°C to OD_{600} 0.4-0.6. Expression of GST-Pob3, GST-Pob3NTD, GST-Pob3CTD, or GST alone was then induced by the addition of isopropyl-1-thio-β-D-galactopyranoside (IPTG) (Invitrogen) to 1 mM and cells were allowed to grow at 37°C for four hours. GST-fusion proteins were purified using a method similar to that described by Ahn *et al.* (1997) and Sengupta *et al.* (2001). Cultures were harvested by centrifugation for 10 minutes at 4°C. Pellets were typically stored at −20°C overnight and resuspended in PBS-NP/PI (phosphate-buffered saline from Invitrogen, 0.1% Igepal Ca-630 known as NP-40 from Sigma, and protease inhibitor cocktail made as described in Ausubel *et al.* [1991]), washed twice and then resuspended in Buffer A (50 mM Tris-Cl pH 8.0, 150 mM NaCl, 0.1% NP-40, 2 mM methionine, and protease-inhibitor cocktail). Cells were then incubated with lysozyme (100 μg/ml) on ice for 15 minutes and then sonciated in two 15-second pulses at setting 10 on a Microson Ultrasonic Cell Disruptor (Heat Systems Ultrasonics, Inc.). To remove insoluble material the mixtures were centrifuged at 12,500 x g for 10 minutes at 4°C. The soluble protein supernate was then added to a 50% glutathione-agarose (Sigma) slurry in PBS (Invitrogen) and incubated at 4°C for 30 minutes with gentle rotation. Glutathione-agarose and bound GST-fusion proteins were then formed into a loose pellet by centrifugation and washed four times with PBS-NP/PI to remove residual unbound proteins. Glutathione-bound GST-fusion proteins were then resuspended in a volume of PBS equal to the agarose-bead volume. The quality and quantity of purified material were assessed by coomassie staining of proteins resolved on 10% SDS-polyacrylamide gels with known amounts of BSA (New England Biolabs) loaded in parallel as protein concentration standards. Protein concentrations were determined using the Gel-doc and Molecular Analyst software. All samples were stored at 4°C and brought to equimolar concentrations with 50% glutathione-agarose bead slurry in PBS prior to use in GST pull-down assays.

b) Isolation of His-tagged recombinant Cdc68 proteins: The pET32-mLIC, pET-68(1-435), pET-68(436-1035), pET-68(436-821), pET-68(436-786), pET-68(308-

642), pET-68(635-1035), pET-68(771-1035), and pET-68(710-1035) plasmids were transformed into *E. coli* BL21-DE3 cells, which were then grown overnight in 2xYT medium containing ampicillin (50 μg/ml). Overnight cultures were diluted 500-fold into fresh medium and grown at 37°C to OD_{600} of 0.4-0.6. These cultures were then induced to express the recombinant proteins by the addition of IPTG to 1 mM and additional incubation at 37°C for four hours. Recombinant proteins were purified under denaturing conditions using a method modified from that described in Novagen's His-bind kits inclusion body purification and resin chromatography manual (Novagen). Cells were pelleted and then washed and resuspended in ice-cold 1 x Binding buffer (Novagen). Cells were then sonciated in two 15-second pulses using setting 10 on a Microson Ultrasonic Cell Disruptor followed by centrifugation at 2700 x g for 15 minutes at 4°C. The pellets were suspended in 1xBinding buffer containing lysozyme (100 μg/ml), incubated on ice for 15 minutes, and centrifuged at 2700 x g for 15 minutes at 4°C. Recombinant proteins in the pellet were solublized by incubation on ice for 1 hour in 1 x Binding buffer containing 6 M urea. Residual insoluble material was removed by centrifugation at 2700 x g for 30 minutes at 4°C and the soluble supernate was transferred to a new microcentrifuge tube containing His-Bind resin, prepared as per Novagen's instructions for purification under denaturing conditions. This mixture was gently mixed by rocking for 10 minutes at room temperature to permit recombinant proteins to associate with the affinity resin. The His-Bind Resin with bound recombinant proteins was washed twice with 1xBinding buffer containing 6 M urea and twice with low-imidazole wash buffer (11 ml 1xBinding buffer, 4.1 ml 1xWash buffer, 6 M urea), and then proteins were eluted in 1xStrip buffer containing 6 M urea. To allow renaturation of recombinant proteins, urea was gradually removed by step-wise dialysis in Buffer A containing 4 M urea, then 2 M urea, and finally Buffer A without urea. Sample purification and quantity were assessed as described above. Proteins were stored at 4°C until use in GST-pulldown assays.

iv) GST-pulldown assays

Prior to use in GST-pulldown assays, purified pET-Cdc68 fusion proteins were centrifuged at 2700 x g to remove any protein precipitate that may have formed, and the supernate was transferred to a new microfuge tube. Equimolar amounts of GST-fused

Pob3 polypeptides or GST alone, and purifed recombinant Cdc68 polypeptides or the pET-tag polypeptide alone (thioredoxin, His_6, and S-protein), were incubated in a 50% glutathione-agarose bead slurry in Buffer A for low-stringency conditions, or Buffer B (50 mM Tris-HCl, 150 mM NaCl, 1% NP-40, 0.5% sodium deoxycholate, 2 mM methionine, and protease-inhibitor cocktail) for high-stringency conditions, all containing BSA (150 μg/ml). Mixtures were rocked gently at 23°C for one hour to allow protein binding and then centrifuged at 300 x g for 1 minute. The supernate from this stage was combined with an equal volume of 2x Laemelli buffer, boiled for 5 minutes and stored at −20°C for later analysis of the unbound fraction. Glutathione-agarose and the bound proteins were then washed five times for 15 minutes each at 23°C in either PBS-NP/PI, for low-stringency conditions, or Buffer B, for high-stringency conditions. After the final wash, the glutathione-agarose slurry and the bound proteins were resuspended in an equal volume of 2x Laemelli loading buffer (Ausubel *et al.* 1991) and boiled for 10 minutes. Samples were then stored at −20°C until assessed by western blot analysis.

v) SDS-polyacrylamide gel electrophoresis and western blot analysis

Proteins were resolved using denaturing polyacrylamide gel electrophoresis (PAGE) as described in Ausubel *et al.* (1991). Typically, a 10% acrylamide gel (30:1 acrylamide:bisacrylamide ratio) was employed to resolve proteins; however, for analysis of the Rad53 protein, a 10% acrylamide gel with a 30:0.4 acrylamide:bisacrylamide ratio was used to assist in resolving the high-molecular-weight phospho-isoforms (Marsolier *et al.* 2000). Rainbow protein molecular-weight markers (Amersham) were also resolved on the gels to allow the molecular weights of proteins to be estimated and to visualize protein migration during electrophoresis. Depending on the application, gels were either stained with coomassie (Ausubel 1991) or transferred to Sequi-blot PVDF membrane (BioRad) using a Trans-blot SD Semi-Dry Transfer Cell (BioRad) in Towbin buffer (25 mM Tris-base, 192 mM glycine, 20% methanol) for 45 minutes at 200 mAmps.

After transfer, membranes were washed in TBST (10 mM Tris-Cl pH 7.4, 140 mM NaCl, 0.1% Tween 20) at 37°C for 10 minutes followed by two washes in TBST at room temperature for 10 minutes each. The membranes were then stained with India ink (only when total protein extracts were being examined) by washing at room temperature for three hours in TBST containing 0.1% India ink (Lek *et al.* 1995). Following this staining,

membranes were washed three times for 10 minutes each in TBST at room temperature, blocked with 5-10% w/v milk powder in TBST from 90 minutes to overnight, washed again in TBST and then incubated with a specific antibody to the protein of interest. Primary-antibody incubations were typically performed in TBST containing 1% w/v milk powder at room temperature for one to three hours. The anti-V5-HRP (Invitrogen), anti-Cdc68 affinity-purified polyclonal (Brewster *et al.* 1998), and anti-Rad53 yC-19 (Santa Cruz Biotechnology) antibodies as well as the HRP-conjugated S-protein were employed here to detect specific antigenic proteins. The anti-V5 antibody was used at a 1:1000 dilution, the anti-Cdc68 and anti-Rad53 antibodies were used at a 1:500 dilution, and the S-protein was used at a 1:8000 dilution. After primary-antibody incubation, membranes were washed three times in TBST at room temperature and, in the case of membranes probed with antibodies that were not directly conjugated to horse radish peroxidase (HRP), the appropriate HRP-conjugated secondary antibody was added at a 1:5000 dilution in TBST containing 1% w/v milk powder (Carnation) and the mixture was incubated for a minimum of 2 hours at room temperature. Antibodies directly conjugated to HRP did not require further incubations and were therefore washed in TBST, and the bound antibody was detected using the LumiGlo Chemiluminescent substrate system (Kierkegaard and Perry Laboratories). Following secondary-antibody incubations, the membranes were washed in TBST and detected using the LumiGlo chemiluminescent substrate system.

5. Gene-expression analysis

i) Northern blotting

Extraction of total RNA from yeast cells, resolution of samples on formaldehyde-agarose gels, and transfer to nylon membranes were performed exactly as described by Xu (1995). DNA probe labelling with [α-^{32}P]dCTP was carried out using the Random Primers DNA Labelling System (Invitrogen). Probes generated in this way were then purified using the QIAquick PCR purification columns (Qiagen). Probes were obtained as follows: 1) plasmid pBR1.129 was digested with *Bam*HI and the 2.0-kbp fragment containing *TUB2* and *YPT1* sequences was purified; 2) plasmid pIC19R was digested with *Bam*HI and *Pst*I and the 1.9-kbp fragment containing *SWI4* sequence was purified; 3) plasmid pUC19-SWI6 was digested with *Eco*RI and the 1.0-kbp fragment containing

SWI6 sequence was purified; 4) plasmid pBAD70 (Table 3) was digested with *Hin*dIII and the 0.8-kbp fragment containing *RNR1* sequence was purified; and 5) plasmid pBAD79 (Table 3) was digested with *Bam*HI and *Eco*RI and the 0.9-kbp fragment containing *RNR3* sequence was purified.

Pre-hybridization of membranes was performed for 4-6 hours at 42°C in 20 ml of prehybridization solution (50 mM Na_3PO_4 pH 6.5, 5x SSC [750 mM NaCl, 75 mM sodium citrate], 50% deionized formamide, 1x Denhardt mix [0.02% Ficoll 400, 0.02% polyvinylpyrrolidone, 0.02% BSA], 1% SDS, and denatured salmon sperm DNA [0.2 mg/ml]). 25 ng of labelled probe DNA was then added to the pre-hybridization solution and incubation at 42°C was continued overnight, at which point the probe solution was removed and the membranes were washed twice at room temperature with 2x SSC containing 0.1% SDS and twice for 20 minutes each at 55°C with 0.2x SSC containing 0.1% SDS.

Membranes were then sealed in bags and exposed to film in light-tight cassettes at −20°C. When this autoradiography was completed, probes were stripped from the membrane by three washes for 20 minutes each in 0.1x SSC containing 1% SDS that had been pre-warmed to 100°C. Membranes were stored at 4°C when consecutive probing was being performed, or at −20°C for long-term storage.

ii) Microarray experiments

An overview of the methodology for microarray experiments is provided in Figure 5. I performed the labelling, hybridization, and scanning steps of the microarray experiments in the Hartzog lab (University of California at Santa Cruz) as per their protocols.

a) Microarray slides: Yeast 6.4K ORF spotted microarray slides (University Health Network Microarray Center, Toronto), on which each spot contains PCR-amplified products corresponding to the complete open reading frame (ORF) of a yeast gene, were used. These slides comprise two replicate loci for approximately 6240 yeast ORFs immobilized on Corning slides.

Prior to use, the slides were blocked as per a Hartzog lab (University of California at Santa Cruz) protocol to help prevent non-specific binding of labelled cDNAs to the slide surface. Slides were placed in blocking solution (50 mM ethanolamine, 0.1 M Tris-Cl pH 9.0, 0.1% SDS) pre-warmed to 50°C and incubated for 15 minutes at this temperature,

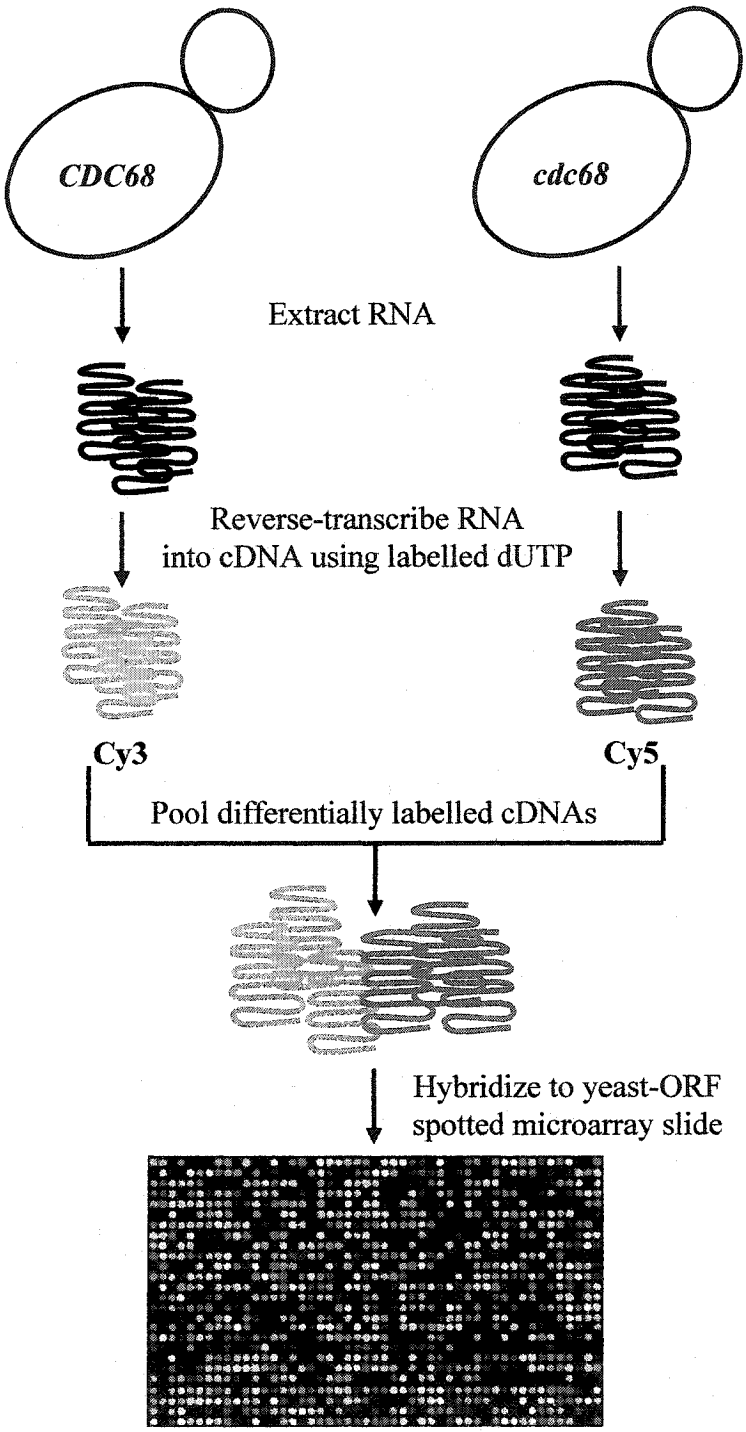

Detect hybridization by scanning the microarray slide image as the different wavelengths of light to excite the Cy3 or Cy5 fluor are applied. A 'red' spot indicates more transcript from the mutant cell, a 'green' spot indicates more transcript from the wild-type cell, and a yellow spot indicates equivalent amounts of transcript from each cell.

Figure 5. Spotted microarray methodology.

then washed twice in dH_2O, once with 4x SSC containing 0.1% SDS at 50°C, and finally twice in dH_2O. Washed slides were then dried by centrifugation at 800 rpm for 4 minutes.

b) RNA extractions, labelling, and microarray hybridization: Total RNA was extracted, using the RNAease Mini kit (Qiagen), from cells of strains KanB 316-A4 Hα, JK121-10D, KanB 316-312, and KanB 316-319 grown to 4.4 x 10^7, 4.2 x 10^7, 3.8 x 10^7, and 1.1 x 10^7 cells/ml, respectively, at 30°C in YM1 liquid medium. The concentrations and purities of the RNA preparations were then assessed using a Gene Quant II RNA/DNA calculator (Pharmacia Biotech) and by resolving approximately 5 μg of each sample by formaldehyde agarose-gel electrophoresis to ensure that the RNA was not degraded based on visual observations of the rRNA bands (data not shown).

RNA was reverse-transcribed using the Superscript II reverse-transcriptase kit (Invitrogen) and following the Hartzog lab protocol;

12.4 μl RNA (10 μg brought up to this volume)

2.5 μl oligo dT primer (Invitrogen)

0.5 μl random oligo primer mix (Invitrogen)

This mixture was heated to 70°C to denature RNA secondary structure.

6.0 μl 5x First strand buffer

3.0 μl 0.1 M dithiothreitol (DTT)

0.6 μl 50x dNTPs (25 mM dATP, dCTP, and dGTP, and 10mM dTTP)

2.0 μl Superscript II reverse transcriptase (200 U/μl)

3 μl Cy3- or Cy5-dUTP

This mixture was then incubated at 42°C for 2 hours. Following this reaction, the RNA was hydrolyzed by adding 1.5 μl 1 M NaOH and 1.0 μl 60 mM EDTA to each reaction and incubating at 65°C for 10 minutes. Unincorporated Cy3- or Cy5-UTP was removed through a series of washes in 1x TE (10 mM Tris-Cl pH 7.4, 1 mM EDTA) and filtration through a microcon-30 filter. At this point, the wild-type control Cy3- or Cy5-labelled cDNA and the mutant labelled cDNA (labelled with the opposite fluorophore) were mixed together, purified from the reaction components using the QIAquick PCR purification kit (Qiagen) and lyophilized, and the resulting pellet was resuspended in 20 μl of dH_2O followed by addition of an equal volume of 2 x hybridization buffer (8x SSC, 0.2% SDS, 0.2 mg polyA /ml). This solution was then filtered to remove insoluble

material, heated to 94°C for 2 minutes to denature the cDNAs, and applied to a blocked microarray slide and incubated in a humidified hybridization chamber at 55°C overnight (approximately 16 hours). Slides were then washed with 2x SSC containing 0.1% SDS to remove the hybridization mixture. Non-specifically associated probe was removed by 1) two five-minute washes at 55°C with 2x SSC containing 0.1% SDS, 2) a 1-minute wash in 0.2x SSC at room temperature, and 3) a 1-minute wash in 0.05x SSC at room temperature. Slides were then dried by centrifugation at 1200 rpm for 3 minutes and scanned for fluorescent signal using a GENPIX 4000B scanner (Axon). To visualize the fluorophores, 635 nm and 532 nm light was passed over each slide and the resulting images corresponding to Cy5 and Cy3 hybridization patterns, respectively, were converted to digitalized images by the GENPIX software. These images were then used to determine signal intensities.

c) Signal intensities and data normalization: The scanned GENPIX images corresponding to the hybridization signals for each of the genes were used to determine the ratios of signal intensity for each of the fluorophores hybridized to every ORF. For each spotted ORF the pixel intensities for one fluorophore were plotted versus the pixel intensities of the other flurophore, and regression analysis using the orthogonal least-squares method was performed using MatLab software (The Mathworks Inc.; analysis performed by Peter Wentzell and Tobias Karakach, Dept. of Chemistry, Dalhousie University) to determine the best-fit straight line through these points. The slope of this line then represented the ratio of hybridization signal intensity for one fluorophore in comparison to that for the other fluorophore. The fluorophore signals associated with the cDNAs generated from cells containing mutant *cdc68* alleles were compared to the fluorophore signals associated with the cDNAs generated from cells containing the wild-type *CDC68* gene (always the ratio of mutant pixel intensities to wild-type pixel intensities). The uncertainties of these ratios were next determined using bootstrapping, where repeated random sampling of pixels from the hybridization signal were plotted and the orthogonal least-squares regression analysis performed for each. If the slopes of the lines determined from these re-sampled plottings show a greater than 10% deviation from the slope originally calculated for a particular spotted ORF then the data from that ORF spot was omitted from further examination. Additionally, data points were removed from

the analysis based on visual inspection of each microarray-slide hybridization image if the spot hybridization signal was distorted due to technical problems (*i.e.* dust particles, pin-strike errors on the slide). As a result, 131, 124, and 95 out of a possible 12,800 hybridization signals were discarded from microarray experiments performed with cDNAs from cells containing *cdc68-mini*, *cdc68-312*, and *cdc68-319*, respectively.

The $\log_2$ value was then calculated for each of the signal-intensity ratios determined from the orthogonal least-squares regression analysis and used to calculate the normalization factors for each sub-grid on a slide (a sub-grid corresponds to the block of 400 ORF spots that are each placed on a slide by the same printing tip when a microarray is made). A global mean normalization was determined for each 'print-tip'/sub-grid and this normalization factor was then applied to the $\log_2$ ratio values for each spot within the appropriate sub-grid (Yang *et al.* 2001; Quackenbush 2002; Park *et al.* 2003). To determine the sub-grid normalization factor, the deviation of the mean $\log_2$ ratio from 0 (which would indicate no difference in transcript abundance between wild-type *CDC68* and *cdc68* mutant cells) for each sub-grid was determined. The mean $\log_2$ deviation was then converted into a numerical factor ($2^{\wedge\text{mean deviation value}}$) that was applied to each of the ratios in the sub-grid dataset. The normalization factors applied for each of the 36 sub-grids per microarray slide are provided in Table 5.

d) Identifying genes with significantly altered expression in *cdc68* mutant cells: Each RNA sample was labelled in separate reactions with either Cy5-dUTP or Cy3-dUTP. Resulting labelled cDNAs generated from RNA extracted from KanB 316-A4 Hα cells (containing wild-type *CDC68*) were used as the control in each case, to which differentially labelled cDNAs made from RNA extracted from KanB 316-312, KanB 316-319, or JK120-10D cells (containing *cdc68-312*, *cdc68-319*, and *cdc68-ΔNTD*, respectively) were then added. A second experiment in which the RNA from cells containing wild-type *CDC68* and mutant *cdc68* alleles were reciprocally labelled was also performed. Therefore, for each gene examined by microarray analysis a total of 4 hybridizations were performed: two from the duplicate spotting of the ORF on a microarray slide that was hybridized with Cy3-labelled cDNAs from *CDC68* cells and Cy5-labelled cDNAs from *cdc68* cells, and two from the duplicate spotting of the ORF on a second microarray slide that was hybridized with Cy5-labelled cDNAs from *CDC68*

Table 5. Microarray slide identification numbers, labelled cell extracts employed for each, and normalization factors.

Slide identification number	Cy3-labelled extract	Cy5-labelled extract	Sub-grid normalization factors for each of the 32 print-tip sub-grids (listed in order from top left to bottom right of the slide)
12437969	KanB 316-A4 Hα	JK120-10D	0.83, 0.85, 0.79, 0.77, 0.80, 0.80, 0.76, 0.76, 0.79, 0.79, 0.78, 0.75, 0.76, 0.75, 0.75, 0.75, 0.72, 0.74, 0.78, 0.72, 0.67, 0.72, 0.70, 0.74, 0.60, 0.64, 0.67, 0.64, 0.60, 0.59, 0.61, 0.59.
12435368	JK120-10D	KanB 316-A4 Hα	1.08, 1.13, 1.27, 1.21, 1.14, 1.12, 1.28, 1.32, 1.10, 1.29, 1.30, 1.41, 1.25, 1.16, 1.26, 1.17, 1.13,1.27, 1.32, 1.31, 1.24, 1.32, 1.33, 1.26, 1.62, 1.67, 1.73, 1.73, 1.84, 1.84, 1.83, 1.85.
12437973	KanB 316-A4 Hα	KanB 316-319	1.05, 1.03, 0.93, 0.84, 0.96, 0.91, 0.87, 0.89, 0.91, 0.99, 0.86, 0.81, 0.91, 0.97, 0.89, 0.87, 0.96, 0.95, 0.94, 0.83, 0.86, 0.97, 0.83, 0.89, 0.72, 0.76, 0.82, 0.77, 0.68, 0.68, 0.68, 0.71.
12435370	KanB 316-319	KanB 316-A4 Hα	1.16, 1.19, 1.24, 1.10, 1.23, 1.28, 1.34, 1.32, 1.25, 1.63, 1.40, 1.38, 1.41, 1.39, 1.41, 1.23, 1.14, 1.31, 1.29, 1.27, 1.14, 1.38, 1.29, 1.14, 1.44, 1.47, 1.67, 1.65, 1.53, 1.52, 1.53, 1.70.
12437933	KanB 316-A4 Hα	KanB 316-312	0.83, 0.81, 0.77, 0.72, 0.82, 0.79, 0.71, 0.70, 0.84, 0.77, 0.67, 0.64, 0.79, 0.75, 0.66, 0.68, 0.84, 0.78, 0.71, 0.67, 0.77, 0.77, 0.70, 0.70, 0.67, 0.65, 0.66, 0.63, 0.64, 0.65, 0.64, 0.62.
12435866	KanB 316-312	KanB 316-A4 Hα	1.77, 1.81,1.97,1.64, 1.76, 1.83, 1.85, 1.69, 1.69, 1.85, 1.77, 1.66, 1.73, 1.67, 1.62, 1.54, 1.54, 1.60, 1.55, 1.58, 1.56, 1.57, 1.51, 1.45, 1.81, 1.66, 1.68, 1.74, 1.71, 1.69, 1.66, 1.79.

cells and Cy3-labelled cDNAs from *cdc68* cells. The $\log_2$ value of the signal-intensity ratio for a spot on one microarray slide was plotted versus the $\log_2$ value of the signal-intensity ratio for the corresponding spot on the dye-swap-experiment microarray slide. These plots, performed for each of the spots on the slide (except spots excluded from the analysis based on the criteria outlined above), are shown in Figures 6, 7, and 8. For any gene where at least two out of the four corresponding ORF spots gave a $\log_2$ ratio greater than +1 (indicating a two-fold or greater increase in transcript abundance in the *cdc68* mutant cells in comparison to wild-type *CDC68* cells) or less than –1 (indicating a two-fold or greater decrease in the transcript abundance in the *cdc68* mutant cells in comparison to wild-type *CDC68* cells), the transcript abundance, and therefore gene expression, was considered to be significantly different in *cdc68* mutant cells. These genes are reported, along with their $\log_2$ ratios and the average fold-change in expression, in Tables 13 to 15.

iii) β-galactosidase assays

The *E. coli lacZ* gene, which encodes the enzyme β-galactosidase, was employed as a reporter for the activation of gene expression from several different promoters. Two colorimetric assays were used to monitor β-galactosidase enzyme activity, which is proportional to the amount of *lacZ* gene expression.

a) Filter lifts: β-galactosidase assays performed on nitrocellulose filters using 5-bromo-4-chloro-3-indolyl-beta-D-galactopyranoside (X-gal) as a substrate were performed as described in Ausubel *et al.* (1991). Cells inoculated as patches onto selective solid medium (to maintain plasmids) were grown overnight at 30°C and then replica-plated to a nitrocellulose filter, which was placed onto YPD solid medium (cell side up) for further incubation and cell growth at 30°C. The filters were then removed and immersed in liquid nitrogen for 30 seconds. The filters were then permitted to thaw and this freeze-thaw cycle was repeated a total of three times. Thawed filters were then incubated (cell side up) at 30°C on a Whatmann filter saturated with assay buffer (2.5 ml Z-buffer, for recipe see (b) below, 6.8 μl β-mercaptoethanol, and 125 μl 2% X-gal solution), in a Petri dish sealed with parafilm. Patches of yeast cells expressing the *lacZ* gene, and therefore generating β-galactosidase enzyme, turned blue in this assay as they metabolized the X-gal substrate. Blue colour development on the nitrocellulose filters

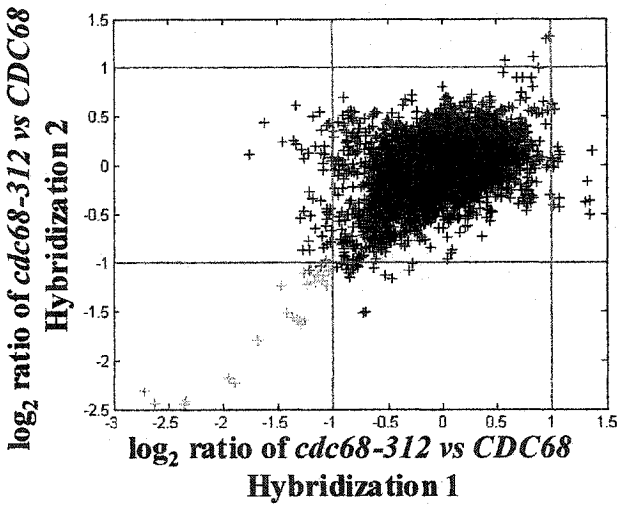

Figure 6. Comparison of *cdc68-312* transcription profiles from two microarray hybridizations. The $\log_2$ ratio of the hybridization signal intensity for *cdc68-312* fluorophore versus that for the *CDC68* fluorophore was determined for each of four spots for a set of approximately 6200 yeast ORFs. These four spots were generated in two different hybridization sets. The $\log_2$ values for each ORF from one hybridization were compared to the $\log_2$ values for each ORF generated in a replicate, dye-swap hybridization. In this way $\log_2$ ratios that consistently showed a greater than two-fold change for a particular gene in comparison to wild-type were identified ($\log_2$ value greater than or equal to +1 or –1). Blue lines indicate the exclusion points for a two-fold change in gene expression with respect to wild-type. Points shown in green that reside within the lower-left section indicate greater than two-fold decreases in transcript abundance for genes in *cdc68-312* cells in comparison to *CDC68* cells for all four replicate spots. Points shown in green that reside within the upper-right section indicate greater than two-fold increases in transcript abundance for genes in *cdc68-312* cells in comparison to *CDC68* cells for all four replicate spots. Magenta points represent genes where only some of the spots had $\log_2$ ratios that were significant (greater than +1 or less than –1). Black points represent genes where the $\log_2$ ratios were not significant.

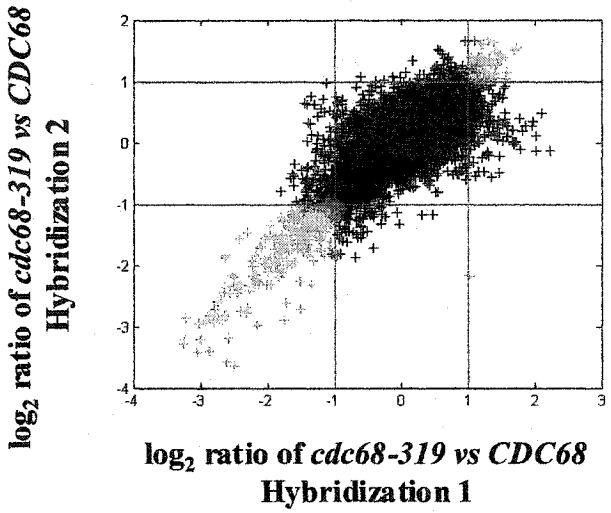

Figure 7. Comparison of *cdc68-319* transcription profiles from two microarray hybridizations. Analysis and graphical representation was as described in the Figure 6 legend.

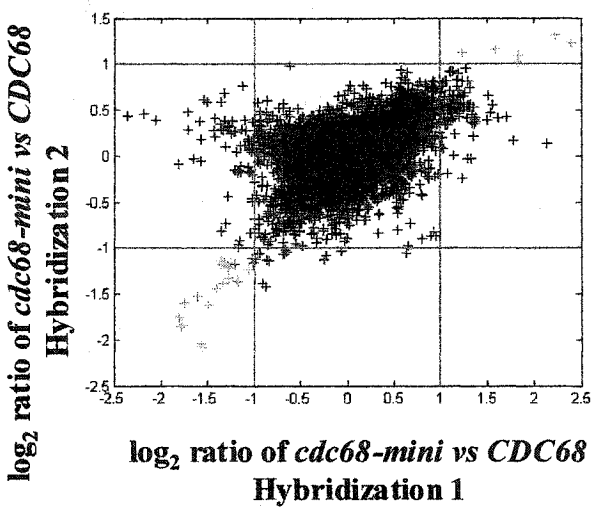

Figure 8. Comparison of *cdc68-mini* transcription profiles from two microarray hybridizations. Analysis and graphical representation was as described in the Figure 6 legend.

was monitored and the time of colour change recorded.

b) Permeabilized-cell assays: These assays were performed essentially as described by Guarente (1983). Cells were grown to a concentration of 5 to 10 x 10^6 cells/ml as determined by Coulter Counter measurement. Cell density for each culture was also determined by OD_{600} measurements. Cells were harvested by centrifugation and cell pellets were stored at −80°C (typically 2-3 days). For cells containing the *prPCL1-lacZ* or 4x*MCB::lacZ* reporters (plasmids pBA537 [Ogas *et al.* 1991] and pBA487 [Verma *et al.* 1992], respectively) the assays generated colorometric changes in an appropriate time frame if a cell pellet corresponding to 2 ml of cell culture was resuspend in 1 ml of Z-buffer (per liter16.1 g $Na_2HPO_4 \cdot 7H_2O$, 5.5 g $NaH_2PO_4 \cdot H_2O$, 0.75 g KCl, and 0.246g $MgSO_4 \cdot 7H_2O$ adjusted to pH 7 with 2.7 ml β-mercaptoethanol added prior to use [Miller 1972]). For cells containing the 4x*SCB::lacZ* reporter on the pBA251 plasmid (Andrews and Herskowitz 1989), the assays generated colorometric changes in an appropriate time frame if a cell pellet corresponding to 0.5 ml of cell culture was resuspended in 1 ml of Z-buffer. These volume changes were accounted for in β-galactosidase activity calculations.

Each of the cell suspensions in Z-buffer was supplemented with 3 drops of chloroform and 2 drops of 0.1% SDS, mixed thoroughly, and incubated at 28°C for 5 minutes. Then 0.2 ml of *o*-nitrophenyl-β-D-galactoside (ONPG; 4mg/ml) in Z-buffer was added to each sample, which were mixed, incubated at 28°C and monitored visually for colour development. When a pale yellow colour had developed the reactions were stopped by the addition of 0.5 ml of 1 M Na_2CO_3 and the time elapsed to colour development was recorded. Cells transformed with a pRS426 vector control were also monitored as a negative control. These cells did not demonstrate any appreciable colour change over the course of the experiment and even when ONPG incubation times were increased to 60 minutes, no significant β-galactosidase activity was observed (data not shown). This indicates that the cells containing the various *lacZ* reporter genes do not themselves contribute significantly to the activity being monitored and that no contaminating activity was present in any of the reagents.

Following the addition of Na_2CO_3, the cells debris and chloroform were removed from the mixture by centrifugation and the OD_{420} of the remaining solution was

determined. The β-galactosidase activity, expressed in Miller units, was then determined using the OD_{600}, the OD_{420}, the reaction time, and the volume of culture in each reaction. For each reporter plasmid and yeast strain, a minimum of two transformants each had a minimum of two independent β-galactosidase assays performed. The β-galactosidase activity from these four experiments (minimally) was then averaged and the standard deviation was determined. These data are reported in Figure 51.

6. Synthetic genetic array (SGA) analysis

Cells from the following strains were employed as 'query' strains in SGA analysis: 1)Y2454 312-8 c1, 2)Y2454 319-5 c1, 3)Y2454 ΔNTD c4 and c8, 4) Y2454 E763G 3 c3, 5)Y2454 E857K 7 c3, 6) Y2454 WT68 c1, and 7) Y2454 YNL NAT. The generation of these strains is described in Materials and Methods sections 2, ii and 2, iii above. SGA screening was performed essentially as described in Tong *et al.* (2001), and a review of the methodology is presented in Figure 55. To begin the SGA screening procedure, cells from each of the query strains were grown in confluent lawns on YEPD medium containing clonNat (100 μg/ml; Werner BioAgents). These lawns were then used to generate an ordered array of double-mutant diploids by mating query cells to cells of the yeast deletion-collection strains (Winzeler *et al.* 1999) using robotics technology. The diploids from this cross were selected on YEPD medium containing clonNAT and geneticin, which select for the presence of the *natMX4* cassette in the query strain and the *kanMX4* cassette used to generate the gene deletion in each of the deletion-collection strains. Diploids were next inoculated onto sporulation medium (described in Tong *et al.* 2001) and grown for several days. A portion of this sporulation mixture was then transferred robotically to synthetic defined medium lacking histidine and arginine but containing canavanine (50 μg/ml); this medium selects for *MAT*a haploids that harbour the *MFA1pr-HIS3* 'magic marker' gene. Due to the *his3* mutation present in all of these cells, diploids and *MATα* cells, which do not express the *MFA1pr-HIS3* gene, are not able to grow on medium lacking histidine. In addition, the canavanine in the medium further inhibits the growth of diploid cells, which contain one copy of the *CAN1* gene. Cells were then transferred robotically and grown under these selective conditions twice and then inoculated to these same conditions with the added presence of geneticin. This selection ensured that only *MAT*a haploids containing a deletion marked with *kanMX4* (which

confers geneticin resistance) from the deletion-collection parental cells will grow. The final selection for double-mutant haploid progeny used synthetic defined medium lacking histidine and arginine and containing clonNAT, geneticin, and canavanine. This combination ensures that only *MAT*a haploids containing the *natMX4* and *kanMX4* markers, from the query stain and the deletion collection strain, respectively, will grow. If no growth or poor growth was observed for a particular double-mutant haploid, this mutational combination was considered a candidate for a synthetic genetic relationship.

The SGA analysis was performed at least twice for each query strain. Only those gene deletions causing growth impairment when combined with the query-strain mutation in both SGA analyses were examined further. A list of 'false-positive' gene deletion strains was identified in the Boone lab (Tong *et al.* 2001). This list indicates haploid deletion strains whose progeny cells typically fail to exhibit robust growth, or any growth at all, after SGA procedures. The mutations in these stains may cause difficulty mating, sporulating, or surviving under the competitive growth conditions that exist during SGA analysis. Approximately 750 deletion mutation strains are in this false-positive category as identified in the Boone lab, and I identified an additional 196 false positives that either fail to grow robustly after SGA procedures or that exhibit poor growth or are absent from the deletion-strain collection in our lab (Results 4, iii). These strains were excluded from my SGA analyses. Additionally, genes in a close proximity to the *natMX4*-tagged locus in the query strain were not included in the analysis, as they represent the 'linkage' group of the *natMX4*-tagged gene. Deletions that are in close proximity to the *natMX4*-marked locus will not readily generate double-mutant haploid progeny due to the fact that the *natMX4* and *kanMX4* markers reside on the same chromosome from the two different haploid parental strains. Thus the only mechanism to generate a single chromosome containing both the *natMX*4 and *kanMX4* markers is to have a recombination event between the two markers. Strains containing these gene deletions do not generate Nat- and geneticin-resistant haploid progeny, not as a result of a synthetic genetic effect, but due to the low frequency with which these doubly marked haploid segregants are produced by recombination. Strains containing gene deletions in the linkage group were therefore excluded from further analysis.

Random-spore analysis as described in Tong *et al.* (2001) was carried out for any gene deletion and query-strain mutation combination that resulted in a slow-growth or lethal phenotype in both of the SGA analyses performed with a given query strain. This method compares the numbers of *MAT*a haploids bearing only a single mutation (*i.e.* only the *natMX4* or the *kanMX4* cassette) that grow to the number of double-mutant *MAT*a haploids that grow. If significantly lower numbers of double-mutant haploids, as determined by growth on medium containing both Nat and geneticin, are found in comparison to the number of either single-mutant haploid, then the double-mutant haploid cells are considered to be synthetically sick. The two mutations in these cells therefore have a synthetic genetic relationship.

For random-spore analysis, cells from the SGA sporulation plates were inoculated into 3 ml of synthetic defined medium lacking histidine and grown for 2 days at 30°C. This cell mixture was then diluted and plated on synthetic medium lacking histidine and arginine but containing canavanine (CAN) and either Nat, or geneticin, or both Nat and geneticin. The SC-HisArg + CAN medium containing Nat alone selects for *MAT*a haploid cells that contain the original query-strain mutation marked with the *natMX4* cassette. The SC-HisArg + CAN medium containing geneticin alone selects for *MAT*a haploid cells that contain the *kanMX4*-marked gene deletion from the deletion-collection strain. The SC-HisArg + CAN medium containing both Nat and geneticin selects for *MAT*a haploid cells containing both the *natMX4*-tagged query-strain mutation and the *kanMX4*-marked gene deletion from the deletion collection. If fewer than half as many colonies as the number expected on the medium containing both Nat and geneticin were observed, then the combination of mutations (the query-strain mutation and the gene deletion from the collection) was said to cause a synthetic growth defect. If no significant number of double-mutant haploid cells were produced, then the random-spore result was scored as synthetically lethal (SL); if less than half the expected number of double-mutant haploid cells was produced, then the random-spore result was scored as synthetically sick (SS); if there was no significant decrease in the number of double-mutant haploids produced, then the random-spore result was scored as 'No', indicating that there was no verified genetic interaction (Appendix 1).

III. RESULTS

1. Characterization of yFACT complex physical interactions

The yeast FACT complex, referred to here as yFACT, comprises the highly abundant essential proteins Cdc68 (also known as Spt16) and Pob3, and the high-mobility-group (HMG) protein Nhp6 (Brewster *et al.* 2001; Ruone *et al.* 2003). Cdc68 and Pob3 share an avid association and bind in a 1:1 stoichiometry to generate a sub-complex of FACT, referred to as CP (Brewster *et al.* 1998; Wittmeyer *et al.* 1999). Nhp6 association with CP to generate FACT is weaker and more complicated, with multiple Nhp6 molecules associating with the nucleosomes and the CP heterodimer associating with this structure (Ruone *et al.* 2003; Rhoades *et al.* 2004). Human FACT is comprised of two subunits, hSpt16 and SSRP1, which are the homologues of yeast Cdc68 and Pob3, respectively (Orphanides *et al.* 1999). In addition to the sequences that share homology with Pob3, SSRP1 contains an added HMG-1 domain as a C-terminal extension. Thus SSRP1 shares regions of homology with two yFACT subunits, Pob3 and Nhp6. Previous research from our lab has shown that a fusion protein of Pob3 and Nhp6 that mimics the hSSRP1 polypeptide is able to provide essential Pob3 function in yeast and alleviates some of the deleterious phenotypes associated with deletion of the Nhp6-encoding genes (Brewster *et al.* 2001). Thus, current evidence suggests that while not every CP dimer in yeast is associated with Nhp6 to form FACT (Brewster *et al.* 2001; Formosa *et al.* 2001), one mechanism of CP association with chromatin is Nhp6-mediated.

This section focuses on structural aspects of the core CP heterodimer. Two approaches to identifying the regions responsible for the interaction between Cdc68 and Pob3 were undertaken: 1) directed two-hybrid studies employing various Cdc68 and Pob3 polypeptides, and 2) *in vitro* pull-down assays with recombinant Cdc68 and Pob3 polypeptides.

i) Cdc68 and Pob3 fail to interact in the yeast two-hybrid system

To identify the regions of Cdc68 responsible for Pob3 binding, a two-hybrid approach was first employed. The yeast two-hybrid system has been used extensively to study protein-protein interactions, and makes use of the well-characterized transactivation of *GAL* genes (Fields and Song 1989). Yeast *GAL* gene promoters contain an upstream activating sequence (UAS) that is able to bind Gal4, a transcriptional activator. The Gal4

protein comprises several separately folding domains, including a DNA-binding domain (Gal4 BD), responsible for binding the UAS, and a transactivation domain (Gal4 AD), responsible for recruiting RNA polymerase to promote transcription. Neither the Gal4 BD nor Gal4 AD is able to activate transcription of *GAL* genes independently. Even when co-expressed in cells as separate polypeptides, these domains are unable to transactivate gene expression, as they no longer physically interact with one another. These two Gal4 domains require a protein 'bridge' to once again bring them into close proximity, at which point they are able to activate transcription (Figure 9).

The yeast two-hybrid system makes use of modified versions of key components of *GAL* expression. Salient features of the system include 1) reporter genes containing a *GAL* promoter fused to various genes that permit expression changes to be easily monitored, and 2) fusions of the proteins of interest to either the Gal4 BD or AD. The protein of interest fused to the Gal4 BD is referred to as the 'bait', while the protein fused to the Gal4 AD is known as the 'prey'. Libraries of DNA sequences encoding a variety of polypeptides may be fused to the Gal4 AD as targets when trying to identify novel protein-protein interactions using the two-hybrid system. When the goal is to characterize binding between two known protein partners, as is the case here, specific polypeptide sequences may also be used as targets. Interactions between two proteins may be characterized by fusing DNA sequences encoding various polypeptides of bait and prey proteins to the DNA sequences encoding the Gal4 BD and AD, respectively, and monitoring activation of reporter genes (Figure 9).

The coding sequences for Cdc68 and Pob3 were fused in frame to the *GAL4* BD and *GAL4* AD sequences present in the pGBT9 or pGAD424 plasmids (Bartel *et al.* 1993), respectively. The reciprocal fusions were also created, with *CDC68* fused to the *GAL4* AD sequences and *POB3* fused to the *GAL4* BD sequences. This was done in case the fusion of one Gal4 domain to the proteins of interest interfered with protein folding or with protein-protein interactions. Additionally, several plasmids were created containing smaller portions of the *CDC68* coding sequence fused to either the *GAL4* BD or *GAL4* AD sequences. The polypeptides encoded by each fusion gene are summarized in Table 6. Since the physical interaction between Cdc68 and Pob3 is well characterized, the combinations of BD-Cdc68 and AD-Pob3, or AD-Cdc68 and BD-Pob3, were expected to

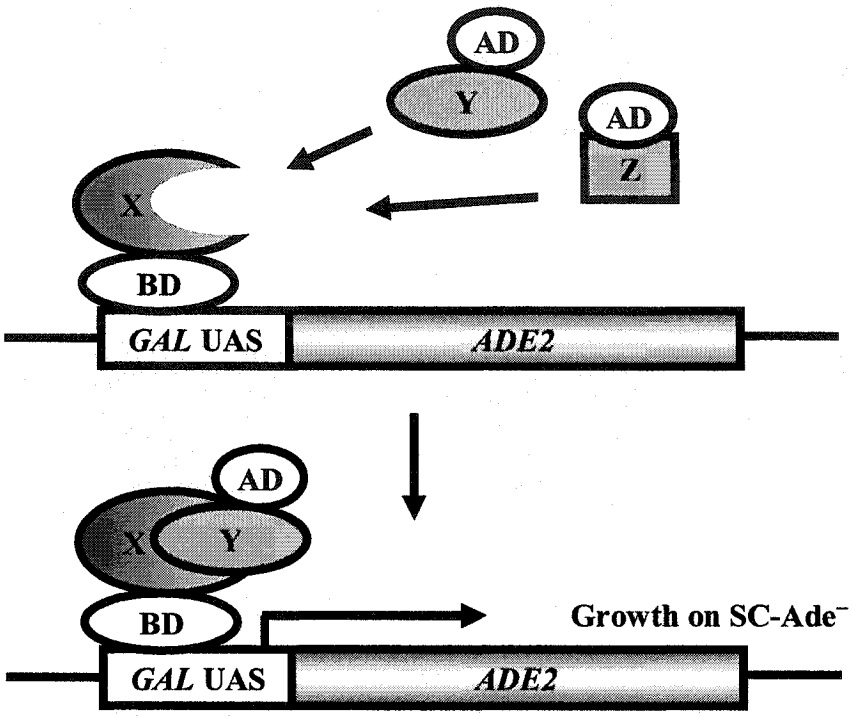

Figure 9. Yeast two-hybrid system. The *GAL2-ADE2* two-hybrid reporter gene is diagramed with the *ADE2* coding region indicated by a partially filled grey box and the *GAL2* promoter, containing a *GAL* UAS sequence, shown as a white box. (Top) The Gal4 DNA-binding domain (BD) is bound to the *GAL* UAS along with its 'bait' protein fusion (X). Two candidate 'prey' proteins (Y and Z) are fused to the Gal4 activation domain (AD). (Bottom) The prey protein Y is able to interact with bait protein X and thus the Gal4 AD is tethered to the Gal4 BD, resulting in *ADE2* gene expression. Cells now make Ade2 protein and become adenine prototrophs, which are able to grow on synthetic medium lacking adenine (SC-Ade). In this way the *GAL2-ADE2* reporter may be used to monitor two-hybrid interactions. The *GAL1-HIS3* and *GAL7-lacZ* reporters are based on the same mechanism, but the readout phenotypes for gene expression in each case are different.

Table 6. Plasmid-encoded fusions of Cdc68 and Pob3 to Gal4 DB and Gal4 AD

Fusion protein name	Primer pair (DNA Sequence)		Amino acids
BD-Cdc68	2H Full CDC68 5' (5'GCGGGATCCATGGAAGAGC TGAATATTGATTTTGACG)	2H Full CDC68 3' (5'GCGGAGCTCCTAATCTC TAAAGTTTGCACCCCTATC A)	1-1035 (full-length)
BD-Cdc68 (1-436)	2H Full CDC68 5'	2H Mega CDC68 3' (5'GCGGAGCTCATTTGTTA AGAAGCGTGGAGGCTCTGT T)	1- 436
BD-Cdc68 (436-1035)	2H Mini CDC68 5' (5'GCGGGATCCTACACCAAAG CCAAATCCCAGATATCAT)	2H Full CDC68 3'	436-1035
BD-Cdc68 (308-642)	2H MID CDC68 5' (5'GCGGGATCCGATCCATCTG AAGAAATGGCCAACAACT)	2H MID CDC68 3' (5'GCGGAGCTCTTGTTTAA AGGTTTCACTCATGCGGTC AC)	308-642
BD-Cdc68 (626-1035)	2H MUT CDC68 5' (5'GCGGGATCCATTACACTAA GATCCAAAGATGGTGACC)	2H Full CDC68 3'	626-1035
AD-Cdc68	2H Full CDC68 5'	2H Full CDC68 3'	1-1035
AD-Cdc68 (1-436)	2H Full CDC68 5'	2H Mega CDC68 3'	1-436
AD-Cdc68 (426-1035)	2H Mini CDC68 5'	2H Full CDC68 3'	436-1035
AD-Cdc68 (308-642)	2H MID CDC68 5'	2H MID CDC68 3'	308-642
AD-Cdc68 (626-1035)	2H MUT CDC68 5'	2H Full CDC68 3'	626-1035
BD-Pob3	2H POB3 5' (5'GCGGGATCCATGAGTACCG ACTTTGATAGAATT)	2H POB3 3' (5'GCGGGATCCCTATTCTA CCTTAGGCTTCTTCGA)	1-552 (full-length)
AD-Pob3	ND	ND	1-552 (full-length)

BD, Gal4 DNA-binding domain fused in frame to the N terminus of the polypeptide chain indicated; AD, Gal4 activation domain fused in frame to the N terminus of the

polypeptided chain indicated. 'Primer pair' indicates the primers used to amplify the DNA sequence coding for the polypeptides of interest. The plasmid construct containing the gene expressing AD-Pob3 was made by N. K. Brewster in our lab (unpublished data) and therefore does not have a primer pair listing here. The 'Amino Acids' column indicates the region of Cdc68 or Pob3 protein, as appropirate, fused to the Gal4 BD or AD.

activate two-hybrid reporter-gene expression. Additionally, the BD- or AD-Cdc68(436-1035) fusion proteins were generated to mimic the amino acid composition of Cdc68-mini, a novel mutant form of Cdc68 containing a large N-terminal deletion but still able to provide essential Cdc68 function in yeast cells (J. Kurniawan, unpublished data, and data not shown). Cdc68-mini is also able to bind Pob3 (see Figure 19), and therefore the BD-Cdc68(436-1035) and AD-Pob3 or AD-Cdc68(436-1035) and BD-Pob3 combinations were also expected to activate reporter-gene expression. To determine if the entire Pob3-binding region is contained within the Cdc68-mini protein, fusions of the sequence corresponding to the region deleted for *cdc68-mini* with *GAL4* BD or AD were also made, encoding BD- or AD-Cdc68(1-436). These polypeptide fusions allowed the association of the Cdc68 N-terminal domain with Pob3 to be examined. Other gene fusions encoding BD- or AD-Cdc68(308-642) and BD- or AD-Cdc68(626-1035) were created to assist in narrowing down the region of Cdc68 responsible for Pob3 binding.

Each of the BD fusions to Cdc68 polypeptides was tested for its ability to physically interact with AD-Pob3, and each of the AD fusions to Cdc68 polypeptides was also tested for its ability to physically interact with BD-Pob3. Pair-wise combinations of the plasmids containing the genes encoding these fusion proteins were then transformed into cells of the two-hybrid yeast strain PJ69-4a (James *et al.* 1996). As controls for detection of two-hybrid interactions, pSE1111, expressing the Snf4 protein fused to the Gal4 AD, and pSE1112, expressing the Snf1 protein fused to the Gal4 BD, were co-transformed into cells of strain PJ69-4a. The physical interaction between Snf4 and Snf1 has been characterized using the yeast two-hybrid system and is widely employed as a positive control in two-hybrid experiments (Bai and Elledge 1997). As an additional control, plasmids containing genes encoding Gal4 BD fused to Gcs1 and Gal4 AD fused to Snc2 were also co-transformed. The two-hybrid interaction between Gcs1 and Snc2 proteins was identified by Dr. P. P. Poon in our lab (personal communication) and the plasmids required were readily available for use as an additional control. To verify that none of the fusion proteins employed could transactivate the reporter genes independently of an interacting partner protein, each fusion protein was introduced into cells of the two-hybrid strain along with the appropriate empty-vector control containing the sequence encoding either the Gal4 BD or Gal4 AD. PJ69-4a yeast cells contain the *GAL1-HIS3*,

GAL7-lacZ, and *GAL2-ADE2* reporter genes, and thus provide three different readout systems for detection of two-hybrid interactions.

Activation of the *GAL1-HIS3* reporter gene was monitored by assessing cell growth on synthetic medium lacking histidine (SC-His) and containing 3-aminotriazole (3AT), a competitive inhibitor of the *HIS3* gene product. When the *GAL1-HIS3* reporter is not activated, no histidine is biosynthesized within these cells, and the cells are histidine auxotrophs and fail to grow on medium lacking histidine. However, there is some 'leaky' or low-level background expression of the *GAL1-HIS3* reporter gene, which results in the generation of some *HIS3* gene product, and as a result some residual growth of cells on SC-His medium is occasionally observed. Addition of 3AT to low concentrations helps to eliminate background cell growth by inhibiting the activity of the *HIS3* gene product. 3AT prevents cells from benefiting from the small amount of His3 produced by 'leaky' reporter-gene expression, and thus ensures that, unless the *GAL1-HIS3* reporter gene is fully activated, cells remain histidine auxotrophs. Cell growth is only observed on SC-His + 3AT medium when the *GAL1-HIS3* reporter is activated by the association of two-hybrid fusion proteins with the UAS. Therefore, growth on SC-His medium containing 3AT is indicative of a positive two-hybrid interaction between the bait and target proteins employed. Similarly, activation of the *GAL2-ADE2* reporter gene can be monitored using cell growth on synthetic medium lacking adenine (SC-Ade). Cells that are unable to express the *GAL2-ADE2* reporter are unable to biosynthesize adenine, and as a result are adenine auxotrophs and fail to thrive on SC-Ade medium. It is only when the *GAL2-ADE2* expression is activated by the association of two-hybrid fusion proteins with the UAS sequence that cells are able to grow on SC-Ade medium. Therefore, growth on SC-Ade medium is indicative of a positive two-hybrid interaction between the bait and target proteins fused to the Gal4 BD and AD, respectively. Activation of *GAL7-lacZ* reporter gene is monitored *via* an assay for the β–galactosidase enzyme produced from the *lacZ* gene. Cells that turned blue during β–galactosidase filter lift assays (Materials and Methods) must have been able to activate transcription of *GAL7-lacZ*, indicating a positive two-hybrid interaction between the bait and prey proteins. Cells that remain white during the assay do not contain any β–galactosidase enzyme from expression of *GAL7-lacZ*, and therefore this result indicates no interaction between the bait and target

Gal4 fusion proteins. Activation of each of these reporters was assessed by the above criteria for each two-hybrid interaction tested during this analysis.

Despite the fact that the association of Cdc68 and Pob3 is well established and stable, the combination of full-length BD-Cdc68 with full-length AD-Pob3 in the two-hybrid system failed to transactivate any of the UAS-driven reporter genes (Figure 10, and data not shown for the *Gal7-lacZ* reporter). No activation of reporter genes was observed if the reciprocal fusion proteins were employed (data not shown). Additionally, none of the BD-Cdc68 polypeptides were unable to activate transcription in the presence of AD-Pob3 (Figure 10), and this same result was obtained with the reciprocal fusions. A summary of all two-hybrid combinations tested and the two-hybrid result for each is provided in Table 7.

There are several possible explanations for the lack of two-hybrid interactions between Cdc68 and Pob3. 1) The Cdc68 and/or Pob3 proteins generated as Gal4 BD or AD fusions are unstable, and therefore not enough of the proteins are present to elicit activation of reporter genes. 2) The Gal4 DNA-binding and activation domains fused to Cdc68 and Pob3 somehow interfere with Cdc68 and Pob3 association. Thus no physical association between the fusion proteins would be possible and subsequently no two-hybrid interaction is observed. 3) The two-hybrid fusions of Cdc68 and Pob3 are incorporated into CP complexes with the endogenous, untagged Cdc68 and Pob3 proteins. As a result, the Gal4-fused Cdc68 and Pob3 proteins are effectively diluted from the target UAS binding site and as a result fail to activate the two-hybrid reporter genes. 4) The two-hybrid fusions of Cdc68 and Pob3 do interact and associate with the UAS of the reporter genes, but the presence of CP at this location is inhibitory to gene expression and therefore no activation of gene expression is observed. Further experiments were undertaken to address some of these possible explanations for the lack of two-hybrid interactions between Cdc68 and Pob3.

To ensure that Cdc68 and Pob3 fusion proteins were present in yeast cells, western blot analyses using anti-Gal4-BD or anti-Gal4-AD antibodies were performed on total protein extracts from cells containing the appropriate plasmid-borne gene fusions (Figure 11). These results indicated that detectible levels of the appropriately sized fusion protein were present in cells for seven of the twelve fusion proteins examined. Neither the BD- or

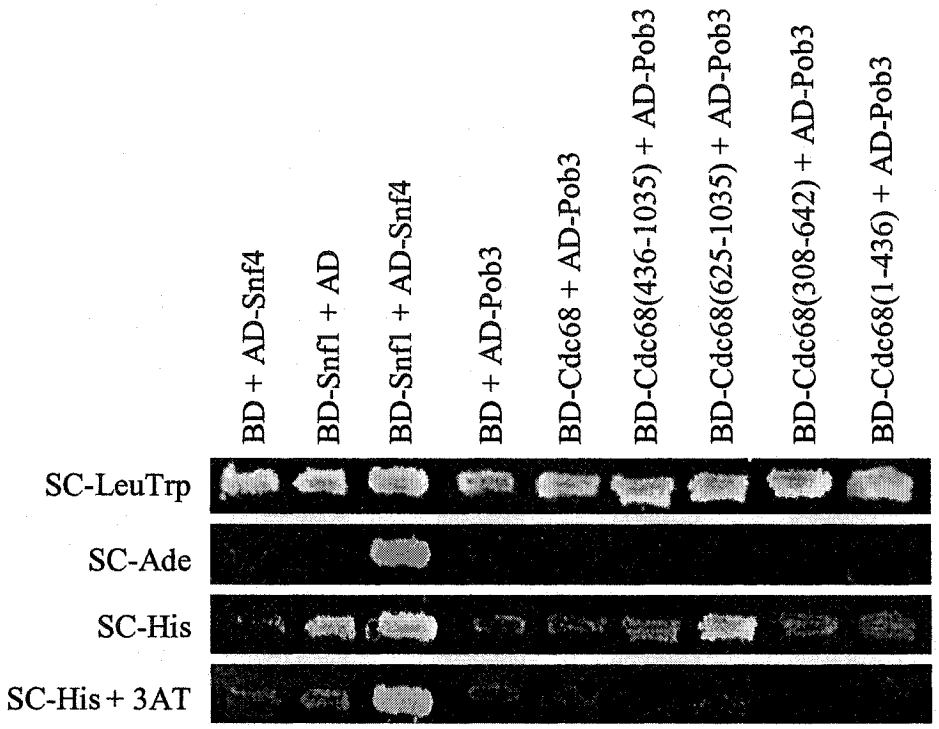

Figure 10. Two-hybrid interactions. Yeast cells expressing the fusion proteins indicated along the top of the panel were spread as patches on solid SC medium lacking leucine (selects for the presence of pGAD424-derived plasmids) and tryptophan (selects for the presence of pGBT9-derived plasmids) and grown for 2 days at 30°C. Cells were then replica-plated to the media indicated at the left. 3AT indicates the presence of 3 mM 3-aminotriazole, a competitive inhibitor of the *HIS3* gene product. Low-level background expression of the *GAL1-HIS3* reporter gene results in the generation of some *HIS3* gene product, and as a result some residual growth of cells on SC-His medium is observed. The presence of 3AT in the medium assists in monitoring activation of this reporter gene by keeping background cell growth to a minimum. BD, Gal4 DNA binding domain; AD, Gal4 activation domain. As can be seen from growth on SC-Ade, expression of the *GAL2-ADE2* reporter gene only occurred in the presence of the positive-control fusion proteins BD-Snf1 and AD-Snf4.

Table 7. Summary of Cdc68 *vs* Pob3 two-hybrid results

Gal4 DNA-binding domain fusion	Gal4 activation domain fusion	Two-hybrid interaction
BD-Cdc68	AD-Pob3	No
BD-Cdc68	AD	No
BD-Cdc68(1-436)	AD-Pob3	No
BD-Cdc68(1-436)	AD	No
BD-Cdc68(436-1035)	AD-Pob3	No
BD-Cdc68(436-1035)	AD	No
BD-Cdc68(308-642)	AD-Pob3	No
BD-Cdc68(308-642)	AD	No
BD-Cdc68(626-1035)	AD-Pob3	No*
BD-Cdc68(626-1035)	AD	No*
BD	AD-Pob3	No
BD-Pob3	AD-Cdc68	No
BD	AD-Cdc68	No
BD-Pob3	AD-Cdc68(1-436)	No
BD	AD-Cdc68(1-436)	No
BD-Pob3	AD-Cdc68(436-1035)	No
BD	AD-Cdc68(436-1035)	No
BD-Pob3	AD-Cdc68(308-642)	No
BD	AD-Cdc68(308-642)	No
BD-Pob3	AD-Cdc68(626-1035)	No
BD	AD-Cdc68(626-1035)	No
BD-Pob3	AD	No

Gal4 DNA-binding domain fusion	Gal4 activation domain fusion	Two-hybrid interaction
BD-Snf1	AD-Snf4	Yes
BD-Snf1	AD	No
BD	AD-Snf4	No
BD-Gcs1	AD-Snc2	Yes
BD-Gcs1	AD	No
BD	AD-Snc2	No
BD	AD	No

Combinations of Gal4 DNA-binding domain fusion polypeptides and Gal4 activation-domain fusion polypeptides employed in two-hybrid assays are indicated. Activation of the two-hybrid reporter genes *GAL2-ADE2*, *GAL1-HIS3*, and *GAL7-lacZ* was monitored by the ability of cells to grow on synthetic complete medium lacking adenine (SC-Ade), to grow on synthetic complete medium lacking histidine and containing 3 mM 3 aminotriazol (SC-His + 3AT), and to turn blue in *lacZ* filter assays, respectively. Combinations that failed to elicit transcription of the reporter genes are indicated as 'No' in the the two-hybrid interaction column. The 'No*' response indicates that the activation of reporters was minimal, with no growth obsereved on SC-Ade and SC-His + 3 mM 3AT, but weak growth seen on SC-His + 2 mM 3AT and slight blue pigment development in *lacZ* filter-lift assays. A 'Yes' in the two-hybrid interaction column indicates that all reporter genes were activated, as evidenced by growth on SC-Ade and SC-His + 3 mM 3AT, and by blue colour development in *lacZ* filter-lift assays.

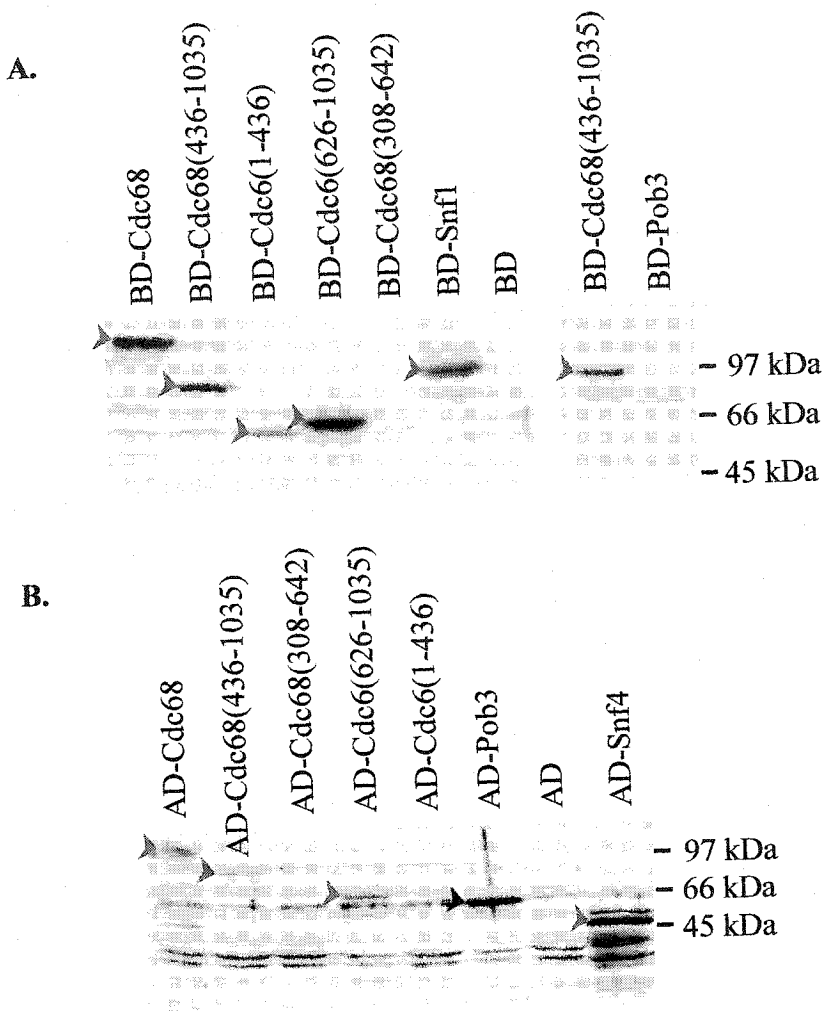

Figure 11. Gal4 BD and AD fusion proteins. Western blot analyses of 10 μg total-protein extracts from yeast using either (A) rabbit polyclonal anti-Gal4-DNA-binding-domain antibody (Santa Cruz) or (B) rabbit polyclonal anti-Gal4-activation-domain antibody (Santa Cruz) are shown. Extracts were from PJ69-4a cells with GBT9 (A) or GAD424 (B) plasmids containing genes encoding the fusion protein indicated across the top of each panel. Polypeptides of the anticipated size for each fusion protein are indicated by red arrowheads in each lane. A black arrowhead is used to indicate the polypeptide detected for AD-Pob3, since it is a lower molecular weight than anticipated. Two lanes containing BD-Cdc68(436-1035) are shown for orientation.

AD-Cdc68(308-642) fusion proteins could be detected, which suggests that a fusion to this region of Cdc68 may generate an unstable protein product that is targeted for degradation. While the BD-Cdc68(1-436) fusion was identified, the AD-Cdc68(1-436) fusion protein could not be detected. The background on blots probed with the anti-Gal4-AD antibody was high in the 60-kDa region, where AD-Cdc68(1-436) would be expected; therefore a faint signal for this fusion protein could have been missed. No hybridization signal corresponding to the expected 80-kDa molecular weight of DB-Pob3 was identified, and a protein slightly smaller than the anticipated 75-kDa protein was observed for AD-Pob3. This smaller protein identified for AD-Pob3 may be a truncation as a result of partial degradation of the fusion protein or as a result of a premature translational stop codon that could have been introduced during cloning. These results indicate that the stabilities and/or composition of the BD- and AD-Pob3 proteins may impede the detection of a two-hybrid interaction with Cdc68 fusion proteins.

To determine if BD-Pob3 and AD-Pob3 are functional protein products, the ability of these fusion proteins to provide essential Pob3 function was assessed. The plasmids encoding BD-Pob3 (pGBT9-based *TRP1* plasmid) and AD-Pob3 (pGAD424-based *LEU2* plasmid) were transformed into haploid yeast cells containing a *pob3Δ::HIS3* or a *pob3Δ::TRP1* chromosomal deletion/replacement, respectively. In both cases, cell viability was maintained by expression of Pob3 from a wild-type *POB3* gene present on a *URA3* plasmid. Transformants were then grown in YNB liquid medium containing uracil, so that cells which failed to inherit the *URA3-POB3* plasmid did not experience any growth impairment due to nutritional deficiencies. However, cells that had lost the *URA3* plasmid containing the gene for Pob3 would only be viable if the BD-Pob3 or AD-Pob3 proteins provide essential Pob3 function. After multiple rounds of growth in YNB medium containing uracil, the cells were spread on solid medium containing uracil and allowed to grow at 30°C until single colonies formed (3-4 days). The plasmid content of cells was assessed by replica-plating colonies to solid synthetic medium lacking either uracil or tryptophan, for cells transformed with pGBT9-based plasmids, or uracil or leucine, for cells transformed with pGAD424-based plasmids. The presence of uracil-auxotrophic cells, indicating absence of the *URA3 POB3* plasmid, that were tryptophan or leucine prototrophs, indicating the presence of pGBT9- or pGAD424-based plasmids

encoding BD-Pob3 and AD-Pob3, respectively, showed that the BD-Pob3 or AD-Pob3 fusion proteins do supply essential Pob3 function (data not shown). Therefore, despite the lack of detectable BD-Pob3 protein and the apparent lower-molecular-weight product detected for AD-Pob3 on western blots, both of these proteins provide essential Pob3 activity. The fact that no BD-Pob3 fusion protein was detected by western blotting is puzzling; however, this was not the only time I was unable to detect, by western blotting with anti-Gal4 antibodies, a two-hybrid fusion protein that generates a biological effect (Results 5, i). To execute Pob3 essential functions, the BD-Pob3 and AD-Pob3 proteins most likely associate with endogenous Cdc68 protein; therefore these fusion proteins are able to bind an untagged version of Cdc68. Furthermore, the ability of the BD-Pob3 and AD-Pob3 proteins to associate with untagged Cdc68 protein in yeast lends support to the hypothesis that perhaps the two-hybrid fusion proteins are titrated away from Gal4-binding sites to other locations of normal CP activity.

A similar approach was taken to determine if the BD- or AD-Cdc68 fusion proteins provide essential Cdc68 functions. The pGBT9- and pGAD424-based plasmids encoding the BD-Cdc68 and AD-Cdc68 polypeptides, respectively, were transformed into haploid yeast cells containing the *cdc68Δ::kanMX4* chromosomal deletion/replacement. Viability of these *cdc68Δ::kanMX4* haploid cells was maintained by a *URA3 CDC68* plasmid. Here again, transformants were grown several times in YNB liquid medium containing uracil to permit the growth of cells that may have failed to inherit the *URA3 CDC68* plasmid. Cells were then transferred to solid medium and allowed to form single colonies at 30°C, which were replica-plated to synthetic media lacking the appropriate nutrients to determine the plasmid complement of cells. No viable uracil-auxotrophic cells were identified from cells transformed with plasmids bearing the genes encoding BD- or AD-Cdc68(1-436), BD- or AD-Cdc68(308-642), or BD- or AD-Cdc68(626-1035). Therefore, these polypeptide fusions of Cdc68 to Gal4 domains are *not* able to provide essential Cdc68 function. In contrast, viable cells that lacked the *URA3 CDC68* plasmid, as evidenced by uracil auxotrophy, were identified from progenitors that had been transformed with plasmids encoding BD- or AD-Cdc68 and BD- or AD-Cdc68(436-1035). Thus, these polypeptide fusions of Cdc68 to Gal4 domains do provide essential Cdc68 function. To execute essential Cdc68 function, these fusion proteins most likely

physically associate with endogenous, untagged Pob3. These findings are in keeping with what is known about the viability of cells containing Cdc68 deletion derivatives. Evans *et al.* (1998) previously reported that polypeptides containing only N-terminal, C-terminal or middle portions of Cdc68, similar to those found in the Cdc68(1-436), Cdc68(626-1035) and Cdc68(308-642) fusion proteins, respectively, are unable to maintain viability when present as the only form of Cdc68. In contrast, Cdc68-mini, a protein whose amino acid sequence closely resembles that of the functional Cdc68(436-1035) fusions, is known to provide essential Cdc68 function in yeast cells (Joelius Kurniawan, unpublished observations, and data not shown).

Cdc68 and Pob3 are highly abundant nuclear proteins present at 10,000 to 50,000 copies per cell (Brewster *et al.* 1998; Wittmeyer *et al.* 1999). The presence of the endogenous, untagged Cdc68 and Pob3 proteins may interfere with the activation of two-hybrid reporter genes by recruiting the two-hybrid Cdc68 and Pob3 proteins to alternative sites, effectively diminishing the amount of two-hybrid fusion proteins available to interact and transactivate the reporter genes. The ability of both BD- and AD-Pob3 proteins as well as BD- and AD-Cdc68 proteins to provide the essential functions of Pob3 and Cdc68 is evidence that these two-hybrid fusion proteins are incorporated into CP and FACT complexes. This lends support to the titration model and helps explain why no two-hybrid interactions are observed for Cdc68 and Pob3. However, while individual tagged versions of Cdc68 or Pob3 may interact with untagged, endogenous Pob3 and Cdc68 proteins, it cannot be ruled out that the interaction between two tagged versions of these proteins may be disrupted by the presence of both Gal4 domains. Additionally, the BD- and AD-Cdc68 proteins may interact with BD- and AD-Pob3 proteins and bind the Gal4 UAS, but the association of this complex with the promoter, in what may be an improper context for FACT function, could block gene expression. However, if this were the case I would anticipate that no Cdc68 or Pob3 fusion to Gal4 domains would result in a positive two-hybrid interaction. While no direct two-hybrid interaction between Cdc68 and Pob3 has been identified, positive two-hybrid interactions with Cdc68 polypeptides have been observed in two-hybrid library screens for novel interacting partners (John, *et al.* 2000; Results 5, i). For the purpose of determining interacting regions of Cdc68 and

Pob3, an alternative approach utilizing recombinant Cdc68 and Pob3 polypeptides in *in vitro* pull-down studies was employed.

ii) *In vitro* pull-down assays show that the middle domain of Cdc68 is responsible for binding Pob3

Recombinant Cdc68 and Pob3 polypeptides were assessed for physical associations by GST (glutatione-S-transferase) pull-down assays. To characterize the regions responsible for the physical association of Cdc68 and Pob3, several genes expressing differentially tagged polypeptides of Cdc68 and Pob3 in bacteria was created.

The genes expressing recombinant Pob3 polypeptides tagged with GST encoded the complete Pob3 protein (amino acids 1-552), the N-terminal domain of Pob3 (amino acids 1-215), or the C-terminal domain of Pob3 (amino acids 178-552) (Figure 12). These proteins are referred to as GST-Pob3, GST-NTDPob3, and GST-CTDPob3, respectively. The GST moiety was used to purify these recombinant proteins from transformants of *E. coli* cells as described in Materials and Methods. Purified GST-Pob3 recombinant proteins resolved by SDS-PAGE and stained with Coomassie are shown in Figure 13.

Recombinant Cdc68 proteins were expressed from gene fusions created in the pET-plasmid system and are therefore designated pET-Cdc68 polypeptides. Eight different recombinant Cdc68 polypeptides were employed in these studies. pET-Cdc68(436-1035) approximates the Cdc68-mini protein, known to bind Pob3 (see Figure 19) and to provide essential Cdc68 function (J. Kurniawan, unpublished observation; data not shown). pET-Cdc68(1-435) corresponds to the N-terminal domain of the Cdc68 protein (N. K. Brewster, unpublished observations). pET-Cdc68(436-821) and pET-Cdc68(436-786) each correspond to the middle domain of Cdc68; however, since the precise boundaries of this domain are not yet resolved, two versions of this region were utilized. pET-Cdc68(308-642) contains portions of both the N-terminal and middle domains. pET-Cdc68(635-1035) contains half of the middle domain as well as the C-terminal domain. pET-Cdc68(771-1035) and pET-Cdc68(710-1035) each contain the C-terminal domain of Cdc68, but since the precise boundary between this and the middle domain is unclear, two polypeptides spanning the boundary region between the two domains were employed(Figure 12). Each recombinant Cdc68 protein is N-terminally fused to the His_6 tag, employed in protein purification, and S-tags, used in detection of these proteins on

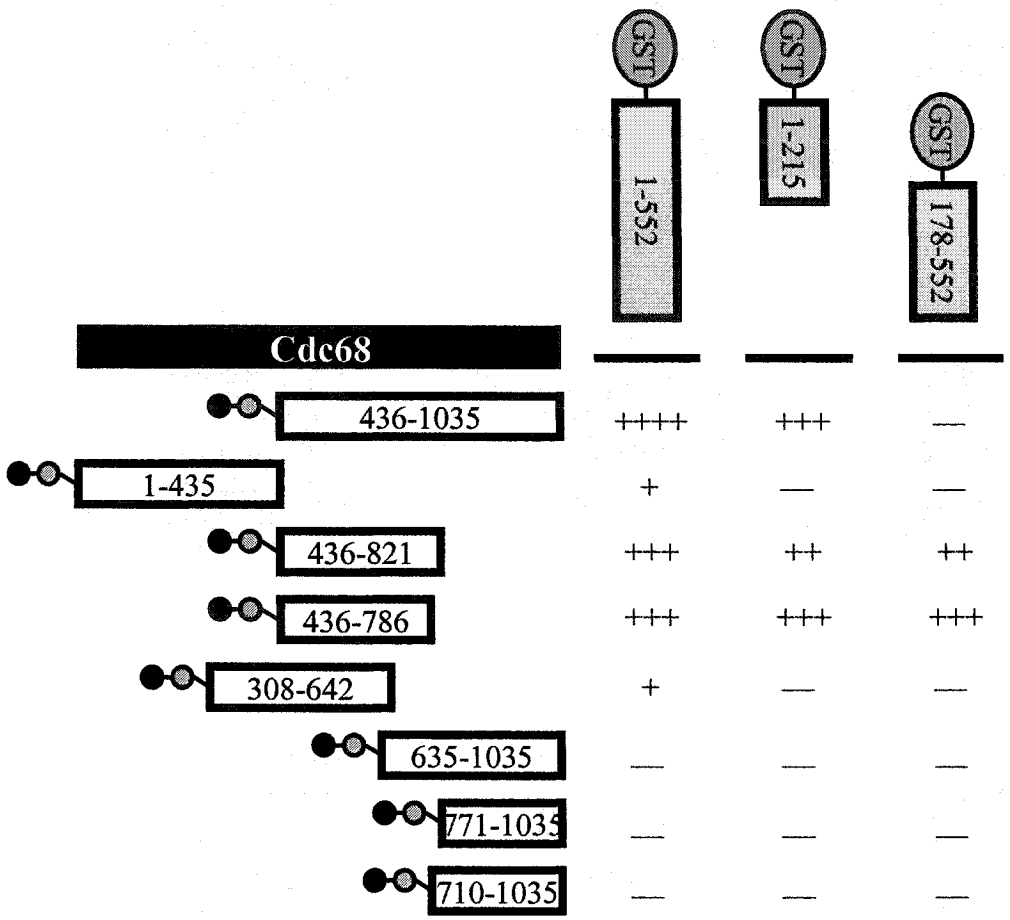

Figure 12. Summary of interactions between Cdc68 and Pob3 as determined by *in vitro* pull-down studies. Recombinant Cdc68 and Pob3 proteins are shown. Cdc68 proteins are shown on the left side as white boxes with the His_6 and S-protein tags shown as black and gray circles at the N-terminal ends of proteins. The Cdc68 residues spanned by each polypeptide are indicated within each box. The full-length Cdc68 protein, spanning residues 1-1035, is shown as a black box at the top for reference. GST-fused Pob3 proteins are shown across the top as gray boxes with the GST tags at the N termini indicated by gray ovals. The numbers inside boxes indicate the portion of Pob3 sequence in each polypeptide. The table summaries GST pull-down results with ++++ = most avid binding, +++ = good binding, ++ = fair binding, + = weak binding, and — = no binding between the indicated polypeptides.

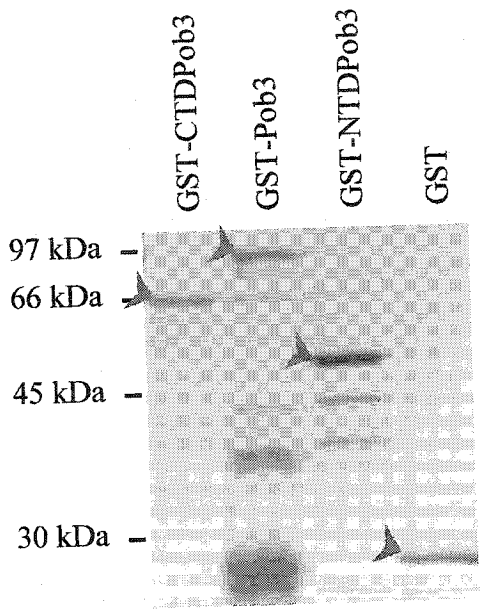

Figure 13. Purified recombinant GST-Pob3 polypeptides used in pull-downs. Recombinant GST-Pob3 fusion proteins purified using gluathione agarose were resolved by SDS-PAGE and stained with Coomassie blue. The portions of Pob3 contained in each GST fusion are: NTDPob3, amino acids 1-215; CTDPob3, amino acids 178-552; and Pob3, amino acids 1–552. In each lane the red arrow indicates the protein product of the appropriate molecular weight.

western blots. His_6 affinity purified material from *E. coli* extracts is shown for each recombinant Cdc68 protein (Figure 14).

GST-Pob3, GST-NTDPob3, GST-CTDPob3, and GST alone were bound to glutathione-agarose beads (Sigma) in equimolar quantities as determined by Coomassie staining of proteins resolved by SDS-PAGE. Equimolar amounts of each recombinant purified pET-Cdc68 polypeptide were then added to the glutathione-bound GST recombinant proteins and incubated at room temperature to permit binding. Bound material was washed in either low-stringency or high-stringency buffers (as indicated in figure legends), resolved by SDS-PAGE, and assessed by western blotting for the presence of S-tagged Cdc68 polypeptides. The presence of Cdc68 polypeptides in the unbound material was also assessed in this manner.

Avid binding was observed between pET-Cdc68(436-1035), which contains the middle and C-terminal domains of Cdc68, and GST-Pob3 (Figure 15, lane 1; Figure 16, panel A, lane 1). In addition to the intact pET-Cdc68(436-1035) polypeptide, a truncated 45-kDa protein species also associated with GST-Pob3. By inference, this tagged 45-kDa truncation of pET-Cdc68(436-1035) must contain the amino-terminal region of the pET-Cdc68(635-1035) protein, and based on size estimates this polypeptide approximates the Cdc68 middle domain (approximately residues 436-688). The more avid association for this 'middle domain' polypeptide fragment of pET-Cdc68(436-1035) than for the intact (middle and C-terminal domain) polypeptide may indicate that the C-terminal domain of Cdc68 somehow impedes the association of Cdc68 with Pob3. The pET-Cdc68(436-1035) polypeptide and its 45-kDa middle-domain truncation also bound GST-NTDPob3 (Figure 16, panel B, lane 1). However, only the 45-kDa middle-domain truncation of pET-Cdc68(436-1035) showed an association with GST-CTDPob3. These observations further support the idea that the C-terminal domain of Cdc68 may mediate interactions with Pob3, in particular the binding of Cdc68 middle domain to the CTD of Pob3.

Consistent with these findings, recombinant Cdc68 polypeptides designed to approximate the middle domain of Cdc68, pET-Cdc68(436-821) and pET-Cdc68(436-786), bound to GST-Pob3, GST-NTDPob3 and GST-CTDPob3 (Figure 16, lane 2; Figure 17). The associations of the recombinant Cdc68 middle-domain polypeptides with full-

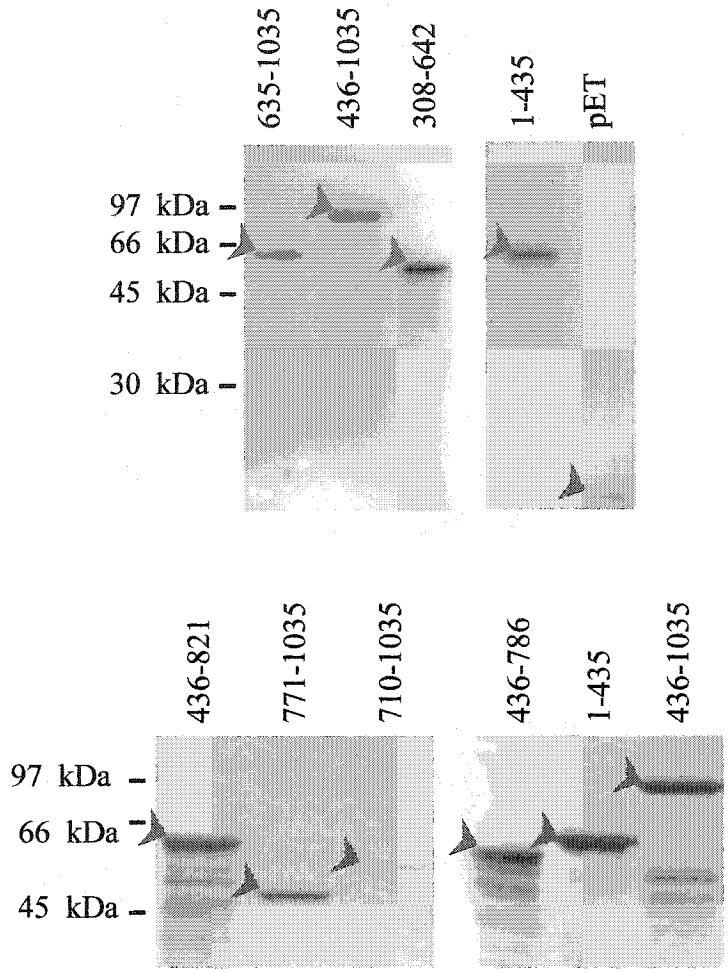

Figure 14. Purified recombinant pET-Cdc68 polypeptides used in pull-downs. His_6 affinity-purified pET-Cdc68 polypeptides were resolved by SDS-PAGE and stained with Coomassie blue. These panels show examples of purified material used in pull-down assays. Numbers across the top of each panel indicate the portion of the Cdc68 polypeptide in each recombinant construct. For some recombinant proteins, more than one example of the purified product is shown. In each lane the red arrow indicates the protein product of the appropriate molecular weight.

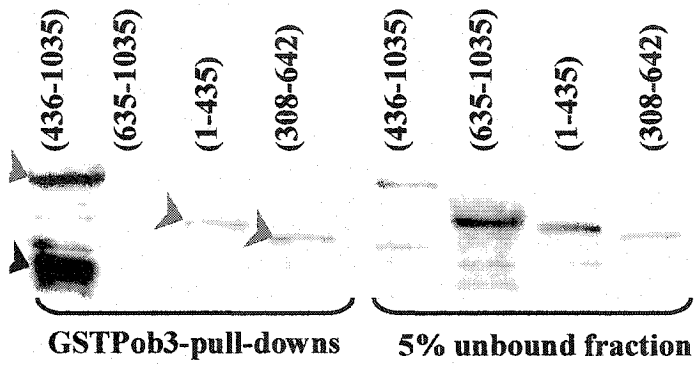

Figure 15. GST-Pob3 pull-downs of recombinant pET-Cdc68 polypeptides. pET-Cdc68 polypeptides (the Cdc68 polypeptide region for each is indicated above the appropriate lane) were incubated with GST-Pob3 or GST alone. Bound and unbound fractions from the pull-downs were resolved by SDS-PAGE and western blots using HRP conjugated S-protein were used to detect recombinant Cdc68 polypeptides. The left panel shows 50% of the material bound to GST-Pob3 during a pull-down performed under low-stringency conditions (30-second exposure) and the right panel shows 5% of the unbound protein from each pull-down (10-second exposure). Proteins bound to GST-Pob3 are indicated by red arrowheads. The 45-kDa truncated product of pET-Cdc68(436-1035) that binds GST-Pob3 is indicated by a black arrowhead. To verify the specificity of binding, each recombinant Cdc68 protein was also incubated with GST-bound agarose beads, and no bound Cdc68 polypeptide was detected in these samples (data not shown). Additional control pull-downs using the pET tag protein (thioredoxin-His_6-S tag) with either GST or GST-Pob3 bound beads were also performed, and in each case no detectable pET protein was observed in the bound material (data not shown).

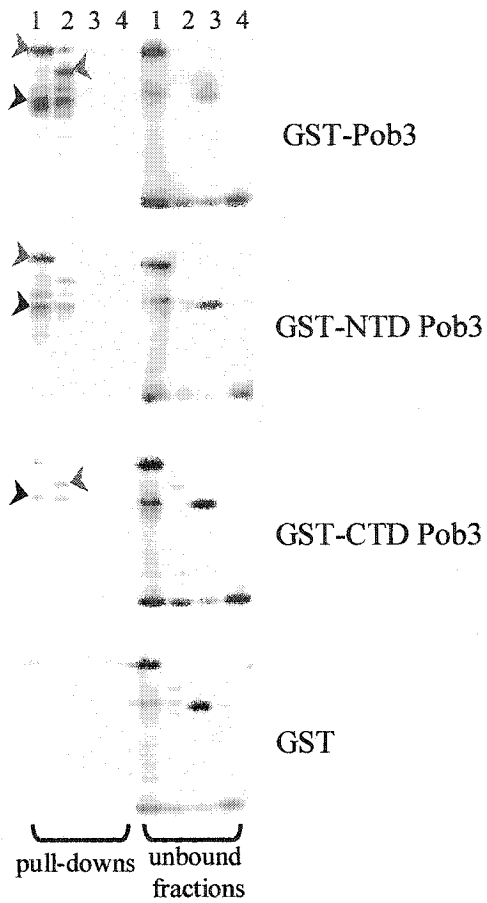

Figure 16. GST pull-downs of pET-Cdc68 recombinant polypeptides with GST-Pob3, GST-NTDPob3, GST-CTDPob3 and GST alone. 25% of bound and 5% of unbound material from GST pull-downs performed under low-stringency conditions with recombinant Cdc68 polypeptides and the GST-polypeptides indicated at the right were analyzed by western blotting (15-second exposures are shown). Lane 1, pET-Cdc68(436-1035); lane 2, pET-Cdc68(436-821); lane 3, Cdc68(771-1035); lane 4, pET protein alone (thioredoxin-His6-Stag). Red arrowheads indicate the bound, intact Cdc68 polypeptides in each case. The 45-kDa truncated protein product from Cdc68(436-1035) is indicated by a black arrowhead.

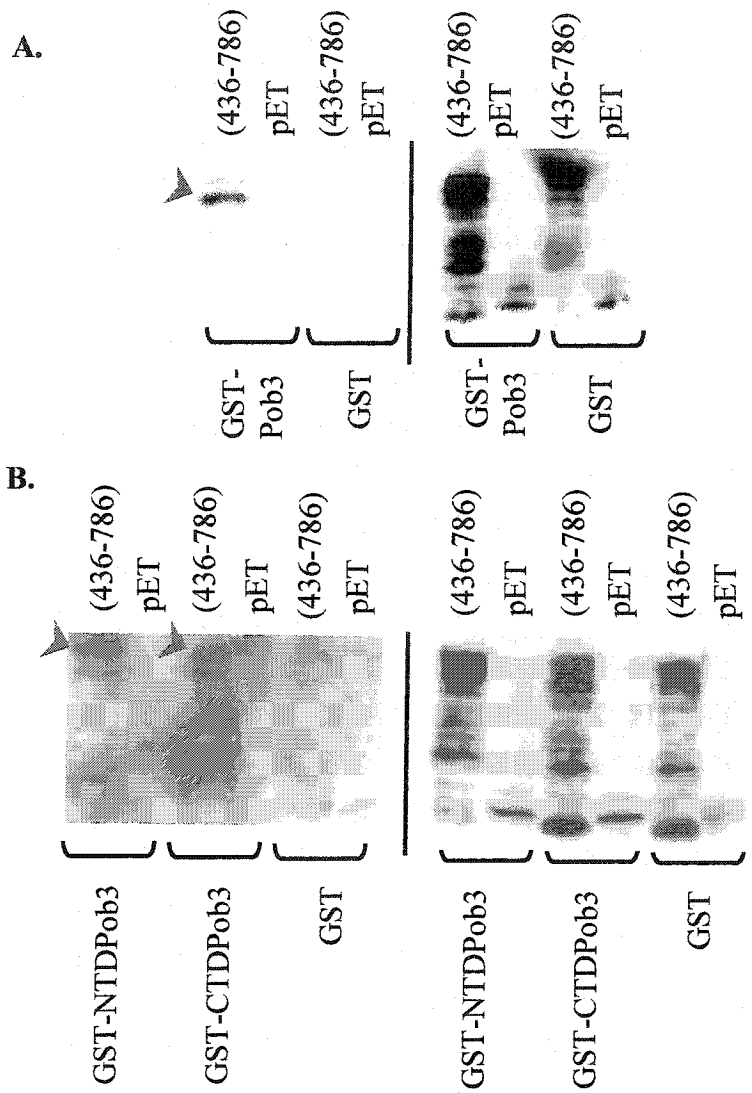

Figure 17. pET-Cdc68(436-786) pull-downs with GST-Pob3, GST-NTDPob3, GST-CTDPob3, and GST. 50% of bound and 5% of unbound material from GST pull-downs performed under high-stringency conditions with GST-fusion proteins (indicated below the appropriate lanes) were analyzed by western blotting (25-second exposures are shown). (A) The left panel shows 50% of bound Cdc68 (436-768) or pET with either GST-Pob3 or GST. (B) The left panel shows 50% of bound Cdc68 (436-768) or pET with either GST-NTDPob3, GST-CTDPob3 or GST. Red arrowheads indicate the bound pET-Cdc68(436-768) intact polypeptide. Right panels in (A) and (B) show 5% of the unbound recombinant protein from each pull-down.

length Pob3 were more avid that their associations with either the NTD or CTD of Pob3 (Figure 16, compare lane 2 panels A, B, and C; Figure 17, compare 9A, lane 1 with 9B, lanes 1 and 3). This difference is to be expected if each domain of Pob3 is partially responsible for Cdc68 middle-domain binding. A decrease in the Cdc68 middle domain bound is therefore observed if either the NTD or CTD of Pob3 is missing.

Cdc68 polypeptides containing only fragments of the middle domain, as is the case for pET-Cdc68(308-642) and pET-Cdc68(635-1035), exhibited little to no association with the GST-fused Pob3 polypeptides. A weak association was observed between pET-Cdc68(308-642) and GST-Pob3 (Figure 15, lane 4) that may be attributed to the presence of the first half of the middle domain. pET-Cdc68(308-642) may contain a disrupted or partial binding site for Pob3, which would account for its weak association with Pob3. No association was observed for pET-Cdc68(308-642) with either the GST-NTDPob3 or GST-CTDPob3 polypeptides (data not shown). pET-Cdc68(635-1035), which contains the second half of the middle domain and the C-terminal domain of Cdc68, was also unable to bind GST-Pob3 (Figure 15, lane 2), GST-NTDPob3, or GST-CTDPob3 (data not shown). These results indicate that disruptions of the middle domain of Cdc68 greatly diminish its ability to bind Pob3.

As already indicated by the failure of pET-Cdc68(635-1035) to bind GST-Pob3, the C-terminal domain of Cdc68 is unable to bind Pob3. pET-Cdc68(710-1035) and pET-Cdc68(771-1035), which both contain the C-terminal domain, did not bind any of the recombinant GST-Pob3 polypeptides (Figure 16, lane 3; data not shown).

The N-terminal domain of Cdc68, expressed in pET-Cdc68(1-435), exhibited a weak, but reproducible, physical interaction with GST-Pob3 (Figure 15, lane 3). No interaction for the Cdc68 N-terminal domain and either GST-NTDPob3 or GST-CTDPob3 was observed (data not shown).

A summary of Cdc68 and Pob3 interactions observed in these GST-pulldown experiments is provided in Figure 12. These data show that the major binding site(s) for Pob3 resides between amino acids 436-786 of Cdc68, which roughly corresponds to the middle domain of Cdc68. The N-terminal domain of Cdc68 is also able to bind Pob3, but this binding is significantly weaker than that exhibited by the Cdc68 middle domain, and therefore is not the principal site of interaction between these two proteins. Pob3

associates with the middle domain of Cdc68 through contacts in both the N-terminal and C-terminal domains. The effects of the binding site(s) within these two domains of Pob3 are additive, with the most avid association of Cdc68 middle domain observed for full-Pob3 protein. An alternative explanation is that the observed binding of the NTD and CTD of Pob3 to Cdc68 could be provided by the 37-residue overlap shared between the GST-NTDPob3 and GST-CTDPob3 polypeptides. However, this stretch of 37 amino acids is not conserved in the Pob3 structural homologues from metazoans, as would be expected for a significant functional aspect of the protein like the Cdc68 binding site. Based on these *in vitro* pull-down results, a model of the Cdc68 and Pob3 protein domains and how they associate to form a CP dimer is shown in Figure 18.

iii) *In vivo* assessment of Cdc68-mini and Cdc68-ΔNTD association with Pob3

The Cdc68-mini protein is able to supply essential function in yeast (J. Kurniawan, unpublished data; data not shown), even though it is missing approximately 40% of the Cdc68 protein sequence, corresponding to most of the N-terminal domain of Cdc68. A gene encoding a more complete resection of the N-terminal domain, *cdc68-ΔNTD*, was generated in our lab by N. K. Brewster (unpublished data). To verify the *in vitro* finding that the N-terminal domain of Cdc68 has little involvement in the physical association of Cdc68 with Pob3, competitive co-immunoprecipitations studies were performed employing cells containing both Cdc68 and Cdc68-mini, or both Cdc68 and Cdc68-ΔNTD proteins. Proteins were purified under native conditions from logarithmically growing yeast cells containing Cdc68, expressed from the chromosomal *CDC68* gene, and Cdc68-mini or Cdc68-ΔNTD, expressed from low-copy plasmids. Cells employed in this experiment also expressed a V5-epitope tagged version of Pob3, from a chromosomally integrated *POB3-V5* gene. Thus the number of copies of *CDC68* genes, both full-length and the N-terminal deletions, was in excess of the *POB3-V5* gene copies per cell by 2-3 fold. Therefore the Cdc68 proteins would have to compete for a limiting supply of Pob3 protein. The Pob3-V5 protein, along with bound protein partners, was then immunoprecipitated from extracts using the anti-V5 antibody (Gibco BRL) with addition of Protein A-agarose beads. As a control for non-specific binding of proteins to the Protein A-agarose beads, these beads were also added to extracts without antibody. Bound and unbound material from the immunoprecipitation was analyzed by western

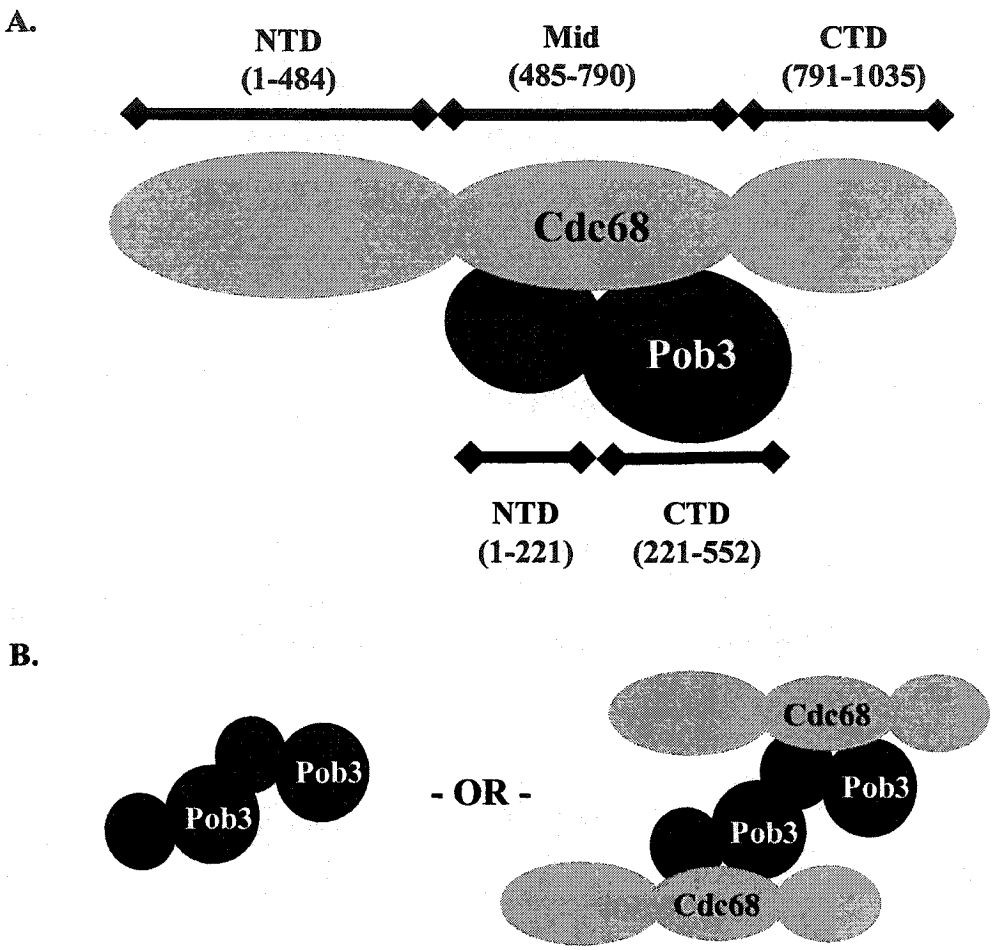

Figure 18. CP structure. (A) The physical association of Cdc68 and Pob3 as determined by *in vitro* pull-down experiments is shown as both the N- and C-terminal domains of Pob3 (black) contacting the middle domain of Cdc68 (grey). The domain architecture for each protein (N. K. Brewster, unpublished data) is indicated, with each domain represented as a oval, and the approximate polypeptide region of each domain is given in parentheses. NTD = N-terminal domain; CTD = C-terminal domain. (B) The *in vitro* physical interaction between the N-terminal domain of Pob3 with the C-terminal domain of Pob3 is shown. It is not known if two Pob3 proteins interact individually or in the context of the CP complex; both scenarios are diagrammed.

bloting using anti-V5 antibody, to ensure that Pob3-V5 had been precipitated, and affinity purified anti-Cdc68 antibody, to detect the Cdc68 polypeptides associated with Pob3. Both Cdc68-mini and Cdc68-ΔNTD bound to Pob3-V5 in the presence of full-length Cdc68 (Figure 19A and B), as indicated by the presence of these proteins in the V5-antibody immunoprecipitate. Full-length Cdc68 protein also associated with Pob3-V5 in the presence of either Cdc68-mini or Cdc68-ΔNTD. These observations indicate that the presence of Cdc68-containing CP dimers does not preclude the dimerization of Pob3 with Cdc68-mini or Cdc68-ΔNTD, and *vice versa*. Cdc68 and Cdc68-mini or Cdc68 and Cdc68-ΔNTD are found in the Pob3-V5 immunoprecipitated material at approximately equal levels when the initial protein abundances are taken into consideration (the abundances of Cdc68-mini and Cdc68-ΔNTD are lower than that of Cdc68 in the supernates of the mock immunoprecipitation reactions). The ability of Cdc68-mini and Cdc68-ΔNTD to associate with Pob3 with approximately the same affinity as full-length Cdc68 suggests that the N-terminal domain of Cdc68 plays a negligible role in the association with Pob3. Previous studies have shown that the Cdc68-Δ922 protein, missing a large portion of the N-terminal domain, is also able to immunopreciptate Pob3 at levels approximating those observed for wild-type Cdc68 protein (Brewster *et al.*, 1998). These findings support the *in vitro* pull-down experimental findings that the N-terminal domain of Cdc68 has only a weak *in vitro* association with Pob3. The avid association of Cdc68 with Pob3 must therefore be the result of a domain within Cdc68-mini and Cdc68-ΔNTD. Both of these proteins contain an intact middle domain, consistent with the *in vitro* pull-down results indicating that the middle domain of Cdc68 is primarily responsible for Pob3 binding.

Similar competitive co-immunoprecipitation studies were attempted with yeast extracts from strains containing a chromosomal *CDC68* gene and a plasmid borne gene encoding only the middle domain of the Cdc68 protein plus a nuclear localization signal and FLAG-epitope tag (plasmid made by N. K. Brewster, unpublished data). However, these experiments were not conclusive, as no protein product of the appropriate size for the Cdc68 middle domain could be identified in western blots of whole-cell extracts probed with either anti-FLAG antibody (Sigma) or affinity purified Cdc68 polyclonal antibody (data not shown). Perhaps the Cdc68 middle domain is simply not stable as a separate

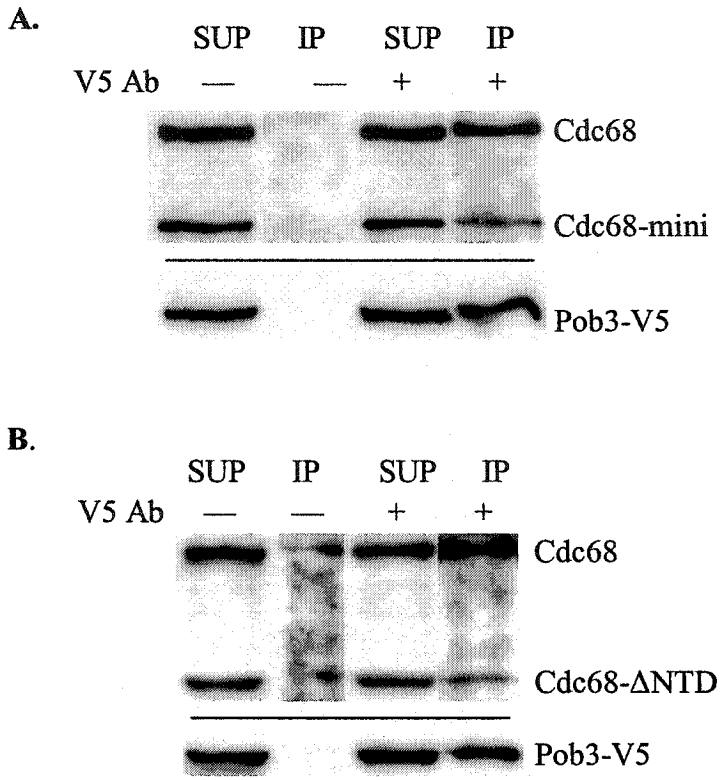

Figure 19. Competitive co-immunoprecipitation of full-length Cdc68 *versus* (A) Cdc68-mini or (B) Cdc68-ΔNTD with Pob3. Protein extracts were obtained from derivatives of strain NB6247 harbouring either (A) pRS314-*CDC68-mini* or (B) pRS315-*CDC68-ΔNTDFLAG* using the glass-bead disruption method under non-denaturing conditions. 2 mg of total protein was then used in an immunoprecipitation with (+) or without (—) 5 μl (0.9 mg/ml) anti-V5-HRP Ab (Invitrogen). 50 μl of 50% Protein-A-agarose bead slurry (Invitrogen) was added to both mixtures, and bound (IP) and unbound (SUP) proteins were analyzed by western blotting with either anti-Cdc68 polyclonal antibody (top portions of panels A and B) or anti-V5-HRP Ab (bottom portions of panels A and B). 15- and 60-second exposures of the SUP and IP lanes, respectively, are shown.

polypeptide, or is particularly labile during the purification process. In any case, no further *in vivo* verification of the Cdc68 middle-domain interaction with Pob3 was achieved from this approach.

iv) Assessment of CP multimerization

CP complex from whole-cell yeast extracts has an apparent molecular weight of 400 kDa based on gel-filtration and size-exclusion chromatography experiments (Brewster *et al.* 1998; Wittmeyer *et al.* 1999), approximately twice the expected 181 kDa for a single dimer of Cdc68 and Pob3. There are several possible explanations for this observation. 1) Equilibrium sedimentation studies suggest that the CP complex has a rod-like shape, with an aspect ratio of 15:1 (Wittmeyer *et al.* 1999). This elongated shape provides a plausible explanation for the observed gel filtration and size-exclusion chromatography profiles, since in both techniques steric hindrance for molecules that do not have a globular shape can influence the elution profiles (Brewster *et al.* 1998; Wittmeyer *et al.* 1999). 2) The CP dimer may associate with other proteins to generate larger complexes. 3) The CP dimer may self-associate to form oligomeric structures. To explore the last possibility, experiments were performed in parallel with those described above to assess protein-protein interactions between two Pob3 proteins and between two Cdc68 proteins.

The yeast two-hybrid fusion genes generated to assess the regions responsible for the physical interaction between Cdc68 and Pob3 were also used to assess the ability of Cdc68 and Pob3 proteins to self-associate. Each BD-fused Cdc68 polypeptide was employed in two-hybrid analysis with each of the AD-fused Cdc68 polypeptides. None of the five pairwise combinations of BD-Cdc68 and AD-Cdc68 polypeptides activated expression of two-hybrid reporter genes (Table 8). Similarly, BD-Pob3 and AD-Pob3 expressed together in yeast were unable to activate expression of the two-hybrid reporter genes (Table 8). These two-hybrid results suggest that one Pob3 protein does not physically associate with a second Pob3 protein. Based on this analysis it would appear that neither Cdc68 nor Pob3 is able to physically associate with itself. However, the inability of full-length, over-expressed Cdc68 and Pob3 Gal4-fusions to activate expression of the two-hybrid reporter genes raises the possibility that these results may not be reflective of the *in vivo* scenario. Problems similar to those described earlier for the detection of the well-established Cdc68 and Pob3 interaction using a two-hybrid

Table 8. Summary of Cdc68 *vs* Cdc68 and Pob3 *vs* Pob3 two-hybrid results

Bait protein (Gal4 DNA-binding domain fusion)	Target protein (Gal4 activation domain fusion)	Two-hybrid interaction
BD-Cdc68	AD-Cdc68	No
BD-Cdc68	AD-Cdc68(1-436)	No
BD-Cdc68	AD-Cdc68(436-1035)	No
BD-Cdc68	AD-Cdc68(308-642)	No
BD-Cdc68	AD-Cdc68(626-1035)	No
BD-Cdc68(1-436)	AD-Cdc68	No
BD-Cdc68(1-436)	AD-Cdc68(1-436)	No
BD-Cdc68(1-436)	AD-Cdc68(436-1035)	No
BD-Cdc68(1-436)	AD-Cdc68(308-642)	No
BD-Cdc68(1-436)	AD-Cdc68(626-1035)	No
BD-Cdc68(436-1035)	AD-Cdc68	No
BD-Cdc68(436-1035)	AD-Cdc68(1-436)	No
BD-Cdc68(436-1035)	AD-Cdc68(436-1035)	No
BD-Cdc68(436-1035)	AD-Cdc68(308-642)	No
BD-Cdc68(436-1035)	AD-Cdc68(626-1035)	No
BD-Cdc68(308-642)	AD-Cdc68	No
BD-Cdc68(308-642)	AD-Cdc68(1-436)	No
BD-Cdc68(308-642)	AD-Cdc68(436-1035)	No
BD-Cdc68(308-642)	AD-Cdc68(308-642)	No
BD-Cdc68(308-642)	AD-Cdc68(626-1035)	No
BD-Cdc68(626-1035)	AD-Cdc68	No*
BD-Cdc68(626-1035)	AD-Cdc68(1-436)	No*
BD-Cdc68(626-1035)	AD-Cdc68(436-1035)	No*
BD-Cdc68(626-1035)	AD-Cdc68(308-642)	No*

Table 8. Summary of Cdc68 *vs* Cdc68 and Pob3 *vs* Pob3 two-hybrid results, continued

Bait protein (Gal4 DNA-binding domain fusion)	Target protein (Gal4 activation domain fusion)	Two-hybrid interaction
BD-Cdc68(626-1035)	AD-Cdc68(626-1035)	No*
BD-Pob3	AD-Pob3	No

Combinations of Gal4 DNA-binding-domain fusion polypeptides and Gal4 activation-domain fusion polypeptides employed in two-hybrid assays are indicated. Activation of the two-hybrid reporter genes *GAL2-ADE2*, *GAL1-HIS3*, and *GAL7-lacZ* was monitored by the ability of cells to grow on synthetic medium lacking adenine (SC-Ade), to grow on synthetic medium lacking histidine and containing 3 mM 3 aminotriazol (SC-His + 3AT), and to turn blue in *lacZ* filter assays, respectively. Combinations that failed to elicit transcription of the reporter genes are indicated as 'No' in the the two-hybrid interaction column. The 'No*' response indicates that the activation of reporters was minimal, with no growth obsereved on SC-Ade and SC-His + 3 mM AT, but weak growth seen on SC-His + 2 mM 3AT and slight blue pigment development in *lacZ* filter-lift assays. A 'Yes' in the two-hybrid interaction column indicates that all reporter genes were activated, as evidenced by growth on SC-Ade and SC-His + 3 mM 3AT, and by blue colour development in *lacZ* filter-lift assays.

approach may also be at play here when assessing interactions between two Cdc68 or two Pob3 proteins using the two-hybrid system. Possible explanations for the lack of observed interaction between two Cdc68 or two Pob3 polypeptides include issues of Gal4-fusion protein stability, Gal4 domains folding to block or interfere with interacting surfaces on Cdc68 and Pob3, titration of the Gal4-fusion proteins to alternative sites through binding with the endogenous, untagged Cdc68 and Pob3 proteins, and the potential for a Cdc68 or Pob3 dimer to be inhibitory to transcription initiation when bound at a reporter-gene promoter.

Purified recombinant Pob3 polypeptides employed above in GST pull-down experiments were also used in similar pull-downs with a differently tagged Pob3 protein. A Pob3-(V5+His_6) protein (Invitrogen) was expressed in *E. coli* cells and purified using a His_6 affinity column. While the *POB3-(V5+His_6)* gene was designed to express full-length Pob3 protein C-terminally tagged with the V5 epitope, a predominant product of 40 kDa was consistently obtained from *E. coli* cells in multiple purifications. Yeast cells expressing the same *POB3-(V5+His_6)* gene generate full-length Pob3-V5-His_6 protein that can be isolated as the intact protein as determined by western blotting (Figure 20A). The 40-kDa protein species purified from *E. coli* cells contains a V5-epitope tag, as it was detected by western blotting using the HRP-conjugated V5 antibody, and therefore likely contains the C-terminal region of the Pob3 protein. Based on size estimates, this truncated species of Pob3-V5 appears to comprise the C-terminal domain of Pob3. Edman sequencing, performed at the NRC in Montreal, was used to identify the amino-terminal peptide sequence of the 40-kDa truncation of Pob3-V5. Results from the Edman sequencing indicated the presence of two slightly different polypeptides in the 40-kDa protein band: the first had the N-terminal sequence of AEAFYEELKEKA and comprised 60% of the sample, while the second species had the N-terminal sequence AVEEKSMAEAFY and comprised approximately 30% of the sample. Both of these sequences match the sequence of yeast Pob3, but from different locations. Thus the 40-kDa Pob3-(V5+His_6) purified from *E. coli* cells contained two polypeptides, one with an amino terminus at residue 221 (the major product) and a second with an amino terminus at residue 214 (the minor product). These positions map to the boundary region of the N- and C-terminal domains of Pob3 as determined by partial proteolysis studies by N. K.

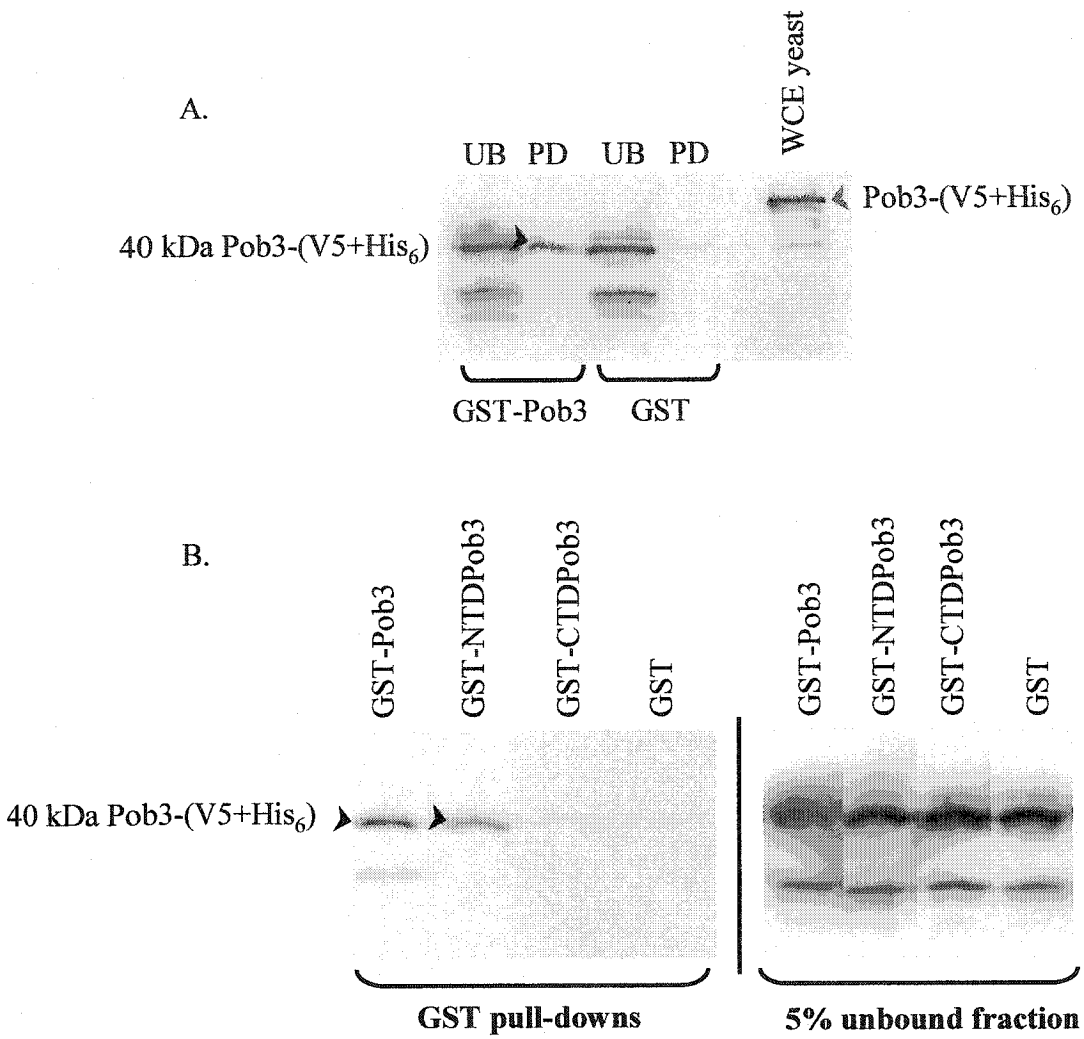

Figure 20. Pob3-Pob3 interaction. Western blots of GST pull-downs using recombinant purified Pob3-(V5+His_6) and (A) GST-Pob3 and GST or (B) GST-Pob3, GST-NTDPob3, GST-CTDPob3 and GST alone. In each case, 50% of pull-down material and 5% of unbound material was loaded per lane and Pob3-(V5+His_6) protein was detected with HRP-conjugated V5 antibody. (A) GST-Pob3 binds the 40-kDa C-terminal truncation of Pob3-V5 (residues 214-552) purified from *E. coli* cells. For comparison, 10 µg of whole-cell extract from cells expressing Pob3-(V5+His_6) (red arrowhead) was also analyzed (lane 6). PD, material from pull-down; UB, unbound fraction. (B) GST-Pob3 and GST-NTDPob3 (residues 1-215) bind the 40-kDa Pob3-(V5+His_6) recombinant polypeptide. Black arrowheads indicate the 40-kDa Pob3-(V5+His_6) polypeptide.

Brewster in our lab (unpublished data). However, those partial-proteolysis studies did not include Edman sequencing for the proteolytic peptide fragments produced, and therefore the boundaries for the two domains have not been specified. It would appear that this Pob3 truncation generated in *E. coli* fortuitously assists in defining these domain boundaries. Presumably the full-length Pob3-(V5+His_6) protein is produced in *E. coli*, but either within the cells themselves or as a result of the purification process becomes cleaved at a site readily accessible to proteolysis, most likely a domain boundary.

The 40-kDa purified Pob-(V5+His_6) polypeptides corresponding to the C-terminal domain of Pob3 were used in *in vitro* pull-down experiments with GST-Pob3, GST-NTDPob3, GST-CTDPob3, or GST alone bound to glutathione-agarose beads. Western blots of bound and unbound material from these experiments were analyzed for the presence of the Pob3-(V5+His_6) polypeptide using the HRP-conjugated V5 antibody (Figure 20A and B). Both GST-Pob3 and GST-NTDPob3 bound the 40-kDa Pob3-(V5+His_6) polypeptides containing the C-terminal domain of Pob3, while the GST-CTDPob3 and GST alone were unable to bind Pob3-V5. These *in vitro* findings indicate that Pob3 is able to self associate *in vitro* through a physical interaction between the C-terminal domain of the protein and the N-terminal domain. The relevance of this finding to the biological situation remains to be determined. This interaction may not occur *in vivo* due to the association of Pob3 with other protein partners, such as Cdc68. However, the possibility exists that this interaction may be responsible for an as-yet unidentified Pob3-Pob3 or CP-CP multimerization.

In summary, the research described in this section has identified the protein domains responsible for the interaction between Pob3 and Cdc68. The middle of three independently folded protein domains of Cdc68 (N. K. Brewster, unpublished data) is responsible for the avid association with Pob3. Some weak physical associations can be identified *in vitro* between the N-terminal domain of Cdc68 and Pob3; however, competitive co-immunoprecipitation experiments examining the *in vivo* association of N-terminal-domain deletion proteins, Cdc68-mini and Cdc68-ΔNTD, with Pob3 indicate that the N-terminally deleted proteins physically associate with Pob3 even in the presence of full-length Cdc68 protein. Additionally, the ratios of Cdc68-mini or Cdc68-ΔNTD to Cdc68 bound to Pob3 closely resemble the input ratios for these proteins, indicating that

not only do these Cdc68 N-terminal-domain deletion proteins bind Pob3, but they do so with an affinity approximately equal to that of the full-length Cdc68 protein. *In vitro* findings suggest a role for both the N- and C-terminal domains of Pob3 in binding Cdc68. The ability of Pob3 to associate with Cdc68 is diminished when either of these domains is missing. Further *in vitro* evidence helps to define the boundary between the N- and C-terminal domains of Pob3 at residues 214-221, and suggests that the N- and C-terminal domains of Pob3 physically associate with one another. The conclusions of this structural analysis are depicted in Figure 18.

2. Isolation and characterization of novel *cdc68* mutant alleles

i) Generation of dominant *cdc68* alleles that cause defects in chromatin structure

To further understand the function of the Cdc68 component of FACT, a selection scheme to identify novel mutant forms of Cdc68 was undertaken. This selection for new *CDC68* mutations was designed to specifically identify mutations that result in anomalous chromatin structure. At the onset of my studies very few *CDC68* alleles had been characterized, and those that had been identified were shown to harbour mutations within the 5' region of the gene. A single allele of *CDC68*, known variously as *cdc68-1* (Prendergast *et al.* 1990; Rowley *et al.* 1991), *spt16-197* (Winston *et al.* 1984; Malone *et al.* 1991) and *cdc68-11* (Lycan *et al.* 1994) as it was identified independently in three different labs, encodes a glycine-to-glutamate substitution at residue 132 in the N-terminal region of Cdc68. A second allele, *cdc68-Δ922* was created in the Singer lab to contain a large N-terminal deletion (see Figure 30; Evans *et al.* 1998). Therefore, a strategy to generate novel mutant alleles of *CDC68* was employed such that the mutations identified would affect the previously uncharacterized C-terminal two-thirds of the protein and cause phenotypes indicative of chromatin structural changes, as evidenced by alterations in transcription.

New dominant mutations affecting Cdc68 were selected for based on alterations in Spt (suppressor of Ty1) reporter-gene expression. Spt reporter genes are classically used to indicate defects in transcription machinery and chromatin structure (Winston *et al.* 1984; Formosa 2003). Typically, the reporter genes employed here, *his4-912δ* and *lys2-128δ*, do not generate functional His4 and Lys2 protein products, resulting in histidine and lysine auxotrophy. Defects in the transcription machinery or chromatin structure can

allow transcription of these reporters from otherwise silenced promoter sites, which ultimately leads to the production of functional His4 and Lys2 enzymes, conferring on cells the ability to grow on media lacking histidine or lysine (Figure 21). Recent literature has proposed a simple and clear model for how these new promoter sites become accessible (Kaplan *et al.* 2003). This new model proposes that mutations in chromatin modulators, such as FACT, cause anomalous conformations in chromatin behind the elongating RNA polymerase. This perturbation in chromatin structure permits DNA that would typically be inaccessible, due to its association with nucleosomes, to be accessible to the transcription initiation machinery. Thus these typically silenced promoters, or cryptic promoters, may now be recognized as sites for transcription initiation.

To introduce mutations in specific regions of *CDC68*, PCR mutagenesis was employed (Muhlrad *et al.* 1992). Regions of the *CDC68* gene, approximately 1 kb in length, were amplified *via* PCR using *Taq* DNA polymerase which lacks proof-reading capabilities. Without the ability to remove mis-incorporated deoxynucleotides, *Taq* DNA polymerase makes one error per 10^4 or 10^5 deoxynucleotides (Zhou *et al.* 1991). Some PCR reactions contained decreased levels of dATP available to the polymerase, thereby increasing the error frequency in these reactions, while other PCR reactions relied solely on the error rate of *Taq* under standard conditions (Materials and Methods). These PCR fragments, along with an appropriately digested plasmid-borne *CDC68* gene (Figure 22), were co-transformed into either *CDC68* or *cdc68-1* yeast cells (AW11-9a and AFO-I2, respectively; see Table 2 for descriptions). Homologous recombination within the organism allowed repair of the gapped plasmid with the linear PCR fragments to regenerate a full-length *CDC68* gene that potentially harboured mutational changes. Transformants were then replica-plated to medium lacking histidine or lysine and allowed to grow at 23°C or 30°C for 3-4 days. Colonies exhibiting an Spt$^-$ phenotype, characterized by the ability to grow on histidine- and lysine-deficient media, were selected and 206 isolates found to be dominant to *CDC68* or *cdc68-1* for their ability to generate Spt$^-$ phenotype (Table 9). To ensure that the Spt$^-$ phenotype was dependent on the presence of the *cdc68* plasmid, two approaches were taken. First, plasmids were isolated from 38 of the transformants that continued to grow under the selective conditions and these plasmids were re-transformed into cells of the starting strains (both

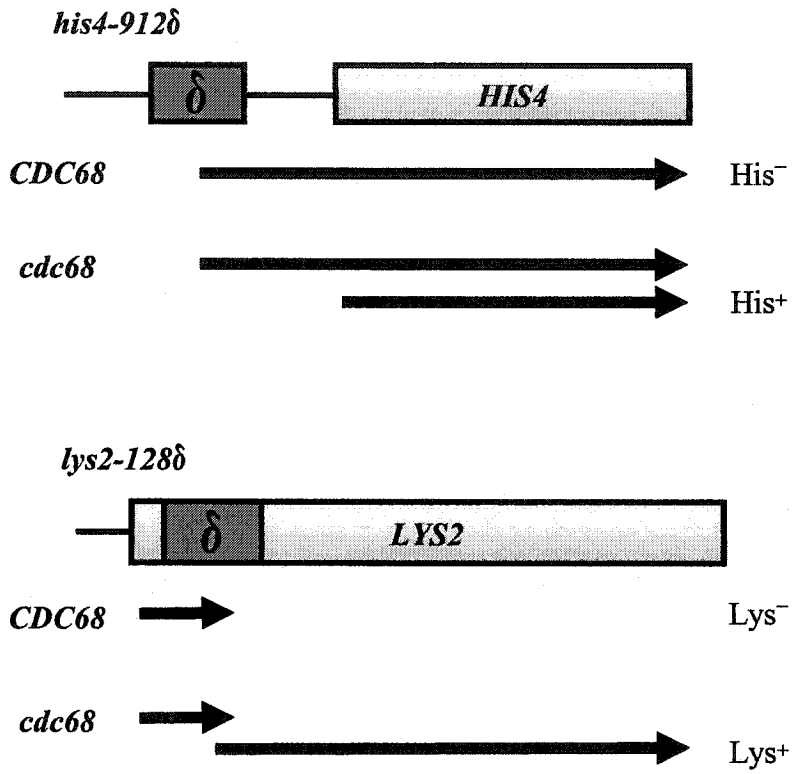

Figure 21. Spt reporter genes. Shaded boxes represent the coding region for the *HIS4* and *LYS2* genes, respectively. Transcripts generated in the wild-type and mutant scenarios are shown as black arrows and the resultant phenotype is given at the right. Ty1 delta-element insertion is indicated by a dark grey box with a δ. (Adapted from Hekmatpanah *et al.* 1991)

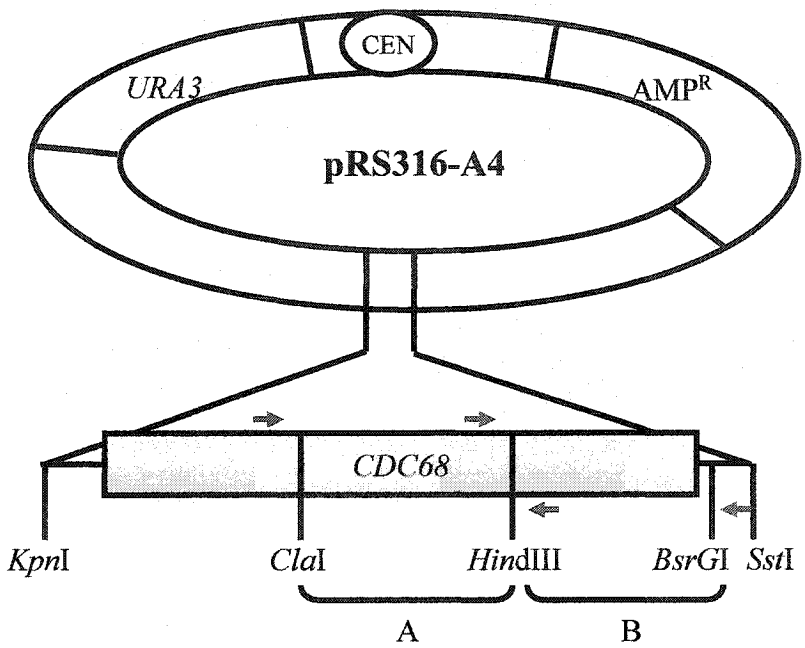

Figure 22. Regions of *CDC68* subjected to PCR mutagenesis. This diagram depicts the 9.1-kbp plasmid pRS316-A4 that was used both as a template to generate the mutagenic PCR fragments (primer pairs indicated as pairs of coloured arrows) and to generate the gapped plasmid for repair. Region A is a 1689-bp portion of *CDC68* (nucleotides 772 – 2461 of the *CDC68* coding sequence) that was PCR-amplified by the blue primer pair; the corresponding gap-repair plasmid was generated by *Cla*I and *Hin*dIII digestion. Region B is a 1463-bp fragment of *CDC68* (from nucleotide 2109 of *CDC68* coding sequence to 375 nucleotides downstream of the *CDC68* stop codon) that was PCR-amplified by the red primer pair; the corresponding gap-repair plasmid was generated by *Hin*dIII and *Bsr*GI digestion. *Kpn*I and *Sst*I sites were used to insert the *CDC68* sequence into the pRS316 vector backbone (Sikorski and Hieter, 1989). The *Hin*dIII and *Sst*I sites shown above are 2.7-kbp apart.

Table 9. Summary of Cdc68 mutants generated and verifications performed

Chromosomal *CDC68* allele (yeast strain)	***CDC68*** **(AW11-9a)**	***cdc68-1*** **(AFO-I2)**
Isolates	122	84
Plasmid loss verification (number of pls-dependent events/ total tested)	122 (71/122)	4/84 (2/4)
Verified by re-transformation (number of pls-dependent events/ total tested)	13/122 (0/13)	25/84 (23/25)
Alleles sequenced	0	11
Sequenced alleles found to contain E763G mutation	ND	9/11
Presence of E763G mutation assessed by *Hin*dIII digest (number containing E763G mutation/ total tested)	ND	78/84 (51/78)

pls – plasmid

E – glutamic acid

G – glycine

763 – refers to the amino acid position in Cdc68 protein

AW11-9a and AFO-I2, regardless of the strain in which the PCR-mutagenized allele was identified) to ensure that the Spt$^-$ phenotype observed was plasmid-dependent. In this way, 23 of the 38 *cdc68* plasmids were shown to regenerate the Spt$^-$ phenotype upon retransformation into *CDC68* or *cdc68-1* cells. For an additional 109 isolates, the Spt$^-$ phenotype was determined to be plasmid-associated based on the results of plasmid-loss experiments, where the selection for the presence of the *URA3* marker-gene on the newly mutagenized plasmid was no longer maintained. Cells within the population that fail to inherit the *cdc68* plasmid will not experience growth impairment under these conditions as the growth medium was supplimented with uracil, histidine and lysine, which would otherwise be required by the uracil auxotrophic and Spt$^+$ starting strains. Single colonies from these cultures were then grown on solid non-selective medium and subsequently replica-plated to conditions that would establish the plasmid and Spt status of colonies. In this way the dependence of the Spt$^-$ phenotype on the plasmid bearing the new *cdc68* mutants was confirmed. Of the 109 isolates tested *via* plasmid loss, 71 were confirmed to be the source of the Spt$^-$ phenotype (Table 9). From the collection of *cdc68* mutant alleles verified to be the source of the Spt$^-$ phenotype by either method, 11 were sequenced to determine the base-pair changes and the resulting amino acid substitutions responsible for the underlying chromatin structure alterations. Table 10 summarizes the mutational changes in the sequenced alleles and Figure 23 shows the associated Spt$^-$ phenotype.

Although approximately two thirds of the *CDC68* gene was subjected to PCR mutagenesis, the mutations associated with an Spt$^-$ phenotype clustered in the carboxy-terminal third of the gene (Figures 24 and 25). The substitution of a glutamate at position 763 with a glycine residue was encoded in 9 of the 11 sequenced alleles. This residue is absolutely conserved in Cdc68 proteins from a wide variety of eukaryotes (Figure 24). The mutation causing this substitution fortuitously abolishes a *Hin*dIII restriction endonuclease recognition site, allowing the remaining new mutant forms to be screened for this mutational change based on restriction digestion pattern. The collection of *cdc68* mutant alleles identified in the AFO-I2 strain was screened in this way by myself, Jeff Coles, and Cheri Adams. The *cdc68* plasmids were extracted from the yeast strains, passaged through *E. coli* and digested in one reaction with both *Hin*dIII and *Sst*I. The

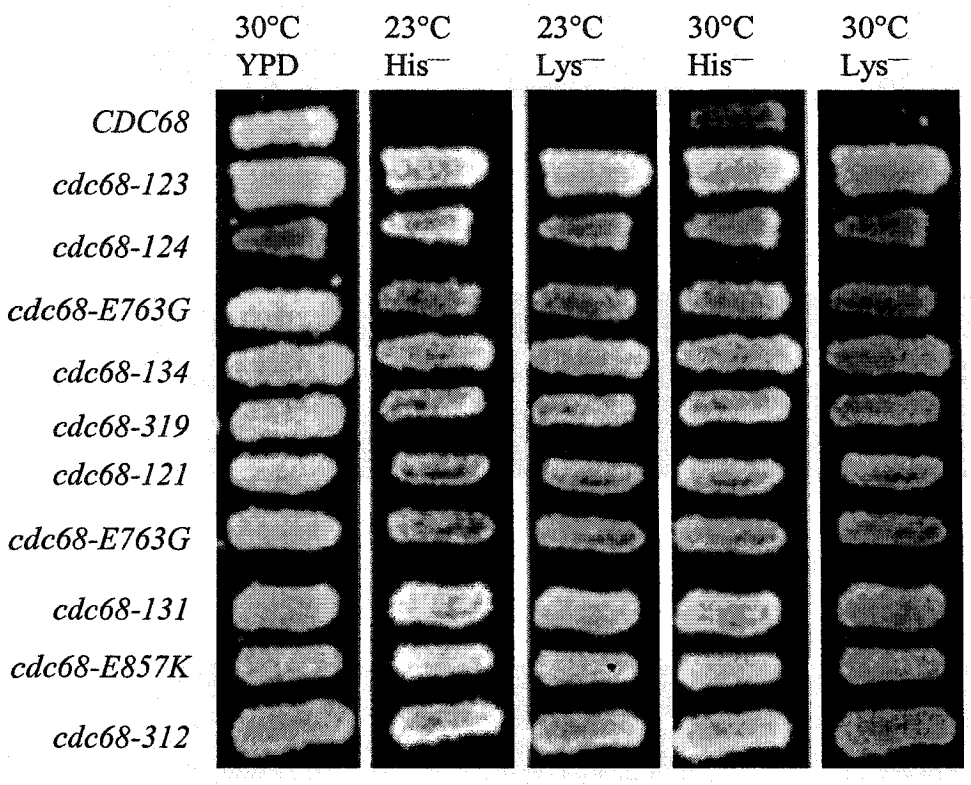

Figure 23. Spt⁻ phenotype of the sequenced *cdc68* alleles generated in this study. Cells were streaked in a patch on YPD medium, grown for two days at 30°C and then replica-plated to the above conditions and permitted to grow an additional 4 days. Note that there are two different *cdc68-E763G* isolates shown here. At the time of this experiment it was not known that these two isolates contained the same mutational change, and as a result this allele is represented twice in the collection of sequenced alleles.

Table 10. Summary of sequence changes in novel *cdc68* alleles.

Allele	Nucleotide substitution(s) in the coding strand	Amino acid substitution(s)
cdc68-E763G (isolate nm24)	A2288G	**E763G**
cdc68-E763G (isolate nm33)	A2288G	**E 763G**
cdc68-E857K (isolate nm34)	G2569A	E857K
cdc68-121 (isolate nm21)	A1088G, A1947G, A2288G	N363S, E649E, **E763G**
cdc68-122 (isolate m22)	T894C, A935T, A1053G, A1350G, T2039C, A2067G, A2288G, A2347G	C298C, E312D, K351K, E450E, L680P, K692K, **E763G**, R783G
cdc68-123 (isolate nm23)	A1967G, A2204G, A2288G	E 656G, E735G, **E736G**
cdc68-124 (isolate m24)	T2081C, T2171C, A2261G, A2288G, T2310C, T2344C	V694A, I 724T, K754R, **E763G**, D770D, F782L
cdc68-131 (isolate nm31)	A2288G, T2298C, T2737A	**E763G**, D766D, W913R
cdc68-134 (isolate m34)	A2174G, A2288G, A2417G, T2444C, T2657C, A2897C, A3017G	K725R, **E763G**, K806R, I815T, V886A, E966A, Y1006C
cdc68-312 (isolate m312)	A2288G, A2350G, T2455C, T2856C, A2936G	**E763G**, R784G, S819P, F9522F, V979V
cdc68-319 (isolate m319)	T2410C, T2765C, T2836C, T2888C, A3010G, T3020C	L804P, T922T, L946S, D963D, D1004G, T1007T

A, C, G, T in the nucleotide substitutions column represent nucleic acid bases and numbers indicate the position in the coding sequence of *CDC68*.

In the amino acids substitutions column, amino acids are represented by their single letter designations and numbers indicate the position of the substitutions in the coded Cdc68 polypeptide sequence. The E763G amino acid substitution is shown in bold to highlight alleles encoding this substitution.

Figure 24. Alignment of Cdc68 protein homologues. Identical and conserved amino acids are shown on a black or grey background, respectively. Amino acids are represented by their standard single-letter abbreviations. ◆ indicates amino acid 763 in the *S. cerevisiae* sequence.

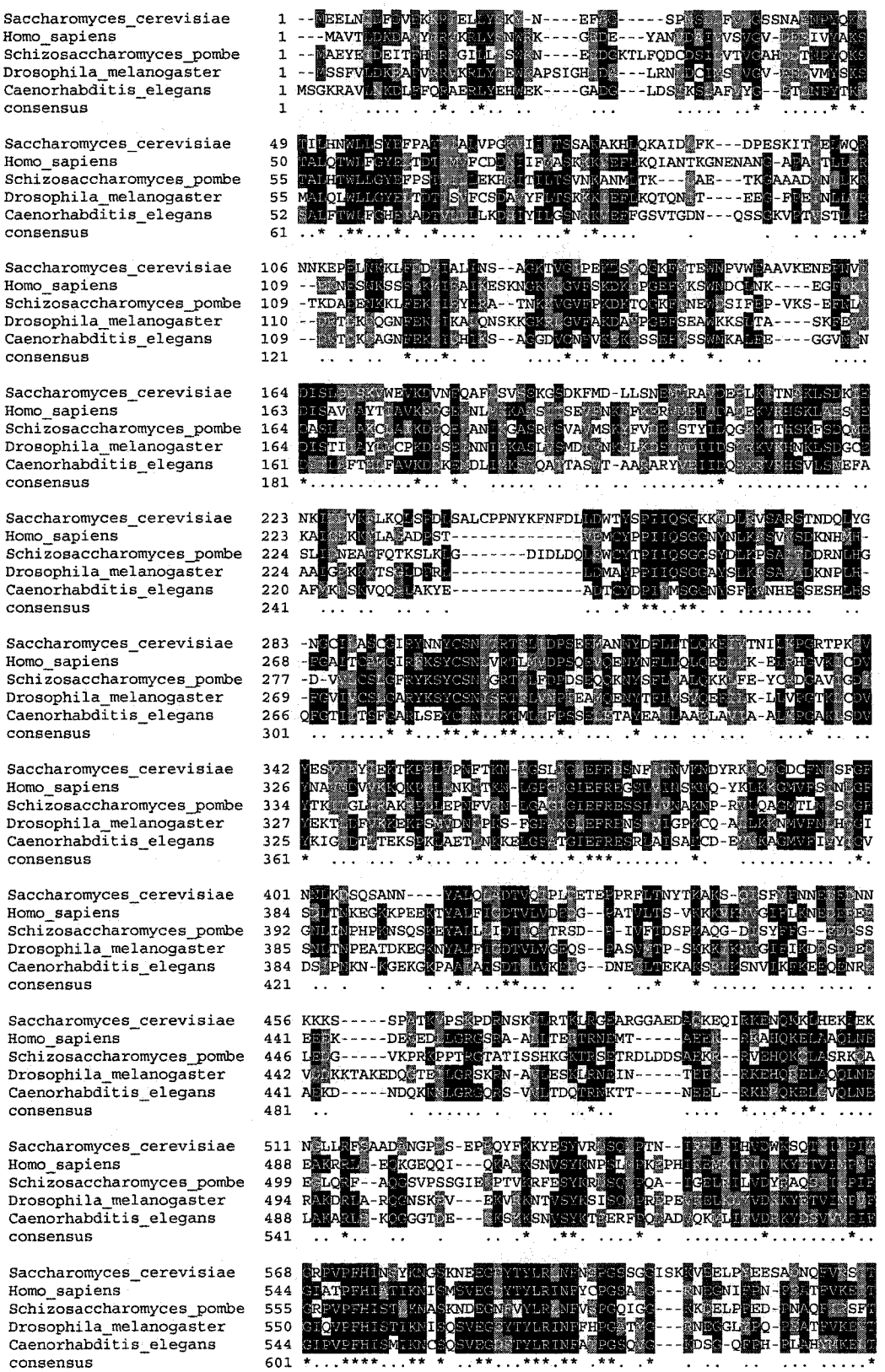
Saccharomyces_cerevisiae
Homo_sapiens
Schizosaccharomyces_pombe
Drosophila_melanogaster
Caenorhabditis_elegans
consensus

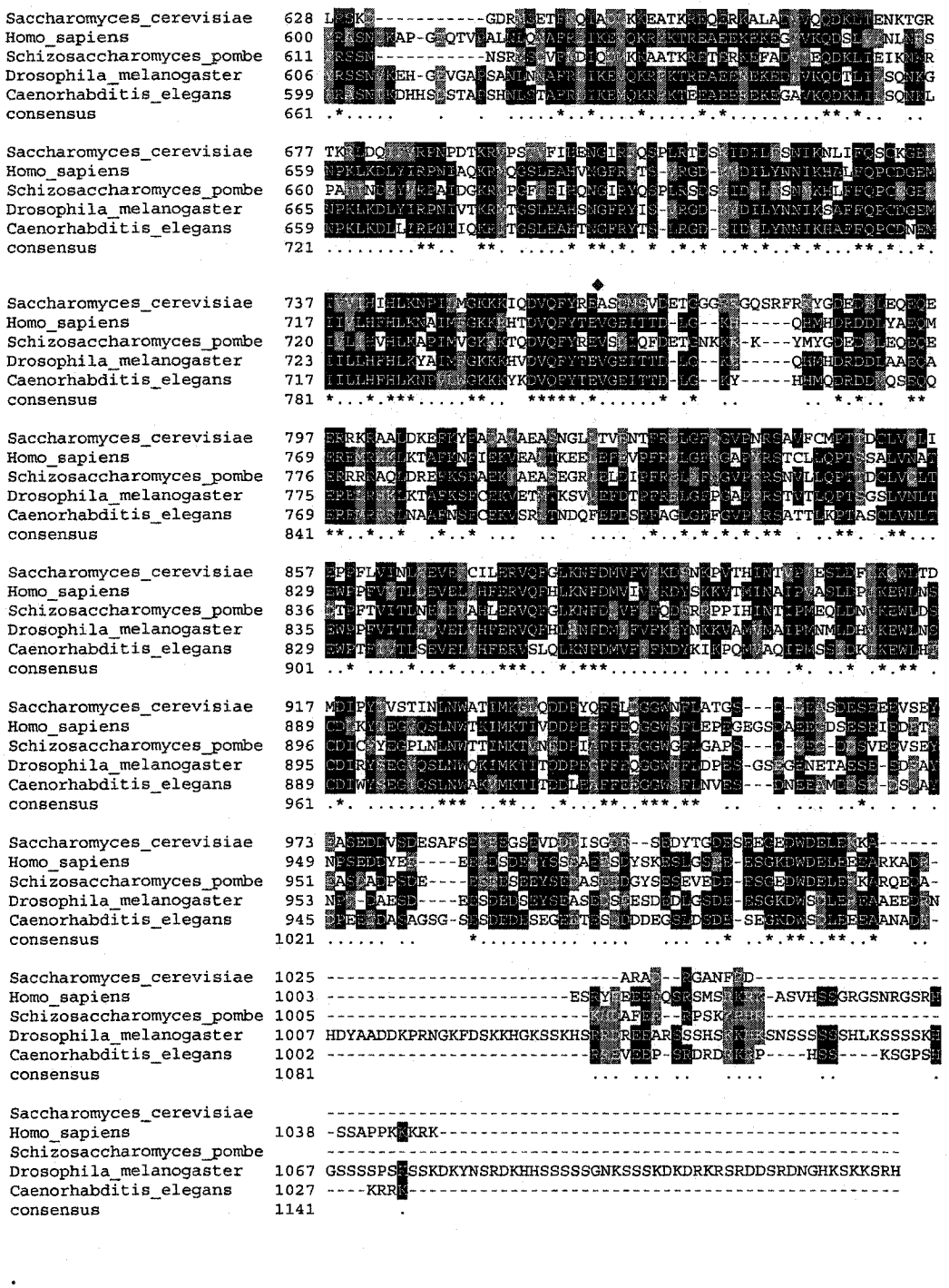
Saccharomyces_cerevisiae
Homo_sapiens
Schizosaccharomyces_pombe
Drosophila_melanogaster
Caenorhabditis_elegans
consensus

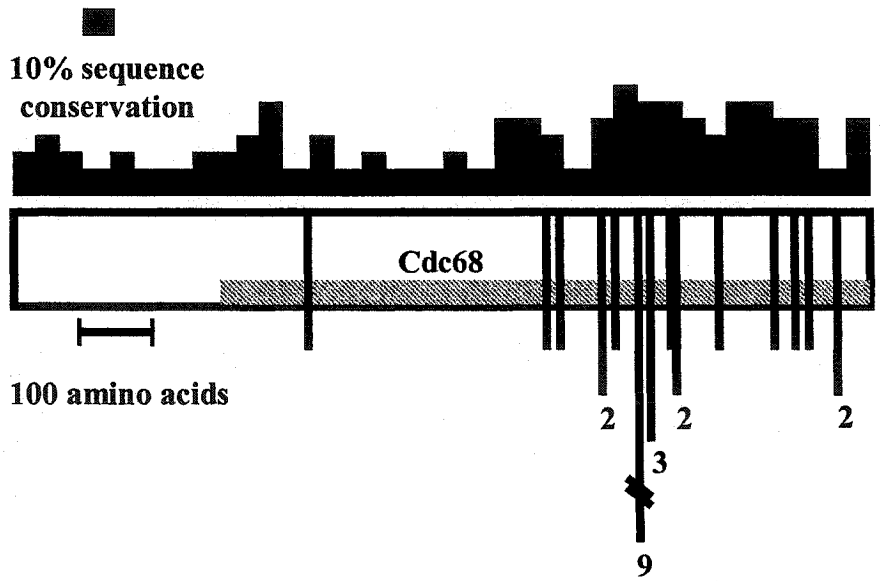

Figure 25. Summary of sequence changes in eleven of the Cdc68 mutant proteins generated in this study. Amino acid substitutions are represented by vertical lines through the Cdc68 protein (white box). Increased length of lines with numbers represents substitutions found in more than one allele. The grey hatched bar indicates the protein-coding region of the gene that was subjected to mutagenesis. The black boxes across the top show the percent sequence conservation in an alignment of Cdc68 proteins from *H. sapiens*, *M. musculus*, *D. melanogaster*, *S. cerevisiae*, and *C. elegans*.

resulting DNA fragments were resolved by agarose gel electrophoresis. This procedure allowed the mutant plasmids to be classified into two groups: 1) those that contained the mutation at codon 763, had therefore lost the *Hin*dIII recognition site, and generate a single 9.1-kbp DNA fragment upon restriction digestion (resulting from cleavage of the plasmid at the unique *Sst*I site; Figure 22), and 2) those that contained the wild-type sequence at codon 763, had therefore retained an intact *Hin*dIII recognition site, and generated 2.7-kbp and 6.4-kbp DNA fragments (resulting from cleavage of the plasmid at both the *Hin*dIII and *Sst*I sites; Figure 22) (Table 9 and data not shown). Future studies with this mutant collection that are now underway in the Singer lab will be facilitated by this classification, as it prevents the repeated characterization of mutants containing the codon-763 substitution. It will be interesting to see if the mutational clustering observed to date is maintained when more alleles from this collection are characterized.

The functional significance of the apparent mutational clustering affecting the C-terminal third of Cdc68 is unclear. These mutations alter what we know to be an independently folded C-terminal domain (CTD) and its junction with the middle domain of Cdc68. While the Cdc68 protein is conserved throughout its length, the C-terminal region is the most highly conserved region (Figures 24 and 25). This region may play a key role in effecting Cdc68-mediated chromatin structural changes, and therefore mutations here may be more likely to produce the observed Spt$^-$ phenotype. However, several N-terminal Cdc68 mutations and deletions display a recessive Spt$^-$ phenotype (section iv below; Malone *et al.* 1991; Evans *et al.* 1998; Formosa *et al.* 2001). Additionally, the region that lacks mutational changes corresponds roughly to the middle domain of the Cdc68 protein (N. K. Brewster, unpublished data). This region is required for Pob3 binding (Figures 12 and 18); thus mutations in this region may not be found because weakening the association with Pob3 no longer produces a Cdc68 protein able to exert a dominant effect. For example, the weakened interaction of mutant Cdc68 with Pob3 may result in less of the novel mutant form incorporated into FACT, thereby lessening the opportunity for this Cdc68 protein to exert a dominant effect. Such mutant proteins may be deleterious for the cell if they are incorporated into FACT. The weakly associated FACT complex may lead to a dominant-lethal phenotype, rather than the

desired Spt⁻ phenotype, by significantly reducing the level of optimally functioning FACT.

ii) New Cdc68 mutants supply essential function

Each of the new Cdc68 mutants generated in this study, for whom the amino acid changes are known, is able to provide essential Cdc68 functions when present as the only version of Cdc68 in yeast. This was determined by transforming each of the plasmid-borne mutant alleles into cells of strain BM64 (Malone *et al.* 1991), a diploid yeast strain containing a disrupting *LEU2* insertion in one chromosomal *CDC68* genes, and then sporulating the resultant transformants. Spore products from complete tetrads were assessed for growth on synthetic medium lacking leucine or uracil to determine if they contained the *spt16-101::LEU2* disrupted chromosomal *CDC68* gene and the *URA3*-marked, plasmid-borne mutant *cdc68* allele. Cells that were both leucine and uracil prototrophs were concluded to be kept alive by the *cdc68* mutant allele (data not shown). Each of the mutant *cdc68* alleles, when present as the only version of *CDC68*, still causes an Spt⁻ phenotype, as determined by growth on medium lacking either histidine or lysine (data not shown). Two of the alleles, *cdc68-312* and *cdc68-319*, also confer temperature sensitivity at 39°C (Figure 27).

The *spt16-101::LEU2* disruption allele still retains the chromosomal *CDC68* sequence. To eliminate the possibility of *cdc68* mutant allele repair through recombination with the remaining chromosomal *CDC68* sequences in *spt16-101::LEU2*, a complete replacement of the *CDC68* coding region with the *kanMX4* cassette (Wach, A. *et al.* 1994) was created in a derivative of the BM64 diploid (Materials and Methods). This new diploid, called KanB, contains a wild-type *CDC68* gene and the *cdc68Δ::kanMX4* deletion/replacement, which confers dominant geneticin resistance. The KanB diploid was then transformed with plasmids containing the following new *cdc68* alleles: *cdc68-E763G* (both isolates), *cdc68-E957K*, *cdc68-121*, *cdc68-123*, *cdc68-124*, *cdc68-131*, *cdc68-134*, *cdc68-312*, and *cdc68-319* (*cdc68-122* was not characterized further due to technical difficulties in obtaining the plasmid bearing this allele). Haploid spore products from complete tetrads shown to contain the *cdc68Δ::kanMX* allele and the plasmid-borne *cdc68* allele, as determined by geneticin resistance and uracil prototrophy, respectively, once again provided evidence that each of these mutant alleles encodes a

protein that is able to provide essential Cdc68 function (data not shown). These KanB haploid segregants containing *cdc68Δ::kanMX* and a plasmid-borne mutant allele of *cdc68* were employed in most subsequent characterizations.

iii) New Cdc68 mutant proteins are present at wild-type levels in cells at 30°C

Since an alteration in the level of Cdc68 protein in cells has been shown to produce an Spt$^-$ phenotype (Malone *et al.* 1991; Xu, Q. *et al.* 1993; Brewster *et al.* 1998), I performed western blot analyses to assess Cdc68 protein levels in the ten KanB haploid segregants containing *cdc68Δ::kanMX4* in the chromosome and kept alive by a centromeric plasmid containing a *cdc68* mutant allele. Total protein extracts were resolved by SDS-PAGE and analyzed by western blotting using affinity-purified polyclonal Cdc68 antibodies. Results showed that Cdc68 protein abundance in each of these strains was not significantly altered in comparison to that in the wild-type control (Figure 26). Thus an altered Cdc68 protein abundance does not account for the Spt$^-$ phenotype caused by these *cdc68* alleles. Further evidence to support this finding comes from the fact that these *cdc68* mutations cause an Spt$^-$ phenotype at both 23°C and 30°C, while overexpression of wild-type *CDC68* only results in an Spt$^-$ phenotype at 30°C, and not at 23°C (data not shown).

iv) N-terminal and C-terminal Cdc68 alterations cause similar phenotypes

To explore the functional nature of Cdc68 protein domains, genetic characterization of *cdc68* mutations encoding deletions or alterations in various regions of the protein was undertaken. Cells containing each of the ten new sequenced alleles of *cdc68* generated in this study (Results 2, i) encoding mutational changes in the C terminus of Cdc68, four *spt16/cdc68* N-terminal point-mutant alleles (Formosa *et al.* 2001) and three *cdc68* N-terminal deletion mutations (Evans *et al.* 1998; N. K. Brewster and J. Kurniawan, unpublished data) were assessed for sensitivities to a range of conditions. In this way, linkages between the mutational changes in specific regions of Cdc68 and associated mutant phenotypes were sought.

Initially, cells bearing my *cdc68* C-terminal mutations *cdc68E763G* (both isolates), *cdc68-E957K*, *cdc68-121*, *cdc68-123*, *cdc68-124*, *cdc68-131*, *cdc68-134*, *cdc68-312*, or *cdc68-319* were characterized for additional growth defects under a variety of conditions. Growth of these cells in the presence of high salt concentrations, sorbitol, caffeine,

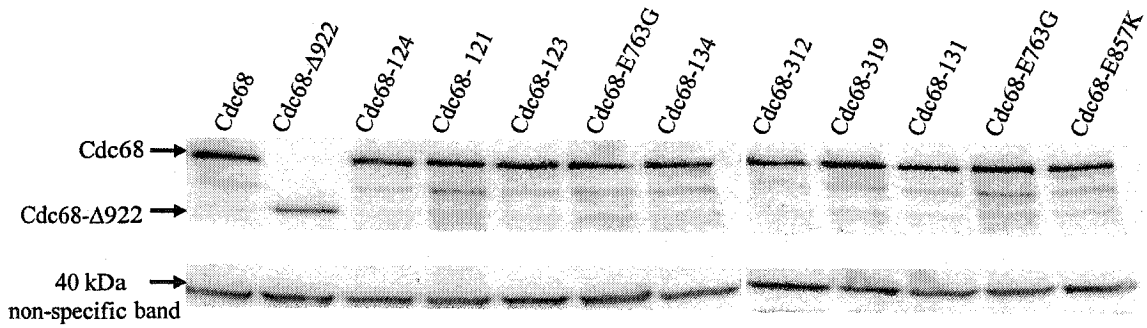

Figure 26. Western blot of total protein extracts from cells containing Cdc68 mutant proteins. The mutant protein present is indicated above the corresponding lane. Cdc68 protein was detected with anti-Cdc68 polyclonal antibodies. 8 μg of total protein extract (determined by Bradford assay) from cells grown logarithmically at 30°C was loaded per lane. India-ink staining of total proteins after transfer (not shown) and a 40-kDa non-specific band detected in each lane were used to ensure equivalent loading and transfer of proteins. Abundance of mutant Cdc68 proteins appears equivalent to that of wild-type Cdc68 controls. Therefore, the Spt^- phenotype observed in these mutant strains at 30°C is not the result of increased Cdc68 dosage.

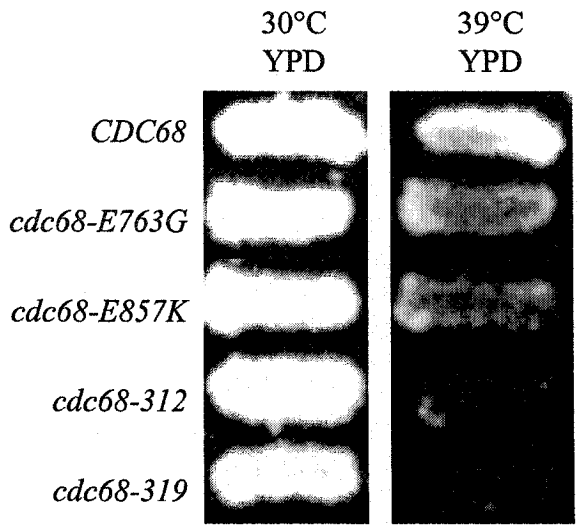

Figure 27. *cdc68-312* and *cdc68-319* temperature sensitivity. Cells were inoculated as patches onto YPD solid medium and allowed to grow for 2 days at 30°C, at which point they were replica-plated to the above conditions and grown for 4 days. All alleles indicated were present on centromeric (*CEN*) plasmids which are maintained at 1-2 copies per cell.

hydroxyurea, mycophenolic acid, 6-azauracil, ethanol, formamide, glycerol, and under conditions of low pH, elevated temperature, inositol deprivation or nitrogen starvation were all assessed. The phenotypes examined are linked to defects in a wide range of cellular processes (Hampsey 1997), and were chosen based on ease of assessment or due to their direct relationship with the already characterized Cdc68 functions of transcription and replication, such as sensitivity to inositol deprivation, hydroxyurea, mycophenolic acid, and 6-azauracil. For the majority of conditions tested, all of the mutant strains were able to grow as well as the wild-type *CDC68* control strain (data not shown). Notable exceptions to this are the 39°C temperature sensitivities (Figure 27) and hydroxyurea sensitivities (Figure 28) exhibited by the *cdc68-312* and *cdc68-319* strains (Table 11).

During the course of my research, the Formosa lab also generated a collection of *spt16/cdc68* mutant alleles using a different selection scheme (Formosa *et al.* 2001). To complement my study of C-terminal *cdc68* mutations I assessed several of the 'Formosa' alleles that encode proteins with N-terminal mutations. These mutant alleles were introduced in my *cdc68Δ::kanMX4* haploid strain by a plasmid-shuffling procedure (Materials and Methods) and assessed for the subset of sensitivities shown above to be associated with the C-terminal mutations. To verify that repair of these alleles during the plasmid-shuffling procedure had not occurred, the plasmid from each of the final strains was extracted and the region known to contain the specific mutations was sequenced (data not shown). Each of these mutants displays an Spt^- phenotype and varying degrees of temperature sensitivity (Figure 29 and Table 11), but did not display any significant sensitivity to hydroxyurea at 30°C. My findings for the phenotypes associated with these mutant alleles are consistent with those reported by the Formosa lab (Formosa *et al.* 2001), except that the maximal permissive growth temperature supported by each allele was slightly greater in most cases. These subtle changes may be the result of the different genetic backgrounds employed, or incubator differences between the two labs.

To further enrich this study, several *CDC68* N-terminal deletion mutations (Figure 30), *cdc68-Δ922* (Evans *et al.* 1998), *cdc68-ΔNTD* (N. K. Brewster, unpublished data), and *cdc68-Δ369* (J. Kurniawan, unpublished data), were also assessed in a similar fashion. These N-terminal deletion mutations each caused temperature and hydroxyurea sensitivities to varying degrees (Figure 31). Additionally, the *cdc68-Δ369* and *cdc68-*

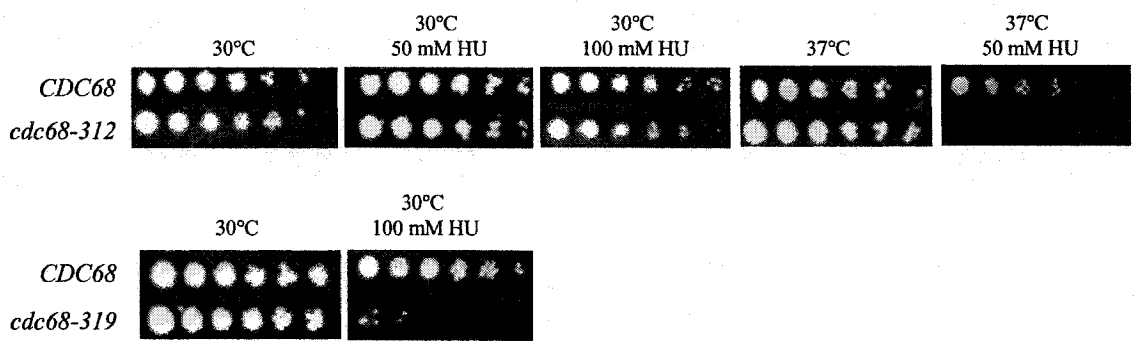

Figure 28. Hydroxyurea sensitivity of *cdc68-312* and *cdc68-319* mutant cells. Cells were grown to log phase in YPD liquid medium at 30°C and concentrations determined by Coulter Counter measurements. Five-fold serial dilutions of cultures were spotted on YPD medium with or without hydroxyurea (HU), starting at a concentration of 1 x 10^7 cells/ml.

Table 11. Phenotypes for N-terminal and C-terminal Cdc68 mutants

Allele	YPD			His^-Lys^-	100 mM HU	
	30°C	37°C	39°C	30°C	30°C	37°C
CDC68	+++	+++	+++	–	+++	+++
cdc68-312	+++	+++	–	+++	+++	–
cdc68-319	+++	++	–	+++	–	–
cdc68-8	+++	+++	–	+++	+++	ND
cdc68-12	+++	+++	–	+++	+++	ND
cdc68-16a	+++	–	–	+++	++	ND
cdc68-24	+++	+++	–	+++	+++	ND
cdc68-ΔNTD	+++	+++	–	+	+++	–
cdc68-Δ922	+++	+++	+	+++	+++	–
cdc68-Δ369	+++	++	–	+++	+	–

Symbols: (+++) good growth; (++) moderate growth; (+) poor growth; (–) no growth

cdc68-312 and *cdc68-319* contain mutations altering the C terminus of Cdc68. *cdc68-8*, *cdc68-12*, *cdc68-16a*, and *cdc68-24* contain point mutations affecting the N-terminal domain (Formosa *et al.* 2001). *cdc68-ΔNTD*, *cdc68-Δ922*, and *cdc68-Δ369* are deleted for regions encoding the N-terminal domain.

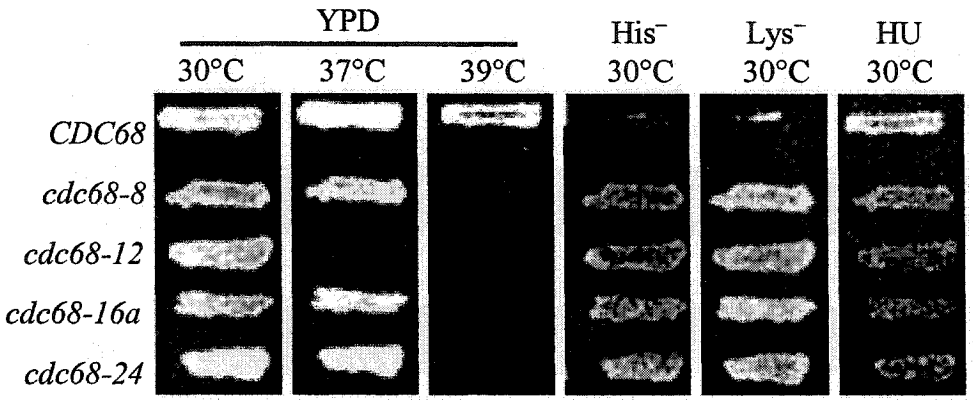

Figure 29. Phenotypes caused by Cdc68 mutant proteins with of N-terminal substitutions. Several *cdc68* alleles containing N-terminal point mutations (Formosa *et al.* 2001) in cells with the *cdc68Δ::kanMX4* chromosomal deletion (haploid spore products from the KanB diploid) were assessed for growth defects. Cells were placed on solid growth medium in patches and permitted to grow at 30°C for 2 days, at which point they were replica-plated to the above conditions and grown for 4 days. HU = YPD medium containing 100 mM hydroxyurea, His− = SC medium lacking histidine, Lys− = SC medium lacking lysine.

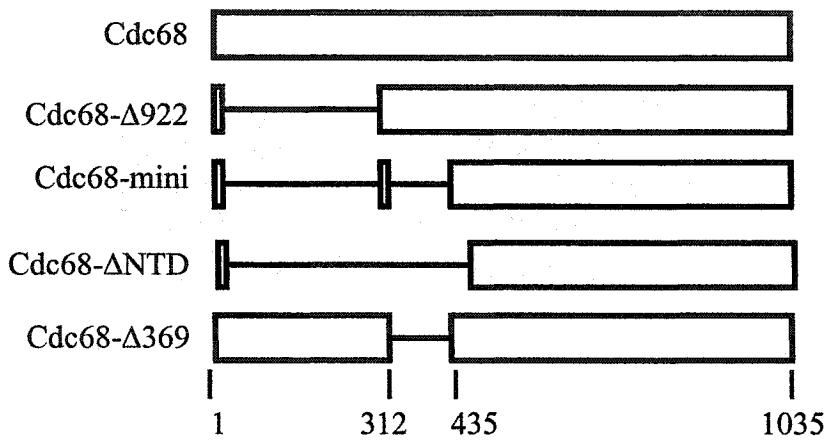

Figure 30. N-terminal deletion mutations of Cdc68. Schematic of protein-coding regions of the various N-terminal deletion alleles of *CDC68* described in this study. Numbers along the bottom indicate codons within the coding region of Cdc68. Boxes indicate intact regions, while lines indicate deleted regions of coding sequence. The intact coding sequence for Cdc68 encodes residues 1-1035, while Cdc68-Δ922 lacks residues 7-307; Cdc68-mini lacks residues 7-307 and 312-435; Cdc68-ΔNTD lacks residues 2-484; and Cdc68-Δ369 lacks residues 312-435.

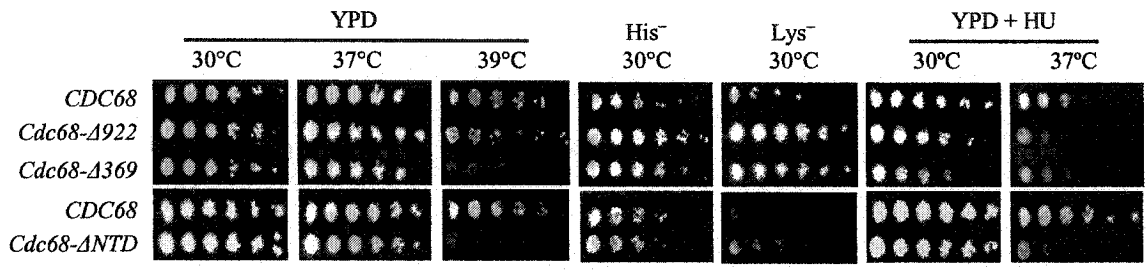

Figure 31. Phenotypes caused by Cdc68 mutant proteins with N-terminal deletions. Several *cdc68* alleles containing N-terminal deletion mutations (Evans *et al.* 1989; J. Kurniawan and N. K. Brewster unpublished observations) present in cells containing a *cdc68Δ::kanMX4* chromosomal deletion (a haploid spore product from the KanB diploid) were assessed for growth defects. Five-fold serial dilutions (starting at 1 x 10^7 cells/ml as determined from cell concentration assessments made using a Coulter Counter) from stationary-phase cultures were spotted and allowed to grow for 4 days. HU = YPD medium containing 50 mM hydroxyurea, His– = SC medium lacking histidine, Lys– = SC medium lacking lysine.

Δ922 deletions produced an Spt⁻ phenotype (Figure 31). The Spt⁻ phenotype associated with *cdc68-Δ922* has been previously reported (Evans *et al.* 1998).

Thus *cdc68* alleles that encode mutations affecting the N- or C-terminal region of the protein can cause a similar subset of phenotypes, namely Spt⁻ phenotype, temperature sensitivity, and hydroxyurea sensitivity. Does this imply that the N- and C-terminal domains of Cdc68 share a common function, or do these independently folded regions of the protein function *via* separate mechanisms that happen to result in similar phenotypic profiles? Strategies to determine the underlying molecular mechanisms leading to the temperature and hydroxyurea phenotypes were pursued to try to distinguish between these two possibilities.

v) Cdc68 N-terminal mutations produce unstable protein products

In a screen for suppressors of the *cdc68-Δ922* temperature sensitivity, J. Kurniawan identified the *cdc68-mini* allele, which encodes a protein containing an additional N-terminal deletion to that encoded by *cdc68-Δ922* (Figure 30). The Cdc68-mini protein is missing approximately 40% of the Cdc68 coding sequence. Remarkably, cells containing the Cdc68-mini protein are Spt⁺ and show no sensitivity to growth at elevated temperatures (J. Kurniawan unpublished data; data not shown). The region deleted in *cdc68-mini* roughly corresponds to the independently folded N-terminal domain of Cdc68 (N. K. Brewster, unpublished data). Based on this finding, a more precise resection of the N-terminal domain, known as *cdc68-ΔNTD*, was generated in our lab by N. K. Brewster (Figure 30). Both the Cdc68-mini and Cdc68-ΔNTD polypeptides provide essential Cdc68 function (data not shown; Figure 31). Moreover, cells containing these mutant alleles display only moderate growth defects. These results indicate that the N-terminal domain of Cdc68 is dispensable for essential Cdc68 function. How then are N-terminal point mutations able to cause more severe phenotypes than the deletion of the domain that harbours these mutational changes? One hypothesis is that mutations in this regions result in unstable protein products, and the resulting loss of essential function at elevated temperatures is due to the destabilization of the entire Cdc68 protein, rather than a consequence of a malfunctioning N-terminal domain. This idea is not unprecedented with *CDC68*: *cdc68-1*, a well-studied allele containing an N-terminal point mutation, is an

example of a *cdc68* mutant allele that produces an unstable protein product (Xu *et al.* 1995).

To test this hypothesis, western-blot experiments were undertaken to determine the stability of Cdc68 mutant proteins at elevated temperature. This analysis included the proteins generated by the NTD point mutant and deletion alleles as well as those from the *cdc68-312* and *cdc68-319* alleles, which contain the C-terminal point mutations described above (Results 2, i). The cells were grown logarithmically at 23°C and then shifted to the restrictive temperature, 39°C, with the addition of cycloheximide (0.5 mg/ml) for a further one-hour incubation. Protein extracts were examined by western blot with affinity-purified anti-Cdc68 polyclonal antibodies. As shown in Figure 32 (lanes 7-10 and 13-20), the abundances of Cdc68 protein for all N-terminal mutants that exhibit temperature sensitivity at 39°C were decreased, with the exception of *cdc68-Δ922* (lanes 3-4). Conversely, the *cdc68-312* and *cdc68-319* C-terminal mutant alleles, shown above to generate temperature-sensitive phenotypes, produced stable protein products at the elevated temperature (Figure 32, lanes 23-26). Thus, it is likely that the majority of mutations affecting the non-essential NTD of Cdc68 cause temperature sensitivities due to decreased mutant-protein stability at elevated temperatures, rather than to loss of a specific functional aspect of the NTD. In contrast, the temperature sensitivity of C-terminal mutations cannot be explained by altered protein stability, and must therefore be attributed to altered Cdc68 protein function. While mutations in both the N- and C-terminal domains of Cdc68 exhibit similar temperature-sensitive phenotypes, the molecular bases for these phenotypes are different.

vi) The temperature-sensitive phenotype of Cdc68 N-terminal mutants can be suppressed by elevated gene dosage

Consistent with the findings that N-terminal *cdc68* mutants encode unstable proteins at elevated temperatures, when these mutant alleles are provided on high-copy plasmids cells show increased maximal permissive growth temperatures (Figure 33A). Thus supplying more of the unstable protein, by expressing multiple copies of the mutant gene, results in the restoration of essential function at elevated temperatures. If the loss of growth activity at elevated temperatures were due to altered N-terminal domain function, then simply supplying more of the dysfunctional Cdc68 protein would not be anticipated

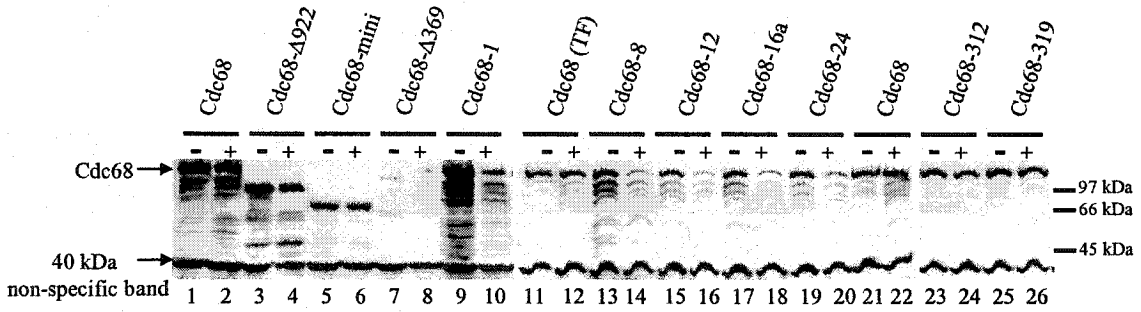

Figure 32. Stabilities of mutant Cdc68 proteins at elevated temperature. Western blots of total protein extracts (8 μg/lane as determined by Bradford assays) made from cells with various alleles of *CDC68* (where Cdc68 (TF) lane designation indicates the KanB-haploid strain containing pTF128 plasmid from the Formosa lab as a wild-type control)growing logarithmically at 23°C (-) or from cells that were shifted to 39°C and then further incubated at this temperature for one hour with addition of cycloheximide (+). Blots were probed with rabbit polyclonal anti-Cdc68 antibody and detected using HRP-conjugated goat anti-rabbit IgG antibody and chemiluminescent substrate. India-ink staining of the membranes prior to antibody binding was used as a loading control. In addition, the non-specific band at 40 kDa is also an indicator of relative loading and transfer.

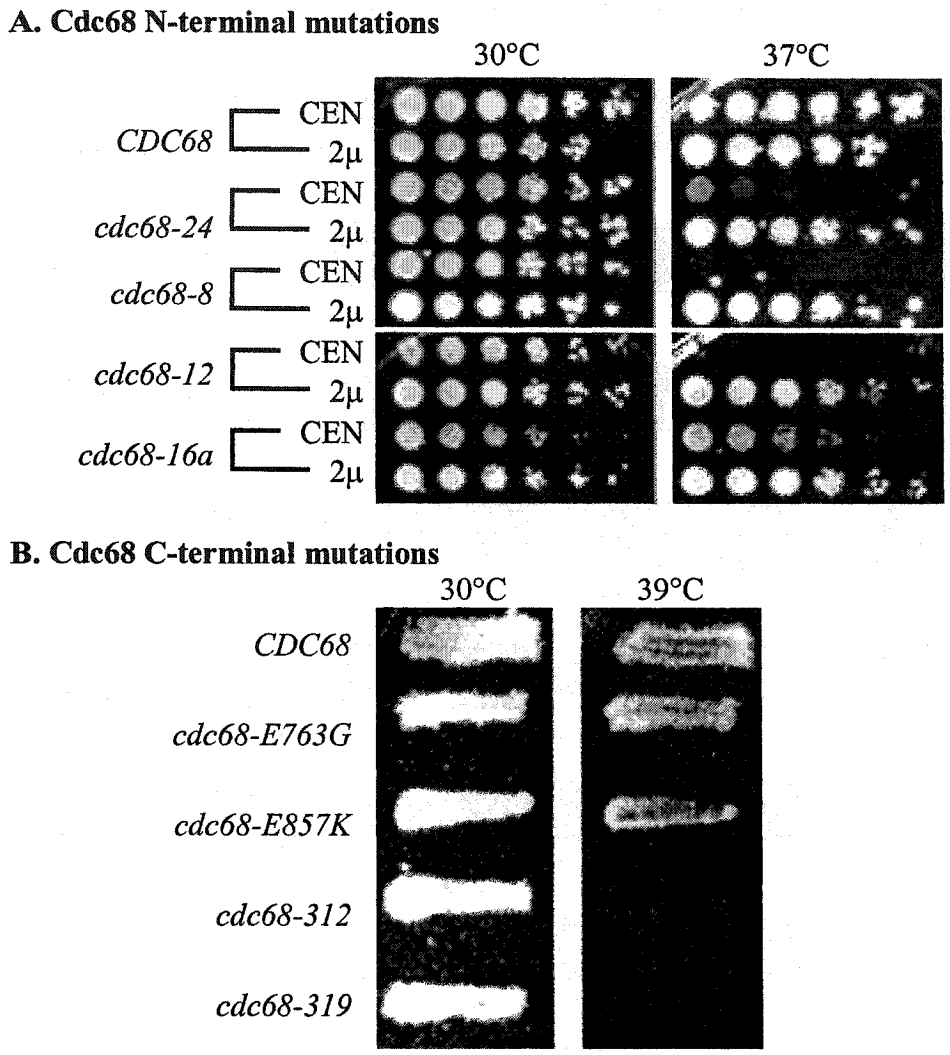

Figure 33. Dosage suppression of the temperature-sensitive phenotype for Cdc68 mutations. (**A**) Cdc68 N-terminal mutations were present in cells on either a centromeric plasmid (*CEN*), which is maintained at 1-2 copies per cell, or on a 2μ-based plasmid, which is maintained at many copies per cell. Five-fold serial dilutions of stationary-phase cultures were spotted on YPD solid medium starting at 1 x 10^7 cells/ml (as determined by Coulter Counter assessments) and permitted to grow for 4 days. (**B**) Cdc68 C-terminal mutations were present in strains on 2μ-based plasmids. Cells were distributed on solid YPD medium as patches and allowed to grow for 2 days at 30°C, and then replica-plated onto YPD solid medium and allowed to grow for 4 days.

to restore growth. However, if the loss of cell viability at elevated temperature is due to the unstable nature of these Cdc68 N-terminally mutated proteins, then by supplying more of the protein to cells the deleterious impact of high temperatures can be alleviated. The C-terminal mutants, *cdc68-312* and *cdc68-319*, generate stable protein products at the elevated temperature (Figure 32, lanes 23-26) but exhibit temperature sensitivity (Figure 27). However, this temperature sensitivity cannot be alleviated by increasing the dosage of the *cdc68-312* or *cdc68-319* gene (Figure 33B). In these cases, supplying more of the dysfunctional, C-terminally mutated protein product does not facilitate growth at elevated temperatures.

vii) The hydroxyurea sensitivities of *cdc68* mutations are not due to defects in the activation of the DNA-replication checkpoint

Hydroxyurea is an agent known to inhibit ribonucleotide reductase, resulting in depleted dNTP pools and leading to stalling during replication and a preponderance of unresolved replication forks (Slater 1973; Skoog and Bjursell 1974; Lopes *et al.* 2001). The unresolved forks are manifested as an accumulation of single-stranded DNA, which is a common trigger for the activation of S-phase checkpoint responses (Lopes *et al.* 2001). These checkpoint responses allow the cell enough time to repair DNA damage and complete DNA replication prior to dividing its DNA contents. Prolonged exposure to hydroxyurea also results in the accumulation of double-strand breaks, which must be repaired for successful replication (Merrill and Holm 1999; D'Amours and Jackson 2001). Mutations in the NTD and the CTD of Cdc68 can result in sensitivity to hydroxyurea (Figures 28, 29, and 31).

Incomplete or unfaithful replication of DNA during S phase results in mutations and genome instability. To prevent cell division when DNA damage is present or DNA replication is incomplete, a block to further cell-cycle progression is imposed in S phase as a result of DNA replication checkpoints. Cells sensitive to prolonged exposure to hydroxyurea (as is the situation when cells are grown on solid medium containing hydroxyurea) may or may not have checkpoint defects (Allen *et al.* 1994; D'Amours and Jackson 2001). In contrast, sensitivity to high doses of hydroxyurea over short periods of time, as in the acute hydroxyurea assay, indicates defects in activation of the replication checkpoint. Exposure is lethal because cells continue to replicate DNA when dNTPs are

in short supply, leading to incomplete replication. In this way, acute hydroxyurea-sensitivity testing identifies defects in the replication checkpoint.

To help establish the molecular basis of the sensitivities to prolonged hydroxyurea treatment during growth on solid medium, I carried out acute hydroxyurea-sensitivity tests on cells with *CDC68*, *cdc68-ΔNTD*, *cdc68-mini*, *cdc68-312*, and *cdc68-319* genotypes (Figures 34 and 35; data not shown). As positive controls in this experiment, I also used *xrs2* and *mre11* deletion strains (Figure 34), which are known to cause defects in replication-checkpoint signalling (D'Amours and Jackson 2001). Negative controls included wild-type strains and a *leu1* deletion strain (Figure 34). The Leu1 protein is an isomerase that operates in the first step of the leucine biosynthesis pathway to convert α-isopropylmalate to β-isopropylmalate, and should have no impact on DNA replication checkpoints, especially since the cells were supplied with exogenous leucine in the growth medium. In addition to these controls, cell concentrations and morphologies after addition of hydroxyurea were monitored to ensure that cells did not proliferate significantly and that the large-bud morphology associated with the hydroxyurea-induced block in the cell cycle was generated (data not shown).

The *cdc68-mini*, *cdc68-ΔNTD* and *cdc68-312* strains did not show decreased viabilities upon acute hydroxyurea treatment at 30°C (data not shown; Figure 34). Since *cdc68-ΔNTD* and *cdc68-312* cells do not show sensitivity to hydroxyurea in prolonged-exposure assays unless they are incubated at elevated temperatures (Figures 28 and 31), a similar acute hydroxyurea assay was performed at 35°C. Even at this elevated temperature, *cdc68-ΔNTD* and *cdc68-312* strains did not lose viability upon acute hydroxyurea treatment (Figure 35). This finding indicates that these *cdc68* mutations do not result in replication-checkpoint defects. The *cdc68-319* cells, however, did show a limited sensitivity to acute hydroxyurea exposure, exhibited as an approximately 5-fold decrease in viability (Figure 34). In comparison to the *mre11Δ* and *xrs2Δ* controls that seen 125-fold and greater than 50-fold reductions in viable cell numbers, respectively, the reduction in *cdc68-319* viability is minimal. This experiment was performed three times and the modest reduction in *cdc68-319* cell viability was exhibited each time. Prolonging the acute hydroxyurea exposure time to 24 hours for *cdc68-319* cells increased the

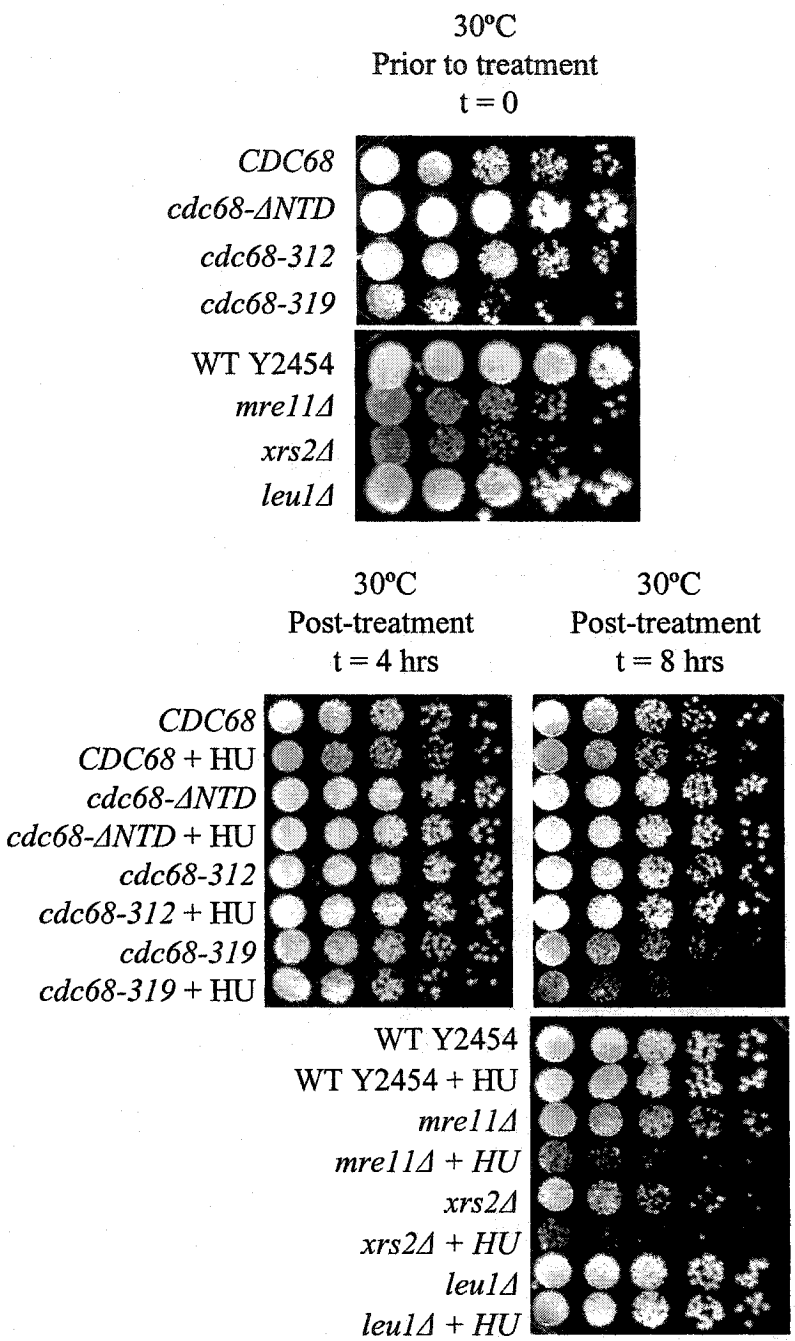

Figure 34. Acute hydroxyurea sensitivity tested at 30°C. The top panel shows the viability of cells grown to log phase at 30°C prior to incubation with hydroxyurea. The bottom panel shows viability after 4 hours or 8 hours of incubation with (+ HU) or without 0.2 M hydroxyurea at 30°C. Cells were spotted on YPD medium and grown for 4 days at 30°C, with the first spot made from cells at $1x10^6$ cells/ml and each subsequent spot a 5-fold serial dilution.

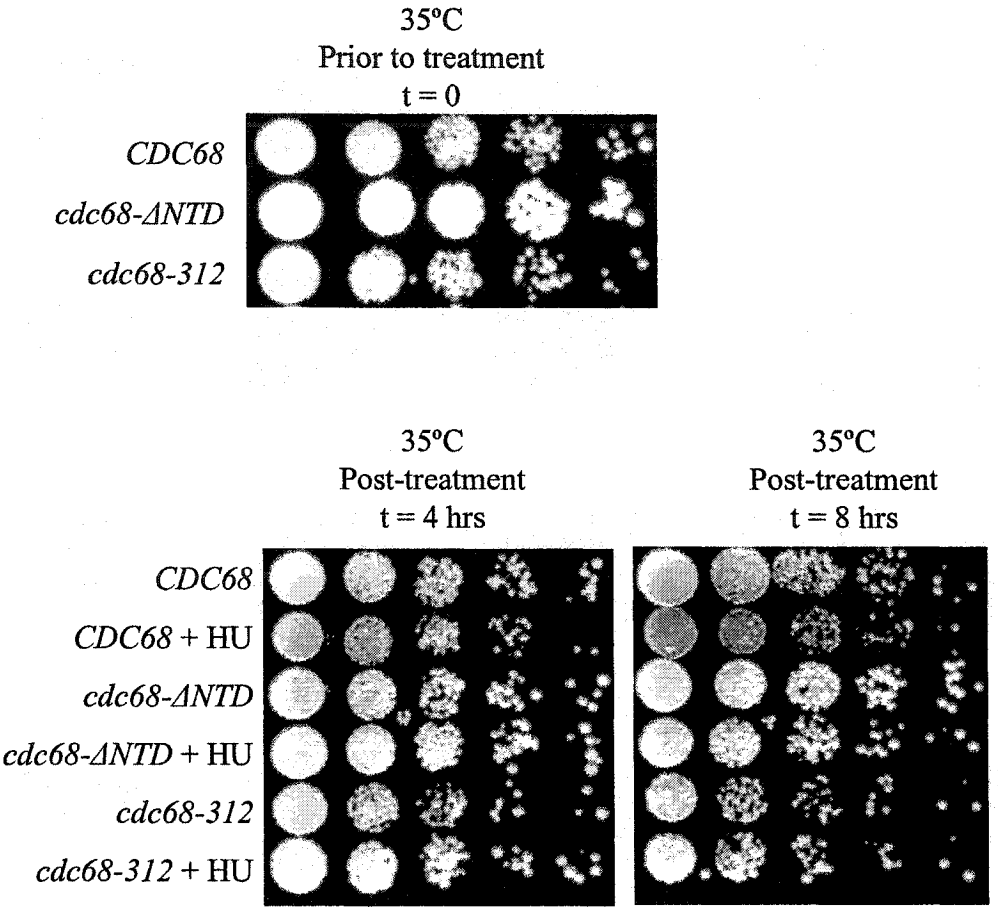

Figure 35. Acute hydroxyurea sensitivity tested at 35°C. The top panel shows the viability of cells grown to log phase at 35°C prior to incubation with hydroxyurea. The bottom panel shows viability after 4 hours or 8 hours of incubation with (+ HU) or without 0.2 M hydroxyurea at 35°C. Cells were spotted on YPD medium and grown for 4 days at 30°C, with the first spot made from cells at $1x10^6$ cells/ml and each subsequent spot a 5-fold serial dilution.

decline in cell viability to 125-fold (data not shown), indicating that this mutation in *CDC68* does indeed cause a mild defect in the replication checkpoint.

It should be noted that all of the strains grown at 35°C exhibited slight (*CDC68* and *cdc68-ΔNTD*) to severe (*cdc68-312*) perturbations in cell morphology that worsened with increased duration at this elevated temperature. Elongated, misshapen and multi-budded cells were observed and, in the case of *cdc68-312*, doubling time became very much extended. At the time of treatment with hydroxyurea approximately 25% of the *cdc68-312* cells growing at 35°C already exhibited anomalous cell morphologies, and by the end of the 8-hour experiment the majority of these cells exhibited anomalous cell morphologies. These huge, multi-budded cells may have interfered with cell concentration assessments, as these measurements were done using a Coulter Counter, which measures light scattering per particle, and therefore one of these large multi-budded cells that represents several nuclear divisions without complete cytokinesis would count as single cell. As a result, the continued growth of these cells at 35°C, even in the absence of hydroxyurea, was difficult to assess. The effect of hydroxyurea on the morphology of these cells is also consequently uncertain. For *CDC68* and *cdc68-ΔNTD* cells at 35°C, approximately 15% of cells were slightly misshapen at the end of the experiment, with large cells and cells with elongated buds. This degree of morphological variation was not an impediment to the assessment of hydroxyurea effects. The large-bud morphology associated with S-phase arrest was still observed for these cells treated with hydroxyurea at 35°C.

viii) Rad53 activation in response to hydroxyurea treatment is impaired in certain *cdc68* mutant strains

As a further measure of the activation of the DNA replication checkpoint, Rad53 phosphorylation status in hydroxyurea-treated cells was assessed. Rad53 is a key player in triggering the replication checkpoint, and is itself activated in response to acute hydroxyurea treatment through phosphorylation by the Mec1 kinase (Sun, Z. *et al.* 1996). This phosphorylated form of Rad53 then induces, through a series of events, the replication block (Allen *et al.* 1994; Sun, Z. *et al.* 1996). The phosphorylated forms of Rad53 may be detected on western blots as lower-mobility isoforms of the protein (Sun *et*

al. 1996; Pellicioli *et al.* 1999). Upon acute hydroxyurea exposure, cells phosphorylate Rad53 within 30 minutes of treatment (Pellicioli *et al.* 1999).

To verify that the Rad53 trigger for the replication checkpoint is activated in *cdc68* mutants treated with hydroxyurea, western blots were used to detect Rad53 protein. A portion of each cell culture used in the acute hydroxyurea experiments described above was harvested both before hydroxyurea treatment and 1, 4, and 8 hours after the addition of hydroxyurea for total protein extraction by TCA precipitation (Foiani *et al.* 1999). Extracts from *CDC68*, *cdc68-312*, *cdc68-319*, and *cdc68-ΔNTD* cells growing either at 30°C or 35°C were then resolved, blotted and probed for Rad53 protein (Figure 36; data not shown). Consistent with the acute-hydroxyurea cell-viability results, all of the mutants tested were able to activate Rad53, as evidenced by the presence of the lower-mobility isoforms which correspond to phosphorylated Rad53. However, changes in the activation status of Rad53, seen as changes in the relative abundance of the phosphorylated forms, were detected in *cdc68* mutant strains. These qualitative decreases in Rad53 phosphorylation were seen by one hour in *cdc68-ΔNTD* cells at either 30°C or 35°C, *cdc68-312* cells at 35°C, and *cdc68-319* cells at 30°C (Figure 36), and were also observed at the 4-hour and 8-hour timepoints for the *cdc68-ΔNTD* and *cdc68-312* cells at 35°C, and *cdc68-319* cells at 30°C (data not shown).

The most severe impairment to Rad53 phosphorylation was observed for the *cdc68-312* cells at 35°C. As described above, at this temperature these cells exhibited considerable growth defects, as evidenced by severe cell-morphology problems. Therefore, Rad53 activation may not occur effectively due to the existing growth defect at the time of hydroxyurea addition.

While Rad53 activation is impaired in these strains, there is still some activation in each, which must be sufficient for efficient replication-checkpoint activation in all but the *cdc68-319* cells, as cell viability upon short-term exposure to a high dosage of hydroxyurea was diminished significantly only in these cells. Since there was a significant amount of phosphorylated Rad53 in the *cdc68-319* cells, perhaps this acute hydroxyurea sensitivity is the result of some other impairment of the replication checkpoint. Rad53 phosphorylation and sensitivity to short-term exposure to high doses

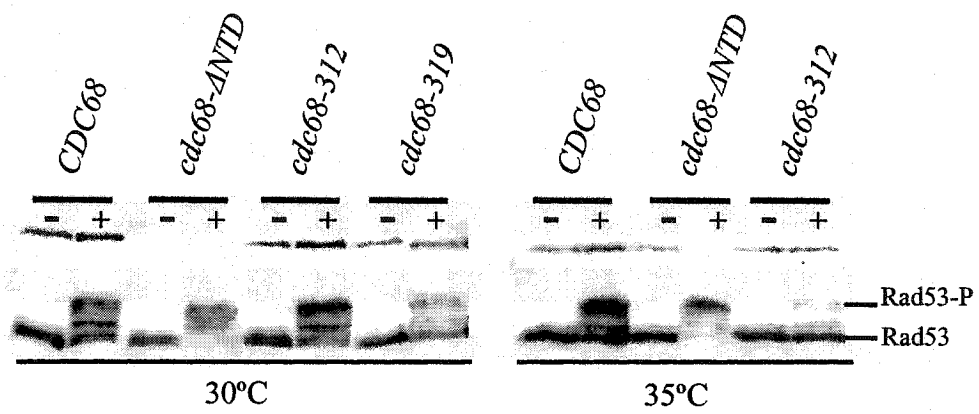

Figure 36. Rad53 phosphorylation in response to hydroxyurea treatment. Extracts from cells growing logarithmically at 30°C or 35°C without treatment (−) or with a 1-hour incubation in medium containing 0.2 M hydroxyurea (+) were prepared using TCA precipitaion. 0.1 mg of extract, as determined by Bradford assays, was loaded per lane on a 10% acrylamide:bis acrylamide (30:0.4) gel, extract contents were resolved electrophoretically and blotted, and Rad53 protein in phosphorylated (Rad53-P) and unphosphorylated forms (Rad53) was detected with anti-Rad53-yC19 antibody (Santa Cruz). Equivalent loading and transfer was verified by India-ink staining (not shown).

of hydroxyurea are not always equivalent measures of replication checkpoint activation (D'Amours and Jackson 2001). In fact, cells containing an *xrs2* or *mre11* deletion mutation, which exhibit exquisite sensitivities to acute exposure to 0.2 M hydroxyurea, do *not* show significant impairment of Rad53 phosphorylation (D'Amours and Jackson 2001). Thus alteration of Rad53 phosphorylation is not the only mechanism to impair the replication checkpoint.

ix) *RNR1* and *RNR3* gene expression in response to hydroxyurea is altered in *cdc68* mutants.

As an additional measure of Rad53 activation, the transcription of the *RNR1* and *RNR3* genes in response to hydroxyurea treatment was monitored. In addition to triggering the activation of proteins responsible for DNA-damage response in cells, the phosphorylated form of Rad53 is also involved in the activation of gene expression in response to DNA damaging agents. Ribonucleotide reductase in yeast is composed of a heterodimeric tetramer ($\alpha 2\ \beta 2$), where the α subuints are encoded by *RNR1* and *RNR3* and the β subunits are encoded by *RNR2* and *RNR4*. The *RNR1* and *RNR3* gene products share approximately 86% sequence identity. Regulation of *RNR1* and *RNR3* is complex, with both gene transcription and enzyme activity altered in response to several different stimuli (Elledge *et al.* 1992, 1993).

To determine if the subtle alterations in Rad53 phosphorylation observed in *cdc68* mutant cells have an impact on Rad53 function, the levels of *RNR1* and *RNR3* transcripts were monitored in response to treatment with hydroxyurea. Portions of the cell cultures used in both the acute hydroxyurea experiments and the Rad53 protein-analysis experiments described above were harvested for RNA extraction before hydroxyurea treatment, and 0.5, 1, and 4 hours after the addition of hydroxyurea. Extracts from *CDC68*, *cdc68-312*, *cdc68-319*, and *cdc68-ΔNTD* cells growing at 30°C and 35°C were then resolved, blotted and probed for *RNR1* or *RNR3* transcripts (Figure 37).

In a fashion similar to the subtle changes observed for Rad53 phosphorylation in *cdc68* mutant alleles, alterations in *RNR1* and *RNR3* RNA abundance were also observed (Figure 37). Specifically, the induction of *RNR1* transcription was delayed and decreased in *cdc68-319* cells treated with hydroxyurea at 30°C in comparison to the levels of *RNR1* RNA obtained from wild-type *CDC68* cells. In contrast, the induction of *RNR1*

Figure 37. *RNR1* and *RNR3* transcript levels in response to hydroxyurea treatment are altered in *cdc68* mutant cells. Total RNA was extracted from growing cells that were treated with hydroxyurea for the times indicated at 30°C (**A** and **B**) or 35°C (**C** and **D**). 10 μg of RNA was loaded per lane, resolved by gel electrophoresis, and blotted to a nylon membrane, and probed with ^{32}P-labelled probes specific for *RNR1*, *RNR3*, or *TUB2* (as a loading control). Densitometry of the resulting hybridization signals was carried out using ImageJ software (US National Institutes of Health; available at http://rsb.info.nih.gov/nih-image/). Signal intensities were normalized to the *TUB2* control value for each lane and then compared to the signal intensity determined for the no-hydroxyurea (t = 0) control for each allele. An example of the Northern blot hybridization signals is shown above the corresponding graphs of those data (A, B, C, D). For hydroxyurea treatment at 30°C, two replicate Northern blots were performed and two different exposures for each transcript were quantitated. The average fold change in transcript abundance in comparison to the no-hydroxyurea control (t = 0) is plotted for each timepoint, along with error bars that indicate the standard deviation. For the cells treated with hydroxyurea at 35°C a single Northern blot was performed and two different exposures for each transcript were quantitated. The average fold change in transcript abundance in comparison to the no-hydroxyurea control (t = 0) is plotted.

Hydroxyurea treatment at 30°C

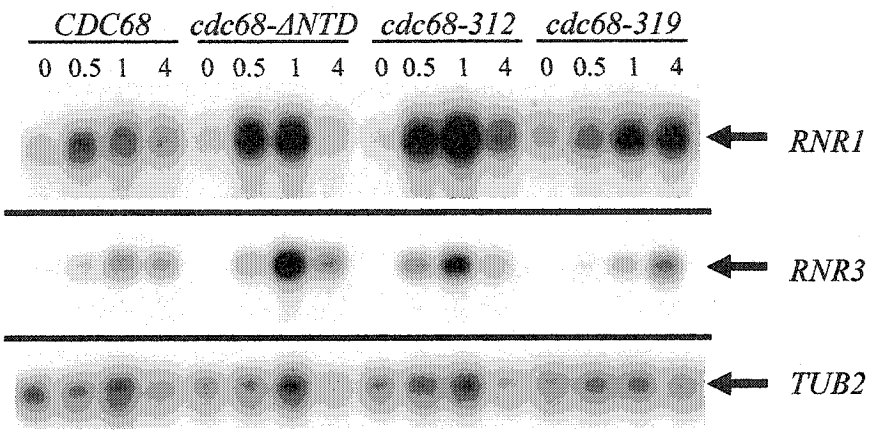

A. *RNR1* 30°C

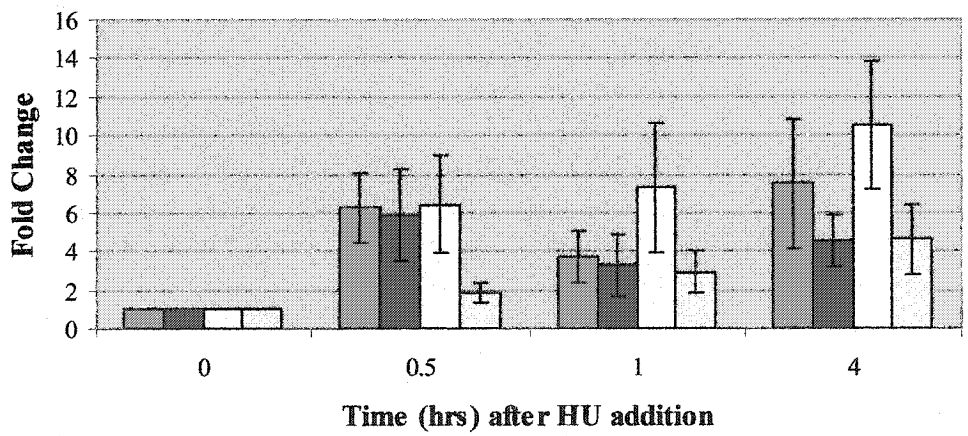

B. *RNR3* 30°C

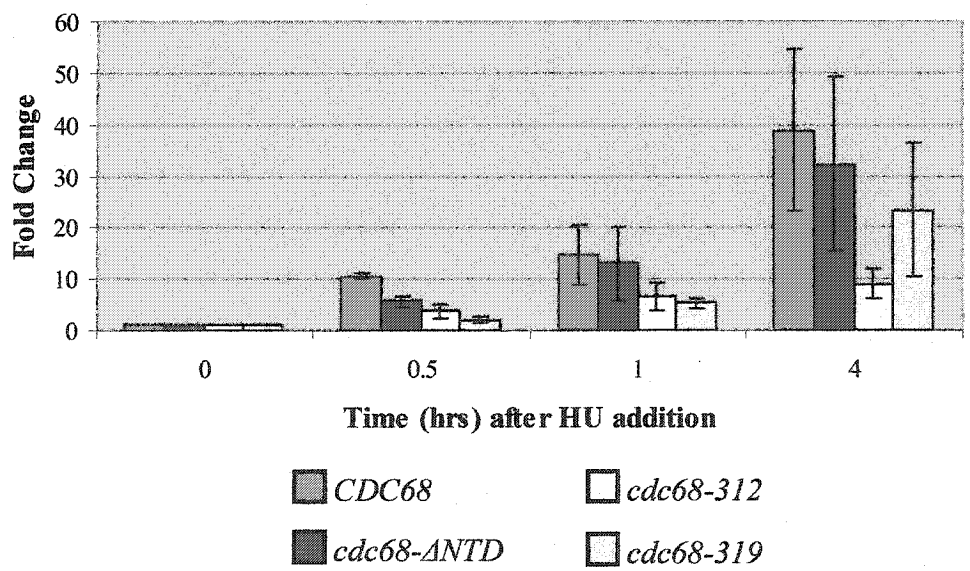

Hydroxyurea treatment at 35°C

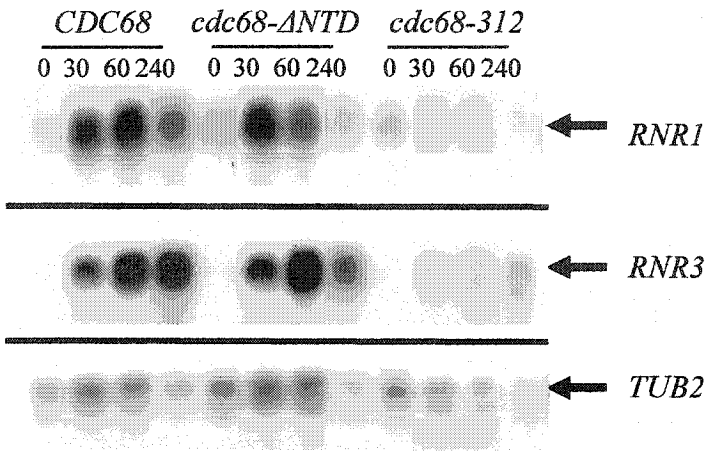

C. *RNR1* 35°C

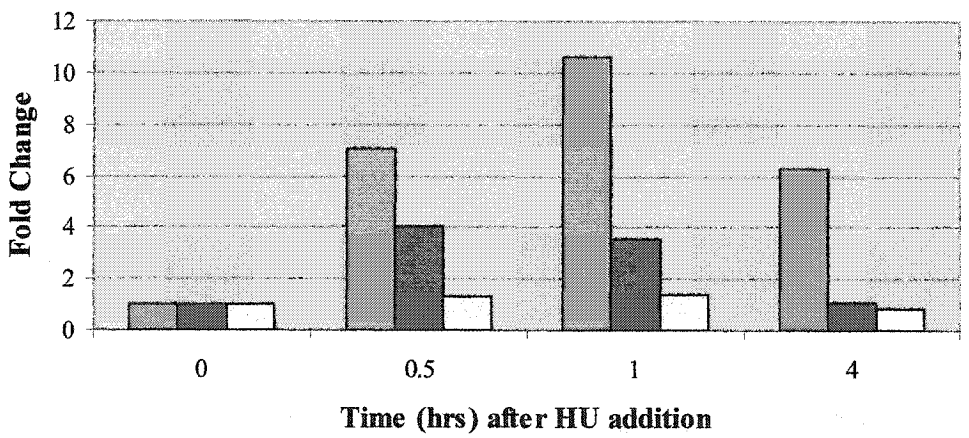

D. *RNR3* 35°C

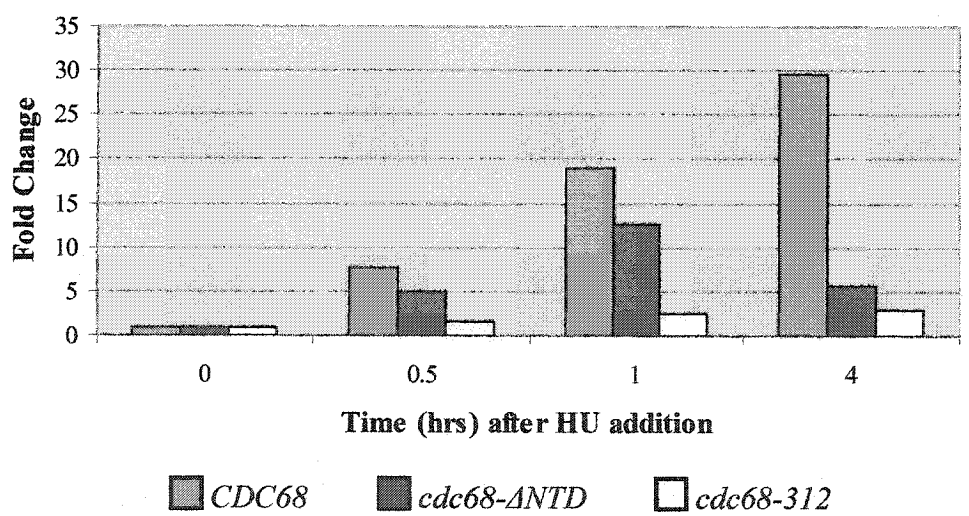

transcription in *cdc68-312* and *cdc68-ΔNTD* cells was similar to wild-type under these conditions (Figure 37A). The induction of *RNR3* transcription in response to hydroxyurea treatment at 30°C was unaffected in *cdc68-ΔNTD* cells, but was decreased in cells containing *cdc68-312* and *cdc68-319* (Figure 37B). For cells growing at 35°C and treated with hydroxyurea, both the *cdc68-ΔNTD* and the *cdc68-312* cells showed significantly lower *RNR1* and *RNR3* transcript abundance in comparison to wild-type *CDC68* cells (Figures 37C and 37D). This pattern is again similar to the slight alterations in Rad53 phosphorylation seen in these cells, as described in the preceeding section. The significance of this finding for the *cdc68-312* cells treated with hydroxyurea at 35°C is uncertain, given the fact that these mutant cells were not proliferating efficiently at this temperature and displayed abnormal cell morphologies. It may be the case that these cells are not able to induce Rad53 phosphorylation or *RNR1* and *RNR3* transcription effectively because they are not growing well at this elevated temperature.

It is interesting that the subtle change in Rad53 phosphorylation in hydroxyurea-treated *cdc68* mutant cells is mirrored by the alterations in *RNR1* and *RNR3* gene induction. This correlation suggests that there may be a functionally significant difference between the Rad53-phosphoisoform activity in *cdc68* mutant cells compared to wild type. The decreased *RNR1* and *RNR3* expression observed in *cdc68* mutant cells may provide a key to the mechanism of the chronic hydroxyurea sensitivities observed for these cells. This possibility is examined further in the following section.

x) Increased dosage of *RNR1* or *RNR3* cannot suppress the hydroxyurea sensitivity of *cdc68* mutants

As described above, hydroxyurea inhibits ribonucleotide reductase, the enzyme that performs the rate-limiting step in dNTP synthesis. Depletion of dNTP pools leads to defects in DNA repair and replication. One feature of acute exposure to hydroxyurea is the activation of a kinase cascade (of which Rad53 is a member) that ultimately results in the induction of the genes encoding ribonucleotide reductase subunits. Any impairment of this induction may lead to deleterious consequences in the presence of hydroxyurea. Since the phosphorylated form of Rad53 is a key mediator in this process, the low levels of activated Rad53 observed for *cdc68* mutants upon hydroxyurea treatment may be an explanation for their heightened hydroxyurea sensitivities (Results 2, iv). There are

several examples in the literature of mutations causing hydroxyurea sensitivity that may be suppressed by overexpressing the genes encoding ribonucleotide reductase subunits (Desany *et al.* 1998; Zhao *et al.* 1998).

To determine if the hydroxyurea sensitivities of *cdc68* mutants could be alleviated by increased dNTP pools, two strategies to increase ribonucleotide reductase enzyme activity were employed: 1) the *RNR1* and *RNR3* genes were ectopically over-expressed from a constitutive promoter, and 2) the *SML1* gene, encoding the inhibitor of Rnr1 and Rnr3 enzyme activity was deleted. The hydroxyurea sensitivities of *cdc68* mutants were then assessed.

Over-expression of *RNR1* or *RNR3* was achieved by transforming constitutively expressing versions of these genes into *cdc68* cells. Plasmids containing fusions of the coding regions of *RNR1* (pBAD070) and *RNR3* (pBAD079) to the constitutively active GAP promoter were obtained from the Elledge lab (Desany *et al.* 1998). By employing these versions of *RNR1* and *RNR3*, the complications of *RNR* gene regulation are averted. Transformants were then assessed for hydroxyurea and temperature sensitivity. Over-expression of either *RNR1* or *RNR3* in this way had no effect on the growth for any *cdc68* mutant strain tested (Figure 38). To ensure that the hydroxyurea concentration was not lethal to wild-type cells during this experiment, *CDC68* cells containing the vector (pBAD054) or the *RNR1* over-expressing plasmid (pBAD070) were also included as growth controls on each plate, but to conserve space are not shown in each instance in Figure 38.

As a second approach to examine the effects of increased ribonucleotide reductase activity on the hydroxyurea sensitivity of *cdc68-ΔNTD*, double-mutant cells deleted for the *SML1* gene, encoding the ribonucleotide reductase inhibitor, were tested. To generate these double-mutant cells, a chromosomally integrated *cdc68-ΔNTD* allele tagged downstream of the coding sequence with the dominant drug-resistance gene, NAT, encoding nourseothricin N-acetyltransferase, was used to replace the wild-type chromosomal *CDC68* gene in cells from the Y2454 strain (Materials and Methods; Results 4, viii). Cells with this genotype were then crossed to *sml1Δ::kanMX4* cells from the yeast gene deletion collection (Winzeler *et al.* 1999), and haploid segregants from this diploid were assessed for resistance to geneticin and clonNAT as indicators of the *SML1*

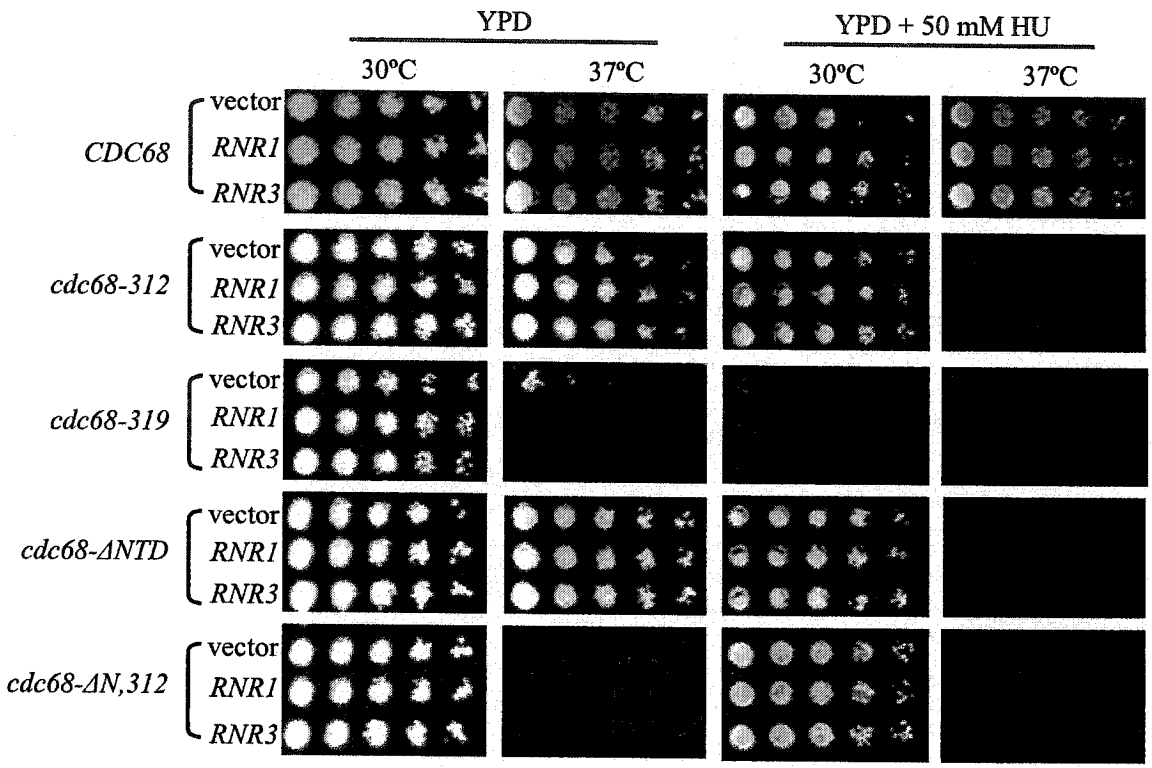

Figure 38. Overexpression of *RNR1* or *RNR3* does not suppress the hydroxyurea sensitivities of *cdc68* mutants. Plasmids pBAD054 (vector control), pBAD070 (constitutive GAP promoter fused to *RNR1*) and pBAD079 (constitutive GAP promoter fused to *RNR3*) were transformed into cells containing the *cdc68* alleles listed at left. Five-fold serial dilutions of stationary-phase cultures were spotted, starting at $1x10^7$ cells/ml.

and *CDC68* status of cells, respectively. Single-mutant segregants of *cdc68-ΔNTD* or *sml1Δ* as well as double-mutant *cdc68-ΔNTD sml1Δ* segregants were identified based on growth in the presence of geneticin and clonNAT drugs. Similarly, as a control in this experiment the wild-type *CDC68* gene was also tagged with the *natMX4* cassette in cells from Y2454, and these cells were also assessed with *sml1Δ::kanMX4* cells; both single- and double-drug resistant spores, indicative of the *CDC68* and *SML1* loci, were chosen for analysis. The hydroxyurea sensitivity of cells from each segregant was then assessed. Consistent with the finding that ectopic over-expression of *RNR1* or *RNR3* cannot alleviate the hydroxyurea sensitivity of *cdc68* mutant cells, deletion of *SML1*, the gene encoding a ribonucleotide reductase inhibitor, was also unable to suppress the hydroxyurea sensitivity of *cdc68-ΔNTD* cells(Figure 39). The hydroxyurea sensitivities of cells containing *cdc68* mutant alleles therefore do not appear to be consequences simply of decreased dNTP pools through impaired activation of the ribonucleotide reductase enzyme.

xi) Genetic analysis of chimeric *cdc68* mutant alleles

The hydroxyurea sensitivities observed for both NTD and CTD Cdc68 mutations raises the question of an overlapping function for these two domains. With this in mind, chimeric *cdc68* mutant alleles consisting of the *cdc68-ΔNTD* deletion with the *cdc68-E763G, cdc68-E857K*, *cdc68-312*, or *cdc68-319* C-terminal point mutations were generated (named *cdc68-ΔN,763*, *cdc68-ΔN,857*, *cdc68-ΔN,312*, and *cdc68-ΔN,319*, respectively). Each of these new mutant alleles, as well as a the wild-type *CDC68* gene, the *cdc68-ΔNTD* allele and the individual point mutant alleles encoding C-terminal substitutions as controls, all on *URA3* centromeric plasmids, was tested to determine if the new mutant allele provides essential Cdc68 function. The new plasmids were transformed into *cdc68Δ::kanMX4* haploid cells that were kept alive by *cdc68-ΔNTD* on a *LEU2* centromeric plasmid. Transformants were selected based on the ability to grow on SC-Ura medium, and cells from the resulting colonies were grown in SC-Ura liquid medium to select for maintenance of the newly introduced, chimeric allele, but permit the growth of cells that had failed to inherit the *LEU2 cdc68-ΔNTD* plasmid. Repeated sessions of growth under these conditions permit the population to become enriched with cells lacking the *LEU2 cdc68-ΔNTD* plasmid. Cells from these cultures were then

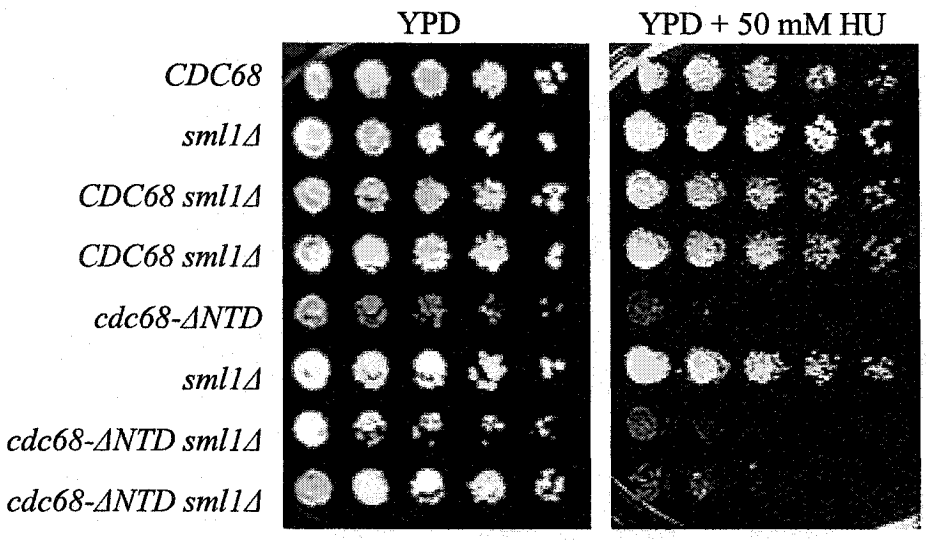

Figure 39. *sml1Δ* is unable to alleviate the hydroxyurea sensitivity of *cdc68-ΔNTD*. Five-fold serial dilutions of stationary-phase cultures were spotted from a starting concentration of 1 x 10^7 cells/ml and allowed to grow for 4 days at 30°C.

allowed to form single colonies on solid SC-Ura medium. These colonies were replica-plated to SC-Ura or SC-Leu to determine plasmid content. Colonies derived from cells that had failed to inherit the *LEU2 cdc68-ΔNTD* plasmid would be unable to grow in the absence of exogenously supplied leucine; thus cells that were leucine auxotrophs but uracil prototrophs must be kept alive by the *cdc68* allele encoded on the *URA3* plasmid. In this way it was shown that each of the chimeric mutant alleles was able to provide essential function as the only version of Cdc68, with the exception of *cdc68-ΔN,319*. This finding is consistent with the idea that the N-terminal and the C-terminal domains of Cdc68 share an overlapping essential function, for when mutations that abrogate the function of either of these domains are present individually viable cells are produced, but the combination of mutational changes in both domains, as evidenced here for *cdc68-ΔN,319*, can result in loss of essential Cdc68 function.

To ensure that *cdc68-ΔN,319* is indeed unable to provide essential function, unlike either of the parental mutations *cdc68-ΔNTD* and *cdc68-319*, additional analysis was performed. The *URA3* plasmids bearing *cdc68-ΔN,319* and *cdc68-ΔNTD* were transformed separately into KanB diploid cells (*cdc68Δ::kanMX4/CDC68*). These diploids were then sporulated and the resulting haploid spores were assessed for growth on medium lacking uracil or containing geneticin. Growth on SC-Ura medium indicates the presence of the plasmid-borne *cdc68* allele, while resistance to geneticin indicates the presence of *cdc68Δ::kanMX4*. Spore products with these two phenotypes must therefore be kept alive by the plasmid-borne *cdc68* allele. No such haploid progeny could be identified from the KanB diploid containing *cdc68-ΔN,319*, and a 2:2 ratio of viable:inviable spore products was observed (data not shown). In each case the two viable spores were sensitive to geneticin, indicating the presence of the wild-type *CDC68* gene, rather than *cdc68Δ::kanMX4*, at the *CDC68* locus. This result is consistent with the inability of *cdc68-ΔN,319* to provide essential function in the absence of a chromosomal version of *CDC68*. The control sporulation from KanB *cdc68-ΔNTD* was able to produce tetrads with four viable spores, and geneticin-resistant, uracil-prototrophic segregants were found (data not shown). Thus the *URA3 cdc68-ΔNTD* plasmid is able to provide essential Cdc68 function in cells containing the *cdc68Δ::kanMX4* chromosomal deletion. The *cdc68-319* allele also provides essential Cdc68 function in the same genetic

background (Results 2, ii). These two experiments together indicate that, while the *cdc68-ΔNTD* allele is able to provide essential Cdc68 function, the doubly mutant *cdc68-ΔN,319* allele is *not*. Further, this finding suggests a synthetic lethal interaction between the *cdc68-ΔNTD* and *cdc68-319* mutations, consistent with an overlapping essential function for the NTD and CTD of Cdc68.

To determine if this evidence of overlapping function between the N and C-terminal domain of Cdc68 is a feature exclusive to the protein encoded by the *cdc68-ΔN,319* allele, phenotypic characterizations of the chimeric alleles found to provide essential Cdc68 function, *cdc68-ΔN,763, cdc68-ΔN,857*, and *cdc68-ΔN,312*, was undertaken. Strains containing each of the chimeric alleles, their C-terminally mutated parental alleles, and *cdc68-ΔNTD* were scored for growth under a variety of conditions. With the exception of *cdc68-ΔN,763*, each of the chimeric mutants, containing both the N-terminal deletion mutation and the C-terminal point mutation(s), was found to cause more severe impairments to growth than did either of the original parental mutations alone (Figure 40; Table 12). Specifically, *cdc68-ΔN,857* resulted in an increased sensitivity to hydroxyurea and a more severe temperature sensitivity, while *cdc68-ΔN,312* displayed an increased sensitivity to growth at elevated temperatures.

In summary, deletion of the dispensable N-terminal domain of Cdc68 results in mild growth defects in response to elevated temperature or hydroxyurea. My collection of C-terminally mutated *cdc68* alleles also shows a similar range of growth defects. These similarities raise the question of weather the dispensable N-terminal domain of Cdc68 shares an overlapping function with the essential C-terminal domain. Based on the genetic evidence presented here, showing that chimeric mutant Cdc68 proteins containing both NTD deletion and C-terminal point mutations cause more severe growth defects than does either parental mutation alone, the answer is yes. For three out of the four chimeric alleles tested, more severe phenotypes are observed for cells when the C-terminal mutations are present in conjunction with a deletion of the NTD. In the instance of *cdc68-ΔN,319*, loss of Cdc68 essential function is indicated.

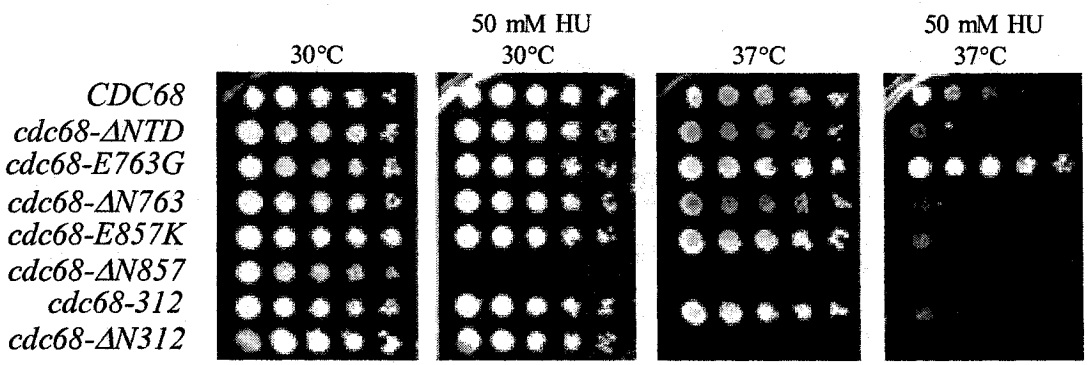

Figure 40. Phenotypes of *cdc68* chimeric alleles containing an NTD deletion and C-terminal point mutation(s). Five-fold serial dilutions of cultures were spotted from a starting concentration of 1 x 10^7 cells/ml on YPD solid medium with or without 50 mM hydroxyurea (HU) and grown for 4 days.

Table12. Phenotypes for *cdc68* mutant alleles contain a deletion of the NTD and C-terminal mutations.

Allele	YPD			YPDS			50 mM HU		HIS^- LYS^-
	30°C	37°C	39°C	30°C	37°C	39°C	30°C	37°C	30°C
CDC68	+++	+++	++	+++	+++	+++	+++	$+^{+}/-$	—
cdc68-ΔNTD	+++	++	—	+++	+++	+++	+++	$^{+}/-$	+
cdc68-E763G	+++	+++	+++	+++	+++	+++	+++	+++	++
cdc68-ΔN,763	+++	++	—	+++	+++	+++	+++	$^{+}/-$	++
cdc68-E857K	+++	+++	—	+++	+++	+++	+++	$^{+}/-$	+++
cdc68-ΔN,857	++	—	—	+	—	—	—	—	+++
cdc68-312	+++	+++	—	+++	+++	+++	+++	$^{+}/-$	+++
cdc68-ΔN,312	+++	—	—	+++	—	—	+++	—	+++

Symbols: (+++) good growth, (++) moderate growth, (+) poor growth, (+/-) intermediate growth between categories, and (—) no growth.

xii) Chimeric N- and C-terminally mutated alleles generate stable protein products

An alternative explanation for the lethality of *cdc68-ΔN,319* and the exacerbated growth defects for *cdc68-ΔN,E857K* and *cdc68-ΔN,312* mutant cells is that these multiply mutated alleles generate unstable protein products. While the *cdc68-ΔNTD* allele and each of the C-terminal mutant alleles, *cdc68-312*, *cdc68-319*, *cdc68-E763G*, and *cdc68-E857K*, encode stable proteins (Figures 26 and 32), the possibility exists that the combination of the *cdc68-ΔNTD* mutation with the C-terminal mutation(s) results in an unstable protein product. To address this issue, the Cdc68 proteins generated from the chimeric alleles were examined in two different ways.

First, to include the Cdc68-ΔN,319 protein in this analysis, viability of yeast cells was maintained by a copy of the *CDC68* gene. Total protein extracts from logarithmically growing *cdc68Δ::kanMX4* cells (haploid segregants of the KanB diploid) at 30°C containing both *CDC68* (on a *LEU2* centromeric plasmid) and a *cdc68-ΔNTD* chimeric allele (on a *URA3* centromeric plasmid) were made and western blot analysis to detect Cdc68 proteins in these extracts was performed. Each of the *cdc68-ΔNTD* chimeric alleles generated a detectable protein product in the presence of *CDC68*, at levels comparable to that of Cdc68-ΔNTD (Figure 41). Since the steady-state levels of Cdc68-ΔN,319 are comparable to those for the other chimeric Cdc68 mutant proteins and for Cdc68-ΔNTD itself, a decreased abundance of this protein is not involved in its inability to provide essential Cdc68 function.

A more detailed look at the Cdc68 chimeric proteins able to provide essential Cdc68 function was also undertaken. The stabilities of the Cdc68-ΔN,763, cdc68-ΔN,857, and Cdc68-ΔN,312 proteins at elevated temperature were determined. Protein extracts were made from cells containing these chimeric proteins, as well as from cells containing their individual progenitor mutant alleles, grown at 23°C or grown at 23°C and then shifted to 38°C for further incubation in the presence of cycloheximide. These extracts were then western blotted and Cdc68 proteins were detected. All three of the chimeric mutants tested in this way proved to produce stable Cdc68 proteins at this elevated temperature (Figure 42). Therefore, the temperature sensitivities observed for these cells are *not* the result of decreased abundance of the Cdc68 protein upon temperature shift.

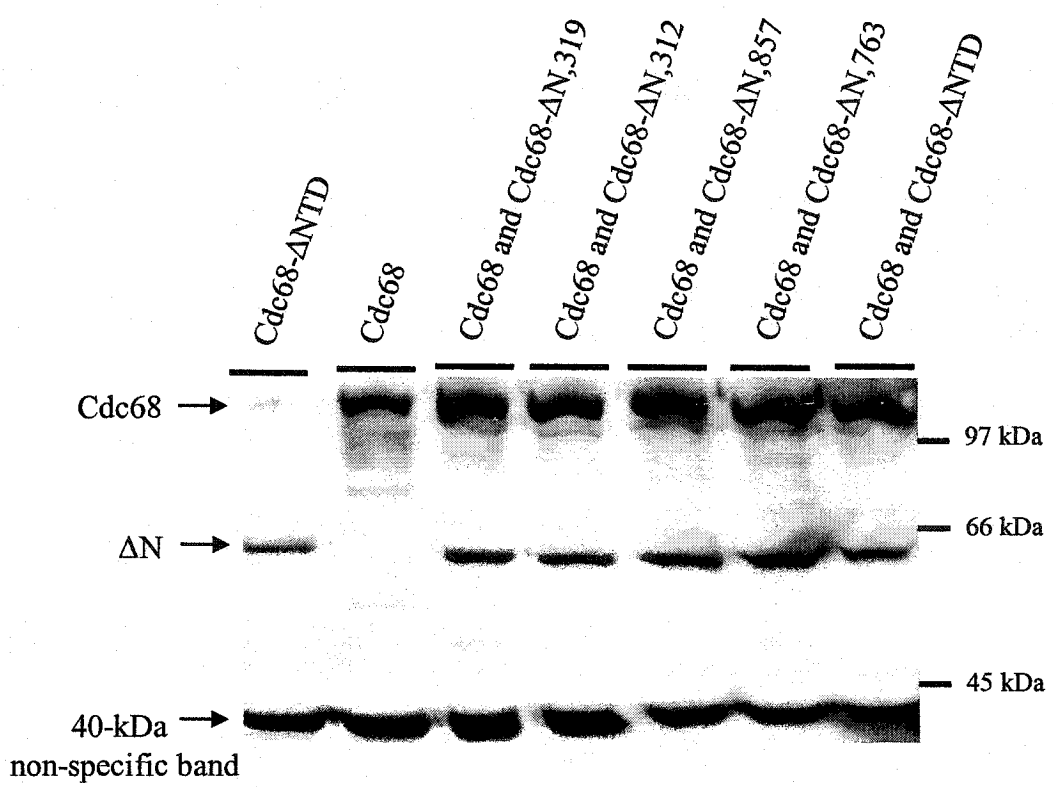

Figure 41. Chimeric Cdc68 proteins are stable in the presence of wild-type Cdc68 protein. Western blots of protein extracts (5 μg/lane) from cells with various alleles of *CDC68* (as indicated across the top) growing logarithmically at 30°C. Blots were probed with affinity-purified rabbit polyclonal anti-Cdc68 antibody and detected using HRP-conjugated goat anti-rabbit IgG antibody and chemiluminescent substrate. India-ink staining of the membranes prior to antibody binding was used as a loading control (not shown). The non-specific band at 40 kDa is also an indicator of relative loading and transfer.

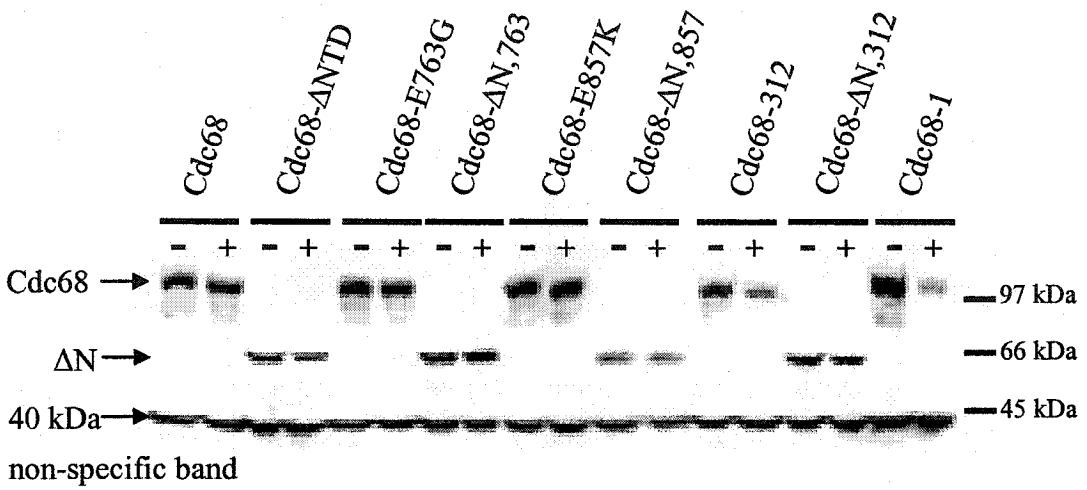

Figure 42. Chimeric Cdc68 proteins are stable at 38°C. Protein extracts (8 μg/lane) were made from cells with various alleles of *CDC68* (as indicated across the top) growing logarithmically at 23°C (-) or shifted in log-phase to the non-permissive temperature (38°C) and incubated at this temperature for one hour with addition of cycloheximide to 0.5mg/ml (+), and resolved electrophoreticlly for western analysis. Blots were probed with affinity-purified rabbit polyclonal anti-Cdc68 antibody and visualized using HRP-conjugated goat anti-rabbit IgG antibody and chemiluminescent substrate. India-ink staining of the membranes prior to antibody binding was used as a loading control (not shown). The non-specific band at 40 kDa is also an indicator of relative loading and transfer.

xiii) Global alterations in transcription caused by *cdc68* mutations

To determine if the overlapping function between the N-terminal domain and the C-terminal domain could be explained by a common influence of these domains on transcription, global alterations in the transcription profiles for cells containing *cdc68* mutations were determined. Two-colour microarray analyses of transcripts was carried out for cells containing *cdc68-mini* (which encodes a protein missing the majority of the N-terminal domain), *cdc68-312* and *cdc68-319* (which both encode proteins containing C-terminal amino acid substitutions) and compared to that for *CDC68* cells. The transcripts from *cdc68* mutant cells were reverse-transcribed and labelled with a fluorophore to generate a cDNA pool, which was mixed with an equivalent but differentially labelled cDNA pool generated from transcripts from wild-type *CDC68* cells. These two mixed pools of cDNA were then hybridized to spotted microarray slides (University Health Network Microarray Center, Toronto), where each spot contains PCR-amplified products corresponding to the open reading frame (ORF) of a yeast gene. Cy3-labelled cDNAs generated from wild-type *CDC68* cells were mixed with Cy5-labelled cDNAs generated from *cdc68-mini*, *cdc68-312*, or *cdc68-319* cells and incubated on a microarray slide to permit hybridization of the labelled cDNAs to the ORF DNA present on each slide. A 'dye-swap' experiment was also performed in which the cDNAs generated from wild-type *CDC68* cells were labelled with Cy5-dUTP and those from *cdc68-mini*, *cdc68-312*, or *cdc68-319* were labelled with Cy3-dUTP. The dye-swap experiment helps control for possible alterations in transcript labelling efficiencies that may result from differences in the incorporation of the Cy5- or Cy3-tagged dUTP moieties by the reverse-transcriptase enzyme.

Cy3 and Cy5 are fluorophores that permit the specific detection of the differentially tagged cDNAs when light of the appropriate wavelength is applied. By measuring the fluorescence intensities of each spotted ORF, a comparison of the relative abundance of a given transcript isolated from a *CDC68* cell *versus* that isolated from a *cdc68* mutant cell may be attained.

a) Genes with altered transcript abundance in *cdc68-mini* cells

Comparisons of the transcript profiles for *cdc68-mini* cells *versus CDC68* cells using microarray analysis identified only a handfull of genes, 17 in all, with significant (greater

than two-fold) changes in transcript abundance. The proteins encoded by these 17 genes can be grouped into four functional classes (as determined using Osprey and the Yeast Grid database gene ontology annotations as of May, 2004): cell growth and maintenance, stress response, metabolism, and 'unknown' (Table 13). For many of these genes, such as *FMP45*, *HBT1*, *YBR281C*, *YDR015C*, *YFL013W-A*, *YGL211W*, and *YNL195C*, very little is known about the functions of the encoded proteins. The remaining genes share only a limited number of common expression attributes. Global transcription regulatory analysis (Lee *et al.* 2002) did not indicate any striking overlap in the transcription factors regulating this entire group of genes. The transcription factor *Hsf1* (heat shock factor), involved in activating expression of a number of genes in response to a range of cellular stressors (Sorger and Pelham 1988; Hahn *et al.* 2004) plays a role in activating the expression of five of the seventeen genes identified here, namely *ALD3*, *HSP12*, *HSP26*, *CUP1-1* and *CUP1-2*, in response to heat shock, oxidative stress or glucose deprivation (Sakurai and Fukasawa 2001; Aranda and del Olmo 2003; Hahn *et al.* 2004; Hahn and Thiele 2004). Additionally, the *ALD3*, *HSP12* and *HSP26* genes are regulated by the association of the general-stress-response transcription factors Msn2 and Msn4 to STREs (stress-response elements) in their promoters (Varela *et al.* 1995; Martinez-Pastor *et al.* 1996; DeRisi *et al.* 1997; Moskvina *et al.* 1998; Aranda and del Olmo 2003). Like Hsf1, the Msn2/4 transcription factors activate gene expression in response to cellular stresses, including heat shock, osmotic stress, and metabolic stress (Estruch 2000), and the Hsf1 and Msn2/4 transcription factors have been shown to work both co-operatively and independently to activate a common gene set in response to various cellular stressors (Amoros and Estruch 2001; Grably *et al.* 2002; Lagorce *et al.* 2003).

Each of the five genes that shows a greater than two-fold increase or decrease in transcript abundance in the *cdc68-mini* cells and is regulated by Hsf1 and/or Msn2/4 encodes a protein involved in cellular adaptations to stress. *HSP12* and *HSP26* both encode heat-shock proteins that act as chaperones in the refolding of denatured proteins that arise as a result of cell perturbations (Praekelt and Meacock 1990; Haslbeck *et al.* 1999; Stromer *et al.* 2004). The expression of molecular chaperones is up-regulated in times of stress, such as fluctuations in temperature, osmolarity and glucose, which may result in unfolded proteins (Varela *et al.* 1995; DeRisi *et al.* 1997; Puig and Perez-Ortin

Table 13. Gene-expression changes greater than two-fold in *cdc68-mini* cells as determined by microarray analysis.

A. Gene expression down-regulated in *cdc68-mini* cells with respect to wild-type expression levels:

Cell growth and maintenance:

Gene Name	Systematic Name	Description	Gene Ontology	Log_2 Ratio				Average Fold-decrease
FMP45	**YDL222C**	The authentic, non-tagged protein was localized to the mitochondria; cell cortex protein	cell organization and biogenesis; cell growth and/or maintenance	-1.28	-1.19	-1.27	-1.20	2.4
HBT1	**YDL223C**	Substrate of the Hub1p ubiquitin-like protein that localizes to the shmoo tip mating projection ; mutants are defective for mating projection formation, thereby implicating Hbt1p in polarized cell morphogenesis	cell organization and biogenesis; cell growth and/or maintenance	-1.76	-1.84	-1.76	-1.81	3.5

Stress response:

Gene Name	Systematic Name	Description	Gene Ontology	Log_2 Ratio				Average Fold-decrease
ALD3	**YMR169C**	Expression induced in response to heat shock, oxidative and osmotic stress. NAD+ is preferred coenzyme.	response to stress; metabolism	-1.16	-1.35	-1.17	-1.34	2.4
HSP12	**YFL014W**	induced by heat shock, entry into stationary phase, depletion of glucose, and addition of lipids fatty acids	response to stress; metabolism	-1.04	-1.22	-1.26	-1.31	2.3
HSP26	**YBR072W**	heat shock protein 26	metabolism; response to stress	-1.55	-2.05	-1.55	-2.03	3.5

Metabolism:

Gene Name	Systematic Name	Description	Gene Ontology	Log2 Ratio				Average Fold-decrease
ALD6	YPL061W	Utilizes NADP+ as the preferred coenzyme. Activated by Mg2+.	metabolism	-1.34	-1.14	-1.34	-1.18	2.4
CAT2	YML042W	Carnitine O-acetyltransferase, peroxisomal and mitochondrial	metabolism	-1.59	-1.52	-1.48	-1.61	2.9
MET6	YER091C	Cobalamin-independent methionine synthase, involved in amino acid biosynthesis; also called N5-methyltetrahydrofolate homocysteine methyltransferase or 5-methyltetrahydropteroyltriglutamate homocysteine methyltransferase	metabolism	-1.24	-1.16	-1.24	-1.16	2.3
STR3	YGL184C	Sulfur TRansfer	metabolism	-1.15	-0.98	-1.19	-1.16	2.2

Unknown:

Gene Name	Systematic Name	Description	Gene Ontology	Log2 Ratio				Average Fold-decrease
RTN2	YDL204W	reticulon gene member of the RTNLA reticulon-like A subfamily	biological process unknown	-1.32	-1.16	-1.31	-1.18	2.4
YDR015C	YDR015C	Hypothetical Systematic	biological process unknown	-1.01	-1.09	-0.96	-1.05	2.0
YFL013W-A	YFL013W-A	Hypothetical Systematic	biological process unknown	-1.31	-1.37	-1.38	-1.43	2.6
YNL195C	YNL195C	NONE	biological process unknown	-1.79	-1.73	-1.74	-1.59	3.3

B. Gene expression that is up-regulated in *cdc68-mini* cells with respect to wild-type expression levels:

Unknown:

Gene Name	Systematic Name	Description	Gene Ontology	Log$_2$ Ratio				Average Fold-increase
CUP1-1	**YHR053C**	Metallothionein, binds copper and mediates resistance to high concentrations of copper and cadmium; locus is variably amplified in different strains, with two copies, CUP1-1 and CUP1-2, in the genomic sequence reference strain S288C	NONE	1.84	1.03	1.85	1.11	2.8
CUP1-2	**YHR055C**	Metallothionein, binds copper and mediates resistance to high concentrations of copper and cadmium; locus is variably amplified in different strains, with two copies, CUP1-1 and CUP1-2, in the genomic sequence reference strain S288C	biological process unknown	2.41	1.25	2.23	1.33	3.7
YBR281C	**YBR281C**	NONE	biological process unknown	1.25	1.14	1.60	1.18	2.5
YGL211W	**YGL211W**	NONE	biological process unknown	3.04	2.96	2.34	3.05	7.3

2000; Aranda and del Olmo 2003). The *CUP1-1* and *CUP1-2* genes are duplicate copies of the *CUP1* gene found in S288c-derived strains. These genes encode proteins involved in regulating copper ion concentrations but, in addition to their role in copper homeostasis, each of these genes is induced in response to the diauxic shift (DeRisi *et al.* 1997; Haurie *et al.* 2001; Hahn and Thiele 2004). The diauxic shift refers to the point when cells switch from fermenting glucose as a primary energy source to utilizing ethanol in aerobic respiration. While a role for Cup1-1 and Cup1-2 proteins at the diauxic shift is unclear, it is interesting that this alternative form of stress, namely glucose limitation, can also induce the expression of these genes. *ALD3* encodes a cytoplasmic aldehyde dehydrogenase whose expression is also induced when the glucose supply becomes limiting and cells begin utilizing ethanol as a fuel (DeRisi *et al.* 1997; Aranda and del Olmo 2003). Aldehyde dehydrogenases assist in one phase of the conversion of ethanol into acetyl-CoA, which may then participate in metabolism by the tricarboxylic acid cycle.

ALD6, which also encodes a cytosolic aldehyde dehydrogenase, was identified here as having decreased transcript levels in *cdc68-mini* cells. The *ALD6* gene is not regulated in the same fashion as *ALD3*, however, as it is not regulated by the Hsf1 or Msn2/4 transcription factors and is typically expressed at high levels even in the presence of glucose (Aranda and del Olmo 2003). The reported alterations in *ALD6* gene expression upon diauxic shift have been variable, with some reports indicating a decline in *ALD6* expression while others demonstrate an increased expression of *ALD6*, depending on the strains and conditions employed (DeRisi *et al.* 1997; Haurie *et al.* 2001; Aranda and del Olmo 2003).

Consistent with the findings that several of the aforementioned genes are regulated in response to cellular stress, the *FMP45* gene, down regulated in *cdc68-mini* cells, has been identified in a screen for genes whose expression is up-regulated in response to osmotic stress (Runner and Brewster 2003), and *FMP45*, *HBT1*, *CAT2*, *RTN2* and *YNL195C* are each induced during the diauxic shift (DeRisi *et al.* 1997; Puig and Perez-Ortin 2000). Thus in total, 10 of the 17 genes identified here as affected by *cdc68-mini* are up-regulated in response to some form of stress, and 9 of these respond specifically to limited glucose levels that arise during the diauxic shift (DeRisi *et al.* 1997). It should be

noted that approximately 1700 genes have been found with a greater than 2-fold alteration in transcript level during the diauxic shift (DeRisi *et al.* 1997), so the nine genes with altered expression patterns identified here are in no way representative of the complexity of the diauxic-shift gene-expression profile. There are several possible explanations for the altered expression in *cdc68-mini* cells of genes regulated by stress conditions. Perhaps *cdc68-mini* cells do not respond to stress as effectively as wild-type *CDC68* cells due problems activating gene expression. Chromatin structural changes due to the presence of Cdc68-mini in FACT could impair or facilitate (depending on the gene in question) gene activation, perhaps specifically by altering the activation of gene expression by the Msn2/4 or Hsf1 transcription factors. Mutant FACT could prevent effective binding of the Msn2/4 or Hsf1 transcription factors to the promoters of genes identified here, or somehow impair subsequent recruitment of RNA polymerase proteins and/or histone-modifiying complexes, which would result in decreased expression. Another possibility is that the mutant FACT complex may not be able to facilitate effectively the passage of RNA polymerase II through the nucleosomal barrier during transcription elongation, which could also result in decreased transcript levels. However, it is difficult to say why this type of 'global' defect in RNA polymerase II transcription would not generate widespread effects in the transcription profile for *cdc68-mini* cells; therefore this scenario is a less-appealing alternative. The fact that so few genes were identified with alterations in transcript levels in *cdc68-mini* cells implies that the *cdc68-mini* mutation has little impact on transcript abundance. A final possibility is that a difference in the glucose levels present in the growth medium of the wild-type *CDC68* cells *versus cdc68-mini* cells used for RNA extraction is the cause of these alterations in transcript levels. If this were the case, then the *CDC68* cells may have been at a different stage in the diauxic shift and therefore the gene-expression profiles would be different. Given the fact that the *cdc68-mini* cells were harvested at a concentration of 4.2×10^7 cells per millilitre of culture while the wild-type *CDC68* cells were harvested at a concentration of 4.4×10^7 cells per millilitre of culture (and that these cells were each grown in medium from the same bottle of YPD), it is difficult to explain these findings simply based on different glucose levels in the medium as a result of differences in cell density. Indeed, the difference in glucose levels between these two cultures could not

have been dramatically different or this difference would have been reflected in changes in transcript abundance for a much larger number of genes.

In summary, the *cdc68-mini* mutation does not cause global alterations in transcript abundance. Thus the N-terminal domain of Cdc68 may be removed with only minor alterations in the gene-expression profile (Table 13). Several of the genes that do display altered transcript abundance in *cdc68-mini* cells compared to *CDC68* cells are induced during stress responses. This finding may indicate that *cdc68-mini* cells do not respond to cellular stress as effectively or in the same fashion as do *CDC68* cells. Specifically, a significant number of the genes identified here as having altered transcript levels in *cdc68-mini* cells are regulated by the Hsf1 and Msn2/4 transcription factors; therefore *cdc68-mini* may alter the ability of these transcription factors to induce gene expression in response to stress.

b) Genes with altered transcript abundance in *cdc68-312* cells

Similar to the microarray findings for *cdc68-mini* cells, in comparing the transcript profile for *cdc68-312* cells to that for wild-type *CDC68* cells, little alteration in gene expression was observed. Thus the *cdc68-312* mutation also has little impact on the regulation of transcript abundance. Only 16 genes were shown to differ in expression by a factor of two or more in *cdc68-312* cells, and all of these genes showed a decrease in transcript abundance in the *cdc68-312* cells (Table 14). No genes were identified with increased transcript abundance in *cdc68-312* cells in comparison to wild-type transcript levels. The 16 genes with decreased transcript abundance in *cdc68-312* cells encode proteins that are involved in cell growth and maintenance, metabolism, and stress response (Table 14). Significant overlap between the altered gene expression patterns for *cdc68-312* and *cdc68-mini* cells was observed, with 9 genes (greater than 50% of the genes identified in each of the microarray experiments) common to both sets. The majority of genes with decreased transcript abundance in *cdc68-312* cells, including *ALD3*, *ALD6*, *CAT2*, *FMP45*, *GPX1*, *HBT1*, *HSP26*, *LEE1*, *SOL4*, *SUC2*, *UIP4*, *YJR096W* and *YNL195C*, have been shown to be induced as a result of fluctuations in osmolarity and/or temperature, or by oxidative or glucose-deprivation stress (DeRisi *et al.* 1997; Inoue *et al.* 1999; Puig and Perez-Ortin 2000; Haurie *et al.* 2001; Boer *et al.* 2003; Runner and Brewster 2003). These findings indicate that, like *cdc68-mini* cells,

Table 14. Gene-expression changes greater than two-fold in *cdc68-312* cells as determined by microarray analysis.

Cell growth and maintenance:

Gene Name(s)	Orf Name	Description	Gene Ontology	Log_2 Ratios				Average Fold-decrease
FMP45	**YDL222C**	The authentic, non-tagged protein was localized to the mitochondria; cell cortex protein	cell organization and biogenesis; cell growth and/or maintenance	-1.21	-1.08	-1.22	-0.77	2.1
HBT1	**YDL223C**	Substrate of the Hub1p ubiquitin-like protein that localizes to the shmoo tip mating projection ; mutants are defective for mating projection formation, thereby implicating Hbt1p in polarized cell morphogenesis	cell organization and biogenesis; cell growth and/or maintenance	-1.29	-1.64	-1.31	-1.58	2.8

Stress response:

Gene Name(s)	Orf Name	Description	Gene Ontology	Log_2 Ratios				Average Fold-decrease
ALD3	**YMR169C**	Expression induced in response to heat shock, oxidative and osmotic stress. NAD+ is preferred coenzyme.	response to stress; metabolism	-1.41	-1.51	-1.36	-1.56	2.8
GPX1	**YKL026C**	Phospholipid hydroperoxide glutathione peroxidase induced by glucose starvation that protects cells from phospholipid hydroperoxides and nonphospholipid peroxides during oxidative stress	response to stress; metabolism	-1.12	-1.03	-1.12	-1.04	2.1

HSP26	**YBR072W**	heat shock protein 26	metabolism; response to stress	-2.35	-2.45	-2.34	-2.42	5.2

Metabolism:

Gene Name(s)	Orf Name	Description	Gene Ontology	Log_2 Ratios				Average Fold-decrease
ALD6	**YPL061W**	Utilizes NADP+ as the preferred coenzyme. Activated by Mg2+.	metabolism	-1.27	-1.11	-1.21	-1.07	2.2
CAT2	**YML042W**	Carnitine O-acetyltransferase, peroxisomal and mitochondrial	metabolism	-1.95	-2.19	-1.90	-2.23	4.2
ECM17	**YJR137C**	ExtraCellular Mutant	metabolism; cell organization and biogenesis; cell growth and/or maintenance	-1.10	-1.19	-1.08	-1.13	2.2
STR3	**YGL184C**	Sulfur TRansfer	metabolism	-1.46	-1.24	-1.23	-1.22	2.4

Carbohydrate metabolism:

Gene Name(s)	Orf Name	Description	Gene Ontology	Log_2 Ratios				Average Fold-decrease
SUC2	**YIL162W**	None	carbohydrate metabolism; metabolism	-1.68	-1.79	-1.67	-1.80	3.3
YJR096W	**YJR096W**	None	carbohydrate metabolism; metabolism	-1.10	-1.03	-1.07	-0.97	2.1

Unknown:

Gene Name(s)	Orf Name	Description	Gene Ontology	Log_2 Ratios				Average Fold-decrease
LEE1	**YPL054W**	Product of gene unknown	biological process unknown	-1.03	-1.09	-1.06	-1.24	2.2
SOL4	**YGR248W**	Similar to SOL3	biological_process unknown	-1.26	-1.58	-1.31	-1.59	2.7
UIP4	**YPL186C**	Ulp1 Interacting Protein 4	biological process unknown	-1.14	-1.13	-1.16	-1.21	2.2
YFL013W-A	**YFL013W-A**	None	biological process unknown	-1.01	-1.07	-1.13	-1.14	2.1
YNL195C	**YNL195C**	None	biological process unknown	-2.71	-2.31	-2.62	-2.44	5.8

cdc68-312 cells may not be able to activate the expression of these genes as effectively as wild-type *CDC68* cells in response to stress. Four of the genes identified here as down-regulated in *cdc68-312* mutant cells, *ALD3*, *GPX1*, *HSP26*, and *LEE1*, are regulated by Hsf1 and/or Msn2/4 transcription factors (Martinez-Pastore *et al.* 1996; DeRisi *et al.* 1997; Moskvina *et al.* 1998; Aranda and del Olmo 2003; Hahn and Thiele 2004). As indicated above for *cdc68-mini*, this may imply that the *cdc68-312* mutation specifically impedes the function of these transcription factors. However, the number of genes identified here as influenced by *cdc68-312* and regulated by Hsf1 and/or Msn2/4 is small compared to the total number of genes regulated by these transcription factors.

Twelve of the 16 genes down-regulated in *cdc68-312* cells are induced during the diauxic shift (DeRisi *et al.* 1997). This may imply that the *CDC68* cells employed in this experiment had limiting amounts of glucose in comparison to the *cdc68-312* cells so that these genes would have been induced in the wild-type cells but not in the *cdc68-312* cells. It seems unlikely that this is the case, however, since the cell concentration was 4.4 x 10^7 cells per millilitre for wild-type *CDC68* cells and 3.8 x 10^7 cells per millilitre for *cdc68-312* cells, a difference of only 13%. Additionally, the fact that a related set of gene-expression changes was seen in the *cdc68-mini* microarray experiment argues that both *cdc68-312* cells and *cdc68-mini* cells would have been in a more glucose-rich environment than the *CDC68* control cells. While both the *cdc68-312* and *cdc68-mini* cells were at slightly lower cell concentrations than the wild-type *CDC68* cells, the changes were small and therefore would not be expected to influence gene expression significantly. An alternative explanation for the similarities between the patterns of *cdc68-312* and *cdc68-mini* transcription changes is that these two mutant alleles cause similar impairments to transcription functions. This similarity between the effects of the *cdc68-312* mutation and *cdc68* mutations encoding N-terminal domain deletions is also observed in the results of SGA analysis (Results 4, vi and viii), and genetic analyses of chimeric mutant alleles containing both the *cdc68-312* point mutations and the N-terminal domain deletion indicate an overlapping function for these two domains (Results 2, xi). The diauxic shift results in a greater than two-fold induction of approximately 700 genes (DeRisi *et al.* 1997); thus the twelve genes identified here which are also induced

during glucose limitation represent a small subset of the gene-expression changes observed during the diauxic shift.

Three of the genes down-regulated in *cdc68-312* mutant cells, *HSP26*, *SUC2*, and *YNL195C*, are regulated by the Ssn6-Tup1 repressor complex, and are induced when the *TUP1* gene is deleted (DeRisi *et al.* 1997; Boukaba *et al.* 2004). Ssn6 and Tup1 are repressors that block the transcription of genes involved in determining mating type and in coping with glucose starvation, hypoxia, DNA damage, and osmotic stress (reviewed in Wahi *et al.* 1998). Many DNA-binding proteins are able to recruit the Ssn6-Tup1 repressor complex to gene promoters, and in turn Tup1 is thought to target histone deacetylation complexes (HDACs) to the promoters (reviewed in Wahi *et al.* 1998; Watson *et al.* 2000). The HDACs deacetylate histones in the promoter region, which promotes Tup1 association with histones to generate a chromatin conformation that is repressive to transcription (Deckert and Struhl 2001; Davie *et al.* 2002). When the appropriate signals are present, not only can Ssn6-Tup1-mediated repression be lost, but this complex can assist in activating gene expression by recruiting histone modifiying and remodelling complexes (Proft and Struhl 2002). Thus an association between Tup1 activities and chromatin structure has clearly been established. One possible mechanism for *cdc68-312*–mediated decreases in the expression of genes may be through mis-regulation of the Ssn6-Tup1 complex. Chromatin structural modifications mediated by the Ssn6-Tup1 complex may not occur as efficiently at the *HSP26*, *SUC2*, and *YNL195C* promoters when the Cdc68-312 protein is part of the FACT complex, leading to decreased transcription of these genes in FACT mutant cells. There are over 200 genes whose expression is increased when the *TUP1* gene is deleted (DeRisi *et al.* 1997), so that the three genes affected by *cdc68-312* represent only a small portion of that gene set. However, as described in the following section, the *cdc68-319* mutation also results in altered expression of genes known to be repressed by the Ssn6-Tup1 complex. The fact that the *cdc68-319* allele, which also encodes a protein containing C-terminal mutations, alters the transcription of Ssn6-Tup1–regulated genes makes a stronger case for an overlapping role in regulating gene expression for these two protein complexes.

In summary, the *cdc68-312* mutation does not alter transcript abundance for the majority of genes. For the few genes whose expression does decrease significantly in

cdc68-312 cells, most are known to be activated in response to cellular stresses, like osmotic, temperature, glucose or oxidative fluctuations. Few common regulatory ties could be identified within this small set of genes, although some of the genes are regulated by the transcription factors Hsf1 and/or Msn2/4, and/or by the repressor Tup1. There may be specific roles for FACT in mediating the activities of these particular transcription activators and repressors. However, given that only one biological sample was employed for these microarray experiments, any changes in gene expression observed need to be further verified by alternative approaches. As a result of this feature, the expression changes observed may be due to subtle differences in the glucose levels in the growth medium of the wild-type cells and that of the mutant *cdc68* cells. The glucose level for the wild-type cells would have had to have been less than that for the *cdc68-312* cells and *cdc68-mini* cells, which show strikingly similar alterations in transcription.

c) Genes with altered transcript abundance in *cdc68-319* cells

In striking contrast to the relatively normal transcription profiles observed for *cdc68-312* or *cdc68-mini* cells, *cdc68-319* mutant cells show significant alterations in gene expression as determined by transcript abundance measurements. As many as 187 genes exhibited a greater than two-fold alteration in transcript abundance in *cdc68-319* cells in comparison to wild-type *CDC68* cells, with 37 genes showing a greater than two-fold increase in transcript abundance and 150 genes showing a greater than two-fold decrease in transcript abundance (Table 15). These genes encode proteins with a range of cellular functions (Table 15), although some common expression attributes were identified for these genes.

c.i.Genes with increased transcript abundance in *cdc68-319* cells

The genes that are up-regulated in the *cdc68-319* cells are predominantly involved in ribosome biogenesis. A total of 23 (*RPA43*, *LSG1*, *RIX7*, *RPL42B*, *RPS17B*, *RPS28B*, *SDA1*, *DHR2*, *DIM1*, *ERB1*, *HCA4*, *MTR4*, *NAN1*, *NOP7*, *NSR1*, *NUG1*, *RIO2*, *RLP7*, *RRP5*, *TSR1*, *UTP14*, *FPR4*, and *NOP13*) of the 37 genes that show a greater than two-fold increase in transcript abundance in *cdc68-319* cells in comparison to *CDC68* cells encode components of the ribosome or proteins involved in ribosome assembly and/or nuclear export (Fath *et al.* 2000; Bassler *et al.* 2001; Nissan *et al.* 2002; Kallstrom *et al.*

Table 15. Genes-expression changes greater than two-fold in *cdc68-319* cells as determined by microarray analysis.

A. Gene expression down-regulated in *cdc68-319* cells with respect to wild-type expression levels:

Transcription:

Gene Name	Systematic Name	Description	Gene Ontology	Log_2 ratios				Average Fold-decrease
GAC1	**YOR178C**	Regulatory subunit for phosphoprotein phosphatase type 1 PP-1 , also known as Glc7p, which regulates glycogen synthase-2	transcription; metabolism; carbohydrate metabolism; cell cycle; cell growth and/or maintenance; response to stress	-1.48	-1.73	-1.53	-1.74	3.1
HPR1	**YDR138W**	Hyperrecombination protein that suppresses intrachromosomal excision recombination	RNA localization; metabolism; transport; cell growth and/or maintenance; DNA recombination; DNA metabolism; transcription	-1.19	-1.16	-1.13	-1.14	2.2
NET1	**YJL076W**	Nucleolar protein involved in exit from mitosis	transcription; metabolism; DNA metabolism; cell organization and biogenesis; cell growth and/or maintenance; cell cycle	-1.72	-1.94	-1.70	-2.00	3.6
PNC1	**YGL037C**	NAD + salvage pathway gene	metabolism; transcription; DNA metabolism; cell organization and biogenesis; cell growth and/or maintenance	-1.70	-2.00	-1.64	-1.98	3.6
RME1	**YGR044C**	mediates cell type control of sporulation; negatively regulates IME1 and sporulation	transcription; metabolism; cell cycle; cell growth and/or maintenance	-1.80	-1.89	-1.80	-1.83	3.6
RPO26	**YPR187W**	subunit common to RNA polymerases I, II, and III	transcription; metabolism	-1.56	-1.24	-1.55	-1.28	2.7

SDS3	**YIL084C**	Suppressor of Defective Silencing 3 Functions are similar to those of SIN3 and RPD3	transcription; metabolism; DNA metabolism; cell organization and biogenesis; cell growth and/or maintenance	-1.00	-1.23	-1.00	-1.22	2.2

Transport:

Gene Name	Systematic Name	Description	Gene Ontology	Log_2 ratios				Average Fold-decrease
ARV1	**YLR242C**	ARE2 Required for Viability 1. similar to Nup120p and C.elegans R05H5.5 protein.	transport; cell growth and/or maintenance; metabolism	-1.40	-1.32	-1.34	-1.27	2.5
GAL2	**YLR081W**	Galactose transport, also able to transport hexoses	carbohydrate metabolism; metabolism; transport; cell growth and/or maintenance	-1.38	-1.56	-1.43	-1.57	2.8
GSG1	**YDR108W**	Subunit of TRAPP transport protein particle , a multi-subunit complex involved in targeting and/or fusion of ER-to-Golgi transport vesicles with their acceptor compartment; protein has late meiotic role, following DNA replication	transport; cell growth and/or maintenance; cell cycle	-1.45	-1.26	-1.34	-1.04	2.4
HXT1	**YHR094C**	Low-affinity glucose transporter of the major facilitator superfamily, expression is induced by Hxk2p in the presence of glucose and repressed by Rgt1p when glucose is limiting	transport; cell growth and/or maintenance	-1.67	-1.75	-1.63	-1.72	3.2
HXT10	**YFL011W**	Putative hexose transporter, expressed at low levels and expression is repressed by glucose	transport; cell growth and/or maintenance;	-1.76	-1.73	-1.88	-1.72	3.4
HXT15	**YDL245C**	Protein of unknown function with similarity to hexose transporter family members, expression is induced by low levels of glucose and repressed by high levels of glucose	transport; cell growth and/or maintenance	-0.92	-1.02	-1.15	-1.01	2.0

HXT3	**YDR345C**	Low affinity glucose transporter of the major facilitator superfamily, expression is induced in low or high glucose conditions	transport; cell growth and/or maintenance	-1.45	-1.42	-1.55	-1.48	2.8
HXT4	**YHR092C**	High-affinity glucose transporter of the major facilitator superfamily, expression is induced by low levels of glucose and repressed by high levels of glucose	transport; cell growth and/or maintenance	-2.20	-2.15	-2.19	-2.13	4.5
HXT5	**YHR096C**	Hexose transporter with moderate affinity for glucose, may function in accumulation of reserve carbohydrates during stress, expression induced by a decrease in growth rate, contains an extended N-terminal domain relative to other HXTs	transport; cell growth and/or maintenance	-1.18	-1.18	-1.16	-1.18	2.3
HXT6	**YDR343C**	High-affinity glucose transporter of the major facilitator superfamily, nearly identical to Hxt7p, expressed at high basal levels relative to other HXTs, repression of expression by high glucose requires SNF3	transport; cell growth and/or maintenance	-2.64	-2.83	-2.67	-2.86	6.7
HXT7	**YDR342C**	High-affinity glucose transporter of the major facilitator superfamily, nearly identical to Hxt6p, expressed at high basal levels relative to other HXTs, expression repressed by high glucose levels	transport; cell growth and/or maintenance	-2.86	-3.39	-3.02	-3.40	9.1
HXT8	**YJL214W**	Protein of unknown function with similarity to hexose transporter family members, expression is induced by low levels of glucose and repressed by high levels of glucose	transport; cell growth and/or maintenance	-2.59	-2.34	-2.39	-2.30	5.3

HXT9	**YJL219W**	Putative hexose transporter that is nearly identical to Hxt11p, has similarity to major facilitator superfamily MFS transporters, expression of HXT9 is regulated by transcription factors Pdr1p and Pdr3p	transport; cell growth and/or maintenance	-2.09	-1.70	-2.07	-1.70	3.7
MON1	**YGL124C**	Protein required for fusion of cvt-vesicles and autophagosomes with the vacuole; associates, as a complex with Ccz1p, with a perivacuolar compartment; potential Cdc28p substrate	protein transport; metabolism; transport; cell growth and/or maintenance; autophagy	-1.12	-1.21	-1.10	-1.14	2.2
STF2	**YGR008C**	ATPase stabilizing factor	response to stress; metabolism; transport; cell growth and/or maintenance	-1.83	-2.17	-1.85	-2.07	4.0
TRS120	**YDR407C**	targeting complex TRAPP component involved in ER to Golgi membrane traffic	transport; cell growth and/or maintenance	-2.72	-2.59	-2.77	-2.62	6.4
VMA5	**YKL080W**	42 kDa subunit of V1 sector	transport; cell growth and/or maintenance; cell organization and biogenesis	-1.09	-1.09	-1.10	-1.04	2.1
YRA2	**YKL214C**	Yeast RNA Annealing protein	RNA localization; metabolism; transport; cell growth and/or maintenance;	-1.41	-1.15	-1.49	-1.23	2.5

Cell growth and maintenance:

Gene Name	Systematic Name	Description	Gene Ontology	Log_2 ratios				Average Fold-decrease
CWH41	**YGL027C**	Glucosidase I, involved in assembly of cell wall beta 1,6 glucan; an ER type II integral membrane N-glycoprotein	cell organization and biogenesis; cell growth and/or maintenance	-0.84	-1.07	-1.21	-1.04	2.1

ECM4	**YKR076W**	ExtraCellular Mutant	cell organization and biogenesis; cell growth and/or maintenance	-1.65	-1.33	-1.59	-1.27	2.8
HBT1	**YDL223C**	Substrate of the Hub1p ubiquitin-like protein that localizes to the shmoo tip mating projection ; mutants are defective for mating projection formation, thereby implicating Hbt1p in polarized cell morphogenesis	cell organization and biogenesis; cell growth and/or maintenance	-1.64	-1.64	-1.52	-1.59	3.0
NCA3	**YJL116C**	With NCA2, regulates proper expression of subunits 6 Atp6p and 8 Atp8p of the Fo-F1 ATP synthase	cell organization and biogenesis; cell growth and/or maintenance	-1.79	-1.78	-1.76	-1.65	3.4
PEX28	**YHR150W**	Similar to PEX24 in Yarrowia lipoytica	cell organization and biogenesis; cell growth and/or maintenance	-2.05	-1.97	-2.01	-1.96	4.0

Protein biosynthesis:

Gene Name	Systematic Name	Description	Gene Ontology	Log_2 ratios				Average Fold-decrease
UGP1	**YKL035W**	UDP-glucose pyrophosphorylase or UTP-glucose-1-phosphate uridylyltransferase	protein biosynthesis; metabolism; carbohydrate metabolism	-1.59	-1.65	-1.72	-1.70	3.2

Cell cycle:

Gene Name	Systematic Name	Description	Gene Ontology	Log_2 ratios				Average Fold-decrease
SMP2	**YMR165C**	involved in plasmid maintenance	metabolism; cell cycle; cell growth and/or maintenance	-1.88	-1.56	-1.76	-1.49	3.2

Stress Response:

Gene Name	Systematic Name	Description	Gene Ontology	Log2 ratios				Average Fold-decrease
ALD3	**YMR169C**	Expression induced in response to heat shock, oxidative and osmotic stress. NAD+ is preferred coenzyme.	response to stress; metabolism	-1.84	-1.98	-1.86	-1.97	3.8
CTT1	**YGR088W**	Cytosolic catalase T, has a role in protection from oxidative damage by hydrogen peroxide	response to stress	-2.15	-2.24	-2.18	-2.28	4.6
GAD1	**YMR250W**	glutamate decarboxylase	response to stress; metabolism	-2.85	-2.85	-2.87	-2.83	7.2
GPX1	**YKL026C**	Phospholipid hydroperoxide glutathione peroxidase induced by glucose starvation that protects cells from phospholipid hydroperoxides and nonphospholipid peroxides during oxidative stress	response to stress; metabolism	-1.79	-1.66	-2.02	-1.58	3.4
GRE3	**YHR104W**	Aldose reductase involved in methylglyoxal, d-xylose and arabinose metabolism; stress induced osmotic, ionic, oxidative, heat shock, starvation and heavy metals ; regulated by the HOG pathway	response to stress; carbohydrate metabolism; metabolism	-1.32	-1.11	-1.37	-1.17	2.4
HSP104	**YLL026W**	plays a major role in the acquisition of tolerance to a variety of stresses such as heat, ethanol, and sodium arsenite, inheritance of [PSI+], and reactivation of mRNA splicing after heat shock.	metabolism; response to stress	-1.94	-1.92	-1.88	-1.91	3.8
HSP12	**YFL014W**	induced by heat shock, entry into stationary phase, depletion of glucose, and addition of lipids fatty acids	response to stress; metabolism	-1.54	-1.43	-1.50	-1.57	2.9
HSP26	**YBR072W**	heat shock protein 26	metabolism; response to stress	-3.24	-3.26	-3.22	-3.20	9.4

HSP42	**YDR171W**	Similar to HSP26; expression is regulated by stress conditions	response to stress; cell organization and biogenesis; cell growth and/or maintenance	-1.16	-1.29	-1.16	-1.24	2.3
MCR1	**YKL150W**	NADH-cytochrome b5 reductase	metabolism; response to stress	-1.66	-1.38	-1.67	-1.36	2.9
TIR1	**YER011W**	Cold-shock induced protein of the Srp1p/Tip1p family of serine-alanine-rich proteins. Encodes a stress-response cell wall mannoprotein and this gene is downregulated at acidic pH.	response to stress	-1.73	-2.91	-2.14	-3.00	5.8
TPS1	**YBR126C**	Probable regulator of glucose influx into the cell & into glycolytic pathway, indirectly regulating glucose-induced signalling activation & inactivation & initial step s of glucose metabolism. Homologue of E. coli otsA protein	carbohydrate metabolism; metabolism; response to stress	-1.43	-1.78	-1.46	-1.72	3.0
TPS2	**YDR074W**	Trehalose-6-phosphate phosphatase	carbohydrate metabolism; metabolism; response to stress	-1.87	-1.52	-1.96	-1.54	3.3
TPS3	**YMR261C**	115 kD regulatory subunit of trehalose-6-phosphate synthase/phosphatase complex	response to stress; carbohydrate metabolism; metabolism	-0.99	-1.14	-1.08	-1.14	2.1
TSL1	**YML100W**	123 kD regulatory subunit of trehalose-6-phosphate synthase/phosphatase complex; homologous to TPS3 gene product	response to stress; carbohydrate metabolism; metabolism	-1.93	-2.32	-1.98	-2.31	4.4
YGP1	**YNL160W**	may be involved in cellular adaptations prior to stationary phase	response to stress	-1.46	-1.73	-1.46	-1.72	3.0

Metabolism:

Gene Name	Systematic Name	Description	Gene Ontology	Log_2 ratios				Average Fold-decrease
ACH1	**YBL015W**	Acetyl-coA hydrolase, primarily localized to mitochondria; required for acetate utilization and for diploid pseudohyphal growth	metabolism	-1.68	-1.23	-1.75	-1.27	2.8
ADH5	**YBR145W**	alcohol dehydrogenase isoenzyme V	metabolism	-1.03	-1.33	-1.04	-1.27	2.3
ALD6	**YPL061W**	Utilizes NADP+ as the preferred coenzyme. Activated by Mg2+.	metabolism	-1.46	-1.11	-0.66	-1.14	2.2
APA2	**YDR530C**	Diadenosine 5 ,5 -P1,P4-tetraphosphate phosphorylase II AP4A phosphorylase , involved in catabolism of bis 5 - nucleosidyl tetraphosphates; has similarity to Apa1p	metabolism	-1.37	-1.15	-1.28	-1.19	2.4
BDH1	**YAL060W**	2R,3R -2,3-butanediol dehydrogenase	metabolism	-2.60	-1.82	-2.61	-1.87	4.8
BNA1	**YJR025C**	3-hydroxyanthranilic acid dioxygenase, required for biosynthesis of nicotinic acid from tryptophan via kynurenine pathway	metabolism	-1.11	-1.38	-1.11	-1.36	2.4
CAT2	**YML042W**	Carnitine O-acetyltransferase, peroxisomal and mitochondrial	metabolism	-2.89	-2.88	-2.90	-2.91	7.4
ECM17	**YJR137C**	ExtraCellular Mutant	metabolism; cell organization and biogenesis; cell growth and/or maintenance	-1.15	-1.10	-1.14	-1.06	2.2
HEM13	**YDR044W**	Coproporphyrinogen III oxidase, an oxygen requiring enzyme that catalyzes the sixth step in the heme biosynthetic pathway; localizes to the mitochondrial inner membrane; transcription is repressed by oxygen and heme via Rox1p and Hap1p	metabolism	-1.83	-1.73	-1.86	-1.85	3.5

HIS6	**YIL020C**	Phosphoribosyl-5-amino-1-phosphoribosyl-4-imidazolecarboxiamide isomerase, catalyzes the fourth step in histidine biosynthesis; mutations cause histidine auxotrophy and sensitivity to Cu, Co, and Ni salts	metabolism	-1.12	-1.45	-1.18	-1.44	2.5
ISF1	**YMR081C**	May regulate NAM7 function, possibly at level of mRNA turnover	metabolism	-1.55	-1.24	-1.44	-1.25	2.6
LEU1	**YGL009C**	LEU1 encodes the second enzyme in leucine biosynthesis.	metabolism	-1.23	-1.28	-1.21	-1.34	2.4
MET6	**YER091C**	Cobalamin-independent methionine synthase, involved in amino acid biosynthesis; also called N5-methyltetrahydrofolate homocysteine methyltransferase or 5-methyltetrahydropteroyltriglutamate homocysteine methyltransferase	metabolism	-1.33	-1.18	-1.33	-1.21	2.4
QCR9	**YGR183C**	7.3 kDa subunit 9 of the ubiquinol cytochrome c oxidoreductase complex	metabolism	-1.08	-0.90	-1.12	-1.01	2.0
SIZ1	**YDR409W**	Sap and mIZ. Contains two known protein motifs: SAP DNA binding and MIZ-finger; ubiquitin-like protein ligase 1	metabolism	-1.38	-1.34	-1.42	-1.37	2.6
SKI3	**YPR189W**	dsRNA virus protection family member, contains 8 copies of the tetratricopeptide TPR domain	metabolism	-1.03	-1.06	-0.96	-1.00	2.0
SOD2	**YHR008C**	Manganese-containing superoxide dismutase	metabolism	-1.24	-1.06	-1.21	-1.10	2.2
SSE2	**YBR169C**	HSP70 family member, highly homologous to Sse1p	metabolism	-1.27	-1.06	-1.23	-1.12	2.3

Signal transduction:

Gene Name	Systematic Name	Description	Gene Ontology	Log_2 ratios				Average Fold-decrease
CMK1	**YFR014C**	Calmodulin-dependent protein kinase	protein amino acid phosphorylation; metabolism; signal transduction	-1.65	-1.60	-1.72	-1.64	3.1
STT4	**YLR305C**	functions in the PKC1 protein kinase pathway, in a pathway with STT1 and MSS4	metabolism; cell organization and biogenesis; cell growth and/or maintenance; signal transduction	-1.05	-1.06	-0.92	-1.15	2.1
TPK1	**YJL164C**	putative catalytic subunit of cAMP-dependent protein kinase	cell organization and biogenesis; cell growth and/or maintenance; protein amino acid phosphorylation; metabolism; signal transduction	-1.30	-1.01	-1.40	-0.96	2.3

DNA metabolism:

Gene Name	Systematic Name	Description	Gene Ontology	Log_2 ratios				Average Fold-decrease
DDR48	**YMR173W**	DNA damage-responsive protein, expression is increased in response to heat-shock stress or treatments that produce DNA lesions	DNA repair; DNA metabolism; response to DNA damage stimulus; response to stress; metabolism	-1.25	-1.07	-1.34	-1.23	2.3

MSC1	**YML128C**	Protein of unknown function, green fluorescent protein GFP -fusion protein localizes to the endoplasmic reticulum; msc1 mutants are defective in directing meiotic recombination events to homologous chromatids	DNA recombination; DNA metabolism; metabolism; cell cycle; cell growth and/or maintenance	-1.96	-1.52	-1.90	-1.54	3.3
YRF1-5	**YLR467W**	Helicase encoded by the Y element of subtelomeric regions, highly expressed in the mutants lacking the telomerase component TLC1; potentially phosphorylated by Cdc28p	response to DNA damage stimulus; DNA recombination; response to stress; DNA metabolism; cell organization and biogenesis; cell growth and/or maintenance; metabolism	-1.51	-1.70	-1.45	-1.61	3.0

Protein degradation:

Gene Name	Systematic Name	Description	Gene Ontology	Log_2 ratios				Average Fold-decrease
LAP4	**YKL103C**	vacuolar aminopeptidase ysc1	protein catabolism; metabolism	-2.48	-2.18	-2.52	-2.16	5.1
TFS1	**YLR178C**	Carboxypeptidase Y inhibitor	protein catabolism; metabolism	-2.62	-2.43	-2.54	-2.44	5.7

Carbohydrate metabolism:

Gene Name	Systematic Name	Description	Gene Ontology	Log_2 ratios				Average Fold-decrease
GLC3	**YEL011W**	Glycogen branching enzyme, involved in glycogen accumulation; green fluorescent protein GFP -fusion protein localizes to the cytoplasm in a punctate pattern	carbohydrate metabolism; metabolism	-1.96	-1.88	-2.01	-1.99	3.9

GLG1	**YKR058W**	self-glucosylating initiator of glycogen synthesis; similar to mammalian glycogenin	carbohydrate metabolism; metabolism	-1.53	-1.21	-1.63	-1.10	2.6
GLK1	**YCL040W**	Glucose phosphorylation	carbohydrate metabolism; metabolism	-2.30	-2.77	-2.29	-2.67	5.8
GND2	**YGR256W**	6-phosphogluconate dehydrogenase, decarboxylating; converts 6-phosphogluconate + NADP to ribulose-5-phosphate + NADPH + CO2	carbohydrate metabolism; metabolism	-1.06	-1.21	-1.01	-1.24	2.2
GPM2	**YDL021W**	Similar to GPM1 phosphoglycerate mutase ; converts 3-phosphoglycerate to 2-phosphoglycerate in glycolysis	carbohydrate metabolism; metabolism	-2.29	-1.46	-2.39	-1.56	4.0
GSY2	**YLR258W**	Glycogen synthase, similar to Gsy1p; expression induced by glucose limitation, nitrogen starvation, heat shock, and stationary phase; activity regulated by cAMP-dependent, Snf1p and Pho85p kinases as well as by the Gac1p-Glc7p phosphatase	carbohydrate metabolism; metabolism	-1.39	-1.39	-1.61	-1.41	2.7
HXK1	**YFR053C**	Hexokinase isoenzyme 1, cytosolic protein that catalyzes phosphorylation of glucose during glucose metabolism, expression is highest during growth on non-glucose carbon sources and is repressed by Hxk2p	carbohydrate metabolism; metabolism	-2.78	-2.88	-3.00	-2.93	7.5
MDH1	**YKL085W**	mitochondrial malate dehydrogenase	carbohydrate metabolism; metabolism	-1.63	-1.18	-1.55	-1.14	2.6
PGM1	**YKL127W**	phosphoglucomutase, minor isoform	carbohydrate metabolism; metabolism	-1.42	-1.54	-1.48	-1.53	2.8
PGM2	**YMR105C**	Phosphoglucomutase	carbohydrate metabolism; metabolism	-2.48	-3.63	-2.58	-3.55	8.9

SDH1	**YKL148C**	Yeast succinate dehydrogenase SDH is a tetramer of non-equivalent subunits--Sdh1p, Sdh2p, Sdh3p, Sdh4p--that couples the oxidation of succinate to the transfer of electrons to ubiquinone.	carbohydrate metabolism; metabolism	-1.50	-1.03	-1.43	-1.26	2.5
SUC2	**YIL162W**	NONE	carbohydrate metabolism; metabolism	-2.66	-2.89	-2.70	-2.86	6.9
TAL1	**YLR354C**	Transaldolase, enzyme in the pentose phosphate pathway	carbohydrate metabolism; metabolism	-1.22	-1.52	-1.20	-1.55	2.6
TDH1	**YJL052W**	Glyceraldehyde-3-phosphate dehydrogenase 1	carbohydrate metabolism; metabolism	-1.03	-1.81	-0.96	-1.83	2.8
XKS1	**YGR194C**	third enzyme in the xylose pathway	carbohydrate metabolism; metabolism	-1.00	-1.03	-1.03	-1.02	2.0
YJR096W	**YJR096W**	NONE	carbohydrate metabolism; metabolism	-1.10	-1.27	-1.10	-1.28	2.3

RNA processing:

Gene Name	Systematic Name	Description	Gene Ontology	Log_2 ratios				Average Fold-decrease
YJU2	**YKL095W**	Essential nuclear protein; putative spliceosomal component involved in mRNA splicing, based on computational analysis of large-scale protein-protein interaction data	RNA processing; metabolism	-1.60	-1.30	-1.78	-1.18	2.8
YLR145W	**YLR145W**	NONE	RNA processing; metabolism	-1.09	-1.08	-1.07	-1.04	2.1

Ribosome biogenesis:

Gene Name	Systematic Name	Description	Gene Ontology	Log_2 ratios				Average Fold-decrease
RRS1	**YOR294W**	Regulator for ribosome synthesis	ribosome biogenesis; cell organization and biogenesis; cell growth and/or maintenance; RNA processing; metabolism	-1.06	-1.24	-0.98	-1.28	2.2

Protein amino acid dephosphorylation:

Gene Name	Systematic Name	Description	Gene Ontology	Log2 ratios				Average Fold-decrease
GIP2	**YER054C**	Glc7-interacting protein; shares homology with PIG2; contains conserved 25 residue motif, called the GVNK motif, also found in GAC1, PIG1, PIG2, and RGI, the mammalian type 1 phosphatase targeting subunit.	protein amino acid dephosphorylation; metabolism	-1.50	-1.07	-1.48	-1.29	2.5

Unknown:

Gene Name	Systematic Name	Description	Gene Ontology	Log_2 ratios				Average Fold-decrease
CUP1-1	**YHR053C**	Metallothionein, binds copper and mediates resistance to high concentrations of copper and cadmium; locus is variably amplified in different strains, with two copies, CUP1-1 and CUP1-2, in the genomic sequence reference strain S288C	biological process unknown	-1.15	-1.83	-1.02	-1.84	2.8

CUP1-2	**YHR055C**	Metallothionein, binds copper and mediates resistance to high concentrations of copper and cadmium; locus is variably amplified in different strains, with two copies, CUP1-1 and CUP1-2, in the genomic sequence reference strain S288C	biological process unknown	-1.32	-2.32	-1.50	-2.27	3.8
DCS2	**YOR173W**	Non-essential protein containing a HIT histidine triad motif; regulated by Msn2p, Msn4p, and the Ras-cAMP-cAPK signalling pathway, transcript accumulates under glucose limitation, similar to Dcs1p	biological process unknown	-2.77	-2.79	-2.76	-2.73	6.8
EMI2	**YDR516C**	Early Meiotic Induction	biological process unknown	-1.56	-1.45	-1.56	-1.43	2.8
FMP12	**YHL021C**	The authentic, non-tagged protein was localized to the mitochondria	biological process unknown	-1.64	-1.39	-1.77	-1.54	3.0
HXT12	**YIL170W**	Protein of unknown function with similarity to hexose transporter family members, possible pseudogene	biological process unknown	-2.13	-2.30	-2.17	-2.14	4.6
HXT12	**YIL171W**	Protein of unknown function with similarity to hexose transporter family members, possible pseudogene	biological process unknown	-1.19	-1.27	-1.34	-1.40	2.5
OM45	**YIL136W**	Protein of unknown function, major constituent of the mitochondrial outer membrane; located on the outer cytosolic face of the outer membrane	biological process unknown	-1.63	-1.51	-1.69	-1.61	3.1
RTN2	**YDL204W**	reticulon gene member of the RTNLA reticulon-like A subfamily	biological process unknown	-2.83	-2.96	-3.03	-3.25	8.1
SOL4	**YGR248W**	Similar to SOL3	biological process unknown	-2.99	-2.97	-3.19	-2.88	8.1
STB5	**YHR178W**	binds Sin3p in two-hybrid assay	biological process unknown	-1.19	-1.76	-1.20	-1.71	2.8
SYM1	**YLR251W**	stress-induced yeast MPV17 homolog	biological process unknown	-1.15	-1.04	-1.12	-0.98	2.1
TIR3	**YIL011W**	TIP1-related	biological process unknown	-1.50	-2.70	-1.71	-2.60	4.7
TIR4	**YOR009W**	NONE	biological process unknown	-2.55	-3.20	-2.55	-3.21	7.5
TMT1	**YER175C**	Trans-aconitate Methyltransferase 1	biological process unknown	-1.27	-1.41	-1.28	-1.40	2.5

UIP4	**YPL186C**	Ulp1 Interacting Protein 4	biological process unknown	-2.20	-2.00	-2.21	-1.92	4.3
YAL061W	**YAL061W**	NONE	biological process unknown	-1.08	-1.27	-1.15	-1.22	2.3
YBP2	**YGL060W**	35% identity with Ybp1p, which is required for the oxidative stress response to peroxides via the the Yap1p transcription factor	biological process unknown	-2.42	-2.44	-2.37	-2.33	5.2
YBR139W	**YBR139W**	NONE	biological process unknown	-1.35	-1.25	-1.34	-1.34	2.5
YBR147W	**YBR147W**	NONE	biological process unknown	-1.11	-0.84	-1.36	-1.03	2.1
YBR281C	**YBR281C**	NONE	biological process unknown	-1.38	-1.85	-1.30	-1.94	3.1
YBR285W	**YBR285W**	NONE	biological process unknown	-1.24	-1.32	-1.00	-1.13	2.3
YCL042W	**YCL042W**	NONE	biological process unknown	-1.36	-1.08	-1.38	-1.15	2.4
YCR013C	**YCR013C**	Protein required for cell viability	biological process unknown	-1.02	-1.18	-1.00	-1.18	2.1
YCR064C	**YCR064C**	Hypothetical Systematic	biological process unknown	-1.82	-1.92	-1.57	-1.93	3.5
YDL124W	**YDL124W**	NONE	biological process unknown	-1.04	-1.30	-1.05	-1.31	2.3
YDR015C	**YDR015C**	Hypothetical Systematic	biological process unknown	-2.39	-2.73	-2.17	-2.28	5.3
YDR020C	**YDR020C**	NONE	biological process unknown	-2.00	-1.61	-2.00	-1.39	3.4
YDR438W	**YDR438W**	NONE	biological process unknown	-1.15	-1.24	-1.23	-1.33	2.4
YEL073C	**YEL073C**	NONE	biological process unknown	-1.48	-1.48	-1.41	-1.33	2.7
YER053C	**YER053C**	NONE	biological process unknown	-1.51	-1.50	-1.51	-1.51	2.8
YER067W	**YER067W**	NONE	biological process unknown	-2.13	-2.28	-2.24	-2.41	4.8
YER128W	**YER128W**	NONE	biological process unknown	-1.34	-1.77	-1.21	-1.58	2.8
YER188W	**YER188W**	Hypothetical Systematic	biological process unknown	-1.22	-1.28	-1.42	-1.27	2.5
YFL013W-A	**YFL013W-A**	NONE	biological process unknown	-1.32	-1.23	-1.37	-1.56	2.6
YGR043C	**YGR043C**	NONE	biological process unknown	-1.08	-1.31	-1.13	-1.33	2.3
YGR205W	**YGR205W**	NONE	biological process unknown	-1.66	-1.21	-1.72	-1.42	2.9
YHL044W	**YHL044W**	NONE	biological process unknown	-1.36	-1.07	-1.28	-0.44	2.1
YHR029C	**YHR029C**	NONE	biological process unknown	-1.96	-2.12	-1.94	-2.04	4.1
YHR087W	**YHR087W**	NONE	biological process unknown	-1.86	-1.73	-2.03	-1.88	3.7
YJR115W	**YJR115W**	NONE	biological process unknown	-1.05	-1.28	-1.11	-1.31	2.3
YKL036C	**YKL036C**	Protein required for cell viability	biological process unknown	-1.14	-1.05	-1.10	-1.09	2.1
YKL151C	**YKL151C**	NONE	biological process unknown	-1.17	-1.25	-1.34	-1.37	2.4
YLR290C	**YLR290C**	NONE	biological process unknown	-1.14	-1.15	-1.17	-1.13	2.2

YMR057C	**YMR057C**	Hypothetical Systematic	biological process unknown	-1.38	-1.53	-1.39	-1.66	2.8
YMR110C	**YMR110C**	NONE	biological process unknown	-0.98	-0.93	-1.03	-1.01	2.0
YMR173W-A	**YMR173W-A**	Hypothetical Systematic	biological process unknown	-1.26	-0.92	-1.25	-1.04	2.2
YNL115C	**YNL115C**	NONE	biological process unknown	-1.43	-1.32	-1.48	-1.31	2.6
YNL194C	**YNL194C**	NONE	biological process unknown	-0.94	-1.18	-1.03	-1.21	2.1
YNL195C	**YNL195C**	NONE	biological process unknown	-2.50	-2.33	-2.42	-2.33	5.3
YNL276C	**YNL276C**	Hypothetical Systematic	biological process unknown	-1.06	-1.71	-1.04	-1.62	2.6
YOL083W	**YOL083W**	NONE	biological process unknown	-1.24	-1.00	-1.21	-0.90	2.1
YOR161C	**YOR161C**	NONE	biological process unknown	-1.01	-1.18	-0.89	-1.08	2.1
YPR146C	**YPR146C**	Hypothetical Systematic	biological process unknown	-2.21	-1.86	-2.09	-2.00	4.1
YPS5	**YGL259W**	Gpi-anchored aspartic protease Yapsin 5	biological process unknown	-1.22	-1.19	-1.21	-1.25	2.3
YSA1	**YBR111C**	Protein with weak homology to D. melanogaster serendipity protein and X. laevis basis fibroblast growth factor	biological process unknown	-1.15	-1.02	-1.15	-1.14	2.2

B. Gene expression up-regulated in *cdc68-319* cells with respect to wild-type expression levels:

Transcription:

Gene Name	Systematic Name	Description	Gene Ontology	Log_2 ratios				Average Fold-increase
ELP3	**YPL086C**	elongator protein; histone and other protein acetyltransferase; has sequence homology to known HATs and NATs	transcription; metabolism	1.06	1.28	1.05	1.17	2.2
ESC1	**YMR219W**	Protein localizesd to the nuclear periphery, involved in telomeric silencing; interacts with PAD4-domain of Sir4p	transcription; metabolism; DNA metabolism; cell organization and biogenesis; cell growth and/or maintenance	1.25	1.05	1.19	0.99	2.2
RPA43	**YOR340C**	RNA polymerase I subunit A43	transcription; metabolism	1.23	1.40	1.18	1.37	2.5

Transport:

Gene Name	Systematic Name	Description	Gene Ontology	Log_2 ratios				Average Fold-increase
FET3	**YMR058W**	Ferro-O2-oxidoreductase required for high-affinity iron uptake and involved in mediating resistance to copper ion toxicity, belongs to class of integral membrane multicopper oxidases	transport; cell growth and/or maintenance	1.24	1.18	1.27	1.16	2.3
LSG1	**YGL099W**	Killer toxin REsistant	sporulation; cell growth and/or maintenance; ribosome biogenesis; protein transport; metabolism; transport; cell organization and biogenesis	1.14	1.27	1.14	1.28	2.3
PHO3	**YBR092C**	Acid phosphatase, constitutive	transport; cell growth and/or maintenance	1.21	1.61	1.24	1.60	2.7
RIX7	**YLL034C**	Putative ATPase of the AAA family, required for export of pre-ribosomal large subunits from the nucleus; distributed between the nucleolus, nucleoplasm, and nuclear periphery depending on growth conditions	ribosome biogenesis; protein transport; metabolism; transport; cell organization and biogenesis; cell growth and/or maintenance	1.59	1.16	1.58	1.04	2.6

Cell growth and maintenance:

Gene Name	Systematic Name	Description	Gene Ontology	Log_2 ratios				Average Fold-increase
DIA1	**YMR316W**	Protein of unknown function, involved in invasive and pseudohyphal growth; green fluorescent protein GFP -fusion protein localizes to the cytoplasm in a punctate pattern	cell organization and biogenesis; cell growth and/or maintenance	1.27	1.35	1.18	1.41	2.5

STE2	**YFL026W**	alpha-factor pheromone receptor; seven-transmembrane domain protein	cell organization and biogenesis; cell growth and/or maintenance	1.06	1.40	1.10	1.25	2.3

Protein biosynthesis:

Gene Name	Systematic Name	Description	Gene Ontology	Log_2 ratios				Average Fold-increase
RPL42B	**YHR141C**	Homology to rat L36a and human L36a	protein biosynthesis; metabolism	1.43	1.14	1.41	1.07	2.4
RPS17B	**YDR447C**	Ribosomal protein 51 rp51 of the small 40s subunit; nearly identical to Rps17Ap and has similarity to rat S17 ribosomal protein	protein biosynthesis; metabolism; cell organization and biogenesis; cell growth and/or maintenance	1.17	1.04	1.19	0.98	2.1
RPS28B	**YLR264W**	Protein component of the small 40S ribosomal subunit; nearly identical to Rps28Bp and has similarity to rat S28 ribosomal protein	protein biosynthesis; metabolism	1.41	1.04	1.42	1.04	2.4

Cell cycle:

Gene Name	Systematic Name	Description	Gene Ontology	Log_2 ratios				Average Fold-increase
SDA1	**YGR245C**	Severe Depolymerization of Actin	cell organization and biogenesis; cell growth and/or maintenance; cell cycle	0.92	1.16	1.08	1.20	2.1

Metabolism:

Gene Name	Systematic Name	Description	Gene Ontology	Log_2 ratios				Average Fold-increase
CHA1	**YCL064C**	catabolism of hydroxy amino acids	metabolism	1.51	1.35	1.42	1.27	2.6
GUA1	**YMR217W**	GMP synthase, an enzyme that catalyzes the second step in the biosynthesis of GMP from inosine 5 -phosphate IMP ; transcription is not subject to regulation by guanine but is negatively regulated by nutrient starvation	metabolism	1.73	1.48	N/A	N/A	3.1

Ribosome biogenesis:

Gene Name	Systematic Name	Description	Gene Ontology	Log_2 ratios				Average Fold-increase
DHR2	**YKL078W**	Predominantly nucleolar DEAH-box RNA helicase, required for 18S rRNA synthesis	ribosome biogenesis; cell organization and biogenesis; cell growth and/or maintenance	1.27	1.02	1.33	1.10	2.3
DIM1	**YPL266W**	Essential 18S rRNA dimethylase, responsible for conserved m6 2 Am6 2 A dimethylation in 3 -terminal loop of 18 S rRNA, part of 90S and 40S pre-particles in nucleolus, involved in pre-ribosomal RNA processing	RNA processing; metabolism; ribosome biogenesis; cell organization and biogenesis; cell growth and/or maintenance	1.29	1.27	1.35	1.34	2.5
ERB1	**YMR049C**	Protein required for maturation of the 25S and 5.8S ribosomal RNAs; homologous to mammalian Bop1	RNA processing; ribosome biogenesis; metabolism; cell organization and biogenesis; cell growth and/or maintenance	1.20	1.29	1.24	1.29	2.4

HCA4	**YJL033W**	Putative nucleolar DEAD box RNA helicase; high-copy number suppression of a U14 snoRNA processing mutant suggests an involvement in 18S rRNA synthesis	RNA processing; ribosome biogenesis; metabolism; cell organization and biogenesis; cell growth and/or maintenance	1.33	1.69	1.41	1.65	2.9
MTR4	**YJL050W**	Dead-box family helicase required for mRNA export from nucleus	RNA processing; ribosome biogenesis; metabolism; cell organization and biogenesis; cell growth and/or maintenance	1.09	1.22	1.11	1.26	2.3
NAN1	**YPL126W**	part of small ribosomal subunit SSU processosome contains U3 snoRNA ; Net1-Associated Nucleolar protein 1	RNA processing; ribosome biogenesis; metabolism; cell organization and biogenesis; cell growth and/or maintenance	1.31	1.12	1.30	1.10	2.3
NOP7	**YGR103W**	Nucleolar protein involved in rRNA processing and 60S ribosomal subunit biogenesis; constituent of several different pre-ribosomal particles	ribosome biogenesis; cell organization and biogenesis; cell growth and/or maintenance; RNA processing; metabolism	0.96	1.66	1.10	1.66	2.6
NSR1	**YGR159C**	Nucleolar protein that binds nuclear localization sequences, required for pre-rRNA processing and ribosome biogenesis	cell organization and biogenesis; cell growth and/or maintenance; RNA processing; ribosome biogenesis; metabolism	1.05	1.25	1.10	1.37	2.3
NUG1	**YER006W**	GTPase that associates with nuclear 60S pre-ribosomes, required for export of 60S ribosomal subuits from the nucleus	RNA processing; ribosome biogenesis; metabolism; cell organization and biogenesis; cell growth and/or maintenance	1.16	1.34	1.20	1.39	2.4

RIO2	**YNL207W**	Protein required for cell viability	RNA processing; ribosome biogenesis; metabolism; cell organization and biogenesis; cell growth and/or maintenance	1.00	1.11	1.02	1.05	2.1
RLP7	**YNL002C**	Significant sequence similarity to RPL7B, but neither can functionally replace the other. Does not correspond to any ribosomal component identified so far, based on its biochemical features	RNA processing; ribosome biogenesis; metabolism; cell organization and biogenesis; cell growth and/or maintenance	1.33	1.36	1.33	1.37	2.5
RRP5	**YMR229C**	Part of small ribosomal subunit SSU processosome contains U3 snoRNA . Rrp5p is the only ribosomal RNA processing trans-acting factor that is required for the synthesis of both 18S and 5.8S rRNAs.	RNA processing; ribosome biogenesis; metabolism; cell organization and biogenesis; cell growth and/or maintenance	1.46	1.31	1.38	1.30	2.6
TSR1	**YDL060W**	Twenty S rRNA accumulation	RNA processing; ribosome biogenesis; metabolism; cell organization and biogenesis; cell growth and/or maintenance	1.13	1.11	1.13	1.03	2.1
UTP14	**YML093W**	Nucleolar protein, component of the small subunit SSU processome containing the U3 snoRNA that is involved in processing of pre-18S rRNA	RNA processing; ribosome biogenesis; metabolism; cell organization and biogenesis; cell growth and/or maintenance	1.06	1.21	1.03	1.21	2.2

Unknown:

Gene Name	Systematic Name	Description	Gene Ontology	Log_2 ratios				Average Fold-increase
FPR4	**YLR449W**	Homolog of homolog of the nucleolar FKBP, Fpr3	biological process unknown	1.09	0.33	1.14	1.15	2.0
NOP13	**YNL175C**	Protein of unknown function, localizes to the nucleolus and nucleoplasm; contains an RNA recognition motif RRM and has similarity to Nop12p, which is required for processing of pre-18S rRNA	biological process unknown	1.47	1.46	1.43	1.47	2.7
PHO12	**YHR215W**	acid phosphotase, nearly identical to Pho11p	biological process unknown	1.12	1.14	1.03	1.17	2.2
TOS7	**YOL019W**	NONE	biological process unknown	1.14	1.26	1.07	1.25	2.3
YFR032C	**YFR032C**	NONE	biological process unknown	1.21	1.15	1.11	1.18	2.2
YML125C	**YML125C**	NONE	biological process unknown	1.50	1.43	1.53	1.41	2.8
YMR310C	**YMR310C**	NONE	biological process unknown	1.15	1.03	N/A	N/A	2.1
YOL079W	**YOL079W**	Hypothetical Systematic	biological process unknown	0.95	1.62	1.04	1.87	2.7
YOR021C	**YOR021C**	NONE	biological process unknown	1.04	1.18	1.03	1.08	2.1

2003; Leger-Silvestre *et al.* 2004). This finding suggests that FACT may have a role in regulating the transcription of genes encoding proteins that function in ribosome biogenesis. However, this conclusion has two caveats: 1) genes involved in ribosome biogenesis often display highly variable results in microarray analyses (Hughes *et al.* 2000; Baetz *et al.* 2001), and 2) all of the genes identified here encoding proteins involved in ribosome biogenesis are down-regulated during the diauxic shift (DeRisi *et al.* 1997). This second point highlights the similarities between the subset of genes identified here as up-regulated and the correlation to down-regulated genes in the diauxic shift experiment. Of the 37 genes up-regulated in *cdc68-319* cells, 35 of them display significant decreases in transcript abundance during the diauxic shift. If the wild-type *CDC68* cells, which were harvested for RNA extractions at 4.4×10^7 cells per millilitre, were experiencing glucose deprivation in comparison to the *cdc68-319* cells, which were harvested for RNA extractions at a cell concentration of only 1.1×10^7 cells per millilitre, then the down-regulation of these genes in the wild-type *CDC68* cells as a result of decreased glucose supply could explain why these transcripts were relatively more abundant in the *cdc68-319* cells. Thus these effects may not be the result of a *cdc68-319* influence on transcription, but instead may be the result of glucose limitation and its influences on transcription in the wild-type *CDC68* cells. As seen below for the genes that show decreased transcript abundance in *cdc68-319* cells, there is significant overlap with genes that are typically up-regulated in response to diauxic growth. So here again the confounding factor of cell concentration and glucose limitation may have had a significant effect on the expression profile observed for *cdc68-319* mutant cells.

There are two genes that show significant increases in transcript abundance in *cdc68-319 cells*, namely *DIA1* and *CHA1*, whose transcription is not affected by diauxic growth conditions. While little is known about the regulation or function of the *DIA1* gene (Kaniak *et al.* 2004), the expression of *CHA1* has been shown to be regulated by the Nhp6A and Nhp6B HMG-box proteins (Moreira and Holmberg 2000). Nhp6 proteins are components of yeast FACT and are responsible in part for FACT association with nucleosomes (Brewster *et al.* 2001; Ruone *et al.* 2003; Rhoades *et al.* 2004). Moreira and Holmberg (2000) showed that Nhp6 is required for full induction of the *CHA1* gene (which encodes a catabolic serine/threonine dehydratase) by serine and threonine, and

also that Nhp6 plays a role in down-regulating the basal transcript level of *CHA1* (Moreira and Holmberg 2000). In the *cdc68-319* cells *CHA1* expression was increased approximately 3-fold in comparison to that in wild-type *CDC68* cells, which may indicate that Cdc68, like Nhp6, is involved in maintaining the repression of *CHA1* and that the Cdc68-319 protein is unable to maintain the same level of repression. Additionally, *CHA1* expression is regulated by the Tup1 repressor (Sabet *et al.* 2003), and as indicated in the preceding section, some genes that are regulated by Tup1 have altered expression in *cdc68* mutant cells. Thus there may be a functional connection between FACT and the repression mediated by Tup1, which is discussed more in the sections below.

c.ii. Genes with decreased transcript abundance in *cdc68-319* cells that are also regulated during the diauxic shift

Of the 150 genes whose transcripts are less abundant in *cdc68-319* cells than in *CDC68* cells, 89 also show increased levels of transcription during the diauxic shift (DeRisi *et al.* 1997). Therefore, changes observed for these transcripts may reflect a decreased glucose concentration in the growth medium for the wild-type *CDC68* cells and a consequent up-regulation of these 89 transcripts due to the diauxic shift, rather than an influence of the *cdc68-319* mutation on the regulation of these genes. However, it cannot be said with certainty that the alterations in transcript abundances for these 89 genes are not effects of the *cdc68-319* mutation, and as a result these genes are not excluded from further comparisons. As indicated above, approximately 700 genes are up-regulated during the diauxic shift (DeRisi *et al.* 1997), so these 89 genes do not represent the entire collection and the possibility exists that the overlap between the expression profiles from these two experiments may not be biologically meaningful. Indeed, there are some genes whose transcription is typically down-regulated in the diauxic shift that showed a decrease in transcript abundance in *cdc68-319* cells. For example the *HXT1* gene, encoding a hexose transporter, showed diminished expression in *cdc68-319* cells, whereas the expression of this gene is typically induced in the presence of glucose (DeRisi *et al.* 1997; Tomas-Cobos *et al.* 2004). Therefore, if the glucose had been greater for the *cdc68-319* cells, then the *HXT1* transcript abundance should have been higher in these cells than in *CDC68* cells, but instead the *HXT1* transcript level was over 3-fold lower in *cdc68-319*

cells than in *CDC68* cells. Additionally, *cdc68-319* cells showed significant decreases in transcript abundances for many metabolic genes involved whose expression does not change as a result of the diauxic shift, including *ADH5*, *ALD6*, *APA2*, *BNA1*, *ECM17*, *HIS6*, *LEU1*, *MET6*, *PGM1*, *QCR9*, *SIZ1*, *SKI3*, *SOD2* (an important factor in response to oxidative stress), *TAL1*, and *TDH1* (Table 15). These gene-expression changes that are not consistent with those observed for the diauxic shift support the idea that *cdc68-319* is the causative agent for the observed expression changes, and not glucose-concentration differences between the mutant and wild-type cultures.

The 61 genes whose transcript abundances were decreased two-fold or more in the *cdc68-319* cells and that are not known to be up-regulated in response to the diauxic shift are discussed in more detail in the following sections (Table 15). Even limiting the analysis to these 61 genes, there were still significantly more gene-expression changes in the *cdc68-319* cells than found for either the *cdc68-312* or *cdc68-mini* cells.

c.iii. Genes with decreased transcript abundance in *cdc68-319* cells that are induced by stress-response transcription factors Msn2/4 and/or Hsf1

The majority of the common genes displaying altered transcript levels in the *cdc68-319* cells and changes during the diauxic shift encode proteins that function in stress response and metabolism. The proteins encoded by these genes respond to limited glucose supplies by mobilizing carbon stores, converting ethanol into acetyl-CoA, or catabolizing alternative sugar sources. Many of these genes have other roles and impacts that may be unrelated to glucose-limiting conditions. For example, 22 of these genes (*ACH1*, *ALD3*, *CTT1*, *DCS2*, *ECM4*, *GLK1*, *GPX1*, *GSY2*, *HSP104*, *HSP12*, *HSP26*, *HSP42*, *HXK1*, *PGM2*, *TPK1*, *TPS1*, *TPS2*, *TSL1*, *YAL061W*, *YGR043C*, *YHR087W* and *YNL194C*) may be expressed in response to other cellular stresses and are activated by the Msn2/4 general-stress-response transcription factors (DeRisi *et al.* 1997; Moskvina *et al.* 1998; Lee *et al.* 2002; Aranda and del Olmo 2003). The fact that these genes all showed decreased transcript abundance in *cdc68-319* cells may indicate a decreased ability of the Msn2/4 transcription factors to activate gene expression. Two other genes, *SMP2* and *TPS3*, that do not show altered gene expression as a result of the diauxic shift (DeRisi *et al.* 1997) and are also regulated by Msn2/4 in response to cellular stresses (Moskvina *et al.* 1998; Lee *et al.* 2002), were found here to have lower transcript abundance in *cdc68-*

319 cells than in *CDC68* cells. Approximately 110 genes have promoters that are bound by Msn2 or Msn4 (Lee *et al.* 2002) or contain the STRE consensus sequence in upstream regions (Moskvina *et al.* 1998). Cells containing *cdc68-319* showed decreased transcript abundance for 24 of these genes (approximately 20%). This is a significant enrichment for Msn2/4-regulated genes, and the fact that some of these Msn2/4-regulated genes are not induced during the diauxic shift makes a more compelling argument for an effect of *cdc68-319* on Msn2/4 regulation.

As indicated above, there is an overlap among genes regulated by the general-stress-response transcription factors and those regulated by the heat-shock transcription factor Hsf1. Ten of the genes (*CUP1-1*, *CUP1-2*, *GSG1*, *HSP104*, *HSP42*, *NCA3*, *PNC1*, *SSE2*, *TSL1*, and *YNL194C*) with decreased levels of transcript in *cdc68-319* cells are regulated by the Hsf1 transcription factor (Lee *et al.* 2002; Hahn and Thiele 2004). Three of these genes are also regulated by Msn2/4. The seven Msn2/4-independent, Hsf1-regulated genes also represent a class of genes involved in stress response, bringing the total number of stress-inducible genes with decreased transcript abundance in *cdc68-319* cells up to 31. Approximately 173 genes have been reported to be regulated by the Hsf1 transcription factor under a variety of conditions (Lee *et al.* 2002; Hahn and Thiele 2004); thus the ten genes identified here does not represent a significant number of the total genes regulated by this factor. It may be that only some of the Hsf1-regulated genes are also influenced by *cdc68-319*, or that the conditions examined do not activate the expression of the majority of Hsf1-mediated genes and therefore no effects on gene expression could be observed for those genes.

c.iv. Genes with decreased transcript abundance in *cdc68-319* cells that are regulated by the Ssn6-Tup1 repressor complex

Microarray analysis of gene expression in *tup1Δ* cells in comparison to wild-type cells identified over 200 genes that are repressed by the Ssn6-Tup1 complex (DeRisi *et al.* 1997). Comparison of the genes identified here as having decreased transcript levels in *cdc68-319* cells to those regulated by Tup1 revealed a set of 24 genes (*EMI2*, *FET3*, *GAL2*, *HEM13*, *HSP26*, *HXT1*, *HXT15*, *HXT3*, *HXT4*, *HXT6*, *HXT7*, *HXT8*, *HXT9*, *STE2*, *SUC2*, *TIR1*, *TIR3*, *TIR4*, *UGP1*, *YER067W*, *YER188W*, *YHL044W*, *YNL195C* and *YPS5*) that may be regulated by both Tup1 and Cdc68. As indicated above, the Tup1 repressor

acts in association with Ssn6 to repress transcription of genes involved in a variety of cellular activities, at least partly through recruitment of chromatin modifying and remodelling complexes (Deckert and Struhl 2001; Davie *et al.* 2002; Proft and Struhl 2002). Mutations in the FACT complex may generate altered chromatin structures that are more tightly repressed by the Ssn6-Tup1 complex, which could result in the decreased transcription seen here for genes regulated by this repressor complex. Seven of the 24 genes whose expression is regulated by both Tup1 and Cdc68 are not subject to alterations in transcription during diauxic growth; therefore the potentially confounding factor of glucose concentrations cannot fully explain the observed overlap in Tup1 and Cdc68 regulation.

c. v. Genes with decreased transcript abundance in *cdc68-319* cells that encode proteins involved in vesicular transport

Of all the Hsp1-regulated genes that were also down-regulated in *cdc68-319* cells, only the *GSG1* gene does *not* display altered expression during the diauxic shift. Therefore, the decreased *GSG1* gene-expression cannot be explained by potentially different glucose concentrations in the growth medium, but is more likely to be an effect of the *cdc68-319* mutation. *GSG1* encodes a member of the TRAPP (transport protein particle) complex, which is comprised of ten components and is involved vesicular transport between the endoplasmic reticulum and the Gogli apparatus (Sacher *et al.* 2001). A second gene encoding a TRAPP component, *TRS120*, was also shown to have approximately six-fold less transcript in the *cdc68-319* cells in comparison to wild-type *CDC68* cells. The fact that these genes are not expressed as abundantly in *cdc68-319* cells may help explain why *cdc68* mutant cells display synthetic growth defects when deleted for genes encoding components of the vesicular-transport machinery (Results 4, v and vi). Two other genes encoding proteins that function in vesicular transport were also found to have decreased transcript levels in *cdc68-319* cells. The *MON1* gene encodes a protein that complexes with Ccz1 and assists in the late stages of transport-vesicle fusion to target membranes (Wang *et al.* 2002, 2003). Cells containing both *cdc68* and *mon1Δ* mutations are synthetically sick, as are cells containing *cdc68* mutations and deletions of other genes involved in vesicular-transport functions similar to those attributed to Mon1 (Results 4). Finally, transcript levels for the *VMA5* gene, encoding a subunit of a vacuolar ATPase

pump (Ho *et al.* 1993), were also decreased significantly in *cdc68-319* cells, and deletions of genes encoding other vacuolar ATPase subunits have been found to cause synthetic growth defects in cells containing *cdc68* mutant alleles (Results 4). This synthetic lethality may therefore be the result of reduced transport activity due to the influence of *cdc68* mutations on transcription, rather than a direct role for Cdc68 in transport functions.

The *MON1* gene, or genes encoding vacuolar ATPases, and subunits of the TRAPP complex can be deleted to produce synthetic sickness or lethality in *cdc68* mutant cells (Results 4). The findings here of decreased gene expression for related genes in *cdc68* mutants may provide a mechanism for the observed genetic interactions. If mutations in *cdc68* result in decreased transcription of genes involved in transport functions, as the microarray data presented here indicates, then deletions of other genes involved in parallel transport functions may result in synthetic growth defects, like those identified below in my SGA analysis (Results 4).

c. vi. Genes with decreased transcript abundance in *cdc68-319* cells that encode proteins involved in cell integrity

During the course of my research I have identified morphological, phenotypic, and genetic findings that indicate a role for Cdc68 in maintaining cell integrity (Results 3). Indeed, several genes involved in maintaining cell integrity, either through alterations to the cell-wall structure itself or through activating the cell-integrity Pkc1-mediated signal-transduction pathway, have decreased transcript abundance in *cdc68-319* cells. These findings are described in detail below (Results 3).

The *STT4* gene encodes a protein kinase that is anchored to the plasma membrane, where it plays an important role in activating the Pkc1-mediated signal-transduction effector protein Rom2 (Yoshida *et al.* 1994; Heinisch *et al.* 1999; Audhya and Emr 2002). In this way, Stt4 is an upstream activator of the Pkc1 pathway and may be a key player in monitoring events at the cell surface and initiating the signalling of cell-surface stress (Yoshida *et al.* 1994; Audhya and Emr 2002). *STT4* transcript abundance is two-fold lower in *cdc68-319* cells than in wild-type *CDC68* cells. This finding may help explain, in part, why this particular mutant allele of *cdc68* causes defects that are consistent with problems in maintaining cell integrity.

Another gene with a clear role in maintaining cell integrity is *CWH41* (calcofluour white hypersensitivity). The *CWH41* gene encodes a glucosidase that is involved in forming the β-1,6 glucan linkages that are critical for anchoring certain cell-wall proteins within the wall matrix (Romero *et al.* 1997; reviewed in Smits *et al.* 1999). In *cdc68-319* cells the level of *CWH41* mRNA was approximately two-fold lower than in wild-type cells. This decrease could have structural implications for the cell wall, and therefore may result in cell-integrity defects. SGA analysis has shown that *cdc68* cells exhibit synthetic growth defects when the *CWH41* gene is also deleted (Results 4). This implies that *cdc68* mutations, in addition to influencing *CWH41* gene expression as indicated by these microarray results, may also influence other parallel activities in mediating cellular integrity. This idea is consistent with the observed cell-integrity defects observed for *cdc68* mutants.

The Tir family of cell-wall mannoproteins is involved in stress-response cell-wall remodelling that occurs as a result of anaerobic growth, decreased pH, or temperature shock (Russo *et al.* 1993; Kowalski *et al.* 1995; Abramova *et al.* 2001). Genes encoding three different Tir proteins, Tir1, Tir3, and Tir4, showed dramatic decreases in transcript abundances in *cdc68-319* cells in comparison to *CDC68* cells, implicating a role for FACT in regulating the expression of these genes (Table 15). Consistent with this finding, it has been proposed that *TIR* gene expression is regulated by HMG-protein association with upstream activating sequences, and deletion of the HMG-protein genes *NHP6A* and *NHP6B* results in increased expression of the *TIR3* gene (Moreira and Holmberg 2000; Cohen *et al.* 2001). Nhp6 proteins are members of the FACT complex and play important roles in mediating FACT activities (Brewster *et al.* 2001; Ruone *et al.* 2003; Rhoades *et al.* 2004). These findings support the idea that FACT, and specifically Cdc68, regulates expression of the *TIR* gene family and thereby is involved in the maintenance of cell integrity under stress conditions.

Other proteins involved in maintaining cell integrity under stress conditions, particularly thermal stress, are involved in the formation of trehalose, a disaccharide that can be incorporated in the cell wall (Hottiger *et al.* 1994; reviewed in Elbein *et al.* 2003). Each of the genes encoding protein components of the trehalose phosphate synthase complex (*TPS1*, *TPS2*, *TPS3*, and *TSL1*) had greatly decreased transcript levels in *cdc68-*

319 cells in comparison to wild-type *CDC68* cells (Table 15). These findings may also explain the decreased thermotolerance of *cdc68-319* cells and other cell-integrity defects associated with cells containing this mutation. This decreased expression also implies that Cdc68, and potentially the FACT complex, mediates expression of genes encoding trehalose synthase. An alternative explanation, however, is that trehalose is stored as a carbon source in response to glucose starvation so that three of the four genes involved in trehalose synthesis are up-regulated during the diauxic shift. As a result, the altered transcription of trehalose phosphate synthase complex genes may be due to glucose limitation in the growth medium of wild-type control cells in comparison to the *cdc68-319* culture.

Microarray studies of gene-expression changes that arise upon deletion of the *GAS1*, *MNN9*, *FKS1*, *KNR4*, or *KRE6* gene which each encode a key component of cell-wall construction, have identified a set 79 genes called the 'cell wall compensatory–dependent gene cluster' that is typically up-regulated in response to cell-wall perturbations (Lagorce *et al.* 2003). My microarray analysis for *cdc68-319* found significant decreases in the transcript abundances for 13 (*DPR48*, *DIA1*, *ECM4*, *HSP12*, *LGK1*, *PNC1*, *STF2, TSL1*, *TFS1*, *YDL124W*, *YGR043C*, *YGP1*, and *YHR087W*) of the 79 members of the cell wall compensatory-dependent gene cluster (Table 15). As a result of the decreased transcription of these genes, *cdc68-319* cells may not be able to cope with environmental stresses that may perturb cell integrity, which is consistent with findings for *cdc68-319* cells that indicate defects in cell integrity (Results 3). The majority of the genes identified here that are in the cell-wall compensatory cluster are involved in carbohydrate metabolism (and are regulated in response to the diauxic shift); however, since the cell wall is largely composed of carbohydrates it is not surprising that the response to cell-wall or cell-integrity stresses alters the expression of genes regulating carbohydrate flux and other metabolic processes in the cell (Lagorce *et al.* 2003). Therefore, the observed changes in the expression of metabolic genes may be due to defects in cell-wall integrity found in *cdc68-319* cells, and not the result of glucose limitations in the *cdc68-319* cells versus wild-type *CDC68* cells.

In summary, the microarray experiments performed here indicate that the *cdc68-mini* and *cdc68-312* mutations have little impact on gene expression, while *cdc68-319* causes

more drastic effects on the transcription profile. A confounding aspect of these experiments may be the small differences in cell concentration, and therefore glucose concentration in the growth medium, of the cells harvested for RNA analysis. It is difficult to imagine that the differences in cell concentration between *CDC68* cells and *cdc68-mini* or *cdc68-312* cells had much impact on transcription profiles, yet several genes that are induced at the diauxic shift were down-regulated in the *cdc68* mutant cells. This trend is further highlighted by the results for *cdc68-319*, where over half of the genes whose expression was altered in the *cdc68-319* cells also show expression changes during the diauxic shift. However, there are still many genes whose expression is not correlated with glucose limitation that were altered in expression in the *cdc68-319* cells. Significant associations between Cdc68-mediated gene regulation and the regulation of gene expression by certain transcription activators and repressors are evident. Additionally, the mRNA for several genes involved in vesicular transport and cell integrity were less abundant in *cdc68-319* cells, a finding that is consistent with, and may provide a mechanism for, several genetic interactions observed for cells containing this mutation (Results 4).

3. Genetic and phenotypic characterization of *cdc68* mutant alleles implicate a role for FACT in mediating cell integrity

i) Complementation of the temperature sensitivity of *cdc68 ssd1-d* cells by *SSD1*

Two of the novel mutant alleles of *cdc68* identified here (Results 2, i) confer temperature sensitivity at 39°C (Figure 27) but produce a stable protein product at the elevated temperature (Figure 32). Therefore, the cells do not fail to proliferate at elevated temperatures due to loss of an unstable Cdc68 protein. Instead, these mutant Cdc68 proteins are functionally impaired at the elevated temperature. Additionally, cells containing increased dosages of *cdc68-312* or *cdc68-319* (on 2μ-based plasmids) are still temperature-sensitive at 39°C (Figure 33B). Overexpression of an unstable protein product often alleviates the temperature sensitivity (Figure 33A; Results 2, vi), and so the inability of *cdc68-312* or *cdc68-319* overexpression to improve cell growth at elevated temperatures is further support that cells containing these mutant alleles of *cdc68* are not temperature-sensitive due to the Cdc68 protein instability. Thus the temperature

sensitivities conferred by *cdc68-312* and *cdc68-319* are more likely due to a loss of function by the mutant Cdc68 proteins encoded by these alleles.

In an effort to understand the mechanism(s) of this temperature sensitivity, a selection for dosage suppressors of *cdc68-312* and/or *cdc68-319* temperature sensitivity was undertaken. The cells employed in these dosage-suppressor selections contained the chromosomal *cdc68Δ::kanMX4* deletion and were kept alive by the presence of the *cdc68-312* or *cdc68-319* gene on a centromeric *URA3* plasmid (these cells were haploid derivatives of the KanB diploid strain). High-copy *LEU2* yeast genomic library plasmids were transformed into these *cdc68-312* and *cdc68-319* cells and transformants were selected on leucine-free medium (SC-Leu) at 30°C. Transformant colonies generated in this way were then replica-plated to YPD and SC-Leu media and incubated at the restrictive temperature of 39°C for 2 to 6 days. Colonies that were able to grow at 39°C were then spread for single-colony growth on SC-Leu medium and grown at 30°C. The resultant single colonies were then tested to ensure that the temperature-resistance phenotype was reproduced. In total, approximately 1 x 10^5 library transformants for both *cdc68-312* and *cdc68-319* cells were assessed, and 64 and 72 dosage-suppressor candidates were identified for *cdc68-312* and *cdc68-319*, respectively.

To ensure that temperature resistance was caused by the presence of a library plasmid, cells from each of the candidate dosage-suppressed derivatives were grown at 30°C in synthetic liquid medium that contained leucine but did not contain uracil. This maintained selection for the *cdc68* plasmid (either *cdc68-312* or *cdc68-319*) but not for the *LEU2* library plasmid. This growth resulted in mixed populations, with some cells that had inherited *LEU2* library plasmids and some that had not. Cells from these cultures were placed on SC solid medium lacking uracil and grown for 3 days at 30°C to allow colony formation. Single colonies were then replica-plated to SC medium lacking either uracil (as a control) or leucine (to determine the status of the *LEU2* library plasmid) and grown at both 30°C and 39°C. If the temperature resistance of the *cdc68-312* or *cdc68-319* cells was linked to the presence of the *LEU2* library plasmid, then only those cells that were able to grow on SC-Leu medium at 30°C would also be able to grow at 39°C. If this was not the case, and cells that were leucine auxotrophs were able to grow at the elevated temperature, then the temperature resistance of the *cdc68-312* or *cdc68-319* cells

was not due to the genomic library plasmid but the result of a chromosomal suppression event. Yeast cells containing *cdc68-312* or *cdc68-319* that exhibited temperature resistance at 39°C only when a *LEU2* yeast genomic library plasmid was present were kept for further analysis.

A plasmid-borne wild-type *CDC68* gene is able to alleviate the temperature sensitivity of cells containing *cdc68-312* or *cdc68-319* (Figure 43). Thus, while the Spt$^-$ phenotype displayed by *cdc68-312* or *cdc68-319* cells is dominant, the temperature sensitivity at 39°C is a recessive phenotype. The possibility therefore existed that the insert in many of the genomic library plasmids contains a wild-type copy of the *CDC68* gene. To identify these cases two approaches were taken.

Initially, the genomic library plasmids were extracted from five dosage-suppressor candidate cells and digested with restriction endonucleases. A common restriction digestion pattern was obtained for all candidate suppressor library plasmids examined in this way, which was consistent with the digestion pattern of chromosomal DNA containing the *CDC68* locus (data not shown). To verify that the wild-type *CDC68* sequence was present on these genomic library plasmids, PCR amplification employing *CDC68*-specific primers was performed using the genomic library plasmids as template. As controls for this amplification, a plasmid known to contain the *CDC68* gene was also used as a PCR template (positive control) as was an 'empty' vector that did not have any insert (negative control). As anticipated, a diagnostic DNA fragment of the expected size for the *CDC68* gene was obtained with each of these genomic library plasmids as well as with the *CDC68* control plasmid, while no DNA fragments were generated from the vector control (data not shown). This result confirmed the restriction-digestion findings, indicating that these five genomic library plasmids identified as 'dosage suppressors' of the *cdc68-312* or *cdc68-319* temperature sensitivity actually contained the wild-type *CDC68* gene. Since this methodology was time-consuming, it was not used further for screening the rest of the candidate suppressors. Instead, an alternative approach to determine if a dosage-suppressor plasmid contains the wild-type *CDC68* gene was employed.

Since the *CDC68* gene is essential, only cells that maintain a copy of this gene are viable. If a yeast genomic library plasmid identified as a dosage suppressor of the *cdc68*

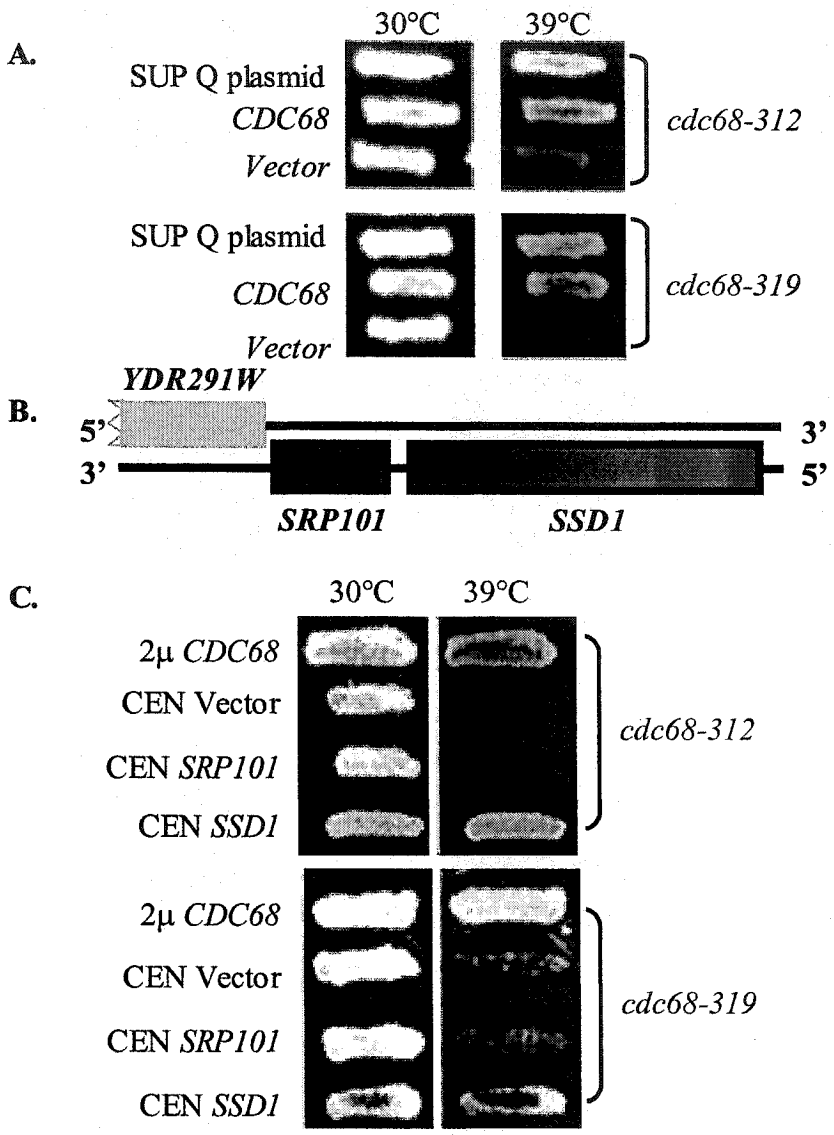

Figure 43. Alleviation of *cdc68-312* and *cdc68-319* temperature sensitivities. (A) *cdc68-312* and *cdc68-319* cells harbouring the 2m-based plasmids indicated on the left were spread as patches on selective medium and grown for 2 days at 30°C, and then replica-plated to YPD medium and incubated for 4 days at either 30°C or 39°C. The yeast genomic library plasmid SUP Q is able to alleviate the temperature sensitivity of both *cdc68-312* and *cdc68-319* cells. **(B)** The yeast genomic DNA insert in library plasmid SUP Q. **(C)** Cells were grown as in (A). The temperature sensitivities of *cdc68-312* and *cdc68-319* cells are alleviated by the presence of a centromeric plasmid containing *SSD1*.

312 or *cdc68-319* temperature sensitivity contains the wild-type *CDC68* gene, then cells harbouring this library plasmid will be able to survive in the absence of the *URA3*-marked *cdc68-312* or *cdc68-319* plasmid. To determine if this was the case, the cells harbouring dosage-suppressor candidates were grown in liquid medium containing uracil but lacking leucine. This growth medium maintains selection for the presence of the *LEU2* genomic library plasmid but does not maintain selection for the *URA3 cdc68* plasmid. The resulting mixed populations, in which some cells have the *URA3* plasmid while others have failed to inherit this plasmid, were then examined by growing these cells on solid SC-Leu medium, and then replica-plating the single colonies that formed to SC medium lacking uracil or leucine. In this way the plasmid complement of the cells could be assessed. Cells that were leucine prototrophs but uracil auxotrophs no longer contained the *URA3*-marked *cdc68-312* or *cdc68-319* plasmid, and therefore Cdc68 function was most likely supplied by the *LEU2* genomic library plasmid (due to a wild-type version of *CDC68* on the genomic DNA insert). For all but one of the plasmid-linked dosage-suppressor candidates, cells were able to survive in the absence of the *URA3*-marked *cdc68-312* or *cdc68-319* plasmid, suggesting that the library plasmid contains a wild-type copy of the *CDC68* gene. As a final verification, colony PCR was performed on a subset of the candidates from the plasmid-loss experiment. Once again a set of *CDC68*-specific primers was employed, and cells that were leucine prototrophic (indicating the presence of the *LEU2* library plasmid) but uracil auxotrophic (indicating the absence of the *URA3*-marked *cdc68-312* or *cdc68-319* plasmid) were used as templates for PCR amplification (Materials and Methods). A diagnostic DNA fragment of the anticipated size was generated from each of the derivatives tested in this way, indicating the presence of the wild-type *CDC68* gene on the yeast genomic library plasmid insert (data not shown).

These experiments identifed a single non-*CDC68* genomic library plasmid, called SUP Q, that would alleviate *cdc68-312* temperature sensitivity (Figure 43A). SUP Q was unable to provide essential function in the absence of the *cdc68-312* plasmid. To identify the yeast genomic DNA insert on SUP Q, a yeast-plasmid extraction was performed and the resulting DNA was transformed into *E. coli* cells of strain JF1754. JF1754 cells contain the *leuB* mutation that can be complemented by the *LEU2* gene of yeast. This

complementation allows straightforward differentiation between *E. coli* transformants harbouring the *LEU2* yeast genomic library plasmid and those with the *URA3 cdc68-312* plasmid, based on the *E. coli* leucine auxotrophic status. The SUP Q library plasmid was purified from *E. coli* and primers specific for vector sequences flanking the genomic DNA insertion site were used in sequencing reactions to determine the region of the yeast genome contained in this plasmid. The sequences generated were then used to query the Saccharomyces Genome Database yeast genomic DNA sequence using a BLAST-N search (Altschul *et al.* 1990). This analysis returned a single significant match for each of the sequences employed, indicating that the yeast genomic DNA insert contained on the SUP Q plasmid spans basepairs 1,042,816 to 1,050,653 (a total of 7837 basepairs) of chromosome IV (Figure 43B). Within this region are the complete coding sequences for *SSD1* and *SRP101* as well as a 3' portion of the coding sequence for *YDR291W*. To determine the gene responsible for the *cdc68-312* temperature-sensitivity suppression, the *SSD1* and *SRP101* genes were individually sub-cloned from the SUP Q yeast genomic library plasmid into both high-copy (2μ) and low-copy (*CEN*) *LEU2* plasmids (Materials and Methods) and assessed for the ability to alleviate the temperature sensitivity of *cdc68-312* and *cdc68-319* cells. The *SSD1* gene was able to suppress the temperature sensitivity of both *cdc68-312* and *cdc68-319* cells, while *SRP101* had no effect (Figure 43C). Additionally, the low-copy *SSD1* plasmid was equally capable of this suppression. The implications of this finding is either that subtle changes in *SSD1* gene dosage are able to suppress the temperature sensitivity of *cdc68-312* and *cdc68-319* cells, or that the *SSD1* low-copy plasmid may be complementing an unanticipated *ssd1* mutant allele in the yeast cells.

SSD1 (suppressor of *SIT4* deletion) has been identified as a suppressor in several genetic screens involving genes encoding proteins that function in a variety of processes, including signal transduction, transcription, mRNA processing, protein transport and cell integrity (Sutton *et al.* 1991a; Stettler *et al.* 1993; Uesono *et al.* 1994; Luukkonen and Seraphin 1999; Kosodo *et al.* 2001; Du and Novick 2002; Kaeberlein and Guarente 2002; McDonald *et al.* 2002). Despite repeated identification of this gene in many labs and biological contexts, little is known about the function of the Ssd1 protein. *SSD1* encodes a protein with sequence homology to a class of exoribonucleases, but while Ssd1 has

been shown to bind nucleic acid *in vitro*, no exoribonuclease activity has been found (Turcq *et al.* 1992; Uesono *et al.* 1997). It has been hypothesized that the pleiotropic effects of *ssd1* mutations may be the result of post-transcriptional regulation that is in some way mediated by the RNA-binding activity of Ssd1 (Uesono *et al.* 1997). In support of this model, genetic evidence has been reported that demonstrates the ability of *SSD1* to alleviate splicing defects in cells containing mutations in genes encoding components of the spliceosome, which is responsible for mRNA processing (Luukkonen and Seraphin 1999).

The *SSD1* locus is polymorphic in yeast laboratory strains, with some strains containing a wild-type *SSD1* gene (also refered to as *SSD1-V*) while others contain *ssd1-d*, a mutant form of the gene that encodes a C-terminally truncated protein product (Sutton *et al.* 1991a; Uesono *et al.* 1997). To determine which of these alleles is present in the cells (derived from the S288c strain) that I used, I isolated the DNA from the *SSD1* chromosomal locus using a gap-repair strategy (Materials and Methods). The plasmid containing the chromosomal *SSD1* sequence from these cells (a KanB haploid derivative) was used as template for DNA sequencing. The DNA sequences for both the coding and non-coding strands of the chromosomal *SSD1* gene were determined, and comparison of these sequences to the published *SSD1* sequence revealed a single change, from C to G at nucleotide 2904. This alteration results in a premature stop codon just after codon 697 in the 1250-codon *SSD1* open reading frame. This sequence alteration has also been identified in the Guarente lab (Massachusettes Institute of Technology, Boston, MA) for the *ssd1-d* allele present in cells from their strain PSY316 (Greg Liszt, personal communication), and in the Boone lab for cells from their W303 derivative (Jorgensen *et al.* 2002). I also identified this same sequence change in cells from strain Y150, a W303 derivative employed in our lab. The finding that our S288c-derived cells have the *ssd1-d* allele at the chromosomal *SSD1* locus, coupled with the fact that the *SSD1* gene subcloned from the yeast genomic library plasmid SUP Q alleviates the temperature sensitivity of *cdc68-312* and *cdc68-319* cells even when present on a low-copy plasmid (Figure 43C), indicate that the 'suppression' phenotype originally characterized for *SSD1* is more likely the result of complementation of the effects of the defective *ssd1-d* allele present in these cells. The nucleotide sequence was determined for the *SSD1* gene

subcloned from the SUP Q library plasmid (Materials and Methods – plasmid pRS315-SSD1) and shown to encode the full-length Ssd1 protein. A single nucleotide difference between the sequence determined for the subcloned *SSD1* gene from the genomic library plasmid and the *SSD1* gene sequence reported in the *Saccharomyces* Genome Database substitutes a cytosine for a thymine at ORF nucleotide 1442, resulting in a switch in the amino acid encoded by codon 481 from serine to phenylalanine. Whether this sequence difference exists in the SUP Q yeast genomic library plasmid or arose during the PCR amplification that generated the subcloned *SSD1* gene remains undetermined. However, the fact remains that both the high-copy yeast genomic library plasmid SUP Q and the subcloned low-copy *SSD1* plasmid are able to complement the temperature sensitivity of *cdc68-312* and *cdc68-319* cells, which suggests that this sequence difference may not significantly impair Ssd1 function. The temperature sensitivity observed for cells containing *cdc68-312* or *cdc68-319* is therefore not the result of the *cdc68* mutation alone, but is due to a synthetic growth defect that arises when these alleles are combined with the *ssd1-d* mutation. This synthetic sickness at elevated temperatures may be complemented by a wild-type *CDC68* or *SSD1* gene (Figure 43C; data not shown).

To determine if the temperature sensitivities observed for other alleles of *cdc68* are also the result of synthetic growth defects in the presence of *ssd1-d*, cells containing *cdc68-1*, *cdc68-Δ922*, or *cdc68-Δ369*, which have been shown to cause temperature sensitivity, were transformed with the low-copy *SSD1* plasmid or an 'empty' vector and then tested for growth at elevated temperatures. In each case, the presence of the low-copy *SSD1* plasmid was able to increase the maximal growth temperature of the *cdc68* mutant yeast cells (Figure 44). The fact that this interaction between *cdc68* and *ssd1-d* is not allele-specific suggests that Cdc68 and Ssd1 work in parallel to mediate a common process. The synthetic growth defect at elevated temperatures between *cdc68* mutations and *ssd1-d* is therefore functionally significant.

ii) Cells containing *cdc68* mutation exhibit phenotypes consistent with defects in cell integrity

Several lines of investigation have indicated a role for Ssd1 in the maintenance of cell integrity (Ibeas *et al.* 2001; Kaeberlein and Guarente 2002; Wheeler *et al.* 2003; Kaeberlein *et al.* 2004; Reinke *et al.* 2004). A significant number of the genes shown to

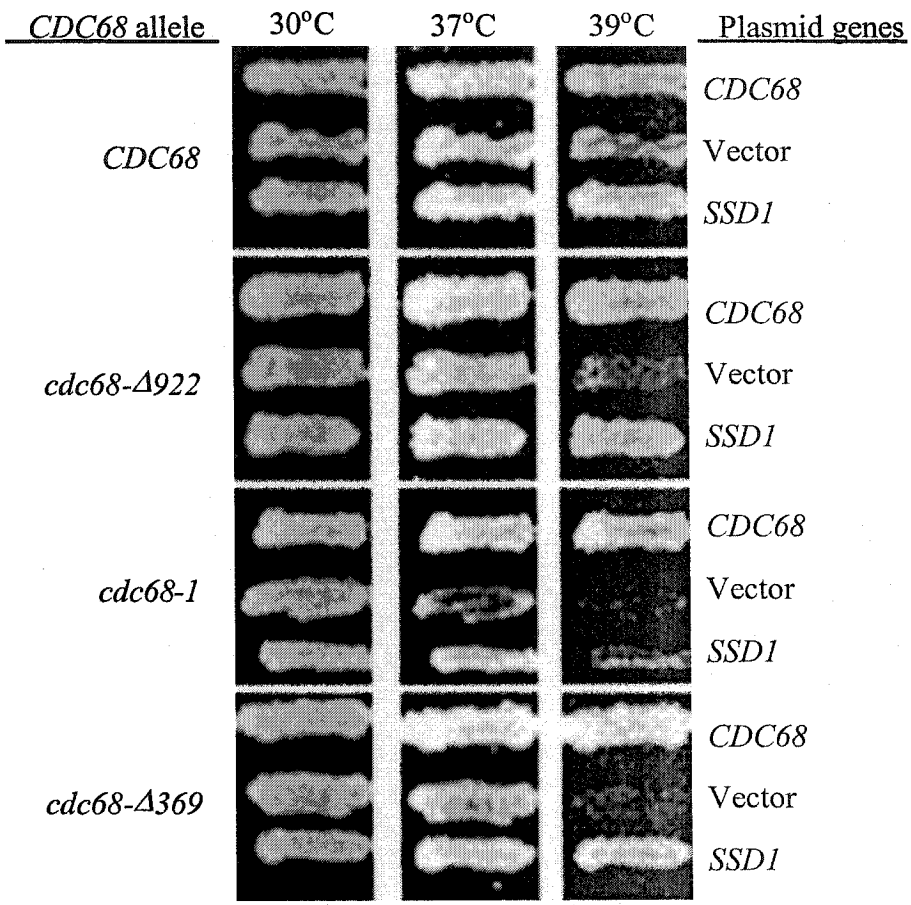

Figure 44. *SSD1* increases the maximal growth temperature for *cdc68* mutant cells. Cells were spread as patches on SC medium lacking leucine and grown for 2 days at 30°C, and then were replica-plated to YPD medium and grown at the temperature indicated for 4 to 5 days. *cdc68* alleles are listed on the left and genes carried on *CEN* plasmids are listed on the right. Similar to the findings reported for *cdc68-312* and *cdc68-319* cells, the low-copy *SSD1* plasmid increases the maximal growth temperature for cells containing *cdc68-1*, *cdc68-Δ922* and *cdc68-Δ369*.

have genetic interactions with *SSD1* can be linked either directly or indirectly to cell morphogenesis and/or the maintenance of cell integrity (Kaeberlein *et al.* 2004). Specifically, allelic variation at the *SSD1* locus leads to alterations in the composition of the yeast cell wall (Ibeas *et al.* 2001; Wheeler *et al.* 2003), and the *ssd1-d* allele results in altered sensitivities to chemical agents, such as sodium dodecylsulphate, caffeine, and calcoflour white, that are associated with perturbation of the cell wall (Martin *et al.* 1996; Kaeberlein and Guarente 2002). The Sit4 protein phosphatase (the genetic interaction with which *SSD1* was named; Sutton *et al.* 1991) is a downstream component of the 'alternative' branch of the Pkc1-signalling pathway as well as the Tor (target of rapamycin) pathway, which both function to maintain cell integrity (Heinisch *et al.* 1999; Reinke *et al.* 2004). Additional recent findings have furthered the functional connection between the Tor signalling pathway and Ssd1 in the maintenance of cell integrity (Reinke *et al.* 2004). Synthetic genetic interactions have been reported between *SSD1* and genes encoding the cell-morphogenesis regulators Cbk1, Pag1, Elm1, and Dhh1 (Moriya and Isono 1999; Du and Novick 2002; Jorgensen *et al.* 2002), as well as genes encoding components of the Pkc1-mediated cell-integrity pathway, namely Bck1, Slt2, Rlm1, and Swi4 (Costigan *et al.* 1992; Watanabe *et al.* 1994; Kaeberlein and Guarente 2002). Indeed, Ssd1 has been proposed to function in parallel with the Pkc1 signalling pathway to maintain cell integrity (Kaeberlein and Guarente 2002; Kaeberlein *et al.* 2004). In light of the genetic interaction identified here between *cdc68* and *ssd1*, phenotypes associated with perturbations of cell integrity were assessed for *cdc68* mutant cells.

Sorbitol-remedied temperature sensitivity is associated with osmotic stabilization capable of suppressing cell lysis at elevated temperatures that is sometimes associated with impaired cell integrity (Hampsey 1997). Deletions of genes encoding components of the Pkc1-mediated cell-integrity pathway often display a lysis phenotype at elevated temperatures that can be suppressed by 1 M sorbitol in the growth medium (Torres *et al.* 1991; Lee and Levin 1992; Levin and Bartlett-Heubusch 1992; Mazzoni *et al.* 1993). Additionally, it has been shown that cells deleted for the genes encoding the Nhp6 component of FACT display sorbitol-remedied temperature sensitivity (Costigan *et al.* 1994). Cells containing *cdc68-312*, *cdc68-319*, *cdc68-Δ922* and *cdc68-Δ369*, mutant alleles of *cdc68* that typically result in temperature sensitivity at 37°C or 39°C, were

therefore tested for the ability of sorbitol to suppress the growth defect at elevated temperatures. The addition of 1 M sorbitol to the growth medium increased the maximal growth temperature for cells containing each of the *cdc68* alleles and the *ssd1-d* allele (Figure 45). The ability of sorbitol to suppress the temperature sensitivity displayed by cells containing a *cdc68* mutant allele and the *ssd1-d* mutation is consistent with an overlapping role for Cdc68 with Ssd1 in the maintenance of cell integrity, particularly at elevated temperatures.

Sodium dodecylsulphate is a detergent that results in cell-wall perturbations, and the presence of *ssd1-d* in combination with mutations of other genes involved in cell integrity has been shown to result in altered sensitivity to this detergent (Moriya and Isono 1999; Du and Novick 2002; Kaeberlein and Guarente 2002). Sensitivity to detergent was tested for *CDC68 ssd1-d*, *cdc68-312 ssd1-d*, and *cdc68-319 ssd1-d* cells in the presence or absence of a low-copy *SSD1* plasmid. Surprisingly, this experiment showed that the *CDC68 ssd1-d* cells were much more sensitive to the presence of detergent in the growth medium than were the *cdc68-312 ssd1-d* or *cdc68-319 ssd1-d* cells, and this sensitivity could not be suppressed by the presence of the plasmid-borne *SSD1* allele (Figure 46). While this result may seem inconsistent with the growth defects at elevated temperatures for these mutants, it is not unprecedented for *ssd1-d* mutations to cause detergent sensitivity when combined with a secondary mutation, yet this same combination of mutations need not result in a growth deficit at elevated temperatures (Du and Novick 2002). Therefore, these two phenotypes of temperature sensitivity and detergent sensitivity need not be associated in the same fashion for all situations in which other mutations are combined with *ssd1-d*. This finding of altered detergent sensitivity does suggest that there is a difference in cell-wall composition and perhaps in cell integrity for *CDC68 ssd1-d* cells in comparison with *cdc68 ssd1-d* cells. This difference between cell integrity in *CDC68 versus cdc68* cells is also manifested in the temperature sensitivity observed for *cdc68* mutant cells. Therefore, alterations in both the temperature sensitivities and the detergent sensitivities for *cdc68* mutant cells are consistent with the idea that cell integrity is affected in these cells.

Mutations of cell-integrity genes in the presence of *ssd1* mutant alleles often result in abnormal cellular morphologies, including elongated and/or misshapen buds or mating

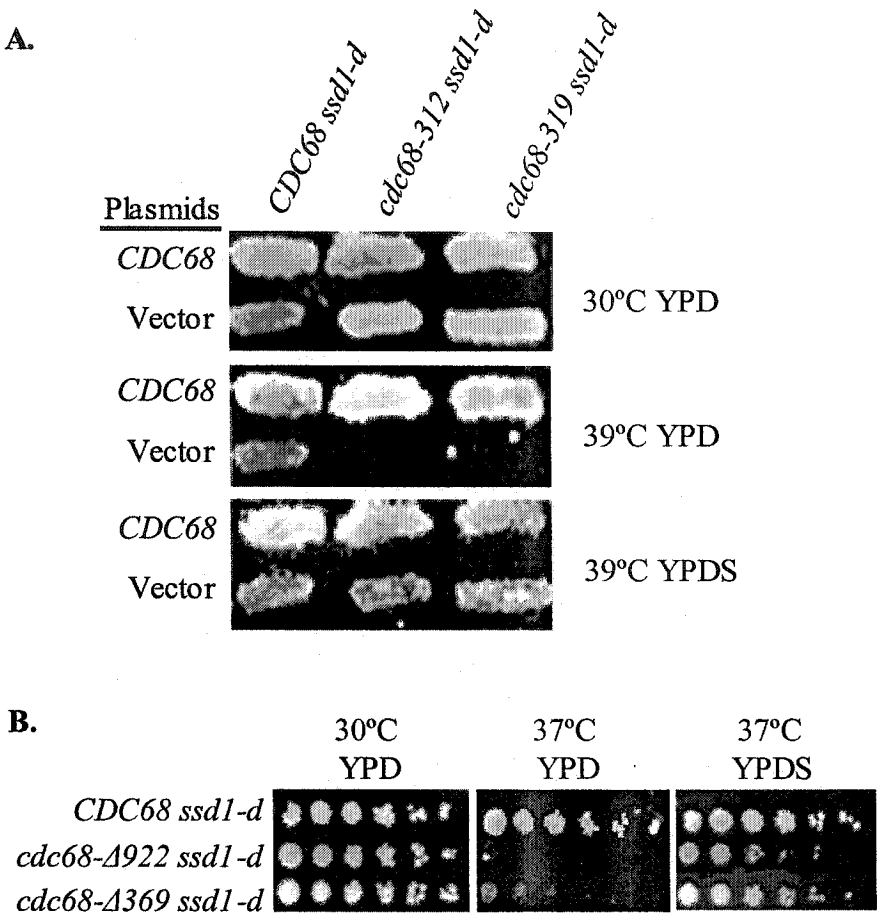

Figure 45. Sorbitol-remedied temperature sensitivity of *cdc68* mutant cells. (A) Cells were distributed in patches on YPD medium and grown 2 days at 30°C, at which time they were replica-plated to the conditions indicated (YPDS = YPD plus 1 M sorbitol) and grown for 4 days. The presence of sorbitol suppresses the temperature sensitivity of *cdc68-312 ssd1-d* and *cdc68-319 ssd1-d* cells. (B) Cultures were growth in YPD liquid medium to stationary phase, adjusted for cell concentration, serially diluted in 5-fold steps, and spotted onto the indicated medium for further growth (4 to 5 days at the temperature indicated). The presence of sorbitol can suppress the temperature sensitivity of *cdc68-Δ922 ssd1-d* and *cdc68-Δ369 ssd1-d* cells.

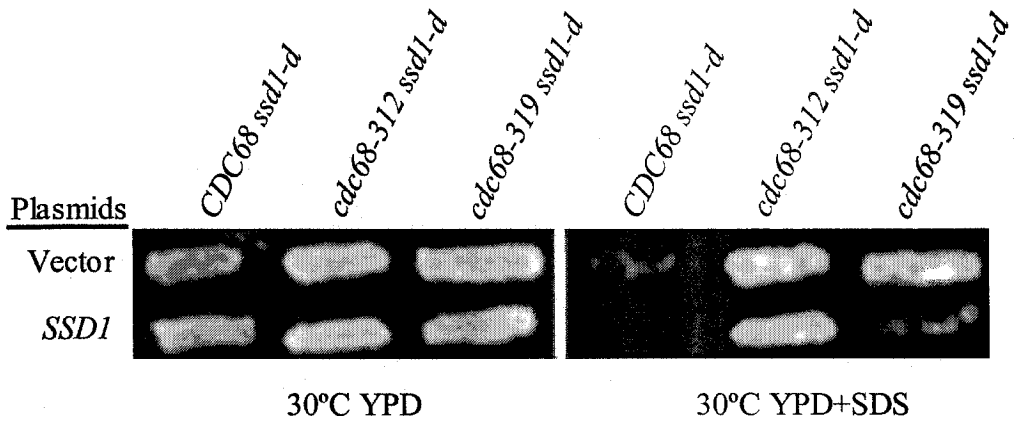

Figure 46. Sodium dodecyl sulfate (SDS) sensitivity of *CDC68 ssd1-d* mutant cells. Cells were plated as distributed in patches on YPD medium and grown 2 days at 30°C, at which time they were replica-plated to the conditions indicated (YPD+SDS = YPD plus 0.02% SDS) and grown for 4 days. Sensitivity to detergents like SDS is a hallmark of cell-integrity perturbations. *CDC68 ssd1-d* cells are sensitive to SDS and this sensitivity cannot be alleviated by the presence of *SSD1*. *cdc68-312 ssd1-d* cells with or without the *SSD1* plasmid are not sensitive to SDS. *cdc68-319 ssd1-d* cells are not sensitive to SDS, but *SSD1* plasmid causes these cells to become sensitive.

projections and growth of cells in 'chains' or as multi-budded forms that indicate defects in cell septation and cytokinesis (Moriya and Isono 1999; Du and Novick 2002; Kaeberlein and Guarente 2002). A similar set of morphological defects, including elongated and misshapen buds and incomplete cytokinesis, was also observed for *cdc68 ssd1-d* cells grown at 30°C, and the number of cells in the population displaying these defects was greatly increased after cells were shifted from 30°C to 38°C for further incubation (Figure 47; data not shown). Diamidino-2-phenylindole (DAPI) staining of DNA in *cdc68 ssd1-d* cells grown at 30°C showed that nuclear division is not significantly affected by the cytokinesis defect, with each of the cells in a multiply budded cell or cell 'chain' containing an individual nuclear staining signal (data not shown). This finding is consistent with the nuclear staining reported for other situations in which mutations combined with the *ssd1-d* mutation result in the formation of 'chains' of cells that have not completely undergone cell septation (Costigan *et al.* 1994; Moriya and Isono 1999). The morphological defects described here are similar to those for cells deleted for the *NHP6* genes; thus the findings reported here are not the first examples of mutations affecting FACT components that result in these types of morphological defects. Cells deleted for *NHP6* genes have elongated buds and thickened bud necks, and a preponderance of the cells fail to complete cytokinesis but display no defect in nuclear division (Costigan *et al.* 1994). These morphologies bear similarities to those that have been reported for cells with defects in the Pkc1 signalling pathway (Costigan *et al.* 1994).

In summary, my findings of sorbitol-remedied temperature sensitivity for *cdc68* mutant cells, alterations in sensitivity to detergent and aberrant cell morophologies all indicate that *cdc68* mutations result in abnormal cell morphogenesis and defects in cell integrity. These findings implicate a role for Cdc68 in mediating cell morphogenesis and integrity.

iii) Genetic interactions between genes encoding Pkc1-pathway components and *cdc68-312* and *cdc68-319* indicate a role for Cdc68 in cell integrity

Ssd1 has been shown to have an overlapping essential function with components of the Pkc1 cell-integrity pathway (Costigan *et al.* 1992; Watanabe *et al.* 1994; Martin *et al.* 1996; Kaeberlein and Guarente 2002). Based on these findings, it has been proposed that Ssd1 and Pkc1 function in parallel to mediate cell integrity (Kaeberlein and Guarente

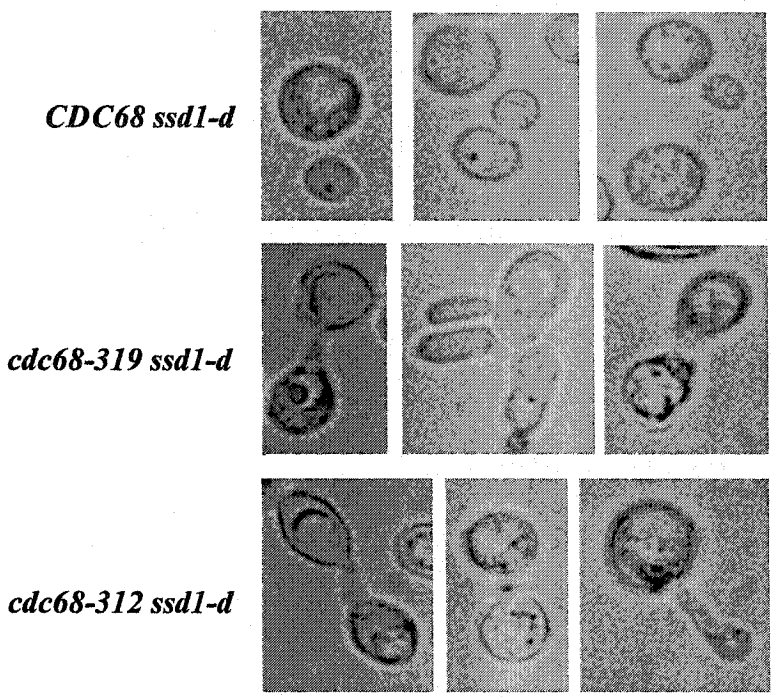

Figure 47. Abnormal cell morphologies associated with *cdc68 ssd1* mutant cells. Cells were grown in YPD liquid medium at 30°C to a concentration of 5 x 10^6 cells/ml, then examined by differential interference contrast microscopy (Model 84489, Carl Zeiss). Representative morphological anomalies found for *cdc68 ssd1* cells, including multiply budded cells, elongated and misshapen buds and cell-separation defects indicted by elongated bud-necks, were chosen for display.

2002). Given the phenotypic and genetic evidence reported above that suggests Cdc68 plays a role in cell integrity and morphogenesis in parallel with Ssd1, genetic interactions between *cdc68* mutants and components of the Pkc1 cell-integrity pathway were sought. Indeed, *NHP6A* has been identified as a dosage suppressor of *bck1-1 spa2Δ* synthetic lethality (Costigan *et al.* 1994). Bck1 is a protein kinase in the Pkc1 signal-transduction cascade, and Spa2 localizes to sites of polarized cell growth and assists in budding and mating-projection formation (Costigan *et al.* 1994; Heinisch *et al.* 1999). Thus, genetic ties between FACT and the Pkc1 signalling pathway have previously been forged and Nhp6 has been postulated to be a downstream effector of Pkc1-mediated functions (Costigan *et al.* 1994).

The Pkc1 signal-transduction cascade is thought to consist of multiple branches (Errede and Levin 1993); signalling through the primary branch of this pathway occurs *via* a phosphorylation relay from the Pkc1 kinase to the Bck1, Mkk1, Mkk2 and Slt2/Mpk1 kinases (reviewed in Heinisch *et al.* 1999). The targets of this phosphorylation cascade include the Rlm1 and the SBF (comprised of Swi4 and Swi6) transcription factors that activate transcription of genes involved in cell-wall remodelling, cell-cycle control, and polarized growth. While it is not yet clear how the Pkc1 kinase becomes activated during times of cellular stress, such as growth at elevated temperature or alteration in the osmotic environment, several cell-surface sensor proteins like Wsc1/Slg1, Wsc2 to 4, and Mid2 serve as initiators of the Pkc1-induction signal (Verna *et al.* 1997; Ketela *et al.* 1999).

To determine if the Pkc1 pathway functions in parallel or in conjunction with Cdc68 to mediate cell integrity, several genetic approaches were used. The first approach was to determine if over-expression of Pkc1-pathway components could alleviate the temperature sensitivities of cells containing *cdc68* mutations. High-copy plasmids containing the genes encoding Wsc1, Pkc1, Slt2, Swi4, and Swi6 were transformed into yeast cells containing *cdc68-312*, *cdc68-319* or *CDC68* on low-copy plasmids and transformants were assessed for growth at elevated temperature. Increased dosage of either *WSC1* or *PKC1* weakly suppressed the temperature sensitivities of *cdc68-312* and *cdc68-319* cells, while increasing dosage of the *SLT2*, *SWI6* or *SWI4* genes had no effect on the temperature sensitivities of these cells (Figures 48A and B). One explanation why

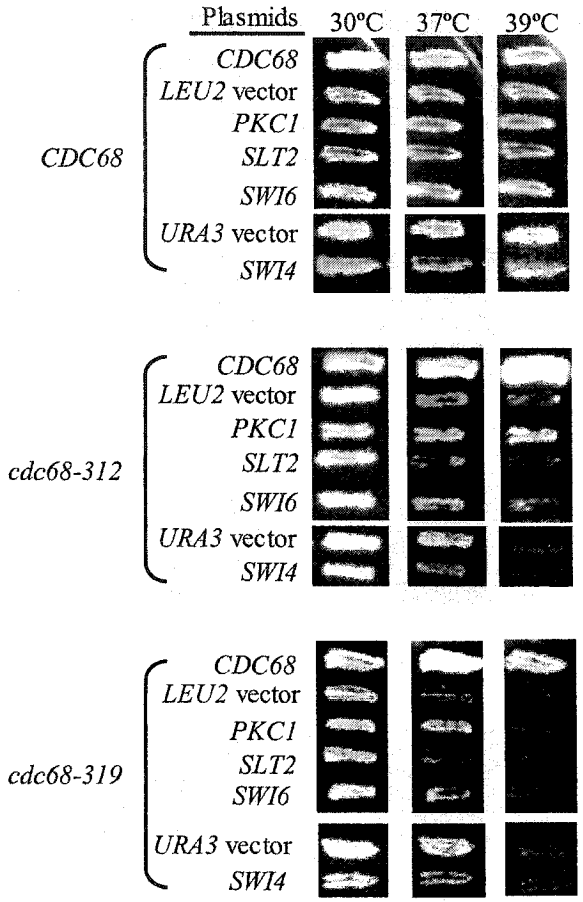

Figure 48. Suppression of the temperature sensitivity of *cdc68-312* and *cdc68-319* by over-expression of genes encoding components of the Pkc1 signaling pathway. Yeast strains containing the allele of *cdc68* listed at far left were transformed with the indicated 2μ-based plasmid. The *CDC68*, *PKC1*, *SLT2*, and *SWI6* plasmids were marked with *LEU2,* and cells containing a *LEU2* vector were used as a growth control. The *SWI4* plasmid was marked with *URA3* and therefore growth of cells containing this plasmid was compared to cells transformed with a *URA3* vector. When a *LEU2* 2μ plasmid was employed, cells containing a *cdc68* allele on a *URA3 CEN* plasmid were used. When a *URA3* 2μ plasmid was employed, cells containing a *cdc68* allele on a *LEU2 CEN* plasmid were used. Strains were distributed as patches on SC medium lacking uracil and leucine, grown for 2 days at 30°C, and then replica-plated to SC medium lacking leucine (for the cells with *LEU2* 2μ plasmids) or uracil (for cells with the *URA3* 2μ plasmids) and incubated for 4 days.

over-expression of genes encoding upstream components of the Pkc1 pathway, like *WSC1* and *PKC1*, is able to suppress the temperature sensitivities of *cdc68-312* and *cdc68-319* cells while over-expression of downstream effectors like Slt2, Swi4, and Swi6 cannot is that over-expression of upstream components of the pathway is able to activate an alternative branch of Pkc1 signalling, while over-expression of downstream elements is not. Thus, suppression by over-expression of *PKC1* or *WSC1* may not be mediated through the activity of the Slt2 arm of the pathway, but may instead be the result of activation of the 'alternative' and less characterized Pck1 pathway containing the Bck2 and Knr4 proteins (Errede and Levin 1993; Wijnen and Futcher 1999; Martin-Yken *et al.* 2002). While the two branches of Pkc1-mediated signal transduction are thought to act in parallel to promote cell integrity, SBF is a common downstream target for each pathway (Madden *et al.* 1997; Heinisch *et al.* 1999; Wijnen and Futcher 1999). Thus, while the pathways may have distinct components and regulatory mechanisms, they also have significant features that overlap, making distinction between these two branches of the Pkc1 pathway difficult. Based on the findings presented above, it may be that Cdc68 mediates activity of the Slt2 branch of the Pkc1 pathway, which may be why over-expression of components in that arm of the pathway has no suppressive effects on the *cdc68* temperature sensitivity. However, the Cdc68 protein may not act as a downstream effector of the Bck2 arm of the Pkc1 pathway, and therefore the temperature sensitivity of *cdc68* mutations may be suppressed by the up-regulation of this alternative Pkc1 pathway that results from the over-expression of *PKC1* and *WSC1*.

A third pathway mediating cell integrity in parallel with Ssd1 and the Pkc1 signal-transduction cascade is thought to involve the Mpt5 protein (Hata *et al.* 1998; Kaeberlein and Guarente 2002). Mpt5 is a member of the Puf family of RNA-binding proteins and acts as a post-transcriptional regulator (Tadauchi *et al.* 2001). Recent work has identified Mpt5-bound transcripts, showing that many Mpt5-associated transcripts are from genes encoding proteins involved in chromatin structure and chromatin modifications (Gerber *et al.* 2004). In addition to its proposed role in mediating cell integrity, Mpt5 has been shown to influence a number of cellular processes including growth at elevated temperatures and Sir-dependent chromatin silencing (Kikuchi *et al.* 1994; Gasser *et al.* 1998). Given the parallel role for Mpt5, along with Pkc1 and Ssd1, in mediating cell

integrity, I also determined the effect of over-expressing *MPT5* on *cdc68-312* and *cdc68-319* temperature sensitivities. Increasing *MPT5* gene dosage had no effect on the temperature sensitivity of cells containing these *cdc68* mutations (Figure 48). Thus the Mpt5-mediated pathway promoting cell integrity either does not influence the same subset of functions as does Cdc68, or may function in concert with Cdc68. In the latter case, increased flux through the Mpt5 pathway by over-expression of *MPT5* may not be able to alleviate the potentially downstream effects of the *cdc68* mutations, and as a result no improvement of growth at the high temperature would be observed for these cells.

To further investigate the relationship between Cdc68 and components of the Pkc1 signalling pathway, I determined the effects of over-expressing the *CDC68* gene in cells deleted for various Pkc1-pathway components or for proteins known to function in cell integrity. In addition to a role in the maintenance of cell integrity, the Pkc1 pathway also influences cell-cycle progression and has been hypothesized to co-ordinate polarized growth and cell cycling (Igual *et al.* 1996). The transcription activator SBF regulates the expression of genes involved in cell-cycle progression from G_1 to S phase (reviewed in Breeden 1996) and has been shown to be a downstream target for both branches of Pkc1 signalling (Madden *et al.* 1997; Heinisch *et al.* 1999; Wijnen and Futcher 1999). With these factors in mind, the effects of deletions of genes known to be regulated by SBF and that also play a role in cell cycling were determined as well. Cells deleted for these genes (Winzeler *et al.* 1999) were transformed with a 2μ-based 'empty' *LEU2* vector or the same vector bearing a wild-type version of the *CDC68* gene. The deletions eliminated *SLG1/WSC1*, *WSC2*, *WSC3*, *WSC4*, and *MID2*, which encode the cell-surface sensors known to initiate signalling through the Pkc1 pathway; *SAC7*, which encodes a GTPase-activating protein found at the plasma membrane and known to assist in activation of the Pkc1 pathway (Madden and Snyder 1998); *BCK1*, *MKK1*, *MKK2*, *SLT2*, *SWI4*, *SWI6*, and *RLM1*, members of the Pkc1 signal-transduction cascade and its known transcription-factor targets (reviewed in Heinisch *et al.* 1999); *BCK2*, encoding a component of the 'alternative' Pkc1-signalling branch that also activates the Swi4 and Swi6 transcription factors (Errede and Levin 1993; Wijnen and Futcher 1999); *CLN3*, which encodes a G_1 cyclin that has been shown to have functions related to those of Bck2 and that also activates the SBF transcription factor (Di Como *et al.* 1995; Wijnen and Futcher 1999);

and *FKS1*, *CLN1*, and *CLN2*, each activated by SBF and functioning in either the production of cell-wall constituents (Igual *et al.* 1996) or in regulating the transition from G_1 to S phase of the cell cycle (Hadwiger *et al.* 1989; Richardson *et al.* 1989). Transformants were tested for growth on rich YPD medium and on SC medium lacking leucine at 30°C, 37°C, and 39°C. High-copy *CDC68* had no significant positive or negative impact on growth of cells from any of the deletion strains under the conditions tested (data not shown). Cells from the majority of strains tested did not display a significant growth defect, even at elevated temperatures; therefore the positive impact on growth that may be the result of increased dosage of *CDC68* was not fully explored. Cells from the deletion-strain collection are known to contain the wild-type *SSD1* gene at its chromosomal locus, and therefore the temperature sensitivities described for cells deleted for a gene encoding a Pkc1-signalling component in combination with the *ssd1-d* allele would not be observed here (Costigan *et al.* 1992; Watanabe *et al.* 1994; Martin *et al.* 1996). However, it is clear from these results that over-expression of *CDC68* has no negative impact on growth of cells containing the aforementioned gene deletions.

As a third approach to characterizing genetic interactions between *CDC68* and genes encoding Pkc1-pathway components and downstream targets of the pathway, synthetic growth defects were assessed for *cdc68* cells deleted for key cell-integrity genes. Synthetic genetic array (SGA) analysis was performed with cells containing the *cdc68-312* and *cdc68-319* alleles integrated at the *CDC68* chromosomal locus. This analysis and its results are described in full in Results 4 vi and vii below, but some of the findings are directly relevant to the Pkc1 signalling pathway and cell integrity, and are therefore highlighted here. SGA analysis was carried out at 30°C, and therefore only gene deletions that cause a synthetic growth defect in combination with *cdc68* mutations at this otherwise permissive growth temperature would be identified. The genetic interactions assessed as described here extends the findings of the SGA analysis by assessing growth of double-mutant cells (containing a gene deletion and a *cdc68* mutant allele) at elevated temperatures in comparison to cells containing only a single mutation (a gene deletion or a *cdc68* mutant allele).

The SGA analysis identified the *SWI4* gene deletion as causing synthetic lethality in cells containing the *cdc68-319::natMX4* allele (Table 21). These results were verified by

random-spore analysis and also by tetrad analysis (Figure 49). No similar synthetic lethality was identified during SGA analysis between the *cdc68-312* allele and *swi4Δ*, although with a false-negative rate in SGA analysis between 17 and 41% (Tong *et al.* 2001, 2004) this interaction could have been missed. As a result of this *cdc68-319 swi4Δ* synthetic-lethality finding, the *cdc68-319* allele was used to test for other genetic interactions with deletions of genes encoding Pkc1-pathway components and downstream targets. During the course of the SGA analysis, tetrad dissections were performed in cases involving *cdc68-319::natMX4* and deletions of the following genes: *WSC4*, *BCK1*, *BCK2*, *MKK1*, *SLT2*, *CLN2*, *CLN3,* and *SWI4*. In each case, the double-mutant (*cdc68-319* and gene-deletion) haploid spores from these diploids germinated just as well as the single-mutant or wild-type spores, with the exception of the *cdc68-319 swi4Δ* combination (Figure 49). Not many haploid segregants containing the *cdc68-319* and *swi4Δ* mutations were viable, and those that were viable generated very small, slow-growing colonies (Figure 49). This finding indicates that this *cdc68* mutation shares an overlapping function with Swi4, which is a downstream transcription regulator of the Pkc1 signalling pathway. However, since Swi4 is a downstream effector for both branches of the Pkc1 signalling pathway, this finding does not assist in determining which branch of the pathway is influenced by the *cdc68* mutation.

Even though none of the other deletions eliminating Pck1 components or related proteins (see previous descriptions), in combination with the *cdc68-319* mutation, showed significant growth impairments by tetrad analysis, the double-mutant haploid cells generated during this process were assessed for growth at elevated temperatures. Cells containing only the *cdc68-319* mutation, only a deletion of *WSC4*, *BCK1*, *BCK2*, *MKK1*, *SLT2*, *CLN2*, *CLN3,* or *SWI4*, or both the *cdc68-319* mutation and one of the gene deletions were tested for growth on rich medium at 30°C and 37°C. To assess the growth at elevated temperatures of the *cdc68-319 swi4Δ* double-mutant cells several of the slow-growing segregants were tested. The *cdc68-319 swi4Δ* double-mutant spores that did germinate produced cells that subsequently grew reasonably well at 30°C. Most of the gene deletions tested did not cause significant growth impairment in combination with the *cdc68-319* mutation (data not shown); however, notable exceptions were the combinations of *cdc68-319 slt2Δ*, *cdc68-319 bck2Δ*, and *cdc68-319 swi4Δ*, which each

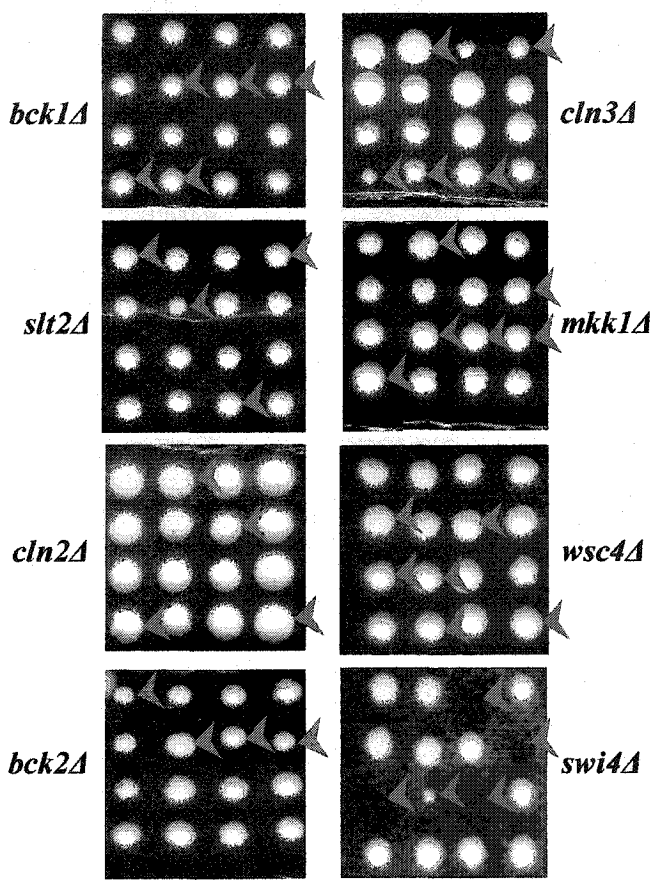

Figure 49. Tetrad analysis of segregants from heterozygous *cdc68-319::natMX4* diploids deleted for genes encoding Pkc1-pathway components. Each column in a panel shows the four spore products from a tetrad produced by a diploid heterozygous for *cdc68-319::natMX4* and the gene deletion indicated beside each panel. Double-mutant segregants (arrowheads) show colony sizes equivalent to those of single-mutant or wild-type segregants in each case, except for *swi4Δ*. The arrowheads indicate where double-mutant *cdc68-319::natMX4 swi4Δ* haploid segregants should have been found based on marker segregation (data not shown). The *cdc68-319::natMX4 swi4Δ* double-mutant spores produce significantly smaller colonies or no colonies at all.

resulted in significantly impaired growth at 37°C in comparison to the single-mutant cells (Figure 50). This finding indicates that Cdc68 and components of each branch of the Pkc1 signalling pathway, specifically Slt2, Bck2, and Swi4, share overlapping essential functions, perhaps in maintaining cell integrity under conditions of elevated temperature. Why deletions of other genes that encode proteins known to function upstream of the Slt2-dependent branch of the pathway did not have the same deleterious effects in combination with *cdc68-319* at elevated temperatures is unclear. However, it is interesting that the activity of SBF is required for both branches of the Pkc1 signalling pathway and that deletion of *SWI4*, the gene that encodes one of the SBF subunits, causes synthetic genetic defects in *cdc68-319* cells. It may therefore be the case that both branches of Pkc1 signalling must be disrupted or additional pressures brought to bear on the cell for the genetic relationship between Cdc68 and cell integrity to be observed.

iv) *cdc68* mutations alter the activity of SBF but do not alter transcript levels for *SWI4* and *SWI6*

In addition to the genetic interaction identified above between *cdc68* and *swi4* mutations, genetic interactions between genes encoding FACT proteins (*CDC68*, *POB3*, and *NHP6*) and those encoding SBF components (*SWI4* and *SWI6*) have been reported (Lycan *et al.* 1994; Sidorova and Breeden 1999). Specifically, increased dosage of Nhp6 protein has been shown to suppress transcription defects that result from specific *swi6* mutant alleles (Sidorova and Breeden 1999). Nhp6 is therefore able to influence the transcription of at least one SBF-regulated gene. Furthermore, this ability of Nhp6 to increase transcription of an SBF-dependent gene requires Swi4, but increased dosage of Nhp6 does not simply result in increased levels of *SWI4* or *SWI6* mRNA (Sidorova and Breeden 1999). The authors suggest that increasing the dosage of Nhp6 may somehow influence the activity of Swi4 to assist in compensating for the impaired function of the Swi6 mutant protein (Sidorova and Breeden 1999).

CDC68 was identified as a bypass mutational suppressor of transcription defects when either *SWI4* or *SWI6* is deleted (Lycan *et al.* 1994). The *cdc68-1* allele, which encodes an unstable Cdc68 protein whose levels are significantly decreased at 37°C (Xu 1995) was also shown to result in diminished transcription of *SWI4* and *SWI6* at 37°C (Lycan *et al.* 1994). In light of new findings that demonstrate a role for Cdc68 and FACT in removing

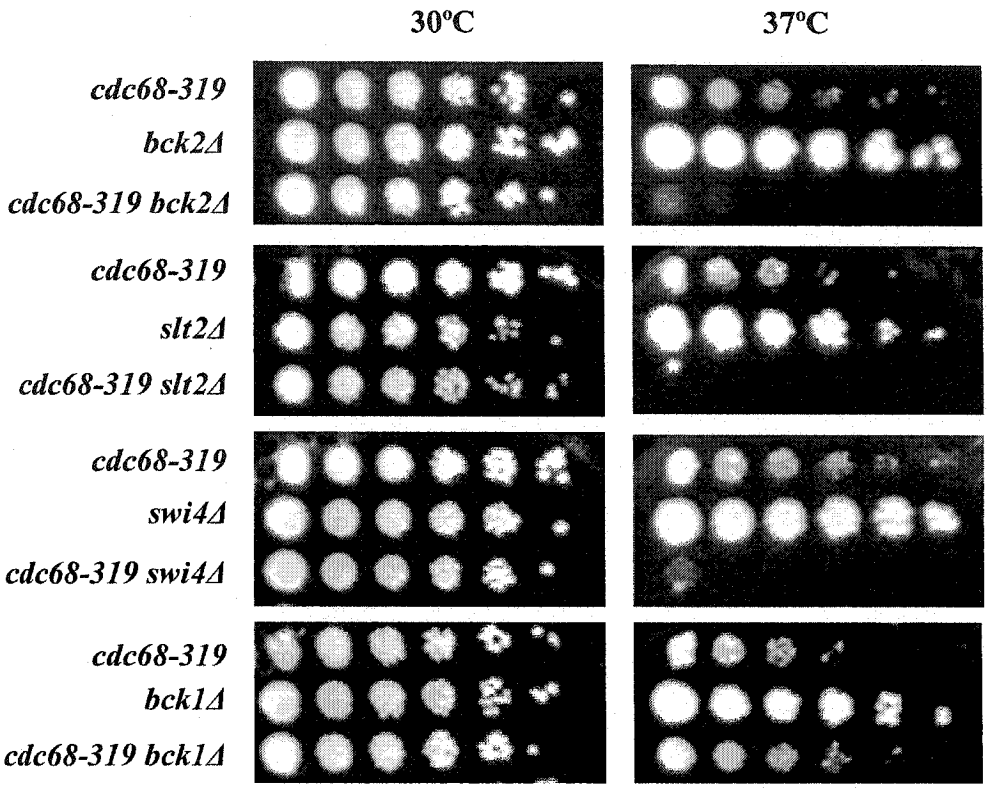

Figure 50. Synthetic growth defect at 37°C for *cdc68-319* cells deleted for genes encoding Pkc1-pathway components. Cultures were grown to stationary phase in YPD liquid medium and the cell concentrations determined. Cultures diluted to an initial concentration of 1 x 10^7 cells/ml were serially diluted in 5-fold steps, spotted onto the indicated medium and allowed to grow for 4 days. While *cdc68-319* caused some degree of temperature sensitivity at 37°C, the combination of *cdc68-319* with *bck2Δ*, *slt2Δ*, and *swi4Δ* led to significant further impairments of growth. Cells containing the double-mutant combination *cdc68-319 bck1Δ* grew as well as *cdc68-319* cells at 37°C.

the nucleosomal barrier during transcription elongation, this decreased abundance of *SWI4* and *SWI6* mRNAs under circumstances that would deplete the labile Cdc68-1 protein from cells may be attributed to the loss of Cdc68 essential function in facilitating transcription elongation. Cells containing *cdc68-1* that are incubated at elevated temperatures show greatly diminished mRNA levels for almost all genes investigated (including *CLN1*, *CLN2*, *CLN3*, *ACT1*, *SAN1*, *ADK1*, and *HTA1/HTB1*) (Lycan *et al.* 1994; Xu 1995), a finding that is compatible with the localization of FACT on genes that are actively transcribed by RNA polymerase II (Mason and Struhl 2003; Saunders *et al.* 2003).

Given the genetic associations between FACT and SBF, both described here and previously characterized (Results 3 iii above; Lycan *et al.* 1994; Sidorova and Breeden 1999; Formosa *et al.* 2001), the activation of SBF reporter genes was assessed in *cdc68* mutant cells. The SBF components, Swi4 and Swi6, have been shown to activate transcription independently of each another. Swi4 activates transcription of a subset of genes independently of Swi6, and Slt2 appears to mediate this type of activation (Baetz *et al.* 2001). Swi6 is known to function in conjunction with Mbp1 in an alternative transcription activator known as MBF (reviewed in Breeden 1996), which regulates the expression of several genes involved in cell-cycle progression, specifically those involved in DNA replication and repair (reviewed in Breeden 1996; Iyer *et al.* 2001). The effects of the *cdc68-312* and *cdc68-319* mutations on SBF, MBF, and Swi4 activation of transcription was assessed using *lacZ* reporter genes regulated by these specific factors. The SBF complex binds a specific DNA sequence, known as an SCB element (reviewed in Breeden 1996), upstream of genes, and the *SCB-lacZ* reporter employed here to monitor SBF activity contains four copies of the SCB consensus sequence upstream of the *lacZ* coding sequence (Andrews and Herskowitz 1989). The MBF complex also binds DNA in a sequence-specific manner, to MCB elements in the promoters of target genes (reviewed in Breeden 1996). The *MCB-lacZ* reporter contains four copies of the MCB sequence element upstream of *lacZ* (Verma *et al.* 1992). The *PCL1* gene, which encodes a G_1 cyclin, is activated in a Swi4 dependent fashion (Baetz *et al.* 2001), and therefore the *PCL1* promoter (*prPCL1*) fused to the *lacZ* gene generates a Swi4-specific activation reporter (Ogas *et al.* 1991).

Each of the *prPCL1-lacZ*, *MCB-lacZ*, and *SCB-lacZ* reporter genes was present on a high-copy *URA3* plasmid. These plasmids were transformed independently into yeast cells containing either a chromosomal wild-type version of *CDC68*, or the *cdc68Δ::kanMX4* chromosomal deletion and a wild-type *CDC68*, *cdc68-312* or *cdc68-319* centromeric *LEU2* plasmids. Transformants were then grown to mid-log phase at 30°C in SC liquid medium lacking uracil, to maintain selection for the plasmids containing the reporter genes. Liquid β-galactosidase assays were then carried out on a minimum of two independent transformants, with a minimum of four replicates for each experiment, as a measure of β-galactosidase enzyme activity, which is proportional to the transcription activation. Only moderate differences in expression of the *MCB-lacZ* reporter were observed, with the mean level of β-galactosidase in *MCB-lacZ* cells between 70 and 76 Miller units for *CDC68* (plasmid or chromosomal) and *cdc68-319* cells (Figure 51A). The level of β–galactosidase activity was decreased by 30% in *MCB-lacZ* cells containing the *cdc68-312* allele (Figure 51A). These results indicate that the influence of Cdc68, as determined by the impact of these particular mutational changes, on the activation of MCB-driven gene expression is minimal. Similarly, no significant alterations in β–galactosidase activity were observed for *cdc68-312* cells containing either the *SCB-lacZ* or *prPCL1-lacZ* reporters (Figure 51B and C). In contrast, dramatic changes in the β-galactosidase activity were observed for cells containing the *SCB-lacZ* or *prPCL1-lacZ* reporters in combination with the *cdc68-319* allele, with approximately 2-fold and 4- to 5-fold increased activity in comparison to wild-type controls, respectively (Figure 51B and C).

These findings indicate that, while the *cdc68-312* mutation has little impact on SBF and Swi4 activity at 30°C, the *cdc68-319* mutation results in greatly increased transcription activation of both SBF and Swi4 targets. This increased activation of SBF- and Swi4-mediated transcription could be a result of 1) increased cellular 'stress' due to the *cdc68-319* mutation that then activates the Pkc1 signalling pathway and generates an increased activation of SBF and Swi4; 2) a direct influence of the *cdc68-319* mutation on the activation of these genes, perhaps by altering chromatin structure in such a way as to facilitate SBF and Swi4 activation; 3) increased mRNA levels for *SWI4* and/or *SWI6*

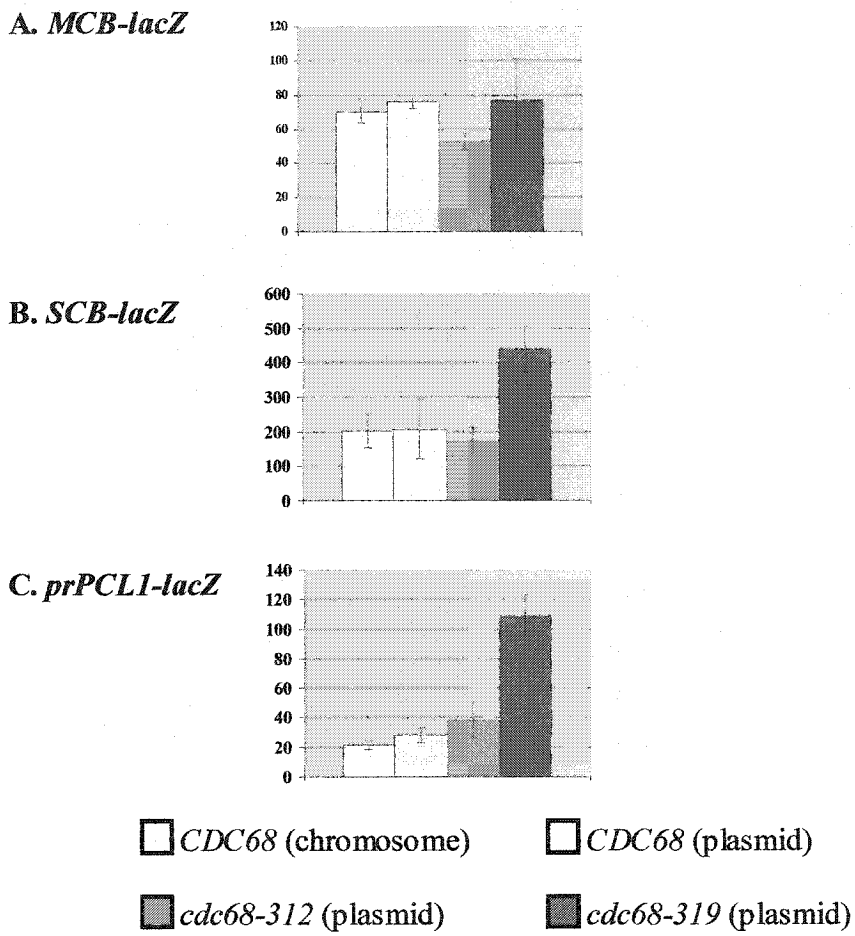

Figure 51. Effects of *cdc68* mutations on MBF, SBF, and Swi4 activation of transcription. The β-galactosidase activities (Miller units) were measured for lysates prepared from log-phase cells grown at 30°C containing (A) *MCB-lacZ*, (B) *SCB-lacZ*, or (C) *prPCL1-lacZ* reporters. Error bars indicate standard deviation.

cdc68-319 cells, which in turn results in higher activities of the SBF and Swi4 transcription factors. It is difficult to distinguish between the first two possibilities. The genetic evidence certainly supports a common function for Cdc68 and SBF, or specifically the Swi4 component of this complex. Microarray experiments using *cdc68-312* and *cdc68-319* cells grown to mid- to late-log phase at 30°C (Results 2, xiii) showed no significant alterations in *SWI4* or *SWI6* transcript levels. To verify this finding and address the third possible mechanism of Cdc68-mediated SBF and Swi4 gene activation, northern blots of RNA extracted from cells grown to mid-log phase at 30°C were probed for *SWI4* and *SWI6* mRNA. Under these conditions no significant changes in *SWI4* or *SWI6* mRNA abundances were observed in *cdc68-312* or *cdc68-319* cells (Figure 52). Therefore, the observed changes in SBF- and Swi4-activated reporter-gene expression in *cdc68-319* cells are not the result of changes in *SWI4* or *SWI6* transcript abundance, and must therefore be due to an overlapping function for Cdc68 and these factors, most likely involving the regulation of gene expression.

In summary, several lines of genetic evidence implicate FACT, and specifically the Cdc68 component of this complex, in maintaining cell integrity and morphogenesis. Cells containing *cdc68* mutant alleles are shown here to display several phenotypes characteristic of defects in these processes, including sorbitol-remedied temperature sensitivity, altered sensitivity to detergent, and abnormal morphologies. The *ssd1-d* allele is shown to cause synthetic lethality in combination with mutant alleles of *cdc68* when cells are grown at elevated temperatures. *SSD1* along with the Pkc1 signal-transduction pathway and an Mpt5-mediated pathway have been implicated in parallel functions maintaining cell integrity and morphogenesis in (Kaeberlein and Guarente 2002). I have shown here that over-expression of the *MPT5* gene does not alter the temperature sensitivity of *cdc68* mutant cells. However, over-expression of genes encoding components of the Pkc1 signal-transduction cascade suppress the high-temperature growth defect of *cdc68* cells. Futhermore, deletions of genes encoding members of each of the two branches of the Pkc1 signalling cascade result in synthetic lethality or growth impairments in *cdc68-319* mutant cells. These findings implicate an overlapping essential function between FACT and the Pkc1 signal-transduction cascade. Key transcription factors responding to Pkc1 signalling are the SBF complex and specifically the Swi4

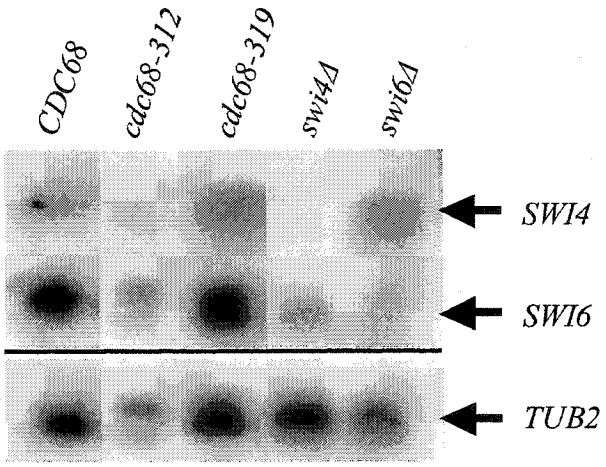

	CDC68	*cdc68-312*	*cdc68-319*
SWI4	**1.0**	**1.3**	**1.3**
SWI6	**1.0**	**0.7**	**1.0**

Figure 52. *SWI4* and *SWI6* transcript abundances are not altered in *cdc68* mutant cells.. Total RNA was extracted from mid-log cells grown at 30°C. Approximately 10 μg of RNA was loaded per lane, resolved by gel electrophoresis, and blotted to a nylon support membrane, which was probed with ^{32}P-labelled probes specific for *SWI4*, *SWI6*, or *TUB2* (as a loading control). Densitometry of the resulting hybridization signals was carried out using ImageJ software (US National Institutes of Health; available at http://rsb.info.nih.gov/nih-image/). Signal intensities were normalized to the *TUB2* control value for each lane and then compared to the signal intensity determined for the wild-type *CDC68* samples. Relative transcript abundances for *SWI4* and *SWI6* in *cdc68* mutant cells in comparison to wild-type *CDC68* cells are shown in the table.

subunit of this transcription activator. The expression of reporter genes designed to measure SBF and Swi4 transactivation is significantly increased in *cdc68-319* mutant cells. This effect is not due to altered mRNA abundance for the *SWI4* and *SWI6* genes. The mechanism of this altered gene activation in *cdc68-319* cells remains uncertain; Cdc68 may act directly to influence the activity of these two transcription activators by alterations in chromatin structure, or it may be that the level of SBF and Swi4 activation is increased as a result of increased Pkc1 signalling in *cdc68* mutant cells. In any case, these findings suggest a novel role for FACT in the maintenance of cell integrity and regulation of cell morphogenesis, a role that is directly linked to the functions of both the Ssd1 and Pkc1-mediated pathways that regulate these processes.

4. Synthetic lethal interactions with novel *cdc68* mutant alleles

A powerful method to obtain insight into gene-product function is to identify other gene products with overlapping activities. Screening for second-site mutations that result in sickness or even lethality when combined with a mutation in the gene of interest is one means to identify such functional relationships. When this occurs, the gene pair is said to be synthetically sick or lethal. Any instance where the phenotypes associated with individual mutations in *geneX* and *geneY* are considerably worsened upon generation of a double-mutant cell containing mutations in both *geneX* and *geneY* is an example of synthetic sickness or lethality.

This type of synthetic sick/lethal relationship between two mutations indicates that the genes in question generate products with overlapping cellular functions. In yeast, the majority of genes can be individually deleted without loss of cell viability and often with only minor consequences on cell proliferation (Winzeler *et al.* 1999). One explanation for this observation is that there are several pathways or proteins within a cell that perform the same or similar functions. Therefore, when one of the pathways is impaired, the cell is still able to meet its requirements though the functioning of a redundant pathway.

Gene pairs exhibiting synthetic sick/lethal relationships can be very informative as they highlight a common functionality between the genes involved. Synthetic lethality between mutations causing partial or impaired function, rather than complete gene deletions, may identify genes whose protein products function within the same pathway or physically interact (Figure 53; Guarente, 1993; Appling 1999). In this way, synthetic

Figure 53. Mechanisms for synthetic lethal interactions. This figure highlights the differences between mechanisms underlying synthetic lethal interactions with non-null mutations (1, 2, and 3) *versus* null mutations (3). (1) depicts a synthetic lethal interaction between non-null mutations affecting the same pathway. (2) displays a mechanism for synthetic lethality between two non-null mutations affecting members of the same protein complex. (3) shows two parallel pathways that act to carry out function 'X'. Individual mutations affecting one of the two pathways have little to no impact on cell viability, whereas impairment of both pathways, by either null or non-null mutations, results in loss of cell viability. Proteins encoded by mutant alleles are shaded shapes.

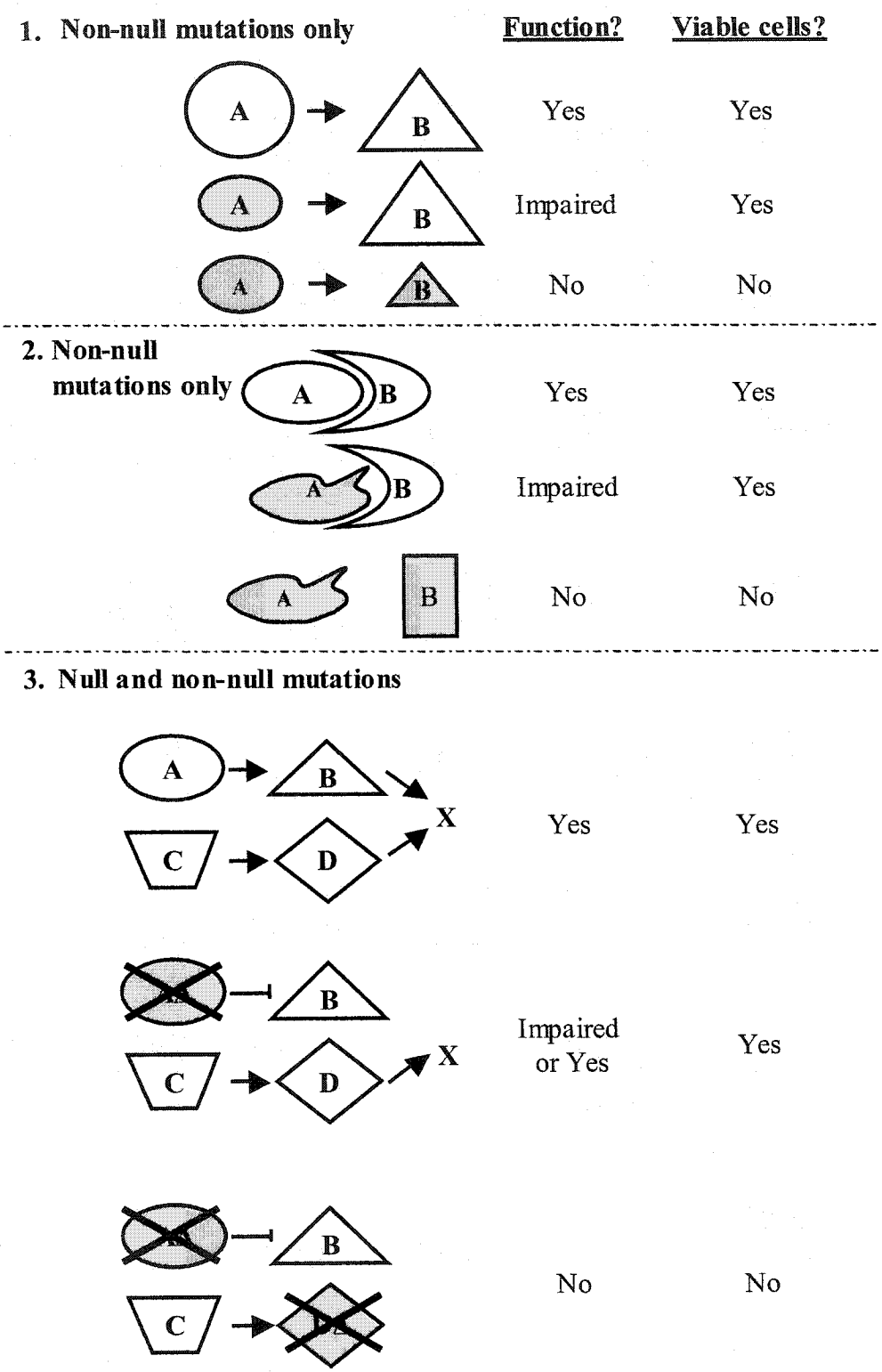

Figure 53. Mechanisms for synthetic lethal interactions.

lethal relationships can be used to assist in identifying the protein components that function in the same pathways as the gene of interest, or function in the same complex. Alternatively, synthetic lethality involving a gene deletion may identify genes whose protein products function in parallel pathways to execute a common molecular function (Figure 53; Guarente, 1993).

Two different synthetic-lethal screening methods have been employed here to identify second-site mutations that result in synthetic lethality with *cdc68* mutations. This analysis made use of several *cdc68* alleles that encode mutations affecting various regions of the protein. Identifying the synthetic-lethal gene partners for each allele permits a degree of functional classification for the various regions of Cdc68 that are affected. For example, alleles that generate an N-terminally mutated Cdc68 protein may identify significantly different synthetic-lethal gene partners than would alleles that generate Cdc68 proteins with C-terminal mutations. By comparing the synthetic-lethal interactions for these two mutant alleles it may be feasible to assign functions to specific regions of the Cdc68 protein based on the functions of the synthetic-lethal partners for that region. The first synthetic-lethal approach that I used made use of a classical colony-sectoring phenotype (Kranz and Holm 1990) to identify mutations that result in synthetic lethality with *cdc68* mutations (Figure 54). The second approach employed the more recently described synthetic genetic array (SGA) analysis (Tong *et al.* 2001), which allows screening through the set of approximately 4700 non-essential yeast gene deletions (Winzeler *et al.* 1999; Tong *et al.* 2001) for synthetic-lethal interactions with *cdc68* mutations (Figure 55).

i) Identification of synthetic lethal interactions with *cdc68-E857K* using a 'classical' synthetic-lethal approach

Classically, synthetic-lethality screens have exploited mutations in the adenine biosynthesis pathway that result in pigmented yeast colonies depending on the cohort of adenine-pathway mutations present (Kranz and Holm 1990; Bender and Pringle 1991). Mutations in the *ade2* gene cause cells to accumulate the *de novo* purine biosynthesis pathway intermediate 5-phosphoribosyl 5-aminoimidazol, which results in pink or reddish pigment accumulation. A mutation in the *ade3* locus is epistatic to an *ade2* mutation and prevents accumulation of the pigment-generating intermediate by blocking

Figure 54. Classical synthetic-lethal screening with *cdc68-E857K*. Derivatives of strain SNL-51B harbouring plasmid pSNLCDC68 (contains *URA3*, *ADE3*, *CDC68* and *GAL1p-CEN4*) and a *TRP1 cdc68-E857K* plasmid, shown at the top, form colonies that are pinkish-red. UV mutagenesis introduces new mutations (*mutX*). Subsequent growth on galactose medium prevents efficient inheritance of the pSNLCDC68 plasmid. Cells that fail to inherit pSNLCDC68 form colonies that are white (shown at left) and therefore do not possess a *mutX* mutation that is synthetically lethal with *cdc68-E857K*. When the *mutX* mutation is synthetically lethal with *cdc68-E857K*, cells that fail to inherit the pSNLCDC68 plasmid will not thrive, leaving only cells that do inherit this plasmid to generate a red, unsectored colony (shown at right).

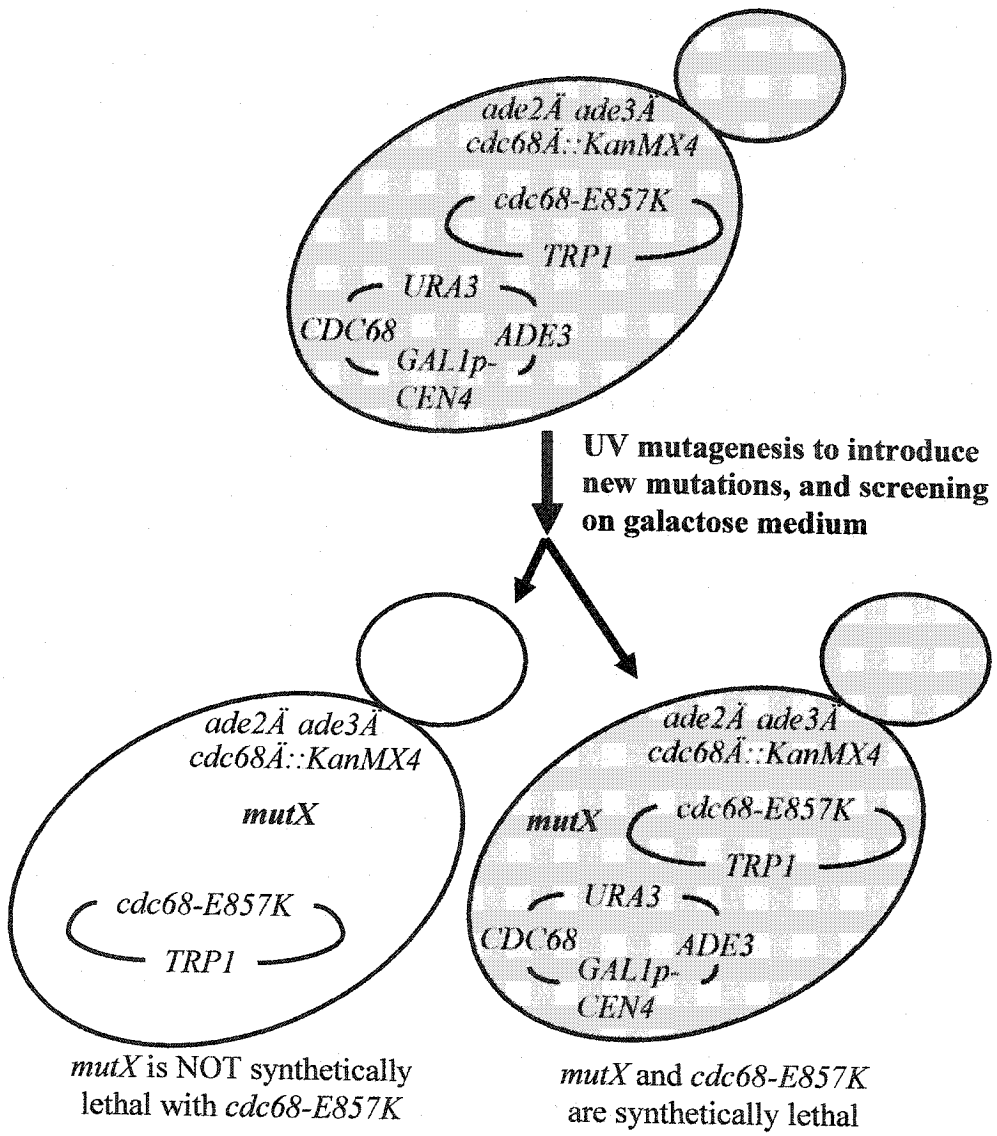
ade2Ä ade3Ä
cdc68Ä::KanMX4
cdc68-E857K
TRP1
URA3
CDC68
ADE3
GAL1p-
CEN4
UV mutagenesis to introduce new mutations, and screening on galactose medium
ade2Ä ade3Ä
cdc68Ä::KanMX4
mutX
cdc68-E857K
TRP1
mutX is NOT synthetically lethal with cdc68-E857K
ade2Ä ade3Ä
cdc68Ä::KanMX4
mutX
cdc68-E857K
TRP1
URA3
CDC68
ADE3
GAL1p-
CEN4
mutX and cdc68-E857K are synthetically lethal

Figure 54

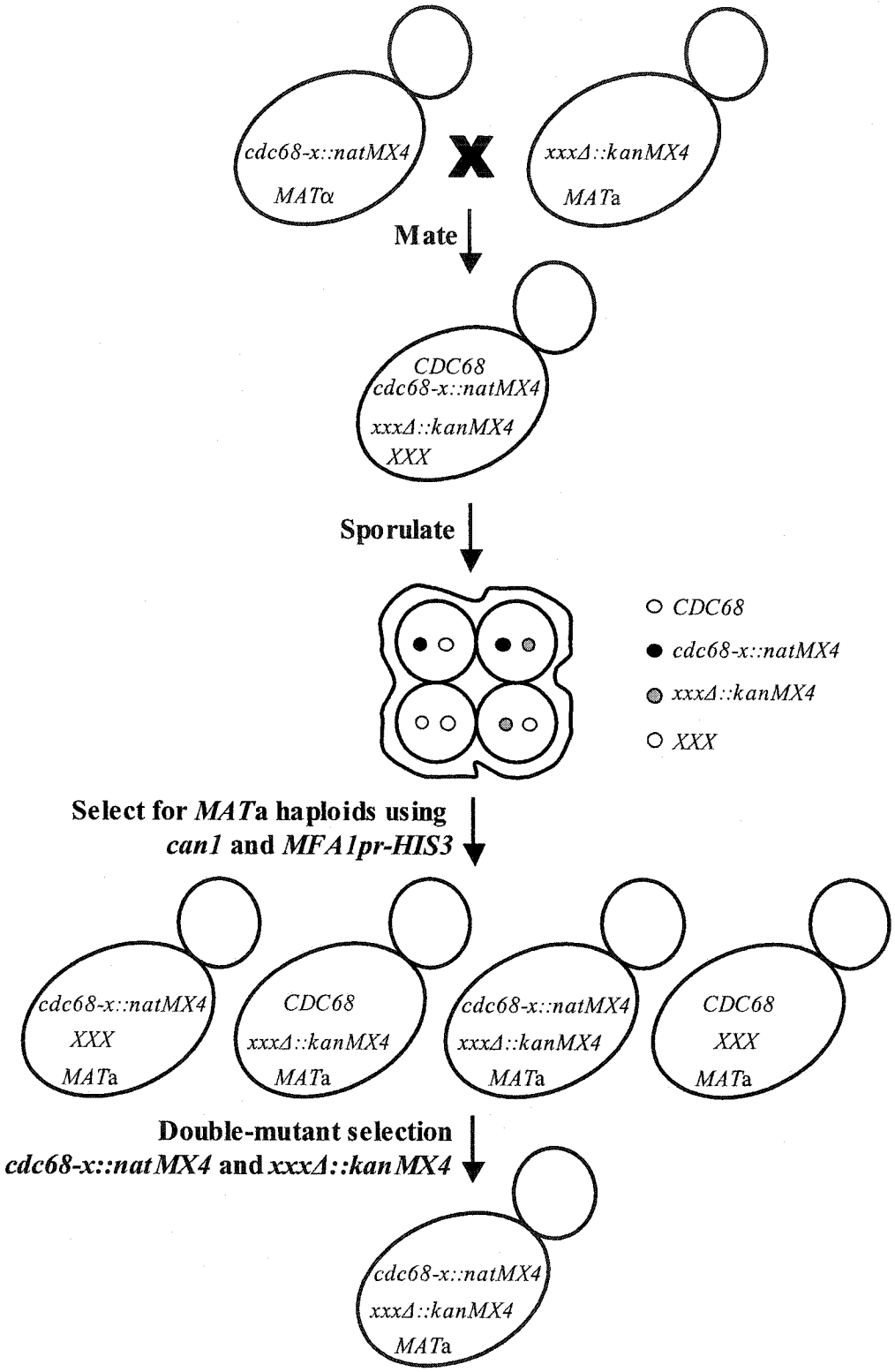

Figure 55. Synthetic genetic array (SGA) analysis. Modified from Tong *et al.* (2001).

the biosynthetic pathway at an earlier step. This prevents the accumulation of the red pigment, since the pathways is blocked before the 5-phosphoribosyl 5-aminoimidazol intermediate is ever produced; therefore, *ade2 ade3* double-mutant cells remain white. Classical synthetic-lethal screens are designed so that monitoring of colony colour, red or white, permits identification of cells containing synthetic-lethal mutations.

Yeast strains SNL-58D and SNL-51B (*cdc68Δ::kanMX4 ade2Δ ade3Δ ura3-52 trp1-Δ1 leu2-3,112* and *MAT*a or *MAT*α, respectively) were generated that contain plasmid pSLCDC68, which harbours the *ADE3*, *URA3* and *CDC68* genes. A second plasmid containing either a wild-type *CDC68* gene (as a control in the experiment) or a mutant *cdc68* allele, *cdc68-E763G*, *cdc68-E857K*, *cdc68-312*, or *cdc68-319*, on a centromeric *LEU2* or *TRP1* backbone, was then introduced. Transformants containing both the *URA3* plasmid pSLCDC68 and a *LEU2* or *TRP1* plasmid were selected. These cells harboured two versions of the *CDC68* gene, which both produce proteins that are able to provide essential Cdc68 function, on differentially marked plasmids (Figure 54), and provided the starting point for synthetic-lethal screening. These cells accumulate red pigment because of the chromosomal *ade2Δ* mutation and the *ADE3* gene provided on pSNLCDC68 that complements the chromosomal *ade3Δ* mutation. However, due to occasional mis-segregation of the pSNLCDC68 plasmid during cell division, some cells may not inherit pSNLCDC68. In these cells, the *ade3Δ* mutation is no longer complemented, so that cells fail to accumulate the pigmented intermediate in *de novo* purine biosynthesis and are therefore white. Of course, when the pSNLCDC68 plasmid is no longer present, cells fail to inherit a wild-type copy of the *CDC68* gene as well as *ADE3*. These cells must therefore rely on the *cdc68* allele on the *LEU2* or *TRP1* plasmid for essential Cdc68 function (Figure 54).

By mutagenizing a population of cells that contain both the pSNLCDC68 plasmid and the *LEU2* or *TRP1 cdc68* plasmid, and then monitoring the resultant colony colour indicative of the ability to thrive in the absence the pSNLCDC68 plasmid, second-site mutations that cause lethality in combination with the plasmid-borne mutant *cdc68* allele may be identified (Figure 54). To increase the frequency of pSNLCDC68 plasmid loss (failure to inherit at mitosis), a galactose-inducible promoter has been incorporated upstream of the centromeric sequence on this plasmid (Barbour *et al.* 2000). The

centromeric sequence is a key player in the segregation of plasmids to both mother and daughter cells. Growth of cells on medium containing galactose results in increased frequency of pSNLCDC68 plasmid mis-segregation as a result of glactose-activated transcription through the centromere (Chlebowicz-Sledziewska and Sledziewski 1985; Barbour *et al.* 2000). The pSNLCDC68 plasmid is therefore not inherited efficiently by both mother and daughter cells on galactose-containing medium (Barbour *et al.* 2000). This increased frequency of pSNLCDC68 mis-segregation results in a higher proportion of white cells in a colony, unless the pSNLCDC68 plasmid is required for cell viability due to a synthetic lethal interaction. In the synthetic-lethal scenario, the only cells able to produce progeny are those that have maintained pSNLCDC68 and therefore accumulate the red-pigment, while those cells that have not inherited the pSNLCDC68 plasmid appear white.

The SNL-58D and SNL-51B derivatives described above containing both pSNLCDC68 and a *TRP1* or *LEU2 cdc68* plasmid, respectively, were spread on SC medium lacking tryptophan or leucine, as appropriate, and containing galactose as the carbon source. Cells were then irradiated with ultraviolet light, at dosages that resulted in approximately 50% mortality, to induce mutations. On the galactose medium, the *GAL1* promoter next to the centromeric sequence on the *CDC68 ADE3 URA3* plasmid is activated, resulting in a reduced fidelity of plasmid inheritance. As a result, many progeny cells fail to inherit the pSNLCDC68 plasmid, resulting in a mixed or sectored colony phenotype where cells that have the plasmid remain red, while the progeny of those cells that failed to inherit the plasmid appear white. When cells fail to inherit a copy of the *ADE3* plasmid they also fail to inherit a wild-type copy of the *CDC68* gene. These cells therefore rely on the mutant allele of *cdc68* for Cdc68 activity. In scenarios where the UV treatment has generated a second-site mutation in a gene that is synthetically lethal with the mutant *cdc68* allele (see Figure 53 for potential mechanisms), cells that do not inherit pSNLCDC68 containing the *ADE3*, *CDC68*, and *URA3* genes will fail to thrive, leaving only those cells that do have this plasmid to form a colony. These colonies remain red even in the presence of galactose.

Prior to screening for synthetic-lethal interactions, the SNL-51B and SNL-58D derivatives containing a plasmid with a *cdc68* mutant allele were each grown on medium

containing galactose to ensure that the plasmid-borne *cdc68* allele is indeed able to provide essential Cdc68 function. In each case, red/white sectored or all-white colonies resulted, which showed that the cells do not require the pSNLCDC68 plasmid for viability (data not shown). These observations ensured that the *cdc68-E763G*, *cdc68-E857K*, *cdc68-312*, and *cdc68-319* alleles do not significantly impair cell growth under the conditions employed for this screen. Efforts using this method focused on the *cdc68-E857K* mutation.

Initial screens for second-site mutations that are synthetically lethal with *cdc68-E857K* were conducted using SNL-51B and SNL-58D derivatives containing a *LEU2* or *TRP1 cdc68-E857K* plasmid, respectively. These cells were subjected to UV mutagenesis on medium lacking leucine or tryptophan as appropriate to maintain selection for the *cdc68-E857K* plasmid, but containing galactose as a carbon source, to promote mis-segregation of the pSNLCDC68 plasmid. Among $3.1x10^3$ colonies from the SNL-51B derivative and $1x10^3$ colonies from the SNL-58D derivative, a total of seven red, unsectored colonies were identified. Cells from these isolates may therefore carry second-site mutations that are synthetically lethal with *cdc68-E857K*. Upon spreading cells from these candidate colonies on SC-Trp or SC-Leu medium containing galactose, the resultant colonies from only five of the seven candidates, all from the SNL-51B screen, were all red and unsectored. As described below, further experiments were performed on these five candidate isolates to ensure that: 1) the synthetic lethality between *cdc68-E857K* and the second-site mutation is genuine and that the pSNLCDC68 plasmid is indeed necessary for cell viability even when negative selection for pSNLCDC68 was applied; 2) the plasmid-borne *cdc68-E857K* allele had not been further mutated during the UV mutagenesis to be unable to provide essential Cdc68 function; and 3) the lethality observed is related to the presence of the *cdc68-E857K* allele, and not due to other genetic interactions.

As a more rigorous test than sectored-colony development to determine the necessity of plasmid pSNLCDC68 for survival, cells were grown in the presence of 5-fluoroorotic acid (5-FOA). 5-FOA is toxic to yeast cells containing a functional pyrimidine biosynthetic pathway, of which the *URA3* gene product is a member (Boeke *et al.* 1984). The pyrimidine synthesis pathway incorporates 5-FOA during the biosynthesis and

eventually produces 5-fluorodeoxy UMP (uridine-5'-monophosphate), an inhibitor of thymidylate synthase, and cells subsequently die as a consequence of thymine starvation (Boeke *et al.* 1984; Rose *et al.* 1990; Santoso and Thornburg 1998). Since the *URA3* gene is present on the pSNLCDC68 plasmid but mutated in the chromosome, when cells are challenged to grow on medium containing 5-FOA only those cells that are viable in the absence of pSNLCDC68 will thrive. Cells that fail to inherit the pSNLCDC68 plasmid will have the potential to form colonies in the presence of 5-FOA, but these cells must therefore be kept alive by the plasmid containing the *cdc68-E857K* allele. If this were the case, then no synthetic lethal interaction between the *cdc68-E857K* mutation and another mutation could exist in these cells. Alternatively, if plasmid pSNLCDC68 really *is* required to maintain cell viability, the synthetic-lethal candidates will be unable to grow in the presence of 5-FOA. Cells from each of the five synthetic-lethal candidates, along with cells of an unmutagenized SNL-51B derivative containing a *TRP1*-marked *cdc68-E857K* plasmid as a control, were assessed for growth on medium containing 5-FOA. The only cells that were able to proliferate under these conditions were those from the unmutagenized control strain (Figure 56). Thus the survival of cells from each of the five synthetic-lethal candidates is dependent upon the presence of the pSNLCDC68 plasmid, which is consistent with the findings from the colony-colour sectoring assay.

To verify that the synthetic lethality observed for each of the candidates is not the result of further mutation of the *cdc68-E857K* plasmid during UV mutangenesis, plasmid shuffling was performed. Cells that had failed to inherit the original *TRP1 cdc68-E857K* plasmid and were therefore kept alive by the pSNLCDC68 plasmid were selected as starting points for the following experiments. These derivatives of the SNL-51B synthetic-lethal candidates, with the pSNLCDC68 plasmid, were transformed with a *TRP1 cdc68-E857K* plasmid that had not been subjected to mutagenic influences. Synthetic-lethal candidate transformant cells able survive in the absence of the pSNLCDC68 plasmid in the presence of this new *TRP1 cdc68-E857K* plasmid must have previously been unable to thrive in the absence of pSNLCDC68 as a result of mutation of the original *TRP1 cdc68-E857K* plasmid. Cell growth in the absence of pSNLCDC68 was assessed on medium containing 5-FOA (Figure 57). In this way, two of the five

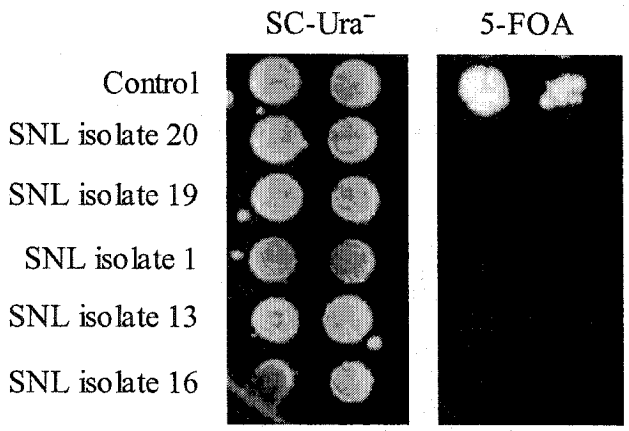

Figure 56. Growth of *cdc68-E857K* synthetic-lethal candidates on 5-fluoroorotate medium. Cells from the SNL-51B derivative bearing pSLNCDC68 and a *TRP1 cdc68-E857K* plasmid that were unmutagenized (control) or identified as synthetic-lethal candidates, isolates 20, 19, 1, 13, and 16, by the colony sectoring assay were inoculated as 5-μl spots from cultures diluted to 2.0×10^6 and 5.5×10^5 c/ml densities on SC medium lacking uracil and on 5-FOA medium. Only the control strain was able to grow on 5-FOA medium, indicating that these cells are not dependent on the *URA3* plasmid pSLNCDC68 plasmid for viability, as expected. Cells from each of the synthetic-lethal candidate strains were unable to grow on medium containing 5-FOA, indicating that these cells are not viable in the absence of the *URA3* plasmid pSLNCDC68.

Figure 57. Two *cdc68-E857K* synthetic-lethal candidates are further confirmed. Cells from the synthetic-lethal candidates, as well as an unmutagenized control strain, bearing pSLNCDC68 and a *TRP1 cdc68-E857K* plasmid were grown multiple times on SC medium containing tryptophan. Cells that had failed to inherit the *TRP1 cdc68-E857K* plasmid were selected and re-transformed with a new *TRP1 CDC68* or *cdc68-E857K* plasmid (indicated along the bottom of each panel). Transformants were tested for growth on medium containing 5-FOA to determine if cells were viable cells in the absence of the *URA3* plasmid pSLNCDC68. Failure to inherit the pSNLCDC68 plasmid has no effect on the viability of the unmutagenized control strain, as evidenced by growth on 5-FOA when either the *CDC68* or *cdc68-E857K* allele is present. SNL isolates 13 and 20 were both able to grow on medium containing 5-FOA in the presence of the new *TRP1 cdc68-E857K* plasmid. Thus these isolates do not have a second mutation that results in synthetic lethality with *cdc68-E857K*. Cells from SNL isolate 1 were unable to grow in the absence of the pSLNCDC68 plasmid, as evidenced by their inability to grow on medium containing 5-FOA, even in the presence of another wild-type *CDC68* plasmid. Therefore SNL isolate 1 does not exhibit a synthetic lethal interaction with *cdc68-E857K*, but instead has a synthetic lethal interaction with some component of the pSLNCDC68 plasmid. SNL isolates 16 and 19 produced viable cells lacking pSLNCDC68, but only in the presence of a second plasmid bearing wild-type *CDC68.* These two isolates did not generate viable cells lacking pSLNCDC68 when the *TRP1 cdc68-E857K* plasmid was present. These observations indicate that these two isolates harbour second-site mutations that are synthetically lethal with *cdc68-E857K*.

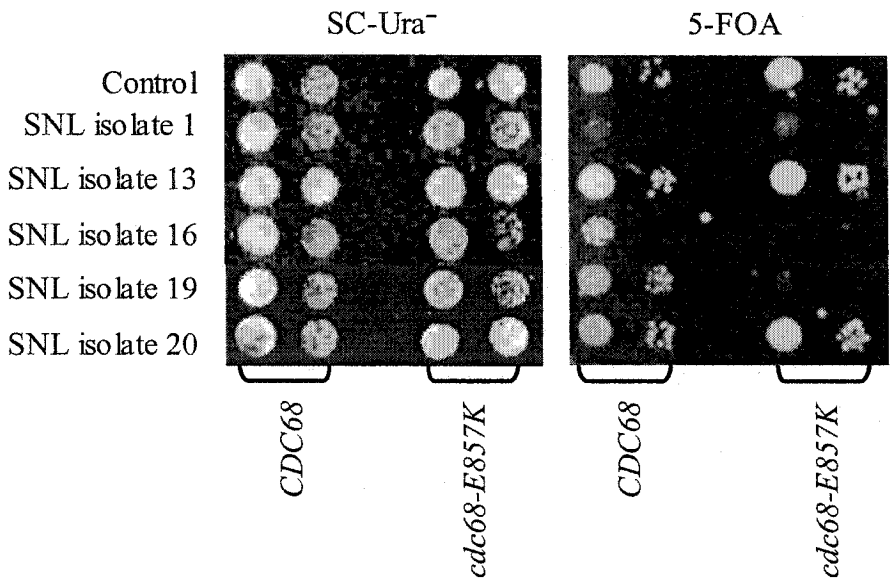
SC-Ura⁻
5-FOA
Control
SNL isolate 1
SNL isolate 13
SNL isolate 16
SNL isolate 19
SNL isolate 20
CDC68
cdc68-E857K
CDC68
cdc68-E857K

Figure 57

synthetic-lethal candidates, isolates 13 and 20, were discarded as they were able to grow on 5-FOA when they harboured the new *cdc68-E857K* plasmid.

To ensure that synthetic lethality is related to the *cdc68-E857K* mutant allele and not to pSNLCDC68 plasmid-related genetic factors, the original *TRP1 cdc68-E857K* plasmid was replaced with a *TRP1* plasmid bearing a wild-type *CDC68* gene, using the plasmid swapping method described above. These synthetic-lethal candidate derivativescontaining pSNLCDC68 and a *TRP1 CDC68* plasmid were grown in the presence of 5-FOA to ensure that, in this situation, the pSNLCDC68 plasmid is no longer required for cell growth. The lethality originally observed with *cdc68-E857K* and the second-site mutation could be alleviated by the presence of pSNLCDC68 or the newly introduced *TRP1 CDC68* plasmid for four of the five original isolates; however, one of the five isolates failed to grow on 5-FOA even when the *TRP1 CDC68* plasmid was present (Figure 57). This finding indicated that the UV-induced mutation is lethal in the absence of genetic factors contained on the pSNLCDC68 plasmid. Therefore the dependence of cell viability on the presence of pSNLCDC68 in this candidate is not due to a synthetic lethal interaction involving *cdc68-E857K*.

These additional experiments support a synthetic lethal interaction between *cdc68-E857K* and a second-site mutation for two of the original five candidates. These two candidates, SNL isolates 16 and 19, have been studied further by Jennifer Stevens, a graduate student in the Singer/Johnston lab, who, in addition to continued screening for synthetic lethal interactions using the methodology described here, has employed a cloning-by-complementation strategy to identify the genes responsible for the synthetic lethality with *cdc68-E857K*. To date, no complementing yeast genomic library plasmid has been identified for SNL isolate 19; however, a yeast genomic library plasmid complementing the synthetic lethal mutation in SNL isolate 16 has been identified (J. R. Stevens, unpublished observation). Sequence analysis shows that this genomic library plasmid contains the complete coding sequences for *BUR2*, *ADY4*, and *YLR227w-B*, as well as partial sequences for the *YLR225c* and *ECM22* genes and some transposon sequence elements. The DNA sequence encompassing the *BUR2* gene was cloned into a plasmid (Materials and Methods) and shown to be the complementing gene on the genomic library plasmid insert (data not shown; J. R. Stevens, unpublished observation).

The *bur2* mutant allele that is synthetically lethal with *cdc68-E857K* was isolated by gap-repair, and sequence analysis determined that this allele contains an insertion at nucleotide 235 of the *BUR2* open reading frame, changing codon 85 from glutamate to arginine and resulting in frame-shift and premature translation termination after the 91st codon. Only about 20% of the Bur2 protein is encoded by this allele. Bur2 functions as a regulatory cyclin for the Bur1 protein kinase, and together the Bur1/Bur2 kinase may be involved in phosphorylating Spt5 (Keogh *et al.* 2003; Pei and Shuman 2003), a protein that binds Spt4 to form a complex involved in regulating transcription elongation (Murray *et al.* 2001; Prelich 2002). Additional synthetic-lethal mutations in the *hir1*, *hir2* and *hir3* genes, involved in nucleosome assembly (Kaufman *et al.* 1998) and regulation of histone gene expression (Osley 1991; Xu *et al.* 1992) with *cdc68-E857K* have been identified by J. R. Stevens using this approach (see Discussion). Based on the functions of theses synthetic-lethal partners, it appears that the *cdc68-E857K* mutation affects the region of Cdc68 required for transcription elongation and histone gene expression or nucleosome assembly. The precise nature of these interactions, *i.e.* whether Cdc68 functions in the same or a parallel pathway to these proteins, remains to be determined.

ii) Synthetic genetic array analysis of *cdc68* mutant alleles

A second method used to screen for synthetic lethal interactions involves the high-throughput mating of cells from a strain containing the mutation of interest, called the 'query' strain, to cells from a collection of approximately 4700 individual yeast gene-replacement strains (Winzeler *et al.* 1999; Tong *et al.* 2001). The systematic generation of double-mutant diploids is the initial step in Synthetic Genetic Array (SGA) analysis (Figure 55; Tong *et al.*, 2001). These diploids are sporulated and *MAT*a haploid progeny are selected for analysis using the 'magic-marker' gene *MFA1pr-HIS3*. This gene is a fusion of the Mating Factor A (*MFA1*) promoter with the *HIS3* coding sequence. *MFA1* is only expressed in *MAT*a haploid cells; therefore this fusion of the *MFA1* promoter with *HIS3* ensures that the His3 protein product is only generated in *MAT*a cells, and as a result only these haploid cells are histidine prototrophs. Using the 'magic marker' ensures that the haploids examined in the final stage of SGA analysis are the products of mating and sporulation, as 1) the initial *MAT*a haploid strain from the deletion collection does not contain the *MFA1pr-HIS3* gene, 2) the *MAT*α haploid 'query' strain containing the

MFA1pr-HIS3 magic marker does not express His3 protein product due to the repression of *MFA1* promoter in *MATα* cells, and 3) diploids do not transcribe from the *MFA1* promoter, so that no His3 protein product is generated in these cells. Thus both of the starting haploids and the diploid generated from that cross are unable to grow on medium lacking histidine, whereas certain haploid products of the cross can do so.

An additional selection against unsporulated diploids makes use of canavanine resistance. The *CAN1* gene encodes an arginine permease that, in addition to permitting the uptake of arginine from the environment, allows the uptake of canavanine, an arginine analog (Fantes 1984). Canavanine incorporation into polypeptide chains in the place of arginine leads to anomalies in protein structure due to a decreased nucleophilicity of the canavanine side chain in comparison to arginine and consequently decreased ionic bond strengths, which lead to a loss of cell viability (Bence and Crooks 2003). When the *CAN1* permease gene is deleted in yeast, canavanine is not taken into cells from the medium and therefore cells are canavanine resistant. The query strain is a *can1Δ* while haploids from the deletion collection are *CAN1*, and the resultant diploids from this cross are *CAN1/can1Δ*. Therefore haploids from the deletion collection, the diploids generated in the cross, and haploid progeny carrying the *CAN1* gene are inhibited by canavanine in the medium. The absence of histidine and the presence of canavanine in the medium after sporulation ensures that *MAT*a haploid progeny from the cross are able to grow (Tong *et al.* 2001).

The dominant drug-resistance markers employed in creating the gene replacements in the deletion strain collection (*kanMX4* cassette; Wach *et al.* 1994) and to tag or delete the gene of interest (*natMX4* cassette; Goldstein *et al.* 1999) are used to select for double-mutant progeny (Tong *et al.* 2001). In most instances double-mutant haploid segregants, containing the gene deletion from the collection and the mutation or deletion of the gene of interest, are able to form colonies and exhibit no growth impairment. However, double-mutant cells that form less robust colonies or no colonies at all are synthetically sick or inviable, respectively. This outcome indicates a shared essential function between the deleted gene in the array and the mutated gene of interest. To determine the complement of gene deletions that share a synthetic lethal relationship with mutations affecting various regions of *CDC68*, I have performed SGA analysis on *natMX4*-tagged

chromosomal integrations of *CDC68* (as a control), *cdc68-E763G*, *cdc68-E857K*, *cdc68-312*, *cdc68-319*, and *cdc68-ΔNTD*.

iii) SGA analysis of *CDC68::natMX4*

SGA analysis was performed with a derivative of the Y2454 'query' strain containing a *CDC68::natMX4* chromosomal integration. Cells from this strain were employed in SGA analysis as a control for subsequent SGA analyses using similarly tagged and integrated *cdc68* mutant alleles. Two SGA screens were carried out with *CDC68::natMX4* to assist in identifying gene-deletion strains that are false positives in SGA analysis in our lab. These screens identified 684 and 926 gene deletions with apparent genetic interactions with *CDC68::natMX4*. Since this allele is wild-type with the exception of the downstream *natMX4* integration, these candidate genetic interactions were either the result of: 1) gene deletions that generate a false positive in SGA analysis due to the fact that that may grow and/or mate poorly, generate diploids that sporulate at low efficiency, and/or generate haploid segregants that germinate poorly; 2) subtle variability in growth efficiency from one screen to the next as a result of technical differences (*i.e.* pin-strike errors, wet plate conditions, etc.) or growth-assessment variations; 3) a gene deletion with a tight physical association to the *CDC68* gene locus, resulting in fewer double-mutant haploid segregants due to the low probability of recombination in this small stretch of DNA; or 4) true synthetic lethality due to genomic perturbation caused by the position of the *natMX4* integration.

The Boone lab has compiled a list of 'standard' false-positive gene-deletion strains that are repeatedly identified in SGA screens (Tong *et al.* 2001). These false-positives are not the result of *bona fide* genetic interactions with the mutation harboured in the query strain, but are due to problems with the viability of cells from the deletion strain itself at some point during the SGA process. 502 out of the 684 and 638 out of the 926 of the gene-deletion candidates identified in each of my *CDC68::natMX4* screens have been previously identified as SGA false positives by the Boone lab (Tong *et al.*, 2001; data not shown). Of the remaining 182 and 288 candidates from each screen, 14 and 18 deletion strains, respectively, were identified as the linkage group for *CDC68::natMX4*. Comparisons of the remaining gene-deletion candidates exhibiting genetic interactions with *CDC68::natMX4* in each SGA screen revealed that 131 gene deletions were

identified in both (Table 16). The fact that these gene deletions were identified in both screens argues against a random technical problem as the cause. The gene-deletion candidates that are not false positives, not part of the *CDC68* linkage group, or not identified in both screens are most likely the result of variation in growth assessment or technical differences between the two SGA analyses. A large subset of the 131 gene deletions identified in both *CDC68::natMX4* screens were also identified in other SGA screens performed in the Singer/Johnston lab using cells from three other query strains each containing a different gene deletion, *ynl035cΔ::natMX4* (see below), *ypt6Δ::natMX4*, and *age1Δ::natMX4*. This finding argues against the insertion of the *natMX4* cassette at the *CDC68* locus as the causative agent for the synthetic lethal and sick interactions observed. Rather, this list of 131 gene deletions identifies additional false-positive strains for SGA analysis in our lab. The causes of these additional false positives are uncertain; they may be the result of slight variations in technique used during the SGA procedure or growth assessment of the colonies. Additionally, these 'extra' false-positive deletion strains may be identified due to technical issues with our deletion collection. In other words, our deletion collection may contain subtle genetic alterations due to the generations of growth that separate out collection from that initially analyzed in the Tong *et al.* (2001) publication. Consistent with this interpretation 158 deletion strains that were not present on the Boone-lab false-positive list exhibited poor growth or were completely absent from our collection (Table 16). 92 of the 158 gene deletion strains exhibiting poor growth in our deletion collection were also found as synthetic-lethal candidates in both of the *CDC68::natMX4* SGA screens. Thus, 92 of the 131 (70%) deletion strains identified as common hits for both *CDC68::natMX4* SGA screens exhibit poor growth or are completely absent from the deletion collection used in our lab. This further supports the idea that the gene deletions exhibiting genetic interactions with *CDC68::natMX4* in both screens are most likely false positives that show impaired growth in SGA analysis due to the gene deletion alone, and not from a synthetic genetic interaction with the *natMX4*-tagged wild-type *CDC68* gene.

Table 16. Additional SGA false-positive gene deletions

Gene name	Systematic name	Deletion array co-ordinates			SGA analysis with *CDC68::natMX4*	Deletion collection scoring
		Plate	Row	Column		
ABF2	YMR072W	14	11	2	X	X
ADH3	YMR083W	14	11	20	X	X
AEP2	YMR282C	6	12	10		X
AEP2	YMR282C	12	11	11	X	X
AGP2	YBR132C	8	11	15		X
ANP1	YEL036C	12	7	10	X	X
APL4	YPR029C	14	16	24		X
ARD1	YHR013C	13	15	8	X	X
ARO1	YDR127W	1	7	13	X	
ATP1	YBL099W	8	15	8	X	X
ATP10	YLR393W	5	13	18	X	X
ATP17	YDR377W	2	10	19	X	X
ATP17	YDR377W	12	7	18		X
ATP7	YKL016C	4	2	4		X
ATP7	YKL016C	12	13	18		X
BCS1	YDR375C	12	7	20	X	X
BCS1	YDR375C	2	10	17		X
BUD25	YER014C-A	2	7	24	X	X
BUD25	YER014C-A	13	5	7	X	X
CBP1	YJL209W	13	13	16	X	X
CBP1	YJL209W	12	11	4		X
CBP2	YHL038C	3	15	4	X	X
CBP2	YHL038C	12	11	14	X	X
CBP3	YPL215W	7	15	4	X	X
CBP6	YBR120C	8	13	23	X	X
CBS1	YDL069C	9	16	22	X	X
CDH1	YGL003C	2	11	5	X	
CEM1	YER061C	2	15	3	X	
COQ1	YBR003W	8	13	2	X	X
COQ2	YNR041C	10	5	12		X
COQ3	YOL096C	14	2	3	X	X
COX10	YPL172C	12	7	15		X
COX10	YPL172C	7	9	4		X
COX11	YPL132W	14	4	10	X	X

COX12	YLR038C	14	14	11		X
COX15	YER141W	11	6	20	X	X
COX17	YLL009C	12	13	6		X
COX18	YGR062C	3	4	24	X	X
COX18	YGR062C	12	9	12	X	X
COX18	YGR062C	13	1	3	X	X
COX18	YGR062C	13	1	1	X	X
COX19	YLL018C-A	15	15	24	X	X
COX19	YLL018C-A	16	10	20	X	X
COX9	YDL067C	16	7	3	X	X
CTK2	YJL006C	11	3	20	X	
CVT9	YPR049C	16	4	20	X	
CYT1	YOR065W	6	7	2	X	X
CYT1	YOR065W	12	9	11	X	X
DAL81	YIR023W	14	7	13	X	
DEG2	YFL001W	15	16	4		X
ELP2	YGR200C	3	4	9		X
EMP24	YGL200C	2	1	15		X
END3	YNL084C	10	2	7	X	X
EUG1	YDR518W	9	2	14	X	X
EXO1	YOR033C	6	11	2		X
FOB1	YDR110W	1	9	7		X
FUI1	YBL042C	13	15	19		X
FUM1	YPL262C	7	6	9		X
GCV3	YAL044C	1	14	8	X	
GIN4	YDR507C	9	4	20	X	X
GLO3	YER122C	11	8	18	X	X
GPD1	YDL022W	8	5	23	X	X
GPM2	YDL021W	8	5	21	X	X
GTR2	YGR163W	3	8	3	X	
HAP3	YBL021C	13	15	15		X
HAP5	YOR358W	7	8	22		X
HPC2	YBR215W	1	4	17		X
HOP2	YGL033W	2	7	5	X	
IFM1	YOL023W	7	16	1	X	X
IFM1	YOL023W	13	8	1	X	X
IFM1	YOL023W	13	8	3	X	X
KAP123	YER110C	11	10	18	X	X
KNH1	YDL049C	8	1	15	X	X

KRE1	YNL322C	6	6	16	X	X
LCB5	YLR260W	5	14	7	X	X
LCB5	YLR260W	12	15	23	X	X
LIP2	YLR239C	13	5	16	X	
LST4	YKL176C	4	15	22	X	
LST7	YGR057C	3	4	18	X	
MAC1	YMR021C	5	1	12		X
MCT1	YOR221C	6	5	9	X	
MEC3	YLR288C	5	10	5	X	X
MEC3	YLR288C	12	13	3	X	X
MRS1	YIR021W	11	16	14	X	X
MSS2	YDL107W	9	3	11	X	X
MSS51	YLR203C	5	6	20	X	X
MSS51	YLR203C	12	15	19	X	X
OAR1	YKL055C	4	14	5	X	
PDR17	YNL264C	10	8	15	X	
PDR18	YNR070W	14	13	18	X	X
PET111	YMR257C	6	16	22	X	X
PET111	YMR257C	12	11	7	X	X
PET122	YER153C	11	4	12		X
PET54	YGR222W	8	6	5	X	X
PET54	YGR222W	12	3	7		X
PET8	YNL003C	10	15	4		X
PEX15	YOL044W	7	14	11	X	
PFD1	YJL179W	4	10	2	X	
PGD1	YGL025C	2	9	17	X	X
PHM8	YER037W	14	13	9	X	
PKH2	YOL100W	14	2	9	X	X
POM152	YMR129W	14	14	16		X
PRS4	YBL068W	1	12	3		X
QCR7	YDR529C	9	16	3	X	X
QCR8	YJL166W	4	10	18	X	X
QCR8	YJL166W	12	13	24	X	X
QRI7	YDL104C	9	3	7	X	X
RAD18	YCR066W	12	15	10	X	
RAD54	YGL163C	9	15	10	X	
RIC1	YLR039C	14	14	13		X
RIM1	YCR028C-A	12	2	16	X	X
RIM21	YNL294C	10	12	19	X	

RLR1	YNL139C	10	6	19		
RPH1	YER169W	11	2	10	X	X
RPL20B	YOR312C	10	1	14	X	
RPL20B	YOR312C	7	12	4		
RPL31A	YDL075W	16	7	7	X	
RPS12	YOR369C	7	6	12	X	
RRP6	YOR001W	6	2	13	X	
RRP8	YDR083W	1	13	11		X
RSM24	YDR175C	12	3	4	X	X
RSM24	YDR175C	1	1	15	X	X
RVS161	YCR009C	1	3	14	X	
SAG1	YJR004C	11	15	1	X	X
SAG1	YJR004C	14	11	11		X
SAS2	YMR127C	14	14	14		X
SCO1	YBR037C	8	9	14	X	X
SCP160	YJL080C	15	13	15	X	
SDH2	YLL041C	13	7	6		X
SHY1	YGR112W	3	14	7		X
SHY1	YGR112W	12	9	4		X
SNF1	YDR477W	16	7	9		X
SPE1	YKL184W	4	13	8	X	
SPS1	YDR523C	16	7	15	X	X
SSA4	YER103W	11	10	10	X	X
SSN3	YPL042C	7	9	15	X	
SSZ1	YHR064C	14	10	21	X	
STV1	YMR054W	14	15	21		X
TAF14	YPL129W	7	5	16	X	X
TDH1	YJL052W	15	1	8		X
UFO1	YML088W	9	7	4		X
VIP1	YLR410W	5	11	20	X	
VPS27	YNR006W	10	9	6	X	
VPS41	YDR080W	1	13	9	X	X
YBT1	YLL048C	14	12	15		X
YCL074W	YCL074W	14	13	15		X
YDL009C	YDL009C	8	5	5	X	X
YDL032W	YDL032W	8	3	11	X	X
YDL057W	YDL057W	9	16	6	X	X
YDL062W	YDL062W	9	16	12		X
YDL063C	YDL063C	9	16	14	X	X

YDL068W	YDL068W	9	16	20	X	X
YDL073W	YDL073W	9	14	4	X	X
YDR128W	YDR128W	1	7	15	X	
YDR230W	YDR230W	2	12	24	X	X
YDR230W	YDR230W	12	5	20	X	X
YDR230W	YDR230W	13	9	11	X	X
YDR332W	YDR332W	2	14	5		X
YDR357C	YDR357C	2	12	17		X
YDR521W	YDR521W	16	7	13		X
YER083C	YER083C	2	13	15		X
YGL220W	YGL220W	3	16	18		X
YGL220W	YGL220W	12	9	16		X
YGL024W	YGL024W	2	9	15	X	
YGR228W	YGR228W	8	6	17		X
YIM2	YMR151W	5	13	19	X	X
YJL003W	YJL003W	11	3	16	X	X
YJR056C	YJR056C	11	11	23	X	
YKE2	YLR200W	5	6	14	X	
YKL162C-A	YKL162C-A	14	5	15		X
YKR074W	YKR074W	14	7	18		X
YLL044W	YLL044W	14	12	13		X
YLR040C	YLR040C	14	14	15		X
YLR050C	YLR050C	14	14	19		X
YLR114C	YLR114C	12	15	9	X	X
YLR201C	YLR201C	5	6	16	X	X
YLR201C	YLR201C	12	15	15	X	X
YLR202C	YLR202C	5	6	18	X	X
YLR202C	YLR202C	12	15	17	X	X
YLR218C	YLR218C	5	4	20		X
YLR270W	YLR270W	5	12	3	X	X
YLR270W	YLR270W	12	13	1	X	X
YML090W	YML090W	14	4	20		X
YML095C-A	YML095C-A	14	6	2	X	
YMR071C	YMR071C	14	9	24	X	X
YMR084W	YMR084W	14	11	22	X	X
YMR114C	YMR114C	14	12	16		X
YMR132C	YMR132C	14	14	20		X
YNL081C	YNL081C	10	2	9	X	X

YNL170W	YNL170W	6	4	3		X
YNL170W	YNL170W	12	9	5		X
YNR071C	YNR071C	14	13	20		X
YOR199W	YOR199W	6	7	5	X	X
YOR199W	YOR199W	12	9	15	X	X
YOR305W	YOR305W	7	14	20	X	X
YOR305W	YOR305W	12	7	3	X	X
YPL030W	YPL030W	7	7	11		X
YTA12	YMR089C	14	13	10	X	X

Deletion of a gene with an 'X' in the 'SGA analysis with *CDC68::natMX4'* column resulted in a synthetic growth defect in combination with *CDC68::natMX4*, a wild-type allele except for the *natMX4* insertion downstream of the *CDC68* coding sequence (Materials and Methods). Further analysis showns that cells from the majority of these deletion stains exhibit poor growth or are absent from the deletion collection used in SGA analysis. A deletion strain that exhibited impaired growth or was completely absent from the yeast gene deletion collection (Winzeler *et al.* 1999) utilized in the Singer/Johnston lab is indicated by an 'X' in the 'deletion collection scoring' column, and have been designated as SGA false-positive in our collection.

Of the remaining 39 deletion strains identified in both of the SGA screens for *CDC68::natMX4*, 32 were found to have growth defects when the only dominant drug-resistance marker for the deletion mutation from the collection is selected. Thus the growth impairment identified at the end of SGA analysis is most likely a function of some aspect of the gene deletion from the collection and not a feature of a synthetic genetic interaction between this gene deletion and *CDC68::natMX4*. These strains have been classified in our lab as SGA false-positive gene deletions additional to those identified in the Boone lab.

In summary, the two SGA screens using the *CDC68::natMX4* query strain provided useful information about the screening procedure. These control screens initially identified a large number of candidate synthetic genetic interactions, but this number could be pared down by eliminating synthetic-lethal candidates containing a gene deletion that: 1) had been previously identified as a false positive in SGA analysis by the Boone lab (Tong *et al.* 2001); 2) exhibit a chromosomal location close to the *CDC68* gene locus and is therefore a member of the *CDC68* linkage group; 3) failed to grow robustly or was not represented at all in the deletion strain collection employed by our lab during this analysis; or 4) failed to grow robustly in SGA procedures even in the absence of the *CDC68::natMX4* marker. From SGA analysis with *CDC68::natMX4*, coupled with examination of growth of cells from the deletion collection strains, an additional list of SGA false-positive deletion strains was compiled, and these strains were not examined when they were repeatedly identified in other SGA screens. Additionally, the *CDC68::natMX4* SGA screens identified 51 and 157 candidates that were *not* common to both screens, did not fall into the linkage group, and were not identified as Boone-lab false-positives. This failure to reproduce the genetic interactions may be the result of subtle growth differences between the replicate experiments due to technical differences (*i.e.* pin-strike errors, wet plates, alterations in growth assessments, etc.). At any rate, this set of non-overlapping deletion strains as SGA candidates with *CDC68::natMX4* illustrates the degree of variability between SGA screens and highlights the importance of replicate screens to narrow down the list of synthetic-lethal gene-deletion candidates studied in subsequent screens.

iv) SGA analysis using *cdc68-E857K::natMX4*

Two SGA screens using cells from a Y2454-derivative in which the *cdc68-E857K* allele had been chromosomally integrated (to replace the *CDC68* allele) and tagged downstream of the stop codon with the *natMX4* cassette (Materials and Methods) identified 992 and 939 candidate genetic interactions initially (Table 17). Gene deletions known to exhibit poor growth upon SGA analysis in the absence of any other secondary mutation were eliminated from these lists, as were genes from the *cdc68-E857K* linkage group, leaving 394 and 242 candidates, respectively (Table 17). Of these, 80 candidates were common to both screens (Appendix 1; Table 17). Each gene deletion was tested further to verify the genetic interaction with *cdc68-E857K* by comparing the number of singly mutated haploid segregants to the number of doubly mutated haploid segregants obtained using random-spore methodology. If no double-mutant segregants were produced while both single-mutant segregants were generated, then the gene deletion was considered to be synthetically lethal with *cdc68-E857K*. If the number of double-mutant segregants was significantly decreased (less than half the expected number of colonies) in comparison to the number of single-mutant segregants, then the gene deletion was considered to be synthetically sick with *cdc68-E857K*. A total of 22 gene deletions were found to cause synthetic lethality or sickness in combination with the *cdc68-E857K* mutation (Table 18; Appendix 1). These synthetic interactions, as well as any known interactions between genes within this data set, are diagrammed in Figure 46. The genes identified affect a spectrum of functions, including transcription, DNA repair and recombination, and membrane transport. Genes are clustered based on the gene ontology (GO) assignments generated using Osprey software and the Yeast GRID database current as of May, 2004. In many cases more than one GO annotation is associated with a gene, and a complete list of GO terms for each gene is given in Table 18.

a) *cdc68-E857K* SGA interactions with genes involved in transcription

Two of the gene deletions, *HIR2* and *HIR3* (histone regulatory), identified in this analysis as synthetically lethal with *cdc68-E857K* have also been shown by a classical synthetic-lethal approach (J. R. Stevens, unpublished data) to cause synthetic lethality in combination with *cdc68-E857K* when mutated (Results 4, i). Similarly, mutations in the *HIR* family of genes (*HIR1*, *HIR2*, *HIR3*, and *HPC2*), which function to regulate histone

Table 17. Number of synthetic-lethal or -sick genetic interactions identified with each *cdc68* allele.

Query-strain allele (tagged with *natMX4*)	SGA interactions in initial screens	SGA interactions after false-positive and linkage-group removal	Interactions identified in multiple SGA screens and tested by random-spore analysis	Interactions verified by random-spore analysis
cdc68-E763G	1039, 1031	346, 328	161	90
cdc68-E857G	992, 939	394, 242	80	22
cdc68-312	1119, 928	398, 400	175	83
cdc68-319	1852, 1170	1025, 1054	392	78
cdc68-ΔNTD	1613*, 1656*, 2394	992*, 968*, 1659	321	96

SGA analysis was performed in duplicate or triplicate (for *cdc68-ΔNTD*) using cells from query-strain derivatives containing the indicated *natMX4*-tagged *cdc68* allele. In each instance, the total number of gene-deletion strains that displayed a synthetic growth defect in combination with the *cdc68* allele is given (second column) as well as the number of strains that displayed a genetic interaction after the SGA false-positive gene-deletion strains were removed (third column). The gene deletions exhibiting synthetic genetic interactions in all SGA screens for a particular allele (fourth column) were then identified and tested using the random-spore method (Materials and Methods). The number of gene deletions that generated a verified synthetic-lethal or synthetic-sick interaction as indicated by random-spore analysis is given in the fifth column. Further information on the results of random-spore analysis is in Appendix 1.

* - for these two SGA screens the datasets were incomplete due to technical problems. As a result, the number of gene-deletion candidates in these two screens is decreased. By using the data from all three screens, however, a minimum of a duplicate SGA dataset was obtained for 94% of the yeast deletion strains. To be considered for verification by random-spore analysis, a deletion candidate needed to be identified in all possible SGA screens. In the 6% of instances where only a single datapoint was available, some were tested by random-spore analysis.

Table 18. Gene deletions that are synthetically sick or lethal in combination with *cdc68-E857K*

Transcription:

Gene Name	Systematic Name	Description	Gene Ontology
CDC73	YLR418C	accessory factor associated with RNA polymerase II by affinity chromatography	transcription; metabolism
HIR3	YJR140C	Transcriptional corepressor involved in the cell cycle-regulated transcription of histone genes HTA1, HTB1, HHT1, and HHT2; involved in position-dependent gene silencing and nucleosome reassembly	cell cycle; transcription; cell growth and/or maintenance; metabolism
HIR2	YOR038C	Non-essential transcriptional corepressor involved in the cell cycle-regulated transcription of histone H2A, H2B, H3, and H4 genes; recruits Swi-Snf complexes to histone gene promoters; promotes heterochromatic gene silencing with Asf1p	transcription; metabolism
LEO1	YOR123C	member of the RNA polymerase II-associated Paf1 complex	transcription; metabolism

Transport:

Gene Name	Systematic Name	Description	Gene Ontology
LYS7	YMR038C	Involved in lysine biosynthesis, oxidative stress protection	transport; cell growth and/or maintenance
VPS4	YPR173C	Defective in vacuolar protein sorting; homologous to mouse SKD1 and to human hVPS4	transport; protein transport; metabolism; cell growth and/or maintenance; cell organization and biogenesis
VPS8	YAL002W	involved in vacuolar protein sorting; required for localization and trafficking of the CPY sorting receptor	transport; cell growth and/or maintenance; cell organization and biogenesis
VPS21	YOR089C	Rab5-like GTPase involved in vacuolar protein sorting and endocytosis post vesicle internalization; geranylgeranylated; geranylgeranylation required for membrane association	transport;cell growth and/or maintenance; protein transport; metabolism

Cell growth and maintenance:

Gene Name	Systematic Name	Description	Gene Ontology
ALF1	YNL148C	alpha-tubulin foldin; protein implicated in folding of alpha tubulin	cell organization and biogenesis; cell growth and/or maintenance
YKL160W (ELF1)	YKL160W	NONE	cell growth and/or maintenance
SWA2	YDR320C	auxilin-like protein	cell organization and biogenesis; cell growth and/or maintenance

Protein biosynthesis:

Gene Name	Systematic Name	Description	Gene Ontology
MNN11	YJL183W	member of a cis Golgi complex that is involved in mannan synthesis, other complex members include Mnn10p, Hoc1p, Anp1p, Mnn9p	protein biosynthesis; metabolism
RPS23B	YPR132W	Ribosomal protein 28 rp28 of the small 40S ribosomal subunit, required for translational accuracy; nearly identical to Rps23Ap and similar to E. coli S12 and rat S23 ribosomal proteins; deletion of both RPS23A and RPS23B is lethal	protein biosynthesis; metabolism

Metabolism:

Gene Name	Systematic Name	Description	Gene Ontology
ERG2	YMR202W	C-8 sterol isomerase, catalyzes the isomerization of the delta-8 double bond to the delta-7 position at an intermediate step in ergosterol biosynthesis	metabolism
SER2	YGR208W	phosphoserine phosphatase	metabolism

DNA metabolism:

Gene Name	Systematic Name	Description	Gene Ontology
HHT1	YBR010W	One of two identical histone H3 proteins see also HHT2 ; core histone required for chromatin assembly, involved in heterochromatin-mediated telomeric and HM silencing; regulated by acetylation, methylation, and mitotic phosphorylation	DNA metabolism; cell organization and biogenesis; metabolism; cell growth and/or maintenance

MRE11	YMR224C	Disp. for premeiotic DNA synthesis, but required for both double strand break formation & resection, synaptonemal complexes, meiotic recombination & viable spores. Localizes to discrete sites in rad50 mutants	DNA repair; DNA metabolism; response to DNA damage stimulus; response to stress; metabolism; DNA recombination; cell cycle;cell growth and/or maintenance
RTT106	YNL206C	Regulator of Ty1 Transposition - same phenotype as RTT101 - RTT105, disruption causes increase in Ty1 transposition. Isolated from the same screen as the other named RTT genes.	DNA recombination; DNA metabolism; metabolism
SGS1	YMR190C	Involved in maintaining genome stability. Homologous to E. coli RecQ and human BLM and WRN proteins that are defective in the cancer-prone disorder Bloom s syndrome and the premature aging disorder Werner s syndrome, respectively	cell cycle; cell growth and/or maintenance; DNA replication; DNA metabolism; metabolism; cell organization and biogenesis

DNA Damage response:

Gene Name	Systematic Name	Description	Gene Ontology
ASF1	YJL115W	anti-silencing protein that causes depression of silent loci when overexpressed	response to DNA damage stimulus; response to stress

Protein Degradation:

Gene Name	Systematic Name	Description	Gene Ontology
RPN4	YDL020C	Involved in ubiquitin degradation pathway. May act as common transcription factor on proteasomal and proteasome-related genes.	protein catabolism; metabolism

Unknown:

Gene Name	Systematic Name	Description	Gene Ontology
NCE4	YPL024W	Negative regulator of Cts1 Expression	biological process unknown

gene expression (Xu *et al.* 1992) and histone deposition onto DNA to form nucleosomes (Sharp *et al.* 2001, 2002), have been identified as synthetically lethal with *spt16-11*, an allele of *CDC68/SPT16* with mutations that flank that of *cdc68-E857K* and generate amino acid substitutions at codons 821 and 859 (Formosa *et al.* 2002). FACT has been shown to bind nucleosomes (Orphanides *et al.* 1999) and is involved in nucleosomal rearrangements during the process of transcription to help facilitate RNA polymerase II passage (Orphanides *et al.* 1999; Belotserkovskaya *et al.* 2003; Kaplan *et al.* 2003; Saunders *et al.* 2003). The observations that FACT is important for nucleosome disassembly in front of the elongating RNA polymerase enzyme (Orphanides *et al.* 1998, 1999) and reassembly of the chromatin structure in the wake its passage (Kaplan *et al.* 2003) are consistent with a role for FACT in histone deposition. Thus this overlapping function between the *HIR* family of genes and *CDC68*, as indicated by genetic interactions with *cdc68-E857K*, is consistent with the roles previously assigned to the respective protein products.

The *HIR* family members *HIR1* and *HPC2* were not identified as synthetically lethal with *cdc68-E857K* in this analysis. However, cells containing *hpc2Δ* are false positive in the SGA analysis and would therefore not have been included in initial analyses. The *hir1Δ* deletion was identified as synthetically sick in only one of the two SGA screens with *cdc68-E857K*. Once the nucleosome-deposition function was highlighted by other SGA results, random-spore methodology was used to test directly for synthetic growth defects arising from the combination of *cdc68-E857K* with *hpc2Δ* and *hir1Δ*. These results indicated that deletion of each of these two *HIR* genes does not confer any further growth impairment on cells when combined with the *cdc68-E857K* mutation. These findings are in contrast to those reported by Formosa *et al.* (2002) for the *spt16-11* allele in combination with *hpc2Δ* or *hir1Δ*. However, the effects of *hpc2Δ* and *hir1Δ* in combination with the *cdc68* mutations examined (Formosa *et al.* 2002) were allele-specific; therefore, *cdc68-E857K* and *spt16-11* need not behave in an identical fashion. Additionally, the severities of the growth defects for cells containing *hir* mutations with *cdc68* alleles could be altered by integration of the *cdc68* allele into the chromosomal locus instead of having it plasmid-borne as shown in the experiments performed by Formosa *et al.* (2002). The differences between the genetic interactions for *spt16-11* and

cdc68-E857K may therefore be the result of differences in the context of the allele, as the *spt16-11* allele was plasmid-borne while *cdc68-E857K* is chromosomally integrated. The involvement of Cdc68 in histone deposition is intriguing and warrants future investigation.

Deletions or mutations of *HIR* genes cause synthetic lethality when other genes whose products have roles in histone deposition, like Asf1 and components of chromatin assembly factor 1 (CAF-1) are mutated (Kaufman *et al.* 1998; Sharp *et al.* 2001; Krawitz *et al.* 2002). This situation suggests that these factors share an overlapping essential function. An analogous functional relationship is observed for *cdc68-E857K asf1Δ* cells (Table 18), but not when deletions of CAF-1 genes are combined with *cdc68-E857K*. These findings for Asf1 and CAF-1 are consistent with those reported by Formosa *et al.* (2002), who tested directly for genetic interactions between *cac1Δ* and *cac2Δ*, which encode two subunits of CAF-1, and *spt16-11* mutation as well as between *cac1Δ* and several mutant alleles of *pob3*, and saw no effects on cell growth. When the *cac1Δ*, *cac2Δ* or *cac3Δ* deletions were tested here for a synthetic growth defects in combination with *cdc68-E857K* using both SGA and random-spore analysis, no growth impairments were identified, indicating that Cdc68 and the components of CAF-1 do not share an overlapping essential function. Formosa *et al.* (2002) also showed that *spt16-11* cells are significantly more temperature sensitive when deleted for *ASF1*, and my random-spore results confirmed the SGA finding that *asf1Δ* is synthetically sick in combination with *cdc68-E857K*. Alterations in the temperature sensitivity of cells containing *spt16-11* and *asf1Δ* as well as the synthetic growth defect identified here for *cdc68-E857K asf1Δ* cells indicate that Cdc68 and Asf1 share an overlapping function, potentially related to nucleosome deposition. To date, no similar genetic interactions have been reported between *cdc68* mutations and genes encoding CAF-1 components. These observations taken together could imply that FACT-mediated nucleosome assembly operates independently of, or may be directly involved in, CAF-1-mediated histone deposition, while the Hir proteins and Asf1 function in parallel pathways to promote nucleosome assembly.

In addition to the genetic interactions observed between *HIR* genes and *cdc68-E857K*, SGA analysis showed that deletions eliminating the Paf-complex components Cdc73 and

Leo1 are synthetically lethal in combination with *cdc68-E857K*. The Paf (RNA polymerase associated factor) complex, consisting of Paf1, Cdc73, Ctr9, Rtf1, and Leo1 (Krogan *et al.* 2002; Mueller and Jaehning 2002; Squazzo *et al.* 2002), physically associates with RNA polymerase II and is involved in transcription initiation and elongation (Shi *et al.* 1996, 1997; Wade *et al.* 1996; Costa and Arndt 2000; Pokholok *et al.* 2002; Squazzo *et al.* 2002; Rondon *et al.* 2004). Genetic and physical interactions between Paf-complex members and FACT components have been previously reported (Costa and Arndt 2000; Krogan *et al.* 2002; Squazzo *et al.* 2002). Affinity purifications have shown that FACT and Paf physically associate in a larger complex (Krogan *et al.* 2002; Squazzo *et al.* 2002). Synthetic lethal interactions have been previously characterized for *paf1Δ spt16-197* (an allele of *CDC68/SPT16* with a point mutation that results in a substitution of glutamate for glycine at residue 132, resulting in an unstable protein product (Winston *et al.* 1984; Malone *et al.* 1991; Xu 1995) and *ctr9Δ spt16-197*, while no synthetic growth defects were observed for cells containing deletions of *rtf1* or *leo1* in combination with *spt16-197* (Costa and Arndt 2000; Squazzo *et al.* 2002). However, a mutant allele of *POB3* was shown to be synthetically lethal in combination with *rtf1Δ* (Costa and Arndt 2000), indicating some overlap between FACT and Rtf1 function.

Despite the number of physical and genetic associations identified to date between FACT and Paf, no genetic interaction has previously been reported between *CDC68* and *CDC73* or *LEO1*. The identification of these two components of Paf as synthetically lethal in combination with *cdc68-E857K* raises questions as to the synthetic effects of this allele in combination with other Paf components. The *paf1Δ* mutation in the yeast deletion collection has been reported as a false positive during SGA analysis (Tong *et al.* 2001), but no significant growth defect was observed for *paf1Δ cdc68-E857K* double-mutant cells in the two SGA screens reported here. A *ctr9* deletion is not present in our current deletion collection; therefore, genetic interactions between *cdc68-E857K* and this component of Paf have not been assessed here. The *RTF1* gene (systematic name *YGL244W*) is located only 55 kbp from the *CDC68* gene (systematic name *YGL207W*) on chromosome VII. This proximity raises the possibility that *rtf1Δ*, even if identified as a synthetic-lethal candidate, may yield a decreased number of double-mutant haploid

segregants generated with *cdc68* alleles due to the linkage of these two genes. However, *rtf1Δ* was not identified in the linkage group for *cdc68-E857K::natMX4* and has not been found as a positive in SGA analysis performed with *CDC68::natMX4*, and therefore probably resides far enough from the *CDC68* locus to allow sufficient double-mutant haploid progeny production during SGA analysis to avoid this pitfall (Results 4, vii below). Taken together, the results of the *cdc68-E857K* SGA analysis indicate that this allele of *CDC68* is only synthetically lethal in combination with deletions of the *CDC73* and *LEO1* components of Paf, while *paf1* and *rtf1* deletions do not result in growth deficits in combination with *cdc68-E857K*. The combined effect of *cdc68-E857K* and *ctf9Δ* remains to be tested. However, the fact that SGA analysis has been estimated to miss between 17 and 41% of genetic interactions ('false negatives') makes interpretation of a negative result from this method difficult without additional investigation (Tong *et al.* 2001, 2004). Given the Paf complex's role in RNA polymerase II transcription and the plethora of previously characterized physical and genetic interactions between FACT and Paf components, it is not surprising to identify additional genetic interactions between these two complexes using SGA. This finding lends support to the validity of this approach for identifying synthetic genetic interacting partners with *cdc68* alleles.

SGA analysis has been performed with *cdc73Δ* cells and 113 deletions with synthetic effects were identified (Tong *et al.* 2004). A subset of these genes was also identified here to have synthetic interactions in SGA analysis with *cdc68-E857K*, namely *HIR2*, *HIR3*, *LEO1*, *LYS7*, *VPS21*, *VPS8*, and *ELF1*, implying that these genes share an overlapping function with both *CDC68* and *CDC73* (Figure 58). The connectivity of the *HIR* genes, *CDC68* and *CDC73* is interesting, as it provides further support for the coupling of transcription elongation and nucleosome displacement/deposition. *LYS7*, a gene whose protein product has been shown to be involved in copper ion homeostasis and lysine biosynthesis (Bhattacharjee *et al.* 1968; Horecka *et al.* 1995), does not obviously fit the picture for a functional association with *CDC68* and *CDC73*. However, SGA analysis has identified *lys7Δ* as synthetically lethal in combination with several factors involved in DNA repair, replication and sister chromatid cohesion, so it would appear that an alternative function for Lys7 is highlighted by these genetic interactions (Huang *et al.* 2003; Tong *et al.* 2004). *VPS21* and *VPS8* (vacuolar protein sorting) both encode

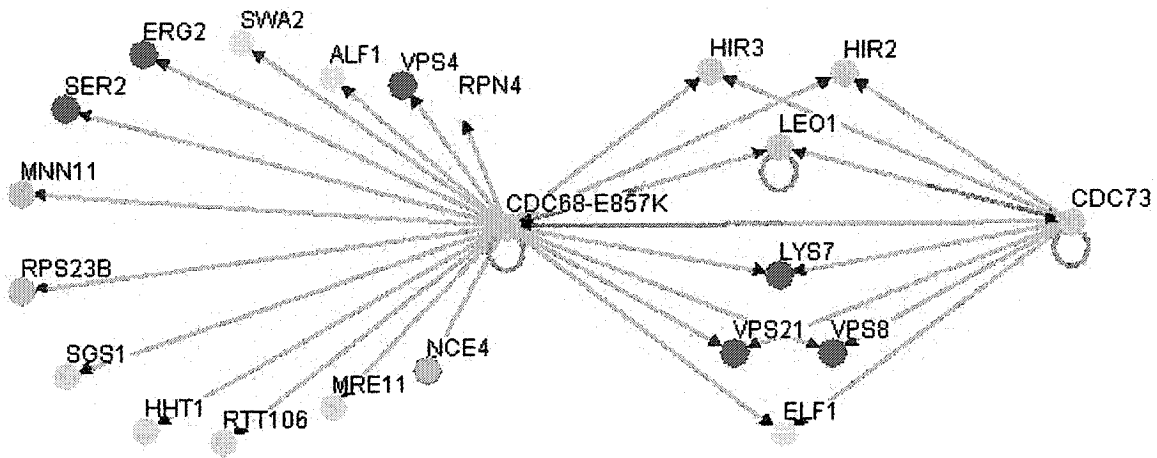

Figure 58. Synthetic genetic interactions web with *cdc68-E857K*. Each gene deletion identified by SGA and verified by random-spore analysis as synthetically sick or lethal in combination with *cdc68-E857K* is indicated here by a coloured node. Node colours are associated with gene ontology annotations and line colours show the type of interaction identified between two genes, as indicated in Appendix 2. The connectivity of the gene deletions on the right side of this figure highlights the overlap between the functional interactions of *cdc68-E857K* and *cdc73Δ* mutations.

proteins affecting transport between the Golgi and endosomal compartments and have been shown to be functionally linked (Chen and Stevens 1996; Horazdovsky *et al.* 1996; Gerrard *et al.* 2000). Once again, the significance of genetic interactions of these two particular genes with *cdc68* and *cdc73* is unclear. However, 21 gene deletions encoding proteins involved in transport have been identified as synthetically lethal with *cdc73Δ*, and other mutant alleles of *cdc68* examined here (Results 4, v and vi below) display a wealth of synthetic lethal interactions with genes involved in transport. Whether these effects are direct remains to be determined. One possible explanation is that mutations in *cdc68* or deletion of *cdc73* impede the transcription of genes required for transport, and as a result further impairment of transport pathways, by loss of genes encoding transport proteins, is lethal. There is no published information pertaining to the *ELF1* gene and its function, other than the reported synthetic lethal interaction with *cdc73Δ* (Tong *et al.* 2004); however the fact that the *ELF1* name is reserved in the *Saccharomyces* Genome Database implies that investigations of this gene are currently underway even though no information has yet been published.

b) *cdc68-E857K* SGA interactions with genes involved in DNA metabolism

In addition to those genes identified as having a synthetic genetic interaction with both *cdc73Δ* and *cdc68-E857K*, an interesting set of genes involved in DNA metabolism, *HHT1*, *MRE11*, *RTT106*, and *SGS1*, was identified as synthetically sick/lethal with *cdc68-E857K* when each gene is deleted.

HHT1 is one of two nearly identical genes encoding histone H3. Deletions of other histone genes, including *HHF1*, which encodes histone H4, and *HTZ1*, which encodes a variant of histone H2A, were identified as synthetically lethal with other *cdc68* alleles (Results 4, vii and viii below). Synthetic lethality between FACT mutations and histone gene deletions is not unprecedented (Formosa *et al.* 2002). Given the role FACT is thought to play as a nucleosome chaperone during RNA polymerase II transcription (Orphanides *et al.* 1999; Formosa *et al.* 2002; Belotserkovskaya *et al.* 2003; Kaplan *et al.* 2003) and FACT involvement in DNA replication (Okuhara *et al.* 1999; Schlesinger and Formosa 2000), where it is hypothesized to play a similar role, disturbances in histone gene dosage that result in synthetic defects are not surprising, as other genes encoding histone chaperone proteins, such as the Hirs also show synthetic genetic relationships

with histone gene mutations (Kaufman *et al.* 1998). Growth defects have been described for cells containing deletions of the genes encoding the H3 and H4 histone proteins with the *spt16-11* mutant allele, and deletion of H2A or H2B genes in *pob3-7* mutant cells also results in growth impairments (Formosa *et al.* 2002). The stoichiometry of H2A/H2B and H3/H4 histone dimers is crucial, and mutations that perturb this balance result in alterations to transcription, silencing defects and chromosome loss (Meeks-Wagner and Hartwell 1986; Clark-Adams *et al.* 1988; Han and Grunstein 1988; Osley 1991; Kaufman *et al.* 1998). The balance of H2A/H2B and H3/H4 dimers also impinges upon FACT function, with alterations resulting in increased levels of H2A/H2B dimer with respect to H3/H4 dimer causing growth deficits for cells containing the *spt16-11* mutant allele (Formosa *et al.* 2002). This finding is mirrored by the synthetic sickness observed here with *cdc68-E857K* and deletion of the *HHT1* gene encoding H3 protein: deletion of *HHT1* may result in decreased H3 protein levels, which in turn would decrease the H3/H4 dimer abundance, decreasing the ratio of H3/H4 to H2A/H2B. Similar sickness was observed for *cdc68-E857K hhf1Δ* double-mutant cells using SGA analysis (Appendix 1); however, this synthetic sickness has not been clearly established by random-spore analysis and is an avenue that merits further investigation. Additionally, deletions of *HHT2* or *HHF2*, which also encode histones H3 and H4, respectively, were not identified in both SGA screens as causing synthetic growth defects in combination with *cdc68-E857K*. The *HHT1-HHF1* and *HHT2-HHF2* gene pairs are divergently transcribed from different loci (Smith and Murray 1983) and the *HHT1* and *HHF1* or *HHT2* and *HHF2* genes are regulated in much the same fashion (Cross and Smith 1988). The synthetic sickness/lethality observed here with *hht1Δ* and *hhf1Δ* in combination with *cdc68-E857K*, but not with *hht2Δ* or *hhf2Δ* with *cdc68-E857K*, may due to differences in the regulation of gene expression for these two gene pairs (Cross and Smith 1988; van der Meijden *et al.* 1998). However, this hypothesis remains to be tested, and genetic interactions between deletions of *HHT2* or *HHF2* and *cdc68-E857K* should be explored further.

Failure to identify the genes encoding histones H2A and H2B as synthetically sick/lethal when deleted in combination with *cdc68-E857K* using SGA analysis is consistent with the findings reported by Formosa *et al.* (2002), who show that while

spt16-11 is synthetically sick when the level of histones H3 and H4 is decreased, a decrease in the levels of histone H2A and H2B actually improves cell growth under certain conditions. This type of genetic interaction would not be identified by the SGA analysis performed here, and may explain why deletions of the genes encoding H2A and H2B are not synthetically lethal with *cdc68-E857K*.

Each of the remaining three genes involved in DNA metabolism whose deletions are synthetically lethal with *cdc68-E857K* was also identified in a screen for genes that, when mutated, permit increased mobility of Ty1 elements in the yeast genome (Scholes *et al.* 2001). Mre11 and Sgs1 had been previously characterized, but Rtt106 (regulation of Ty1 transposition) was a previously uncharacterized open reading frame. Ty1 elements are retrotransposons (Boeke *et al.* 1985) that, while readily transcribed, do not typically mobilize or spread to alternative sites within the yeast genome due to inhibition by host factors (Roth 2000). For a Ty1 element to insert into alternative sites within the genome it must be transcribed, and then, by the actions of a reverse transcriptase encoded within the transposon element itself, this transcript is converted into a cDNA intermediate which may be integrated at a new genomic site (Roth 2000). Mutations affecting host factors that prevent transposition at any stage, either by regulating transcript or cDNA stability or by mediating recombination and integration events, allow increased Ty1 mobility (Conte *et al.* 1998; Lee *et al.* 1998; Scholes *et al.* 2001). *RTT* gene products have roles in each of the above processes and can be grouped into functional classes that include DNA repair, replication and genome stability. Little is known about Rtt106 other than the fact that deletion of this gene results in increased Ty1 mobility, implicating this gene in one of the aforementioned functions (Scholes *et al.* 2001). The synthetic lethality of *cdc68-E857K* with genes of this type also implies that *CDC68* has an overlapping function with these genes in DNA repair, replication and/or genome stability.

In addition to allowing increased mobility of Ty1 elements when altered by mutation, Sgs1 and Mre11 have other, better characterized roles. Mre11 possesses endonucleolytic and exonucleolytic activities that assist in its function as a member of the MRX complex (Paull and Gellert 1998), involved in DNA recombination, repair (D'Amours and Jackson 2001; Trujillo *et al.* 2003) and replication-fork stabilization during DNA replication (Mirzoeva and Petrini 2003). Therefore, the synthetic lethal interaction observed for

cdc68-E857K mre11Δ cells implies that the *cdc68-E857K* mutation may also impinge on one or more of these functions. FACT has been previously implicated in both DNA repair (Keller *et al.* 2001; Yarnell *et al.* 2001; Keller and Lu 2002; Zeng *et al.* 2002; Krohn *et al.* 2003) and replication (Okuhara *et al.* 1999; Wittmeyer *et al.* 1999; Schlesinger and Formosa 2000), although its involvement in these processes remains unclear. This novel genetic interaction between FACT and the MRX complex may assist in elucidating the nature of FACT activity in these processes. The MRX complex is comprised of Mre11, Rad50, and Xrs2; however, only the deletion of *MRE11* was identified by SGA and random-spore analysis as synthetically lethal with *cdc68-E857K*. Deletions of *XRS2* or *RAD50* in combination with *cdc68-E857K* failed to produce cells exhibiting any growth deficit in either of the two SGA screens. The reason for this difference between MRX mutations remains unclear, but further genetic investigations of the interactions between genes encoding FACT and MRX components are warranted. The MRX complex is discussed more extensively in Results 4, vii below, as deletion of each gene for this complex was identified as synthetically sick/lethal with *cdc68-ΔNTD*.

The role for *SGS1* in Ty1 mobility has been explored in more detail than that of *MRE11* or *RTT106* (Bryk *et al.* 2001). Deletion of *SGS1* results in increased recombination among Ty1 elements, which leads to as much as a 79-fold increase in Ty1 mobility (Bryk *et al.* 2001). *SGS1* encodes a RecQ-family DNA helicase that shares homology to the BLM and WRN RecQ helicases in humans, in which mutations cause Bloom's and Werner's syndrome, respectively, characterized by increased susceptibility to cancer and premature ageing (Mohaghegh *et al.* 2001; Khakhar *et al.* 2003). Helicases assist in unwinding the DNA helix and melting the basepair associations to allow exposure of the single-stranded templates required for replication (Khakhar *et al.* 2003). Cdc68, in the context of FACT, has been shown to be a DNA unwinding factor (DUF): it was based on this activity that the *Xenopus* version of FACT, known as DUF, was identified (Okuhara *et al.* 1999). The Sgs1 helicase has been shown to affect replication-fork progression, DNA repair and recombination (Fabre *et al.* 2002; Myung and Kolodner 2002; Khakhar *et al.* 2003; Versini *et al.* 2003), and the synthetic lethal relationship between *sgs1Δ* and *cdc68-E857K* further strengthens the ties associating Cdc68 with these processes and specifically implicates the mutation at codon 857 as

disrupting one or more of these functions. Many, but not all, Sgs1 functions occur in conjunction with the topoisomerase Top3 (Onodera *et al.* 2002); however, *top3Δ* was identified as synthetically lethal in combination with *cdc68-E857K* in only one of the two SGA screens. As a result, the genetic interaction between *TOP3* and *CDC68* has not been pursued further, although this would be an intriguing area of future investigation as it may shed light on the role of FACT in DNA replication and/or repair.

While no genetic or physical interactions were identified in the Yeast GRID database resources between the DNA-metabolism genes (Figure 58), the ties between Mre11, Sgs1, and Rtt106 are apparent as each is implicated in DNA repair, replication and recombination, three processes that are intimately connected and therefore difficult to distinguish genetically. Sensitivities to the DNA-damaging agent methyl methanesulphonate have been identified for cells containing any of these gene deletions (Chang *et al.* 2002), and deletion of the *RAD50* gene, encoding an MRX component, is synthetically lethal in combination with *sgs1Δ*. The associations of Cdc68 activity with those of Mre11 and Sgs1 are especially intriguing and may well highlight a role for FACT in remodelling chromatin to regulate DNA replication, repair and recombination.

c) Additional *cdc68-E857K* SGA interactions and conclusions

The connections between *CDC68* function and the remaining 8 gene deletions identified as synthetically lethal in combination with *cdc68-E857K* are not easily made. One exception to this may be that *nce4Δ*, found to cause synthetic lethality with *cdc68-E857K*, cause synthetic sickness when combined with deletions of 10 different genes involved in DNA repair and/or replication (Tong *et al.* 2004) and has been shown to cause sensitivity to the DNA-damaging agent methyl methanesulphonate (Chang *et al.* 2002). Thus the Nce4 protein appears to affect DNA repair and/or replication, which is consistent with what is known about the function of Ccd68. The protein products encoded by these remaining 7 genes affect a range of biological processes, including metabolism, protein synthesis and protein degradation. These interactions may not be a direct result of altered *cdc68-E857K* activity, but may be an indirect consequence of altered expression patterns of genes that are themselves synthetically lethal with *cdc68*. Overall, the collection of genes with a synthetic sick/lethal phenotype when deleted in combination with *cdc68-E857K* highlight the Cdc68 functions that are impaired by this point mutation, namely

transcription, nucleosome deposition, DNA repair and DNA replication. Each of these functions has been associated with FACT previously, but the precise roles for Cdc68 in these activities are still unclear. Further investigations into the interactions identified here, particularly for those genes encoding proteins involved in nucleosome structure, like the *HIR* genes and *HHT1*, those involved in transcription, like *CDC73* and *LEO1*, and those functioning in DNA metabolism, like *MRE11* and *SGS1*, will undoubtedly shed more light on this subject.

An intriguing model for FACT activity that unifies some of the genetic interactions identified in this section is that impairments to chromatin assembly, as a result of *CDC68*, *HIR*, *ASF1* or histone gene mutations, may lead to stalling during DNA replication as a result of nucleosome 'mismanagement' and may even lead to DNA damage, which has been described for mutations in genes encoding the human CAF-1 histone-chaperone complex (Ye *et al.* 2003). Stalled replication forks and DNA damage, including double-strand breaks caused by replication-fork stalling, activate the S-phase checkpoint, and proteins involved in recombination/repair, like Sgs1 and Mre11, become necessary to re-start stalled forks and repair lesions in the DNA. A similar situation may be applied to transcription, where mutations in *CDC68*, *HIR*, *ASF1* or histone genes leads to improperly 'managed' nucleosomes and therefore difficulties or 'stalling' during transcription, which are then further exacerbated by mutations in other genes encoding proteins that mediate transcription, such as *CDC73* and *LEO1*.

v) Synthetic genetic array analysis with *cdc68-E763G::natMX4*

SGA screens employing cells containing a *natMX4*-tagged, chromosomally integrated *cdc68-E763G* allele were performed in duplicate and identified 1039 and 1031 candidate synthetic-lethal deletions. Of these, only 346 and 328 deletions did not fall into the SGA false-positive category, and 161 of these gene deletions were identified in both SGA screens as synthetically sick or lethal in combination with *cdc68-E763G* (Table 17). These 161 gene deletions were then further tested using random-spore methodology to verify the synthetic genetic relationship with *cdc68-E763G* (Appendix 1). Cells from twelve diploid strains containing gene deletions that had been identified by SGA analysis as synthetically sick or lethal with *cdc68-E763G::natMX4* were also examined by tetrad analysis to verify that the results generated by random-spore analysis were an accurate

reflection of genetic interactions (Figure 59; Appendix 1). Of the twelve deletions assessed in this fashion, six had been shown by random-spore analysis to cause synthetic sickness or lethality when combined with *cdc68-E763G*, while the other six had not displayed any synthetic defects in combination with *cdc68-E763G*. The results of tetrad analysis confirmed the random-spore findings, with all six deletions identified as synthetically sick or lethal by random-spore analysis generating smaller colonies (or none at all) from double-mutant spore products during tetrad analysis, while the six deletions identified as causing no growth defect in combination with *cdc68-E763G* using random-spore analysis also showing no growth defect for double-mutant haploid segregants obtained through tetrad analysis (Figure 59, and data not shown).

In total, 90 of the SGA candidates containing different gene deletions were verified as resulting in synthetic sickness or lethality with *cdc68-E763G* using random-spore methodology (data not shown; summarized in Tables 17 and 19). The connectivity, or previously identified genetic and physical interactions, between genes within this set of 90 displaying synthetic sickness or lethality with *cdc68-E763G* is shown in Figures 60 and 61. In these 'gene webs' each gene is indicated by a coloured node, coded by gene-ontology annotations (legend given in Appendix 2), and for this set of genes a high degree of connectivity is observed for *ARL3*, *GYP1*, *HOC1*, *CHS1*, *SMI1*, *CDC73* and *SET2*, known as 'hub' nodes, within this dataset. The genes identified in the set share a synthetic lethal or sick relationship with, *cdc68-E763G*, which indicates overlapping essential function(s) for the encoded proteins. In turn, the genes within the dataset may themselves have synthetic lethal or sick relationships with one another, indicating that they too share overlapping essential functions. Identifying this type of genetic-interactions web assists in determining the nature of the impaired molecular function.

a) *cdc68-E763G* SGA interactions with genes involved in transport

The 90 genes identified as synthetically sick or lethal with *cdc68-E763G* can be grouped into several functional classes (visulaized Osprey software using the Yeast GRID database as a source current to May, 2004), including transcription, cell growth and maintenance, and cell-cycle maintenance; however, by far the largest functional category represented is that of intracellular transport, with 43 genes (Table 19). Figure 62

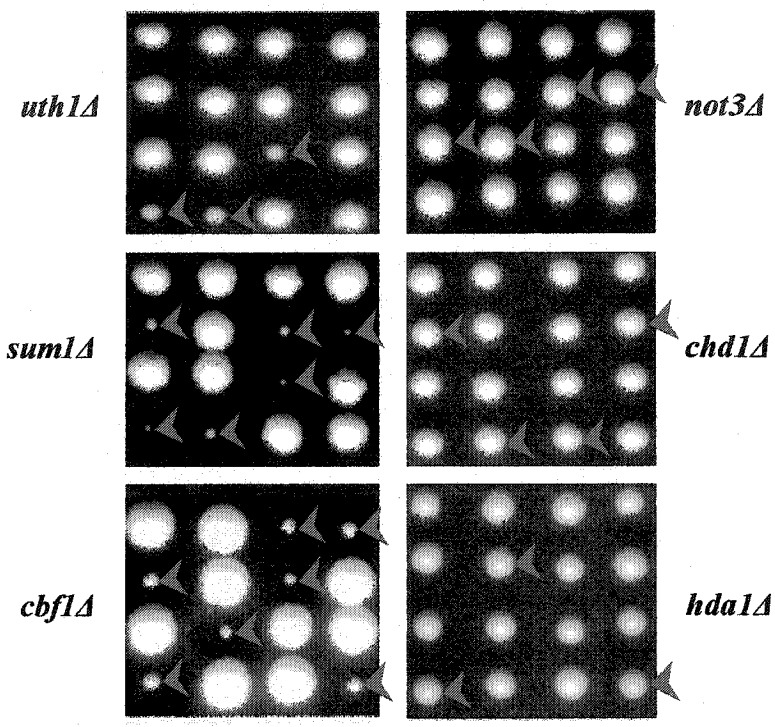

Figure 59. Tetrad analysis of *cdc68-E763G::natMX4* synthetic lethality. Each panel shows the four spores (from top to bottom) generated from four tetrads (from left to right) produced from diploids containing *cdc68-E763G::natMX4* and the gene deletion indicated beside each panel. Random-spore analysis for the crosses involving *uth1Δ*, *sum1Δ*, and *cbf1Δ* indicated that these gene deletions are each synthetically sick or lethal in combination with *cdc68-E763G* and, as can be seen above, the double-mutant spores (arrowheads) generated significantly decreased colony sizes, consistent with the random-spore findings. In contrast, random-spore analysis for the crosses involving *not3Δ*, *chd1Δ*, and *hda1Δ* gene deletions in combination with *cdc68-E763G* did display any significant growth impairment for double mutants and the tetrad analysis confirmed these finding, since the double-mutant segregants from these diploids (arrowheads) grew as robustly as wild-type cells.

Table 19. Gene deletions that are synthetically sick or lethal in combination with *cdc68-E763G*.

Transcription:

Gene Name	Systematic Name	Description	Gene Ontology
CAF40	YNL288W	CCR4 Associated Factor 40 kDa	transcription; metabolism
CDC73	YLR418C	accessory factor associated with RNA polymerase II by affinity chromatography	transcription; metabolism
DST1	YGL043W	General transcription elongation factor TFIIS, enables RNA polymerase II to read through blocks to elongation by stimulating cleavage of nascent transcripts stalled at transcription arrest sites	transcription; metabolism; DNA recombination; DNA metabolism; cell cycle; cell growth and/or maintenance
MED1	YPR070W	Subunit 1 of the Mediator complex essential for transcriptional regulation	transcription; metabolism
PLO1	YPR179C	Subunit of a possibly tetrameric trichostatin A-sensitive class II histone deacetylase complex that contains an Hda1p homodimer and an Hda2p-Hda3p heterodimer; required for the activity of the complex; has similarity to Hda2p	metabolism; DNA metabolism; cell organization and biogenesis; cell growth and/or maintenance; transcription
SET2	YJL168C	Contains a SET or TROMO domain at the N-terminus of the protein. Methyltransferase activity is important for transcriptional repression activity	metabolism; DNA metabolism; cell organization and biogenesis; cell growth and/or maintenance; transcription
SUM1	YDR310C	Suppresor of mar1-1 sir2 mutation	transcription; metabolism; DNA metabolism; cell organization and biogenesis; cell growth and/or maintenance; cell cycle

Transport:

Gene Name	Systematic Name	Description	Gene Ontology
AGE2	YIL044C	ADP-ribosylation factor ARF GTPase activating protein GAP effector	transport; cell growth and/or maintenance
APL4	YPR029C	Gamma-adaptin, large subunit of the clathrin-associated protein AP complex	transport; cell growth and/or maintenance

APL6	YGR261C	beta3-like subunit of the yeast AP-3 complex which functions in transport of alkaline phosphatase to the vacuole via the alternate pathway, suppressor of loss of casein kinase 1 function	transport; cell growth and/or maintenance; cell organization and biogenesis
APM2	YHL019C	homologous to the medium chain of mammalian clathrin-associated protein complex	transport; cell growth and/or maintenance
APS3	YJL024C	sigma3-like subunit of the yeast AP-3 complex which functions in transport of alkaline phosphatase to the vacuole via the alternate pathway, suppressor of loss of casein kinase 1 function	transport; cell growth and/or maintenance; cell organization and biogenesis
ARL1	YBR164C	Encodes a regulator of membrane traffic. Hydrolyzes GTP; myristylated; in soluble fraction. Part of the carboxypeptidase Y pathway.	transport; cell growth and/or maintenance; protein transport; metabolism
ARL3	YPL051W	Similar to ADP-ribosylation factor. Part of the carboxypeptidase Y pathway.	protein transport; transport; cell growth and/or maintenance
CCZ1	YBR131W	Calcium Caffeine Zinc sensitivity	protein transport; metabolism; transport; cell growth and/or maintenance; cell organization and biogenesis; autophagy
COD2	YNL041C	Conserved Oligomeric Golgi complex 6 Complexed with Cog8p; interacts with Cog2p	transport; cell growth and/or maintenance
COD5	YGL005C	Conserved Oligomeric Golgi complex 7 Complexed with Cog8p	transport; cell growth and/or maintenance
DID2	YKR035W-A	Class E protein of the vacuolar protein-sorting Vps pathway, associates reversibly with the late endosome, has human ortholog that may be altered in breast tumors	protein transport; metabolism; transport; cell growth and/or maintenance
DRS2	YAL026C	Integral membrane Ca 2+ -ATPase involved in cleavage of the 20S precursor of the 18S rRNA; potential aminophospholipid translocase required to form a specific class of secretory vesicles that accumulate upon actin cytoskeleton disruption	transport; cell growth and/or maintenance; protein transport; RNA processing; ribosome biogenesis; metabolism; cell organization and biogenesis
GOS1	YHL031C	SNARE protein with a C-terminal membrane anchor GOlgi Snare	transport; cell growth and/or maintenance

GSG1	YDR108W	Subunit of TRAPP transport protein particle , a multi-subunit complex involved in targeting and/or fusion of ER-to-Golgi transport vesicles with their acceptor compartment; protein has late meiotic role, following DNA replication	transport; cell growth and/or maintenance; cell cycle
GUP1	YGL084C	Multimembrane-spanning protein and putative glycerol transporter that is essential for proton symport of glycerol; Gup2p homolog	transport; cell growth and/or maintenance; metabolism
GYP1	YOR070C	Cis-golgi GTPase-activating protein GAP for the Rab family members Ypt1p in vivo and for Ypt1p, Sec4p, Ypt7p, and Ypt51p in vitro ; involved in vesicle docking and fusion	transport; cell growth and/or maintenance
MID1	YNL291C	N-glycosylated integral plasma membrane protein	transport; cell growth and/or maintenance
MON2	YNL297C	Peripheral membrane protein with a role in endocytosis and vacuole integrity, interacts with Arl1p and localizes to the endosome; member of the Sec7p family of proteins	protein transport; metabolism; transport; cell growth and/or maintenance
MSO1	YNR049C	multicopy suppressor of sec1; small hydrophilic protein, enriched in microsomal membrane fraction, interacts with Sec1p	transport; cell growth and/or maintenance; sporulation
PEP8	YJL053W	Plays a role in delivery of proteins to the vacuole	transport; protein transport; metabolism; cell growth and/or maintenance; cell organization and biogenesis
PMR1	YGL167C	Pmr1p, a member of the SERCA family of CaATPases, plays an important role in the transport of Ca++ into Golgi.	transport; cell growth and/or maintenance
RAV1	YJR033C	Regulator of H+ -ATPase in vacuolar membrane	transport; cell growth and/or maintenance; cell organization and biogenesis
RAV2	YDR202C	Regulator of H+ -ATPase in Vacuolar membrane	transport; cell growth and/or maintenance; cell organization and biogenesis
RIC1	YLR039C	Ribosome Control Ric1p binds to Rgp1p, on the Golgi, and the complex catalyses nucleotide exchange on Ypt6p.	protein transport; transport; cell growth and/or maintenance

RER1	YCL001W	Protein involved in retention of membrane proteins, including Sec12p, in the ER; localized to Golgi, where it may function in returning membrane proteins to the ER	transport; cell growth and/or maintenance
RGP1	YDR137W	Ric1p-Rgp1p is an exchange factor, and peripheral membrane protein complex restricted to the Golgi.	protein transport; transport; cell growth and/or maintenance
SEC22	YLR268W	Identified in a screen for dense cells that accumulated invertase at the non-permissive temperature, SEC22 encodes a v-SNARE present on ER to Golgi vesicles and is involved in anterograde and retrograde transport between the ER and Golgi	transport; cell growth and/or maintenance
SYS1	YJL004C	Multicopy suppressor of ypt6 null mutation	transport; cell growth and/or maintenance; cell organization and biogenesis
VAC8	YEL013W	Phosphorylated vacuolar membrane protein that interacts with Atg13p, required for the cytoplasm-to-vacuole targeting Cvt pathway; interacts with Nvj1p to form nucleus-vacuole junctions	autophagy; cell growth and/or maintenance; cell organization and biogenesis; protein transport; metabolism; transport
VAM3	YOR106W	Syntaxin-related protein; required for vacuolar assembly; PEP12 homolog	transport; cell growth and/or maintenance; cell organization and biogenesis
VPS1	YKR001C	involved in vacuolar protein sorting and normal organization of intracellular membranes; probably required for membrane-protein retention in a late Golgi compartment	protein transport; metabolism; transport; cell growth and/or maintenance; cell organization and biogenesis
VPS17	YOR132W	Peripheral membrane protein required for vacuolar protein sorting	transport; cell growth and/or maintenance; cell organization and biogenesis
VPS21	YOR089C	Rab5-like GTPase involved in vacuolar protein sorting and endocytosis post vesicle internalization; geranylgeranylated; geranylgeranylation required for membrane association	transport; cell growth and/or maintenance; protein transport; metabolism
VPS29	YHR012W	Vacuolar protein sorting	transport; cell growth and/or maintenance; cell organization and biogenesis
VPS30	YPL120W	Required for sorting and delivery of soluble hydrolases to the vacuole.	protein transport; metabolism; transport; cell growth and/or maintenance; autophagy

VPS35	YJL154C	Protein involved in vacuolar sorting	transport; protein transport; metabolism; cell growth and/or maintenance; cell organization and biogenesis
VPS38	YLR360W	involved in vacuolar protein targeting	transport; cell growth and/or maintenance; cell organization and biogenesis
VPS4	YPR173C	Defective in vacuolar protein sorting; homologous to mouse SKD1 and to human hVPS4	transport; protein transport; metabolism; cell growth and/or maintenance; cell organization and biogenesis
VPS5	YOR069W	Vacuolar Protein Sorting. component of the retromer coat that retrieves proteins from late endosomes.	transport; protein transport; metabolism; cell growth and/or maintenance; cell organization and biogenesis
VPS67	YKR020W	whiskey whi mutant; forms a tetramer with VPS52, VPS53, and VPS54	protein transport; metabolism; transport; cell growth and/or maintenance; budding;cell organization and biogenesis
VPS74	YDR372C	NONE	protein transport; metabolism; transport; cell growth and/or maintenance
VPS8	YAL002W	involved in vacuolar protein sorting; required for localization and trafficking of the CPY sorting receptor	transport; cell growth and/or maintenance; cell organization and biogenesis
YIP3	YNL044W	Interacts with YPT proteins	transport; cell growth and/or maintenance
YPT7	YML001W	Gtp-binding protein of the rab family; required for homotypic fusion event in vacuole inheritance, for endosome-endosome fusion, and for fusion of endosomes to vacuoles when expressed from high copy plasmid	cell organization and biogenesis; cell growth and/or maintenance; transport

Cell growth and/ or maintenance:

Gene Name	Systematic Name	Description	Gene Ontology
BUD14	YAR014C	Protein involved in bud-site selection; diploid mutants display a random budding pattern instead of the wild-type bipolar pattern	cell organization and biogenesis; cell growth and/or maintenance
CCW12	YLR110C	NONE	cell organization and biogenesis; cell growth and/or maintenance
CWH41	YGL027C	Glucosidase I, involved in assembly of cell wall beta 1,6 glucan; an ER type II integral membrane N-glycoprotein	cell organization and biogenesiscell growth and/or maintenance
GAS1	YMR307W	Glycophospholipid-anchored surface protein	cell organization and biogenesis; cell growth and/or maintenance
GEF1	YJR040W	Integral membrane protein highly homologous to voltage-gated chloride channels from humans, mice and fish	cell growth and/or maintenance
UTH1	YKR042W	Youth, involved in determining yeast longevity	cell organization and biogenesis; cell growth and/or maintenance
WHI3	YNL197C	RNA binding protein that binds to and sequesters the G1 cyclin CLN3 mRNA; regulates cell fate and dose-dependently inhibits passage through Start by regulating the critical cell size requirement necessary for cell cycle progression	cell organization and biogenesis; cell growth and/or maintenance
YGL020C	YGL020C	Spore Wall Formation. Mitochondrial Distribution and Morphology	cell organization and biogenesis; cell growth and/or maintenance
YOR068C	YOR068C	[Abnormal]Vacuole Morphology	cell organization and biogenesis; cell growth and/or maintenance

Protein biosynthesis:

Gene Name	Systematic Name	Description	Gene Ontology
HOC1	YJR075W	Homologous to OCH1, an alpha-1,6-mannosyltransferase; Golgi-localized, type II integral membrane protein	protein biosynthesis; cell organization and biogenesis; metabolism; cell growth and/or maintenance; carbohydrate metabolism

MNN11	YJL183W	member of a cis Golgi complex that is involved in mannan synthesis, other complex members include Mnn10p, Hoc1p, Anp1p, Mnn9p	protein biosynthesis; metabolism
MNN2	YBR015C	Probable type II membrane protein involved in mannan synthesis. Catalyzes addition of first mannose to branches on poly 1,6-mannose backbone of outer chain of cell wall N-linked mannans.	protein biosynthesis; metabolism
OST3	YOR085W	Gamma subunit of the oligosaccharyltransferase complex of the ER lumen, which catalyzes asparagine-linked glycosylation of newly synthesized proteins; Ost3p is important for N-glycosylation of a subset of proteins	protein biosynthesis; metabolism
RPL34B	YIL052C	Homology to rat L34	protein biosynthesis; metabolism
SPF1	YEL031W	Sensitivity to a killer toxin SMK toxin produced by Pichia Farinosa	protein biosynthesis; metabolism; cell growth and/or maintenance
SRO9	YCL037C	Associates with translating ribosomes; may function in the cytoplasm to modulate mRNA translation; may be involved in organization of actin filaments	protein biosynthesis; metabolism
TEF4	YKL081W	Translation elongation factor EF-1gamma	protein biosynthesis; metabolism

Cell cycle:

Gene Name	Systematic Name	Description	Gene Ontology
CBF1	YJR060W	centromere binding factor; binds in vivo to CDE I sites in centromeres and some promoters , and induces DNA bending, required for mitotic segregation and normal growth rate	metabolism; cell cycle; cell growth and/or maintenance
CLB3	YDL155W	Involved in mitotic induction and perhaps in DNA replication and spindle assembly	cell cycle; cell growth and/or maintenance
YGR089W	YGR089W	Protein that exhibits physical and genetic interactions with Rpb8p, which is a subunit of RNA polymerases I, II, and III; computational analysis of large-scale protein-protein interaction data suggests a role in chromosome segregation	cell cycle; cell growth and/or maintenance

Stress Response:

Gene Name	Systematic Name	Description	Gene Ontology
ELM1	YKL048C	cell morphology	cell growth and/or maintenance; protein amino acid phosphorylation; metabolism; response to stress; budding; cell organization and biogenesis
TPS1	YBR126C	Probable regulator of glucose influx into the cell & into glycolytic pathway, indirectly regulating glucose-induced signalling activation & inactivation & initial step s of glucose metabolism. Homologue of E. coli otsA protein	carbohydrate metabolism; metabolism; response to stress
WHI2	YOR043W	Protein required, with binding partner Psr1p, for full activation of the general stress response, possibly through Msn2p dephosphorylation; regulates growth during the diauxic shift; negative regulator of G1 cyclin expression	response to stress

Metabolism:

Gene Name	Systematic Name	Description	Gene Ontology
BRE5	YNR051C	protein of unknown function	metabolism
CHO2	YGR157W	First step in the methylation pathway for phosphatidylcholine biosynthesis	metabolism
PHO80	YOL001W	Negative regulator of PHO81 and PHO5	metabolism
URE2	YNL229C	Nitrogen catabolite repression regulator that acts by inhibition of GLN3 in good nitrogen source. Altered form of Ure2p creates [URE3] prion.	metabolism

Signal transduction:

Gene Name	Systematic Name	Description	Gene Ontology
BEM4	YPL161C	Involved in polarity establishment and bud emergence; interacts with the Rho1p small GTP-binding protein	signal transduction; cell organization and biogenesis; cell growth and/or maintenance

SAC7	YDR389W	GTPase activating protein GAP for Rho1p, involved in signaling to the actin cytoskeleton, null mutations suppress tor2 mutations and temperature sensitive mutations in actin; potential Cdc28p substrate	signal transduction; cell cycle; cell growth and/or maintenance; cell organization and biogenesis

DNA repair:

Gene Name	Systematic Name	Description	Gene Ontology
MRE11	YMR224C	Disp. for premeiotic DNA synthesis, but required for both double strand break formation & resection, synaptonemal complexes, meiotic recombination & viable spores. Localizes to discrete sites in rad50 mutants	DNA repair; DNA metabolism; response to DNA damage stimulus; response to stress; metabolism; DNA recombination; cell cycle; cell growth and/or maintenance

Budding:

Gene Name	Systematic Name	Description	Gene Ontology
CHS1	YNL192W	disrupts mating and sporulation efficiently	budding; cell growth and/or maintenance

Protein degradation:

Gene Name	Systematic Name	Description	Gene Ontology
BST1	YFL025C	Negatively regulates COPII vesicle formation	cell organization and biogenesis; cell growth and/or maintenance; protein catabolism; metabolism

Carbohydrate metabolism:

Gene Name	Systematic Name	Description	Gene Ontology
SMI1	YGR229C	Protein involved in 1,3 -beta-glucan synthesis, possibly through regulation of cell wall glucan and chitin synthesis; chromatin binding protein	carbohydrate metabolism; metabolism; cell organization and biogenesis; cell growth and/or maintenance

Unknown:

Gene Name	Systematic Name	Description	Gene Ontology
KRE25	YNL296W	Hypothetical ORF	UNKNOWN

PKR1	YMR123W	Pichia farinosa Killer toxin Resistance	biological process unknown
VPS60	YDR486C	vacuolar protein sorting putative	biological process unknown
YDR203W	YDR203W	Hypothetical ORF	NONE
YEL043W	YEL043W	NONE	biological process unknown
YLR111W	YLR111W	Hypothetical ORF	NONE
YLR171W	YLR171W	Hypothetical ORF	NONE
YPR090W	YPR089W	NONE	biological process unknown

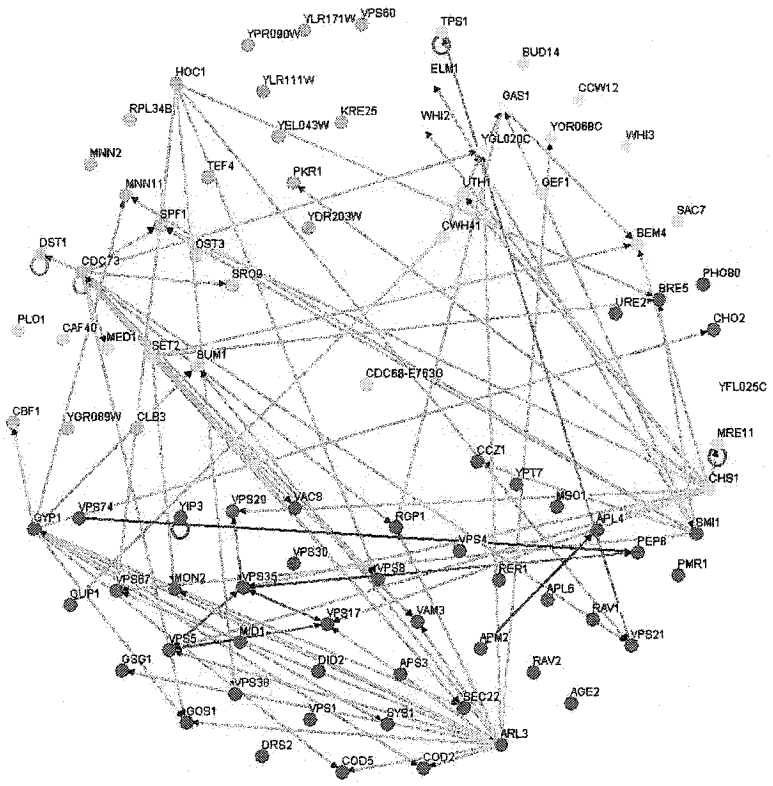

Figure 60. Synthetic genetic interactions involving *cdc68-E763G*. Each gene deletion identified by SGA and verified by random-spore analysis to be synthetically sick or lethal in combination with *cdc68-E763G* is indicated by a coloured node, and previously identified genetic or physical interactions between two genes are indicated by coloured lines (see Appendix 2 for legend). The *cdc68-E763G* mutant gene is shown in the middle of the web and should have green lines, indicating a synthetic sick or lethal interaction, connecting it all of the gene deletions shown, but for clarity these lines have been omitted. A high degree of connectivity can be seen in this group of genetic interactions, which indicates overlapping functions. The key 'hubs' of interactions are displayed more clearly in Figure 61.

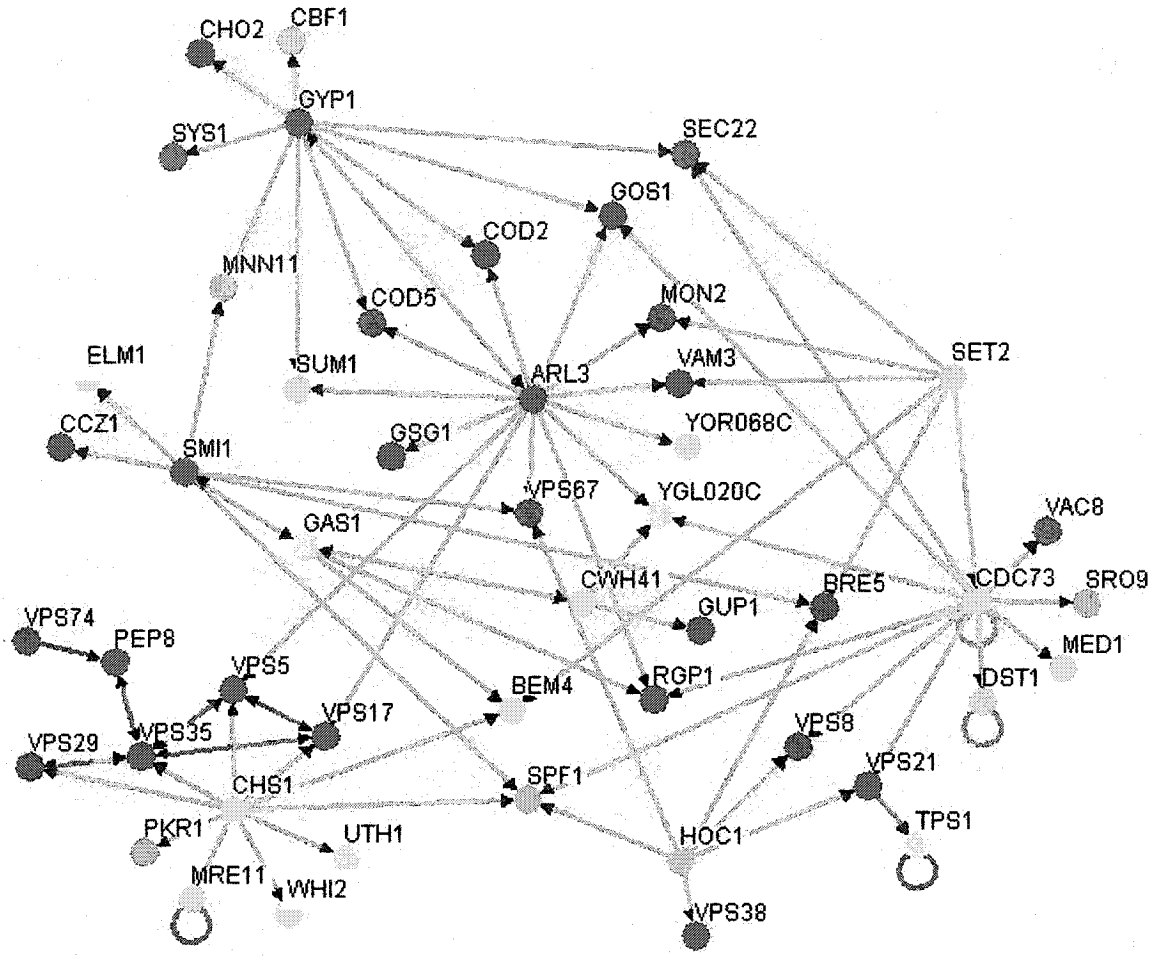

Figure 61. Connectivity of synthetic genetic interactions with *cdc68-E763G*. Of the 90 genes identified as having a synthetic genetic relationship when deleted along with the *cdc68-E763G* mutation, the 49 with previously identified genetic or physical interactions are shown. These 49 genes show a high degree of connectivity, with 79 interactions among them. The legend for line and node colours is given in Appendix 2.

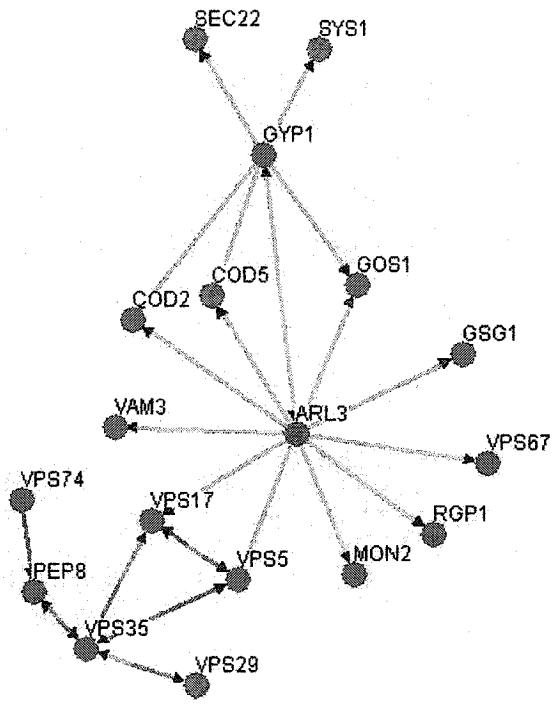

Figure 62. Interacting genes involved in vesicular transport whose deletions cause synthetic sickmess or lethality in combination with *cdc68-E763G*. Of the 43 genes with genetic interactions with *cdc68-E763G* and that function in transport, the 18 shown here had been previously reported to interact either physically or genetically. Each of the genes encoding retromer-complex components (*VPS17*, *VPS5*, *VPS35*, *VPS29*, and *PEP8*/*VPS26*), which mediates retrograde transport from the endosome to the Golgi (Seaman *et al.* 1998), is identified here.

highlights the connectivity of these transport hits, showing 18 of these 43 genes. The majority of the transport genes identified as synthetically lethal with *cdc68-E763G* function in the Golgi complex, or mediating trafficking from the *trans*-Golgi network (TGN) to the endosome.

Transport between the TGN and endosomes is primarily mediated by clathrin-coated vesicles, so named for the clathrin lattice that forms the structural coat around the vesicle during the budding process (reviewed in Hirst and Robinson 1998). A clathrin 'coat' is comprised of a tetramer of heavy-chain and light-chain molecules that form a 'honeycomb'-type of icosahedral structure on the surface of the membrane that is then altered to deform the membrane and permit vesicle budding (Hirst and Robinson 1998). There are physical associations between clathrin structural elements and membrane adaptor proteins (AP), which comprise there are three different complexes AP-1, AP-2, and AP-3, functioning in different stages of transport (Hirst and Robinson 1998). The AP complexes, while not required for clathrin assembly on membranes, Sit4 reside between the membrane and clathrin coat and may facilitate and/or regulate clathrin deposition and also assist in cargo selection. AP-1 is comprised of Apl2, Apl4, Apm1, and Aps1 and potentially Apm2 as an 'alternative' subunit, and this tetramer functions primarily for transport between the TGN and the endosome (Hirst and Robinson 1998). Both *aps1Δ* and *apm2Δ* deletions were identified here as synthetically lethal in combination with the *cdc68-E763G* mutation. Derivatives of the *apl2Δ* deletion strain are false positives in SGA analysis (Tong *et al.* 2001), and therefore this deletion was not studied further here; however, *apl2Δ* and *cdc68-E763G* was a lethal combination in both of the SGA screens. In addition to this synthetic lethality with deletions of AP-1 genes, synthetic lethality or sickness was seen for deletions of the genes encoding the AP-3 subunits Apl6, Apl5, Apm3, and Aps3 in combination with *cdc68-E763G* using SGA and random-spore analysis. The AP-3 complex resembles a clathrin adaptor complex in structure and composition, but is thought to act independently of clathrin to facilitate transport from the TGN (Vowels and Payne 1998; Rehling *et al.* 1999; Yeung *et al.* 1999). While only *apl6Δ* and *aps3Δ* were clearly identified here as synthetically sick with *cdc68-E763G*, *apl5Δ* and *amp3Δ* were each found in one of the two SGA screens as synthetically sick or lethal in combination with *cdc68-E763G*. Thus the genetic relationships between *cdc68-*

E763G and the genes encoding other AP-1 and AP-3 subunits could be examined further. No genetic interactions were identified with genes encoding members of the AP-2 complex, which functions in clathrin-mediated transport at the plasma membrane and is not associated with the TGN. This distinction in localization of the AP-1 and AP-3 complexes in comparison to AP-2 and the genetic relationships for each with *cdc68-E763G*, in addition to the genetic interactions identified with other factors functioning in Golgi-to-endosome transport, suggests that the transport stage influenced is significant. Perhaps *cdc68-E763G* mutations disrupt transport in a stage-specific fashion, influencing Golgi-to-endosome transport.

Other genes affecting clathrin-coated vesicle traffic between the TGN and endosomal compartments were also identified here as synthetically sick or lethal with *cdc68-E763G*. It has been hypothesised that Vps1, the yeast dynamin homologue which is a GTPase involved in recruiting factors and/or providing the energy required for vesicle scission (Hill and Robinson, 2001; reviewed in Hirst *et al.* 1998), may facilitate all clathrin-mediated transport events (Vater *et al.* 1992; Bensen *et al.* 2000; Hill *et al.* 2001; Gurunathan *et al.* 2002). The *ARL3* gene (ADP-ribosylation factor-like) encodes a GTPase involved in vesicular transport at the Golgi, and the deletion of this gene is synthetically lethal in combination with *cdc68-E763G* (Lee and Huang 2001; Setty *et al.* 2003). Arls and Arfs are thought to assist in recruiting coat components to the site of vesicle formation and may also affect in cargo selection. When bound to GTP, Arls and Arfs associate with the membrane, while the GDP-bound form releases these coat components from the membrane or vesicle surface. In this way the switch from GTP-bound to GDP-bound Arl or Arf is crucial, and is regulated by GTPase activating proteins (GAPs) and guanine nucleotide exchange factors (GEFs). One GAP involved at the TGN in vesicular transport is Age2 (Poon *et al.* 2001), which was also identified here as gene deletion with synthetic lethality in combination with *cdc68-E763G*. The Mon2 GEF was also identified here as synthetically lethal with *cdc68-E763G*, and has been hypothesized to mediate the guanine exchange cycle for Arl1 and Arl3 (Jochum *et al.* 2002; Setty *et al.* 2003). The *CCZ1* gene, whose deletion was identified here as causing synthetic lethality in combination with *cdc68-E763G*, encodes a GEF functioning in the endosomal and vacuolar compartments. Ccz1 is important for the late stages of vesicle fusion with target

membranes (Wang *et al.* 2002, 2003) along with the Mon2 homologue Mon1 and the endosomal GTPase Ypt7 (Kucharczyk *et al.* 2000, 2001; Wang *et al.* 2002). Another complex comprised of Vps8 and the GTPase Vps21 operates in Golgi-to-endosome transport (Horazdovsky *et al.* 1996; Gerrard *et al.* 2000), and deletions of the genes encoding these components were identified here as synthetically lethal with *cdc68-E763G*. Both the *cdc68-E857K* and *cdc73Δ* mutations were also identified as synthetically sick or lethal with deletions of *VPS8* or *VPS21* (Results 4, v; Tong *et al.* 2004); therefore *cdc68-E763G* is not the only transcription-related mutation with genetic interactions with these transport components. Each of these factors, Vps1, Arl3, Mon2, Age2, Ccz1,Ypt7, Vps8 and Vps21, can be associated with vesicular transport at the Golgi or endosomal compartments. The synthetic sickness or lethality caused by combining each of these gene deletions with *cdc68-E763G* suggests that this mutation somehow disrupts transport, particularly at the Golgi-to-endosomal stage.

When proteins involved in stage-specific transport are tethered to the transport vesicle itself, they generally are retrieved from the target organelle back to the original donor organelle for future transport events. This process is known as retrograde transport. Gene deletions encoding proteins involved in retrograde transport from the endosome to the Golgi were also identified as synthetically lethal in combination with *cdc68-E763G*. Deletions of each of the five genes encoding components of the retromer complex, comprised of Vps35, Vps29, Vps26/Pep8, Vps5, and Vps17 (Seaman *et al.* 1998), which operates in retrograde transport from the endosome to the Golgi, were identified as synthetically lethal with *cdc68-E763G* by SGA analysis (Figures 61 and 62). The GARP (Golgi-associated retrograde protein) complex, composed of Vps67 (also known as Vps51), Vps52 (also known as Sac2), Vps53, and Vps54, also functions in retrograde transport from the endosome to the Golgi (Conibear *et al.* 2003), and deletion of the *VPS61* gene was found here to be synthetically lethal with *cdc68-E763G*. Of the remaining components of GARP, deletions of *VPS52/SAC2* and *VPS53* are both SGA false positives and were therefore not studied beyond the initial SGA analyses. However, *vps53Δ* did cause synthetic lethality with *cdc68-E763G* in both screens, while *vps52Δ* caused synthetic lethality in cells with *cdc6-E763G* in one of the two SGA screens. (A deletion of *VPS54* is not present in our deletion collection and therefore is not included in

the dataset here.) These findings further support a role for Cdc68 in transport, and highlight a specific role in transport between the Golgi and endosomal compartments.

Based on these findings, two additional genes, encoding Ric1 and the GTPase Arl1 involved in Golgi-to-endosome transport and retrieval, were tested for synthetic growth defects when deleted in *cdc68-E763G* cells. Ric1 interacts with Rgp1 and serves as a GEF for Ypt6, and operates in retrieval of Golgi proteins from the endosome. Arl1 physically interacts with Arl3, which localizes Arl1 to membranes during transport (Setty *et al.* 2003). Arl1 and Arl3 affect the tethering other factors, including the GARP complex (see above), to vesicles during retrograde transport from the endosome to the Golgi (Panic *et al.* 2003a, 2003b). Deletions of *RIC1* and *ARL1* are synthetically lethal with 44 and 21, respectively, of the genes identified as synthetically sick or lethal with *cdc68-E763G*, indicating that several of the genes identified here share overlapping essential functions with Ric1 and Arl1 (Tong *et al.* 2004). Due to this finding, and the fact that a physically associating protein for each, Rgp1 and Arl3, respectively, was identified here as synthetically lethal when the gene was deleted, I decided to examine the synthetic lethality of *ric1Δ* and *arl1Δ* deletions in combination with *cdc68-E763G* by random-spore analysis. Results showed that deletion of either *ric1* or *arl1* results in synthetic sickness or lethality for cells containing *cdc68-E763G*. These findings are consistent with overlapping functions for *cdc68-E763G* in Golgi-to-endosome transport. This result also illustrates how genetic interactions can occasionally be missed during SGA analysis, which has a false-negative rate of between 17 and 40% (Tong *et al.* 2001, 2004).

Other interesting genetic interactions within this set related to Golgi or Golgi-to-endosomal transport involve Gyp1, a Golgi-localized GAP, and Yip3. Both of these proteins interact with Ypt7, which mediates vesicle fusion (Vollmer *et al.* 1999; Calero and Collins 2002). *RAV1* and *RAV2* encode two of the three components of the RAVE complex (regulator of the (H+)-ATPase of the vacuolar and endosomal membranes), an ATPase regulating the acidity of the vacuole and endosomal compartments (Seol *et al.* 2001). The components of this complex have been shown to be synthetically lethal in combination with deletions of other genes encoding proteins involved in Golgi-to-endosomal transport. The *DRS2* and *PMR1* genes each encode another type of ATPase,

ones involved in mediating calcium levels, and these proteins are thought to influence transport between the TGN and the endosome or within the Golgi itself, respectively (Rudolph *et al.* 1989; Hua *et al.* 2002). Both *GOS1* and *SYS1* have been identified as multicopy suppressors of deleterious phenotypes associated with *ypt6Δ* or *ric1Δ*, which affect Golgi-to-endosome transport, indicating a role for Sys1 at this transport stage (Tsukada and Gallwitz 1996; Bensen *et al.* 2001). More recently, Sys1 has been shown to recognize an acetylated form of Arl3 and recruits this protein to the Golgi (Behnia *et al.* 2004). Subunits of both the TRAPP (transport protein particle) and COG (conserved oligomeric Golgi) complexes, involved in vesicle maturation in the Golgi, were also identified as causing synthetic defects in combination with *cdc68-E763G*. The web of synthetic genetic interactions involving many of these genes is also convincing evidence that they encode proteins with overlapping molecular functions (Figures 61 and 62).

The results of SGA and random-spore analysis identified a large number of gene deletions affecting vesicular transport, with a preponderance of these genes encoding proteins that operate in the Golgi or endosomal transport processes, that result in synthetic sickness or lethality when combined with the *cdc68-E763G* mutation. While a direct connection between Cdc68, a chromatin modulator, and vesicular transport is difficult to rationalize, these results do seem to implicate that Cdc68 impacts on membrane trafficking. It should be noted that mutations or deletions of other genes, such as *CDC73*, *SET2*, *DST1*, *CDC45* and *RAD50*, involved in transcription, repair and/or replication, have also been found through SGA analysis to have genetic interactions with genes involved in vesicle transport (Tong *et al.* 2001, 2004; Krogan *et al.* 2003b). In some cases, physical interactions have been identified between components involved in transport and those involved in transcription, replication, or repair (Ho *et al.* 2002; Krogan *et al.* 2003b). While to my knowledge no single gene deletion or mutation involved in transcription, repair or replication has identified through SGA analysis as many components of the transport machinery as has the *cdc68-E763G* mutation (or, as described in the next section, the *cdc68-312* mutation), there is overlap in the genes identified here and those found in other SGA screens using mutations or deletions of other genes encoding transcription, repair or replication machinery. For example, SGA analysis identified 21 genes involved in transport functions as causing cells to be sick or

lethal when deleted in combination with *cdc73Δ*, and at least five of those genes, *VPS8*, *VPS21*, *RIC1*, *RGP1* and *YPT6*, are intimately involved in transport between the TGN and the endosome (Krogan *et al.* 2003b; Tong *et al.* 2004). Additionally, seven of the genes encoding proteins involved in transport have been shown to cause synthetic genetic effects when deleted in *cdc68-E763G* or *cdc73Δ* cells (Figure 60; Krogan *et al.*, 2003b; Tong *et al.* 2004). The significance of this finding is currently not clear, but it is interesting that a recently identified 13-member complex called SWR-C, shown to have ATP-dependent nucleosome-remodelling activity, to assist in the incorporation of the histone H2A variant H2A.Z into nucleosomes, and to be in involved in transcription elongation, contains seven components affecting vacuolar protein sorting (VPS) (Bonangelino *et al.* 2002; Krogan *et al.* 2003b). Krogan *et al.* (2003b) indicate that each of these components has been shown to reside in the nucleus, and that their effects on transport must therefore be indirect. Be this as it may, the implication that mutations affecting a complex involved in transcription elongation and modification of chromatin structure are capable of causing defects in transport is still clear. An analogous situation maybe at play in the synthetic defects reported here between *cdc68* mutations and deletions of genes encoding vesicular-transport proteins.

There are several possible explanations for these synthetic genetic interactions involving *CDC68*. The first is that the *cdc68-E763G* mutation influences the expression of a gene or subset of genes involved in vesicular transport and, as a result, further insults to the transport processes are not tolerated. If this is the case, the influence of *cdc68-E763G* on transport is an indirect effect of its involvement in transcription. The second possibility is that one or more of the components involved in vesicular transport also operates in the nucleus to mediate transcription, replication and/or repair. In an instance where *cdc68* is mutated, the transport component(s) may be inappropriately sequestered in its nuclear function and, as a result, cytoplasmic transport functions suffer. Further perturbations to transport activities therefore result in cell growth defects or lethality. A third possibility is that a downstream event requires proper functioning of Gogli-to-endosome transport as well as proper chromatin structure, and that these two pathways each contribute in parallel to the downstream function. For example, each of these functions, chromatin modulation and vesicular transport, may contribute to the generation

of a stable cell-wall architecture, and therefore perturbations in both of these pathways result in a more deleterious impact on the cell.

Another hypothesis for these synthetic lethal interactions is more technical in nature, and implicates the *natMX4* integration event downstream of the *cdc68-E763G* mutant allele as somehow disrupting expression of the neighbouring *CHC1* gene, which encodes the clathrin heavy-chain subunit. As indicated above, clathrin heavy chain plays an important role in the transport of vesicles from the TGN to the endosome, as a component of the vesicle coat. Some of the gene deletions identified here as causing synthetic defects in combination with *cdc68-E763G* have also been identified as causing synthetic sickness or lethality in combination with temperature-sensitive *chc1* mutations, including *apl4*, *drs2*, *ric1*, *vps1*, *vps5*, *vps21*, and *vps17* (Chen *et al.* 1999; Yeung *et al.* 1999; Bensen *et al.* 2000, 2001). However, this hypothesis would mean that the other tagged *cdc68* alleles generated for use in SGA analysis using the same approach (Materials and Methods), including the wild-type *CDC68::natMX4* control, resulted from genome integration events that are somehow different from the intergration event in this particular allele, for the myriad of transport defects found to be synthetically lethal or sick for the *cdc68-E763G::natMX4* allele are not identified for the other alleles, with the exception of *cdc68-312::natMX4* (Results 4, vi). The *cdc68-E763G* and *cdc68-312* alleles both contain the point mutation that generates a glutamate-to-glycine substitution at codon 763, although the *cdc68-312* allele contains additional mutations (Table 10). Not surprisingly, these two alleles behave very similarly in SGA analysis and share approximately 60% overlap in the gene deletions that cause synthetic sickness or lethality. A few transport-gene deletions are synthetically sick or lethal in combination with every *cdc68* allele used here in SGA analysis, but only *cdc68-E763G* and *cdc68-312* identify such large cohorts of genes involved in vesicular transport, suggesting that the mutation causing the E763G substitution may specifically impair membrane trafficking processes, in particular in the Golgi and endosomal compartments, or that this stage of transport has an overlapping function with a Cdc68-mediated function.

b) *cdc68-E763G* SGA interactions with genes involved in cell integrity and morphogenesis

I show in part three of Results (above) that the Cdc68 component of FACT affects the maintenance of cell integrity, and vesicular transport is also critical for cell-wall stability and morphogenesis. Therefore, these roles in maintaining cell integrity may be the overlapping functions for Cdc68 and vesicular transport. When yeast cells undergo morphological changes and growth, materials within the cell must be directed to the areas of growth or repair. A number of findings have made ties between transport, cell-wall maintenance and cell morphogenesis (Pruyne and Bretscher 2000a, 2000b). For example, in times of stress the internal chitin stores located in the TGN and endosome are mobilized to the cell surface, presumably to assist in strengthening the cell wall (Valdivia and Schekman 2003). Also, many of the post-translational modifications that occur on proteins directed to the cell wall, for example glycosylation, occur within membrane-bound organelles like the Golgi. Mutations in transport machinery that impair the glycosylation of proteins result in altered expression of genes encoding the enzymes required for these modifications (Yamamoto and Jigami 2002). Recent SGA screens employing deletions of genes encoding proteins responsible for the assembly of β-1,3-glucan, the major constituent of the cell wall, have identified several genes involved in transport, namely *BRE5*, *RIC1*, *RGP1*, and several *VPS* genes, including genes identified here as synthetically lethal with *cdc68-E763G* (Lesage *et al.* 2004). Many genes encoding proteins involved in cell morphogenesis and cell-wall maintenance, including *GAS1*, *BUD14*, *BEM1*, *SAC7*, *CHS1*, *HOC1*, *MNN11*, *MNN2*, *OST3*, *SMI1*, *SPF1*, *ELM1*, *CCW12*, and *CWH41*, are identified here as synthetically lethal when deleted in *cdc68-E763G* cells. Many of these genes encode a protein that is itself a glycosylated component of the plasma membrane or cell wall, is involved directly in the production of glucans, mannans, or chitin, or is involved in the addition of these moieties to form glycoproteins that operate at the cell wall. As described above (Results 3), several different *cdc68* mutations confer phenotypes consistent with cell-wall integrity and cell-morphogenesis defects. The identification of the above genes as causing synthetic lethality when deleted with *cdc68-E763G* is further evidence that *cdc68* mutations influence cell-wall architecture and that these proteins therefore share an overlapping function with Cdc68. This overlapping function is most likely indirect and the result of Cdc68-mediated effects on transcription of genes involved in cell integrity, in particular

the transcription of genes that are activated by the Pkc1 signal-transduction pathway (Results 3).

c) *cdc68-E763G* SGA interactions with genes involved in transcription

Several other interesting gene deletions identified here as resulting in synthetic growth impairments when combined with the *cdc68-E763G* mutation are more readily interpretable in the context of known Cdc68 functions. As described above for the *cdc68-E857K* mutation, *cdc73Δ* was also identified here as causing synthetic sickness with *cdc68-E763G*. Cdc73 is a member of the Paf complex, which associates with RNA polymerase II, assists in transcription initiation and elongation, and physically and genetically interacts with FACT (Shi *et al.* 1996, 1997; Wade *et al.* 1996; Costa and Arndt 2000; Krogan *et al.* 2002; Pokholok *et al.* 2002; Squazzo *et al.* 2002; Rondon *et al.* 2004). Other factors directly related to Paf1-complex functions, and specifically to Cdc73, were also identified here as synthetically sick or lethal with *cdc68-E763G* (Figures 60 and 61). These are described below.

The *SET2* gene encodes a histone methyltransferase that methylates histone H3 at lysine 36, but this modification only takes place when the Paf complex is present to assist in recruiting Set2 to sites of RNA polymerase II activity (Strahl *et al.* 2002; Krogan *et al.* 2003c). Indeed, Set2 physically associates with RNA polymerase II components, an association that is dependent on the phosphorylation of the C-terminal tail of Rpb1, the largest subunit of RNA polymerase II, by Ctk1, a protein kinase (Li *et al.* 2002; Hampsey and Reinberg 2003; Li *et al.* 2003; Xiao *et al.* 2003). The Paf1 complex associates with RNA polymerase II during both transcription initiation and elongation (Shi *et al.* 1997; Pokholok *et al.* 2002), and the hyper-phosphorylation of the C-terminal domain of Rbp1, specifically as mediated by the Ctk1 kinase, is a modification associated with the actively elongating RNA polymerase (Komarnitsky *et al.* 2000; Cho *et al.* 2001). Additionally, Set2 itself has been localized to the region of actively elongating RNA polymerase II (Krogan *et al.* 2003c), indicating a role for Set2 in RNA polymerase II transcription elongation (Hampsey and Reinberg 2003). My finding that cells containing *set2Δ* and the *cdc68-E763G* mutation are synthetically sick is a novel and exciting finding. Both Set2 and Cdc68 have been shown to function in transcription elongation and are related to the

Paf1 complex, physically and functionally. These functional ties between FACT and the Set2 methlytransferase merit further investigation.

SET2 has genetic interactions with the *DST1* gene, which encodes the TFIIS (transcription elongation factor S-II) component of RNA polymerase II ((Krogan *et al.* 2003b; Li *et al.* 2003). TFIIS assists in RNA polymerase II transcription 're-start' after pausing, where the RNA polymerase II catalytic site loses contact with the 3' end of the transcript, by stimulating cleavage of the nascent transcript (Izban and Luse 1992; Wind and Reines 2000). SGA and random-spore analysis indicate that the combination of a *dst1Δ* and *cdc68-E763G* causes synthetic sickness. This genetic association between *DST1* and *CDC68* is not unprecedented, for a genetic interaction has been reported between the *spt16-197* allele and *dst1Δ* that results in a mild growth defect (Orphanides *et al.* 1999; Lindstrom and Hartzog 2001). There are several additional genetic ties associating TFIIS and Cdc68 function.

Lindstrom and Hartzog (2001) also show that *dst1Δ* is synthetically sick with *bur1* mutations, *ctk1Δ* and *rpb1* mutations. Genetic interactions similar to these described for *dst1Δ* have also been identified for *cdc68* mutations. Findings presented above (Results 4, i) indicate that mutations in *cdc68* cause synthetic lethality in combination with a *bur2* mutation. Bur2 encodes the regulatory subunit of the Bur1 kinase and this Bur1/Bur2 complex appears to play a role similar to that of the Ctk1 kinase during transcription by phosphorylating elongation factors. Additionally, certain *rpb1* mutations have been shown to suppress *cdc68* mutations (J. Kurniawan, unpublished data). Taken together, these similar genetic interactions suggest an overlapping essential function in transcription elongation for TFIIS and FACT.

Genetic interactions for *cdc73Δ*, *set2Δ*, and *dst1Δ* as determined by SGA analysis have been reported (Krogan *et al.* 2003b). Interestingly, only 5 gene deletions were shown to cause synthetic growth defects with all three mutations. Since *cdc73Δ*, *set2Δ*, and *dst1Δ* have each been identified here as synthetically sick with *cdc68-E763G*, I assessed the overlap between the deletions identified as synthetically sick or lethal in these four instances and found that only *sec22Δ* results in synthetically sick cells in all four cases. Sec22 is a v-SNARE (soluble NSF-attachment protein receptor) involved in vesicular transport between the endoplasmic reticulum and the Golgi. As can be seen in

Figure 61, 6 gene deletions with synthetic interactions with *set2Δ*, 13 gene deletions with synthetic interactions with *cdc73Δ* and 1 gene deletion with synthetic interactions with *dst1Δ* are also identified as synthetically sick or lethal with *cdc68-E763G*. Once again the majority of these genes encode proteins involved in vesicular transport. These findings further strengthen the functional ties between vesicular transport and components involved in transcription elongation, although the biological significance of these ties remain unclear.

In addition to Set2, the Set1 and Set3 complexes, known as COMPASS and Set3-complex, also contain histone methyltransferase activity. None of the genes encoding components of these complexes was identified here as synthetically lethal in combination with *cdc68-E763G*. However, in addition to having histone methyltransferase activity the Set3 complex also contains histone deacetylase capabilities, provided by Hst1 and Hos2 (Pijnappel *et al.* 2001). In addition to acting in the Set3 complex, Hst1 physically interacts with Sum1 to mediate histone deacetylation involved in silencing gene expression at telomeres and the silent mating-type loci as well as in regulating transcription of a subset of genes involved in sporulation (Xie *et al.* 1999; Sutton *et al.* 2001b). A *sum1* deletion is synthetically lethal in combination with *cdc68-E763G*, tying histone deacetylation to chromatin structural changes mediated by FACT. Another histone deacetylase complex in yeast is comprised of Hda1 (the catalytic subunit), Hda2 and Plo1 (also known as Hda3; Wu *et al.* 2001). Here again a gene encoding a regulatory subunit of this histone deacetylase complex, namely *PLO1* (a.k.a. *HDA3*), was identified as synthetically sick in combination with the *cdc68-E763G* mutation. These findings, together with those for Set2 above, indicate a tie between FACT function and nucleosome modifications such as methylation and deacetylation. While associations between FACT and histone methylation or deacetylation have not previously been reported, it has been shown that the Cdc68 subunit of FACT interacts physically and genetically with the Sas3 histone acetyltransferase (John *et al.* 2000). The role(s) of FACT in conjunction with histone modifications remains to be determined; FACT may be a substrate for modifications by these complexes, may assist in localizing histone-modifying complexes to sites of action, or may recognize specific histone modifications when binding or depositing histones.

Finally, consistent with the localization of FACT to both initiation and elongation stages of transcription, the *cdc68-E763G* mutation is shown here to cause synthetic sickness in cells when combined with *med1Δ*, eliminating a component of the Mediator complex (Balciunas *et al.* 1999; Mason and Struhl 2003). The Mediator complex in yeast consists of approximately 20 subunits and is important for regulation of RNA polymerase II transcription initiation, but is not found in association with the elongating polymerase (Pokholok *et al.* 2002). This synthetic genetic interaction between Mediator and FACT suggests an overlapping function between these two complexes, potentially involving transcription initiation (Mason and Struhl 2003).

In summary, the SGA results for the *cdc68-E763G* allele demonstrate strong genetic ties with genes encoding proteins that function in vesicular transport, particularly between the TGN and the endosomal compartments, and in cell integrity and morphogenesis. It is difficult to imagine a direct role for Cdc68 in these functions. However, given the role Cdc68 plays in RNA polymerase II transcription, it may be that this *cdc68* mutation causes alterations in transcription that impinge upon genes encoding proteins that mediate vesicular transport and/or cell integrity. Further perturbations to these functions by deletion of genes involved in these processes may therefore be expected to generate synthetic growth defects. The processes of vesicular transport and cell integrity are intimately connected, as proteins and glucans required for the synthesis of the cell wall must be modified and transported from internal organelles to the cell surface. Additionally, during times of cell-wall growth or repair, new materials must be transported to the proper sites on the cell surface; defects in transport can therefore result in cell-wall integrity and polarized-growth impairments. In addition to these synthetic lethal relationships, several novel genetic associations are identified here between *cdc68* and deletions of genes involved in transcription initiation and elongation as well as in histone modification, namely *med1Δ*, *cdc73Δ*, *dst1Δ*, *set2Δ*, *sum1Δ*, and *plo1Δ/hda3Δ*. These findings may highlight novel roles for Cdc68 and FACT in mediating histone modification as well as deposition, and certainly continue to strengthen the case for FACT activity during transcription.

vi) Synthetic genetic array analysis with *cdc68-312::natMX4*

Two SGA screens were performed with a derivative of the Y2454 strain that contains the *cdc68-312* allele tagged with the *natMX4* cassette. The *cdc68-312* allele is closely related to *cdc68-E763G* as it too contains the mutational change that results in the glutamate-to-glycine substitution at residue 763. However, the *cdc68-312* allele contains two additional point mutations that result in non-conservative substitutions at residues 784 and 819, which make this allele more deleterious than *cdc68-E763G* as indicated by the severity of mutant phenotypes (Results 2). The SGA analysis (Table 17) identified approximately 1000 gene deletions as synthetically sick or lethal in combination with *cdc68-312*; however, only 175 of these deletions were identified in both screens and are not members of the linkage group or typically identified as false positives in SGA analysis. Each of these gene deletions was then further tested for growth defects in combination with *cdc68-312* using random-spore methodology, and in this way 83 of the initial candidates were verified as causing synthetic growth defects in combination with *cdc68-312* (Appendix 1; Table 20). Figure 63 shows these gene deletions clustered into functional groups based on gene ontology descriptions using the Yeast GRID database as a source, with previously identified interactions between genes within the set also displayed. Of the 83 genes that cause synthetic growth defects when deleted with *cdc68-312*, 43 have previously characterized genetic or physical interactions within the group (Figure 64). A high degree of connectivity is observed for this set of genes, with 68 previously identified genetic and physical interactions within the 43-gene set.

a) Common SGA interactions for *cdc68-E763G* and *cdc68-312* with genes involved in transport, cell integrity and morphogenesis

As was the case for the *cdc68-E763G* allele, many genes encoding components of the vesicular-transport machinery, 40 in total, were identified here as synthetically sick or lethal with *cdc68-312*. Several of these genes were also identified as synthetically lethal with *cdc68-E763G* and many encode proteins that function in transport from the TGN to the endosome. Once again, a large number of genes encoding proteins involved in cell integrity and morphogenesis were also identified. Among them are Skn7, a transcription factor that regulates expression of cell-wall biosynthetic components, Gas1, a

Table 20. Gene deletions that are synthetically sick or lethal in combination with *cdc68-312*.

Transcription:

Gene Name	Systematic Name	Description	Gene Ontology
CAF40	YNL288W	CCR4 Associated Factor 40 kDa	transcription; metabolism
OPI1	YHL020C	Transcriptional regulator of a variety of genes; phosphorylation by protein kinase A stimulates Opi1p function in negative regulation of phospholipid biosynthetic genes	metabolism; transcription
PLO1	YPR179C	Subunit of a possibly tetrameric trichostatin A-sensitive class II histone deacetylase complex that contains an Hda1p homodimer and an Hda2p-Hda3p heterodimer; required for the activity of the complex; has similarity to Hda2p	metabolism; DNA metabolism; cell organization and biogenesis; cell growth and/or maintenance; transcription
RTG3	YBL103C	bHLH/Zip transcription factor which regulates CIT2 gene expression	transcription; metabolism
SKN7	YHR206W	Protein with similarity to DNA-binding region of heat shock transcription factors	response to stress; metabolism; transcription
SUM1	YDR310C	Suppresor of mar1-1 sir2 mutation	transcription; metabolism; DNA metabolism; cell organization and biogenesis; cell growth and/or maintenance; cell cycle

Transport:

Gene Name	Systematic Name	Description	Gene Ontology
AGE2	YIL044C	ADP-ribosylation factor ARF GTPase activating protein GAP effector	transport; cell growth and/or maintenance
APL4	YPR029C	Gamma-adaptin, large subunit of the clathrin-associated protein AP complex	transport; cell growth and/or maintenance
APL5	YPL195W	Delta-like subunit of the yeast AP-3 complex which functions in transport of alkaline phosphatase to the vacuole via the alternate pathway, suppressor of loss of casein kinase 1 function	transport; cell growth and/or maintenance; cell organization and biogenesis

APL6	YGR261C	beta3-like subunit of the yeast AP-3 complex which functions in transport of alkaline phosphatase to the vacuole via the alternate pathway, suppressor of loss of casein kinase 1 function	transport; cell growth and/or maintenance; cell organization and biogenesis
APM1	YPL259C	medium subunit of the clathrin-associated protein complex	transport; cell growth and/or maintenance
APS1	YLR170C	Involved in a subset of clathrin functions at the Golgi	transport; cell growth and/or maintenance
ARL1	YBR164C	Encodes a regulator of membrane traffic. Hydrolyzes GTP; myristylated; in soluble fraction. Part of the carboxypeptidase Y pathway.	transport; cell growth and/or maintenance; protein transport; metabolism
ARL3	YPL051W	Similar to ADP-ribosylation factor. Part of the carboxypeptidase Y pathway.	protein transport; transport; cell growth and/or maintenance
COD2	YNL041C	Conserved Oligomeric Golgi complex 6 Complexed with Cog8p; interacts with Cog2p	transport; cell growth and/or maintenance
COD5	YGL005C	Conserved Oligomeric Golgi complex 7 Complexed with Cog8p	transport; cell growth and/or maintenance
DOR1	YML071C	Conserved Oligomeric Golgi complex 8 dependent on RIC1	transport; cell growth and/or maintenance
DRS2	YAL026C	Integral membrane Ca 2+ -ATPase involved in cleavage of the 20S precursor of the 18S rRNA; potential aminophospholipid translocase required to form a specific class of secretory vesicles that accumulate upon actin cytoskeleton disruption	transport; cell growth and/or maintenance; protein transport; RNA processing; ribosome biogenesis; metabolism; cell organization and biogenesis
GSG1	YDR108W	Subunit of TRAPP transport protein particle , a multi-subunit complex involved in targeting and/or fusion of ER-to-Golgi transport vesicles with their acceptor compartment; protein has late meiotic role, following DNA replication	transport; cell growth and/or maintenance; cell cycle
GUP1	YGL084C	Multimembrane-spanning protein and putative glycerol transporter that is essential for proton symport of glycerol; Gup2p homolog	transport; cell growth and/or maintenance; metabolism
GYP1	YOR070C	Cis-golgi GTPase-activating protein GAP for the Rab family members Ypt1p in vivo and for Ypt1p, Sec4p, Ypt7p, and Ypt51p in vitro ; involved in vesicle docking and fusion	transport; cell growth and/or maintenance

LYS7	YMR038C	Involved in lysine biosynthesis, oxidative stress protection	transport; cell growth and/or maintenance
MON1	YGL124C	Protein required for fusion of cvt-vesicles and autophagosomes with the vacuole; associates, as a complex with Ccz1p, with a perivacuolar compartment; potential Cdc28p substrate	protein transport; metabolism; transport; cell growth and/or maintenance; autophagy
PEP8	YJL053W	Plays a role in delivery of proteins to the vacuole	transport; protein transport; metabolism; cell growth and/or maintenance; cell organization and biogenesis
RAV2	YDR202C	Regulator of H+ -ATPase in Vacuolar membrane	transport; cell growth and/or maintenance; cell organization and biogenesis
RER1	YCL001W	Protein involved in retention of membrane proteins, including Sec12p, in the ER; localized to Golgi, where it may function in returning membrane proteins to the ER	transport; cell growth and/or maintenance
RGP1	YDR137W	Ric1p-Rgp1p is an exchange factor, and peripheral membrane protein complex restricted to the Golgi.	protein transport; transport; cell growth and/or maintenance
RUD3	YOR216C	Novel matrix protein that is involved in the structural organization of the cis-Golgi. Relieves uso1-1 transport defect; golgin-160 related protein.	transport; cell growth and/or maintenance
SEC28	YIL076W	Part of a heptameric protein complex that regulates retrograde Golgi-to-ER protein traffic in eukaryotic cells; coatomer forms the COP I vesicle coat whose functions are essential	transport; cell growth and/or maintenance
SEC66	YBR171W	glycoprotein complexed with Sec62p and Sec63p in the Sec63 complex, an integral endoplasmic reticulum membrane protein complex required for translocation of presecretory proteins	transport; protein transport; metabolism; cell growth and/or maintenance
VAC8	YEL013W	Phosphorylated vacuolar membrane protein that interacts with Atg13p, required for the cytoplasm-to-vacuole targeting Cvt pathway; interacts with Nvj1p to form nucleus-vacuole junctions	autophagy; cell growth and/or maintenance; cell organization and biogenesis; protein transport; metabolism; transport

VAM3	YOR106W	Syntaxin-related protein; required for vacuolar assembly; PEP12 homolog	transport; cell growth and/or maintenance; cell organization and biogenesis
VMA6	YLR447C	vacuolar ATPase V0 domain subunit d 36 kDa	transport; cell growth and/or maintenance; cell organization and biogenesis
VPS1	YKR001C	involved in vacuolar protein sorting and normal organization of intracellular membranes; probably required for membrane-protein retention in a late Golgi compartment	protein transport; metabolism; transport; cell growth and/or maintenance; cell organization and biogenesis
VPS17	YOR132W	Peripheral membrane protein required for vacuolar protein sorting	transport; cell growth and/or maintenance; cell organization and biogenesis
VPS21	YOR089C	Rab5-like GTPase involved in vacuolar protein sorting and endocytosis post vesicle internalization; geranylgeranylated; geranylgeranylation required for membrane association	transport; cell growth and/or maintenance; protein transport; metabolism
VPS38	YLR360W	involved in vacuolar protein targeting	transport; cell growth and/or maintenance; cell organization and biogenesis
VPS4	YPR173C	Defective in vacuolar protein sorting; homologous to mouse SKD1 and to human hVPS4	transport; protein transport; metabolism; cell growth and/or maintenance; cell organization and biogenesis
VPS5	YOR069W	Vacuolar Protein Sorting. component of the retromer coat that retrieves proteins from late endosomes.	transport; protein transport; metabolism; cell growth and/or maintenance; cell organization and biogenesis
VPS67	YKR020W	whiskey whi mutant; forms a tetramer with VPS52, VPS53, and VPS54	protein transport; metabolism; transport; cell growth and/or maintenance; budding; cell organization and biogenesis
VPS72	YDR485C	NONE	protein transport; metabolism; transport; cell growth and/or maintenance

VPS74	YDR372C	NONE	protein transport; metabolism; transport; cell growth and/or maintenance
VTA1	YLR181C	Has coiled-coil domains and is involved in class E vacuolar-protein sorting; binds to Vps20 and Vps4 and may regulate Vps4 function	transport; cell growth and/or maintenance; cell organization and biogenesis
YDR153C	YDR153C	Protein containing an N-terminal epsin-like domain involved in clathrin recruitment and traffic between the Golgi and endosomes; associates with the clathrin adaptor Gga2p, clathrin adaptor complex AP-1, and clathrin	transport; cell growth and/or maintenance; cell organization and biogenesis
YIP3	YNL044W	Interacts with YPT proteins	transport; cell growth and/or maintenance
YPT7	YML001W	Gtp-binding protein of the rab family; required for homotypic fusion event in vacuole inheritance, for endosome-endosome fusion, and for fusion of endosomes to vacuoles when expressed from high copy plasmid	cell organization and biogenesis; cell growth and/or maintenance; transport

Cell growth and/ or maintenance:

Gene Name	Systematic Name	Description	Gene Ontology
BUD14	YAR014C	Protein involved in bud-site selection; diploid mutants display a random budding pattern instead of the wild-type bipolar pattern	cell organization and biogenesis; cell growth and/or maintenance
GAS1	YMR307W	Glycophospholipid-anchored surface protein	cell organization and biogenesis; cell growth and/or maintenance
VAM6	YDL077C	Required for the vacuolar morphogenesis in yeast	cell organization and biogenesis; cell growth and/or maintenance
WHI3	YNL197C	RNA binding protein that binds to and sequesters the G1 cyclin CLN3 mRNA; regulates cell fate and dose-dependently inhibits passage through Start by regulating the critical cell size requirement necessary for cell cycle progression	cell organization and biogenesis; cell growth and/or maintenance
YGL020C	YGL020C	Spore Wall Formation. Mitochondrial Distribution and Morphology	cell organization and biogenesis; cell growth and/or maintenance
YOR068C	YOR068C	[Abnormal]Vacuole Morphology	cell organization and biogenesis; cell growth and/or maintenance

Protein biosynthesis:

Gene Name	Systematic Name	Description	Gene Ontology
MNN2	YBR015C	Probable type II membrane protein involved in mannan synthesis. Catalyzes addition of first mannose to branches on poly 1,6-mannose backbone of outer chain of cell wall N-linked mannans.	protein biosynthesis; metabolism
MNN11	YJL183W	member of a cis Golgi complex that is involved in mannan synthesis, other complex members include Mnn10p, Hoc1p, Anp1p, Mnn9p	protein biosynthesis; metabolism
RPL34B	YIL052C	Homology to rat L34	protein biosynthesis; metabolism
SPF1	YEL031W	Sensitivity to a killer toxin SMK toxin produced by Pichia Farinosa	protein biosynthesis; metabolism; cell growth and/or maintenance
TEF4	YKL081W	Translation elongation factor EF-1gamma	protein biosynthesis; metabolism

Stress response:

Gene Name	Systematic Name	Description	Gene Ontology
ELM1	YKL048C	cell morphology	cell growth and/or maintenance; protein amino acid phosphorylation; metabolism; response to stress; budding; cell organization and biogenesis
OXR1	YPL196W	OXidation Resistance	response to stress; metabolism
WHI2	YOR043W	Protein required, with binding partner Psr1p, for full activation of the general stress response, possibly through Msn2p dephosphorylation; regulates growth during the diauxic shift; negative regulator of G1 cyclin expression	response to stress

Metabolism:

Gene Name	Systematic Name	Description	Gene Ontology
CHO2	YGR157W	First step in the methylation pathway for phosphatidylcholine biosynthesis	metabolism

PSD1	YNL169C	Converts phosphatidylserine to phosphatidylethanolamine. Mitochondrial Psd1p provides ~90% of total cellular phosphatidylserine decarboxylase activity.	metabolsim
URE2	YNL229C	Nitrogen catabolite repression regulator that acts by inhibition of GLN3 in good nitrogen source. Altered form of Ure2p creates [URE3] prion.	metabolism

Signal transduction:

Gene Name	Systematic Name	Description	Gene Ontology
SAC7	YDR389W	GTPase activating protein GAP for Rho1p, involved in signaling to the actin cytoskeleton, null mutations suppress tor2 mutations and temperature sensitive mutations in actin; potential Cdc28p substrate	signal transduction; cell cycle; cell growth and/or maintenance; cell organization and biogenesis
RTG2	YGL252C	Protein involved in interorganelle communication between mitochondria, peroxisomes, and nucleus. Likely role of Rtg2p is to antagonize Mks1p, a negative regulator of RTG target gene activation.	signal transduction

DNA repair:

Gene Name	Systematic Name	Description	Gene Ontology
MRE11	YMR224C	Disp. for premeiotic DNA synthesis, but required for both double strand break formation & resection, synaptonemal complexes, meiotic recombination & viable spores. Localizes to discrete sites in rad50 mutants	DNA repair; DNA metabolism; response to DNA damage stimulus; response to stress; metabolism; DNA recombination; cell cycle; cell growth and/or maintenance

Protein degradation:

Gene Name	Systematic Name	Description	Gene Ontology
RPN10	YHR200W	homolog of the mammalian S5a protein, component of 26S proteasome	protein catabolism; metabolism

Carbohydrate metabolism:

Gene Name	Systematic Name	Description	Gene Ontology
SMI1	YGR229C	Protein involved in 1,3 -beta-glucan synthesis, possibly through regulation of cell wall glucan and chitin synthesis; chromatin binding protein	carbohydrate metabolism; metabolism; cell organization and biogenesis; cell growth and/or maintenance

Unknown:

Gene Name	Systematic Name	Description	Gene Ontology
KRE25	YNL296W	Hypothetical ORF	UNKNOWN
NBP2	YDR162C	interacts with Nap1, which is involved in histone assembly	biological process unknown
PSL10	YDR126W	Spore Wall Formation	biological process unknown
PSP1	YDR505C	high-copy suppressor of cdc17 DNA polymerase alpha mutations	biological process unknown
VPS60	YDR486C	vacuolar protein sorting putative	biological process unknown
YAL058C-A	YAL056C-A	Hypothetical ORF	NONE
YDL206W	YDL206W	NONE	biological process unknown
YDR203W	YDR203W	Hypothetical ORF	NONE
YEL043W	YEL043W	NONE	biological process unknown
YIL110W	YIL110W	NONE	biological_process unknown
YLR111W	YLR111W	Hypothetical ORF	NONE
YLR169W	YLR169W	Hypothetical ORF	NONE
YLR171W	YLR171W	Hypothetical ORF	NONE
YMR003W	YMR003W	NONE	biological_process unknown
YPR090W	YPR089W	NONE	biological process unknown

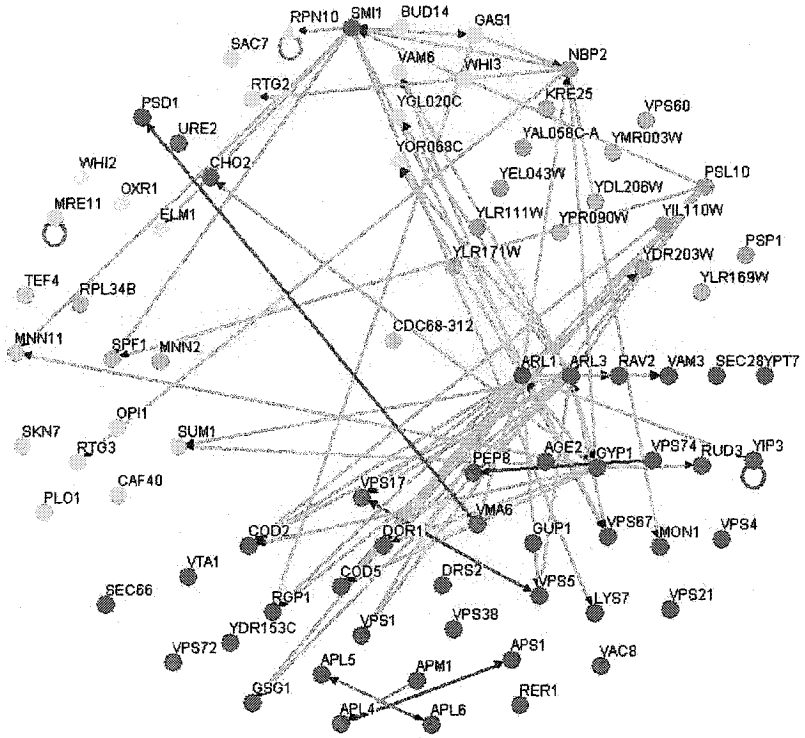

Figure 63. Synthetic genetic interactions involving *cdc68-312*. Each gene deletion identified by SGA and verified by random-spore analysis as synthetically sick or lethal in combination with *cdc68-312* is indicated by a coloured node, and previously identified genetic or physical interactions between two genes are indicated by coloured lines (see Appendix 2 for legend). The *cdc68-312* mutant gene is shown in the middle of the web and should have green lines, indicating a synthetic sick or lethal interaction, connecting it to all of the gene deletions shown, but for clarity these lines have been omitted. A high degree of connectivity can be seen in this group of genetic interactions, which indicates overlapping functions. The key 'hubs' of interactions are displayed in Figure 64.

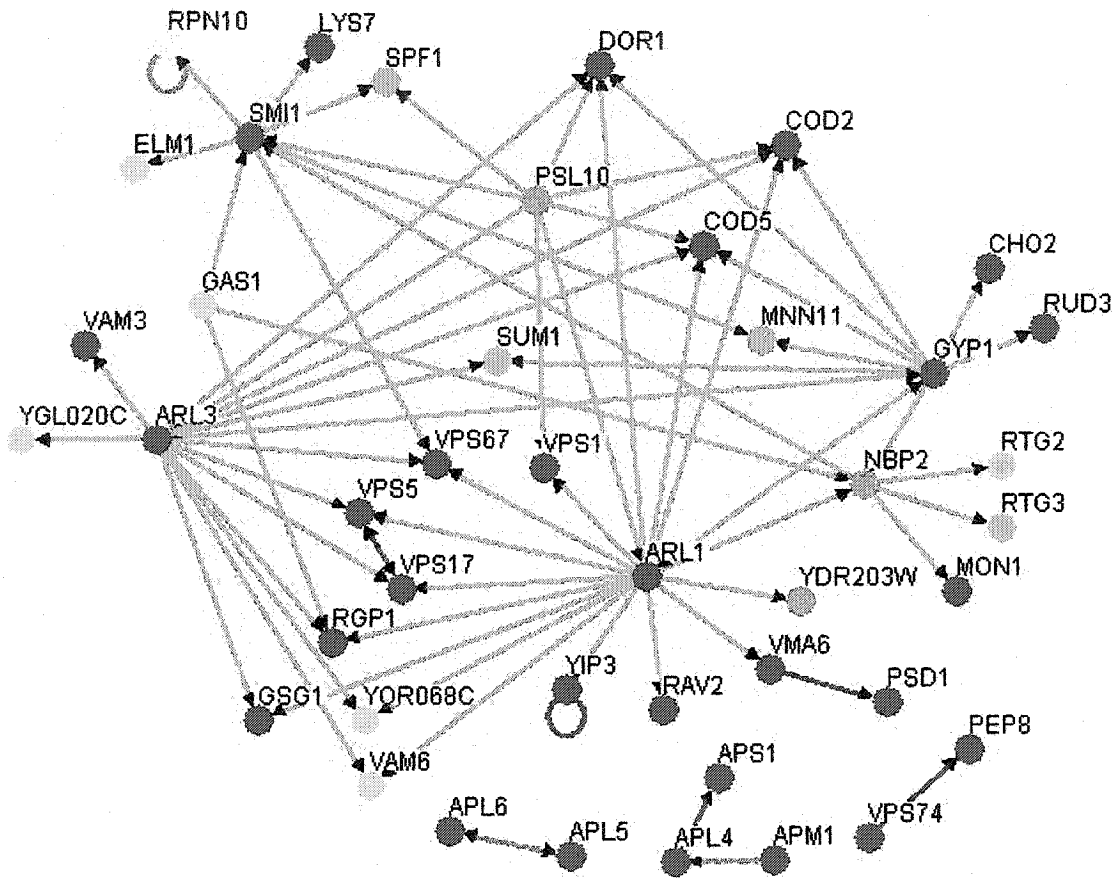

Figure 64. Connectivity of synthetic genetic interactions with *cdc68-312*. Of the 83 genes identified as having a synthetic genetic relationship when deleted in in combination with *cdc68-312*, the 43 with previously identified genetic or physical interactions are shown. These 43 genes show a high degree of connectivity, with 68 interactions among them. The legend for line and node colours is given in Appendix 2.

glucanosyltransferase located on the external face of the plasma membrane, *Elm1*, a kinase involved in polarized growth and bud-neck formation, Bud14, a protein that assists in bud-site selection, Smi1/Knr4, a regulator of Pkc1-pathway Slt2 kinase that is able to stimulate glucan synthesis, and Mnn2 and Mnn11, involved in mannan synthesis and conjugation to proteins. These findings have the same implications for the *cdc68-312* allele as they did for *cdc68-E763G* and indicate a role for Cdc68 in transport and cell morphogenesis, two processes that are intimately connected.

An alternative possibility is that the *natMX4* integration downstream of these two *cdc68* alleles somehow affects activity of the neighboring *CHC1* gene, which encodes clathrin heavy chain. However, neither the *natMX4*-tagged wild-type *CDC68* gene nor *cdc68-E857K* allele identified a significant number of genes involved in vesicular transport or cell integrity and morphogenesis through SGA analysis. These alleles were all tagged using the identical one-step genomic fragment-swap procedure (Materials and Methods). An effect on the neighboring *CHC1* gene would therefore have to have arisen through some anomalous integration event that would have had to have occurred independently for these two alleles. A more appealing explanation is that these two alleles have a large number of common genetic interactions because they contain a common point mutation and therefore have similar effects. Of the 90 and 83 genes identified as causing synthetic sickness or lethality when deleted with *cdc68-E763G* and *cdc68-312*, respectively, 53 of them, or approximately 60%, are common to both datasets (Figure 65).

b) *cdc68-312* SGA interactions with genes involved in transcription

In addition to the genetic interactions identified for *cdc68-312* with genes encoding transport and morphogenesis proteins, interactions involving transcription functions were found. Like the *cdc68-E763G* allele, the *cdc68-312* allele causes synthetic sickness with *sum1Δ* and *plo1Δ*, which eliminate proteins that associate with histone deacetylases. The *opi1Δ* deletion was identified here as synthetically lethal with *cdc68-312*. The *OPI1* gene encodes a transcription repressor for genes involved in inositol and phospholipids biosynthesis, but the Opi1 protein also associates with the Sin3 histone deacetylase (Wagner *et al.* 2001). One possible explanation for these findings is that when *cdc68* is mutated histone deacetylases do not function as effectively, and therefore loss of other

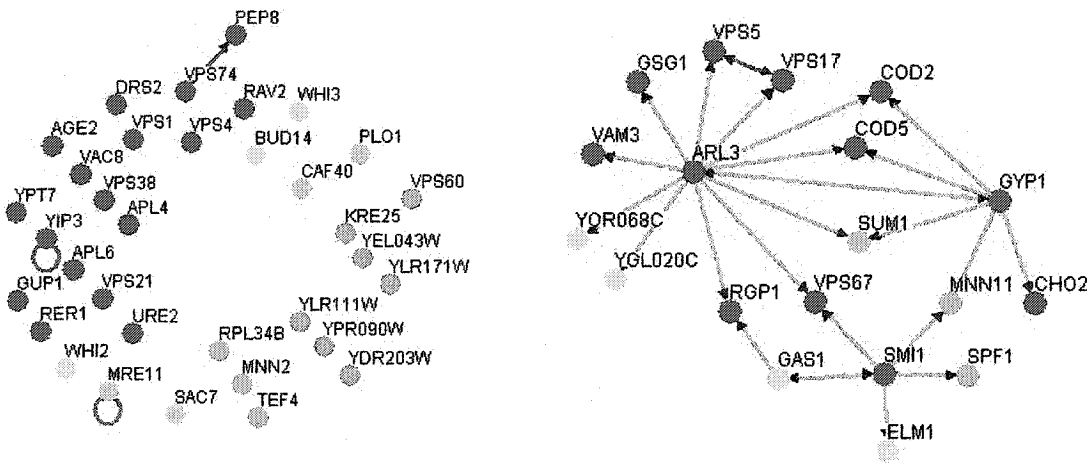

Figure 65. Gene deletions causing growth defects with both *cdc68-E763G* and *cdc68-312*. The 53 gene deletions identified as synthetically sick or lethal when combined with *cdc68-E763G* and *cdc68-312* are indicated as coloured nodes (colour coding is given in Appendix 2). The gene cluster on the left represents 'loner nodes' that do not have previously identified genetic or physical interactions with other genes in this dataset. The gene cluster on the right shows previously identified genetic or physical interactions within the dataset.

factors that assist in histone deacetylase activities impairs cell growth. A less direct overlapping function between Cdc68 and these histone deacetylase partners could be in regulating the transcription of an essential gene or several genes within the cell. Therefore, when both the Cdc68 function and histone deacetylase functions are impaired the cell is no longer viable.

RTG3 encodes a transcription factor responsible for the induction of several metabolic genes and whose import into the nucleus is regulated in part by Rtg2 (Sekito *et al.* 2000, 2002). Both *rtg2Δ* and *rtg3Δ* were identified here as synthetically lethal in combination with *cdc68-312*. Perhaps Cdc68 shares an overlapping role in the expression of an essential gene that is typically induced by Rtg3, so when both of these components are functionally impaired cell viability is compromised. Interestingly, *rtg2Δ* and *rtg3Δ* both have synthetic genetic interactions with *nbp2Δ* (Tong *et al.* 2004), which was also identified here as synthetically lethal in combination with *cdc68-312*. Little is known about the function of Nbp2, but it is a Nap1-binding protein as the name implies, and seems to play a role in assisting cell proliferation and cell-wall integrity at elevated temperatures in conjunction with the Pkc1-mediated signal transduction cascade (Ohkuni *et al.* 2003). Nap1 is involved in nucleosome assembly and mediates the nuclear import of histones H2A and H2B, and has also been shown to physically associate with the histone variant H2A.Z, a substitute for H2A found in nucleosomes of some active genes (Gavin *et al.* 2002; Kobor *et al.* 2004). While *nap1Δ* was not identified as having a genetic interaction with *cdc68-312* by SGA analysis, it will be interesting to ecamine the connection between Cdc68 and Nbp2 activities, and if Rtg2 and Rtg3 functions are also involved.

CAF40 (Ccr4 associated factor 40 kDa) encodes a member of the Ccr4-Not complex, which is comprised of approximately nine subunits in yeast and thought to affect RNA stability and transcription initiation (Liu *et al.* 1998; Chen *et al.* 2001). Of the nine subunits of the Ccr4-Not complex, two are essential and would therefore not be identified here and four are gene deletions that commonly cause false positives in SGA analysis. These four Ccr4-Not component were therefore not included in the list of candidates for either *cdc68-E763G* or *cdc68-312*; however, all four of these deletions showed significant growth defects in each of the screens with *cdc68-E763G* and *cdc68-312*,

which could indicate further genetic ties between Ccr4-Not and FACT. Of the remaining three Ccr4-Not components only the *caf40Δ* deletion was identified as synthetically lethal and sick with *cdc68-312* and *cdc68-E763G*, respectively, in each of the screens (Tables 19 and 20). While several physical and genetic interactions have been identified between Ccr4-Not components and RNA polymerase II components, implicating Ccr4-Not in transcription and particularly in RNA polymerase II transcription initiation (Liu *et al.* 2001; Collart 2003), none of these interactions involve *CAF40* specifically. To date the molecular function of Caf40 is unclear. The synthetic genetic relationship between a *caf40Δ* and *cdc68* alleles raises questions about the relationship between Cdc68 and Ccr4-Not activities, and further investigations into the genetic interactions between *cdc68* mutants and deletions of other Ccr4-Not genes is warranted. Given an involvement of Ccr4-Not in RNA stability and particularly in RNA polymerase II transcription initiation, future experiments in this area may identify effects of FACT or these processes as well.

vii) Synthetic genetic array analysis with *cdc68-319::natMX4*

SGA analysis using cells containing the *cdc68-319* allele tagged with the *natMX4* cassette was performed in duplicate (Winzeler *et al.* 1999). Approximately 1500 gene deletions caused synthetic growth defects in cells when the *cdc68-319* allele was also present, and 392 of these deletions were identified in both SGA screens and are not fall into the linkage-group or false-positives categories (Table 17). These 392 candidates were then tested using random-spore analysis, and 22 were also tested by tetrad analysis, to further assess the growth defects of double-mutant cells (data not shown; Appendix 1). In this way, 78 deletions were verified as causing synthetic growth defects in *cdc68-319* cells (Figure 66; Table 21). The connectivity within this group of 78 genes is high, with a total of 83 previously

identified physical and genetic interactions between 45 of the genes identified (Figure 67). Major 'hub' nodes or highly connected genes within this set are *CDC73*, with a striking 26 genetic interactions with genes that show growth defects in combination with *cdc68-319*, *CTF4*, *CTF18*, *ARP6* and *GIM3*.

a) *cdc68-319* SGA interactions with genes involved in transcription

The connections between *cdc68-319* and transcription-related processes within this dataset are abundant. Several genes previously identified as causing synthetic growth

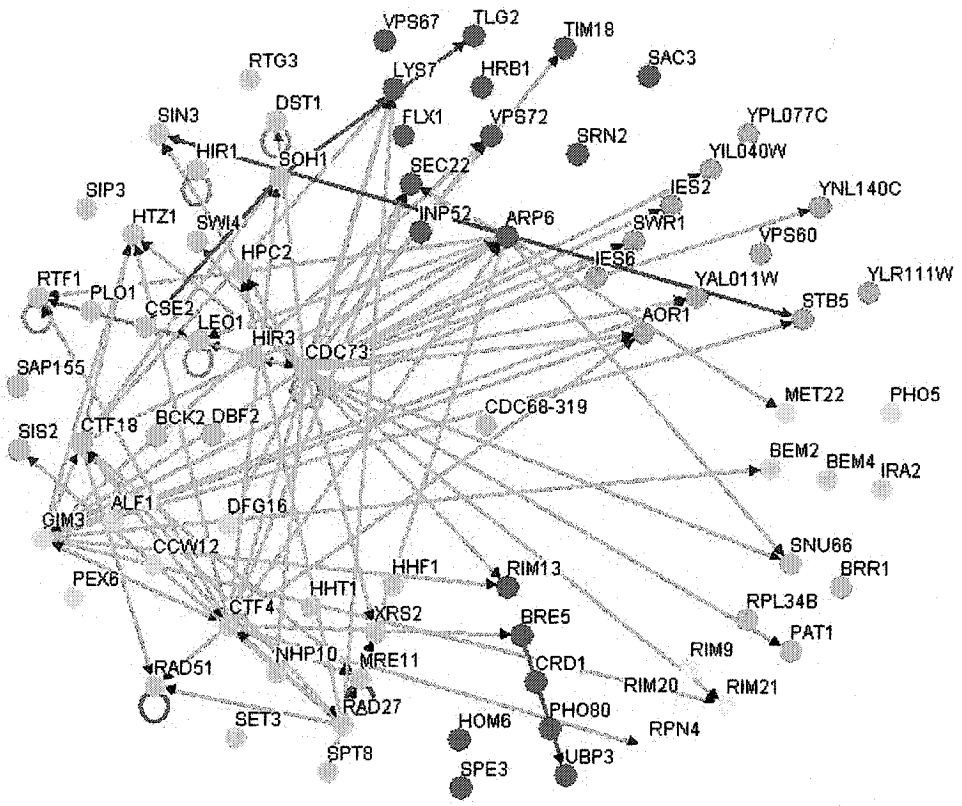

Figure 66. Synthetic genetic interactions with *cdc68-319*. Each gene deletion identified by SGA and verified by random-spore analysis as synthetically sick or lethal in combination with *cdc68-319* is indicated by a coloured node, and previously identified genetic or physical interactions between two genes are indicated by coloured lines (see Appendix 2 for legend). The *cdc68-319* mutant gene is shown in the middle of the web and should have green lines, indicating a synthetic sick or lethal interaction, connecting it to all of the genes shown, but for clarity these lines have been omitted. A high degree of connectivity can be seen in this group of genetic interactions, which indicates overlapping functions. Key 'hubs' of interaction are displayed in Figure 67.

Table 21. Gene deletions that are synthetically sick or lethal in combination with *cdc68-319*.

Transcription:

Gene Name	Systematic Name	Description	Gene Ontology
CDC73	YLR418C	accessory factor associated with RNA polymerase II by affinity chromatography	transcription; metabolism
CSE2	YNR010W	Component of the Med9/10 module, which is a subcomplex within the RNA polymerase II Mediator complex; required for regulation of RNA polymerase II activity	transcription; metabolism; cell cycle; cell growth and/or maintenance
DST1	YGL043W	General transcription elongation factor TFIIS, enables RNA polymerase II to read through blocks to elongation by stimulating cleavage of nascent transcripts stalled at transcription arrest sites	transcription; metabolism; DNA recombination; DNA metabolism; cell cycle; cell growth and/or maintenance
HIR1	YBL008W	Non-essential transcriptional corepressor involved in the cell cycle-regulated transcription of histone H2A, H2B, H3 and H4 genes; contributes to nucleosome formation, heterochromatic gene silencing, and formation of functional kinetochores	transcription; metabolism
HIR3	YJR140C	Transcriptional corepressor involved in the cell cycle-regulated transcription of histone genes HTA1, HTB1, HHT1, and HHT2; involved in position-dependent gene silencing and nucleosome reassembly	cell cycle; transcription; cell growth and/or maintenance; metabolism
HPC2	YBR215W	Protein required for normal cell-cycle regulation of histone gene transcription	cell cycle; transcription; cell growth and/or maintenance; metabolism
HTZ1	YOL012C	Histone-related protein that can suppress histone H4 point mutation	transcription; metabolism; DNA metabolism; cell organization and biogenesis; cell growth and/or maintenance
LEO1	YOR123C	member of the RNA polymerase II-associated Paf1 complex	transcription; metabolism

PLO1	YPR179C	Subunit of a possibly tetrameric trichostatin A-sensitive class II histone deacetylase complex that contains an Hda1p homodimer and an Hda2p-Hda3p heterodimer; required for the activity of the complex; has similarity to Hda2p	metabolism; DNA metabolism; cell organization and biogenesis; cell growth and/or maintenance; transcription
RTF1	YGL244W	Directly or indirectly regulates DNA-binding properties of Spt15p, TATA box-binding protein, and relative activities of different TATA elements. Member of RNA polymerase II-associated Paf1 complex.	transcription; metabolism
RTG3	YBL103C	bHLH/Zip transcription factor which regulates CIT2 gene expression	transcription; metabolism
SIN3	YOL004W	DNA binding protein involved in transcriptional regulation	transcription; metabolism; DNA metabolism; cell organization and biogenesis; cell growth and/or maintenance
SIP3	YNL257C	Protein that activates transcription through interaction with DNA-bound Snf1p, C-terminal region has a putative leucine zipper motif; potential Cdc28p substrate	transcription; metabolism
SOH1	YGL127C	Soh1p has limited sequence similarity to RNA polymerases and interacts with a DNA repair protein, Rad5p, in a two-hybrid system assay; may provide a link between recombination in direct repeats and transcription	transcription; metabolism; DNA repair; DNA metabolism; response to DNA damage stimulus; response to stress
SWI4	YER111C	Involved in cell cycle dependent gene expression	cell cycle; cell growth and/or maintenance; transcription; metabolism

Transport:

Gene Name	Systematic Name	Description	Gene Ontology
ARP6	YLR085C	Actin-related protein. Part of the carboxypeptidase Y pathway.	protein transport; metabolism; transport; cell growth and/or maintenance

FLX1	YIL134W	Protein required for transport of flavin adenine dinucleotide FAD from mitochondria, where it is synthesized from riboflavin, to the cytosol	transport; cell growth and/or maintenance
HRB1	YNL004W	an ORF of unknown function located in a centromeric region duplicated between chromosomes III and XIV	protein transport; metabolism; transport; cell growth and/or maintenance
INP52	YNL106C	Synaptojanin-like protein	transport; cell growth and/or maintenance; metabolism; cell organization and biogenesis
LYS7	YMR038C	Involved in lysine biosynthesis, oxidative stress protection	transport; cell growth and/or maintenance
SAC3	YDR159W	A component of the nuclear pore that is involved in the nuclear export of both mRNA and protein	cell organization and biogenesis; cell growth and/or maintenance; cell cycle; protein transport; metabolism; transport; RNA localization
SEC22	YLR268W	Identified in a screen for dense cells that accumulated invertase at the non-permissive temperature, SEC22 encodes a v-SNARE present on ER to Golgi vesicles and is involved in anterograde and retrograde transport between the ER and Golgi	transport; cell growth and/or maintenance
SRN2	YLR119W	Suppressor of rna1-1 mutation	protein transport; metabolism; transport; cell growth and/or maintenance
TIM18	YOR297C	mitochondrial inner membrane translocase	protein transport; metabolism; transport; cell growth and/or maintenance
TLG2	YOL018C	member of the syntaxin family of t-SNAREs	transport; cell growth and/or maintenance

VPS67	YKR020W	whiskey whi mutant; forms a tetramer with VPS52, VPS53, and VPS54	protein transport; metabolism; transport; cell growth and/or maintenance; budding; cell organization and biogenesis
VPS72	YDR485C	NONE	protein transport; metabolism; transport; cell growth and/or maintenance

Cell growth and maintenance:

Gene Name	Systematic Name	Description	Gene Ontology
ALF1	YNL148C	alpha-tubulin foldin; protein implicated in folding of alpha tubulin	cell organization and biogenesis; cell growth and/or maintenance
CCW12	YLR110C	NONE	cell organization and biogenesis; cell growth and/or maintenance
DFG16	YOR030W	Probable multiple transmembrane protein, involved in invasive growth upon nitrogen starvation	cell organization and biogenesis; cell growth and/or maintenance
GIM3	YNL153C	Prefoldin subunit 4; putative homolog of subunit 4 of bovine prefoldin, a chaperone comprised of six subunits	cell organization and biogenesis; cell growth and/or maintenance
PEX6	YNL329C	Required for peroxisome assembly	cell organization and biogenesis; cell growth and/or maintenance

Protein biosynthesis:

Gene Name	Systematic Name	Description	Gene Ontology
PAT1	YCR077C	Necessary for accurate chromosome transmission during cell; Involved in mRNA turnover	cell cycle; cell growth and/or maintenance; protein biosynthesis; metabolism
RPL34B	YIL052C	Homology to rat L34	protein biosynthesis; metabolism

Cell cycle:

Gene Name	Systematic Name	Description	Gene Ontology
BCK2	YER167W	Rich in serine/threonine residues and functions in the protein kinase C mediated pathway	cell cycle; cell growth and/or maintenance
CTF18	YMR078C	Subunit of a complex with Ctf8p that shares some subunits with Replication Factor C and is required for sister chromatid cohesion; may have overlapping functions with Rad24p in the DNA damage replication checkpoint	cell cycle; cell growth and/or maintenance
DBF2	YGR092W	Kinase required for late nuclear division. Cdc15 promotes the exit from mitosis by directly switching on the kinase activity of Dbf2.	cell cycle; cell growth and/or maintenance; protein amino acid phosphorylation; metabolism
SAP155	YFR040W	155 kDa SIT4 protein phosphatase-associated protein	cell cycle; cell growth and/or maintenance
SIS2	YKR072C	Involved in cell cycle control and ion homeostasis	cell cycle; cell growth and/or maintenance; response to stress; metabolism

Stress response:

Gene Name	Systematic Name	Description	Gene Ontology
MET22	YOL064C	Bisphosphate-3 -nucleotidase, involved in salt tolerance and methionine biogenesis; dephosphorylates 3 -phosphoadenosine-5 -phosphate and 3 -phosphoadenosine-5 -phosphosulfate, intermediates of the sulfate assimilation pathway	metabolism; response to stress
PHO5	YBR093C	Acid phosphatase, repressible	metabolism; response to stress

Metabolism:

Gene Name	Systematic Name	Description	Gene Ontology
BRE5	YNR051C	protein of unknown function	metabolism
CRD1	YDL142C	Cardiolipin synthase; produces cardiolipin, which is an important constituent of mitochondrial membranes; required for normal mitochondrial membrane potential and function	metabolism; cell organization and biogenesis; cell growth and/or maintenance

HOM6	YJR139C	catalyzes third step in common pathway for methionine and threonine biosynthesis	metabolism
PHO80	YOL001W	Negative regulator of PHO81 and PHO5	metabolism
RIM13	YMR154C	Regulator of IME2 RIM	metabolism
SPE3	YPR069C	biosynthesis of spermidine	metabolism
UBP3	YER151C	Possible role for UBP3 in controlling the activity or assembly of the SIR protein complex.	metabolism

Signal transduction:

Gene Name	Systematic Name	Description	Gene Ontology
BEM2	YER155C	Protein with role in bud emergence	cell organization and biogenesis; cell growth and/or maintenance; budding; signal transduction
BEM4	YPL161C	Involved in polarity establishment and bud emergence; interacts with the Rho1p small GTP-binding protein	signal transduction; cell organization and biogenesis; cell growth and/or maintenance
IRA2	YOL081W	Negatively regulates cAPK by antagonizing CDC25	signal transduction

DNA metabolism:

Gene Name	Systematic Name	Description	Gene Ontology
CTF4	YPR135W	Chromatin-associated protein, required for sister chromatid cohesion; interacts with DNA polymerase alpha Pol1p and may link DNA synthesis to sister chromatid cohesion	cell cycle; cell growth and/or maintenance; DNA replication; DNA metabolism; metabolism; DNA repair; response to DNA damage stimulus; response to stress
HHF1	YBR009C	One of two identical histone H4 proteins see also HHF2 ; core histone required for chromatin assembly and chromosome function; contributes to telomeric silencing; N-terminal domain involved in maintaining genomic integrity	DNA metabolism; cell organization and biogenesis; metabolism; cell growth and/or maintenance

HHT1	YBR010W	One of two identical histone H3 proteins see also HHT2 ; core histone required for chromatin assembly, involved in heterochromatin-mediated telomeric and HM silencing; regulated by acetylation, methylation, and mitotic phosphorylation	DNA metabolism; cell organization and biogenesis; metabolism; cell growth and/or maintenance
NHP10	YDL002C	Non-Histone Protein 10	DNA metabolism; cell organization and biogenesis; metabolism; cell growth and/or maintenance
MRE11	YMR224C	Disp. for premeiotic DNA synthesis, but required for both double strand break formation & resection, synaptonemal complexes, meiotic recombination & viable spores. Localizes to discrete sites in rad50 mutants	DNA repair; DNA metabolism; response to DNA damage stimulus; response to stress; metabolism; DNA recombination; cell cycle; cell growth and/or maintenance
RAD27	YKL113C	5 to 3 exonuclease, 5 flap endonuclease, required for Okazaki fragment processing and maturation as well as for long-patch base-excision repair; member of the S. pombe RAD2/FEN1 family	DNA replication; DNA metabolism; cell cycle; metabolism; cell growth and/or maintenance; DNA repair; response to DNA damage stimulus; response to stress; DNA recombination
RAD51	YER095W	Strand exchange protein, forms a helical filament with DNA that searches for homology; involved in the recombinational repair of double-strand breaks in DNA during vegetative growth and meiosis; homolog of Dmc1p and bacterial RecA protein	DNA repair; DNA metabolism; response to DNA damage stimulus; DNA recombination; response to stress; metabolism; cell cycle; cell growth and/or maintenance; cell organization and biogenesis
SET3	YKR029C	NAD-dependant histone deacetylase activity	metabolism; DNA metabolism; cell organization and biogenesis; cell growth and/or maintenance; cell cycle

SPT8	YLR055C	Subunit of the SAGA transcriptional regulatory complex but not present in SAGA-like complex SLIK/SALSA, required for SAGA-mediated inhibition at some promoters	DNA metabolism; cell organization and biogenesis; metabolism; cell growth and/or maintenance
XRS2	YDR369C	classified as an early recombination function, required for DNA repair but dispensable for mitotic recombination xrs2 is hyper-Rec during vegatative growth , required for double strand breaks, meiotic recombination and spore viability	DNA repair; DNA metabolism; response to DNA damage stimulus; response to stress; metabolism; DNA recombination; cell cycle; cell growth and/or maintenance

Protein degradation:

Gene Name	Systematic Name	Description	Gene Ontology
RIM20	YOR275C	Regulator of IME2	metabolism; protein catabolism; sporulation; cell growth and/or maintenance; cell organization and biogenesis
RPN4	YDL020C	Involved in ubiquitin degradation pathway. May act as common transcription factor on proteasomal and proteasome-related genes.	protein catabolism; metabolism

RNA processing:

Gene Name	Systematic Name	Description	Gene Ontology
BRR1	YPR057W	Protein involved in snRNP biogenesis	RNA processing; metabolism
SNU66	YOR308C	66kD U4/U6.U5 snRNP associated protein	RNA processing; metabolism

Sporulation:

Gene Name	Systematic Name	Description	Gene Ontology
RIM21	YNL294C	Regulator of IME2	sporulation; cell growth and/or maintenance; cell organization and biogenesis

RIM9	YMR063W	Regulator of IME2 RIM required for IME1 expression	sporulation; cell growth and/or maintenance

Unknown:

Gene Name	Systematic Name	Description	Gene Ontology
AOR1	YBR231C	Protein of unknown function, localizes to the nucleus	biological process unknown
IES2	YNL215W	Protein that associates with the INO80 chromatin remodeling complex under low-salt conditions	biological process unknown;
IES6	YEL044W	Protein that associates with the INO80 chromatin remodeling complex under low-salt conditions	biological process unknown;
STB5	YHR178W	binds Sin3p in two-hybrid assay	NONE
SWR1	YDR334W	NONE	biological process unknown
VPS60	YDR486C	vacuolar protein sorting putative	biological process unknown
YAL011W	YAL011W	Hypothetical ORF	biological process unknown
YIL040W	YIL040W	Protein of unknown function, localizes to the endoplasmic reticulum	biological process unknown;
YLR111W	YLR111W	Hypothetical ORF	NONE
YNL140C	YNL140C	Hypothetical ORF	NONE
YPL077C	YPL077C	NONE	biological process unknown

defects when deleted with other mutant *cdc68* alleles are found here as well, such as *CDC73* and *LEO1*, encoding two components of the Paf1 complex. In addition to these genetic interactions with the Paf1 complex, *rtf1Δ* was also identified as synthetically sick in combination with *cdc68-319*. However, due to the proximity of *RTF1* to *CDC68* on chromosome VII (55 kbp separate these two genes), fewer double-mutant segregants may be generated as a result of the relative rarity of crossover events in this short stretch of DNA. Therefore, to confirm the synthetic growth defect observed by SGA and random-spore analysis for *rtf1Δ*, tetrad analysis was performed. Double-mutant haploid segregants were infrequent, but they did produce smaller colonies than their single-mutant siblings, indicating that there is indeed a deleterious synthetic interaction between *rtf1Δ* and *cdc68-319*. These findings indicate that further perturbations to Cdc68-319 protein function by disrupting the function of the Paf1 complex results in lethality or slow growth. As indicated in sections above, synthetic lethal interactions between mutations in Paf1-complex genes and FACT mutations are not unprecedented (Costa and Arndt 2000; Squazzo *et al.* 2002). The number of genes shown here to be synthetically sick or lethal in combination with either *cdc73Δ* or *cdc68-319* (Figure 67; Tong *et al.*, 2004) is further evidence that the functions of the Paf1 and FACT complexes overlap significantly. Since the *cdc73Δ* and *cdc68-319* share a larger number of common genetic interactions than *cdc73Δ* and any other *cdc68* allele examined here, *cdc68-319* must impact the cell in a similar way as *cdc73Δ*. This similarity emphasizes the possibility of a transcription-elongation defect *cdc68-319* cells. For some of the genes that share an overlapping function with both Cdc68 and Cdc73 as evidenced by synthetic growth defects, it is difficult to ascribe functional links between the proteins they encode and the known functions of Cdc68 and Cdc73. However, a significant number are also involved in transcription and in chromatin modulation.

The implications of synthetic growth defects resulting from deletion of *DST1* in combination with *cdc68* mutations are discussed above (Results 4, iv). The identification here of *dst1Δ* as synthetically lethal with *cdc68-319* further strengthens the ties between this mutation and effects on transcription elongation. *SOH1* encodes an elongation factor not identified here in SGA screens with any other *cdc68* mutation, but *soh1Δ* is synthetically lethal in combination with *cdc68-319*. While the function of Soh1 in

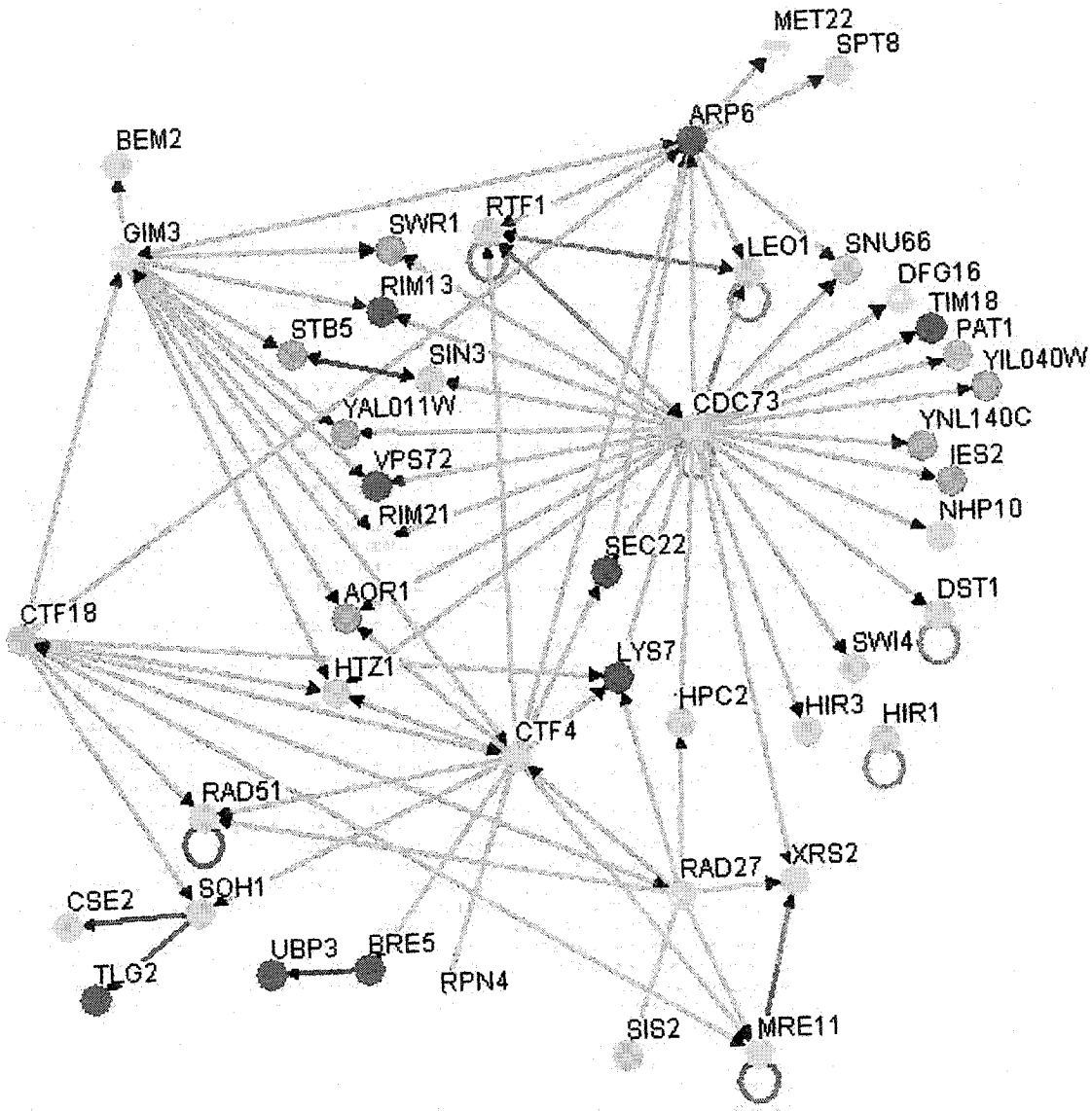

Figure 67. Connectivity of synthetic genetic interactions with *cdc68-319*. Of the 78 genes identified as having a synthetic genetic relationship when deleted in the *cdc68-319* cells, the 45 with previously identified genetic or physical interactions are shown. These 45 genes show a high degree of connectivity, with 83 interactions among them. The legend for line and node colours is given in Appendix 2.

transcription is unclear, mutations in *soh1* cause synthetic growth defects when combined with mutations in genes encoding RNA polymerase II components, and two-hybrid analysis indicates that Soh1 physically interacts with RNA polymerase II and Mediator components (Fan *et al.* 1996; Ito *et al.* 2002). Recent findings have also shown a synthetic growth defect for cells containing both *soh1Δ* and *dst1Δ*, and this finding as well as other genetic associations implicates Soh1 in transcription elongation (Krogan *et al.* 2003b; Malagon *et al.* 2004). This interaction is not present on the interactions webs shown in Figures 66 or 67 because the SGA-identified interactions for *dst1Δ* are not yet present in the Yeast GRID database, which I have used as the sole source for generating the interaction webs.

One of the physical interactions for Soh1 is a two-hybrid interaction with the Cse2 protein, a component of the Mediator complex that functions in transcription initiation (Ito *et al.* 2002). Cells containing the *cdc68-319* mutation show a synthetic growth defect when *CSE2* is deleted, which may implicate Cdc68 in transcription-initiation processes. The synthetic growth defects observed between *cdc68-319* and deletions of genes encoding the transcription factors Rtg3, Sip3, and Swi4 imply that Cdc68 may be important for transcription factor activities, such as recruiting histone-modifying complexes or the polymerase itself (the implications of *cdc68-319* and *swi4Δ* synthetic lethality are more fully explored in Results 3). These interactions could also indicate that Cdc68 and these transcription factors are involved in regulating the transcription of an essential gene, so that when FACT is mutated and the transcription factor is absent this essential gene product is no longer generated. The genetic associations of *cdc68* with genes involved in the initial phases of RNA polymerase II recruitment to promoters and transcription initiation continues to support a role for FACT in these processes as well as its role in transcription elongation. FACT may be a key player in mediating the switch from one phase of transcription to the next.

The deletions *soh1Δ*, *dst1Δ*, *cdc73Δ*, or *set2Δ*, which all show synthetic lethality with *cdc68* mutations, also result in synthetic growth defects when combined with deletions of genes encoding SWR-C complex members (Krogan *et al.* 2003b; Malagon *et al.* 2004). SWR-C is composed of eight non-essential proteins (Vps71/Swc6, Swr1, Arp6, Yaf9, Vps72/Swc2, Aor1/Swc5, Yal011w/Swc1 and Ylr385c/Swc7) and five essential proteins

(Arp4, Act1, God1/Swc4, Rvb1, and Rvb2), and is involved in alterations to chromatin structure during transcription elongation (Krogan *et al.* 2003b; Kobor *et al.* 2004; Mizuguchi *et al.* 2004). The Swr1 component of this complex is an ATPase similar to those of the Snf2 family, known to function in ATP-dependent nucleosome remodelling complexes (Mizuguchi *et al.* 2004). Accordingly, a role for SWR-C in ATP-dependent chromatin remodelling has recently been defined. SWR-C physically associates with the histone variant H2A.Z and facilitates the incorporation of this histone into nucleosomes on transcriptionally active DNA templates (Krogan *et al.* 2003b; Kobor *et al.* 2004; Mizuguchi *et al.* 2004). The presence of this histone H2A variant in nucleosomes is associated with preventing the spread of silencing at telomeric regions and is associated with transcriptionally active regions of DNA (Krogan *et al.* 2003b; Mizuguchi *et al.* 2004). The incorporation of H2A.Z into nucleosomes occurs primarily at genes adjacent to silenced or 'heterochromatic' DNA regions (*i.e.* telomeres), but there are additional sites of incorporation throughout the genome, the significance of which is currently uncertain (Krogan *et al.* 2003b; Kobor *et al.* 2004; Mizuguchi *et al.* 2004). Given the synthetic growth defects when a deletion of the H2A.Z gene *HTZ1* is combined with *dst1Δ*, *set2Δ*, or *cdc73Δ*, it is possible that incorporation of H2A.Z is important during transcription elongation (Krogan *et al.* 2003b; Malagon *et al.* 2004). My SGA analysis with *cdc68-319* also identified *htz1Δ*, and deletions of five of the eight genes encoding nonessential members of the SWR-C complex (*ARP6*, *VPS72/SWC2*, *AOR1/SWC5*, *SWR1*, and *YAL011w/SWC1*) as synthetically lethal. The other three non-essential members of SWR-C showed little to no growth defects in either of the SGA screens using *cdc68-319*. However, given the genetic ties identified here with genes encoding other SWR-C members, the interactions between these three members as well as interactions with the genes encoding essential complex components and *cdc68* merits further investigation. The evidence presented here is the first linking FACT and SWR-C activities. FACT is thought to interact with the H2A/H2B dimer to 'loosen' its association with the rest of the nucleosome core during transcription elongation; therefore it would be interesting to know if SWR-C is also involved in this activity, perhaps by specifically replacing the H2A/H2B dimer with an H2A.Z/H2B dimer during the

elongation process. Further studies in this area will undoubtedly lead to new insight into the mechanism of FACT activity as a histone chaperone.

SWR-C shares components with the INO80 histone-remodelling complex and the NuA4 histone-acetyltranserase complex (Kobor *et al.* 2004). The genes encoding the Ies2, Ies6, and Nhp10 components of the INO80 remodelling complex are identified here as synthetically lethal when deleted in combination with *cdc68-319* (Shen *et al.* 2000; Gavin *et al.* 2002; Shen 2003). The synthetic lethality of *nhp10Δ* with *cdc68-319* could be related more directly to the FACT complex, which includes Nhp6 proteins that are highly similar to Nhp10, but no physical association between the Cdc68-Pob3 dimer and Nhp10 has yet been shown (Brewster *et al.* 2001). The INO80 complex includes at least six other non-essential proteins, but gene deletions for these were not identified here as causing a growth defect with *cdc68-319*. It may be that deletion of only a subset of INO80 components impairs function in ways that functionally overlap with those of Cdc68; however, a redundant role for FACT and INO80 in mediating chromatin structural alterations seems a likely prospect.

Deletions of genes encoding members of histone-modifying complexes were identified as synthetically sick or lethal with *cdc68-319*, including *plo1Δ/hda3Δ*, *set3Δ*, and *sin3Δ*, which all encode members of histone deacetylase complexes (Set3 encodes a histone methyltransferase), and *spt8Δ*, a member of the SAGA histone acetyltransferase. In each case there are additional members to these complexes that were not identified here. These results suggest that Cdc68 functions in parallel to many histone-modifiying and/or -remodelling factors, and are consistent with roles for FACT in histone deposition as well as in transcription, replication and repair. It is clear that the *cdc68-319* mutation perturbs these FACT-mediated processes, as further impairments to histone modification or remodelling result in impaired growth or lethality.

The role for FACT as a histone 'chaperone' or functioning in histone deposition is further supported by the SGA finding that *cdc68* mutations are lethal in combination with loss of other histone chaperones or with histone dosage alterations. The *cdc68-E857K* SGA analysis identified synthetic genetic interactions with deletions of *HIR* genes (Results 4, i and iv). Similarly, the identification of three of the four *HIR* genes as synthetically lethal with *cdc68-319* suggests that the histone 'chaperone' function of

Cdc68 may be impaired as a result of the *cdc68-319* mutations. Transcription elongation may be hampered in cells with Cdc68-319 protein as a result of an inability of FACT complexes containing this protein to efficiently remove the nucleosomal block in front of, or redeposit histones as nucleosomes behind, the elongating RNA polymerase II enzyme. The failure to identify the *hir2Δ* gene deletion as causing a synthetic defect in *cdc68-319* cells should be further explored, in addition to the combination of this *cdc68* mutation with other chromatin-chaperone mutations such as *asf1Δ* and deletions of genes encoding CAF-1 subunits. Also similar to the findings for *cdc68-E857K* (Results 4, iv), deletions of the *HHT1* and *HHF1* genes encoding histone proteins H3 and H4 are identified here as synthetically lethal with *cdc68-319*. Histone dosage plays a key role in mediating nucleosome structure, and perturbations in the balance of histone proteins can result in chromatin defects that may be exacerbated by mutations altering FACT. It is interesting that, once again, deletions of the *HHT2* and *HHF2* divergently transcribed gene pair were not recognized through SGA analysis as causing growth impairments with a *cdc68* mutation. Genetic interactions between other histone gene deletions and *cdc68* mutations could be assessed to determine if the gene-specific effects seen here are significant.

b) *cdc68-319* SGA interactions with genes involved in DNA replication and repair

The nucleosomal barrier to DNA access needs to be dealt with in processes other than transcription. Nucleosomal structure has been shown to influence DNA replication, repair and sister-chromatid cohesion (Milutinovic *et al.* 2002; Bailis and Forsburg 2003; Gonzalez-Barrera *et al.* 2003; Ye *et al.* 2003; Cobb *et al.* 2004). Several of the genes showing SGA interactions with *cdc68-319* are involved in these latter processes. While a role for FACT in DNA repair and replication has been established, the mechanisms of action and the factors involved is still largely unknown (Wittmeyer *et al.* 1999; Schlesinger and Formosa 2000; Keller *et al.* 2001; Yarnell *et al.* 2001; Zeng *et al.* 2002; Mayer *et al.* 2004). A role for FACT in sister-chromatid cohesion has not previously been reported. However, it is difficult at times to resolve the functions of sister-chromatid cohesion, DNA replication and DNA repair, as many of the factors involved operate in all three processes (Edwards *et al.* 2003; Kenna and Skibbens 2003; Mayer *et al.* 2004).

Deletion of the *RAD27* gene was found to cause synthetic sickness when cells were also carrying the *cdc68-319* allele. Rad27 is a 5'-to-3' exonuclease responsible for Okazaki-fragment processing during replication and for the excision of DNA damage during repair (Moreau *et al.* 2001; Parenteau and Wellinger 2002; Sun *et al.* 2003). This finding further associates FACT function with DNA replication and repair.

As shown in Figure 67, *rad27Δ* and *ctf4Δ* is a lethal combination, suggesting an overlapping essential function for this pair (Formosa and Nittis 1999; Tong *et al.* 2004). Two key components in sister-chromatid cohesion, Ctf4 and Ctf18 (chromosome transmission fidelity), physically interact are required for genome stability (Hanna *et al.* 2001). Both of these proteins also associate with the replication machinery. Ctf4 was originally identified as a factor that binds to DNA polymerase α in the same affinity-purification procedure used to isolate Cdc68 and Pob3 (Wittmeyer and Formosa 1997). Deletion of *CTF4* in combination with a *cdc68* mutation has been shown to result in impaired cell growth (Wittneyer and Formosa, 1997; Wittmeyer *et al.* 1999); therefore, the finding here that *ctf4Δ* causes synthetic sickness in *cdc68-319* cells is not surprising. Genetic interactions have also been reported between *ctf4Δ* and *pob3* mutations and between *ctf18Δ/chl12Δ* and *pob3* mutations (Schlesinger and Formosa 2000). In addition to its physical interactions with Ctf4, Ctf18 is a member of an alternative RFC (replication factor C) complex that promotes sister-chromatid cohesion and facilitates DNA-polymerase switching during replication (Schlesinger and Formosa 2000; Hanna *et al.* 2001; Mayer *et al.* 2001). The SGA and random-spore analysis indicate an overlapping function shared between Ctf18 and Cdc68, based on the synthetic sickness observed for cells containing both *ctf18Δ* and *cdc68-319*. This interaction further confirms the findings from the Formosa lab that indicate Cdc68 and FACT affect replication, but a role in sister-chromatid cohesion is also implicated by these findings.

Rad51, Mre11 and Xrs2 are all involved in double-strand-break repair, and also have been shown to be involved in sister-chromatid exchange during meiosis (reviewed in Paques and Haber 1999; Gonzalez-Barrera *et al.* 2003). Rad51 binds ssDNA intermediates generated during homologous recombination or double-strand break repair and assists in ssDNA strand invasion into the repair-template DNA duplex (Paques and Haber 1999; Sugawara *et al.* 2003; Davis and Symington 2004). To perform this task

Rad51 associates with Rad52, Rad54, and Rad55 (Sugawara *et al.* 2003). Deletions of *RAD52* and *RAD55* each showed synthetic growth defects in one of the two SGA screens performed with *cdc68-319*, and the *rad54Δ cdc68-319* cells failed to thrive in both SGA screens. Cells with *rad54Δ* are often identified as false positives by SGA analysis, and therefore this information was not included in the dataset. The relationship between *cdc68-319* and Rad51-mediated double-strand-break repair could be further investigated. Mre11 (an 3'-to-5' exonuclease), Rad50 (an ATPase) and Xrs2 (has DNA-binding activity) make up the MRX complex, which functions in recombination and double-strand-break repair. Xrs2 assists in targeting the MRX complex to DNA ends, and Mre11 is able to remove or 'chew back' some of the dsDNA to reveal a ssDNA template to be used during DNA repair (Paull and Gellert 1998; Trujillo *et al.* 2003). The structure of Rad50 resembles that of the highly conserved class of structural-maintenance-of-chromosomes (SMC) proteins (Anderson *et al.* 2001; Hopfner *et al.* 2001). It has been shown that the human homologue of MRX travels with the replication fork along with PCNA (proliferating cell nuclear antigen) but is further recruited to this site during times of DNA damage (Mirzoeva and Petrini 2003). This association suggests that MRX plays a role in replication even in the absence of DNA damage, but is further required upon DNA damage to both assist in repair and signal checkpoint activation (reviewed in Cobb *et al.* 2004). Both *mre11Δ* and *xrs2Δ* were found to cause synthetic growth defects in cells containing *cdc68-319*. Cells containing *rad50Δ* and *cdc68-319* were also synthetically defective, but the *rad50Δ* cells produce false-positive results in SGA and therefore further experiments are required to verify this observation. Mutations in any gene encoding MRX subunits or the *cdc68-319* mutation result in sensitivity to hydroxyurea, a DNA-damaging agent known to induce double-strand breaks. The genetic evidence here suggests that FACT, Rad51 and MRX may have overlapping roles in double-strand-break repair. An interesting and related function in sister-chromatid cohesion is also possible, since both Rad51 and Mre11 have been shown to assist in resolving homologous-recombination events between sister chromatids and the MRX complex resembles cohesion complexes (Anderson *et al.* 2001; Hopfner *et al.* 2001; Gonzalez-Barrera *et al.* 2003; Hopfner and Tainer 2003).

Microtubules are the links between spindle pole bodies and the kinetochores on chromosomes, and are responsible for the physical segregation of sister chromatids during mitosis. Microtubules are comprised of α and β tubulin subunits, and several chaperones in yeast are involved in the proper folding and functioning of tubulin. Two genes, *GIM3* and *ALF1*, encoding proteins involved in tubulin chaperonin activity were identified here as causing synthetic sickness when deleted in *cdc68-319* cells. Gim3 is a member of the prefoldin complex, a tubulin chaperonin made up of Gim1 to Gim6 (Geissler *et al.* 1998). Alf1 is a post-chaperonin co-factor that assists in folding α tubulin (reviewed in Lopez-Fanarraga *et al.* 2001). Each of these proteins works in concert with additional factors to mediate the folding of tubulin; however, of the genes encoding these additional factors (*CIN1*, *RBL2*, *PAC2*, *GIM1*, *GIM4*, and *GIM5*), two are false positives in SGA analysis (*GIM1* and *GIM6*) and the others each scored as synthetically sick or lethal in combination with *cdc68-319* in only one of the two SGA screens. The *gim2Δ* deletion was identified as causing synthetic sickness in *cdc68-319* cells using SGA analysis, but this interaction was not confirmed by random-spore analysis. As seen in Figure 67, deletion of *GIM3* has been found to cause synthetic growth defects in combination with a large number of mutations affecting transcription and replication-related processes. Recent work has also found synthetic genetic interactions between deletions of prefoldin-subunit genes and deletions of several genes encoding proteins involved in transcription and replication, including *set2Δ*, *dst1Δ*, *sas2Δ*, *hat2Δ*, *top3Δ*, and *cdc45Δ* to name a few (Mayer *et al.* 2001; Malagon *et al.* 2004; Tong *et al.* 2004). Deletions of two transcription-related genes, *dst1Δ* and *rpb9Δ*, encoding a subunit of RNA polymerase II, have also been found to cause sensitivity to the microtubule-de-polymerizing drug benomyl (Malagon *et al.* 2004). These genetic ties between tubulin folding and transcription and replication are interesting, but the direct implications are still uncertain. Perhaps these synthetic genetic effects stem from decreased transcription of a gene involved in tubulin structure as a result of *cdc68* defects or defects in other genes involved in transcription. If, on the other hand, Cdc68 does play a role in sister-chromatid cohesion, then perhaps perturbations in the machinery used to ensure that sister-chromatid segregation occurs efficiently would lead to growth defects or lethality.

In summary, there are many novel synthetic genetic interactions with *cdc68* identified from the SGA analysis employing *cdc68-319*. A strong resemblance is observed between the interactions identified for this allele of *cdc68* and those found with *cdc73Δ* (Krogan *et al.* 2003b; Tong *et al.* 2004). This correspondence implies that the Cdc68 activities impaired as a result of the *cdc68-319* mutations closely resemble those that fail when Cdc73 is absent. Many gene products involved in transcription, or in histone remodelling, modification, deposition and dosage, when absent, cause synthetic growth defects with *cdc68-319*, indicating a overlapping role for Cdc68 in each of these functions. The first evidence of an overlapping function for FACT and the SWR-C histone-remodelling complex is presented here, indicating that FACT may play a role in the incorporation of the histone variant H2A.Z into chromatin. Additional functions identified here include a role for Cdc68 in repair of DNA double-strand breaks and/or perhaps in sister-chromatid cohesion. The latter would be a previously unexplored area of FACT function.

viii) Synthetic genetic array analysis with *cdc68-ΔNTD-FLAG::natMX4*

SGA analysis of *cdc68-ΔNTD-FLAG::natMX4* cells mated to cells from the deletion collection was carried out in triplicate (Table 17). The mutations in 1600 to 2400 gene deletion strains were identified as causing synthetic growth defects in combination with *cdc68-ΔNTD*. In this analysis, the linkage group for *cdc68-ΔNTD* contained a surprisingly small number of gene deletions. It is unclear why this particular *natMX4*-tagged mutant allele did not result in decreased numbers of double-mutant haploid progeny for gene deletions in the vicinity of the *CDC68* chromosomal locus. To ensure that the *natMX4* integration was indeed at the correct chromosomal locus, tetrad analysis was performed for crosses of *cdc68-ΔNTD-FLAG::natMX4* query-strain cells and *CDC68::natMX4* query-strain cells with *mig2Δ::kanMX4* and *pst2Δ::kanXM4* cells from the deletion collection. The *MIG2* (*YGL209w*) gene is 2 kbp upstream of the *CDC68* locus on chromosome VII while the *PST1* (*YDR055w*) gene is on chromosome IV and is therefore unlinked to the *CDC68* locus, and was used as a control for the production of double-mutant haploid segregants. Between 10 and 20 tetrads were dissected for each cross and, consistent with the *natMX4* cassette located downstream of the *CDC68* or *cdc68-ΔNTD* genes, no double-mutant haploid segregants were identified from the cross with *mig2Δ::kanMX4* (Figure 68). In contrast, the control cross using *pst1Δ::kanMX4*

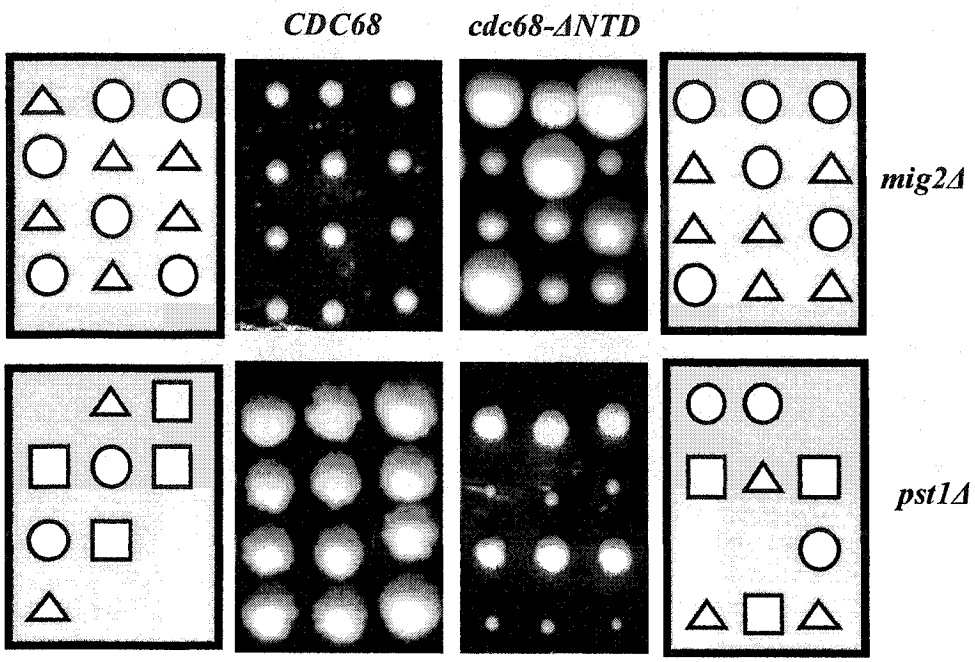

Figure 68. Tetrad analysis to verify chromosomal location of the *natMX4* cassette in cells from the *cdc68-ΔNTD::natMX4* query strain. Each panel shows the spore products from three tetrads from diploids heterozygous for *CDC68::natMX4* and *mig2Δ::kanMX4* (top left quadrant), *CDC68::natMX4* and *pst2Δ::kanMX4* (lower left quadrant), *cdc68-ΔNTD::natMX4* and *mig2Δ::kanMX4* (top right quadrant), *cdc68-ΔNTD::natMX4* and *pst2Δ::kanMX4* (lower right quadrant) that were derived from single-mutant or 'marked' haploid parents. The *MIG2* gene is 2 kbp from the *CDC68* locus on chromosome VII, while and the *PST1* gene is on chromosome IV. As expected for a *natMX4* integration event close to the *CDC68* locus, no double-drug-resistant spore products were identified from the *CDC68::natMX4 mig2Δ::kanMX4* and *cdc68-ΔNTD::natMX4 mig2Δ::kanMX4* heterozygous diploids. Double-drug-resistant spore products were identified from the *pst1Δ::kanMX4* heterozygous diploids. Panels adjacent to each tetrad photo indicate genotypes: no symbol – no drug-resistance cassettes, square - both *natMX4* and *kan MX4* drug-resistance cassettes, circle – *kanMX4* drug-resistance cassette, triangle – *natMX4* drug-resistance cassette.

frequently generated double-mutant haploid progeny, consistent with the *kanMX4* and *natMX4* markers segregating independently (Figure 68). These results, in addition to those verifications done when generating the yeast strain containing the *cdc68-ΔNTD-FLAG::natMX4* chromosomal integration (Materials and Methods), confirm that the *natMX4* marker is indeed integrated downstream of the *cdc68-ΔNTD*, and only at this site. The inability to clearly identify a robust linkage group for the *cdc68-ΔNTD-FLAG::natMX4* allele by SGA analysis is not understood. Nonetheless, the SGA analysis performed here has identified many synthetic genetic interactions with *cdc68-ΔNTD-FLAG::natMX4* that have been verified by random-spore analysis.

Of the greater than 1000 possible synthetic genetic interactions identified by SGA analysis with *cdc68-ΔNTD*, only 321 interactions were identified in all screens (see Table 17 legend). Each of these 321 deletions that may result in synthetic growth defects when combined with *cdc68-ΔNTD* was then further tested using random-spore analysis (data not shown; Table 17; Appendix 1). Based on the results of random-spore analysis, 96 deletions were found to cause growth impairments when *cdc68-ΔNTD* was present (Figure 69; Table 22; Appendix 1). Genes encoding proteins involved in several cellular functions were identified, with the major functional classes involving transcription, DNA metabolism, and transport (Figure 69; Table 22). There are many previously identified genetic and physical interactions between the genes in this dataset. In total, 47 of the genes identified here have at least one interaction with another gene in the group (Figure 70). In total, these 47 genes identify 78 genetic or physical interactions within the set; *HOC1* (8 interactions), *RAD27* (11 interactions), *RAD50* (13 interactions), *POL32* (8 interactions), and *DEP1* (10 interactions) represent gene 'hubs' with multiple interactions within the set (Figure 70).

Several of the genetic interactions shown here for *cdc68-ΔNTD* are also seen for other *cdc68* alleles. Eighteen of the twenty five interactions with genes encoding vesicular-transport proteins observed for *cdc68-ΔNTD* were also identified for *cdc68-E763G* and/or *cdc68-312*. The conclusion of this finding is that the *cdc68-ΔNTD* mutation also disrupts some aspect of Cdc68 function that influences transport, particularly between the Golgi and endosomal compartments, since many genes encoding proteins that function in transport share an overlapping function with that lacking for Cdc68-ΔNTD. How direct a

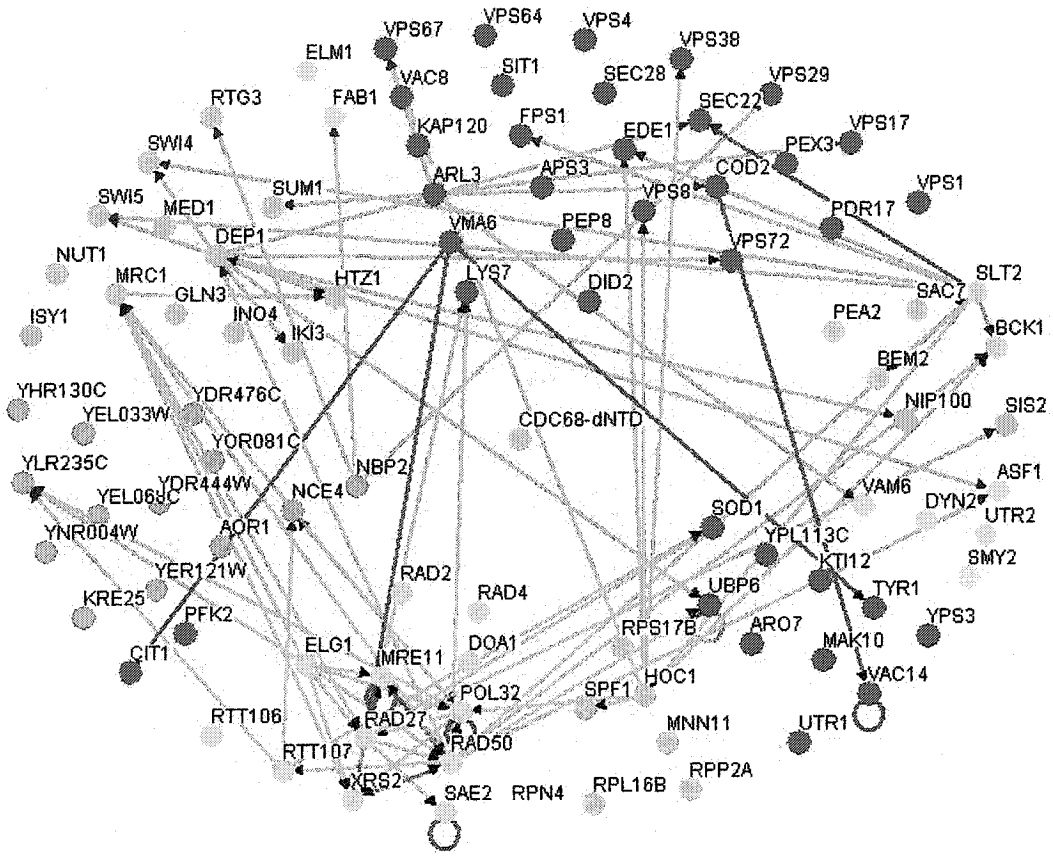

Figure 69. Synthetic genetic interactions with *cdc68-ΔNTD*. Each gene deletion identified by SGA and verified by random-spore analysis as causing synthetic sickness or lethality in combination with *cdc68-ΔNTD* is indicated by a coloured node, and genetic or physical interactions between two genes are indicated by coloured lines (see Appendix 2 for legend). The *cdc68-ΔNTD* mutant gene is shown in the middle of the web and should have green lines, indicating a synthetic sick or lethal interaction, connecting it to all of the genes shown, but for clarity these lines have been omitted. A high degree of connectivity can be seen in this group of genetic interactions, which indicates overlapping functions. Key 'hubs' of interaction are displayed in Figure 70.

Table 22. Gene deletions that are synthetically sick or lethal in combination with *cdc68-ΔNTD*.

Transcription:

Gene Name	Systematic Name	Description	Gene Ontology
DEP1	YAL013W	Transcriptional modulator involved in the regulation of structural genes involved in phospholipid biosynthesis, also participates in regulation of metabolically unrelated genes as well as maintenance of mating efficiency and sporulation	metabolism; transcription
GLN3	YER040W	Responsible for nitrogen catabolite repression NCR -sensitive transcription. During nitrogen starvation, Gln3 is nuclear. Under excess nitrogen, Gln3 is cytoplasmic. Also regulates glutamine-repressible gene products.	metabolism; transcription
HTZ1	YOL012C	Histone-related protein that can suppress histone H4 point mutation	transcription; metabolism; DNA metabolism; cell organization and biogenesis; cell growth and/or maintenance
IKI3	YLR384C	Subunit of RNA polymerase II elongator complex, which is a histone acetyltransferase; involved in maintaining structural integrity of the complex; iki3 mutations confer resistance to the K. lactis toxin zymocin	transcription; metabolism
INO4	YOL108C	Transcription factor required for derepression of inositol-choline-regulated genes involved in phospholipid synthesis	metabolism; transcription
MED1	YPR070W	Subunit 1 of the Mediator complex essential for transcriptional regulation	transcription; metabolism
MRC1	YCL061C	Mediator of the Replication Checkpoint; required for full activation of Rad53p in response to replication stress.	transcription; metabolism; DNA metabolism; cell organization and biogenesis; cell growth and/or maintenance; cell cycle
NUT1	YGL151W	Component of the RNA polymerase II mediator complex, which is required for transcriptional activation and also has a role in basal transcription	transcription; metabolism
RTG3	YBL103C	bHLH/Zip transcription factor which regulates CIT2 gene expression	transcription; metabolism

SUM1	YDR310C	Suppresor of mar1-1 sir2 mutation	transcription; metabolism; DNA metabolism; cell organization and biogenesis; cell growth and/or maintenance; cell cycle
SWI4	YER111C	Involved in cell cycle dependent gene expression	cell cycle; cell growth and/or maintenance; transcription; metabolism
SWI5	YDR146C	Transcription factor that activates transcription of genes expressed in G1 phase and at the G1/M boundary; localization to the nucleus occurs during G1 and appears to be regulated by phosphorylation by Cdc28p kinase	cell cycle; transcription; cell growth and/or maintenance; metabolism

Transport:

Gene Name	Systematic Name	Description	Gene Ontology
APS3	YJL024C	sigma3-like subunit of the yeast AP-3 complex which functions in transport of alkaline phosphatase to the vacuole via the alternate pathway, suppressor of loss of casein kinase 1 function	transport; cell growth and/or maintenance; cell organization and biogenesis
ARL3	YPL051W	Similar to ADP-ribosylation factor. Part of the carboxypeptidase Y pathway.	protein transport; transport; cell growth and/or maintenance
COD2	YNL041C	Conserved Oigomeric Golgi complex 6 Complexed with Cog8p; interacts with Cog2p	transport; cell growth and/or maintenance
DID2	YKR035W-A	Class E protein of the vacuolar protein-sorting Vps pathway, associates reversibly with the late endosome, has human ortholog that may be altered in breast tumors	protein transport; metabolism; transport; cell growth and/or maintenanc
EDE1	YBL047C	EH domain protein involved in endocytosis	transport; cell growth and/or maintenance
FPS1	YLL043W	Suppressor of tps1/fdp1 and member of the MIP family of transmembrane channels; may be involved in glycerol efflux	transport; cell growth and/or maintenance
KAP120	YPL125W	karyopherin	protein transport; metabolism; transport; cell growth and/or maintenance;
LYS7	YMR038C	Involved in lysine biosynthesis, oxidative stress protection	transport; cell growth and/or maintenance;
PDR17	YNL264C	involved in pleiotropic drug resistance by controlling lipids in various cellular compartments; putative phosphatidylinositol transfer protein.	metabolism; transport; cell growth and/or maintenance

PEP8	YJL053W	Plays a role in delivery of proteins to the vacuole	transport; protein transport; metabolism; cell growth and/or maintenance; cell organization and biogenesis
PEX3	YDR329C	48-kDa peroxisomal integral membrane protein	cell organization and biogenesis; cell growth and/or maintenance; protein transport; metabolism; transport
SEC22	YLR268W	Identified in a screen for dense cells that accumulated invertase at the non-permissive temperature, SEC22 encodes a v-SNARE present on ER to Golgi vesicles and is involved in anterograde and retrograde transport between the ER and Golgi	transport; cell growth and/or maintenance
SEC28	YIL076W	Part of a heptameric protein complex that regulates retrograde Golgi-to-ER protein traffic in eukaryotic cells; coatomer forms the COP I vesicle coat whose functions are essential	transport; cell growth and/or maintenance
SIT1	YEL065W	Ferrioxamine B transporter, member of the ARN family of transporters that specifically recognizes siderophore-iron chelates; transcription is induced during iron deprivation and diauxic shift; potentially phosphorylated by Cdc28p	transport; cell growth and/or maintenance
VAC8	YEL013W	Phosphorylated vacuolar membrane protein that interacts with Atg13p, required for the cytoplasm-to-vacuole targeting Cvt pathway; interacts with Nvj1p to form nucleus-vacuole junctions	autophagy; cell growth and/or maintenance; cell organization and biogenesis; protein transport; metabolism; transport
VMA6	YLR447C	vacuolar ATPase V0 domain subunit d 36 kDa	transport; cell growth and/or maintenance; cell organization and biogenesis
VPS1	YKR001C	involved in vacuolar protein sorting and normal organization of intracellular membranes; probably required for membrane-protein retention in a late Golgi compartment	protein transport; metabolism; transport; cell growth and/or maintenance; cell organization and biogenesis
VPS17	YOR132W	Peripheral membrane protein required for vacuolar protein sorting	transport; cell growth and/or maintenance; cell organization and biogenesis
VPS29	YHR012W	vacuolar protein sorting	transport; cell growth and/or maintenance; cell organization and biogenesis

VPS38	YLR360W	involved in vacuolar protein targeting	transport; cell growth and/or maintenance; cell organization and biogenesis
VPS4	YPR173C	Defective in vacuolar protein sorting; homologous to mouse SKD1 and to human hVPS4	transport; protein transport; metabolism; cell growth and/or maintenance; cell organization and biogenesis
VPS64	YDR200C	NONE	protein transport; metabolism; transport; cell growth and/or maintenance; cell cycle
VPS67	YKR020W	whiskey whi mutant; forms a tetramer with VPS52, VPS53, and VPS54	protein transport; metabolism; transport; cell growth and/or maintenance; budding; cell organization and biogenesis
VPS72	YDR485C	NONE	protein transport; metabolism; transport; cell growth and/or maintenance
VPS8	YAL002W	involved in vacuolar protein sorting; required for localization and trafficking of the CPY sorting receptor	transport; cell growth and/or maintenance; cell organization and biogenesis

Cell growth and maintenance:

Gene Name	Systematic Name	Description	Gene Ontology
DYN2	YDR424C	Cytoplasmic light chain dynein, microtubule motor protein	cell organization and biogenesis; cell growth and/or maintenance
SMY2	YBR172C	partial suppressor of myo2-66	cell organization and biogenesis; cell growth and/or maintenance
UTR2	YEL040W	alias: Congo Red Hypersensitivity	cell organization and biogenesis; cell growth and/or maintenance
VAM6	YDL077C	Required for the vacuolar morphogenesis in yeast	cell organization and biogenesis; cell growth and/or maintenance

Protein biosynthesis:

Gene Name	Systematic Name	Description	Gene Ontology
HOC1	YJR075W	Homologous to OCH1, an alpha-1,6-mannosyltransferase; Golgi-localized, type II integral membrane protein	protein biosynthesis; cell organization and biogenesis; metabolism; cell growth and/or maintenance; carbohydrate metabolism
MNN11	YJL183W	member of a cis Golgi complex that is involved in mannan synthesis, other complex members include Mnn10p, Hoc1p, Anp1p, Mnn9p	protein biosynthesis; metabolism
RPL16B	YNL069C	Homology to rat ribosomal protein L13a	protein biosynthesis; metabolism
RPP2A	YOL039W	Homology to rat P2, human P2, and E.coli L12eIB	protein biosynthesis; metabolism
RPS17B	YDR447C	Ribosomal protein 51 rp51 of the small 40s subunit; nearly identical to Rps17Ap and has similarity to rat S17 ribosomal protein	protein biosynthesis; metabolism; cell organization and biogenesis; cell growth and/or maintenance
SPF1	YEL031W	Sensitivity to a killer toxin SMK toxin produced by Pichia Farinosa	protein biosynthesis; metabolism; cell growth and/or maintenance

Cell cycle:

Gene Name	Systematic Name	Description	Gene Ontology
NIP100	YPL174C	Nuclear import protein	cell cycle; cell growth and/or maintenance
SIS2	YKR072C	Involved in cell cycle control and ion homeostasis	cell cycle; cell growth and/or maintenance; response to stress; metabolism

Stress response:

Gene Name	Systematic Name	Description	Gene Ontology
ELM1	YKL048C	cell morphology	cell growth and/or maintenance; protein amino acid phosphorylation; metabolism; response to stress; budding; cell organization and biogenesis

FAB1	YFR019W	1-phosphatidylinositol-3-phosphate 5-kinase; vacuolar membrane kinase that generates phosphatidylinositol 3,5 P2, which is involved in vacuolar sorting and homeostasis	response to stress; cell organization and biogenesis; cell growth and/or maintenance; metabolism

Metabolism:

Gene Name	Systematic Name	Description	Gene Ontology
ARO7	YPR060C	Chorismate mutase, catalyzes the conversion of chorismate to prephenate to initiate the tyrosine/phenylalanine-specific branch of aromatic amino acid biosynthesis	metabolism
KTI12	YKL110C	Protein involved in resistance to K. lactis killer toxin; RNA polymerase II Elongator associated protein	cell growth and/or maintenance; metabolism
MAK10	YEL053C	Glucose-repressible protein	metabolism
SOD1	YJR104C	Cu, Zn superoxide dismutase	metabolism; cell growth and/or maintenance
TYR1	YBR166C	Step of tyrosine biosynthesis pathway	metabolism
UBP6	YFR010W	deubiquitinating enzyme putative	metabolism
UTR1	YJR049C	associated with ferric reductase	metabolism; cell growth and/or maintenance
VAC14	YLR386W	VACuole morphology and inheritance mutant. Vac14 is essential for the regulated synthesis of PtdIns 3,5 P 2 , for control of trafficking of some proteins to the vacuole lumen via the MVB, and for maintenance of vacuole size and acidity.	metabolism; cell organization and biogenesis; cell growth and/or maintenance
YPL113C	YPL113C	NONE	metabolism
YPS3	YLR121C	Gpi-anchored aspartic protease Yapsin 3	metabolism

Signal transduction:

Gene Name	Systematic Name	Description	Gene Ontology
BCK1	YJL095W	bypass requirement for protein kinase C homolog	protein amino acid phosphorylation; metabolism; signal transduction; cell organization and biogenesis; cell growth and/or maintenance
BEM2	YER155C	Protein with role in bud emergence	cell organization and biogenesis; cell growth and/or maintenance; budding; signal transduction

PEA2	YER149C	Pea2p is localized with Spa2p to sites of polarized growth and is required for efficient mating and bipolar budding; it is required for pheromone-induced shmoo formation	cell organization and biogenesis; cell growth and/or maintenance; budding; signal transduction
SAC7	YDR389W	GTPase activating protein GAP for Rho1p, involved in signaling to the actin cytoskeleton, null mutations suppress tor2 mutations and temperature sensitive mutations in actin; potential Cdc28p substrate	signal transduction; cell cycle; cell growth and/or maintenance; cell organization and biogenesis
SLT2	YHR030C	Suppressor of lyt2	protein amino acid phosphorylation; metabolism; signal transduction; cell organization and biogenesis; cell growth and/or maintenance

DNA metabolism:

Gene Name	Systematic Name	Description	Gene Ontology
DOA1	YKL213C	WD repeat protein required for ubiquitin-mediated protein degradation, forms complex with Cdc48p, plays a role in controlling cellular ubiquitin concentration; also promotes efficient NHEJ in postdiauxic/stationary phase	protein catabolism; metabolism; DNA repair; DNA metabolism; response to DNA damage stimulus; response to stress
ELG1	YOR144C	Enhanced Level of Genomic instability, Repressor of Ty1 Transposition	DNA recombination; DNA metabolism; metabolism
MRE11	YMR224C	Disp. for premeiotic DNA synthesis, but required for both double strand break formation & resection, synaptonemal complexes, meiotic recombination & viable spores. Localizes to discrete sites in rad50 mutants	DNA repair; DNA metabolism; response to DNA damage stimulus; response to stress; metabolism; DNA recombination; cell cycle; cell growth and/or maintenance
POL32	YJR043C	Polymerase-associated gene	DNA replication; DNA metabolism; cell cycle; metabolism; cell growth and/or maintenance; DNA repair; response to DNA damage stimulus; response to stress

RAD2	YGR258C	Single-stranded DNA endonuclease, cleaves single-stranded DNA during nucleotide excision repair to excise damaged DNA; subunit of Nucleotide Excision Repair Factor 3 NEF3 ; homolog of human XPG protein	DNA repair; DNA metabolism; response to DNA damage stimulus; response to stress; metabolism
RAD27	YKL113C	5 to 3 exonuclease, 5 flap endonuclease, required for Okazaki fragment processing and maturation as well as for long-patch base-excision repair; member of the S. pombe RAD2/FEN1 family	DNA replication; DNA metabolism; cell cycle; metabolism; cell growth and/or maintenance; DNA repair; response to DNA damage stimulus; response to stress; DNA recombination
RAD4	YER162C	Protein that recognizes and binds damaged DNA with Rad23p during nucleotide excision repair; subunit of Nuclear Excision Repair Factor 2 NEF2 ; homolog of human XPC protein	DNA repair; DNA metabolism; response to DNA damage stimulus; response to stress; metabolism
RAD50	YNL250W	Subunit of MRX complex, with Mre11p and Xrs2p, involved in processing double-strand DNA breaks in vegetative cells, initiation of meiotic DSBs, telomere maintenance, and nonhomologous end joining	DNA repair; DNA metabolism; response to DNA damage stimulus; response to stress; metabolism; DNA recombination; cell cycle; cell growth and/or maintenance; cell organization and biogenesis
RTT106	YNL206C	Regulator of Ty1 Transposition - same phenotype as RTT101 - RTT105, disruption causes increase in Ty1 transposition. Isolated from the same screen as the other named RTT genes.	DNA recombination; DNA metabolism; metabolism
RTT107	YHR154W	Regulator of Ty1 Transposition; Establishes Silent Chromatin	DNA recombination; DNA metabolism; metabolism
SAE2	YGL175C	Involved in meiotic recombination and chromosome metabolism	DNA recombination; DNA metabolism; metabolism; cell cycle; cell growth and/or maintenance
XRS2	YDR369C	classified as an early recombination function, required for DNA repair but dispensable for mitotic recombination xrs2 is hyper-Rec during vegatative growth , required for double strand breaks, meiotic recombination and spore viability	DNA repair; DNA metabolism; response to DNA damage stimulus; response to stress; metabolism; DNA recombination; cell cycle; cell growth and/or maintenance

DNA damage response:

Gene Name	Systematic Name	Description	Gene Ontology
ASF1	YJL115W	anti-silencing protein that causes depression of silent loci when overexpressed	response to DNA damage stimulus; response to stress

Protein Degradation:

Gene Name	Systematic Name	Description	Gene Ontology
RPN4	YDL020C	Involved in ubiquitin degradation pathway. May act as common transcription factor on proteasomal and proteasome-related genes.	protein catabolism; metabolism

Carbohydrate metabolism:

Gene Name	Systematic Name	Description	Gene Ontology
CIT1	YNR001C	citrate synthase. Nuclear encoded mitochondrial protein.	carbohydrate metabolism; metabolism
PFK2	YMR205C	phosphofructokinase beta subunit	carbohydrate metabolism; metabolism

RNA processing:

Gene Name	Systematic Name	Description	Gene Ontology
ISY1	YJR050W	Interacts with Syf1p, Prp39p and Ypl213wp.	RNA processing; metabolism

Unknown:

Gene Name	Systematic Name	Description	Gene Ontology
AOR1	YBR231C	Protein of unknown function, localizes to the nucleus	biological process unknown
KRE25	YNL296W	hypothetical ORF	UNKNOWN
NBP2	YDR162C	interacts with Nap1, which is involved in histone assembly	biological process unknown
NCE4	YPL024W	Negative regulator of Cts1 Expression	biological process unknown
YDR444W	YDR444W	NONE	biological process unknown
YDR476C	YDR476C	NONE	biological process unknown
YEL033W	YEL033W	Hypothetical ORF	NONE

YEL068C	YEL068C	Hypothetical ORF	NONE
YER121W	YER121W	Hypothetical ORF	NONE
YHR130C	YHR130C	Hypothetical ORF	NONE
YLR235C	YLR235C	Involved in meiotic nuclear division.	NONE
YNR004W	YNR004W	NONE	biological process unknown
YOR081C	YOR081C	Protein of unknown function, localizes to lipid particles; potential Cdc28p substrate	biological process unknown

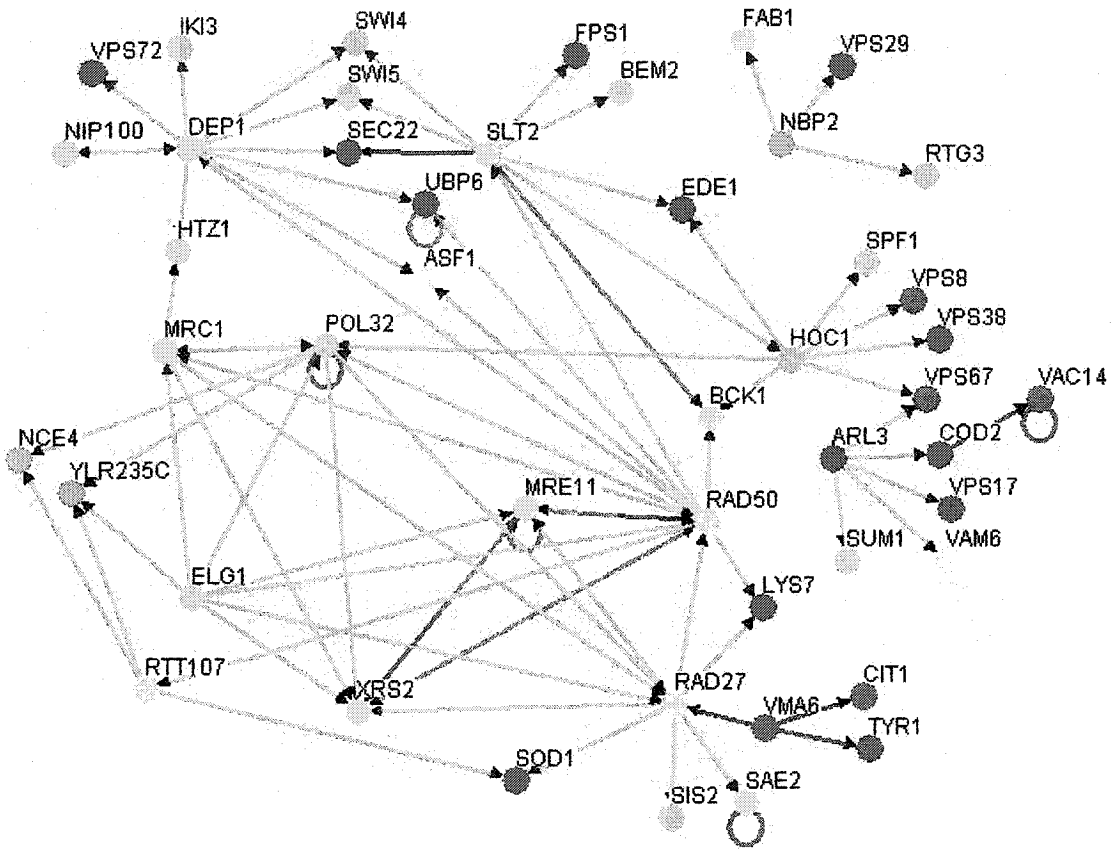

Figure 70. Connectivity of synthetic genetic interactions with *cdc68-ΔNTD*. Of the 96 genes identified as having a synthetic genetic relationship when deleted in the presence of the *cdc68-ΔNTD* mutation, the 47 with previously identified genetic or physical interactions are shown. These 47 genes show a high degree of connectivity, with 78 interactions among them. The legend for line and node colours is given in Appendix 2.

connection exists between Cdc68 activity and vesicular transport remains to be discerned. Genetic interactions between *cdc68-E763G* or *cdc68-312* and genes encoding proteins involved in cell morphogenesis and integrity, such as *HOC1*, *MNN11*, *SPF1* and *ELM1*, have been described above, and *cdc68-ΔNTD* has genetic ties to these processes as well. Loss of the N-terminal domain of Cdc68 seems to impair aspects of cell integrity. Synthetic growth impairments for double-mutant cells containing *cdc68-ΔNTD* in combination with *swi4Δ*, *bck1Δ*, or *slt2Δ*, all encoding components of the Pkc1-mediated signal-transduction cascade, also implicate the N-terminal domain of Cdc68 in cell morphogenesis.

a) *cdc68-ΔNTD* SGA interactions with genes involved in transcription

Several genes involved in transcription-related processes were also found here to cause synthetic sickness or lethality when deleted in *cdc68-ΔNTD* cells. Unlike the situation for other *cdc68* alleles, deletions of Paf1-complex components did not result in synthetic growth defects, indicating that the N-terminal domain of Cdc68 may not share an overlapping function with this complex. Double-mutant cells containing *cdc68-ΔNTD* and deletions of *NUT1* or *MED1*, two of the genes encoding Mediator components, did exhibit growth impairments. This interaction implies that the N-terminal domain of Cdc68 may be involved in transcription initiation. Five genes encoding transcription factors, *GLN3*, *INO4*, *RTG3 SWI4*, and *SWI5*, were shown here to result in sick or lethal phenotypes when deleted in combination with *cdc68-ΔNTD*. These findings indicate that Cdc68 may play a role in the activation of a common gene or genes in each case, and in removing both the transcription factor and the means to modulate chromatin structure cell growth is impaired. Cdc68 may play a role in promoter-proximal chromatin alterations that assist in transcription initiation. The Dep1 protein also functions in transcription, and causes synthetic growth defects when deleted in combination with a myriad of other genes encoding proteins involved in transcription-related processes, including components of the Paf1 complex and the NuA4 histone acetyltransferase complex, several histone deacetylase and methlytransferase complex members as well as Hir proteins (Tong *et al.* 2004). While Dep1 is not well characterized, it has been described as a global regulator of transcription (Lamping *et al.* 1994), which is similar to early descriptions of FACT components. There is a significant overlap between the lists of

gene deletions found to cause growth defects in *dep1Δ* cells and that identified with *cdc68* mutant alleles. Interest in the function of Dep1 may increase given these recent findings.

Components of histone-modifying and remodelling complexes were also identified in this analysis. Sum1, as described above, assists in histone deacetylation to maintain a silencing chromatin conformation. Iki3 is involved in maintaining the structural integrity of the Elongator complex, six-member histone-acetyltransferase complex (Elp1/Iki3, Elp2, Elp3, Elp4, Elp5/Iki1, Elp6) involved in transcription elongation (Wittschieben *et al.* 1999; Frohloff *et al.* 2001; Winkler *et al.* 2001). Cells with *iki3Δ* and *cdc68-ΔNTD* are inviable (cells containing *elp3Δ* along with *cdc68-ΔNTD* were also inviable SGA analysis, but this latter phenotype was not verified by the results of random-spore analysis). Due to the essential nature of the *ELP5* gene it is not part of the yeast gene deletion collection, but each of the other non-essential genes encoding Elongator subunits is present and these deletions were identified in some of the SGA screens as growth-impaired with *cdc68-ΔNTD*. Mutation of genes encoding Elongator proteins have been shown to alter gene-expression profiles, suggesting that Elongator assists in the transcription of many yeast genes (Krogan and Greenblatt 2001). The genetic interactions identified here suggest that FACT and Elongator have overlapping essential function. Whether this is due to an overlap in regulation of gene expression for particular gene(s) is uncertain, but given that both complexes function in transcription elongation this is likely the overlapping essential function that is disrupted when both complexes are mutated.

Deletions of the *AOR1/SWC5* and *VPS27/SWC2* genes, which encode SWR-C components, were also found to cause growth impairments in combination with the *cdc68-ΔNTD* allele. Cells containing *vps71Δ/swc6Δ* and *cdc68-ΔNTD* were also growth impaired in SGA analysis, but the results of random-spore assessment of this interaction are unclear at present. As described in Results, part 4 v(a), SWR-C has ATP-dependent nucleosome-remodelling activities and is involved in the replacement of H2A/H2B dimers with H2A.Z/H2B dimers during transcription elongation (Krogan *et al.* 2003b; Kobor *et al.* 2004; Mizuguchi *et al.* 2004). Deletion of the *HTZ1* gene encoding the histone H2A.Z variant is also synthetically lethal with *cdc68-ΔNTD*. These findings are similar to those reported above for *cdc68-319* and further connect FACT and SWR-C

activities, but the full implications of this fundamental connection remain to be determined.

Eliminating the N-terminal domain of Cdc68 must somehow impair Cdc68 function in histone deposition as well, since cells fail to thrive when Cdc68-ΔNTD cells lack the chromatin assembly factor,Asf1. Cells containing either *cdc68-ΔNTD* or *cdc68-E857K* are growth-impaired when combined with *asf1Δ*. Unlike the findings with *cdc68-E857K*, none of the *HIR* genes were identified by SGA analysis as synthetically sick or lethal when deleted in combination with *cdc68-ΔNTD*. This finding suggests that the C-terminal mutation in *cdc68-E857K* and the deletion of the N-terminal domain of Cdc68 encoded by *cdc68-ΔNTD* may disrupt Cdc68 chromatin assembly in different ways.

b) *cdc68-ΔNTD* SGA interactions with genes involved in DNA replication and repair

Many of the genes identified by SGA analysis with *cdc68-ΔNTD* encode proteins that function in DNA repair and replication, and which also may have roles in sister-chromatid cohesion. The initial phases of DNA replication require that an RNA primer be synthesized to serve as a starting point in the replication process. Cdc68 and Pob3 have been found associated with DNA polymerase α, the polymerase responsible for this priming reaction and the initial 20-30 deoxynucleotides of DNA extension (Wittmeyer and Formosa 1997; Wittmeyer *et al.* 1999). Polymerase α is then replaced by DNA polymerase δ and the PCNA (proliferating cell nuclear antigen) complex (reviewed in Kim *et al.*, 2003; Maga and Hubscher 2003). *POL32* encodes one of three subunits of DNA polymerase δ and when deleted in *cdc68-ΔNTD* cells is shown here to result in growth impairment. PCNA assists in maintaining the processivity of DNA polymerase δ and is loaded onto the DNA template by the replication factor C (RFC) complex (Maga and Hubscher 2003). RFC consists of five essential proteins Rfc1 to Rfc5; alternative forms of RFC have been characterized in which Rfc1 is replaced by other factors (Mayer *et al.* 2001; Naiki *et al.* 2001; Kanellis *et al.* 2003). These alternative RFC complexes are thought to assist in regulating RFC functions during various processes, and may assist in polymerase switching. One such alternative RFC complex is generated by the replacement of Rfc1 with Ctf18, Ctf8 and Dcc1 to form an alternative RFC complex involved in sister-chromatid cohesion, while another alternative RFC complex is formed

when Rfc1 is replaced by Elg1 (Mayer *et al.* 2001; Kanellis *et al.* 2003). The Elg1-RFC derivative is thought to be important for lagging-strand synthesis and Okazaki-fragment maturation (Kanellis *et al.* 2003). Originally, *ELG1* was identified as a member of the regulator-of-Ty1 retrotransposition (*RTT*) gene family and recent studies suggest that it is important for the prevention of gross chromosomal rearrangements (Scholes *et al.* 2001; Kanellis *et al.* 2003). Thus Elg1 plays an important role in maintaining genome integrity. Here I show that deletion of the *ELG1* gene results in synthetic sickness in the presence of *cdc68-ΔNTD*, indicating a possible role for the N-terminal domain of Cdc68 in DNA replication and/or genome stability.

An additional protein that assists in the processing of Okazaki fragments is the Rad27 endo/exonuclease (Lieber 1997; Ayyagari *et al.* 2003; Sun *et al.* 2003). In addition to its role in DNA replication, Rad27 also functions during DNA base-excision repair and has been identified as a member of the *RTT* gene family, so like many other genes involved in these processes, Rad27 operates during DNA replication and DNA repair, and helps maintain genome stability (Klungland and Lindahl 1997; Sundararajan *et al.* 2003). Many of the genes with roles in DNA repair and replication identified here as causing synthetic growth defects when deleted in combination with *cdc68-ΔNTD* also have genetic interactions with *RAD27* (Figure 58). SGA analysis shows that *rad27Δ cdc68-319* (Results 4, vii) and *rad27 cdc68-ΔNTD* cells are growth-impaired, which shows that Cdc68 influences some of the same functions as Rad27. DNA replication requires the removal of histones from the DNA template and the assembly of new nucleosomes on the replicated DNA strands. Disruption in this process of chromatin assembly and disassembly around the replication fork can lead to replication-fork stalling. This may be how mutations affecting FACT perturb DNA replication, by causing replication-fork stalling due to inadequate chromatin assembly or disassembly during replication. When the Cdc68-ΔNTD protein is present in the FACT complex, the process of chromatin assembly during replication may be impaired, and as a result, any further mutation in the replication machinery, such as those indicated above, results in cell growth defects or lethality. Thus, the N-terminal domain of Cdc68 is likely important for mediating chromatin functions during replication.

This same scenario for FACT activity can be applied to defects in checkpoint activation and repair processes. If replication-fork pausing is not resolved and replication restarted efficiently, DNA double-strand breaks can arise. This damage activates checkpoints that signal the presence of DNA damage and assist in recruiting repair machinery to the site of damage. When checkpoint or repair activities are not functioning properly, double-strand breaks may not be resolved, resulting in mutations and genome instability. Checkpoint sensors are activated as a result of stalled replication forks or DNA damage during S phase. Mec1 is a sensor kinase that is activated in this way and one of the targets of this activity is Mrc1 (Osborn and Elledge 2003). Mec1 directly phosphorylates Mrc1, which then assists in restarting stalled replication forks and also activates repair proteins (Katou *et al.* 2003; Osborn and Elledge 2003; Cobb *et al.* 2004). Mrc1 carries out these roles in conjunction with Tof1 (Katou *et al.* 2003), but only the deletion of *mrc1Δ* was found here by SGA analysis to interact genetically with *cdc68-ΔNTD*. An additional phosphorylation substrate for Mec1 and for Tel1, the other DNA checkpoint sensor kinase in yeast, in response to replication stress is Sae2 (Baroni *et al.* 2004). Sae2 is involved in double-strand-break repair and may modulate the activity of the MRX complex in this process (Rattray *et al.* 2001; Baroni *et al.* 2004). The MRX complex and the function of each of its components (Mre11, Rad50, and Xrs2) is described above (Results 4, vii). MRX is involved in DNA replication (as it is found at the replication fork), doublestrand-break repair, DNA-damage checkpoint signalling, and potentially also in sister-chromatid cohesion (Mirzoeva and Petrini 2003; Cobb *et al.* 2004). The SGA and random-spore analyses performed here have revealed that cells containing *cdc68-ΔNTD* and gene deletions of *SAE2*, *MRE11*, *RAD50*, and *XRS2* are growth-impaired. These results indicate that defects in checkpoint signalling or repair processes are linked to Cdc68 function, specifically the function of the N-terminal domain. Each of these genetic interactions with *cdc68-ΔNTD* may be explained by defects in chromatin structure that result in stalled replication forks, as these factors are all involved in replication-fork restart. However, given the overlapping roles for each of these factors in repair and in sister-chromatid cohesion, which both require interfacing with chromatin structure, it is difficult to pinpoint a precise role for FACT based on these findings. These defects could be generated by an inability of FACT to disassemble or

reassemble histones directly, or by an inability of FACT to recruit other factors involved in nucleosome-modifying or -remodelling complexes. Additionally, chromatin structural perturbations caused by loss of the N-terminal domain of Cdc68 could result in impaired DNA-damage signalling or loss of sister-chromatid associations. Further research in this area will undoubtedly lead to exciting discoveries about the nature of FACT function in DNA repair, replication and perhaps sister-chromatid cohesion.

Other synthetic genetic interactions with *cdc68-ΔNTD* and deletions of genes encoding DNA-repair proteins were also found. In addition to their roles in DNA double-strand break repair, Sae2, Mre11, Rad50, and Xrs2 have each been found to function in the nonhomologous-end-joining (NHEJ) repair pathway (Wilson 2002; Yu *et al.* 2004). The *DOA1* gene was also identified in this same screen as Sae2 and MRX components as functioning in NHEJ repair (Wilson 2002), and *doa1Δ cdc68-ΔNTD* cells were shown by SGA and random-spore analysis to be growth-impaired. Genes encoding two components of nucleotide excision repair, *RAD2* and *RAD4*, were also found to cause growth defects when deleted in combination with *cdc68-ΔNTD*. Rad2 is an exonuclease in the same family of proteins as Rad27 and may have an overlapping function in Okazaki-fragment processing (Sun *et al.* 2003). Mutations in *rad2* and *rad4* alleles that disrupt nucleotide excision repair also result in chromosomal non-disjunction and aneuploidy, which implies a role for Rad2 and Rad4 in genome integrity (Howlett and Schiestl 2004). Several genes identified as causing synthetic growth defects in combination with *cdc68-ΔNTD* are members of the *RTT* gene family, including Mre11, Xrs2, Rad50, Sae2, and Rad27. Rtt107 (also known as Esc4) has recently been identified as a Mec1 phosphoryaltion substrate and has been shown to play a role in response to DNA damage (Rouse 2004). The *RTT106* gene also belong to this family, but its function is yet to be determined (Scholes *et al.* 2001).

In summary, it appears that loss of the non-essential N-terminal domain of Cdc68 leads to impairment of several FACT-mediated functions, including transcription, DNA replication, DNA repair and genome stability. In addition to these functions, a role for the N-terminal domain in intracellular transport is also implied, although FACT involvement in this process remains unclear and may be indirect, through effects of a transcription-related activity. The most striking feature of Cdc68 N-terminal domain function is its

involvement in DNA replication and repair. The genetic findings presented here assist in understanding FACT association with these processes and provide a solid basis for further investigations in this area.

ix) Classification of *cdc68* mutant alleles based on synthetic genetic array analysis

SGA analysis of mutant alleles of *cdc68* allows broad classification of these mutations based on the cohort of gene deletions with which they display synthetic genetic interactions. The multiple alleles of *cdc68* employed here for SGA analysis have identified many overlapping but also unique genetic interactions. By examining the subset of interactions for each mutant allele, associated functions for the regions affected by each mutation may be inferred. Allele-specific synthetic lethal interactions allow categorization of the functional consequences of the structural alteration encoded by each. I have compared the genes identified in each screen and determined the percentage of overlap within the datasets in each instance (Table 23).

SGA analysis using the *cdc68-E857K* allele identified approximately five times fewer genetic interactions than did any other *cdc68* allele. This outcome implies that the amino acid substitution encoded by *cdc68-E857K* is less disruptive to Cdc68 functions than are the other mutations identified and studied here, which is consistent with the phenotypes associated with cells containing this allele. Each of the other alleles, *cdc68-E763G*, *cdc68-312*, *cdc68-319*, and *cdc68-ΔNTD*, identify approximately 100 genes as causing synthetic sickness or lethality when deleted (Table 23). Thus each of these alleles affects multiple Cdc68 functions in more deleterious fashion than does *cdc68-E857K*. Due to the relatively small number of genetic interactions identified for *cdc68-E857K*, the percentage of overlap with any other allele appears higher. Functionally, it would appear that the Cdc68-319 protein is most similar in function to Cdc68-E857K, since the *cdc68-319* and *cdc68-E857K* mutant alleles are the only ones that cause synthetic growth defects when Hir proteins or histone dosages are altered, potentially indicating an impairment in chromatin assembly effect for each.

There is a significant overlap between the genetic effects of the *cdc68-E763G* and *cdc68-312* alleles, which is not surprising given that these two alleles share a common mutational change (Table 23; Figure 65). As described above, the majority of genes

Table 23. Overlap between SGA analyses datasets for each allele of *cdc68*.

Allele	*cdc68-E857K*	*cdc68-E763G*	*cdc68-312*	*cdc68-319*	*cdc68-ΔNTD*
cdc68-E857K	100% (22)	7% (6)	6% (5)	10% (8)	9% (9)
cdc68-E763G	27% (6)	100% (90)	65% (53)	17% (13)	24% (23)
cdc68-312	23% (5)	60% (53)	100% (83)	12% (9)	24% (23)
cdc68-319	36% (8)	14% (13)	10% (9)	100% (78)	15% (14)
cdc68-ΔNTD	41% (9)	26% (23)	28% (23)	18% (14)	100% (96)

The number of common gene deletions identified for each pair-wise combination of the *cdc68* alleles employed in SGA analysis is given in brackets. Also shown is the percentage this number represents of the total number of gene deletions identified with the *cdc68* allele indicated in the top row. In this way significant overlaps in the *cdc68-E763G* and *cdc68-312* datasets, the *cdc68-E763G* and *cdc68-ΔNTD* datasets, and the *cdc68-312* and *cdc68-ΔNTD* datasets were identified.

shared between these datasets encode proteins involved in vesicular transport (Figure 65). The next most significant overlap between datasets occurs between *cdc68-E763G* and *cdc68-ΔNTD* or between *cdc68-312* and *cdc68-ΔNTD*, with approximately a quarter of the SGA-identified genetic interactions for these datasets in common. Half of the common genes identified for each of these *cdc68* alleles encode proteins involved in vesicular transport, implying that the major overlapping function affected by these three alleles involves intracellular trafficking. An alternative hypothesis for this overlap is that in making these three chromosomally tagged alleles the insertion of the *natMX4* cassette downstream of the *cdc68* locus has in each case disrupted the *CHC1* gene encoding clathrin heavy chain. If so, then for six different *natMX4* insertions (one for each of the five *cdc68* alleles, and one for the wild-type *CDC68* gene as a control) at the same position downstream of the *CDC68* locus, half of the insertion events may have altered *CHC1* function while the other half did not. This seems an unlikely occurrence considering the mechanism of homologous recombination that would have occurred to insert these replacement cassettes into the chromomsome. A more appealing explanation is that the three mutant alleles showing genetic interactions with significant numbers of genes encoding transport components each impinge on transport function in some manner, perhaps through indirect effects of transcription processes that involve FACT.

All alleles of *cdc68* used in SGA analyses have identified genetic interactions with genes encoding components involved in transcription and DNA metabolism, but *cdc68-319* and *cdc68-ΔNTD* have the largest numbers of interacting genes involved in these functions. It is striking that these alleles, which alter Cdc68 protein structure in very different ways, are so similar in genetic interactions. The implication that there are overlapping functions for the N-terminal domain of Cdc68 and the C-terminal domain altered by *cdc68-319* has also been observed in genetic analysis of chimeric mutant alleles containing both the N-terminal deletion from *cdc68-ΔNTD* and C-terminal point mutations of *cdc68-319* (Results 2, xi and xii). The combination of mutations generates a *cdc68* allele that is unable to provide essential functions. SGA analysis has revealed synthetic genetic interactions for *cdc68-ΔNTD* or *cdc68-319* in combination with genes encoding SWR-C components, MRX components, and Rad27. Perhaps it is through disruption of parallel functions performed by the N-terminal and C-terminal domains of

Cdc68 to those mediated by one of these complexes that the *cdc68-ΔN,319* allele results in loss of essential function.

In summary, each of the *cdc68* alleles examined by SGA analysis has identified genetic interactions that are unique and others that are commonly shared. The unique interactions for each allele potentially represent aspects of Cdc68 function that are impaired as a result of protein structural changes encoded only by that particular mutant allele. The SGA analysis highlights overlapping functions between Cdc68 N-terminal domain deletions and Cdc68 proteins with C-terminal point mutations. Together these findings assist in functional assignments for regions of the Cdc68 protein.

x) Comparison of synthetic genetic interactions identified with *cdc68* mutants to those for other genes

One advantage to using multiple mutant alleles of *cdc68* in SGA analysis is that a broad spectrum of Cdc68 functions is affected by these alleles. Due to the essential nature of *CDC68*, complete gene deletions cannot be studied. Therefore, to ascertain a more comprehensive picture of Cdc68-mediated functions, multiple mutant alleles encoding alterations at various points in the protein were employed. As indicated in section ix above, each allele generated specific genetic associations as well as others that comprise a more global category. I have compiled a complete set of genetic interactions identified from all *cdc68* mutant alleles employed in SGA analysis and have compared this dataset to the genetic-interaction datasets reported for several other mutations using SGA analysis (Figure 71). In total, 246 genes have been identified here as causing synthetic growth impairments when deleted in combination with a *cdc68* mutation. This set of genetic interactions shares significant overlap with a set of genes identified as synthetically sick or lethal in combination with *cdc73Δ* or with a mutant allele of *cdc45* (Tong *et al.* 2004).

As indicated above, Cdc73 is a member of the Paf1 complex which functions in RNA polymerase II transcription elongation. SGA analysis using *cdc73Δ* identified 111 gene deletions that resulted in synthetic growth defects (Tong *et al.* 2004). Of these 111 genes, 46 (40%) are also identified as causing synthetic impairments when deleted in combination with a *cdc68* mutation (Figure 72). This finding is consistent with similar

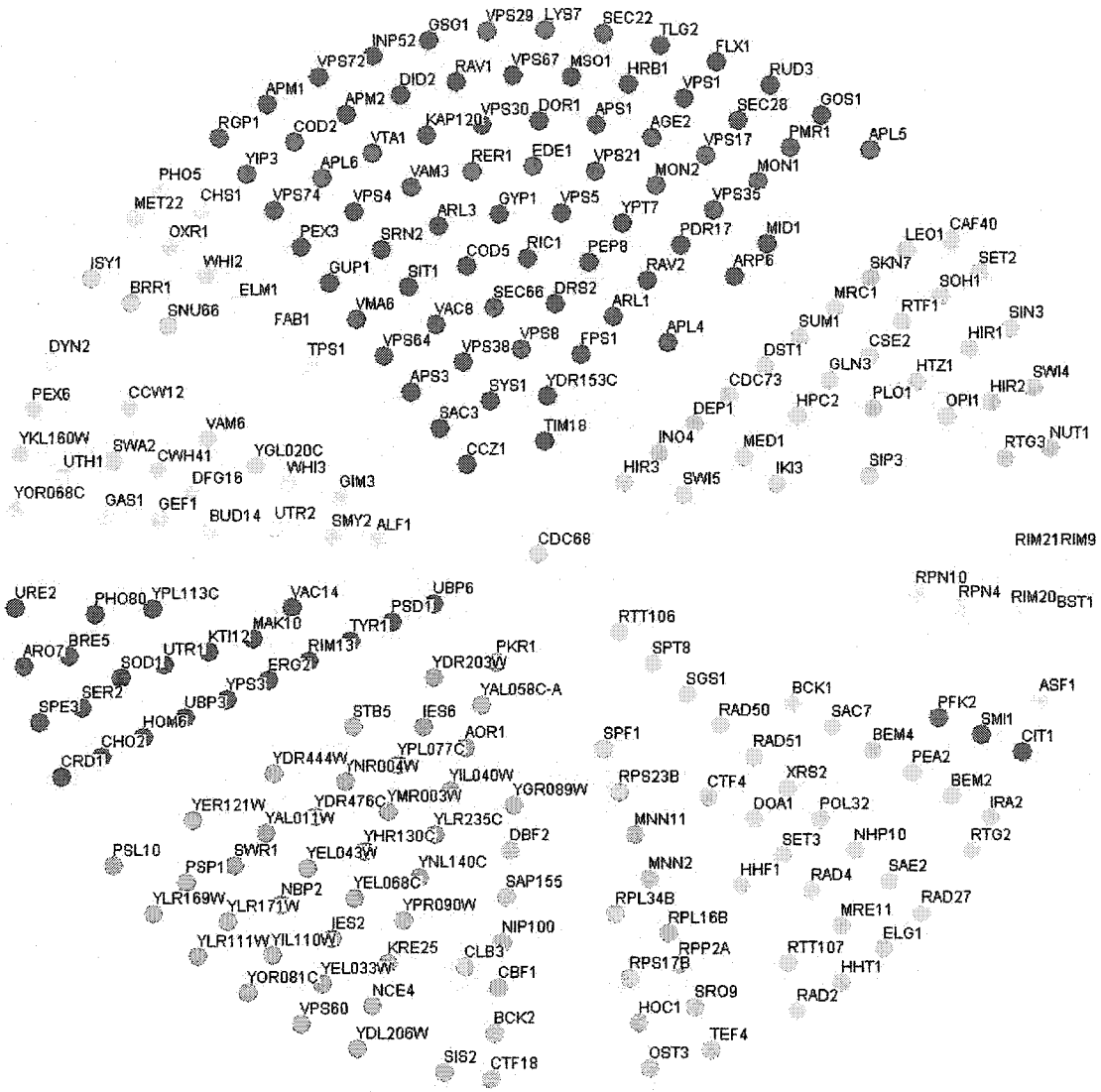

Figure 71. Synthetic genetic interactions web for *cdc68*. The 246 gene deletions identified by SGA and verified by random-spore analysis to be synthetically sick or lethal in combination with *cdc68-E857K*, *cdc68-E763G, cdc68-312, cdc68-319,* or *cdc68-ΔNTD* are indicated by coloured nodes (see Appendix 2 for legend). The *CDC68* gene is indicated in the middle and is connected by synthetic genetic effects to all of the genes indicated. Major functional classifications of interacting genes include transcription, DNA metabolism, metabolism and transport.

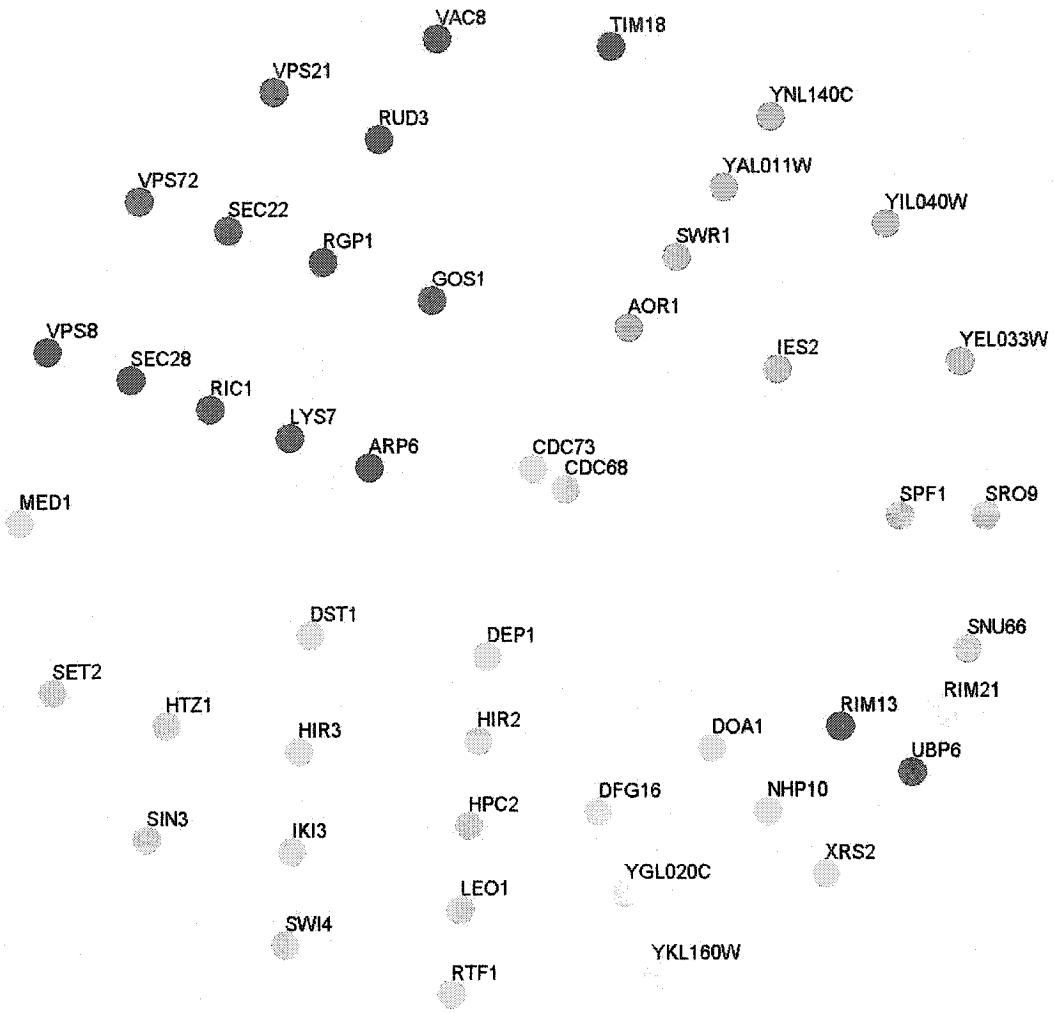

Figure 72. Common genetic interactions identified in SGA screens with *cdc68* mutant alleles and with *cdc73Δ*. SGA analysis with cells containing *cdc73Δ* has identified 111 gene deletions that resulted in a synthetic growth defect (Tong *et al.* 2004). Of these 111 genes, 46 were also identified in SGA analysis carried out here using *cdc68* mutant alleles. The 46 genes common to both datasets are displayed above with *CDC68* and *CDC73* in the center to indicate that they were the common query genes. The majority of common genes encode proteins involved in transcription or transport. See Appendix 2 for node colour codes.

functions for Cdc73 and Cdc68, most likely in transcription elongation, *CDC45* is an essential gene that encodes a protein that functions at the replication fork and assists in DNA strand elongation during replication. A mutant allele of *cdc45* employed in SGA analysis identified 94 genes with synthetic genetic interactions (Tong *et al.* 2004). Of these 94 genes, 37 (39%) were also found to be synthetically sick or lethal when deleted in combination with a *cdc68* mutation (Figure 73). This overlap implies a significant degree of similarity between certain Cdc68 functions and those performed by Cdc45 in replication.

In conclusion, SGA analysis has been a powerful tool for identifying genetic interactions. It has highlighted many functional relationships that were not previously known for Cdc68 and will undoubtedly move FACT-related research to exciting new areas.

5. Identification of Ynl035c as a novel interacting partner with Cdc68

i) Ynl035c physically interacts with the Cdc68(436-1035) polypeptide in the yeast two-hybrid assay

In addition to the directed two-hybrid analysis discussed in Section 1(i) above, the Gal4 DNA-binding domain (BD) fusions with Cdc68 polypeptides and with Pob3 were used in a selection scheme to identify interacting proteins encoded by yeast genomic libraries containing genes encoding Gal4 activation-domain (AD) polypeptide fusions.

Derivatives of strain PJ69-4a yeast cells containing pGBT9-based plasmids bearing the genes expressing BD-Pob3, BD-Cdc68, BD-Cdc68(1-436), BD-Cdc68(436-1035), BD-Cdc68(625-1035), or BD-Cdc68(308-642) were transformed with plasmids from the YL1, YL2 and YL3 yeast genomic two-hybrid libraries. These library plasmids contain segments of yeast genomic DNA fused to the *GAL4* activation domain sequence and therefore express a range of AD-fused yeast polypeptides. Transformants containing both a pGBT9-based plasmid and a library plasmid, as determined by growth on medium lacking both leucine and tryptophan, were replica-plated to medium lacking adenine (SC-Ade) to monitor expression of the *GAL2-ADE2* reporter gene (Figure 9). Table 24 summarizes the number of library-plasmid transformants assessed for each of the starting strains indicated above. Transformants that grew on SC-Ade medium were chosen for further study. These cells, with candidate two-hybrid interactions, could have acquired

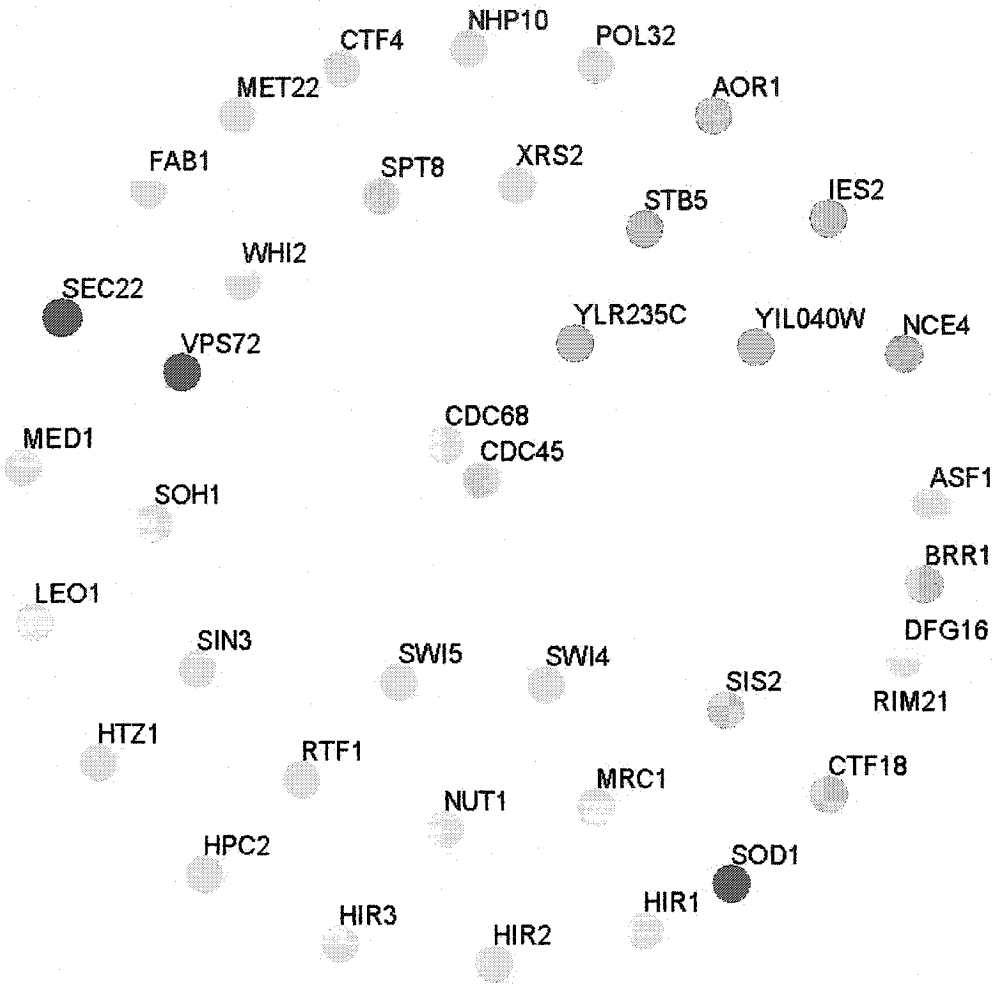

Figure 73. Common genetic interactions identified in SGA screens with *cdc68* mutant alleles and *cdc45*. SGA analysis with *cdc45* cells identified 94 gene deletions that resulted in a synthetic growth defect (Tong *et al.*, 2004). Of these 94 genes, 37 were also identified in SGA analysis performed here using *cdc68* mutant alleles. The 37 genes common to both datasets are displayed above with *CDC68* and *CDC45* in the center to indicate that they were the common query genes. The majority of common genes encode proteins involved in transcription or transport. See Appendix 2 for node colour codes.

the ability to grow on SC-Ade medium by 1) activating transcription of the *GAL2-ADE2* reporter gene by bringing the Gal4 BD and AD into close proximity at the promoter site, indicating that the 'bait' (polypeptide fused to the Gal4 BD) and 'prey' (polypeptide fused to the Gal4 AD) polypeptides physically interact, or 2) activation of the *GAL2-ADE2* reporter gene by the polypeptide fused to the Gal4 AD, without the assistance of additional protein factors, or 3) complementation of the adenine deficiency by the presence of an Ade2 polypeptide fused to the Gal4 AD. This last possibility therefore bypasses the need for expression of *GAL2-ADE2* to restore growth on SC-Ade medium. The first possibility is a positive two-hybrid interaction and identifies proteins that physically interact with the bait polypeptide, which may further our understanding of bait protein function. The second and third possibilities are two-hybrid false positives, since in both cases the AD-fused polypeptide acts independently of the BD-fused polypeptide and does not identify a polypeptide interaction with the bait protein.

The number of yeast two-hybrid candidate isolates identified for each bait protein employed is provided in Table 24. Library plasmids from each candidate isolate were then further tested to see whether adenine prototrophy results in the absence of the bait protein. Plasmid preparations from two-hybrid candidate cells, mixtures of the pGBT9-based plasmid, marked with *TRP1*, and yeast two-hybrid library plasmids, marked with *LEU2*, were transformed into *E. coli* cells of strain JF1754, which contain a *leuB* mutation and as a result are not able to biosynthesize leucine. The yeast *LEU2* gene complements the *leuB* mutation in *E. coli*, allowing these transformant cells to grow in the absence of exogenously supplied leucine (Ratzkin and Carbon 1977). By transforming the plasmid mixture obtained from yeast cells into JF1754 cells, *E. coli* transformants containing the *LEU2*-marked library plasmid could be selected based on leucine protrophy. The library plasmids were then purified from *E. coli* cells and transformed back into yeast PJ69-4a derivatives, which were replica-plated to SC-Ade medium to determine auxotrophic status. In this way, library plasmids encoding polypeptides that themselves confer adenine prototrophy were identified as false positives and discarded.

Of the 112 two-hybrid candidates initially identified, only one candidate was not discarded as a false positive. This two-hybrid plasmid was initially identified with the.

Table 24. Summary of two-hybrid library screening

'Bait' protein	Number of transformants examined from each YL-library	Candidates identified	Verified two-hybrid interactions
BD-Cdc68	YL1: 28296 YL2: 18532 YL3: 29968	10	0
BD-Cdc68(1-436)	YL1: 35292 YL2: 34792 YL3: 20092	29	0
BD-Cdc68(436-1035)	YL1: 20116 YL2: 20436 YL3: 22692	18	1
BD-Cdc68(308-642)	YL1: 14450 YL2: 24328 YL3: 16040	18	0
BD-Cdc68(626-1035)	YL1: 11074 YL2: 15988 YL3: 10760	17	0
BD-Pob3	YL1: 35952 YL2: 46456 YL3: 27512	20	0

BD: Gal4 DNA-binding domain fused in frame to the N-terminus of the polypeptide chain indicated; YL1, YL2, and YL3: two-hybrid libraries which contain the DNA sequence for GAL4 AD fused to yeast genomic DNA in three different reading frames. Candidates for two-hybrid interactions were identified by growth on SC-Ade medium.

BD-Cdc68(436-1035) protein. The sequence of the genomic DNA fused to GAL4 AD in this library plasmid, designated pMH1, was determined and shown to encode amino acids 140-389 of the Ynl035c protein.

Very little is known about the non-essential Ynl035c protein other than that it contains WD-40 domains and a putative nuclear localization signal. Indeed, by large-scale protein localization analyses Ynl035c appears to localize to the yeast nucleus (Shcherbik *et al.* 2002; Huh *et al.* 2003). WD-40 domains, named for the conserved tryptophan and aspartate residues present at the C terminus of this 40-residue domain, are important for mediating protein-protein interactions. The number of WD-40 domains in the Ynl035c protein is uncertain, as different programs designed to predict domain structures based on sequence data, such as Simple Modular Architecture Research Tool (Schultz *et al.* 1998; Letunic *et al.* 2004), *P*rotein families database of alignments and HMMs (Finn, in prepartation), and the National Cancer Biology Institutes' Conserved Domain Architecture Retrieval Tool (Geer *et al.* 2002), identify as few as three and as many as seven WD-40 domains for this protein. All programs identify three WD-40 domains that span Ynl035c residues 47-87, 138-177, and 283-321. Two of these WD-40 domains are encoded in the AD-Ynl035c two-hybrid library polypeptide that is able to bind BD-Cdc68(436-1035). It has been shown that seven WD-40 domains are able to fold into a 'propeller' conformation that binds proteins (van der Voorn and Ploegh 1992); however, there need not be a complete set of seven repeats in a given protein.

The closest yeast homologues of Ynl035c, including Hat2, Utp13, Caf4, and Sif2, themselves contain WD-40 domains, and the regions of homology are confined to the WD-40 domains. These proteins are involved in a wide range of functions; therefore little functional information about Ynl035c can be gleaned from recognizing the presence of this domain structure. However, WD-40 proteins have roles in diverse chromatin-related functions (Henikoff 2003), such as nucleosome deposition (Verreault *et al.* 1996) and deacetylation of histones (Furuyama *et al.* 2003). Thus the physical association of Ynl035c with Cdc68(436-1035) is intriguing. A BLASTP search of all protein database resources using the Ynl035c protein sequence identifies homologues for this protein in several eukaryotes, including *S. pombe*, *M. musculus*, *H. sapiens*, *A. thaliana*, and *D. melanogaster*, which when aligned share 21-34% identity and 42-50% conservation

with *S. cerevisiae* Ynl035c (data not shown). The region of sequence conservation in these potential homologues extends beyond the WD-40 domains to span the entire length of the protein. No function has been assigned to any of these putative homologues to date.

Ynl035c has also been identified in large-scale affinity purifications as a factor interacting with Kin1, a serine/threonine kinase, and Kap104, a protein that binds nuclear-localization signals to facilitate nuclear import of proteins (Ho *et al.* 2002). The significance of these interactions remains to be determined.

The ability of Ynl035c to physically associate with other Cdc68 polypeptides was also assessed through two-hybrid assays. The pMH1 plasmid encoding AD-Ynl035c polypeptide that interacts with BD-Cdc68(436-1035) was transformed into PJ69-4a derivatives containing the other BD-Cdc68 and BD-Pob3 polypeptides employed in this study to test for two-hybrid interactions. Transformants containing both pMH1 and a pGBT9-based plasmid were selected by growth on medium lacking leucine and tryptophan. These cells were then grown as patches on SC-LeuTrp solid medium and replica-plated to SC-Ade medium or to nitrocellulose filters for β–galactosidase assays. Growth on SC-Ade medium and blue pigment development during the β–galactosidase assay indicated activation of the *GAL2-ADE2* and *GAL7-lacZ* reporters, respectively. Based on these criteria, no two-hybrid interaction was observed between any of the other BD-Cdc68 polypeptides and the AD-Ynl035c polypeptide encoded by pMH1 (Figure 74; data not shown). By this analysis it appears that AD-Ynl035c preferentially associates with the BD-Cdc68(436-1035) polypeptide, which contains the middle and C-terminal domains of Cdc68. The failure of AD-Ynl035c to interact with BD-Cdc68(1-1035) may be due to a number of factors: 1) full-length Cdc68 fused to BD may be folded in such a way as to preclude interaction with AD-Ynl035c, either as a result of the positioning of the BD with respect to the Cdc68 protein or due to the presence of the Cdc68 N-terminal domain; 2) BD-Cdc68 may be titered away from the *GAL2* promoter UAS of the reporter gene due to interactions with endogenous, untagged Pob3 or other cellular factors, and as a result is not available for AD-Ynl035c binding to activate the reporter gene. In addition to these reasons, BD-Cdc68(1-436), BD-(308-642) or BD-626-1035)may fail to produce two-hybrid interactions with AD-Ynl035c if these polypeptides either lack or disrupt the

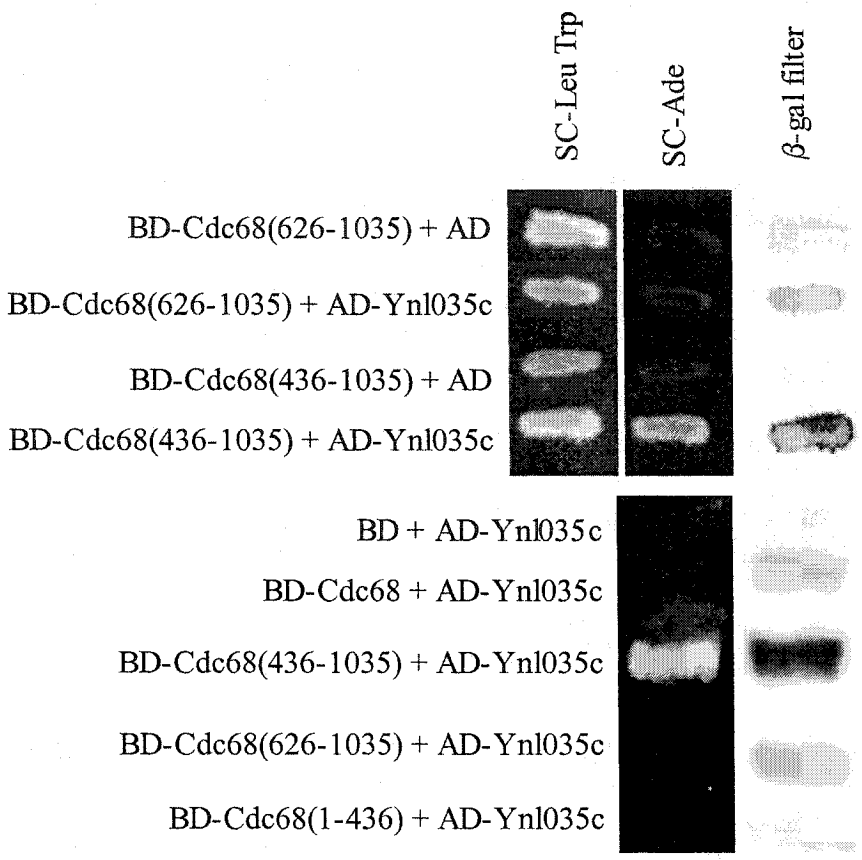

Figure 74. BD-Cdc68(436-1035) interacts with AD-Ynl035c. Cells of strain PJ69-4a derivataives containing the plasmids encoding the fusion proteins indicated at left were spread as patches on medium lacking leucine and tryptophan (SC-Leu Trp), grown for 2 days at 30°C and then replica-plated to SC-Leu Trp and to SC-Ade and grown for 3 to 4 days at 30°C or replica-plated to a nitrocellulose filter and used in β–galactosidase assays (β-gal filter). As indicated by growth on SC-Ade medium and blue colour development during the β–galactosidase assay, only the BD-Cdc68(436-1035) polypeptide was able to interact with AD-Ynl035c to activate *GAL2-ADE2* and *GAL7-lacZ* reporter-gene expression. Faint colour development during the β–galacotsidase assay was observed for BD-Cdc68(626-1035) and BD-Cdc68 with both AD and AD-Ynl035c (β-gal filter column, and data not shown).

Ynl035c-binding site. It should be noted that western blot analysis with anti-Gal4-activation-domain antibodies (Santa Cruz) of extracts from cells containing the AD-Ynl035c with any of the BD-Cdc68 fusion polypeptides assessed did not identify a protein product corresponding to the anticipated size for AD-Ynl035c (data not shown). Therefore, the failure of the AD-Ynl035c polypeptide fusion to ellicit a two-hybrid response with most BD-Cdc68 fusions could be the result of protein instability that is somehow only alleviated in the presence of BD-Cdc68(436-1035).

ii) Phenotypic analysis of *ynl035cΔ*

The nourseothricin (Nat) resistance cassette (Goldstein and McCusker 1999) was used to replace one of the *YNL035c* chromosomal genes (Materials and Methods) in cells from the BM64 yeast strain, an isogentic relative of my KanB diploid strain. employed in the studies of *cdc68* mutant alleles (see section 2 above). These diploids were sporulated and resultant haploid segregants were assessed for growth on medium containing Nat. A 2:2 segregation pattern was observed for resistance to Nat, indicating that the diploid strain contained only one insertion of the *NatMX4* cassette. Eighteen haploid *ynl035cΔ::natMX4* segregants, as determined by growth on medium containing Nat, as well as wild-type *YNL035c* control segregants, were assessed for growth under a wide range of conditions. A growth phenotype associated with *ynl035cΔ* may assist in elucidating a molecular function for the Ynl035c protein product. Growth at 23°C, 30°C, 35°C, 37°C, and 39°C on YPD medium was characterized. The Spt status of *ynl035cΔ* cells containing the *his4-912δ* and *lys2-128δ* reporter genes was assessed by monitoring cell growth on SC-His and SC-Lys media. The ability of *ynl035cΔ* cells to grow on medium containing a range of concentrations of the DNA-damaging agents methyl methanesulphonate, phleomycin, 4-nitroquinoline oxide, cisplatin, and hydroxyurea (which was also tested at both 30°C and 35°C) was determined. Growth of *ynl035cΔ* cells was also assessed in the presence of sodium dodecyl sulphate, high salt concentrations, caffeine, the nucleotide analogues 6-azauracil and mycophenolic acid, and sorbitol (tested at 30°C, 37°C, and 39°C). In each instance, growth of *ynl035cΔ* cells was comparable to that of wild-type cells (data not shown).

iii) Characterization of genetic interactions for *YNL035c* and *CDC68*

Two approaches to characterizing genetic interactions between *YNL035c* and *CDC68* were undertaken. The first involved phenotypic analysis of double-mutant *ynl035cΔ* cells containing various *cdc68* mutant alleles, while the second investigated the effects of over-expressing *YNL035c* in *cdc68* mutant cells.

To test for genetic interactions between *ynl035cΔ* and *cdc68* mutant alleles the *ynl035cΔ* haploids were mated to haploid *cdc68Δ::kanMX4* segregants containing *URA3* centromeric plasmids carrying *CDC68*, *cdc68-1*, *cdc68-Δ922*, *cdc68-Δ368*, *cdc68-mini*, *cdc68-E857K*, *cdc68-E763G*, *cdc68-312*, or *cdc68-319*. The resultant diploids were sporulated and haploid segregants were selected that were geneticin-resistant, indicating the presence of the *cdc68Δ::kanMX4* replacement, Nat-resistant, indicating the presence of *ynl035cΔ::natMX4*, and uracil-prototrophic, indicating the presence of a *CDC68* plasmid. Four double-mutant haploid segregants and, as controls, two of each single-mutant haploid segregant were assessed under the conditions described above for *ynl035cΔ* alone. No synthetic enhancement or lethality was observed when the *ynl035cΔ* was combined with any of the *cdc68* mutant alleles (data not shown). These observations suggest that the Ynl035c protein does not share an overlapping or parallel function with any that are compromised by the *cdc68* mutant alleles. Consistent with this finding, the *ynl035cΔ* in the yeast deletion collection was not found to be synthetically lethal with the *cdc68-E763G*, *cdc68-E857K*, *cdc68-312*, *cdc68-319* or *cdc68-ΔNTD* alleles in synthetic genetic array analysis (Results 4).

The second approach to identify genetic interactions between *YNL035c* and *cdc68* mutations was to monitor the effects of over-expressing *YNL035c* in *cdc68* mutant cells. A 2μ-based, *YNL035c* plasmid was introduced into KanB-derived haploid *cdc68Δ::kanMX4* segregants harbouring centromeric plasmids encoding *CDC68*, *cdc68-1*, *cdc68-Δ922*, *cdc68-Δ368*, *cdc68-mini*, *cdc68-312* and *cdc68-319*. Cell growth of transformants was assessed over a range of temperatures (23°C, 30°C, 35°C, 37°C, 39°C) on both YPD and synthetic complete media, on medium lacking hisidine or lysine (to monitor Spt reporter-gene activation), and on media containing caffeine, sodium dodecyl sulphate, high salt concentrations, sorbitol (at 30°C and 39°C), hydroxyurea (at 30°C and 35°C), 6-azauracil and mycophenolic acid. Once again, under almost all of the condition

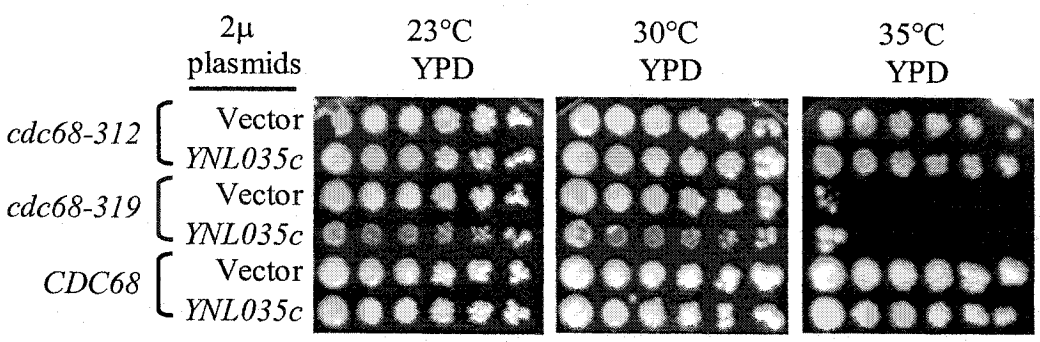

Figure 75. Over-expression of *YNL035c* causes a synthetic growth defect in *cdc68-319* cells. Five-fold serial dilutions of cultures bearing the genes indicated at left on either *CDC68 CEN* plasmids or 2μ-based plasmids were spotted starting with a concentration of $1x10^7$ cells/ml. Cells were grown on YPD medium at the indicated temperature for 3-5 days.

tested no growth enhancement or impairment was observed for cells over-expressing *YNL035c* in comparison to the same cells containing an empty vector as a control (data not shown). The one exception was the growth impairment seen on YPD medium at 23°C and 30°C for *cdc68-319* cells containing the high-copy *YNL035c* plasmid (Figure 75). Serial dilutions of these *cdc68-319* yeast cultures grown on YPD medium at 23°C or 30°C show a significant decline in the robustness of growth. While the viability of cells did not seem to be affected by this combination, the density of cell growth, or perhaps cell size, seemed to be affected. While the effect is subtle, this result has been reproduced in three independent trials. This finding provides genetic evidence that *CDC68* and *YNL035c* may be functionally related, which supports the physical association identified by two-hybrid analysis.

iv) Synthetic genetic array analysis of *ynl035cΔ*

In an effort to understand the function of *YNL035c*, synthetic genetic array analysis (Tong *et al.* 2001) using *ynl035cΔ* was performed. Synthetic lethal relationships identify genes that affect common cellular functions. Through SGA analysis with *ynl035cΔ* an understanding of this as-yet uncharacterized gene's function was anticipated.
Two independent SGA screens identified 840 and 941 synthetic-lethal candidates with *ynl035cΔ::natMX4*. The number of candidates was decreased to 168 and 182 by discarding deletion strains identified as 'false positives' by the Boone lab (Tong *et al.* 2001) or our own lab (Results 4, iii), and by eliminating genes in the genetic linkage group for *YNL035c*. The linkage group found in this way for *ynl035cΔ* contained 14 of the genes residing between *HDA1* (*YNL021w*) and *YNL050c*, including *ynl035cΔ::kanMX4* from the deletion collection. Gene deletions resulting in synthetic growth impairment or lethality were then sorted further by choosing for future study only those that resulted in growth impairment in combination with *ynl035cΔ* in both SGA trials, giving a final list of 29 candidate gene deletions (Table 25).

Assessment of these 29 gene candidates by random-spore methodology (Tong *et al.*, 2001). By this analysis, the number of viable double-mutant progeny, harbouring both *ynl035cΔ::natMX4* and *geneXΔ::kanMX4* from the deletion collection, was not significantly lower than the number of single-mutant progeny, either *ynl035cΔ::natMX4* or *geneXΔ::kanMX4* for any of the candidates. Therefore *none* of the synthetic-lethal

Table 25. Gene deletions identified as synthetic-lethal with *ynl035cΔ* by SGA analysis

Gene name	Systematic name	SGA scoring	RSA scoring
ARP6	YLR085c	lethal	False
CBP1	YJL209w	lethal	False
CCE1	YKL011c	lethal	False
GPD1	YDL022w	lethal	False
GTR1	YML121w	slg	False
IES6	YEL044w	lethal	False
MKS1	YNL076w	slg	False
NPL6	YMR091c	lethal	False
NUT1	YGL151w	lethal	False
RAD4	YER162c	slg	False
RAD54	YGL163c	slg	False
RTS1	YOR014c	slg	False
SCS7	YMR272c	lethal	False
SIC1	YLR079w	slg	False
SOH1	YGL127c	slg	False
SPE2	YOL052c	slg	False
SPL2	YHR136c	lethal	False
TPS2	YDR074w	slg	False
UBC8	YEL012w	lethal	False
VPS4	YPR173c	slg	False
VPS8	YAL002w	slg	False
WHI3	YNL197c	slg	False
YDR467c	YDR467c	slg	False
YEL033w	YEL033w	slg	False
YGL214w	YGL214w	lethal	False

Table 25. Gene deletions identified as synthetic lethal with *ynl035cΔ* in SGA analysis, continued

Gene name	Systematic name	SGA scoring	RSA scoring
YHL013c	YHL013c	lethal	False
YIL121w	YIL121w	lethal	False
YJR084w	YJR084w	lethal	False
YPL077c	YPL077c	slg	False

Deletions of the genes identified as being synthetic-lethal (lethal) or sick (slg, slow growth) in combination with *ynl035cΔ*. Each of these candidates was then tested by random-spore anlaysis (RSA) to verify the synthetic relationship. False, no synthetic relationship.

candidates identified initially in SGA give a *bona fide* synthetic lethal interaction with *ynl035cΔ* as determined by random-spore analysis. As a control during the random-spore analysis, segregants from diploid cells containing the *ynl035cΔ* and a *YNL035c*-linked gene deletion were also evalulated. As anticipated, no viable double-mutant progeny were obtained from this control, verifying that the random-spore process was functioning as it should.The Boone lab (Toronto) has reported (Tong *et al.* 2001) rates of false-positive synthetic lethal interactions using SGA greater than 50%. Other gene deletions used in SGA in the Singer/Johnston lab and elsewhere have also resulted in no verifiable synthetic-lethal interactions (S. M. Lewis, unpublished data; M. J. Dobson, personal communication). Thus the finding here of no verifiable synthetic-lethal interactions is not unprecedented.

The lack of synthetic lethal interactions with *ynl035cΔ*, while not particularly informative in terms of elucidating Ynl035c function, may provide a clue about the redundancy of Ynl035c function. There are many WD-40 proteins in yeast, and several of these reside in the nucleus along with FACT. In the absence of Ynl035c, these other WD-40 proteins may be able to provide a substitute activity, and as a result of this redundant function, no growth impairments or synthetic lethal interactions may be identified for *ynl035cΔ* cells. Another possibility is that Ynl035c function is only required for a specific subset of cellular functions, *i.e.* pseudohypheal growth, and conditions that would monitor these functions have not been characterized in the approaches taken to date.

To summarize the findings reported in this section, a Ynl035c-derived polypeptide is shown here to interact physically with Cdc68(436-1035) in the two-hybrid assay. By the same criteria, Ynl035c does not interact with full-length or any other Cdc68 derivative tested, or with Pob3. As evidence in support of the validity of this two-hybrid physical interaction, at least one genetic interaction between Ynl035c and mutant Cdc68 proteins has been identified. Specifically, when Ynl035c is over-expressed in *cdc68-319* cells growth on YPD medium at 23°C and 30°C is much less robust. This finding implies that increased dosage of Ynl035c may impede Cdc68-319 mutant protein function. To identify a molecular function for Ynl035c, SGA analysis and phenotypic characterization was carried out. Of the ~4700 gene deletions tested with *ynl035cΔ*, no double-mutant combination was found to be synthetically lethal. Additionally, no deleterious phenotype

could be associated with *ynl035cΔ* under any of the conditions tested. Either Ynl035c function is redundant, perhaps shareing an overlapping function with an essential protein (which would not be identified using SGA analysis), or the conditions applied in genetic assessments did not necessitate Ynl035c functions.

IV. DISCUSSION

1. FACT structure

i) Domain structure of FACT

The FACT complex in yeast is composed of three proteins, Cdc68, Pob3, and Nhp6 (Wittmeyer and Formosa 1997; Brewster *et al.* 1998, 2001; Wittmeyer *et al.* 1999; Formosa *et al.* 2001). The stable core of this complex is a dimer made up of the Cdc68 and Pob3 proteins, with Nhp6, a small protein comprising an HMG-box domain, weakly associated (Brewster *et al.* 2001; Formosa *et al.* 2001). The metazoan homologue of FACT contains only two proteins, a Cdc68 homologue known as SPT16 and SSRP1, and a single protein homologous to both Pob3 and Nhp6 (LeRoy *et al.* 1998; Orphanides *et al.* 1998). The domain structure of the yeast FACT subunits Cdc68 and Pob3 was determined in our lab by analysis of peptide fragments generated by partial proteolysis (N. K. Brewster, unpublished results). This approach takes advantage of the fact that the regions of a protein more vulnerable to proteolytic degradation often link folded domains. As a result, limited proteolytic degradation can generate polypeptides that correspond to independently folded domains. The results of this analysis have assigned approximate domain boundaries for Cdc68 and Pob3 based on the sizes of the polypeptides generated from partial proteolysis, identifying three independently folded domains in the Cdc68 protein (an N-terminal domain of residues 1-484, a middle domain of residues 485-790, and a C-terminal domain of residues 791-1035), while the Pob3 protein contains two domains (an N-terminal domain of residues 1-221 and a C-terminal domain of residues 221-552). The C-terminal domain boundary for Pob3 was confirmed by Edman sequencing of a proteolytic fragment of recombinant purified Pob3.

ii) Domains responsible for the association of Cdc68 and Pob3

With the domain analysis in mind, constructs to express recombinant Cdc68 and Pob3 proteins were generated and the resulting polypeptides were employed in a series of *in vitro* binding assays to determine the regions responsible for the association of Cdc68 with Pob3. Recombinant proteins were designed to mimic individually folded domains. Additional constructs were also made that expressed portions of these domains, to try to identify subsections of each domain that may be responsible for binding. The results of these assays showed that the middle domain of Cdc68 is responsible for binding Pob3

and associates with both the N-terminal and C-terminal domains of the Pob3 protein. Consistent with this finding, when recombinant polypeptides containing only a portion of the middle domain of Cdc68 were employed in binding assays, the association with Pob3 was decreased. This indicates that the intact middle domain is required for avid association of Pob3, and when only portions of the middle domain are available some regions important for binding Pob3 may be lost, resulting in decreased Pob3 association.

Competitive co-immunoprecipation studies designed to evaluate the *in vivo* interaction between Cdc68 and Pob3 were also performed. The ability of Cdc68 polypeptides missing the N-terminal domain to associate with a limiting amount of Pob3 in the presence of wild-type Cdc68 protein was determined. Results of these studies showed that a Cdc68 protein lacking the N-terminal domain completes effectively with the wild-type Cdc68 protein for Pob3 binding. Thus the middle and C-terminal domains of Cdc68 must be sufficient for stable association with Pob3 *in vivo*. This finding is consistent with the *in vitro* binding assays that assign Pob3-binding function to the middle domain of Cdc68.

Yeast FACT structure determined in this study is consistent with the reported physical associations between metazoan FACT subunits as determined from similar binding assays using purified recombinant polypeptides of SPT16 and SSRP1 from *H. sapiens* and *D. melanogaster* (Keller and Lu 2002; Shimojima *et al.* 2003). A significant difference between the *in vitro* studies performed here and those described for metazoan FACT is that the recombinant polypeptides employed in my studies correspond to the protein domains determined experimentally, while the *in vitro* studies of metazoan FACT used polypeptides that often corresponde to truncations of the SPT16 or SSRP1 domains (as predicted by the yeast studies). As a result of these fragmented domains, some potential SPT16/SSRP1 interactions may have been missed.

The *in vitro* binding studies employing human (h) recombinant proteins (Keller and Lu 2002) showed that hSSRP1 residues that would roughly correspond to the N-terminal domain of Pob3, based on sequence alignments, are able to associate with full-length hSPT16, but with greatly decreased affinity in comparison to full-length hSSRP1 association with full-length hSPT16. This is consistent with the concept that some of the binding sites responsible for the association of Pob3 or hSSRP1 with Cdc68 or hSPT16,

respectively, are contained within the C-terminal domain of Pob3 or homologous region in SSRP1. Therefore, when only some of the residues responsible for Pob3/hSSRP1 association with Cdc68/hSPT16 are present, the avidity of binding between the two is diminished. Further i*n vitro* binding studies employing hSSRP1 residues corresponding to the C-terminal domain of Pob3, minus approximately 50 residues from the N-terminal end of this domain, failed to show an interaction with hSPT16 protein. This apparent discrepancy between the *in vitro* findings for Cdc68 and Pob3 binding in comparison to hSPT16 and hSSRP1 interaction may exist because the region of the hSSRP1 protein that was used most likely is a domain truncation, and therefore the failure to bind hSPT16 may be the result of improper protein folding or loss of peptide sequences involved in binding. Consistent with the findings presented here describing the region of Cdc68 responsible for binding Pob3, a purified recombinant hSPT16 polypeptide approximating the N-terminal domain of Cdc68 was unable to bind to full-length hSSRP1 *in vitro*, while a hSPT16 polypeptide homologous to a portion of the middle domain of Cdc68 was able to bind hSSRP1, although at decreased affinity compared to the binding of full-length hSPT16 to hSSRP1 (Keller and Lu 2002). This latter observation may be the result of truncation of the hSPT16 middle domain, so that only some of the peptides able to associate with hSSRP1 were present.

The *in vitro* binding studies employing recombinant *Drosophila* (d) proteins have shown that two different dSSRP1 polypeptides, containing regions homologous to the yeast Pob3 N-terminal domain and a significant portion of the C-terminal domain, were unable to associate with dSPT16 (Shimojima *et al.* 2003). This result conflicts with both the *in vitro* findings presented here for recombinant yeast Cdc68 and Pob3 and those using human recombinant SPT16 and SSRP1 (Keller and Lu 2002). A possible explanation for this difference may be the presence in the *Drosophila* peptides of residues corresponding to only a partial domain, which could result in misfolding of the recombinant polypeptide or may block dSPT16 association with the dSSRP1 sequences homologous to the N-terminal domain of the yeast Pob3 protein. Consistent with this idea, a larger dSSRP1 recombinant protein containing sequences that correspond with intact N- and C-terminal domains of Pob3 was able to bind effectively *in vitro* with dSPT16. Full-length dSSRP1 was able to associate with dSPT16 polypeptides containing

sequences homologous to the complete or partial middle domain of yeast Cdc68. This finding is consistent with the association of the middle domain of Cdc68 with Pob3 and the observations of the homolgous region from hSPT16 associating with hSSRP1 (Keller and Lu 2002).

One aspect of yeast FACT structure that was not examined in my studies is the association of Nhp6 with the Cdc68-Pob3 dimer. *In vivo* studies previously carried out in our lab employing a Pob3-Nhp6 fusion protein, in which the sequence encoding the Nhp6 protein is fused in frame to the Pob3 coding sequence in a design analogous to that of the metazoan SSRP1 protein, indicated that this fusion protein is able to provide essential Pob3 function and also provides a subset of Nhp6 functions (Brewster *et al.* 2001). This finding implies that the restricted positioning of the Nhp6 protein in this fusion must be at least similar to the natural positioning of Nhp6 with respect to the rest of yeast FACT; otherwise, the Pob3 and Nhp6 proteins would not be able to perform their cellular functions. It would therefore not be surprising to identify a physical interaction between the C-terminal domain of Pob3 and the Nhp6 protein, although this association has not been tested directly. A weak two-hybrid interaction has been reported between Cdc68 and Nhp6 (Formosa *et al.* 2001). This interaction may be indirect, occurring *via* a bridge of other nuclear proteins, or may represent one of the ways Nhp6 is associated with Cdc68 and Pob3 to form FACT in yeast. The *in vitro* binding studies employing recombinant human or *Drosophila* SSRP1 polypeptides containing the HMG-box domain that would correspond to Nhp6 provide an unclear picture of the association of this region with SPT16. In the studies using a hSSRP1 HMG-box polypeptide with hSPT16 (Keller and Lu 2002), no binding between these two was seen, but binding was observed in the studies employing a dSSRP1 HMG-box polypeptide and dSPT16 (Shimojima *et al.* 2003). This difference may be the result of the presence of 'extra' residues in the dSSRP1 polypeptide upstream of the HMG-box domain, and therefore corresponding to part of the yeast Pob3 C-terminal domain, which is shown here to associate with Cdc68. Thus these *in vitro* studies make it difficult to discern if the HMG-box domain or Nhp6 protein (in yeast) is able to bind metazoan SPT16 or yeast Cdc68.

Conclusions from the comparisons of *in vitro* binding assays performed with recombinant polypeptides from human, *Drosophila* or yeast FACT proteins are:

1) The middle domain of yeast Cdc68 protein, or sequences homologous to this domain in metazoan SPT16, are required for the association with Pob3 or SSRP1, respectively.

2) Fragments of yeast Cdc68 middle-domain sequence, or of sequences homologous to this domain in metazoan SPT16, have weakened but detectable association with Pob3/SSRP1. This finding suggests that there may be two binding sites for Pob3 within the middle domain of the Cdc68 protein, associating with the Pob3 N-terminal and C-terminal domains.

3) The *in vitro* studies using human recombinant polypeptides indicate that the region homologous to the N-terminal domain of yeast Pob3 is required for hSSRP1 binding to hSPT16, while the *in vitro* studies using *Drosoplila* recombinant polypeptides show that the region homologous to the C-terminal domain of yeast Pob3 is required for dSSRP1 binding to dSPT16. These findings are consistent with the results described here indicating that both the N-terminal and the C-terminal domains of Pob3 bind Cdc68.

4) The regions responsible for Nhp6 association with the FACT complex remain uncertain, but given the homology of SSRP1 to both Pob3 and Nhp6, the positioning of Nhp6 relative to the rest of FACT is most likely similar and therefore Nhp6 would be associated in the vicinity of the C-terminal domain of Pob3.

iii) FACT multimerization?

As purified from yeast cell extracts, FACT has an apparent molecular weight of approximately 400 kDa (Brewster *et al.* 1998; Wittmeyer *et al.* 1999). FACT purified in this way probably does not contain the Nhp6 protein, since Nhp6 association with the Cdc68 and Pob3 dimer is not stable under the conditions employed in these initial characterizations of yeast FACT (Brewster *et al.* 2001; Formosa *et al.* 2002). FACT containing a monomer of Cdc68 (molecular weight 118 kDa) and a monomer of Pob3 (molecular weight 63 kDa) should have an apparent molecular weight of approximately 181 kDa, for a single dimer. Therefore, the observed properties for FACT containing one Cdc68 and one Pob3 molecule predict a complex of approximately twice the anticipated size for this dimer. This size discrepancy could be accounted for if two Cdc68/Pob3 dimers were associated to form a tetrameric complex, and the evidence that two Pob3 proteins are able to interact supports this possibility.

In vitro binding assays using recombinant full-length Pob3 and a polypeptide containing the C-terminal domain of Pob3 showed a significant affinity between these two polypeptides. Further dissection of this binding indicated that the N-terminal domain of Pob3 associates with the C-terminal domain of Pob3 *in vitro*. The *in vitro* binding of two Pob3 monomers shown here raises the possibility of FACT multimerization, an idea that is supported by co-immunoprecipiation experiments performed in our lab (N. K. Brewster, unpubished data). These experiments showed that, when cells contain two differentially tagged versions of Cdc68, an immunoprecipitation against one of the tags pulled down the alternatively labelled Cdc68 protein. This indicates that these two different forms of Cdc68 can co-exist in a complex. This same type of co-immunoprecipitation experiment was also performed with differentially tagged Pob3 proteins with a similar result, indicating that two different forms of Pob3 can co-exist in a complex. This type of multimerization could place the *in vitro* finding of a Pob3/Pob3 physical association in a biologically meaningful context, as one of the interactions that may assist in stabilizing the FACT multimer. The nature and biological significance of FACT multimerization remains to be determined.

The unexpectedly large molecular size of purified yeast FACT has been previously attributed to a rod-like shape for this complex, as determined by equilibrium sedimentation studies (Wittmeyer *et al.* 1999). The deviation of yeast FACT from a globular shape, as a rod with an aspect ratio of 15:1, provides a plausible explanation for the low mobility observed in gel filtration and size-exclusion chromatography experiments (Brewster *et al.* 1998; Wittmeyer *et al.* 1999). A third explanation for the apparent molecular weight of FACT is that FACT purifies with additional proteins. FACT has been shown to interact with Chd1, the Paf1 complex (Krogan *et al.* 2002; Squazzo *et al.* 2002), the casein kinase II (CKII) complex (Keller and Lu 2002), and several other proteins, and the presence of some of these factors in association with FACT could explain these findings.

Human FACT co-purifies with CKII at an apparent molecular weight of 700 kDa based on gel filtration chromatography (Keller *et al.* 2001). When complexes containing both FACT and CKII are reconstituted from purified recombinant proteins, a similar molecular weight of 670 kDa is observed (Keller and Lu 2002). Thus it appears that no

other cellular factors were present in the purified preparation. However, there is once again a size discrepancy between the expected molecular weight of 360 kDa for the complex if only a monomer of each component was present (SPT16, SSRP1, and each of four subunits of CKII) and the apparent molecular weight of 670 kDa. The authors speculate that there may be two SPT16/SSRP1 dimers present for each CKII tetramer, which would generate a complex with an expected molecular weight of 580 kDa (Keller and Lu 2002). The hypothesized existence of this type of mulitmeric complex of FACT may help provide an *in vivo* relevance for the physical interaction that I detected between the N-terminal domain of Pob3 and the C-terminal domain of Pob3, in stabilizing the formation of such a complex. Nonetheless, the 400-kDa FACT as purified from yeast cell extracts is not as large as expected for two FACT dimers plus a CKII tetramer; therefore this form of the complex does not easily explain the unexpected high apparent molecular weight for yeast FACT.

iv) FACT physical associations with other proteins

As noted above, FACT co-purifies or physically interacts with many other factors including nucleosomes, histone dimers, DNA polymerase α, the Paf1 complex, CKII, Sas3, TFIIE, GAGA factor, and Chd1 (Orphanides *et al.* 1999; Wittmeyer *et al.* 1999; John *et al.* 2000; Kang *et al.* 2000; Keller and Lu 2002; Krogan *et al.* 2002; Squazzo *et al.* 2002; Belotserkovskaya *et al.* 2003; Shimojima *et al.* 2003). I have identified an additional novel physical interaction for a FACT component with Ynl035c, a protein of unknown function, using a yeast two-hybrid approach. For many of these interactions the region or regions of FACT responsible for the physical association are known. A summary of the physical associations of FACT is depicted in Figure 76, using yeast FACT as a template for these interactions even though some of the interactions were identified in other systems and have not yet been confirmed in yeast. The functional implications for many of these interactions are discussed below.

2. FACT functional studies

i) Mechanism generating the Spt phenotype in Cdc68 mutants

The Spt reporter genes contain insertions of δ elements from Ty retrotransposons that generate novel transcription initiation sites or transcription termination sites (Figure 21), that result in the production of transcripts that do not encode functional versions of the

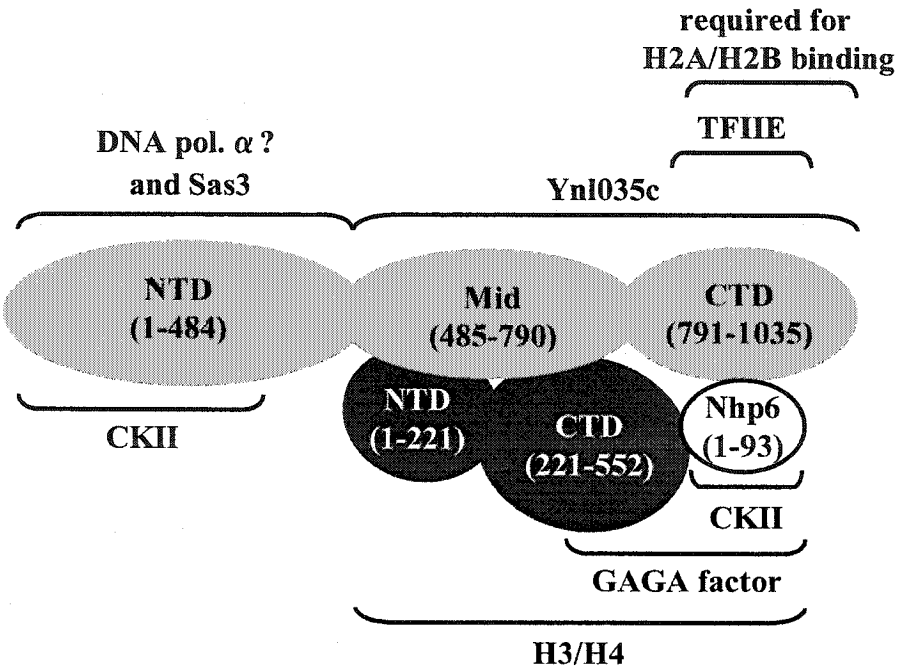

Figure 76. FACT physical associations. Yeast FACT is shown,with grey shaded ovals representing the three domains of the Cdc68 protein, black ovals representing the two Pob3 domains, and a white oval representing the Nhp6 protein. The regions known to be responsible for physical association of FACT with various proteins or complexes are indicated above or below each component. Certain FACT physical interactions, such as the association of FACT with the Paf1 complex or with Chd1, are not indicated, since the region responsible for the association has not been determined. Physical associations identified in other systems have been 'mapped' onto the yeast proteins using polypeptide sequence alignments.

affected genes (Winston *et al.* 1984; Winston *et al.* 1987; Fassler and Winston 1988). Mutations in genes encoding components of the transcription machinery or proteins that regulate chromatin structure alter the transcription pattern to allow additional, functional transcripts to be produced from these Spt reporter genes (Clark-Adams *et al.* 1988; Fassler and Winston 1988). Mutations that result in these additional transcripts confer an Spt^- phenotype. Recent research from the Winston and Struhl labs provides compelling evidence that an Spt^- phenotype can be the result of transcription initiation at cryptic promoters (Kaplan *et al.* 2003; Mason and Struhl 2003). These cryptic promoters become accessible as a result of aberrant chromatin structure, specifically caused by decreased nucleosome densities within coding regions (Kaplan *et al.* 2003). The model for this, as it relates to FACT, is that during the process of transcription elongation by RNA polymerase II the nucleosomes in front of the polymerase are partially disassembled by FACT-mediated removal of a histone H2A/H2B dimer (Figure 2) (Orphanides *et al.* 1999; Belotserkovskaya *et al.* 2003; Saunders *et al.* 2003). Then, in the wake of the elongating polymerase, FACT replaces the H2A/H2B dimer to assist in reassembly of the nucleosome and re-establishment of the appropriate chromatin conformation (Figure 2) (Kaplan *et al.* 2003; Mason and Struhl 2003). When FACT is mutated it may not perform this reassembly of nucleosomes efficiently, which results in the observed decreased density of nucleosomes within the coding sequence of a gene. The DNA, no longer properly packaged into chromatin, becomes more accessible to the transcription initiation machinery, which may recognize otherwise cryptic promoter sequences within the coding region of a gene and initiate transcription at these positions. This results in the production of smaller transcripts for a gene due to internal transcription initiation (Xu 1995; Kaplan *et al.* 2003; Mason and Struhl 2003). The recognition of these cryptic promoters can result in an Spt^- phenotype, as use of alternative promoters leads to functional transcription from the Spt reporter genes (Figure 21).

One of the initial goals of my research was to generate novel mutations in the *CDC68* gene that confer an Spt^- phenotype even in the presence of the wild-type *CDC68* gene. A collection of new *cdc68* alleles that cause a dominant Spt^- phenotype was identified and some of these alleles were sequenced. The non-conservative substitutions encoded by these new *cdc68* alleles cluster in the region spanning residues 656 to 1004 of the Cdc68

protein. The mutagenesis that generated these *cdc68* alleles had an equal opportunity to generate mutational changes affecting residues 265 to 1035 (approximately 75% of the protein; Figure 25), yet the Spt$^-$ alleles isolated in this way encode a significantly higher number of non-conservative substitutions in the latter third of the protein (Table 10 and Figure 25). Given the physical associations for the regions of the protein (Figure 76) subjected to mutagenesis, it seems likely that there is functional significance to this mutational clustering in the C-terminal portion of Cdc68. These mutations cluster in the end of the middle domain, the boundary region between the middle and C-terminal domains, and the C-terminal domain. Mutational changes have not yet been found in the central portion of the middle domain, which is involved in binding Cdc68 to Pob3. It could be that such mutations are not able to generate a dominant Spt$^-$ phenotype, potentially as a result of the interference with Pob3 binding.

The associations of hFACT with the histone H2A/H2B dimer has been shown to require the C-terminal 230 residues of hSPT16 (Belotserkovskaya *et al.* 2003), which corresponds approximately to the C-terminal domain of the yeast Cdc68 protein (Figure 76). It is therefore plausible that mutations in this domain of Cdc68 may influence the association of the H2A/H2B dimer with FACT and thereby prevent proper nucleosome reassembly in the wake of RNA polymerase II, thus resulting in an Spt$^-$ phenotype. The histone proteins are highly basic and histone chaperones typically have a highly acidic domain that is involved in the interaction with histone proteins (Belotserkovskaya *et al.* 2003); consistent with this relationship, the C-terminal domain of Cdc68 contains an acidic region spanning residues 957-1021 (56% glutamate or aspartate). Some of the mutational changes in the new Spt alleles of *cdc68* generated in this study encode substitutions in this region, replacing acidic amino acids with neutral amino acids. In addition to these substitutions, several other substitutions that do not fall within the acidic also result in the substitution of acidic amino acid with neutral or basic amino acids. These types of substitution may alter the ability of the mutant Cdc68 proteins to bind the basic histone proteins by eliminating potential ionic interactions.

Fourteen novel mutant alleles of *cdc68/spt16* have been identified in the Formosa lab based on the inability to support robust cell growth at elevated temperatures (Formosa *et al.* 2001). Nine of these alleles also cause an Spt$^-$ phenotype. The mutational changes

encoded by these alleles are scattered throughout the Cdc68 protein (Formosa *et al.* 2001), with four alleles encoding mutational changes in the N-terminal domain of Cdc68, one allele encoding mutational changes in the middle domain, and four alleles encoding mutational changes in the C-terminal domain. These results imply that there may be multiple ways to mutate the Cdc68 protein to produce an Spt$^-$ phenotype, or perhaps that each of these mutations somehow influences the region(s) of the Cdc68 protein involved in histone binding. The explanation for how the four C-terminal-domain point-mutant alleles generate an Spt$^-$ phenotype could involve perturbation of the interaction between this domain and the histone H2A/H2B dimer, as described above for my C-terminal point mutations. As for the N-terminal-domain point mutations, I have shown that the four alleles (*spt16-8*, *spt16-12*, *spt16-16a*, and *spt16-24*) encoding these mutational changes generate unstable protein products at elevated temperatures. These alleles may result in an Spt$^-$ phenotype because of alterations in protein abundance or conformational changes that influence other FACT domains. This explanation could be extended to the *cdc68-1* allele, which also results in an Spt$^-$ phenotype. This allele encodes a glycine-to-glutamate substitution at residue 132 in the N-terminal domain, which results in an unstable protein product (Xu *et al.* 1995; Figure 32).

Two alleles encoding partial deletions of the N-terminal domain, *cdc68-Δ369* and *cdc68-Δ922*, also result in an Spt$^-$ phenotype (Figure 31). The *cdc68-Δ369* allele, like other N-terminal-domain mutations, encodes a protein product that is unstable, even at a permissive growth temperature. The *cdc68- Δ922* allele is the only N-terminal mutation characterized to date that does not generate an unstable protein product at elevated temperatures (Figure 32). The N-terminal domain fragment encoded by this allele may somehow influence the association of FACT with other proteins as a result of interference by the misfolded truncated domain. Absence of the entire N-terminal domain, as is the case for proteins encoded by *cdc68-mini or cdc68-ΔNTD*, does not confer an Spt$^-$ phenotype, which suggests that this domain of the Cdc68 protein is not important for nucleosome reassembly in the context of transcription, as described above. This finding further supports the idea that mutations in this domain that generate an Spt$^-$ phenotype may do so as a result of influences on the structure and/or stability of the other Cdc68 domains.

ii) *cdc68* alleles categorized by impact on FACT functions

Several lines of investigation were initiated in this work to examine the functional impact of the proteins encoded by different *cdc68* mutant alleles. The results of these studies allow a certain degree of functional assignment for specific mutant Cdc68 proteins. Based on the SGA analysis, there appear to be three principal functions a mutant allele may affect: transcription-related process, membrane-transport functions, and DNA repair and replication. The first alleles described below encode proteins with more significant impact on transcription-related processes, given the cohort of genetic interactions identified by SGA analysis, while alleles in the second group have little impact on transcription but display remarkable influences on membrane transport. Alleles in the third class of alleles encode proteins that influence DNA replication and repair functions. An allele may impinge on more than one of these FACT-related functions, and there is evidence that some of the alleles influence a common functional process.

Two alleles identified in this study, *cdc68-E857K* and *cdc68-319*, encode Cdc68 mutant proteins that have dramatic impacts on transcription-related processes. While *cdc68-319* has a more deleterious effect on cells, as reflected in a wider range of associated growth defects and a significantly longer list of genetic interactions for this allele, the comparatively few genetic interactions identified for *cdc68-E857K* include several genes encoding proteins with transcription-related functions (Tables 18 and 21). As well as the SGA genetic interactions indicating that the Cdc68-319 mutant protein influences transcription, microarray experiments showed significantly more transcript-level alterations in *cdc68-319* cells than in cells containing either the *cdc68-312* or *cdc68-mini* allele. This finding supports the hypothesis that the mutant protein encoded by *cdc68-319* has a more dramatic impact on FACT activity for transcription than does *cdc68-312* or *cdc68-mini*. Also, the *cdc68-319* mutation has significant influences on the transcription of two *lacZ* reporter genes regulated by the SBF transcription factor or by the Swi4 component of SBF. The significance of these particular findings is discussed below in the context of a role for FACT in maintaining cell integrity and regulating morphogenesis, but they also demonstrate the impact of the *cdc68-319* mutation on transcription processes.

In addition to the SGA analysis findings for *cdc68-E857K*, classical synthetic-lethal screening with this allele revealed synthetic genetic relationships with mutations in the *BUR2* gene, which encodes the regulatory subunit of a kinase whose targets are involved in transcription elongation (Keogh *et al.* 2003; Pei and Shuman 2003), and with the *HIR* genes (*HIR1*, *HIR2*, and *HIR3*), which encode histone chaperones involved in regulating histone gene expression and function (Kaufman *et al.* 1998; J. R. Stevens, unpublished observations). The Bur2 and Hir proteins are involved in the process of transcription; the identification of synthetic genetic relationships between *cdc68-E857K* and mutations in the genes encoding these proteins suggests that the mutant Cdc68 protein somehow affects the transcription process. These findings are in agreement with those from the SGA analysis, which also indicate that *cdc68-E857K* cells are growth-impaired when *HIR* genes are deleted. (Derivatives of the yeast deletion strain harbouring the *BUR2* gene deletion are false-positives in SGA analysis, due to poor growth, and are excluded from meaningful interpretation.) The effects of combining the *cdc68-E763G*, *cdc68-312*, *cdc68-319*, and *cdc68-ΔNTD* alleles with each of the mutations identified in the *cdc68-E857K* classical synthetic-lethal screening further support the *cdc68* classification scheme, as only the *cdc68-319* allele caused synthetic sickness when combined with the *bur2*, *hir1*, *hir2*, and *hir3* mutations (J. R. Stevens, unpublished observations). No growth defect was observed for cells containing *cdc68-E763G*, *cdc68-312*, or *cdc68-ΔNTD* in combination with the *bur2*, *hir1*, *hir2*, or *hir3* mutations (J. R. Stevens, unpublished observations). Here again these findings are in agreement with those from SGA analysis, where deletions of *HIR* genes were found to cause synthetic sickness in combination with *cdc68-319* but not when combined with *cdc68-E763G*, *cdc68-312*, or *cdc68-ΔNTD*. The analysis of *cdc68* mutant alleles that are synthetically lethal in combination with mutations in *BUR2* and the *HIR* genes has been extended to include the mutant *cdc68/spt16* alleles generated in the Formosa lab (Formosa *et al.* 2002)and a similar dichotomy has been observed, with certain *cdc68* alleles resulting in synthetic lethality with the *bur2* and *hir* mutations while other *cdc68* alleles are not synthetically lethal with these mutations (J. R. Stevens, unpublished observations). Of the four *cdc68* alleles from the Formosa collection that are synthetically lethal in combination with *bur2* and *hir* mutations, three encode substitutions in the C-terminal domain of the protein and one

allele encodes multiple substitutions in the N-terminal domain and generates an unstable protein product. Thus certain *cdc68* alleles have significant influences on transcription, while other alleles have comparatively little impact on this process.

The *cdc68-E763G* and *cdc68-312* mutant alleles (and to a lesser extent the *cdc68-ΔNTD* allele, as discussed below) each identified a significant number of genetic interactions with deletions of genes encoding components of the membrane-transport machinery. As alluded to above, *cdc68-E763G* and *cdc68-312* did not generate a large number of synthetic lethal interactions with components of the transcription machinery and this finding has been further confirmed by directed studies examining the impact of these mutations in combination with *HIR* gene deletions or the *bur2* mutant allele (J. R. Stevens, unpublished observations). The microarray experiments performed with *cdc68-312* are consistent with the observations from SGA implying that this allele has little impact on transcription, as the global transcription profile for *cdc68-312* cells was not drastically different from that of cells containing wild-type *CDC68*. Other methods to examine transcription in *cdc68-312* cells, including Northern blotting and β-galactosidase assays to monitor the expression of *lacZ* reporter genes, also showed little deviation from wild-type expression patterns.

As indicated in the Results section, the significance of the synthetic lethal interactions between the *cdc68-E763G* and *cdc68-312* alleles and deletions of genes encoding vesicular-transport components is unclear. It could be that, while these two mutant alleles do not influence the transcription of a broad spectrum of genes, they may significantly influence the transcription of a particular gene, or genes, involved in vesicular transport. In this model, when further stress is placed on transport functions by deleting genes encoding transport components, the result is synthetically lethal. Alternatively, the connection between these *cdc68* mutations and those affecting vesicular transport could be that they each impair a common process, such as the maintenance of cell integrity. Phenotypes associated with *cdc68-312* are consistent with a role for FACT in maintaining cell integrity or regulating cell morphogenesis. One of the key means of regulating these processes is the targeting of intracellular components to the plasma membrane in response to cellular stress or cell shape restructuring. If transport processes required for these functions are impaired, then cell integrity may be compromised. Several lines of

investigation have demonstrated the importance of membrane trafficking in maintaining cell integrity (Pruyne and Bretscher 2000a, 2000b; Yamamoto and Jigami 2002; Valdivia and Schekman 2003; Lesage *et al.* 2004). Thus, one plausible explanation for the observed genetic interactions between mutations in FACT and mutation in genes encoding vesicular-transport functions may be overlapping roles in the maintenance of cell integrity.

The third 'class' of *cdc68* mutations, characterized by the DNA repair and replication impairment, contains the *cdc68-319* and *cdc68-ΔNTD* alleles. These two mutant alleles each display synthetic genetic relationships with deletions of genes encoding components of the DNA repair or replication machinery (Tables 21 and 22).

While the *cdc68-319* mutant allele, as described above, has a significant impact on transcription, it also impinges upon DNA repair and replication. It may be expected that if the *cdc68-319* mutant allele results in a protein that is unable to associate effectively with histones H2A/H2B (due to substitutions encoded by *cdc68-319* that affect the region known to be required for histone binding), this impairment may influence all FACT histone-chaperone functions. Cells containing the *cdc68-319* allele show a wide range of phenotypes (Table 31; Figures 27, 28, 45, 46, and 47) and are more severely impaired than are cells containing other *cdc68* alleles encoding C-terminal point mutations, like *cdc68-E857*, *cdc68-E763G*, and *cdc68-312*. While these other C-terminal mutants may also interfere to some degree with Cdc68 and H2A/H2B interactions, the disruption of this interaction may not be as severe as when the Cdc68-319 protein is present. Alternatively, the presence of multiple mutational changes in the Cdc68-319 protein may impact more than one Cdc68 function.

The *cdc68-ΔNTD* allele, which encodes a protein lacking the N-terminal domain, displays a broad spectrum of genetic interactions with genes encoding components of the DNA repair and replication machinery, suggesting that the N-terminal domain of Cdc68 is important for FACT-mediated functions in these processes. Human FACT has been shown to associate with the CKII tetramer in response to DNA damage (Keller *et al.* 2001; Keller and Lu 2002), and this association is at least in part stabilized by interactions involving a region of the hSPT16 protein that corresponds to a large portion of the N-terminal domain of yeast Cdc68 (Figure 76). While it has not yet been

established that interaction between yeast FACT and CKII is involved in DNA-damage responses, the physical association between FACT and CKII is conserved in yeast (Krogan *et al.* 2002). If the interaction between sequences in the N-terminal domain of Cdc68 and CKII is also important for DNA repair in yeast, then it stands to reason that a Cdc68 protein lacking the N-terminal domain, as encoded by *cdc68-ΔNTD* allele, would impair DNA-repair functions. This is consistent with the synthetic lethal interactions identified in this study for *cdc68-ΔNTD* using SGA analysis.

The N-terminal domain of Cdc68 may also be involved in the association of FACT with DNA polymerase α (Wittmeyer *et al.* 1999), which would be consistent with a role for the N-terminal domain in DNA replication. During purifications of FACT associated with the DNA polymerase α complex, a 58-kDa proteolytic fragment of Cdc68 was often observed in the fractions associated with DNA polymerase α (Wittmeyer *et al.* 1999). This proteolytic Cdc68 polypetide was no longer associated with Pob3 but was able to bind DNA plolymerase α in the absence of the rest of FACT (Wittmeyer *et al.* 1999). These characteristics are consistent with those of the N-terminal domain of Cdc68, which has a molecular weight of approximately 55 kDa and is not responsible for the association of Cdc68 with Pob3. While there are other potential explanations for this proteolytic fragment, the evidence suggests that this fragment may be the N-terminal domain of Cdc68. The possibility that the association of FACT with DNA polymerase α may be mediated by the N-terminal domain of Cdc68 is intriguing and merits further investigations, and would certainly solidify the genetic evidence presented here which implicates the N-terminal domain of Cdc68 in DNA replication.

The N-terminal domain of Cdc68 has also been shown to interact with the Sas3 protein in yeast two-hybrid assays (Figure 76; John *et al.* 2000). Sas3 is the catalytic subunit of the yeast NuA3 histone acetyltransferase complex (John *et al.* 2000), which has been implicated in mediating transcription processes (Howe *et al.* 2002; Oki *et al.* 2004). Since the role of NuA3-mediated histone modification is unclear, it is difficult to speculate on the biological consequences that may result from loss of the FACT/NuA3 association, as would be expected to be the case in cells expressing the *cdc68-ΔNTD* allele. However, given this physical association it seems likely that these two complexes function together to modulate chromatin structure.

iii) C-terminal substitutions show that the Cdc68 C-terminal and N-terminal domains share an overlapping function

While SGA analysis provides evidence that specific alterations in the Cdc68 protein can have more dramatic effects on certain functional aspects of Cdc68, similar genetic interactions and phenotypes are sometimes observed for cells expressing N-terminally (*i.e.* the protein generated by *cdc68-ΔNTD*) or C-terminally (*i.e.* the proteins generated by *cdc68-312* and *cdc68-319*) mutated Cdc68 proteins. One example of this is sensitivity to hydroxyurea, a chemical inhibitor of ribonucleotide reductase that can result in double-strand DNA breaks (Slater 1973; Skoog and Bjursell 1974); hydroxyurea sensitivity was observed for cells containing *cdc68-312*, *cdc68-319*, or *cdc68-ΔNTD* alleles (Figures 28, 31 and 40). The similar hydroxyurea sensitivities, combined with the fact that cells containing either *cdc68-ΔNTD* or *cdc68-319* show synthetic growth impairments when genes encoding proteins that function in DNA replication or repair are deleted, suggest a degree of overlapping function for the N-terminal and C-terminal domains of Cdc68. In addition to allele specific genetic interactions identified using SGA, there are also areas where the genetic interactions for different alleles display some degree of overlap. For example, each of the mutant alleles examined by SGA analysis displays synthetic lethality with deletion of the *MRE11* gene, involved in DNA repair and replication functions. To determine whether the N-terminal and C-terminal domains influence a common function, chimeric mutant alleles encoding proteins lacking the N-terminal domain of Cdc68 and also containing C-terminal point mutations were generated. These chimeric alleles typically resulted in an exacerbation of the hydroxyurea-sensitivity or temperature-sensitivity phenotypes associated with the parental mutations. These findings support the idea that the N-terminal and C-terminal domains share some overlapping function, and given the enhanced hydroxyurea sensitivities, the overlapping function may be involved in DNA repair or replication.

Further investigations designed to examine potential mechanisms that may result in hydroxyurea sensitivity were carried out to elucidate the roles of Cdc68 in DNA replication and repair. Cells containing mutant alleles of *cdc68* known to cause sensitivity to chronic exposure to hydroxyurea in the growth medium were assessed for sensitivities to short-term, high-dosage hydroxyurea exposure. Loss of cell viability as a result of this

type of acute hydroxyurea exposure is indicative of defects in replication-checkpoint activation (Allen *et al.* 1994; D'Amours and Jackson 2001). If cells are unable to activate the replication-checkpoint upon hydroxyurea exposure, they continue to replicate potentially damaged DNA under conditions of nucleotide depletion, therefore generating incomplete and mutated genomes. Cells containing *cdc68* mutant alleles did not display dramatic sensitivities to acute hydroxyurea exposure, although *cdc68-319* cells did suffer some diminished viability. These results indicate that the *cdc68-312*, *cdc68-mini* and *cdc68-ΔNTD* alleles do not impair the activation of the replication checkpoint, although *cdc68-319* may slightly affect this activation. Thus a checkpoint failure is not the mechanism underlying the hydroxyurea sensitivities observed for cells bearing these mutant *cdc68* alleles.

An additional response to the stress caused by hydroxyurea is the activation of the Rad53 kinase. Rad53 is a key cellular mediator of DNA-damage response activities whose kinase activity is itself activated through phosphorylation events triggered by the presence of DNA damage (Allen *et al.* 1994; Sun *et al.* 1996). To determine if the Rad53 kinase is activated effectively in *cdc68* mutant cells under DNA-damage conditions the Rad53 protein was characterized after hydroxyurea treatment. In each case, the Rad53 phosphoisoforms, indicative of Rad53 phosphorylation and activation, were detected. This finding shows that Rad53 is activated in response to DNA damage induced by hydroxyurea in *cdc68* mutant cells. However, there were alterations in the kinetics of Rad53 phosphorylation, with potentially less Rad53 phosphoisoform identified in certain *cdc68* mutants. One of the transcription responses regulated by the phosphorylated forms of Rad53 is the activation of transcription of *RNR1* and *RNR3*, the genes encoding the large subunit of the ribonucleotide reductase enzyme. To determine if the subtle alterations in Rad53 phosphorylation observed in *cdc68* cells had an impact on Rad53 function, the levels of *RNR1* and *RNR3* transcripts were monitored in response to treatment with hydroxyurea. Consistent with the subtle changes observed in Rad53 phosphorylation in *cdc68* mutant cells, slight changes in the levels of *RNR1* and *RNR3* transcripts were also observed for certain *cdc68* alleles. To determine if the alterations in *RNR* transcript levels observed in *cdc68* mutant cells upon hydroxyurea treatment could explain the sensitivity to chronic exposure to hydroxyurea observed for these cells, two

approaches to increase the abundance of Rnr proteins were undertaken. However, neither the ectopic over-expression of the *RNR1* or *RNR3* genes nor the elevation of active ribonucleotide reductase by elimination of the inhibitor protein, Sml1, were able to suppress the hydroxyurea sensitivities of *cdc68* mutant cells. Therefore, the subtle changes in *RNR* transcript levels observed in *cdc68* mutant cells in response to hydroxyurea do not account for the hydroxyurea sensitivities observed for these cells.

These findings suggest that while Rad53 activation, as measured both by phosphorylation status and by activation of the *RNR1* and *RNR3* genes, in response to DNA damage is sufficient to activate the DNA replication checkpoint, there may be mild perturbations in this activation in *cdc68* mutants. The differences in Rad53 activation in cdc68 mutant cells *versus* wild-type cells are not enough to significantly impair activation of the DNA replication checkpoint in response to hydroxyurea treatment, since cell viability upon high-dose short-term exposure to hydroxyurea was not drastically decreased. Additionally, the changes in *RNR* gene expression observed in *cdc68* mutant cells exposed to high-dose short-term exposure to hydroxyurea do not explain the chronic hydroxyurea sensitivities observed for these mutants.

While there is evidence for an overlapping function for the N-terminal domain and C-terminal domains of Cdc68 that may center on DNA replication or repair functions, this overlapping essential function does not appear to be the result of perturbations to Rad53 functions. Therefore, unlike the Asf1 histone chaperone that has been intimately connected with Rad53 functions in response to DNA damage (Emili *et al.* 2001; Hu *et al.* 2001), no strong ties between FACT and Rad53 functions were observed here. Thus, the mechanism of FACT involvement in response to DNA damage most likely occurs through some route other than those mediated by Rad53.

iv) FACT and cell integrity

A novel role for FACT in the maintenance of cell integrity is supported by several findings reported here. The initial identification of *SSD1* as a dosage suppressor of the temperature sensitivities conferred by the *cdc68-312* and *cdc68-319* mutant alleles was discovered to be the fortuitous result of complementation of a defective *ssd1-d* allele present in the cells employed in this study. One implication of this finding is that the *cdc68* mutant cells are synthetically sick at elevated temperatures when *ssd1-d* is also

present. Evaluation of the temperature sensitivities caused by other *cdc68* mutant alleles revealed that the effects of *SSD1* are not allele-specific, but rather that the presence of the wild-type *SSD1* gene increases the maximal permissive growth temperature in each case.

Similar types of genetic interactions between a variety of mutant alleles and the *ssd1-d* mutant allele have been reported (Sutton *et al.* 1991b; Stettler *et al.* 1993) (Uesono *et al.* 1994; Luukkonen and Seraphin 1999; Kosodo *et al.* 2001; Du and Novick 2002; McDonald *et al.* 2002). However, recent work has implicated the Ssd1 protein in the maintenance of cell integrity in parallel with the Pkc1-signalling-pathway component Swi4 (Kaeberlein and Guarente 2002). Phenotypes associated with *cdc68-312* or *cdc68-319* mutant cells, including sorbitol-remedied temperature sensitivity, altered sensitivity to detergent, and aberrant cellular morphologies, are consistent with defective cell integrity and morphogenesis. Since genetic evidence linking the Nhp6 component of FACT with Pkc1 signalling had been described (Costigan *et al.* 1994) and it had been shown that *cdc68* mutations have an impact on SBF-regulated gene expression (Lycan *et al.* 1994), ties between the *cdc68-312* and *cdc68-319* mutant alleles and genes encoding Pkc1-singalling-pathway components were sought. Increased dosage of either the *WSC1* or *PKC1* genes in *cdc68-312* or *cdc68-319* cells suppressed the temperature sensitivities of these cells (Figure 48). Additionally, the *cdc68-319* mutation was found to cause synthetic growth impairments at elevated temperatures in cells deleted for genes encoding Pkc1-pathway components, including Swi4, Slt2, and Bck2 (Figures 49 and 50). These findings are consistent with the Pkc1 signalling pathway operating either upstream of or in parallel with FACT to mediate cell integrity.

Alterations in the activities of SBF-regulated reporter genes have been seen when mutant alleles of *cdc68* are present or when the Nhp6 protein is overproduced (Lycan *et al.* 1994; Sidorova and Breeden 1999; Formosa *et al.* 2001). Specifically, the *cdc68-1* allele and seven of the fourteen new *cdc68* mutant alleles reported by the Formosa lab alter expression of a *HO-lacZ* reporter gene (Lycan *et al.* 1994; Formosa *et al.* 2001). Expression of the *HO* gene is regulated, in part, by the SBF transcription factor (Breeden and Mikesell 1991). Since SBF is a downstream effector of the Pkc1 signalling pathway, the influences of the *cdc68-312* and *cdc68-319* mutations on SBF, MBF, and Swi4 gene expression were determined. The *cdc68-319* allele had considerable influence on gene

expression from either the SCB- or Swi4-regulated *lacZ* reporter genes, while the *cdc68-312* mutation had little impact on gene expression for any of the three reporters tested (Figure 51). The increased expression from SBF- and Swi4-dependent genes was not the result of alterations in *SWI4* or *SWI6* transcript abundance (Figure 52). Given the observed associations between FACT and SBF-related transcription activity, it seems likely that FACT has a direct influence on the ability of SBF and Swi4 to activate transcription. In *Drosophila*, FACT has been shown to physically associate with the GAGA transcription factor and influence its ability to alter chromatin structure at promoters (Shimojima *et al.* 2003). Perhaps yeast FACT plays a similar role in assisting SBF, or Swi4 alone, at promoters by modulating chromatin structure. However, unlike the GAGA-factor scenario, yeast FACT has not been found to associate physically with the SBF transcription factor (B. Andrews, personal communication).

Connections similar to those reported here between FACT and the maintenance of cell integrity have been reported for the Paf1 complex and the maintenance of cell integrity (Chang *et al.* 1999; Porter *et al.* 2002). Studies of the Paf1 complex demonstrate a role for this complex in regulating the expression of genes involved in the maintenance of cell integrity and implicate Paf1 as a downstream effector of the Pkc1 signalling pathway (Chang *et al.* 1999; Porter *et al.* 2002). Although the influence of Paf1 on transcription is much more global (Pokholok *et al.* 2002; Krogan *et al.* 2003a; Rondon *et al.* 2004), these findings established functional connections between the Paf1 complex and SBF or MBF in the regulation of gene expression (Porter *et al.* 2002). Given the physical association and functional connections between the Paf1 complex and FACT (Costa and Arndt 2000; Krogan *et al.* 2002; Squazzo *et al.* 2002), it is possible that these two complexes play similar roles in cell integrity through their respective roles in regulating transcription.

3. Concluding remarks

The research findings presented here begin to establish connections between structural features of FACT and the functions of FACT. I have shown that the middle domain of the Cdc68 protein is the primary site for the association of this protein with Pob3, which binds to this domain of Cdc68 through interactions with its N-terminal and C-terminal domains. These findings assist in synthesizing the results of similar studies using metazoan FACT (Keller and Lu 2002; Shimojima *et al.* 2003).

Studies presented here on the N-terminal domain of the Cdc68 component of FACT indicate that this domain is important for mediating FACT activities in DNA repair and replication. Recent findings that shed light on the mechanism of FACT activity during transcription (Orphanides *et al.* 1999; Belotserkovskaya *et al.* 2003; Kaplan *et al.* 2003; Mason and Struhl 2003; Saunders *et al.* 2003) have been extremely beneficial to our understanding of FACT. However, our understanding of FACT function in DNA repair and replication remains incomplete. These areas of FACT activity will undoubtedly receive considerable attention in future research endeavours.

The isolation and characterization of novel mutant *cdc68* alleles encoding substitutions in the C-terminal region of the Cdc68 protein have allowed a dissection of the functions associated with this region, with certain mutant alleles influencing transcription processes in more dramatic ways than other alleles, that seem to impact more on transport functions.

Additionally, some of these C-terminally mutated Cdc68 proteins have identified a role for FACT in maintaining cell integrity. This function also appears to be related to FACT activity in transcription, with FACT as a potential downstream effector of Pkc1 signalling. This activity is most likely influenced by FACT-mediated alteration of chromatin structure. While the mechanism of this effect remains unclear, it appears that FACT is able to alter the activities of the SBF and Swi4 transcription factors. FACT alterations to chromatin structure may therefore be required for full activation of gene expression by certain transcription factors.

Appendix 1. Summary of random-spore verification of genetic interactions with *cdc68* alleles employed in SGA analysis

Genetic interaction Gene name	Genetic interaction Systematic name	*cdc68-E857K*	*cdc68-E763G*	*cdc68-312*	*cdc68-319*	*cdc68-ΔNTD*
ADE8	YDR408C					M
AGE2	YIL044C		SL	SL		NT
AKR2	YOR034C				M	
ALD2	YMR170C				M	
ALF1	YNL148C	SS	M	No	SS	No
AOR1	YBR231C				SL	SS
APG12	YBR217W				M	
APL4	YPR029C		SS	SS		
APL5	YPL195W			SS		
APL6	YGR261C		SS	SS		
APM1	YPL259C			SS		
APM2	YHL019C		SS			M
APS1	YLR170C			SS		
APS3	YJL024C		SS			SS
ARD1	YHR013C	M				
ARL1	YBR164C		SS	SL		
ARL3	YPL051W		SL	SL		SS
ARO2	YGL148W				NT	
ARO7	YPR060C					SS
ARP6	YLR085C				SL	
ASF1	YJL115W	SS		No		SS
BCK1	YJL095W				No	SS
BCK2	YER167W				SS	
BEM2	YER155C				SS	SL
BEM4	YPL161C		SS	No	SS	
BRE5	YNR051C		SL		SS	
BRR1	YPR057W				SS	
BST1	YFL025C		SS			
BUD14	YAR014C		SS	SL		
CAC2	YML102W				M	
CAF40	YNL288W		SS	SL	No	
CBF1	YJR060W		SS			
CBP1	YJL209W		NT	NT	NT	NT
CCW12	YLR110C		SS		SS	
CCZ1	YBR131W		SL			
CDC26	YFR036W					M
CDC73	YLR418C	SL	SS		SL	
CHO2	YGR157W		SS	SS		
CHS1	YNL192W		SS			NT
CIK1	YMR198W	M	NT	No	No	

Genetic interaction Gene name	Genetic interaction Systematic name	*cdc68-E857K*	*cdc68-E763G*	*cdc68-312*	*cdc68-319*	*cdc68-ΔNTD*
CIT1	YNR001C					SS
CKI1	YLR133W					M
CLB3	YDL155W		SL	No	No	
CLN3	YAL040C				No	M
COD2	YNL041C		SL	SL		SS
COD5	YGL005C		SL	SL		
CRD1	YDL142C				SS	
CSE2	YNR010W	M	No		SS	
CTF18	YMR078C	M			SS	
CTF4	YPR135W				SS	
CWH41	YGL027C		SS			
DAL4	YIR028W	M				
DBF2	YGR092W				SL	
DEP1	YAL013W				No	SS
DFG16	YOR030W	No	No		SL	No
DID2	YKR035W-A		SS		No	SL
DOA1	YKL213C	M	No	No	No	SS
DOR1	YML071C		No	SL		
DRS2	YAL026C		SL	SL		
DST1	YGL043W	M	SS	No	SS	
DYN2	YDR424C					SS
ECM25	YJL201W		No	M		
EDE1	YBL047C					SS
ELG1	YOR144C					SS
ELM1	YKL048C	M	SS	SL		SS
ENT4	YLL038C			No	M	
ERG2	YMR202W	SS				
ERG5	YMR015C		M	No		No
ERV14	YGL054C				M	
FAB1	YFR019W					SL
FLX1	YIL134W				SS	
FPS1	YLL043W				No	SS
GAS1	YMR307W		SS	SL	M	
GDA1	YEL042W			M		
GEF1	YJR040W		SL			NT
GIM3	YNL153C				SS	M
GLN3	YER040W	M				SS
GOS1	YHL031C		SL			
GOT1	YMR292W			M		
GPD1	YDL022W		NT	NT	NT	NT
GRD19	YOR357C		M	No		
GSG1	YDR108W		SL	SS		
GSH1	YJL101C	NT			NT	
GSH2	YOL049W				NT	

Genetic interaction Gene name	Genetic interaction Systematic name	*cdc68-E857K*	*cdc68-E763G*	*cdc68-312*	*cdc68-319*	*cdc68-ΔNTD*
GTR1	YML121W				M	
GUP1	YGL084C		SL	SL		
GYP1	YOR070C		SL	SL		
HDA1	YNL021W		No	No	No	
HHF1	YBR009C	M	No		SL	
HHT1	YBR010W	SS		No	SL	
HIR1	YBL008W	No		No	SS	
HIR2	YOR038C	SS		No	No	
HIR3	YJR140C	SL		No	SL	
HOC1	YJR075W		SS	No		SS
HOM6	YJR139C				SS	No
HOR2	YER062C				M	
HOT1	YMR172W				M	
HPC2	YBR215W	No			SL	
HRB1	YNL004W				SS	
HTZ1	YOL012C	M			SS	SL
IES2	YNL215W	No			SS	
IES6	YEL044W				SL	
IKI3	YLR384C					SL
INO4	YOL108C					SL
INP52	YNL106C				SL	
IRA2	YOL081W			No	SS	
ISY1	YJR050W					SL
KAP120	YPL125W					SS
KEX2	YNL238W		M	No	NT	
KRE25	YNL296W		SL	SL		SL
KTI12	YKL110C					SS
LEO1	YOR123C	SL			SL	
LYS7	YMR038C	SS		SS	SS	SL
MAK10	YEL053C				No	SS
MED1	YPR070W		SS		M	SS
MET22	YOL064C				SS	
MID1	YNL291C		SS	No	M	No
MNN11	YJL183W	SS	SL	SL	No	SS
MNN2	YBR015C		SS	SS		
MON1	YGL124C			SS	No	
MON2	YNL297C		SS	No		
MRC1	YCL060C	M			No	SS
MRE11	YMR224C	SL	SL	SL	SS	SS
MSO1	YNR049C		SS			
NBP2	YDR162C			SL		SL
NCE4	YPL024W	SS		No	No	SL
NHP10	YDL002C				SS	
NIP100	YPL174C					SS

Genetic interaction Gene name	Genetic interaction Systematic name	*cdc68-E857K*	*cdc68-E763G*	*cdc68-312*	*cdc68-319*	*cdc68-ΔNTD*
NOP12	YOL041C				M	
NUT1	YGL151W				No	SS (LINKED)
OPI1	YHL020C		No	SL		
OST3	YOR085W		SS			
OXR1	YPL196W			SS		No
PAT1	YCR077C				SL	
PCH2	YBR186W					M
PDR17	YNL264C					SS
PEA2	YER149C					SL
PEP8	YJL053W		SL	SL		SL
PEX3	YDR329C					SS
PEX6	YNL329C				SS	
PFK2	YMR205C	No				SL
PHO5	YBR093C	No			SS	
PHO80	YOL001W		SL		SS	
PKR1	YMR123W		SL			
PLO1	YPR179C	No	SS	SS	SS	
PMR1	YGL167C		SS (LINKED)			
POL32	YJR043C				No	SS
PRB1	YEL060C				M	No
PSD1	YNL169C			SS		
PSL10	YDR126W			SL		
PSP1	YDR505C			SS		
RAD2	YGR258C		No			SL
RAD27	YKL113C				SS	SS
RAD4	YER162C				M	SL
RAD50	YNL250W					SS
RAD51	YER095W				SS	
RAD55	YDR076W					M
RAV1	YJR033C		SL			
RAV2	YDR202C		SL	SL		
RER1	YCL001W		SS	SS		
RGP1	YDR137W		SL	SL		
RIC1	YLR039C		SL			
RIM13	YMR154C			M	SL	
RIM20	YOR275C		M		SL	
RIM21	YNL294C	No	M		SS	
RIM9	YMR063W				SL	
ROT2	YBR229C		M	M		
RPL15B	YMR121C		NT			
RPL16B	YNL069C				M	SS
RPL34B	YIL052C		SS	SS	SL	No
RPN10	YHR200W			SS		

Genetic interaction Gene name	Genetic interaction Systematic name	*cdc68-E857K*	*cdc68-E763G*	*cdc68-312*	*cdc68-319*	*cdc68-ΔNTD*
RPN4	YDL020C	SS			SS	SL
RPP2A	YOL039W					SS
RPS17B	YDR447C				No	SL
RPS21A	YKR057W	M				
RPS23B	YPR132W	SS			No	
RPS24A	YER074W	M				M
RPS6A	YPL090C		M	No	No	
RTF1	YGL244W				SS (LINKED)	
RTG2	YGL252C			SS (LINKED)		
RTG3	YBL103c			SS	SS	SS
RTT103	YDR289C			M		
RTT106	YNL206C	SL		M		SS
RTT107	YHR154W					SS
RTT109	YLL002W	M				
RUD3	YOR216C			SS		
SAC3	YDR159W				SS	M
SAC7	YDR389W		SL	SL	No	SL
SAE2	YGL175C				No	SS (LINKED)
SAP155	YFR040W		M		SS	No
SAS3	YBL052C					M
SBP1	YHL034C		M			
SCS7	YMR272C	No	No	No	NT	NT
SEC22	YLR268W		SL		SL	SS
SEC28	YIL076W			SS	No	SS
SEC66	YBR171W			SS		
SEO1	YAL067C				NT	
SER2	YGR208W	SS				
SET2	YJL168C		SS	No		No
SET3	YKR029C				SS	
SGS1	YMR190C	SS		No	No	No
SIC1	YLR079W	M			No	
SIN3	YOL004W				SS	
SIP3	YNL257C		No		SS	No
SIS2	YKR072C				SS	SS
SIT1	YEL065W	M				SS
SKN7	YHR206W			SS		
SLA1	YBL007C	M			No	
SLT2	YHR030C				No	SS
SMI1	YGR229C		SS	SS	No	
SMY2	YBR172C				No	SS
SNU66	YOR308C				SL	
SOD1	YJR104C	No	NT	NT	NT	SL

Genetic interaction Gene name	Genetic interaction Systematic name	*cdc68-E857K*	*cdc68-E763G*	*cdc68-312*	*cdc68-319*	*cdc68-ΔNTD*
SOH1	YGL127C				SL	
SPE2	YOL052C	No	NT			No
SPE3	YPR069C	No			SS	
SPF1	YEL031W		SS	SL		SL
SPT2	YER161C				No	M
SPT8	YLR055C				SS	
SRN2	YLR119W	No			SL	
SRO9	YCL037C		SS			
STB5	YHR178W				SS	
SUM1	YDR310C		SS	SS		SL
SWA2	YDR320C	SS			No	
SWI4	YER111C				SL	SS
SWI5	YDR146C					SS
SWR1	YDR334W				SL	
SYS1	YJL004C		SL			
TEF4	YKL081W		SL	SL		
THR4	YCR053W		M			
TIM18	YOR297C				SS	
TLG2	YOL018C				SS	
TOF1	YNL273W					M
TPS1	YBR126C	No	SS		No	No
TUS1	YLR425W			M		
TYR1	YBR166C				No	SS
UBP3	YER151C				SS	
UBP6	YFR010W				No	SL
UBP8	YMR223W		No	M		
URE2	YNL229C		SS	SS		No
UTH1	YKR042W		SS	No	No	
UTR1	YJR049C					SS
UTR2	YEL040W					SS
VAC14	YLR386W					SS
VAC8	YEL013W		SS	SS		SS
VAM3	YOR106W		SS	SL	No	NT
VAM6	YDL077C			SL	No	SL
VMA6	YLR447C	No	NT	SL		SL
VPS1	YKR001C		SL	SL		SS
VPS13	YLL040C		M	No		
VPS17	YOR132W		SS	SS		SS
VPS21	YOR089C	SS	SS	SS	No	No
VPS29	YHR012W		SL			SS
VPS30	YPL120W		SS	NT		
VPS35	YJL154C		SS			
VPS38	YLR360W		SL	SL	M	SS
VPS4	YPR173C	SL	SS	SS	M	SS

Genetic interaction Gene name	**Genetic interaction Systematic name**	***cdc68-E857K***	***cdc68-E763G***	***cdc68-312***	***cdc68-319***	***cdc68-ΔNTD***
VPS5	YOR069W		SL	SL		
VPS60	YDR486C		SL	SL	SS	No
VPS64	YDR200C				No	SS
VPS67	YKR020W		SL	SL	SS	SS
VPS71	YML041C					M
VPS72	YDR485C			SS	SL	SL
VPS74	YDR372C		SL	SL		
VPS8	YAL002W	SS	SS	No	No	SL
VTA1	YLR181C		M	SS		No
WHI2	YOR043W		SS	SL		No
WHI3	YNL197C		SS	SS	No	
XRS2	YDR369C			No	SL	SS
YAL011W	YAL011W				SL	
YAL058C-A	YAL058C-A		No	SS		
YBL083C	YBL083C			M		
YDL076C	YDL076C					M
YDL206W	YDL206W			SL		No
YDR153C	YDR153C		M	SS		
YDR203W	YDR203W		SS	SS		
YDR247W	YDR247W					M
YDR444W	YDR444W					SS
YDR476C	YDR476C					SS
YEL033W	YEL033W	M		No		SS
YEL043W	YEL043W		SL	SL		
YEL068C	YEL068C					SS
YER066W	YER066W		No			M
YER121W	YER121W					SS
YGL020C	YGL020C		SL	SS		
YGR089W	YGR089W		SL			
YHL035C	YHL035C				No	M
YHR130C	YHR130C					SS
YIL040W	YIL040W			NT	SS	NT
YIL110W	YIL110W			SS	No	
YIL121W	YIL121W		No		NT	
YIP3	YNL044W		SS	SS		
YJR087W	YJR087W					M
YKL160W	YKL160W	SS			No	
YLR111W	YLR111W		SS	SS	SS	
YLR169W	YLR169W			SS		
YLR171W	YLR171W		SS	SS		
YLR235C	YLR235C			No	No	SS
YML013C-A	YML013C-A	M			M	
YML095C-A	YML095C-A			M		
YMR003W	YMR003W		No	SS	No	NT

Genetic interaction Gene name	**Genetic interaction Systematic name**	***cdc68-E857K***	***cdc68-E763G***	***cdc68-312***	***cdc68-319***	***cdc68-ΔNTD***
YMR148W	YMR148W			M		
Y1	YER005W			M		
YNL140C	YNL140C				SS	M
YNL146W	YNL146W					M
YNR004W	YNR004W					SS
YOR068C	YOR068C		SL	SL		
YOR081C	YOR081C					SL
YOR154W	YOR154W		No	M	No	
YPL077C	YPL077C				SS	
YPL113C	YPL113C					SL
YPL170W	YPL170W					M
YPR064W	YPR064W					M
YPR090W	YPR090W		SS	SL		
YPS3	YLR121C					SS
YPT7	YML001W		SS	SS	No	
YSA1	YBR111C		M	M		No

All random-spore assessments of genetic interactions identified by SGA with any gene deletion that showed a verified synthetic genetic interaction with a *cdc68* allele are presented above. Blank = not determined; NT = No test (no growth on SGA sporulation plate); No = no genetic interaction by random-spore analysis; M = maybe a genetic interaction, but difficult to assess by the random-spore method; SS = synthetic-sick genetic interaction; SL = synthetic-lethal genetic interaction; (LINKED) = gene deletion resides close to the tagged *cdc68* allele, so the genetic relationship may be the result of linkage; Shaded boxes above or underlined entries below = genetic interactions also verified by tetrad analysis.

Additional gene deletions identified through SGA analysis that did not exhibit a genetic interaction with any *cdc68* allele when assessed by random spore analysis:
cdc68-E857K – CAC1, CAC2, CAC3, CSG2, DCC1, FKS1, IDH2, KAR3, LEU3, NFI1, PAC10, PIB2, RAD52, RPS28A, RTS1, SUR1, TPS2, VID22, YAF9, YBR255W, YGL045W, YKL162C-A, YKR007W, YLR128W, YLR391W, YMR086W, YNL179C, and YOR013W.
cdc68-E763G – BMH1, CCH1, CHD1, COD4, ECM21, ERD1, FAP1, GYP8, INO2, ISW1, ISW2, ITC1, JSN1, KRE11, NOT3, MCK1, MLH1, MRL1, PER1, PSP2, SHE10,

SIP3, SKY1, SSH4, TPM1, TPS2, TRS33, UBC13, YBL104C, YCK1, YCK2, YCK3, YER007C-A, YGL045W, YGL168W, YGL235W, YJL169W, YJR070C, YJR084W, YKL063C, YKR007W, YKR035C, and YMR192W.

cdc68-312 – AAH1, ASF1, CCH1, CSG2, ERV46, FAA3, GRS1, HOG1, HXK2, IES1, INO2, MCK1, MMS2, MRL1, NMD2, PEP1, PER1, RTS1, SED1, SNX4, SOK1, SST2, TRS33, UBC13, UBI4, UBR2, YFL034W, YFR008W, YGL045W, YGL149W, YGL161C, YGL165C, YGL168W, YKL063C, YKL076C, YLR126C, YNL077W, YNL224C, YNL326C, and YNR005C.

cdc68-319 – ADH6, AHC1, APG2, APG5, ASE1, ASI3, AUT7, BMH1, BRE1, BRE2, BUL1, CCH1, CIN4, CLA4, CLN2, COS10, CPT1, CSG2, CUP2, CVT17, CYK3, DCC1, DDR48, DHH1, DNF1, DSS4, ECM12, ECM8, EFT1, EPT1, ESC1, FBP1, FLO10, FRE2, FUN11, FUN19, FYV4, GIT1, GND2, GPX2, HAC1, HAT1, HAT2, HRD3, HXT2, IMD3, IOC3, IST3, ISW1, ISW2, JNM1, KAR3, KIN4, LEU3, LGE1, MCM16, MET13, MET32, MIG1, MKC7, MKK1, MKS1, MLC2, MLH3, MNS1, MPA43, MRK1, MYO3, NAT1, NEM1, NGL3, NOP16, NRP1, NTH1, NUP2, OGG1, ORM2, PAC10, PAN6, PBP2, PDC5, PDE2, PEX1, PEX14, PEX19, PEX21, PHO3, PHO8, PHO87, PHO90, PPG1, PPN1, PPQ1, PTK1, PUS4, PUS5, RAD1, RAD10, RAD14, RAD52, RAD57, RED1, WSC4, RGD1, RPL19A, RPL19B, RPL34A, RPL8A, RPL9A, RPS0A, RPS16A, RPS19A, RPS28B, RPS4A, RPS4B, RRD1, SAP30, SCS3, SDF1, SDL1, SDS3, SET6, SFA1, SIA1, SIF2, SIR1, SKI2, SNC2, SNF4, SNT1, SPE4, SRC1, SSK1, STP3, SUB1, SWD3, THI3, TOP1, TOS9, TPM1, TRF5, TSA1, UBI4, UBP2, VID27, YAL037W, YAL049C, YAP1801, YAR028W, YAR029W, YBL028C, YBL060W, YBR090C, YBR090C-A, YBR100W, YBR101C, YBR194W, YBR219C, YBR242W, YBR255W, YBR261C, YBR262C, YBR281C, YCL006C, YDL023C, YDL033C, YDL162C, YDR090C, YDR287W, YDR431W, YDR438W, YEL048C, YER084W, YFL032W, YFL034W, YGL045W, YGL059W, YGL110C, YGL140C, YGL161C, YGL164C, YGR071C, YGR125W, YHR121W, YHR151C, YIL077C, YIL112W, YIL141W, YIL167W, YJL182C, YJL193W, YJR079W, YJR088C, YJR146W, YKL053C-A, YKL098W, YKL174C, YKR032W, YKR065C, YLL014W, YLL032C, YLR126C, YLR190W, YLR225C, YLR376C, YLR414C, YLR427W, YLR455W, YMR126C, YMR140W, YMR191W, YMR262W, YNG1, YNL035C,

YNL056W, YNL077W, YNL105W, YNL168C, YOL002C, YOL046C, YOL050C, YOR013W, YOR024W, YOR042W, YOR135C, YOR277C, YOR298W, YOR304C-A, YOR314W, YOR318C, YOR343C, YOR365C, YPL041C, YPL071C, YPL080C, YPL088W, YPL182C, YPL205C, YPL207W, YPL246C, YPR031W, YPR053C, YPR071W, YPR153W, YPT11, and YTA7.

cdc68-ΔNTD – AKL1, APE3, APG17, AQR1, ARN2, ARP1, ASN1, ATX1, BMH2, BNI4, BUL1, CAF16, CAP2, CHA1, CKB2, CLN1, COX5A, CSR2, CUP2, CWC27, CYK3, DCC1, DLD1, DOS2, ECM7, ECM8, EFT1, ELA1, ELP3, ERD1, ERV46, ESC2, FIG2, FPR1, FUS3, GAL10, GPX2, GRS1, HNT2, HSC82, IDH2, JSN1, LAG1, LSB1, MBP1, MFA2, MRK1, MUP3, NRP1, NUM1, OGG1, OST5, PAN6, PDB1, PEX2, PHO8, PMS1, PPH22, PRM3, PUT2, RAD52, RHR2, RIM101, RPL21B, RPL41A, RPS18B, RPS4B, RSA3, SER1, SFA1, SFB2, SFL1, SHU1, SIA1, SIP3, SIW14, SNZ2, SPS19, SRC1, SRP40, SSA1, STE24, SYM1, TAL1, TEP1, TFP1, THI3, THO1, TRP3, UBC13, UBC8, UBP2, URH1, VPS75, WSC2, WTM1, YAP1801, YAT2, YBL060W, YBL104C, YBR225W, YBR255W, YBR271W, YBR287W, YDL176W, YDR219C, YDR332W, YDR338C, YDR340W, YDR417C, YDR426C, YEL014C, YER181C, YFR039C, YFR045W, YGL007W, YGL081W, YGR018C, YIL077C, YJL028W, YJL160C, YJL192C, YJR020W, YJR038C, YJR070C, YJR116W, YKL056C, YKR065C, YKR077W, YKR078W, YLL030C, YLL049W, YLR128W, YLR149C, YLR247C, YLR374C, YLR414C, YLR415C, YLR431C, YLR445W, YLR455W, YML035C-A, YMR135W-A, YMR140W, YMR147W, YMR187C, YMR193C-A, YMR206W, YMR310C, YNL144C, YNL191W, YNL254C, YNL285W, YNR014W, YNR029C, YOL037C, YOL053C-A, YOL106W, YOR024W, YOR044W, YOR049C, YOR108W, YOR121C, YOR138C, YOR305W, YOR320C, YOR324C, YPL041C, YPL182C, YPL208W, YPR045C, YPR059C, YPR093C, YRO2, and ZRC1.

Appendix 2. Colour indexes for genetic interactions webs.

Gene ontologies associated with node colours:

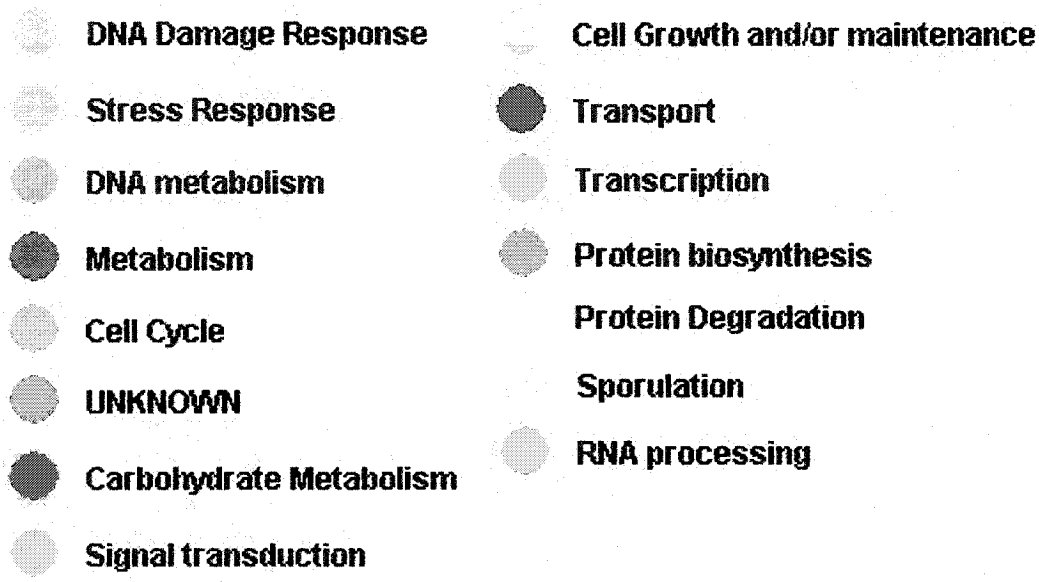

Experimental methods associated with vertex colours:

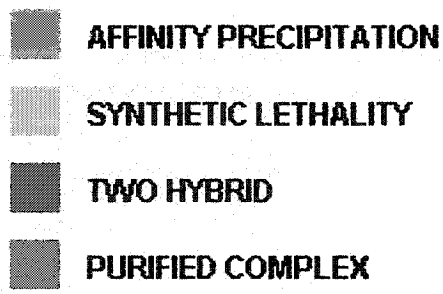

Colour legends for Figures 58, 60-67, and 69-73.

REFERENCES

Abramova, N. E., B. D. Cohen, O. Sertil, R. Kapoor, K. J. Davies and C. V. Lowry (2001) Regulatory mechanisms controlling expression of the *DAN/TIR* mannoprotein genes during anaerobic remodeling of the cell wall in *Saccharomyces cerevisiae*. *Genetics* **157**: 1169-1177.

Ahn, Y. T., X. L. Wu, S. Biswal, S. Velmurugan, F. C. Volkert and M. Jayaram (1997) The 2μ-plasmid-encoded Rep1 and Rep2 proteins interact with each other and colocalize to the *Saccharomyces cerevisiae* nucleus. *J Bacteriol* **179**: 7497-7506.

Allen, J. B., Z. Zhou, W. Siede, E. C. Friedberg and S. J. Elledge (1994) The SAD1/RAD53 protein kinase controls multiple checkpoints and DNA damage-induced transcription in yeast. *Genes Dev* **8**: 2401-2415.

Altheim, B. A. and M. C. Schultz (1999) Histone modification governs the cell cycle regulation of a replication-independent chromatin assembly pathway in *Saccharomyces cerevisiae*. *Proc Natl Acad Sci U S A* **96**: 1345-1350.

Altschul, S. F., W. Gish, W. Miller, E. W. Myers and D. J. Lipman (1990) Basic local alignment search tool. *J Mol Biol* **215**: 403-410.

Amoros, M. and F. Estruch (2001) Hsf1p and Msn2/4p cooperate in the expression of *Saccharomyces cerevisiae* genes *HSP26* and *HSP104* in a gene- and stress type-dependent manner. *Mol Microbiol* **39**: 1523-1532.

Anderson, D. E., K. M. Trujillo, P. Sung and H. P. Erickson (2001) Structure of the Rad50·Mre11 DNA repair complex from *Saccharomyces cerevisiae* by electron microscopy. *J Biol Chem* **276**: 37027-37033.

Andrews, B. J. and I. Herskowitz (1989) Identification of a DNA binding factor involved in cell-cycle control of the yeast *HO* gene. *Cell* **57**: 21-29.

Appling, D. R. (1999) Genetic approaches to the study of protein-protein interactions. *Methods* **19**: 338-349.

Aranda, A. and M. del Olmo (2003) Response to acetaldehyde stress in the yeast *Saccharomyces cerevisiae* involves a strain-dependent regulation of several *ALD* genes and is mediated by the general stress response pathway. *Yeast* **20**: 747-759.

Arents, G., R. W. Burlingame, B. C. Wang, W. E. Love and E. N. Moudrianakis (1991) The nucleosomal core histone octamer at 3.1 Å resolution: a tripartite protein assembly and a left-handed superhelix. *Proc Natl Acad Sci U S A* **88**: 10148-10152.

Audhya, A. and S. D. Emr (2002) Stt4 PI 4-kinase localizes to the plasma membrane and functions in the Pkc1-mediated MAP kinase cascade. *Dev Cell* **2**: 593-605.

Ausubel, F. M., R. Brent, R. E. Kingston, D. D. Moore, J. G. Seidman, J. A. Smith, and K. Struhl (1991) Current Protocols in Molecular Biology. New York, NY, Wiley Interscience.

Ayyagari, R., X. V. Gomes, D. A. Gordenin and P. M. Burgers (2003) Okazaki fragment maturation in yeast. I. Distribution of functions between FEN1 and DNA2. *J Biol Chem* **278**: 1618-1625.

Bae, S. H., D. W. Kim, J. Kim, J. H. Kim, D. H. Kim, H. D. Kim, H. Y. Kang and Y. S. Seo (2002) Coupling of DNA helicase and endonuclease activities of yeast Dna2 facilitates Okazaki fragment processing. *J Biol Chem* **277**: 26632-26641.

Baetz, K., J. Moffat, J. Haynes, M. Chang and B. Andrews (2001) Transcriptional coregulation by the cell integrity mitogen-activated protein kinase Slt2 and the cell cycle regulator Swi4. *Mol Cell Biol* **21**: 6515-6528.

Bai, C. and S. J. Elledge (1997) Gene identification using the yeast two-hybrid system. *Methods Enzymol* **283**: 141-156.

Bailis, J. M. and S. L. Forsburg (2003) It's all in the timing: linking S phase to chromatin structure and chromosome dynamics. *Cell Cycle* **2**: 303-306.

Balciunas, D., C. Galman, H. Ronne and S. Bjorklund (1999) The Med1 subunit of the yeast mediator complex is involved in both transcriptional activation and repression. *Proc Natl Acad Sci U S A* **96**: 376-381.

Barbour, L., Y. Zhu and W. Xiao (2000) Improving synthetic lethal screens by regulating the yeast centromere sequence. *Genome* **43**: 910-917.

Baroni, E., V. Viscardi, H. Cartagena-Lirola, G. Lucchini and M. P. Longhese (2004) The functions of budding yeast Sae2 in the DNA damage response require Mec1- and Tel1-dependent phosphorylation. *Mol Cell Biol* **24**: 4151-4165.

Bartel, P., C. T. Chien, R. Sternglanz and S. Fields (1993) Elimination of false positives that arise in using the two-hybrid system. *Biotechniques* **14**: 920-924.

Bassler, J., P. Grandi, O. Gadal, T. Lessmann, E. Petfalski, D. Tollervey, J. Lechner and E. Hurt (2001) Identification of a 60S preribosomal particle that is closely linked to nuclear export. *Mol Cell* **8**: 517-529.

Behnia, R., B. Panic, J. R. Whyte and S. Munro (2004) Targeting of the Arf-like GTPase Arl3p to the Golgi requires N-terminal acetylation and the membrane protein Sys1p. *Nat Cell Biol* **6**: 405-413.

Belmont, A. S. and K. Bruce (1994) Visualization of G1 chromosomes: a folded, twisted, supercoiled chromonema model of interphase chromatid structure. *J Cell Biol* **127**: 287-302.

Belotserkovskaya, R., S. Oh, V. A. Bondarenko, G. Orphanides, V. M. Studitsky and D. Reinberg (2003) FACT facilitates transcription-dependent nucleosome alteration. *Science* **301**: 1090-1093.

Belotserkovskaya, R. and D. Reinberg (2004) Facts about FACT and transcript elongation through chromatin. *Curr Opin Genet Dev* **14**: 139-146.

Belotserkovskaya, R., A. Saunders, J. T. Lis and D. Reinberg (2004) Transcription through chromatin: understanding a complex FACT. *Biochim Biophys Acta* **1677**: 87-99.

Bence, A. K. and P. A. Crooks (2003) The mechanism of L-canavanine cytotoxicity: arginyl tRNA synthetase as a novel target for anticancer drug discovery. *J Enzyme Inhib Med Chem* **18**: 383-394.

Bender, A. and J. R. Pringle (1991) Use of a screen for synthetic lethal and multicopy suppressee mutants to identify two new genes involved in morphogenesis in *Saccharomyces cerevisiae*. *Mol Cell Biol* **11**: 1295-1305.

Bensen, E. S., G. Costaguta and G. S. Payne (2000) Synthetic genetic interactions with temperature-sensitive clathrin in *Saccharomyces cerevisiae*. Roles for synaptojanin-like Inp53p and dynamin-related Vps1p in clathrin-dependent protein sorting at the *trans*-Golgi network. *Genetics* **154**: 83-97.

Bensen, E. S., B. G. Yeung and G. S. Payne (2001) Ric1p and the Ypt6p GTPase function in a common pathway required for localization of *trans*-Golgi network membrane proteins. *Mol Biol Cell* **12**: 13-26.

Bhattacharjee, J. K., A. F. Tucci and M. Strassman (1968) Accumulation of α-ketoglutaric acid in yeast mutants requiring lysine. *Arch Biochem Biophys* **123**: 235-239.

Boeke, J. D., F. LaCroute and G. R. Fink (1984) A positive selection for mutants lacking orotidine-5'-phosphate decarboxylase activity in yeast: 5-fluoro-orotic acid resistance. *Mol Gen Genet* **197**: 345-346.

Boeke, J. D., D. J. Garfinkel, C. A. Styles and G. R. Fink (1985) Ty elements transpose through an RNA intermediate. *Cell* **40**: 491-500.

Boer, V. M., J. H. de Winde, J. T. Pronk and M. D. Piper (2003) The genome-wide transcriptional responses of *Saccharomyces cerevisiae* grown on glucose in aerobic chemostat cultures limited for carbon, nitrogen, phosphorus, or sulfur. *J Biol Chem* **278**: 3265-3274.

Bonangelino, C. J., E. M. Chavez and J. S. Bonifacino (2002) Genomic screen for vacuolar protein sorting genes in *Saccharomyces cerevisiae*. *Mol Biol Cell* **13**: 2486-2501.

Boukaba, A., E. I. Georgieva, F. A. Myers, A. W. Thorne, G. Lopez-Rodas, C. Crane-Robinson and L. Franco (2004) A short-range gradient of histone H3 acetylation and Tup1p redistribution at the promoter of the *Saccharomyces cerevisiae SUC2* gene. *J Biol Chem* **279**: 7678-7684.

Boulikas, T. (1990) Poly(ADP-ribosylated) histones in chromatin replication. *J Biol Chem* **265**: 14638-14647.

Boy de la Tour, E. and U. K. Laemmli (1988) The metaphase scaffold is helically folded: sister chromatids have predominantly opposite helical handedness. *Cell* **55**: 937-944.

Breeden, L. (1996) Start-specific transcription in yeast. *Curr Top Microbiol Immunol* **208**: 95-127.

Breeden, L. and G. E. Mikesell (1991) Cell cycle-specific expression of the SWI4 transcription factor is required for the cell cycle regulation of *HO* transcription. *Genes Dev* **5**: 1183-1190.

Brewster, N. K., G. C. Johnston and R. A. Singer (1998) Characterization of the CP complex, an abundant dimer of Cdc68 and Pob3 proteins that regulates yeast transcriptional activation and chromatin repression. *J Biol Chem* **273**: 21972-21979.

Brewster, N. K., G. C. Johnston and R. A. Singer (2001) A bipartite yeast SSRP1 analog comprised of Pob3 and Nhp6 proteins modulates transcription. *Mol Cell Biol* **21**: 3491-3502.

Brown, C. E., T. Lechner, L. Howe and J. L. Workman (2000) The many HATs of transcription coactivators. *Trends Biochem Sci* **25**: 15-19.

Bryk, M., M. Banerjee, D. Conte, Jr. and M. J. Curcio (2001) The Sgs1 helicase of *Saccharomyces cerevisiae* inhibits retrotransposition of Ty1 multimeric arrays. *Mol Cell Biol* **21**: 5374-5388.

Budd, M. E. and J. L. Campbell (1997) A yeast replicative helicase, Dna2 helicase, interacts with yeast FEN-1 nuclease in carrying out its essential function. *Mol Cell Biol* **17**: 2136-2142.

Bustin, M. (1999) Regulation of DNA-dependent activities by the functional motifs of the high-mobility-group chromosomal proteins. *Mol Cell Biol* **19**: 5237-5246.

Calero, M. and R. N. Collins (2002) *Saccharomyces cerevisiae* Pra1p/Yip3p interacts with Yip1p and Rab proteins. *Biochem Biophys Res Commun* **290**: 676-681.

Carrozza, M. J., R. T. Utley, J. L. Workman and J. Cote (2003) The diverse functions of histone acetyltransferase complexes. *Trends Genet* **19**: 321-329.

Chang, M., M. Bellaoui, C. Boone and G. W. Brown (2002) A genome-wide screen for methyl methanesulfonate-sensitive mutants reveals genes required for S phase progression in the presence of DNA damage. *Proc Natl Acad Sci U S A* **99**: 16934-16939.

Chang, M., D. French-Cornay, H. Y. Fan, H. Klein, C. L. Denis and J. A. Jaehning (1999) A complex containing RNA polymerase II, Paf1p, Cdc73p, Hpr1p, and Ccr4p plays a role in protein kinase C signaling. *Mol Cell Biol* **19**: 1056-1067.

Chen, H., V. I. Slepnev, P. P. Di Fiore and P. De Camilli (1999) The interaction of epsin and Eps15 with the clathrin adaptor AP-2 is inhibited by mitotic phosphorylation and enhanced by stimulation-dependent dephosphorylation in nerve terminals. *J Biol Chem* **274**: 3257-3260.

Chen, J., J. Rappsilber, Y. C. Chiang, P. Russell, M. Mann and C. L. Denis (2001) Purification and characterization of the 1.0 MDa CCR4-NOT complex identifies two novel components of the complex. *J Mol Biol* **314**: 683-694.

Chen, Y. J. and T. H. Stevens (1996) The *VPS8* gene is required for localization and trafficking of the CPY sorting receptor in *Saccharomyces cerevisiae*. *Eur J Cell Biol* **70**: 289-297.

Chlebowicz-Sledziewska, E. and A. Z. Sledziewski (1985) Construction of multicopy yeast plasmids with regulated centromere function. *Gene* **39**: 25-31.

Cho, E. J., M. S. Kobor, M. Kim, J. Greenblatt and S. Buratowski (2001) Opposing effects of Ctk1 kinase and Fcp1 phosphatase at Ser 2 of the RNA polymerase II C-terminal domain. *Genes Dev* **15**: 3319-3329.

Christianson, T. W., R. S. Sikorski, M. Dante, J. H. Shero and P. Hieter (1992) Multifunctional yeast high-copy-number shuttle vectors. *Gene* **110**: 119-122.

Clark-Adams, C. D., D. Norris, M. A. Osley, J. S. Fassler and F. Winston (1988) Changes in histone gene dosage alter transcription in yeast. *Genes Dev* **2**: 150-159.

Cobb, J. A., K. Shimada and S. M. Gasser (2004) Redundancy, insult-specific sensors and thresholds: Unlocking the S-phase checkpoint response. *Curr Opin Genet Dev* **14**: 292-300.

Cocker, J. H., S. Piatti, C. Santocanale, K. Nasmyth and J. F. Diffley (1996) An essential role for the Cdc6 protein in forming the pre-replicative complexes of budding yeast. *Nature* **379**: 180-182.

Cohen, B. D., O. Sertil, N. E. Abramova, K. J. Davies and C. V. Lowry (2001) Induction and repression of *DAN1* and the family of anaerobic mannoprotein genes in *Saccharomyces cerevisiae* occurs through a complex array of regulatory sites. *Nucleic Acids Res* **29**: 799-808.

Collart, M. A. (2003) Global control of gene expression in yeast by the Ccr4-Not complex. *Gene* **313**: 1-16.

Conibear, E., J. N. Cleck and T. H. Stevens (2003) Vps51p mediates the association of the GARP (Vps52/53/54) complex with the late Golgi t-SNARE Tlg1p. *Mol Biol Cell* **14**: 1610-1623.

Conte, D., Jr., E. Barber, M. Banerjee, D. J. Garfinkel and M. J. Curcio (1998) Posttranslational regulation of Ty1 retrotransposition by mitogen-activated protein kinase Fus3. *Mol Cell Biol* **18**: 2502-2513.

Costa, P. J. and K. M. Arndt (2000) Synthetic lethal interactions suggest a role for the *Saccharomyces cerevisiae* Rtf1 protein in transcription elongation. *Genetics* **156**: 535-547.

Costigan, C., S. Gehrung and M. Snyder (1992) A synthetic lethal screen identifies SLK1, a novel protein kinase homolog implicated in yeast cell morphogenesis and cell growth. *Mol Cell Biol* **12**: 1162-1178.

Costigan, C., D. Kolodrubetz and M. Snyder (1994) NHP6A and NHP6B, which encode HMG1-like proteins, are candidates for downstream components of the yeast SLT2 mitogen-activated protein kinase pathway. *Mol Cell Biol* **14**: 2391-2403.

Cross, S. L. and M. M. Smith (1988) Comparison of the structure and cell cycle expression of mRNAs encoded by two histone H3-H4 loci in *Saccharomyces cerevisiae*. *Mol Cell Biol* **8**: 945-954.

D'Amours, D. and S. P. Jackson (2001) The yeast Xrs2 complex functions in S phase checkpoint regulation. *Genes Dev* **15**: 2238-2249.

Davie, J. K., R. J. Trumbly and S. Y. Dent (2002) Histone-dependent association of Tup1-Ssn6 with repressed genes *in vivo*. *Mol Cell Biol* **22**: 693-703.

Davis, A. P. and L. S. Symington (2004) *RAD51*-dependent break-induced replication in yeast. *Mol Cell Biol* **24**: 2344-2351.

Deckert, J. and K. Struhl (2001) Histone acetylation at promoters is differentially affected by specific activators and repressors. *Mol Cell Biol* **21**: 2726-2735.

DeRisi, J. L., V. R. Iyer and P. O. Brown (1997) Exploring the metabolic and genetic control of gene expression on a genomic scale. *Science* **278**: 680-686.

Desany, B. A., A. A. Alcasabas, J. B. Bachant and S. J. Elledge (1998) Recovery from DNA replicational stress is the essential function of the S-phase checkpoint pathway. *Genes Dev* **12**: 2956-2970.

Di Como, C. J., H. Chang and K. T. Arndt (1995) Activation of CLN1 and CLN2 G1 cyclin gene expression by BCK2. *Mol Cell Biol* **15**: 1835-1846.

Dover, J., J. Schneider, M. A. Tawiah-Boateng, A. Wood, K. Dean, M. Johnston and A. Shilatifard (2002) Methylation of histone H3 by COMPASS requires ubiquitination of histone H2B by Rad6. *J Biol Chem* **277**: 28368-28371.

Du, L. L. and P. Novick (2002) Pag1p, a novel protein associated with protein kinase Cbk1p, is required for cell morphogenesis and proliferation in *Saccharomyces cerevisiae*. *Mol Biol Cell* **13**: 503-514.

Edwards, S., C. M. Li, D. L. Levy, J. Brown, P. M. Snow and J. L. Campbell (2003) *Saccharomyces cerevisiae* DNA polymerase ϵ and polymerase σ interact physically and functionally, suggesting a role for polymerase ϵ in sister chromatid cohesion. *Mol Cell Biol* **23**: 2733-2748.

Elbein, A. D., Y. T. Pan, I. Pastuszak and D. Carroll (2003) New insights on trehalose: a multifunctional molecule. *Glycobiology* **13**: 17R-27R.

Elledge, S. J., Z. Zhou and J. B. Allen (1992) Ribonucleotide reductase: regulation, regulation, regulation. *Trends Biochem Sci* **17**: 119-123.

Elledge, S. J., Z. Zhou, J. B. Allen and T. A. Navas (1993) DNA damage and cell cycle regulation of ribonucleotide reductase. *Bioessays* **15**: 333-339.

Emili, A., D. M. Schieltz, J. R. Yates, 3rd and L. H. Hartwell (2001) Dynamic interaction of DNA damage checkpoint protein Rad53 with chromatin assembly factor Asf1. *Mol Cell* **7**: 13-20.

Errede, B. and D. E. Levin (1993) A conserved kinase cascade for MAP kinase activation in yeast. *Curr Opin Cell Biol* **5**: 254-260.

Estruch, F. (2000) Stress-controlled transcription factors, stress-induced genes and stress tolerance in budding yeast. *FEMS Microbiol Rev* **24**: 469-486.

Evans, D. H., N. K. Brewster, Q. Xu, A. Rowley, B. A. Altheim, G. C. Johnston and R. A. Singer (1998) The yeast protein complex containing Cdc68 and Pob3 mediates core-promoter repression through the Cdc68 N-terminal domain. *Genetics* **150**: 1393-1405.

Fabre, F., A. Chan, W. D. Heyer and S. Gangloff (2002) Alternate pathways involving Sgs1/Top3, Mus81/ Mms4, and Srs2 prevent formation of toxic recombination intermediates from single-stranded gaps created by DNA replication. *Proc Natl Acad Sci U S A* **99**: 16887-16892.

Fan, H. Y., K. K. Cheng and H. L. Klein (1996) Mutations in the RNA polymerase II transcription machinery suppress the hyperrecombination mutant hpr1 {Delta} *Saccharomyces cerevisiae*. *Genetics* **142**: 749-759.

Fantes, P. A. and C., J. (1984) Canavanine resistance and mechanism of arginine uptake in the fission yeast *Schizosaccharomyces pombe*. *J Gen Microbiol* **130**: 3265-3273.

Fassler, J. S. and F. Winston (1988) Isolation and analysis of a novel class of suppressor of Ty insertion mutations in *Saccharomyces cerevisiae*. *Genetics* **118**: 203-212.

Fath, S., P. Milkereit, A. V. Podtelejnikov, N. Bischler, P. Schultz, M. Bier, M. Mann and H. Tschochner (2000) Association of yeast RNA polymerase I with a nucleolar substructure active in rRNA synthesis and processing. *J Cell Biol* **149**: 575-590.

Fazzio, T. G. and T. Tsukiyama (2003) Chromatin remodeling *in vivo*: Evidence for a nucleosome sliding mechanism. *Mol Cell* **12**: 1333-1340.

Ferreiro, J. A., N. G. Powell, N. Karabetsou, N. A. Kent, J. Mellor and R. Waters (2004) Cbf1p modulates chromatin structure, transcription and repair at the *Saccharomyces cerevisiae MET16* locus. *Nucleic Acids Res* **32**: 1617-1626.

Fields, S. and O. Song (1989) A novel genetic system to detect protein-protein interactions. *Nature* **340**: 245-246.

Finn, R. D. (In prepartation) iPfam: Visualisation of protein-protein interactions at domains and amino acid resolutions.

Fischle, W., Y. Wang and C. D. Allis (2003) Histone and chromatin cross-talk. *Curr Opin Cell Biol* **15**: 172-183.

Flaus, A. and T. Owen-Hughes (2001) Mechanisms for ATP-dependent chromatin remodelling. *Curr Opin Genet Dev* **11**: 148-154.

Foiani, M., G. Liberi, S. Piatti, and P. Plevani (1999) *Saccharomyces cerevisiae* as a model system to study DNA replication. Eukaryotic DNA replication. A practical approach. S. Cotterill. Oxford, UK, Oxford University Press: 185-200.

Formosa, T. (2003) Changing the DNA landscape: putting a SPN on chromatin. *Curr Top Microbiol Immunol* **274**: 171-201.

Formosa, T. and T. Nittis (1999) *Dna2* mutants reveal interactions with Dna polymerase α and Ctf4, a Pol α accessory factor, and show that full Dna2 helicase activity is not essential for growth. *Genetics* **151**: 1459-1470.

Formosa, T., P. Eriksson, J. Wittmeyer, J. Ginn, Y. Yu and D. J. Stillman (2001) Spt16-Pob3 and the HMG protein Nhp6 combine to form the nucleosome-binding factor SPN. *EMBO J* **20**: 3506-3517.

Formosa, T., S. Ruone, M. D. Adams, A. E. Olsen, P. Eriksson, Y. Yu, A. R. Rhoades, P. D. Kaufman and D. J. Stillman (2002) Defects in *SPT16* or *POB3* (yFACT) in

Saccharomyces cerevisiae cause dependence on the Hir/Hpc pathway: Polymerase passage may degrade chromatin structure. *Genetics* **162**: 1557-1571.

Frohloff, F., L. Fichtner, D. Jablonowski, K. D. Breunig and R. Schaffrath (2001) *Saccharomyces cerevisiae* Elongator mutations confer resistance to the *Kluyveromyces lactis* zymocin. *EMBO J* **20**: 1993-2003.

Furuyama, T., F. Tie and P. J. Harte (2003) Polycomb group proteins ESC and E(Z) are present in multiple distinct complexes that undergo dynamic changes during development. *Genesis* **35**: 114-124.

Gaillard, P. H., E. M. Martini, P. D. Kaufman, B. Stillman, E. Moustacchi and G. Almouzni (1996) Chromatin assembly coupled to DNA repair: a new role for chromatin assembly factor I. *Cell* **86**: 887-896.

Gartenberg, M. R. (2000) The Sir proteins of *Saccharomyces cerevisiae*: mediators of transcriptional silencing and much more. *Curr Opin Microbiol* **3**: 132-137.

Gasser, S. M., M. Gotta, H. Renauld, T. Laroche and M. Cockell (1998) Nuclear organization and silencing: trafficking of Sir proteins. *Novartis Found Symp* **214**: 114-126; discussion 126-132.

Gavin, I., P. J. Horn and C. L. Peterson (2001) SWI/SNF chromatin remodeling requires changes in DNA topology. *Mol Cell* **7**: 97-104.

Gavin, A. C., M. Bosche, R. Krause, P. Grandi, M. Marzioch, A. Bauer, J. Schultz, J. M. Rick, A. M. Michon, C. M. Cruciat, M. Remor, C. Hofert, M. Schelder, M. Brajenovic, H. Ruffner, A. Merino, K. Klein, M. Hudak, D. Dickson, T. Rudi, V. Gnau, A. Bauch, S. Bastuck, B. Huhse, C. Leutwein, M. A. Heurtier, R. R. Copley, A. Edelmann, E. Querfurth, V. Rybin, G. Drewes, M. Raida, T. Bouwmeester, P. Bork, B. Seraphin, B. Kuster, G. Neubauer and G. Superti-Furga (2002) Functional organization of the yeast proteome by systematic analysis of protein complexes. *Nature* **415**: 141-147.

Geer, L. Y., M. Domrachev, D. J. Lipman and S. H. Bryant (2002) CDART: protein homology by domain architecture. *Genome Res* **12**: 1619-1623.

Geissler, S., K. Siegers and E. Schiebel (1998) A novel protein complex promoting formation of functional alpha- and gamma-tubulin. *EMBO J* **17**: 952-966.

Gerber, J., K. Neumann, C. Prohl, U. Muhlenhoff and R. Lill (2004) The yeast scaffold proteins Isu1p and Isu2p are required inside mitochondria for maturation of cytosolic Fe/S proteins. *Mol Cell Biol* **24**: 4848-4857.

Gerrard, S. R., N. J. Bryant and T. H. Stevens (2000) *VPS21* controls entry of endocytosed and biosynthetic proteins into the yeast prevacuolar compartment. *Mol Biol Cell* **11**: 613-626.

Gietz, R. D. and A. Sugino (1988) New yeast-*Escherichia coli* shuttle vectors constructed with *in vitro* mutagenized yeast genes lacking six-base pair restriction sites. *Gene* **74**: 527-534.

Glowczewski, L., P. Yang, T. Kalashnikova, M. S. Santisteban and M. M. Smith (2000) Histone-histone interactions and centromere function. *Mol Cell Biol* **20**: 5700-5711.

Goldstein, A. L. and J. H. McCusker (1999) Three new dominant drug resistance cassettes for gene disruption in *Saccharomyces cerevisiae*. *Yeast* **15**: 1541-1553.

Gonzalez-Barrera, S., F. Cortes-Ledesma, R. E. Wellinger and A. Aguilera (2003) Equal sister chromatid exchange is a major mechanism of double-strand break repair in yeast. *Mol Cell* **11**: 1661-1671.

Grably, M. R., A. Stanhill, O. Tell and D. Engelberg (2002) HSF and Msn2/4p can exclusively or cooperatively activate the yeast *HSP104* gene. *Mol Microbiol* **44**: 21-35.

Grunstein, M. (1997) Histone acetylation in chromatin structure and transcription. *Nature* **389**: 349-352.

Guarente, L. (1993) Strategies for the identification of interacting proteins. *Proc Natl Acad Sci U S A* **90**: 1639-1641.

Gurunathan, S., D. David and J. E. Gerst (2002) Dynamin and clathrin are required for the biogenesis of a distinct class of secretory vesicles in yeast. *EMBO J* **21**: 602-614.

Guthrie, C., and G. R. Fink (1991) Guide to yeast genetics and molecular biology. San Diego, CA, Academic Press.

Hadwiger, J. A., C. Wittenberg, H. E. Richardson, M. de Barros Lopes and S. I. Reed (1989) A family of cyclin homologs that control the G1 phase in yeast. *Proc Natl Acad Sci U S A* **86**: 6255-6259.

Hahn, J. S., Z. Hu, D. J. Thiele and V. R. Iyer (2004) Genome-wide analysis of the biology of stress responses through heat shock transcription factor. *Mol Cell Biol* **24**: 5249-5256.

Hahn, J. S. and D. J. Thiele (2004) Activation of the *Saccharomyces cerevisiae* heat shock transcription factor under glucose starvation conditions by Snf1 protein kinase. *J Biol Chem* **279**: 5169-5176.

Hampsey, M. (1997) A review of phenotypes in *Saccharomyces cerevisiae*. *Yeast* **13**: 1099-1133.

Hampsey, M. and D. Reinberg (2003) Tails of intrigue: phosphorylation of RNA polymerase II mediates histone methylation. *Cell* **113**: 429-432.

Han, M. and M. Grunstein (1988) Nucleosome loss activates yeast downstream promoters *in vivo*. *Cell* **55**: 1137-1145.

Hanna, J. S., E. S. Kroll, V. Lundblad and F. A. Spencer (2001) Saccharomyces cerevisiae CTF18 and CTF4 are required for sister chromatid cohesion. *Mol Cell Biol* **21**: 3144-3158.

Hartwell, L. H. (1967) Macromolecule synthesis in temperature-sensitive mutants of yeast. *J Bacteriol* **93**: 1662-1670.

Hartzog, G. A., M. A. Basrai, S. L. Ricupero-Hovasse, P. Hieter and F. Winston (1996) Identification and analysis of a functional human homolog of the *SPT4* gene of *Saccharomyces cerevisiae*. *Mol Cell Biol* **16**: 2848-2856.

Hartzog, G. A., T. Wada, H. Handa and F. Winston (1998) Evidence that Spt4, Spt5, and Spt6 control transcription elongation by RNA polymerase II in *Saccharomyces cerevisiae*. *Genes Dev* **12**: 357-369.

Haslbeck, M., S. Walke, T. Stromer, M. Ehrnsperger, H. E. White, S. Chen, H. R. Saibil and J. Buchner (1999) Hsp26: a temperature-regulated chaperone. *EMBO J* **18**: 6744-6751.

Hata, H., H. Mitsui, H. Liu, Y. Bai, C. L. Denis, Y. Shimizu and A. Sakai (1998) Dhh1p, a putative RNA helicase, associates with the general transcription factors Pop2p and Ccr4p from *Saccharomyces cerevisiae*. *Genetics* **148**: 571-579.

Haurie, V., M. Perrot, T. Mini, P. Jeno, F. Sagliocco and H. Boucherie (2001) The transcriptional activator Cat8p provides a major contribution to the reprogramming of carbon metabolism during the diauxic shift in *Saccharomyces cerevisiae*. *J Biol Chem* **276**: 76-85.

Havas, K., A. Flaus, M. Phelan, R. Kingston, P. A. Wade, D. M. Lilley and T. Owen-Hughes (2000) Generation of superhelical torsion by ATP-dependent chromatin remodeling activities. *Cell* **103**: 1133-1142.

Heinisch, J. J., A. Lorberg, H. P. Schmitz and J. J. Jacoby (1999) The protein kinase C-mediated MAP kinase pathway involved in the maintenance of cellular integrity in *Saccharomyces cerevisiae*. *Mol Microbiol* **32**: 671-680.

Henikoff, S. (2003) Gene regulation: Versatile assembler. *Nature* **423**: 814-815, 817.

Henry, K. W., A. Wyce, W. S. Lo, L. J. Duggan, N. C. Emre, C. F. Kao, L. Pillus, A. Shilatifard, M. A. Osley and S. L. Berger (2003) Transcriptional activation via sequential histone H2B ubiquitylation and deubiquitylation, mediated by SAGA-associated Ubp8. *Genes Dev* **17**: 2648-2663.

Hill, E., J. van Der Kaay, C. P. Downes and E. Smythe (2001) The role of dynamin and its binding partners in coated pit invagination and scission. *J Cell Biol* **152**: 309-323.

Hirst, J. and M. S. Robinson (1998) Clathrin and adaptors. *Biochim Biophys Acta* **1404**: 173-193.

Ho, M. N., K. J. Hill, M. A. Lindorfer and T. H. Stevens (1993) Isolation of vacuolar membrane H(+)-ATPase-deficient yeast mutants; the *VMA5* and *VMA4* genes are essential for assembly and activity of the vacuolar H(+)-ATPase. *J Biol Chem* **268**: 221-227.

Ho, Y., A. Gruhler, A. Heilbut, G. D. Bader, L. Moore, S. L. Adams, A. Millar, P. Taylor, K. Bennett, K. Boutilier, L. Yang, C. Wolting, I. Donaldson, S. Schandorff, J. Shewnarane, M. Vo, J. Taggart, M. Goudreault, B. Muskat, C. Alfarano, D. Dewar, Z. Lin, K. Michalickova, A. R. Willems, H. Sassi, P. A. Nielsen, K. J. Rasmussen, J. R. Andersen, L. E. Johansen, L. H. Hansen, H. Jespersen, A. Podtelejnikov, E. Nielsen, J. Crawford, V. Poulsen, B. D. Sorensen, J. Matthiesen, R. C. Hendrickson, F. Gleeson, T. Pawson, M. F. Moran, D. Durocher, M. Mann, C. W. Hogue, D. Figeys and M. Tyers (2002) Systematic identification of protein complexes in *Saccharomyces cerevisiae* by mass spectrometry. *Nature* **415**: 180-183.

Hoffman, C. S. (1997) Preparation of yeast DNA, RNA, and proteins. Current Protocols in Molecular Biology: 13.11.11-13.11.14.

Hopfner, K. P., A. Karcher, L. Craig, T. T. Woo, J. P. Carney and J. A. Tainer (2001) Structural biochemistry and interaction architecture of the DNA double-strand break repair Mre11 nuclease and Rad50-ATPase. *Cell* **105**: 473-485.

Hopfner, K. P. and J. A. Tainer (2003) Rad50/SMC proteins and ABC transporters: unifying concepts from high-resolution structures. *Curr Opin Struct Biol* **13**: 249-255.

Horazdovsky, B. F., C. R. Cowles, P. Mustol, M. Holmes and S. D. Emr (1996) A novel RING finger protein, Vps8p, functionally interacts with the small GTPase, Vps21p, to facilitate soluble vacuolar protein localization. *J Biol Chem* **271**: 33607-33615.

Horecka, J., P. T. Kinsey and G. F. Sprague, Jr. (1995) Cloning and characterization of the *Saccharomyces cerevisiae LYS7* gene: evidence for function outside of lysine biosynthesis. *Gene* **162**: 87-92.

Horz, W. and H. G. Zachau (1980) Deoxyribonuclease II as a probe for chromatin structure. I. Location of cleavage sites. *J Mol Biol* **144**: 305-327.

Hottiger, T., C. De Virgilio, M. N. Hall, T. Boller and A. Wiemken (1994) The role of trehalose synthesis for the acquisition of thermotolerance in yeast. II. Physiological concentrations of trehalose increase the thermal stability of proteins *in vitro*. *Eur J Biochem* **219**: 187-193.

Howe, L., T. Kusch, N. Muster, R. Chaterji, J. R. Yates, 3rd and J. L. Workman (2002) Yng1p modulates the activity of Sas3p as a component of the yeast NuA3 Hhistone acetyltransferase complex. *Mol Cell Biol* **22**: 5047-5053.

Howlett, N. G. and R. H. Schiestl (2004) Nucleotide excision repair deficiency causes elevated levels of chromosome gain in *Saccharomyces cerevisiae*. *DNA Repair* **3**: 127-134.

Hu, F., A. A. Alcasabas and S. J. Elledge (2001) Asf1 links Rad53 to control of chromatin assembly. *Genes Dev* **15**: 1061-1066.

Hua, Z., P. Fatheddin and T. R. Graham (2002) An essential subfamily of Drs2p-related P-type ATPases is required for protein trafficking between Golgi complex and endosomal/vacuolar system. *Mol Biol Cell* **13**: 3162-3177.

Huang, M. E., A. G. Rio, A. Nicolas and R. D. Kolodner (2003) A genomewide screen in *Saccharomyces cerevisiae* for genes that suppress the accumulation of mutations. *Proc Natl Acad Sci U S A* **100**: 11529-11534.

Hughes, T. R., M. J. Marton, A. R. Jones, C. J. Roberts, R. Stoughton, C. D. Armour, H. A. Bennett, E. Coffey, H. Dai, Y. D. He, M. J. Kidd, A. M. King, M. R. Meyer, D. Slade, P. Y. Lum, S. B. Stepaniants, D. D. Shoemaker, D. Gachotte, K. Chakraburtty, J. Simon, M. Bard and S. H. Friend (2000) Functional discovery *via* a compendium of expression profiles. *Cell* **102**: 109-126.

Huh, W. K., J. V. Falvo, L. C. Gerke, A. S. Carroll, R. W. Howson, J. S. Weissman and E. K. O'Shea (2003) Global analysis of protein localization in budding yeast. *Nature* **425**: 686-691.

Ibeas, J. I., D. J. Yun, B. Damsz, M. L. Narasimhan, Y. Uesono, J. C. Ribas, H. Lee, P. M. Hasegawa, R. A. Bressan and J. M. Pardo (2001) Resistance to the plant PR-5 protein osmotin in the model fungus *Saccharomyces cerevisiae* is mediated by the regulatory effects of *SSD1* on cell wall composition. *Plant J* **25**: 271-280.

Igual, J. C., A. L. Johnson and L. H. Johnston (1996) Coordinated regulation of gene expression by the cell cycle transcription factor Swi4 and the protein kinase C MAP kinase pathway for yeast cell integrity. *EMBO J* **15**: 5001-5013.

Iizuka, M. and M. M. Smith (2003) Functional consequences of histone modifications. *Curr Opin Genet Dev* **13**: 154-160.

Inoue, Y., T. Matsuda, K. Sugiyama, S. Izawa and A. Kimura (1999) Genetic analysis of glutathione peroxidase in oxidative stress response of *Saccharomyces cerevisiae*. *J Biol Chem* **274**: 27002-27009.

Ito, H., Y. Fukuda, K. Murata and A. Kimura (1983) Transformation of intact yeast cells treated with alkali cations. *J Bacteriol* **153**: 163-168.

Ito, T., M. Bulger, R. Kobayashi and J. T. Kadonaga (1996) *Drosophila* NAP-1 is a core histone chaperone that functions in ATP-facilitated assembly of regularly spaced nucleosomal arrays. *Mol Cell Biol* **16**: 3112-3124.

Ito, T., K. Ota, H. Kubota, Y. Yamaguchi, T. Chiba, K. Sakuraba and M. Yoshida (2002) Roles for the two-hybrid system in exploration of the yeast protein interactome. *Mol Cell Proteomics* **1**: 561-566.

Iyer, V. R., C. E. Horak, C. S. Scafe, D. Botstein, M. Snyder and P. O. Brown (2001) Genomic binding sites of the yeast cell-cycle transcription factors SBF and MBF. *Nature* **409**: 533-538.

Izban, M. G. and D. S. Luse (1992) The RNA polymerase II ternary complex cleaves the nascent transcript in a 3'----5' direction in the presence of elongation factor SII. *Genes Dev* **6**: 1342-1356.

Jacobs, S. A. and S. Khorasanizadeh (2002) Structure of HP1 chromodomain bound to a lysine 9-methylated histone H3 tail. *Science* **295**: 2080-2083.

James, P., J. Halladay and E. A. Craig (1996) Genomic libraries and a host strain designed for highly efficient two-hybrid selection in yeast. *Genetics* **144**: 1425-1436.

Jenuwein, T. (2001) Re-SET-ting heterochromatin by histone methyltransferases. *Trends Cell Biol* **11**: 266-273.

Jochum, A., D. Jackson, H. Schwarz, R. Pipkorn and B. Singer-Kruger (2002) Yeast Ysl2p, homologous to Sec7 domain guanine nucleotide exchange factors, functions in endocytosis and maintenance of vacuole integrity and interacts with the Arf-Like small GTPase Arl1p. *Mol Cell Biol* **22**: 4914-4928.

John, S., L. Howe, S. T. Tafrov, P. A. Grant, R. Sternglanz and J. L. Workman (2000) The something about silencing protein, Sas3, is the catalytic subunit of NuA3, a yTAF(II)30-containing HAT complex that interacts with the Spt16 subunit of the yeast CP (Cdc68/Pob3)-FACT complex. *Genes Dev* **14**: 1196-1208.

Johnston, G. C., Pringle, J. R., Hartwell, L. H. (1977) Coordination of growth with cell division in the yeast *Saccharomyces cerevisiae*. *Exp Cell Res* **105**: 79-98.

Johnston, L. H. and A. L. Johnson (1993) Budding yeast mutants showing constitutive basal levels of expression of DNA synthesis genes. *Mol Gen Genet* **240**: 36-42.

Jorgensen, P., B. Nelson, M. D. Robinson, Y. Chen, B. Andrews, M. Tyers and C. Boone (2002) High-resolution genetic mapping with ordered arrays of *Saccharomyces cerevisiae* deletion mutants. *Genetics* **162**: 1091-1099.

Jung, Y. and S. J. Lippard (2003) Nature of full-length HMGB1 binding to cisplatin-modified DNA. *Biochemistry* **42**: 2664-2671.

Kaeberlein, M. and L. Guarente (2002) *Saccharomyces cerevisiae MPT5* and *SSD1* function in parallel pathways to promote cell wall integrity. *Genetics* **160**: 83-95.

Kaeberlein, M., A. A. Andalis, G. B. Liszt, G. R. Fink and L. Guarente (2004) *Saccharomyces cerevisiae SSD1-V* confers longevity by a Sir2p-independent mechanism. *Genetics* **166**: 1661-1672.

Kallstrom, G., J. Hedges and A. Johnson (2003) The putative GTPases Nog1p and Lsg1p are required for 60S ribosomal subunit biogenesis and are localized to the nucleus and cytoplasm, respectively. *Mol Cell Biol* **23**: 4344-4355.

Kanellis, P., R. Agyei and D. Durocher (2003) Elg1 forms an alternative PCNA-interacting RFC complex required to maintain genome stability. *Curr Biol* **13**: 1583-1595.

Kang, S. W., T. Kuzuhara and M. Horikoshi (2000) Functional interaction of general transcription initiation factor TFIIE with general chromatin factor *SPT16/CDC68*. *Genes Cells* **5**: 251-263.

Kaniak, A., Z. Xue, D. Macool, J. H. Kim and M. Johnston (2004) Regulatory network connecting two glucose signal transduction pathways in *Saccharomyces cerevisiae*. *Eukaryot Cell* **3**: 221-231.

Kaplan, C. D., L. Laprade and F. Winston (2003) Transcription elongation factors repress transcription initiation from cryptic sites. *Science* **301**: 1096-1099.

Katou, Y., Y. Kanoh, M. Bando, H. Noguchi, H. Tanaka, T. Ashikari, K. Sugimoto and K. Shirahige (2003) S-phase checkpoint proteins Tof1 and Mrc1 form a stable replication-pausing complex. *Nature* **424**: 1078-1083.

Kaufman, P. D., J. L. Cohen and M. A. Osley (1998) Hir proteins are required for position-dependent gene silencing in *Saccharomyces cerevisiae* in the absence of chromatin assembly factor I. *Mol Cell Biol* **18**: 4793-4806.

Keith, K. C., R. E. Baker, Y. Chen, K. Harris, S. Stoler and M. Fitzgerald-Hayes (1999) Analysis of primary structural determinants that distinguish the centromere-specific function of histone variant Cse4p from histone H3. *Mol Cell Biol* **19**: 6130-6139.

Keith, K. C. and M. Fitzgerald-Hayes (2000) *CSE4* genetically interacts with the *Saccharomyces cerevisiae* centromere DNA elements CDE I and CDE II but not CDE

III. Implications for the path of the centromere DNA around a Cse4p variant nucleosome. *Genetics* **156**: 973-981.

Keller, D. M. and H. Lu (2002) p53 serine 392 phosphorylation increases after UV through induction of the assembly of the CK2·hSPT16·SSRP1 complex. *J Biol Chem* **277**: 50206-50213.

Keller, D. M., X. Zeng, Y. Wang, Q. H. Zhang, M. Kapoor, H. Shu, R. Goodman, G. Lozano, Y. Zhao and H. Lu (2001) A DNA damage-induced p53 serine 392 kinase complex contains CK2, hSpt16, and SSRP1. *Mol Cell* **7**: 283-292.

Kelley, D. E., D. G. Stokes and R. P. Perry (1999) CHD1 interacts with SSRP1 and depends on both its chromodomain and its ATPase/helicase-like domain for proper association with chromatin. *Chromosoma* **108**: 10-25.

Kenna, M. A. and R. V. Skibbens (2003) Mechanical link between cohesion establishment and DNA replication: Ctf7p/Eco1p, a cohesion establishment factor, associates with three different replication factor C complexes. *Mol Cell Biol* **23**: 2999-3007.

Kent, N. A., S. M. Eibert and J. Mellor (2004) Cbf1p is required for chromatin remodeling at promoter-proximal CACGTG motifs in yeast. *J Biol Chem* **279**: 27116-27123.

Keogh, M. C., V. Podolny and S. Buratowski (2003) Bur1 kinase is required for efficient transcription elongation by RNA polymerase II. *Mol Cell Biol* **23**: 7005-7018.

Ketela, T., R. Green and H. Bussey (1999) *Saccharomyces cerevisiae* Mid2p is a potential cell wall stress sensor and upstream activator of the *PKC1-MPK1* cell integrity pathway. *J Bacteriol* **181**: 3330-3340.

Khakhar, R. R., J. A. Cobb, L. Bjergbaek, I. D. Hickson and S. M. Gasser (2003) RecQ helicases: multiple roles in genome maintenance. *Trends Cell Biol* **13**: 493-501.

Khan, A. U. and M. Hampsey (2002) Connecting the DOTs: covalent histone modifications and the formation of silent chromatin. *Trends Genet* **18**: 387-389.

Kikuchi, Y., Y. Oka, M. Kobayashi, Y. Uesono, A. Toh-e and A. Kikuchi (1994) A new yeast gene, *HTR1*, required for growth at high temperature, is needed for recovery from mating pheromone-induced G1 arrest. *Mol Gen Genet* **245**: 107-116.

Kim, J. and S. A. MacNeill (2003) Genome stability: a new member of the RFC family. *Curr Biol* **13**: R873-R875.

Klungland, A. and T. Lindahl (1997) Second pathway for completion of human DNA base excision-repair: reconstitution with purified proteins and requirement for DNase IV (FEN1). *EMBO J* **16**: 3341-3348.

Kobor, M. S., S. Venkatasubrahmanyam, M. D. Meneghini, J. W. Gin, J. L. Jennings, A. J. Link, H. D. Madhani and J. Rine (2004) A protein complex containing the conserved Swi2/Snf2-related ATPase Swr1p deposits histone variant H2A.Z into euchromatin. *PLoS Biol* **2**: 587-599.

Kolodrubetz, D. and A. Burgum (1990) Duplicated *NHP6* genes of *Saccharomyces cerevisiae* encode proteins homologous to bovine high mobility group protein 1. *J Biol Chem* **265**: 3234-3239.

Komarnitsky, P., E. J. Cho and S. Buratowski (2000) Different phosphorylated forms of RNA polymerase II and associated mRNA processing factors during transcription. *Genes Dev* **14**: 2452-2460.

Kornberg, R. D. and Y. Lorch (1999) Twenty-five years of the nucleosome, fundamental particle of the eukaryote chromosome. *Cell* **98**: 285-294.

Kosodo, Y., K. Imai, A. Hirata, Y. Noda, A. Takatsuki, H. Adachi and K. Yoda (2001) Multicopy suppressors of the *sly1* temperature-sensitive mutation in the ER-Golgi vesicular transport in *Saccharomyces cerevisiae*. *Yeast* **18**: 1003-1014.

Kowalski, L. R., K. Kondo and M. Inouye (1995) Cold-shock induction of a family of TIP1-related proteins associated with the membrane in *Saccharomyces cerevisiae*. *Mol Microbiol* **15**: 341-353.

Kranz, J. E. and C. Holm (1990) Cloning by function: an alternative approach for identifying yeast homologs of genes from other organisms. *Proc Natl Acad Sci U S A* **87**: 6629-6633.

Krawitz, D. C., T. Kama and P. D. Kaufman (2002) Chromatin assembly factor I mutants defective for PCNA binding require Asf1/Hir proteins for silencing. *Mol Cell Biol* **22**: 614-625.

Krogan, N. J. and J. F. Greenblatt (2001) Characterization of a six-subunit holo-elongator complex required for the regulated expression of a group of genes in *Saccharomyces cerevisiae*. *Mol Cell Biol* **21**: 8203-8212.

Krogan, N. J., M. Kim, S. H. Ahn, G. Zhong, M. S. Kobor, G. Cagney, A. Emili, A. Shilatifard, S. Buratowski and J. F. Greenblatt (2002) RNA polymerase II elongation factors of *Saccharomyces cerevisiae*: a targeted proteomics approach. *Mol Cell Biol* **22**: 6979-6992.

Krogan, N. J., J. Dover, A. Wood, J. Schneider, J. Heidt, M. A. Boateng, K. Dean, O. W. Ryan, A. Golshani, M. Johnston, J. F. Greenblatt and A. Shilatifard (2003a) The Paf1 complex is required for histone H3 methylation by COMPASS and Dot1p: linking transcriptional elongation to histone methylation. *Mol Cell* **11**: 721-729.

Krogan, N. J., M. C. Keogh, N. Datta, C. Sawa, O. W. Ryan, H. Ding, R. A. Haw, J. Pootoolal, A. Tong, V. Canadien, D. P. Richards, X. Wu, A. Emili, T. R. Hughes, S. Buratowski and J. F. Greenblatt (2003b) A Snf2 family ATPase complex required for recruitment of the histone H2A variant Htz1. *Mol Cell* **12**: 1565-1576.

Krogan, N. J., M. Kim, A. Tong, A. Golshani, G. Cagney, V. Canadien, D. P. Richards, B. K. Beattie, A. Emili, C. Boone, A. Shilatifard, S. Buratowski and J. Greenblatt (2003c) Methylation of histone H3 by Set2 in *Saccharomyces cerevisiae* is linked to transcriptional elongation by RNA polymerase II. *Mol Cell Biol* **23**: 4207-4218.

Krohn, N. M., C. Stemmer, P. Fojan, R. Grimm and K. D. Grasser (2003) Protein kinase CK2 phosphorylates the high mobility group domain protein SSRP1, inducing the recognition of UV-damaged DNA. *J Biol Chem* **278**: 12710-12715.

Krude, T. (1995) Chromatin assembly factor 1 (CAF-1) colocalizes with replication foci in HeLa cell nuclei. *Exp Cell Res* **220**: 304-311.

Krude, T. and C. Keller (2001) Chromatin assembly during S phase: contributions from histone deposition, DNA replication and the cell division cycle. *Cell Mol Life Sci* **58**: 665-672.

Kucharczyk, R., S. Dupre, S. Avaro, R. Haguenauer-Tsapis, P. P. Slonimski and J. Rytka (2000) The novel protein Ccz1p required for vacuolar assembly in *Saccharomyces cerevisiae* functions in the same transport pathway as Ypt7p. *J Cell Sci* **113 Pt 23**: 4301-4311.

Kucharczyk, R., A. M. Kierzek, P. P. Slonimski and J. Rytka (2001) The Ccz1 protein interacts with Ypt7 GTPase during fusion of multiple transport intermediates with the vacuole in *S. cerevisiae*. *J Cell Sci* **114**: 3137-3145.

Lagorce, A., N. C. Hauser, D. Labourdette, C. Rodriguez, H. Martin-Yken, J. Arroyo, J. D. Hoheisel and J. Francois (2003) Genome-wide analysis of the response to cell wall mutations in the yeast *Saccharomyces cerevisiae*. *J Biol Chem* **278**: 20345-20357.

Lamping, E., J. Luckl, F. Paltauf, S. A. Henry and S. D. Kohlwein (1994) Isolation and characterization of a mutant of *Saccharomyces cerevisiae* with pleiotropic deficiencies in transcriptional activation and repression. *Genetics* **137**: 55-65.

Landry, J., A. Sutton, S. T. Tafrov, R. C. Heller, J. Stebbins, L. Pillus and R. Sternglanz (2000) The silencing protein SIR2 and its homologs are NAD-dependent protein deacetylases. *Proc Natl Acad Sci U S A* **97**: 5807-5811.

Langst, G. and P. B. Becker (2001) Nucleosome mobilization and positioning by ISWI-containing chromatin-remodeling factors. *J Cell Sci* **114**: 2561-2568.

Langst, G. and P. B. Becker (2004) Nucleosome remodeling: one mechanism, many phenomena? *Biochim Biophys Acta* **1677**: 58-63.

Lee, F. J. and C. F. Huang (2001) Purification, properties, and analysis of yARL3. *Methods Enzymol* **329**: 417-423.

Lee, K. S. and D. E. Levin (1992) Dominant mutations in a gene encoding a putative protein kinase (*BCK1*) bypass the requirement for a *Saccharomyces cerevisiae* protein kinase C homolog. *Mol Cell Biol* **12**: 172-182.

Lee, B. S., C. P. Lichtenstein, B. Faiola, L. A. Rinckel, W. Wysock, M. J. Curcio and D. J. Garfinkel (1998) Posttranslational inhibition of Ty1 retrotransposition by nucleotide excision repair/transcription factor TFIIH subunits Ssl2p and Rad3p. *Genetics* **148**: 1743-1761.

Lee, T. I., N. J. Rinaldi, F. Robert, D. T. Odom, Z. Bar-Joseph, G. K. Gerber, N. M. Hannett, C. T. Harbison, C. M. Thompson, I. Simon, J. Zeitlinger, E. G. Jennings, H. L. Murray, D. B. Gordon, B. Ren, J. J. Wyrick, J. B. Tagne, T. L. Volkert, E.

Fraenkel, D. K. Gifford and R. A. Young (2002) Transcriptional regulatory networks in *Saccharomyces cerevisiae*. *Science* **298**: 799-804.

Leger-Silvestre, I., P. Milkereit, S. Ferreira-Cerca, C. Saveanu, J. C. Rousselle, V. Choesmel, C. Guinefoleau, N. Gas and P. E. Gleizes (2004) The ribosomal protein Rps15p is required for nuclear exit of the 40S subunit precursors in yeast. *EMBO J* **23**: 2336-2347.

Lek, L. H., E. B. Yang, D. F. Wang and L. Y. Cheng (1995) Comparison of the sensitivity of different India inks staining of electro-blotted proteins on filter membranes. *J Biochem Biophys Methods* **30**: 9-20.

LeRoy, G., G. Orphanides, W. S. Lane and D. Reinberg (1998) Requirement of RSF and FACT for transcription of chromatin templates in vitro. *Science* **282**: 1900-1904.

Lesage, G., A. M. Sdicu, P. Menard, J. Shapiro, S. Hussein and H. Bussey (2004) Analysis of beta-1,3-glucan assembly in *Saccharomyces cerevisiae* using a synthetic interaction network and altered sensitivity to caspofungin. *Genetics* **167**: 35-49.

Letunic, I., R. R. Copley, S. Schmidt, F. D. Ciccarelli, T. Doerks, J. Schultz, C. P. Ponting and P. Bork (2004) SMART 4.0: towards genomic data integration. *Nucleic Acids Res* **32 Database issue**: D142-D144.

Levin, D. E. and E. Bartlett-Heubusch (1992) Mutants in the *S. cerevisiae PKC1* gene display a cell cycle-specific osmotic stability defect. *J Cell Biol* **116**: 1221-1229.

Li, B., L. Howe, S. Anderson, J. R. Yates, 3rd and J. L. Workman (2003) The Set2 histone methyltransferase functions through the phosphorylated carboxyl-terminal domain of RNA polymerase II. *J Biol Chem* **278**: 8897-8903.

Li, J., D. Moazed and S. P. Gygi (2002) Association of the histone methyltransferase Set2 with RNA polymerase II plays a role in transcription elongation. *J Biol Chem* **277**: 49383-49388.

Lieber, M. R. (1997) The FEN-1 family of structure-specific nucleases in eukaryotic DNA replication, recombination and repair. *Bioessays* **19**: 233-240.

Lindstrom, D. L. and G. A. Hartzog (2001) Genetic interactions of Spt4-Spt5 and TFIIS with the RNA polymerase II CTD and CTD modifying enzymes in *Saccharomyces cerevisiae*. *Genetics* **159**: 487-497.

Liu, H. Y., V. Badarinarayana, D. C. Audino, J. Rappsilber, M. Mann and C. L. Denis (1998) The NOT proteins are part of the CCR4 transcriptional complex and affect gene expression both positively and negatively. *EMBO J* **17**: 1096-1106.

Liu, H. Y., Y. C. Chiang, J. Pan, J. Chen, C. Salvadore, D. C. Audino, V. Badarinarayana, V. Palaniswamy, B. Anderson and C. L. Denis (2001) Characterization of CAF4 and CAF16 reveals a functional connection between the CCR4-NOT complex and a subset of SRB proteins of the RNA polymerase II holoenzyme. *J Biol Chem* **276**: 7541-7548.

Lopes, M., C. Cotta-Ramusino, A. Pellicioli, G. Liberi, P. Plevani, M. Muzi-Falconi, C. S. Newlon and M. Foiani (2001) The DNA replication checkpoint response stabilizes stalled replication forks. *Nature* **412**: 557-561.

Lopez-Fanarraga, M., J. Avila, A. Guasch, M. Coll and J. C. Zabala (2001) Review: postchaperonin tubulin folding cofactors and their role in microtubule dynamics. *J Struct Biol* **135**: 219-229.

Lorain, S., S. Demczuk, V. Lamour, S. Toth, A. Aurias, B. A. Roe and M. Lipinski (1996) Structural Organization of the WD repeat protein-encoding gene HIRA in the DiGeorge syndrome critical region of human chromosome 22. *Genome Res* **6**: 43-50.

Loyola, A. and G. Almouzni (2004) Histone chaperones, a supporting role in the limelight. *Biochim Biophys Acta* **1677**: 3-11.

Luger, K., A. W. Mader, R. K. Richmond, D. F. Sargent and T. J. Richmond (1997) Crystal structure of the nucleosome core particle at 2.8 Å resolution. *Nature* **389**: 251-260.

Luukkonen, B. G. and B. Seraphin (1999) A conditional U5 snRNA mutation affecting pre-mRNA splicing and nuclear pre-mRNA retention identifies *SSD1/SRK1* as a general splicing mutant suppressor. *Nucleic Acids Res* **27**: 3455-3465.

Lycan, D., G. Mikesell, M. Bunger and L. Breeden (1994) Differential effects of Cdc68 on cell cycle-regulated promoters in *Saccharomyces cerevisiae*. *Mol Cell Biol* **14**: 7455-7465.

Madden, K. and M. Snyder (1998) Cell polarity and morphogenesis in budding yeast. *Annu Rev Microbiol* **52**: 687-744.

Madden, K., Y. J. Sheu, K. Baetz, B. Andrews and M. Snyder (1997) SBF cell cycle regulator as a target of the yeast PKC-MAP kinase pathway. *Science* **275**: 1781-1784.

Maga, G. and U. Hubscher (2003) Proliferating cell nuclear antigen (PCNA): a dancer with many partners. *J Cell Sci* **116**: 3051-3060.

Malagon, F., A. H. Tong, B. K. Shafer and J. N. Strathern (2004) Genetic interactions of *DST1* in *Saccharomyces cerevisiae* suggest a role of TFIIS in the initiation-elongation transition. *Genetics* **166**: 1215-1227.

Malone, E. A., C. D. Clark, A. Chiang and F. Winston (1991) Mutations in *SPT16/CDC68* suppress *cis*- and *trans*-acting mutations that affect promoter function in *Saccharomyces cerevisiae*. *Mol Cell Biol* **11**: 5710-5717.

Marsolier, M. C., P. Roussel, C. Leroy and C. Mann (2000) Involvement of the PP2C-like phosphatase Ptc2p in the DNA checkpoint pathways of *Saccharomyces cerevisiae*. *Genetics* **154**: 1523-1532.

Martens, J. A. and F. Winston (2002) Evidence that Swi/Snf directly represses transcription in *S. cerevisiae*. *Genes Dev* **16**: 2231-2236.

Martens, J. A. and F. Winston (2003) Recent advances in understanding chromatin remodeling by Swi/Snf complexes. *Curr Opin Genet Dev* **13**: 136-142.

Martin, H., M. C. Castellanos, R. Cenamor, M. Sanchez, M. Molina and C. Nombela (1996) Molecular and functional characterization of a mutant allele of the mitogen-activated protein-kinase gene *SLT2* (*MPK1*) rescued from yeast autolytic mutants. *Curr Genet* **29**: 516-522.

Martinez-Pastor, M. T., G. Marchler, C. Schuller, A. Marchler-Bauer, H. Ruis and F. Estruch (1996) The *Saccharomyces cerevisiae* zinc finger proteins Msn2p and Msn4p are required for transcriptional induction through the stress response element (STRE). *EMBO J* **15**: 2227-2235.

Martin-Yken, H., A. Dagkessamanskaia, D. Talibi and J. Francois (2002) *KNR4* is a member of the *PKC1* signalling pathway and genetically interacts with *BCK2*, a gene involved in cell cycle progression in *Saccharomyces cerevisiae*. *Curr Genet* **41**: 323-332.

Mason, P. B. and K. Struhl (2003) The FACT complex travels with elongating RNA polymerase II and is important for the fidelity of transcriptional initiation in vivo. *Mol Cell Biol* **23**: 8323-8333.

Mayer, M. L., S. P. Gygi, R. Aebersold and P. Hieter (2001) Identification of RFC(Ctf18p, Ctf8p, Dcc1p): an alternative RFC complex required for sister chromatid cohesion in *S. cerevisiae*. *Mol Cell* **7**: 959-970.

Mayer, M. L., I. Pot, M. Chang, H. Xu, V. Aneliunas, T. Kwok, R. Newitt, R. Aebersold, C. Boone, G. W. Brown and P. Hieter (2004) Identification of protein complexes required for efficient sister chromatid cohesion. *Mol Biol Cell* **15**: 1736-1745.

Mazzoni, C., P. Zarov, A. Rambourg and C. Mann (1993) The *SLT2* (*MPK1*) MAP kinase homolog is involved in polarized cell growth in *Saccharomyces cerevisiae*. *J Cell Biol* **123**: 1821-1833.

McDonald, H. B., A. H. Helfant, E. M. Mahony, S. K. Khosla and L. Goetsch (2002) Mutational analysis reveals a role for the C terminus of the proteasome subunit Rpt4p in spindle pole body duplication in *Saccharomyces cerevisiae*. *Genetics* **162**: 705-720.

Meeks-Wagner, D. and L. H. Hartwell (1986) Normal stoichiometry of histone dimer sets is necessary for high fidelity of mitotic chromosome transmission. *Cell* **44**: 43-52.

Megee, P. C., B. A. Morgan and M. M. Smith (1995) Histone H4 and the maintenance of genome integrity. *Genes Dev* **9**: 1716-1727.

Mello, J. A. and G. Almouzni (2001) The ins and outs of nucleosome assembly. *Curr Opin Genet Dev* **11**: 136-141.

Mello, J. A., H. H. Sillje, D. M. Roche, D. B. Kirschner, E. A. Nigg and G. Almouzni (2002) Human Asf1 and CAF-1 interact and synergize in a repair-coupled nucleosome assembly pathway. *EMBO Rep* **3**: 329-334.

Mellor, J. and A. Morillon (2004) ISWI complexes in *Saccharomyces cerevisiae*. *Biochim Biophys Acta* **1677**: 100-112.

Meluh, P. B., P. Yang, L. Glowczewski, D. Koshland and M. M. Smith (1998) Cse4p is a component of the core centromere of *Saccharomyces cerevisiae*. *Cell* **94**: 607-613.

Meneghini, M. D., M. Wu and H. D. Madhani (2003) Conserved histone variant H2A.Z protects euchromatin from the ectopic spread of silent heterochromatin. *Cell* **112**: 725-736.

Merrill, B. J. and C. Holm (1999) A requirement for recombinational repair in *Saccharomyces cerevisiae* is caused by DNA replication defects of *mec1* mutants. *Genetics* **153**: 595-605.

Messing, J. (1983) New M13 vectors for cloning. *Methods Enzymol* **101**: 20-78.

Miles, J. and T. Formosa (1992) Protein affinity chromatography with purified yeast DNA polymerase α detects proteins that bind to DNA polymerase. *Proc Natl Acad Sci U S A* **89**: 1276-1280.

Miller, J. H. (1972) Experiments in molecular genetics. Cold Spring Harbor, NY, Cold Spring Harbor Laboratory Press.

Milutinovic, S., Q. Zhuang and M. Szyf (2002) Proliferating cell nuclear antigen associates with histone deacetylase activity, integrating DNA replication and chromatin modification. *J Biol Chem* **277**: 20974-20978.

Min, J., Y. Zhang and R. M. Xu (2003) Structural basis for specific binding of Polycomb chromodomain to histone H3 methylated at Lys 27. *Genes Dev* **17**: 1823-1828.

Mirzoeva, O. K. and J. H. Petrini (2003) DNA replication-dependent nuclear dynamics of the Mre11 complex. *Mol Cancer Res* **1**: 207-218.

Mizuguchi, G., X. Shen, J. Landry, W. H. Wu, S. Sen and C. Wu (2004) ATP-driven exchange of histone H2AZ variant catalyzed by SWR1 chromatin remodeling complex. *Science* **303**: 343-348.

Moggs, J. G., P. Grandi, J. P. Quivy, Z. O. Jonsson, U. Hubscher, P. B. Becker and G. Almouzni (2000) A CAF-1-PCNA-mediated chromatin assembly pathway triggered by sensing DNA damage. *Mol Cell Biol* **20**: 1206-1218.

Mohaghegh, P., J. K. Karow, R. M. Brosh Jr, Jr., V. A. Bohr and I. D. Hickson (2001) The Bloom's and Werner's syndrome proteins are DNA structure-specific helicases. *Nucleic Acids Res* **29**: 2843-2849.

Moran, L., D. Norris and M. A. Osley (1990) A yeast H2A-H2B promoter can be regulated by changes in histone gene copy number. *Genes Dev* **4**: 752-763.

Moreau, S., E. A. Morgan and L. S. Symington (2001) Overlapping functions of the *Saccharomyces cerevisiae* Mre11, Exo1 and Rad27 nucleases in DNA metabolism. *Genetics* **159**: 1423-1433.

Moreira, J. M. and S. Holmberg (2000) Chromatin-mediated transcriptional regulation by the yeast architectural factors NHP6A and NHP6B. *EMBO J* **19**: 6804-6813.

Moriya, H. and K. Isono (1999) Analysis of genetic interactions between *DHH1*, *SSD1* and *ELM1* indicates their involvement in cellular morphology determination in *Saccharomyces cerevisiae*. *Yeast* **15**: 481-496.

Mosammaparast, N., C. S. Ewart and L. F. Pemberton (2002) A role for nucleosome assembly protein 1 in the nuclear transport of histones H2A and H2B. *EMBO J* **21**: 6527-6538.

Moskvina, E., C. Schuller, C. T. Maurer, W. H. Mager and H. Ruis (1998) A search in the genome of *Saccharomyces cerevisiae* for genes regulated *via* stress response elements. *Yeast* **14**: 1041-1050.

Mueller, C. L. and J. A. Jaehning (2002) Ctr9, Rtf1, and Leo1 are components of the Paf1/RNA polymerase II complex. *Mol Cell Biol* **22**: 1971-1980.

Muhlrad, D., R. Hunter and R. Parker (1992) A rapid method for localized mutagenesis of yeast genes. *Yeast* **8**: 79-82.

Murray, S., R. Udupa, S. Yao, G. Hartzog and G. Prelich (2001) Phosphorylation of the RNA polymerase II carboxy-terminal domain by the Bur1 cyclin-dependent kinase. *Mol Cell Biol* **21**: 4089-4096.

Myung, K. and R. D. Kolodner (2002) Suppression of genome instability by redundant S-phase checkpoint pathways in *Saccharomyces cerevisiae*. *Proc Natl Acad Sci U S A* **99**: 4500-4507.

Naiki, T., T. Kondo, D. Nakada, K. Matsumoto and K. Sugimoto (2001) Chl12 (Ctf18) forms a novel replication factor C-related complex and functions redundantly with Rad24 in the DNA replication checkpoint pathway. *Mol Cell Biol* **21**: 5838-5845.

Narlikar, G. J., M. L. Phelan and R. E. Kingston (2001) Generation and interconversion of multiple distinct nucleosomal states as a mechanism for catalyzing chromatin fluidity. *Mol Cell* **8**: 1219-1230.

Nemeth, A. and G. Langst (2004) Chromatin higher order structure: opening up chromatin for transcription. *Brief Funct Genomic Proteomic* **2**: 334-343.

Ng, H. H., F. Robert, R. A. Young and K. Struhl (2002) Genome-wide location and regulated recruitment of the RSC nucleosome-remodeling complex. *Genes Dev* **16**: 806-819.

Niedenthal, R. K., M. Sen-Gupta, A. Wilmen and J. H. Hegemann (1993) Cpf1 protein induced bending of yeast centromere DNA element I. *Nucleic Acids Res* **21**: 4726-4733.

Nielsen, P. R., D. Nietlispach, H. R. Mott, J. Callaghan, A. Bannister, T. Kouzarides, A. G. Murzin, N. V. Murzina and E. D. Laue (2002) Structure of the HP1 chromodomain bound to histone H3 methylated at lysine 9. *Nature* **416**: 103-107.

Nissan, T. A., J. Bassler, E. Petfalski, D. Tollervey and E. Hurt (2002) 60S pre-ribosome formation viewed from assembly in the nucleolus until export to the cytoplasm. *EMBO J* **21**: 5539-5547.

Ogas, J., B. J. Andrews and I. Herskowitz (1991) Transcriptional activation of *CLN1*, *CLN2*, and a putative new G1 cyclin (*HCS26*) by *SWI4*, a positive regulator of G1-specific transcription. *Cell* **66**: 1015-1026.

Ohkuni, K., A. Okuda and A. Kikuchi (2003) Yeast Nap1-binding protein Nbp2p is required for mitotic growth at high temperatures and for cell wall integrity. *Genetics* **165**: 517-529.

Oki, M., L. Valenzuela, T. Chiba, T. Ito and R. T. Kamakaka (2004) Barrier proteins remodel and modify chromatin to restrict silenced domains. *Mol Cell Biol* **24**: 1956-1967.

Okuhara, K., K. Ohta, H. Seo, M. Shioda, T. Yamada, Y. Tanaka, N. Dohmae, Y. Seyama, T. Shibata and H. Murofushi (1999) A DNA unwinding factor involved in DNA replication in cell-free extracts of *Xenopus* eggs. *Curr Biol* **9**: 341-350.

Onodera, R., M. Seki, A. Ui, Y. Satoh, A. Miyajima, F. Onoda and T. Enomoto (2002) Functional and physical interaction between Sgs1 and Top3 and Sgs1-independent function of Top3 in DNA recombination repair. *Genes Genet Syst* **77**: 11-21.

Orphanides, G., G. LeRoy, C. H. Chang, D. S. Luse and D. Reinberg (1998) FACT, a factor that facilitates transcript elongation through nucleosomes. *Cell* **92**: 105-116.

Orphanides, G., W. H. Wu, W. S. Lane, M. Hampsey and D. Reinberg (1999) The chromatin-specific transcription elongation factor FACT comprises human SPT16 and SSRP1 proteins. *Nature* **400**: 284-288.

Osborn, A. J. and S. J. Elledge (2003) Mrc1 is a replication fork component whose phosphorylation in response to DNA replication stress activates Rad53. *Genes Dev* **17**: 1755-1767.

Osley, M. A. (1991) The regulation of histone synthesis in the cell cycle. *Annu Rev Biochem* **60**: 827-861.

Osley, M. A. (2004) H2B ubiquitylation: the end is in sight. *Biochim Biophys Acta* **1677**: 74-78.

Osley, M. A. and L. M. Hereford (1981) Yeast histone genes show dosage compensation. *Cell* **24**: 377-384.

Osley, M. A. and D. Lycan (1987) *Trans*-acting regulatory mutations that alter transcription of *Saccharomyces cerevisiae* histone genes. *Mol Cell Biol* **7**: 4204-4210.

Panic, B., O. Perisic, D. B. Veprintsev, R. L. Williams and S. Munro (2003a) Structural basis for Arl1-dependent targeting of homodimeric GRIP domains to the Golgi apparatus. *Mol Cell* **12**: 863-874.

Panic, B., J. R. Whyte and S. Munro (2003b) The ARF-like GTPases Arl1p and Arl3p act in a pathway that interacts with vesicle-tethering factors at the Golgi apparatus. *Curr Biol* **13**: 405-410.

Pappas, D. L., Jr., R. Frisch and M. Weinreich (2004) The NAD(+)-dependent Sir2p histone deacetylase is a negative regulator of chromosomal DNA replication. *Genes Dev* **18**: 769-781.

Paques, F. and J. E. Haber (1999) Multiple pathways of recombination induced by double-strand breaks in *Saccharomyces cerevisiae*. *Microbiol Mol Biol Rev* **63**: 349-404.

Parenteau, J. and R. J. Wellinger (2002) Differential processing of leading- and lagging-strand ends at *Saccharomyces cerevisiae* telomeres revealed by the absence of Rad27p nuclease. *Genetics* **162**: 1583-1594.

Park, T., S. G. Yi, S. H. Kang, S. Lee, Y. S. Lee and R. Simon (2003) Evaluation of normalization methods for microarray data. *BMC Bioinformatics* **4**: 33-46.

Paull, T. T. and M. Gellert (1998) The 3' to 5' exonuclease activity of Mre 11 facilitates repair of DNA double-strand breaks. *Mol Cell* **1**: 969-979.

Pei, Y. and S. Shuman (2003) Characterization of the *Schizosaccharomyces pombe* Cdk9/Pch1 protein kinase: Spt5 phosphorylation, autophosphorylation, and mutational analysis. *J Biol Chem* **278**: 43346-43356.

Pellicioli, A., C. Lucca, G. Liberi, F. Marini, M. Lopes, P. Plevani, A. Romano, P. P. Di Fiore and M. Foiani (1999) Activation of Rad53 kinase in response to DNA damage and its effect in modulating phosphorylation of the lagging strand DNA polymerase. *EMBO J* **18**: 6561-6572.

Peterson, C. L. (2002) Chromatin remodeling: nucleosomes bulging at the seams. *Curr Biol* **12**: R245-R247.

Peterson, C. L. and J. L. Workman (2000) Promoter targeting and chromatin remodeling by the SWI/SNF complex. *Curr Opin Genet Dev* **10**: 187-192.

Pijnappel, W. W., D. Schaft, A. Roguev, A. Shevchenko, H. Tekotte, M. Wilm, G. Rigaut, B. Seraphin, R. Aasland and A. F. Stewart (2001) The *S. cerevisiae* SET3 complex includes two histone deacetylases, Hos2 and Hst1, and is a meiotic-specific repressor of the sporulation gene program. *Genes Dev* **15**: 2991-3004.

Pokholok, D. K., N. M. Hannett and R. A. Young (2002) Exchange of RNA polymerase II initiation and elongation factors during gene expression in vivo. *Mol Cell* **9**: 799-809.

Poon, P. P., S. F. Nothwehr, R. A. Singer and G. C. Johnston (2001) The Gcs1 and Age2 ArfGAP proteins provide overlapping essential function for transport from the yeast *trans*-Golgi network. *J Cell Biol* **155**: 1239-1250.

Porter, S. E., T. M. Washburn, M. Chang and J. A. Jaehning (2002) The yeast Paf1-RNA polymerase II complex is required for full expression of a subset of cell cycle-regulated genes. *Eukaryot Cell* **1**: 830-842.

Praekelt, U. M. and P. A. Meacock (1990) *HSP12*, a new small heat shock gene of *Saccharomyces cerevisiae*: analysis of structure, regulation and function. *Mol Gen Genet* **223**: 97-106.

Prelich, G. (2002) RNA polymerase II carboxy-terminal domain kinases: emerging clues to their function. *Eukaryot Cell* **1**: 153-162.

Prendergast, J. A., L. E. Murray, A. Rowley, D. R. Carruthers, R. A. Singer and G. C. Johnston (1990) Size selection identifies new genes that regulate *Saccharomyces cerevisiae* cell proliferation. *Genetics* **124**: 81-90.

Proft, M. and K. Struhl (2002) Hog1 kinase converts the Sko1-Cyc8-Tup1 repressor complex into an activator that recruits SAGA and SWI/SNF in response to osmotic stress. *Mol Cell* **9**: 1307-1317.

Pruyne, D. and A. Bretscher (2000a) Polarization of cell growth in yeast. *J Cell Sci* **113 (Pt 4)**: 571-585.

Pruyne, D. and A. Bretscher (2000b) Polarization of cell growth in yeast. I. Establishment and maintenance of polarity states. *J Cell Sci* **113 (Pt 3)**: 365-375.

Puig, S. and J. E. Perez-Ortin (2000) Stress response and expression patterns in wine fermentations of yeast genes induced at the diauxic shift. *Yeast* **16**: 139-148.

Qin, S. and M. R. Parthun (2002) Histone H3 and the histone acetyltransferase Hat1p contribute to DNA double-strand break repair. *Mol Cell Biol* **22**: 8353-8365.

Quackenbush, J. (2002) Microarray data normalization and transformation. *Nat Genet* **32 Suppl**: 496-501.

Rattray, A. J., C. B. McGill, B. K. Shafer and J. N. Strathern (2001) Fidelity of mitotic double-strand-break repair in *Saccharomyces cerevisiae*: a role for *SAE2/COM1*. *Genetics* **158**: 109-122.

Ratzkin, B. and J. Carbon (1977) Functional expression of cloned yeast DNA in *Escherichia coli*. *Proc Natl Acad Sci U S A* **74**: 487-491.

Ray-Gallet, D., J. P. Quivy, C. Scamps, E. M. Martini, M. Lipinski and G. Almouzni (2002) HIRA is critical for a nucleosome assembly pathway independent of DNA synthesis. *Mol Cell* **9**: 1091-1100.

Redon, C., D. Pilch, E. Rogakou, O. Sedelnikova, K. Newrock and W. Bonner (2002) Histone H2A variants H2AX and H2AZ. *Curr Opin Genet Dev* **12**: 162-169.

Rehling, P., T. Darsow, D. J. Katzmann and S. D. Emr (1999) Formation of AP-3 transport intermediates requires Vps41 function. *Nat Cell Biol* **1**: 346-353.

Reinke, A., S. Anderson, J. M. McCaffery, J. Yates, 3rd, S. Aronova, S. Chu, S. Fairclough, C. Iverson, K. P. Wedaman and T. Powers (2004) TOR complex 1 includes a novel component, Tco89p (YPL180w), and cooperates with Ssd1p to maintain cellular integrity in *Saccharomyces cerevisiae*. *J Biol Chem* **279**: 14752-14762.

Rhoades, A. R., S. Ruone and T. Formosa (2004) Structural features of nucleosomes reorganized by yeast FACT and its HMG box component, Nhp6. *Mol Cell Biol* **24**: 3907-3917.

Rhodes, D. (1997) Chromatin structure. The nucleosome core all wrapped up. *Nature* **389**: 231-233.

Richardson, H. E., C. Wittenberg, F. Cross and S. I. Reed (1989) An essential G1 function for cyclin-like proteins in yeast. *Cell* **59**: 1127-1133.

Ridgway, P. and G. Almouzni (2000) CAF-1 and the inheritance of chromatin states: at the crossroads of DNA replication and repair. *J Cell Sci* **113 (Pt 15)**: 2647-2658.

Robinson, K. M. and M. C. Schultz (2003) Replication-independent assembly of nucleosome arrays in a novel yeast chromatin reconstitution system involves antisilencing factor Asf1p and chromodomain protein Chd1p. *Mol Cell Biol* **23**: 7937-7946.

Romero, P. A., G. J. Dijkgraaf, S. Shahinian, A. Herscovics and H. Bussey (1997) The yeast *CWH41* gene encodes glucosidase I. *Glycobiology* **7**: 997-1004.

Rondon, A. G., M. Gallardo, M. Garcia-Rubio and A. Aguilera (2004) Molecular evidence indicating that the yeast PAF complex is required for transcription elongation. *EMBO Rep* **5**: 47-53.

Rose, D., W. Thomas and C. Holm (1990) Segregation of recombined chromosomes in meiosis I requires DNA topoisomerase II. *Cell* **60**: 1009-1017.

Roth, J. F. (2000) The yeast Ty virus-like particles. *Yeast* **16**: 785-795.

Rouse, J. (2004) Esc4p, a new target of Mec1p (ATR), promotes resumption of DNA synthesis after DNA damage. *EMBO J* **23**: 1188-1197.

Rowley, A., R. A. Singer and G. C. Johnston (1991) *CDC68*, a yeast gene that affects regulation of cell proliferation and transcription, encodes a protein with a highly acidic carboxyl terminus. *Mol Cell Biol* **11**: 5718-5726.

Rudolph, H. K., A. Antebi, G. R. Fink, C. M. Buckley, T. E. Dorman, J. LeVitre, L. S. Davidow, J. I. Mao and D. T. Moir (1989) The yeast secretory pathway is perturbed by mutations in *PMR1*, a member of a Ca^{2+} ATPase family. *Cell* **58**: 133-145.

Rundlett, S. E., A. A. Carmen, R. Kobayashi, S. Bavykin, B. M. Turner and M. Grunstein (1996) *HDA1* and *RPD3* are members of distinct yeast histone deacetylase complexes that regulate silencing and transcription. *Proc Natl Acad Sci U S A* **93**: 14503-14508.

Runner, V. M. and J. L. Brewster (2003) A genetic screen for yeast genes induced by sustained osmotic stress. *Yeast* **20**: 913-920.

Ruone, S., A. R. Rhoades and T. Formosa (2003) Multiple Nhp6 molecules are required to recruit Spt16-Pob3 to form yFACT complexes and to reorganize nucleosomes. *J Biol Chem* **278**: 45288-45295.

Rusche, L. N., A. L. Kirchmaier and J. Rine (2003) The establishment, inheritance, and function of silenced chromatin in *Saccharomyces cerevisiae*. *Annu Rev Biochem* **72**: 481-516.

Russo, P., M. Simonen, A. Uimari, T. Teesalu and M. Makarow (1993) Dual regulation by heat and nutrient stress of the yeast *HSP150* gene encoding a secretory glycoprotein. *Mol Gen Genet* **239**: 273-280.

Sabet, N., F. Tong, J. P. Madigan, S. Volo, M. M. Smith and R. H. Morse (2003) Global and specific transcriptional repression by the histone H3 amino terminus in yeast. *Proc Natl Acad Sci U S A* **100**: 4084-4089.

Sacher, M., J. Barrowman, W. Wang, J. Horecka, Y. Zhang, M. Pypaert and S. Ferro-Novick (2001) TRAPP I implicated in the specificity of tethering in ER-to-Golgi transport. *Mol Cell* **7**: 433-442.

Sakurai, H. and T. Fukasawa (2001) A novel domain of the yeast heat shock factor that regulates its activation function. *Biochem Biophys Res Commun* **285**: 696-701.

Sambrook, J., E. F. Fitsch, T. Maniatis (1989) Molecular Cloning: A laboratory manual. New York, NY, Cold Spring Harbor Laboratory Press.

Sanger, F., S. Nicklen and A. R. Coulson (1977) DNA sequencing with chain-terminating inhibitors. *Proc Natl Acad Sci U S A* **74**: 5463-5467.

Santoso, D. and R. Thornburg (1998) Uridine 5'-monophosphate synthase is transcriptionally regulated by pyrimidine levels in *Nicotiana plumbaginifolia*. *Plant Physiol* **116**: 815-821.

Saunders, A., J. Werner, E. D. Andrulis, T. Nakayama, S. Hirose, D. Reinberg and J. T. Lis (2003) Tracking FACT and the RNA polymerase II elongation complex through chromatin in vivo. *Science* **301**: 1094-1096.

Schlesinger, M. B. and T. Formosa (2000) *POB3* is required for both transcription and replication in the yeast *Saccharomyces cerevisiae*. *Genetics* **155**: 1593-1606.

Scholes, D. T., M. Banerjee, B. Bowen and M. J. Curcio (2001) Multiple regulators of Ty1 transposition in *Saccharomyces cerevisiae* have conserved roles in genome maintenance. *Genetics* **159**: 1449-1465.

Schultz, J., F. Milpetz, P. Bork and C. P. Ponting (1998) SMART, a simple modular architecture research tool: identification of signaling domains. *Proc Natl Acad Sci U S A* **95**: 5857-5864.

Schwartz, M. F., S. J. Lee, J. K. Duong, S. Eminaga and D. F. Stern (2003) FHA domain-mediated DNA checkpoint regulation of Rad53. *Cell Cycle* **2**: 384-396.

Seaman, M. N., J. M. McCaffery and S. D. Emr (1998) A membrane coat complex essential for endosome-to-Golgi retrograde transport in yeast. *J Cell Biol* **142**: 665-681.

Sekito, T., J. Thornton and R. A. Butow (2000) Mitochondria-to-nuclear signaling is regulated by the subcellular localization of the transcription factors Rtg1p and Rtg3p. *Mol Biol Cell* **11**: 2103-2115.

Sekito, T., Z. Liu, J. Thornton and R. A. Butow (2002) RTG-dependent mitochondria-to-nucleus signaling is regulated by *MKS1* and is linked to formation of yeast prion [URE3]. *Mol Biol Cell* **13**: 795-804.

Sengupta, A., K. Blomqvist, A. J. Pickett, Y. Zhang, J. S. Chew and M. J. Dobson (2001) Functional domains of yeast plasmid-encoded Rep proteins. *J Bacteriol* **183**: 2306-2315.

Seol, J. H., A. Shevchenko and R. J. Deshaies (2001) Skp1 forms multiple protein complexes, including RAVE, a regulator of V-ATPase assembly. *Nat Cell Biol* **3**: 384-391.

Setty, S. R., M. E. Shin, A. Yoshino, M. S. Marks and C. G. Burd (2003) Golgi recruitment of GRIP domain proteins by Arf-like GTPase 1 is regulated by Arf-like GTPase 3. *Curr Biol* **13**: 401-404.

Sharp, J. A., E. T. Fouts, D. C. Krawitz and P. D. Kaufman (2001) Yeast histone deposition protein Asf1p requires Hir proteins and PCNA for heterochromatic silencing. *Curr Biol* **11**: 463-473.

Sharp, J. A., A. A. Franco, M. A. Osley and P. D. Kaufman (2002) Chromatin assembly factor I and Hir proteins contribute to building functional kinetochores in *S. cerevisiae*. *Genes Dev* **16**: 85-100.

Shcherbik, N., S. Kumar and D. S. Haines (2002) Substrate proteolysis is inhibited by dominant-negative Nedd4 and Rsp5 mutants harboring alterations in WW domain 1. *J Cell Sci* **115**: 1041-1048.

Shen, X. (2003) Preparation and Analysis of the INO80 Complex. *Methods Enzymol* **377**: 401-412.

Shen, X., G. Mizuguchi, A. Hamiche and C. Wu (2000) A chromatin remodelling complex involved in transcription and DNA processing. *Nature* **406**: 541-544.

Sherr, C. J. (2004) Principles of tumor suppression. *Cell* **116**: 235-246.

Shi, X., M. Chang, A. J. Wolf, C. H. Chang, A. A. Frazer-Abel, P. A. Wade, Z. F. Burton and J. A. Jaehning (1997) Cdc73p and Paf1p are found in a novel RNA polymerase II-containing complex distinct from the Srbp-containing holoenzyme. *Mol Cell Biol* **17**: 1160-1169.

Shi, X., A. Finkelstein, A. J. Wolf, P. A. Wade, Z. F. Burton and J. A. Jaehning (1996) Paf1p, an RNA polymerase II-associated factor in *Saccharomyces cerevisiae*, may have both positive and negative roles in transcription. *Mol Cell Biol* **16**: 669-676.

Shibahara, K. and B. Stillman (1999) Replication-dependent marking of DNA by PCNA facilitates CAF-1-coupled inheritance of chromatin. *Cell* **96**: 575-585.

Shimojima, T., M. Okada, T. Nakayama, H. Ueda, K. Okawa, A. Iwamatsu, H. Handa and S. Hirose (2003) *Drosophila* FACT contributes to Hox gene expression through physical and functional interactions with GAGA factor. *Genes Dev* **17**: 1605-1616.

Shore, D. (2000) The Sir2 protein family: A novel deacetylase for gene silencing and more. *Proc Natl Acad Sci U S A* **97**: 14030-14032.

Sidorova, J. and L. Breeden (1999) The *MSN1* and *NHP6A* genes suppress *SWI6* defects in *Saccharomyces cerevisiae*. *Genetics* **151**: 45-55.

Sikorski, R. S. and P. Hieter (1989) A system of shuttle vectors and yeast host strains designed for efficient manipulation of DNA in *Saccharomyces cerevisiae*. *Genetics* **122**: 19-27.

Simic, R., D. L. Lindstrom, H. G. Tran, K. L. Roinick, P. J. Costa, A. D. Johnson, G. A. Hartzog and K. M. Arndt (2003) Chromatin remodeling protein Chd1 interacts with transcription elongation factors and localizes to transcribed genes. *EMBO J* **22**: 1846-1856.

Skoog, L. and G. Bjursell (1974) Nuclear and cytoplasmic pools of deoxyribonucleoside triphosphates in Chinese hamster ovary cells. *J Biol Chem* **249**: 6434-6438.

Slater, M. L. (1973) Effect of reversible inhibition of deoxyribonucleic acid synthesis on the yeast cell cycle. *J Bacteriol* **113**: 263-270.

Slee, E. A., D. J. O'Connor and X. Lu (2004) To die or not to die: how does p53 decide? *Oncogene* **23**: 2809-2818.

Smith, M. M. and K. Murray (1983) Yeast H3 and H4 histone messenger RNAs are transcribed from two non-allelic gene sets. *J Mol Biol* **169**: 641-661.

Smith, S. and B. Stillman (1989) Purification and characterization of CAF-I, a human cell factor required for chromatin assembly during DNA replication in vitro. *Cell* **58**: 15-25.

Smith, C. M., Z. W. Haimberger, C. O. Johnson, A. J. Wolf, P. R. Gafken, Z. Zhang, M. R. Parthun and D. E. Gottschling (2002) Heritable chromatin structure: mapping "memory" in histones H3 and H4. *Proc Natl Acad Sci U S A* **99 (Suppl 4)**: 16454-16461.

Smith, J. S., C. B. Brachmann, I. Celic, M. A. Kenna, S. Muhammad, V. J. Starai, J. L. Avalos, J. C. Escalante-Semerena, C. Grubmeyer, C. Wolberger and J. D. Boeke (2000) A phylogenetically conserved NAD+-dependent protein deacetylase activity in the Sir2 protein family. *Proc Natl Acad Sci U S A* **97**: 6658-6663.

Smits, G. J., J. C. Kapteyn, H. van den Ende and F. M. Klis (1999) Cell wall dynamics in yeast. *Curr Opin Microbiol* **2**: 348-352.

Sorger, P. K. and H. R. Pelham (1988) Yeast heat shock factor is an essential DNA-binding protein that exhibits temperature-dependent phosphorylation. *Cell* **54**: 855-864.

Squazzo, S. L., P. J. Costa, D. L. Lindstrom, K. E. Kumer, R. Simic, J. L. Jennings, A. J. Link, K. M. Arndt and G. A. Hartzog (2002) The Paf1 complex physically and functionally associates with transcription elongation factors *in vivo*. *EMBO J* **21**: 1764-1774.

Stettler, S., N. Chiannilkulchai, S. Hermann-Le Denmat, D. Lalo, F. Lacroute, A. Sentenac and P. Thuriaux (1993) A general suppressor of RNA polymerase I, II and III mutations in *Saccharomyces cerevisiae*. *Mol Gen Genet* **239**: 169-176.

Strahl, B. D. and C. D. Allis (2000) The language of covalent histone modifications. *Nature* **403**: 41-45.

Strahl, B. D., P. A. Grant, S. D. Briggs, Z. W. Sun, J. R. Bone, J. A. Caldwell, S. Mollah, R. G. Cook, J. Shabanowitz, D. F. Hunt and C. D. Allis (2002) Set2 is a nucleosomal histone H3-selective methyltransferase that mediates transcriptional repression. *Mol Cell Biol* **22**: 1298-1306.

Stromer, T., E. Fischer, K. Richter, M. Haslbeck and J. Buchner (2004) Analysis of the regulation of the molecular chaperone Hsp26 by temperature-induced dissociation: the N-terminal domail is important for oligomer assembly and the binding of unfolding proteins. *J Biol Chem* **279**: 11222-11228.

Struhl, K. (1998) Histone acetylation and transcriptional regulatory mechanisms. *Genes Dev* **12**: 599-606.

Sugawara, N., X. Wang and J. E. Haber (2003) In vivo roles of Rad52, Rad54, and Rad55 proteins in Rad51-mediated recombination. *Mol Cell* **12**: 209-219.

Sun, X., D. Thrower, J. Qiu, P. Wu, L. Zheng, M. Zhou, J. Bachant, D. M. Wilson, 3rd and B. Shen (2003) Complementary functions of the *Saccharomyces cerevisiae* Rad2

family nucleases in Okazaki fragment maturation, mutation avoidance, and chromosome stability. *DNA Repair* **2**: 925-940.

Sun, Z., D. S. Fay, F. Marini, M. Foiani and D. F. Stern (1996) Spk1/Rad53 is regulated by Mec1-dependent protein phosphorylation in DNA replication and damage checkpoint pathways. *Genes Dev* **10**: 395-406.

Sun, Z. W. and C. D. Allis (2002) Ubiquitination of histone H2B regulates H3 methylation and gene silencing in yeast. *Nature* **418**: 104-108.

Sundararajan, A., B. S. Lee and D. J. Garfinkel (2003) The Rad27 (Fen-1) nuclease inhibits Ty1 mobility in *Saccharomyces cerevisiae*. *Genetics* **163**: 55-67.

Suto, R. K., M. J. Clarkson, D. J. Tremethick and K. Luger (2000) Crystal structure of a nucleosome core particle containing the variant histone H2A.Z. *Nat Struct Biol* **7**: 1121-1124.

Sutton, A., D. Immanuel and K. T. Arndt (1991a) The SIT4 protein phosphatase functions in late G1 for progression into S phase. *Mol Cell Biol* **11**: 2133-2148.

Sutton, A., F. Lin and K. T. Arndt (1991b) The SIT4 protein phosphatase is required in late G1 for progression into S phase. *Cold Spring Harb Symp Quant Biol* **56**: 75-81.

Sutton, A., J. Bucaria, M. A. Osley and R. Sternglanz (2001a) Yeast ASF1 protein is required for cell cycle regulation of histone gene transcription. *Genetics* **158**: 587-596.

Sutton, A., R. C. Heller, J. Landry, J. S. Choy, A. Sirko and R. Sternglanz (2001b) A novel form of transcriptional silencing by Sum1-1 requires Hst1 and the origin recognition complex. *Mol Cell Biol* **21**: 3514-3522.

Tadauchi, T., K. Matsumoto, I. Herskowitz and K. Irie (2001) Post-transcriptional regulation through the *HO* 3'-UTR by Mpt5, a yeast homolog of Pumilio and FBF. *EMBO J* **20**: 552-561.

Tanner, K. G., J. Landry, R. Sternglanz and J. M. Denu (2000) Silent information regulator 2 family of NAD- dependent histone/protein deacetylases generates a unique product, 1-O-acetyl-ADP-ribose. *Proc Natl Acad Sci U S A* **97**: 14178-14182.

Tomas-Cobos, L., L. Casadome, G. Mas, P. Sanz and F. Posas (2004) Expression of the *HXT1* low affinity glucose transporter requires the coordinated activities of the HOG and glucose signalling pathways. *J Biol Chem* **279**: 22010-22019.

Tong, A. H., M. Evangelista, A. B. Parsons, H. Xu, G. D. Bader, N. Page, M. Robinson, S. Raghibizadeh, C. W. Hogue, H. Bussey, B. Andrews, M. Tyers and C. Boone (2001) Systematic genetic analysis with ordered arrays of yeast deletion mutants. *Science* **294**: 2364-2368.

Tong, A. H., G. Lesage, G. D. Bader, H. Ding, H. Xu, X. Xin, J. Young, G. F. Berriz, R. L. Brost, M. Chang, Y. Chen, X. Cheng, G. Chua, H. Friesen, D. S. Goldberg, J. Haynes, C. Humphries, G. He, S. Hussein, L. Ke, N. Krogan, Z. Li, J. N. Levinson, H. Lu, P. Menard, C. Munyana, A. B. Parsons, O. Ryan, R. Tonikian, T. Roberts, A. M. Sdicu, J. Shapiro, B. Sheikh, B. Suter, S. L. Wong, L. V. Zhang, H. Zhu, C. G. Burd, S. Munro, C. Sander, J. Rine, J. Greenblatt, M. Peter, A. Bretscher, G. Bell, F. P.

Roth, G. W. Brown, B. Andrews, H. Bussey and C. Boone (2004) Global mapping of the yeast genetic interaction network. *Science* **303**: 808-813.

Torres, L., H. Martin, M. I. Garcia-Saez, J. Arroyo, M. Molina, M. Sanchez and C. Nombela (1991) A protein kinase gene complements the lytic phenotype of *Saccharomyces cerevisiae lyt2* mutants. *Mol Microbiol* **5**: 2845-2854.

Trujillo, K. M., D. H. Roh, L. Chen, S. Van Komen, A. Tomkinson and P. Sung (2003) Yeast Xrs2 binds DNA and helps target Rad50 and Mre11 to DNA ends. *J Biol Chem* **278**: 48957-48964.

Tsuchiya, E., T. Hosotani and T. Miyakawa (1998) A mutation in *NPS1/STH1*, an essential gene encoding a component of a novel chromatin-remodeling complex RSC, alters the chromatin structure of *Saccharomyces cerevisiae* centromeres. *Nucleic Acids Res* **26**: 3286-3292.

Tsukada, M. and D. Gallwitz (1996) Isolation and characterization of *SYS* genes from yeast, multicopy suppressors of the functional loss of the transport GTPase Ypt6p. *J Cell Sci* **109 (Pt 10)**: 2471-2481.

Turcq, B., K. F. Dobinson, N. Serizawa and A. M. Lambowitz (1992) A protein required for RNA processing and splicing in *Neurospora* mitochondria is related to gene products involved in cell cycle protein phosphatase functions. *Proc Natl Acad Sci U S A* **89**: 1676-1680.

Tyler, J. K., C. R. Adams, S. R. Chen, R. Kobayashi, R. T. Kamakaka and J. T. Kadonaga (1999) The RCAF complex mediates chromatin assembly during DNA replication and repair. *Nature* **402**: 555-560.

Uesono, Y., A. Fujita, A. Toh-e and Y. Kikuchi (1994) The *MCS1/SSD1/SRK1/SSL1* gene is involved in stable maintenance of the chromosome in yeast. *Gene* **143**: 135-138.

Uesono, Y., A. Toh-e and Y. Kikuchi (1997) Ssd1p of *Saccharomyces cerevisiae* associates with RNA. *J Biol Chem* **272**: 16103-16109.

Valdivia, R. H. and R. Schekman (2003) The yeasts Rho1p and Pkc1p regulate the transport of chitin synthase III (Chs3p) from internal stores to the plasma membrane. *Proc Natl Acad Sci U S A* **100**: 10287-10292.

van der Meijden, C. M., P. S. Vaughan, A. Staal, W. Albig, D. Doenecke, J. L. Stein, G. S. Stein and A. J. van Wijnen (1998) Selective expression of specific histone H4 genes reflects distinctions in transcription factor interactions with divergent H4 promoter elements. *Biochim Biophys Acta* **1442**: 82-100.

van der Voorn, L. and H. L. Ploegh (1992) The WD-40 repeat. *FEBS Lett* **307**: 131-134.

Van Hooser, A. A., Ouspenski, II, H. C. Gregson, D. A. Starr, T. J. Yen, M. L. Goldberg, K. Yokomori, W. C. Earnshaw, K. F. Sullivan and B. R. Brinkley (2001) Specification of kinetochore-forming chromatin by the histone H3 variant CENP-A. *J Cell Sci* **114**: 3529-3542.

Varela, J. C., U. M. Praekelt, P. A. Meacock, R. J. Planta and W. H. Mager (1995) The *Saccharomyces cerevisiae HSP12* gene is activated by the high-osmolarity glycerol pathway and negatively regulated by protein kinase A. *Mol Cell Biol* **15**: 6232-6245.

Vater, C. A., C. K. Raymond, K. Ekena, I. Howald-Stevenson and T. H. Stevens (1992) The VPS1 protein, a homolog of dynamin required for vacuolar protein sorting in *Saccharomyces cerevisiae*, is a GTPase with two functionally separable domains. *J Cell Biol* **119**: 773-786.

Verma, R., J. Smiley, B. Andrews and J. L. Campbell (1992) Regulation of the yeast DNA replication genes through the Mlu I cell cycle box is dependent on SWI6. *Proc Natl Acad Sci U S A* **89**: 9479-9483.

Verna, J., A. Lodder, K. Lee, A. Vagts and R. Ballester (1997) A family of genes required for maintenance of cell wall integrity and for the stress response in *Saccharomyces cerevisiae*. *Proc Natl Acad Sci U S A* **94**: 13804-13809.

Verreault, A., P. D. Kaufman, R. Kobayashi and B. Stillman (1996) Nucleosome assembly by a complex of CAF-1 and acetylated histones H3/H4. *Cell* **87**: 95-104.

Versini, G., I. Comet, M. Wu, L. Hoopes, E. Schwob and P. Pasero (2003) The yeast Sgs1 helicase is differentially required for genomic and ribosomal DNA replication. *EMBO J* **22**: 1939-1949.

Vollmer, P., E. Will, D. Scheglmann, M. Strom and D. Gallwitz (1999) Primary structure and biochemical characterization of yeast GTPase-activating proteins with substrate preference for the transport GTPase Ypt7p. *Eur J Biochem* **260**: 284-290.

Vowels, J. J. and G. S. Payne (1998) A dileucine-like sorting signal directs transport into an AP-3-dependent, clathrin-independent pathway to the yeast vacuole. *EMBO J* **17**: 2482-2493.

Wach, A., A. Brachat, C. Rebischung, S. Steiner, K. Pokorni, S. te Heesen, and P. Philippsen (1998) PCR-based gene targeting in *Saccharomyces cerevisiae*. Methods in Microbiology. **26**. A. Brown. San Diego, CA, Academic Press.

Wach, A., A. Brachat, R. Pohlmann and P. Philippsen (1994) New heterologous modules for classical or PCR-based gene disruptions in *Saccharomyces cerevisiae*. *Yeast* **10**: 1793-1808.

Wada, T., G. Orphanides, J. Hasegawa, D. K. Kim, D. Shima, Y. Yamaguchi, A. Fukuda, K. Hisatake, S. Oh, D. Reinberg and H. Handa (2000) FACT relieves DSIF/NELF-mediated inhibition of transcriptional elongation and reveals functional differences between P-TEFb and TFIIH. *Mol Cell* **5**: 1067-1072.

Wada, T., T. Takagi, Y. Yamaguchi, A. Ferdous, T. Imai, S. Hirose, S. Sugimoto, K. Yano, G. A. Hartzog, F. Winston, S. Buratowski and H. Handa (1998a) DSIF, a novel transcription elongation factor that regulates RNA polymerase II processivity, is composed of human Spt4 and Spt5 homologs. *Genes Dev* **12**: 343-356.

Wada, T., T. Takagi, Y. Yamaguchi, D. Watanabe and H. Handa (1998b) Evidence that P-TEFb alleviates the negative effect of DSIF on RNA polymerase II-dependent transcription in vitro. *EMBO J* **17**: 7395-7403.

Wade, P. A., W. Werel, R. C. Fentzke, N. E. Thompson, J. F. Leykam, R. R. Burgess, J. A. Jaehning and Z. F. Burton (1996) A novel collection of accessory factors associated with yeast RNA polymerase II. *Protein Expr Purif* **8**: 85-90.

Wagner, C., M. Dietz, J. Wittmann, A. Albrecht and H. J. Schuller (2001) The negative regulator Opi1 of phospholipid biosynthesis in yeast contacts the pleiotropic repressor Sin3 and the transcriptional activator Ino2. *Mol Microbiol* **41**: 155-166.

Wahi, M., K. Komachi and A. D. Johnson (1998) Gene regulation by the yeast Ssn6-Tup1 corepressor. *Cold Spring Harb Symp Quant Biol* **63**: 447-457.

Wang, C. W., P. E. Stromhaug, J. Shima and D. J. Klionsky (2002) The Ccz1-Mon1 protein complex is required for the late step of multiple vacuole delivery pathways. *J Biol Chem* **277**: 47917-47927.

Wang, C. W., P. E. Stromhaug, E. J. Kauffman, L. S. Weisman and D. J. Klionsky (2003) Yeast homotypic vacuole fusion requires the Ccz1-Mon1 complex during the tethering/docking stage. *J Cell Biol* **163**: 973-985.

Watanabe, M., C. Y. Chen and D. E. Levin (1994) *Saccharomyces cerevisiae PKC1* encodes a protein kinase C (PKC) homolog with a substrate specificity similar to that of mammalian PKC. *J Biol Chem* **269**: 16829-16836.

Watson, A. D., D. G. Edmondson, J. R. Bone, Y. Mukai, Y. Yu, W. Du, D. J. Stillman and S. Y. Roth (2000) Ssn6-Tup1 interacts with class I histone deacetylases required for repression. *Genes Dev* **14**: 2737-2744.

Wheeler, R. T., M. Kupiec, P. Magnelli, C. Abeijon and G. R. Fink (2003) A *Saccharomyces cerevisiae* mutant with increased virulence. *Proc Natl Acad Sci U S A* **100**: 2766-2770.

White, C. L., R. K. Suto and K. Luger (2001) Structure of the yeast nucleosome core particle reveals fundamental changes in internucleosome interactions. *EMBO J* **20**: 5207-5218.

Wijnen, H. and B. Futcher (1999) Genetic analysis of the shared role of *CLN3* and *BCK2* at the G_1-S transition in *Saccharomyces cerevisiae*. *Genetics* **153**: 1131-1143.

Wilson, T. E. (2002) A genomics-based screen for yeast mutants with an altered recombination/end-joining repair ratio. *Genetics* **162**: 677-688.

Wind, M. and D. Reines (2000) Transcription elongation factor SII. *Bioessays* **22**: 327-336.

Winkler, G. S., T. G. Petrakis, S. Ethelberg, M. Tokunaga, H. Erdjument-Bromage, P. Tempst and J. Q. Svejstrup (2001) RNA polymerase II elongator holoenzyme is composed of two discrete subcomplexes. *J Biol Chem* **276**: 32743-32749.

Winston, F., D. T. Chaleff, B. Valent and G. R. Fink (1984) Mutations affecting Ty-mediated expression of the *HIS4* gene of *Saccharomyces cerevisiae*. *Genetics* **107**: 179-197.

Winston, F., C. Dollard, E. A. Malone, J. Clare, J. G. Kapakos, P. Farabaugh and P. L. Minehart (1987) Three genes are required for *trans*-activation of Ty transcription in yeast. *Genetics* **115**: 649-656.

Winzeler, E. A., D. D. Shoemaker, A. Astromoff, H. Liang, K. Anderson, B. Andre, R. Bangham, R. Benito, J. D. Boeke, H. Bussey, A. M. Chu, C. Connelly, K. Davis, F. Dietrich, S. W. Dow, M. El Bakkoury, F. Foury, S. H. Friend, E. Gentalen, G. Giaever, J. H. Hegemann, T. Jones, M. Laub, H. Liao, N. Liebundguth, D. J. Lockhart, A. Lucau-Danila, N. Lussier, N. M'Rabet, P. Mendard, M. Mittmann, C. Pai, C. Rebischung, J. L. Revuelta, L. Riles, C. J. Roberts, P. Ross-MacDonald, B. Scherens, M. Snyder, S. Sookhai-Mahadeo, R. K. Storms, S. Veronneau, M. Voet, G. Volckaert, T. R. Ward, R. Wysocki, G. S. Yen, K. Yu, K. Zimmermann, P. Philippsen, M. Johnston., and R. W. Davis (1999) Functional characterization of the *S. cerevisiae* genome by gene deletion and parallel analysis. *Science* **285**: 901-906.

Wittmeyer, J. and T. Formosa (1997) The *Saccharomyces cerevisiae* DNA polymerase α catalytic subunit interacts with Cdc68/Spt16 and with Pob3, a protein similar to an HMG1-like protein. *Mol Cell Biol* **17**: 4178-4190.

Wittmeyer, J., L. Joss and T. Formosa (1999) Spt16 and Pob3 of *Saccharomyces cerevisiae* form an essential, abundant heterodimer that is nuclear, chromatin-associated, and copurifies with DNA polymerase α. *Biochemistry* **38**: 8961-8971.

Wittschieben, B. O., G. Otero, T. de Bizemont, J. Fellows, H. Erdjument-Bromage, R. Ohba, Y. Li, C. D. Allis, P. Tempst and J. Q. Svejstrup (1999) A novel histone acetyltransferase is an integral subunit of elongating RNA polymerase II holoenzyme. *Mol Cell* **4**: 123-128.

Wood, A., N. J. Krogan, J. Dover, J. Schneider, J. Heidt, M. A. Boateng, K. Dean, A. Golshani, Y. Zhang, J. F. Greenblatt, M. Johnston and A. Shilatifard (2003) Bre1, an E3 ubiquitin ligase required for recruitment and substrate selection of Rad6 at a promoter. *Mol Cell* **11**: 267-274.

Wu, J., A. A. Carmen, R. Kobayashi, N. Suka and M. Grunstein (2001) HDA2 and HDA3 are related proteins that interact with and are essential for the activity of the yeast histone deacetylase HDA1. *Proc Natl Acad Sci U S A* **98**: 4391-4396.

Xiao, T., H. Hall, K. O. Kizer, Y. Shibata, M. C. Hall, C. H. Borchers and B. D. Strahl (2003) Phosphorylation of RNA polymerase II CTD regulates H3 methylation in yeast. *Genes Dev* **17**: 654-663.

Xie, J., M. Pierce, V. Gailus-Durner, M. Wagner, E. Winter and A. K. Vershon (1999) Sum1 and Hst1 repress middle sporulation-specific gene expression during mitosis in *Saccharomyces cerevisiae*. *EMBO J* **18**: 6448-6454.

Xu, H., U. J. Kim, T. Schuster and M. Grunstein (1992) Identification of a new set of cell cycle-regulatory genes that regulate S-phase transcription of histone genes in *Saccharomyces cerevisiae*. *Mol Cell Biol* **12**: 5249-5259.

Xu, Q., G. C. Johnston and R. A. Singer (1993) The *Saccharomyces cerevisiae* Cdc68 transcription activator is antagonized by San1, a protein implicated in transcriptional silencing. *Mol Cell Biol* **13**: 7553-7565.

Xu, Q. (1995) Yeast proteins that modulate Cdc68 transcriptional activity. PhD thesis, Department of Biochemistry & Molecular Biology, Dalhousie University, Halifax, N.S., Canada.

Yamamoto, K. and Y. Jigami (2002) Mutation of *TRS130*, which encodes a component of the TRAPP II complex, activates transcription of *OCH1* in *Saccharomyces cerevisiae*. *Curr Genet* **42**: 85-93.

Yang, M. C., Q. G. Ruan, J. J. Yang, S. Eckenrode, S. Wu, R. A. McIndoe and J. X. She (2001) A statistical method for flagging weak spots improves normalization and ratio estimates in microarrays. *Physiol Genomics* **7**: 45-53.

Yarnell, A. T., S. Oh, D. Reinberg and S. J. Lippard (2001) Interaction of FACT, SSRP1, and the high mobility group (HMG) domain of SSRP1 with DNA damaged by the anticancer drug cisplatin. *J Biol Chem* **276**: 25736-25741.

Ye, X., A. A. Franco, H. Santos, D. M. Nelson, P. D. Kaufman and P. D. Adams (2003) Defective S phase chromatin assembly causes DNA damage, activation of the S phase checkpoint, and S phase arrest. *Mol Cell* **11**: 341-351.

Yeung, B. G., H. L. Phan and G. S. Payne (1999) Adaptor complex-independent clathrin function in yeast. *Mol Biol Cell* **10**: 3643-3659.

Yoshida, S., Y. Ohya, M. Goebl, A. Nakano and Y. Anraku (1994) A novel gene, *STT4*, encodes a phosphatidylinositol 4-kinase in the PKC1 protein kinase pathway of *Saccharomyces cerevisiae*. *J Biol Chem* **269**: 1166-1172.

Yu, J., K. Marshall, M. Yamaguchi, J. E. Haber and C. F. Weil (2004) Microhomology-dependent end joining and repair of transposon-induced DNA hairpins by host factors in *Saccharomyces cerevisiae*. *Mol Cell Biol* **24**: 1351-1364.

Zeng, S. X., M. S. Dai, D. M. Keller and H. Lu (2002) SSRP1 functions as a co-activator of the transcriptional activator p63. *EMBO J* **21**: 5487-5497.

Zhao, X., E. G. Muller and R. Rothstein (1998) A suppressor of two essential checkpoint genes identifies a novel protein that negatively affects dNTP pools. *Mol Cell* **2**: 329-340.

Zhou, Y. H., X. P. Zhang and R. H. Ebright (1991) Random mutagenesis of gene-sized DNA molecules by use of PCR with *Taq* DNA polymerase. *Nucleic Acids Res* **19**: 6052.